Polymer Deformation. II. Drawing of Polyethylene Single Crystals

P. H. GEIL,* *Camille Dreyfus Laboratory, Research Triangle Institute, Durham, North Carolina*

Synopsis

The effect of molecular weight average and distribution, defect type, fold plane type and orientation, and the presence of fold domain boundaries on the deformation characteristics of polyethylene single crystals drawn on a Mylar substrate has been investigated. Defect content is suggested to have a bigger effect than either molecular weight or distribution. Fold plans of the {100} type are shown to deform in a different fashion than those of the {110} type. Boundaries between {100} and {110} fold domains are greatly susceptible to failure whereas those between neighboring {110} fold domains are not. Clear evidence for deformation through {110} twinning and a crystal transformation is shown. Plastic deformation without molecular unfolding or fracture occurs in many polyethylene crystals for elongation up to at least 150%.

The morphology of oriented crystalline polymers is at present unknown. Although small-angle x-ray diffraction measurements indicate the presence of some form of periodic structure, electron microscope observations of drawn films and fibers, except for a few cases, have revealed no corresponding structure. (These results are reviewed in Chapter VII of ref. 1, referred to as I below.) Because of the limited applicability of electron microscopy to the determination of the morphology of fully oriented polymer, it was believed more useful to investigate the various stages of the deformation process itself and attempt to deduce not only the deformation mechanism but also the structure of the resulting material from these results. For deformation by drawing it was suggested that the use of single crystals as specimens would probably be the most desirable. Some initial investigations in this area are also described in I.

It is believed desirable to describe at the present time some of our subsequent results. In this and in papers III and IV[2,3] are described: (a) A number of observations on the drawing of both diamond-shaped and truncated polyethylene crystals; (b) observations on the effect of annealing drawn polyethylene crystals as a function of temperature, time, and amount of draw; (c) observations on the drawing of nylon 6 and polyoxymethylene crystals and a comparison with the results for polyethylene.

* Present address: Case Institute of Technology, Cleveland, Ohio.

EXPERIMENTAL AND RESULTS

Sample Preparation

We shall consider the following types of polyethylene single crystals. (A) Those grown from a 0.1% tetrachloroethylene solution of an Alathon (E. I. du Pont de Nemours & Co., Inc.) melt index 3.3 linear polyethylene by ambient cooling are diamond-shaped and are similar to those described as type A in I.[1]   (B) These were grown from a 0.1% solution of an Alathon melt index 4.7 polymer in tetrachloroethylene by ambient cooling.   (C) These were grown from 0.01% Marlex 6050 (Philips Chemical Company) (melt index 5.0) linear polyethylene solution in carbon tetrachloroethylene at 80°C.   The solution was filtered to a near gel, then rinsed twice with fresh solvent at 80°C.   The diamond-shaped crystals of types A and B are hollow pyramids in which pleats form during collapse whereas in C the resulting crystals are often finely corrugated.   (D) These were grown from a 0.05% Marlex 6050 solution in xylene at 88°C. and filtered at that temperature.   The crystals are truncated.   (E) Those grown from a 0.1% Fortiflex 60–500 (Celanese Corporation of America) (melt index 5.0) linear polyethylene solution in xylene at 85° and then cooled to room temperature are also truncated.

The appropriate crystals were deposited on Mylar (E. I. du Pont de Nemours & Co., Inc.) films in small stretchers and drawn the desired amount.   It was found that some 0.001 in. Mylar films could be drawn as much as 200% in certain directions.   The maximum draw varied with the particular roll of Mylar used, the direction of draw relative to the roll direction, and with the smoothness of the cut edge of the strips.   After evaporation of the solvent and stretching the desired amount, the samples were shadowed with platinum, stripped with poly(acrylic acid) and backed with carbon (see Chap. 1, ref. 1 for details).   The elongations listed for the various samples below are overall elongations of the substrate.

It has been suggested[1,4] that shadowing a polymer with metal or carbon results in some form of bonding between the shadowing material and the surface of the polymer.   In many of the following micrographs some black spots are seen in regions of the substrate not covered with the polyethylene crystals.   These spots consist of small fibers of poly(ethylene terephthalate) drawn from the Mylar surface when the replica was removed.   On curled up portions of the replica they can be observed to be on the order of 0.1 μ long and to be oriented normal to the replica.   Cracks within the crystals can be readily identified since the fibers are also found there.   In some portions of the replica, sheets of the Mylar are found attached to the replica. The structure of these sheets has not yet been investigated.   The Mylar adheres to the replica only in those regions which have been coated with platinum; poly(acrylic acid) alone will not adhere sufficiently well to result in the effects observed.

Effect of Molecular Characteristics

In I we reported that when type A crystals are drawn up to 100% most of the deformation takes place plastically. If drawn parallel to the **a** axis, little or no visible signs of the internal deformation can be seen in bright-field microscopy except for the overall change in shape and thickness of the crystal (Figs. VII-33 and 34 of I). When drawn at an angle to the **a** axis, ripples or striations developed which were usually parallel to the **a** axis, although occasionally parallel to {310} planes. In many cases the ripples developed in only two (opposite) of the four fold domains (Fig. VII-32 of I). Only occasionally were cracks found in the crystals; these appeared to develop in the thinnest regions of the ripples and at relatively large elongation (Fig. VII-37 of I). Subsequent experiments indicate that the appearance of the ripples is somewhat variable. In the crystals shown in Figure 1, type A

Fig. 1. Type A crystals drawn 25%. The draw direction is indicated by the arrows. The scale represents 1 μ and the shadowing angle is $\tan^{-1} 2/8.5$ for all figures. The long fibers in the upper right were formed when the crystals were stripped from the Mylar.

but from a different preparation than those described in I, the ripples are almost invisible, being very broad and shallow. They are visible in dark field. Diffraction patterns from these crystals indicate the presence of reflections from two different unit cells as described in I and later in this paper. The variation in ripple visibility may be an artifact due to differences in the shadowing process or may be due to actual differences in the crystals

and their adhesion to the substrate. It should be noted that these crystals were shadowed from such a direction that the ripples were parallel to the shadow direction and thus should be nearly invisible. Cracks were still relatively rare.
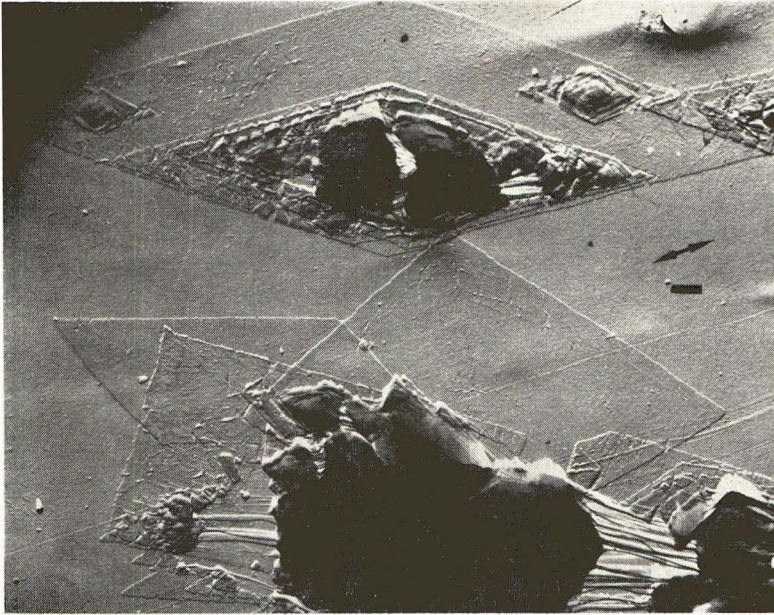

Fig. 2. Type B crystals drawn 50%.

The deformation of type B crystals is nearly the same as type A, with some evidence for a few more cracks (Fig. 2). The {310} type ripples can be seen on the upper crystal in Figure 2, with some irregular cracks near the end of the long axis. In the single lamella crystal at the lower center of the figure, drawn almost parallel to the **b** axis, an irregular crack is present along the fold domain boundary as well as several making an angle with the growth face.

Large cracks and numerous fibers often form in regions of the crystal containing overgrowths. No structure is visible in these fibers, even at high magnification. Those which are above the substrate, appearing black in Figure 2, seem to be surrounded with a layer of carbon and/or platinum. Their relative darkness in the image is difficult to explain in terms of their thickness. Furthermore, the shadows, as at the lower left, sometimes appear larger than the essentially circular fibers. Electron diffraction patterns, resembling x-ray fiber patterns and including the (002) reflections, can be obtained from regions containing numerous such fibers. The annealing of these fibers is described in III.[2] Usually the cracks in regions containing overgrowths extend through the entire crystal, although occasionally the basal layer will remain attached to the substrate, probably deforming in a manner similar to that in regions only one lamella thick. It

is also possible for all of the lamellae in an overgrowth to deform uniformly with no evidence of cracks (Fig. 10).

Fibers of irregular orientation, one end of which is attached to a region more than one lamella thick (overgrowth, pleat, or overlapping crystals), are also occasionally found on the replicas used for this work. These fibers form during stripping of the replica and thus are coated only with carbon (see Fig. 1).

There is a marked contrast in the drawability of type C crystals and those of type A and B. At elongations of as low as 10% large cracks are seen in the type C crystals. They are oriented nearly perpendicular to the draw direction (Fig. 3). These cracks appear to be preferentially aligned along {100}, {010} and nongrowth face {110} planes, although other directions also are possible (Figs. 3 and 4). The edges of the cracks, however, are usually not linear (Fig. 5). No fibers are drawn across these cracks. It is believed that the fracture does not result in breaking of the molecules but rather follows an irregular course on a molecular scale, corresponding to the ends of the molecules.

Fig. 3. Type C crystals drawn 10%. All of the overgrowths and thin edges are believed to have developed from low molecular weight polymer crystallizing during evaporation of the solvent. Fine corrugations resulting from collapse of the crystal during solvent removal can be seen here and in Fig. 4.

One notes that despite the fact that the crystals were filtered and rinsed twice at the growth temperature, there was apparently a large amount of polymer remaining in solution. The difference in amount present on Figures 3 and 4 is believed a result of draining away the excess solvent dur-
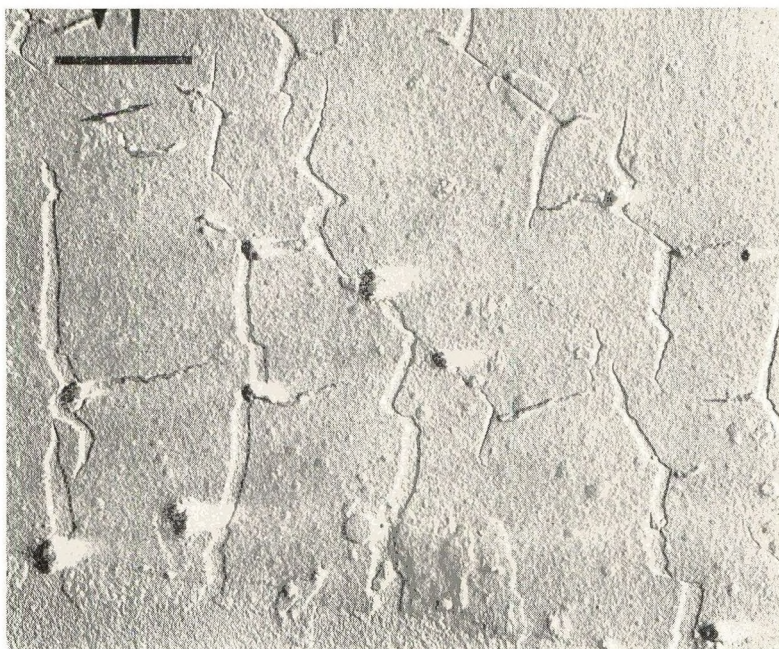
Fig. 4. Type C crystal drawn 25%.

Fig. 5. A portion of the crystal in Fig. 4 at higher magnification.

ing the preparation of the sample in Figure 4, while all of the solvent was allowed to evaporate in the case of the sample in Figure 3. The presence of these considerable quantities of low molecular weight material in the polymer used for these type C crystals, as will be discussed in the last section of this paper, may contribute to their apparent brittleness. When drawn 100%, the entire crystal appears to break up into small pieces on the order of 100 A. in size, these pieces being considerably thinner than the original lamella.

The failure of type C crystals by fracture is also apparent in their electron diffraction patterns and dark-field micrographs. (For observations of the other type crystals see a later section.) The electron diffraction patterns of the drawn type C crystals contain many more orders of reflections than types A and B drawn an equivalent amount, the latter having only one or two orders. In addition, the reflections consist of discrete spots for type C and appear arced for types A and B. When type C crystals are drawn 10%, only the normal reflections of the polyethylene orthorhombic unit cell are found. At 25% draw a few patterns show the presence of discrete spots from the second modification (see Fig. 10 and also Fig. VII-35 in I) while with 100% elongation all of the reflections have spread into arcs and considerable intensity is present in the new reflections.

Dark-field micrographs of type C crystals drawn 10% resemble those of undrawn crystals, except for the cracks. Moiré patterns and Bragg extinction fringes extending over micron-sized regions are visible. Other than the cracks, the only visible sign of deformation in the dark-field micrographs is the presence in some of the crystals of a set of parallel striations. Within a given crystal they make a constant angle with the axes, but this angle varies from crystal to crystal. With 25% elongation the striations are present in the majority of the crystals. In many cases they appear to resemble those described later for truncated crystals (Fig. 11) in being sharply defined. In other cases their appearance suggests they are due to ripples in the crystals resulting from the lateral contraction accompanying the elongation.

Although there is a difference in the molecular weight distribution in the polymers used for the type D and E crystals (that used for type E has a narrow distribution, much of the very high and low molecular weight material being absent[5]), they appear to deform in nearly the same manner. There is a slight indication of more and larger cracks in the type D crystals than in type E when drawn parallel to the **b** axis. No cracks are observed at elongations up to 150% in E and 50% in D (maximum studied) when drawn parallel to the **a** axis. Their deformation is described in the next section.

Effect of Fold Plane and Fold Domain Boundary Orientation

As indicated in I (Figs. VII-31 and 32) and as seen in Figure 4 of this paper, one finds that the pairs of {110} fold domains with the same growth face orientation behave similarly in deformation but that the other two

domains may behave differently. We have been unable to determine any definite reason for the selection of a particular pair of fold domains; it does not depend on the relative orientation of the growth faces and the draw direction. It may be related to the method of collapse of the pyramids during solvent removal.

In diamond-shaped polyethylene crystals one usually sees no effect of the fold domain boundary, boundaries across which the fold plane changes direction, on the deformation characteristics when drawn on Mylar. Figure 2 is the only micrograph we have in which a significant crack has formed along a fold domain boundary. Cracks or ripples often terminate at the boundary suggesting that the fold plane orientation is important. In addition, fibers are drawn across a crack only if it makes an angle with the fold planes. However, there is apparently no weakening of the crystal as a result of a change in direction of the folds.

The situation in the case of a phase boundary, as defined by Burbank,[1,6] is considerably different however. Those boundaries across which both the fold plane direction and the type of fold change, appear to be particu-

Fig. 6. Type E crystals drawn 25%. Note the Mylar fibers in the cracks and on the substrate.

larly weak (Fig. 6). Cracks along these boundaries appear at elongations as low as 10% and probably lower. In the few crystals in which the cracks are sufficiently wide one can observe fibers drawn across the opening. These phase boundary cracks are irregular in direction (Fig. 7), suggesting that the boundary itself may not follow a straight line. The boundary be-

Fig. 7. (100) fold domain of a type E crystal which had been drawn 50%. The pleat parallel to **b** is on the right side of the figure.

tween the {100} and {110} fold domains in truncated polyethylene crystals apparently does not correspond to a low index crystallographic plane, the angular width of the {100} domain varying with the crystallization temperature.[1,7] It is possible that the observed cracks follow the phase boundary, the variations in direction corresponding to small changes in growth temperature.

As seen in Figure 6, cracks and ripples parallel to the **a** axis develop in the {110} fold domains when the **a** axis is at an angle to the draw direction. The deformation of these domains appears similar to that observed in the case of diamond shaped crystals. In Figure 6 the cracks are readily identified by the black dots corresponding to the small fibers of Mylar.

The deformation of the {100} domains is considerably different from that of the {110}. Striations resembling slip bands and zigzag cracks develop when the **a** axis is at an angle to the draw direction. These cracks and striations are not quite parallel to the {110} growth faces of the neighboring domains. Because of the deformation both during crystal collapse and drawing, it is difficult to determine their crystallographic orientation, but it is believed likely they are parallel to {110} planes. When drawn parallel to **b**, both {110} and {1$\bar{1}$0} slip bands and cracks can be observed in the same domain; if drawn at an angle to **b**, only one set of bands and predominantly one crack direction are found. The bands are in the ⟨110⟩ direction most nearly parallel to the draw direction.

Fig. 8. Type E crystals drawn 150%. In the crystal on the bottom, the **a** axis is nearly parallel to the draw direction whereas in the crystal in the center it is almost normal to the draw direction.

In both the diamond-shaped crystals and the truncated crystals the cracks, once formed, do not appear to separate to any great extent with further elongation. Even at 150% elongation (Fig. 8) the cracks in crystals with the **a** axis at an angle to the draw direction are no larger or more numerous than those observed in crystals drawn 10–25%. Throughout the entire range of elongation few or no cracks are observed in crystals oriented such that the **a** axis is nearly parallel to the draw direction. Although it has not been possible to accurately measure the thickness of the crystals, because of the variable thickness edge composed of low molecular weight polymer and formed during solvent evaporation, it is obvious that the crystals are becoming thinner during the elongation. In addition, in the range of 100–150% elongation both the crystal and the Mylar substrate develop a granular appearance on the 250 A. size scale with that of the Mylar being slightly smaller (Fig. 9). This granularity is over and above that due to the shadowing material itself.

Electron Diffraction and Dark-Field Microscopy

As reported in I, electron diffraction patterns from drawn polyethylene single crystals contain not only the normal $hk0$ reflections from the orthorhombic unit cell defined by Bunn[3] but also several new reflections. At present we have been able to observe three of these reflections. Their spacings of 4.5_5, 3.8_5 and 3.5_5 are in good agreement with those given for a
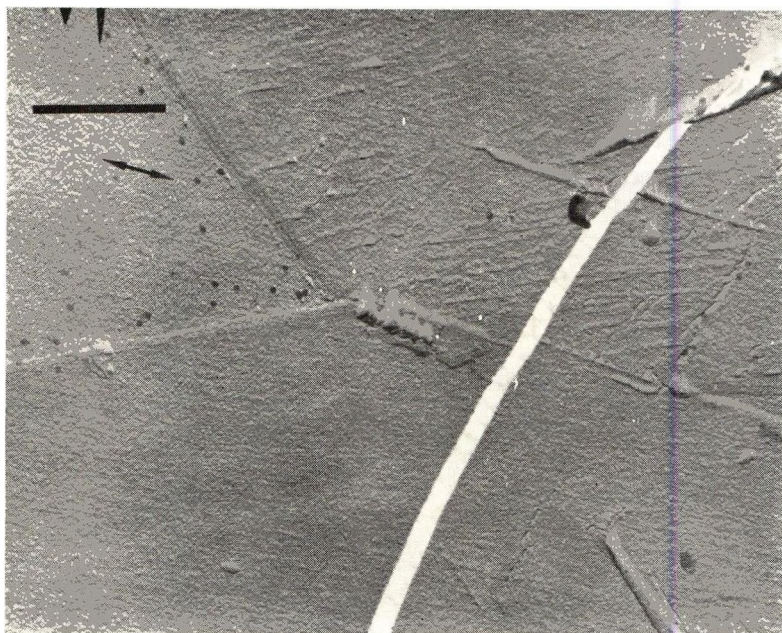
Fig. 9. Portions of type E crystals drawn 150%.

monoclinic unit cell in drawn[9] or pressed[10] polyethylene. (The chain packing defined in these two papers is essentially the same, although the unit cells listed are defined differently.) In terms of the cell defined by Tanaka, Seto, and Hara[10] these reflections are 010, 200, and $2\bar{1}0$, respectively.

In Figure 10 is shown a diffraction pattern in which both the new and old reflections can be seen. The crystal giving rise to the pattern is also shown. A tracing of the diffraction pattern in Figure 10 is shown in Figure 12c with the reflections labeled. One notes, in comparing the monoclinic and orthorhombic reflections in Figure 10, that the monoclinic (010) planes have the same orientation as one set of the orthorhombic {110} planes. The planes giving rise to the 200 reflections appear to have arisen from the other set of {110} planes. The latter set of {110} planes rotated during the transformation toward a more parallel alignment with the draw direction. The $2\bar{1}0$ reflection of the monoclinic cell corresponds to the orthorhombic 200 reflection. Both of the letter sets of planes rotated slightly during the transformations. Similar conclusions apply to the pattern shown in I (Fig. VII-35).

In addition, one finds that the entire orthorhombic pattern is rotated with respect to the crystal. The draw direction in the micrograph is nearly parallel to the $1\bar{1}0$ growth face whereas in the diffraction pattern it is parallel to the [020] direction. In addition, the other reflections do not correspond to the observed faces of the crystal. The only indication of the original lattice is a weak $1\bar{1}0$ reflection near the new 200 reflections (labeled 110_I in Figure 12).

Fig. 10. Diffraction pattern from a type A crystal drawn 25%. The pattern is correctly oriented with respect to the crystal. A tracing of this pattern with the reflections labeled is shown in Fig. 12c.

Dark-field micrographs give a clear indication of the presence of deformation within the crystal even when none is visible in the bright-field micrographs of the replicas. With the replica technique utilized for this work, the crystal remains attached to the replicating material and, therefore, diffraction patterns, dark-field micrographs and bright-field micrographs at high magnification can be obtained, in sequential order, from the same crystal. Dark-field micrographs of crystals drawn 10 and 25% are shown in Figure 11. Regardless of the draw directions, at elongations on the order of 50% and less, fine striations are observed parallel to the **a** axis in those fold domains which are contributing to the diffraction pattern. Oftentimes, as in Figures 11a and 11c, more widely spaced striations can also be seen. There is also a change in appearance at the fold domain boundaries.
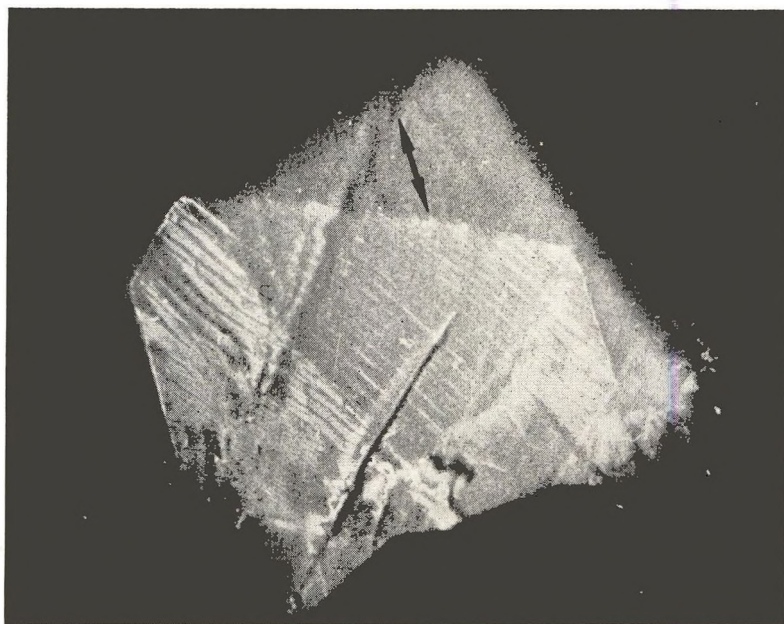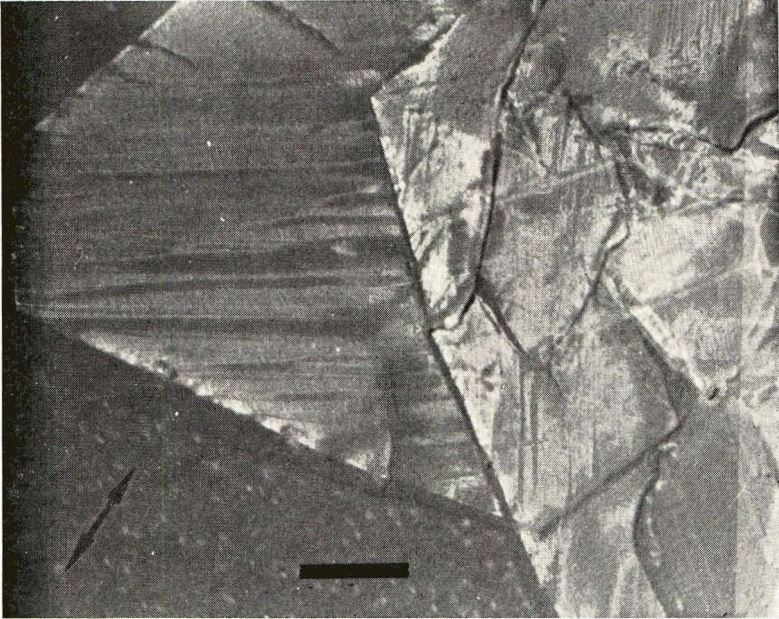
(a)

(b)

Fig. 11. (Caption on page 3827.)

In Figure 11b one notes that the crystal drawn parallel to its **a** axis was contributing only a very small amount to the diffraction pattern.   This is not due to the size of the aperture used, the aperture being so large that it
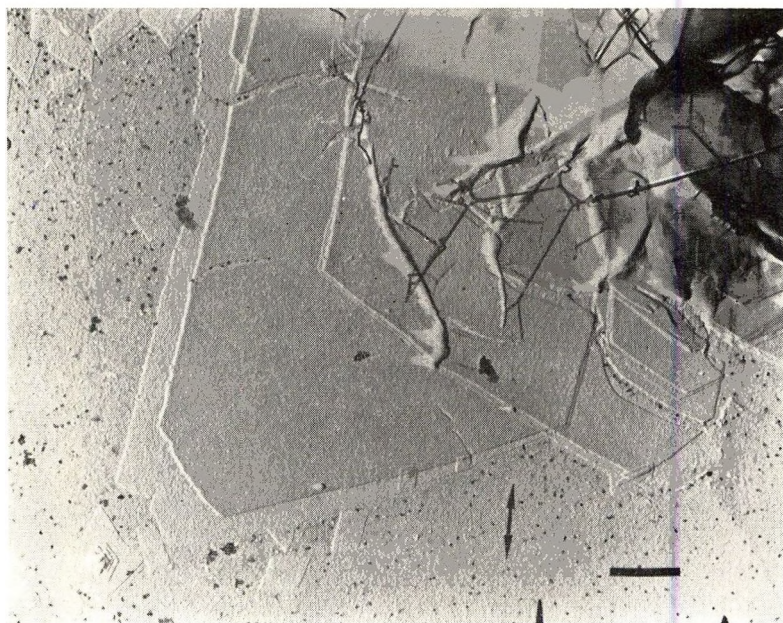
(c)

(d)

would include all ⎰110⎱ and ⎰200⎱ reflections within about $^1/_6$ of the diffraction ring.   One must thus conclude that the lattice in this crystal is everywhere (except near the center pleat) tilted such as not to reflect in the direction shown.   The region of the pattern chosen for the dark field pattern

(e)

(f)

Fig. 11. Dark-field micrographs of type E crystals drawn (a) 10% nearly parallel to a {110} growth face: (b) 10% parallel to **a** and **b**; and (c) 25%. (110) reflections were used in all cases. Bright-field micrographs of the crystals are shown in (d), (e), and (f), respectively.

should have included a $1\bar{1}0$ reflection. The crystal drawn parallel to its **b** axis in this micrograph cracked badly when drawn rather than deforming plastically. Although the widely spaced striations, which probably correspond to the surface ripples noted earlier, are not present, one still observes the finely spaced striations parallel to the **a** axis (not visible in reproduction). These striations have a spacing of about 200 A. Inasmuch as

a
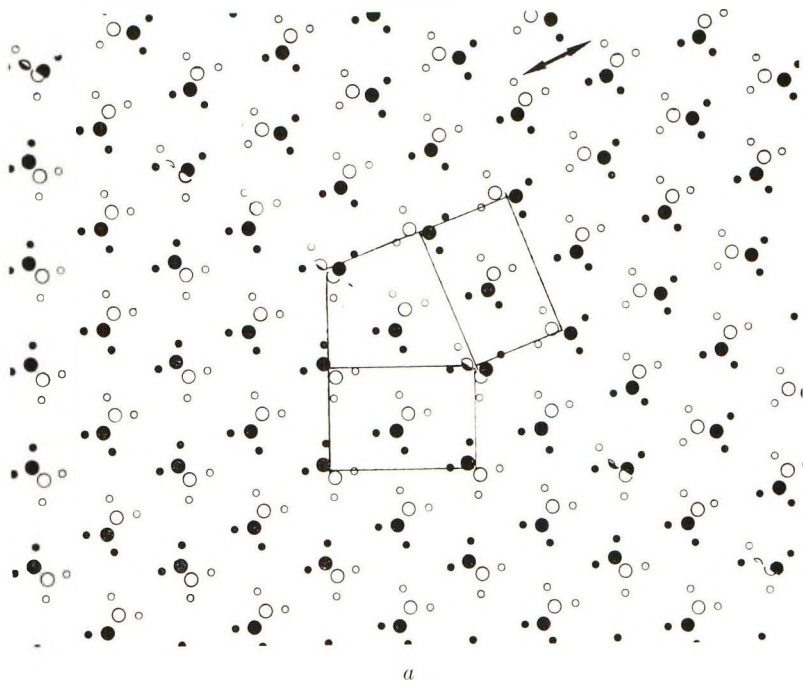
these are dark-field micrographs and because of the size of the aperture used, the striations probably should be interpreted in terms of tilting of the molecules. For instance, they are not slip bands in the normal sense. In the case of the surface ripples and striations present when **b** is nearly parallel to the draw direction, tilting accompanied by slip along the molecular axes probably occurs, giving rise to the striations seen in both dark and bright field. It is possible that slip perpendicular to the molecular axes also accompanies the deformation, particularly in view of the necessity of accommodating the lateral contraction.

The deformation accompanying the transformation from orthorhombic to monoclinic unit cell may also contribute to the formation of the striations. We have been unable, due to lack of a sufficiently small objective aperture, to determine which portions of the crystal are contributing to the monoclinic cell reflections.

The cause of the large amount of material in the thin border of one of the crystals in Figures 11c and 11f is not known. One notes that its deformation characteristics, as indicated by the dark-field micrograph, differs from that of the bulk of the crystal to which it is attached.

With elongations on the order of 100% or more, only small portions of the crystal remain in a diffracting position when the sample is normal to the beam. Most of the remainder of the reflections in patterns from these crystals is found to come from regions two or more lamellae thick. A tilting stage was not available to determine the orientation of the molecules in that portion of the crystal only one lamella thick. Inasmuch as the crystals are
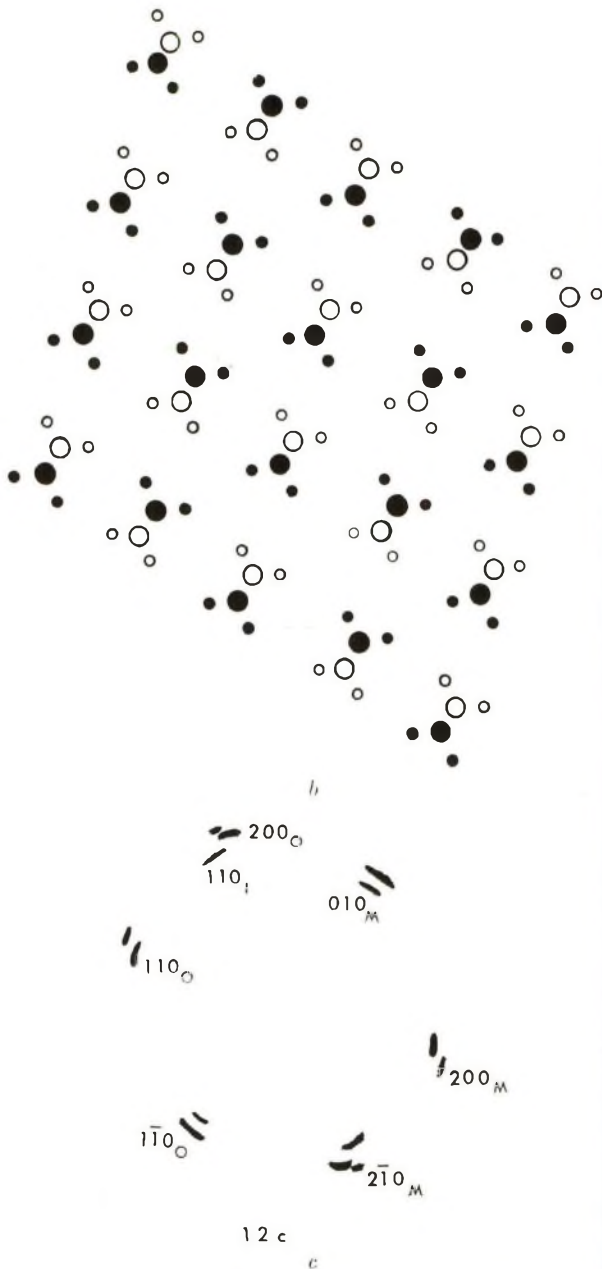
Fig. 12. (a) Polyethylene unit cell in (110) twin; (b) the monoclinic unit cell postulated by Tanaka et. al.[10] Both of the lattices are properly oriented to correspond to the diffraction pattern (c) which is a tracing of that shown in Fig. 10.

considerably thinner than before drawing, the molecules must be tilted through a substantial angle.

DISCUSSION

The first question to be considered is how closely does the deformation observed here correspond to that undergone by the lamellae in bulk polymers when they are drawn.   We believe that the resemblance is closer than one might at first expect.   The lamellae appear to adhere rather uniformly to the Mylar substrate, as shown both by their almost uniform deformation and by the drawing out of fibers when overgrowths are stripped from the substrate.   Regions in which the overgrowths were originally in contact with the substrate are often badly distorted and fibrillar when observed in the microscope (Fig. 1).   Slippage of the lamellae in overgrowths with respect to a basal lamellae in contact with the substrate indicates that the lamella–substrate adhesion is greater than the lamella–lamella adhesion. In the case of bulk polymers the adhesion between the lamella and the substrate is probably replaced by the presence of "tie" molecules joining adjacent lamellae.[1]   If sufficient of these are present, the neighboring lamellae should deform simultaneously whereas if few are present slippage and brittle failure can occur.   The presence of extended chain lamellae[11,12] will, of course, also influence the deformation characteristics of bulk polymers.   Another point of resemblance between the deformation reported here and that occurring when bulk polymers are drawn is the apparent ease of deformation when the draw direction is parallel to the **b** axis.   As reviewed in I, when bulk polyethylene is drawn, one finds that the [011] direction first tends to rotate toward the draw direction and that this is followed by further alignment of the **c** axis.   In the case of single crystals one finds cracks and ripples or striations when the draw direction is parallel to **b** whereas when the draw direction is parallel to **a** a more uniform deformation, which probably requires more energy, occurs. Furthermore, as discussed below, twinning can occur leading to the orientation of **b** in the draw direction.   The tilting of the molecules in the ripples when **b** is properly oriented corresponds to the alignment of [011]. Finally one finds in both bulk and single crystal polyethylene (using a Mylar substrate) that portions of the lattice are transformed from the normal orthorhombic to a monoclinic unit cell.

It should be noted that these results show quite clearly that unfolding of the molecules need not occur for plastic deformations of polymer lamellae up to at least 150%.   In some cases, and depending on the crack orientation, fibers can be drawn across cracks developing in the crystal.   Diffraction patterns indicate the chains are aligned along the fiber axis and possibly may be unfolded.   In the bulk of the crystal the gradual change in thickness during draw suggests that, instead of unfolding, some form of tilt and slip occurs.   It is of interest that when cracks do form, in at least some polyethylene crystals (types A, B, D, and E), they will often develop at quite low elongations, along lines of visible deformation where the crystal has gotten thinner, but they do not widen during further elongation.   This effect, at least in part, may be due to the adhesion of the remainder of the crystal to the Mylar.

The ripples appear to broaden with elongation. They are not visible, for instance, on most type E crystals drawn 50% or more, presumably because they have spread sufficiently that the bulk of the crystal has become thinner. Their development in dark-field micrographs has not yet been sufficiently studied. They appear to become somewhat less sharply defined with increasing elongation. Further study of this effect using a different shadowing direction than used in this work is also needed.

As shown above, the type of fold definitely affects the deformation characteristics of polyethylene. The {100} fold domains appear to be much more susceptible to cracking than the {110} domains when the draw direction is nearly parallel to the b axis. The variation in deformation characteristics can also be seen in the dark-field micrographs (Fig. 11a). Although it is believed likely that it is the type of fold that is affecting the deformation properties, there perhaps being a greater internal strain associated with the {100} folds, it may also be that the deformation occurring as a result of collapse of the pyramids during solvent evaporation is affecting the subsequent deformation during drawing.

It is also apparent that the {110}–{100} phase boundaries are highly susceptible to failure. This is probably due to considerable strain in these regions as a result of the necessity of matching the sloping fold surfaces in the adjacent {100} and {110} domains (see Chapter II, ref. 1 for a discussion).

There probably is not a great difference between the cracks and the "slip bands" in the {100} domains (Fig. 7); in both cases cracks probably form along {110} planes, widening in those cases in which several bands intersect and forming a zigzag crack, or with opposite surfaces of the cracks slipping past each other if only one system is present. It should be noted that opposite sides of these cracks are presumably connected by strained molecules, the fold plane, if it is (100), being at an angle to the cracks. The deformation along these cracks is readily apparent when the crystals are annealed (see paper III of this series[2]).

The relative effects of molecular weight, molecular weight average and distribution, and linearity of the molecules are not yet completely clear. The results presented here suggest only a small effect due to molecular weight distribution. Type E, which probably contains a smaller amount of low molecular weight polymer, if any cocrystallizes with the higher molecular weight polymer, appears to crack somewhat less readily than type D. On the other hand, there is a significant difference between type A and B and type C, cracking without the formation of fibers occurring readily, and in various directions, in type C. It is suggested that this may be due to the incorporation of a few more defects such as branches, in the type A and B polymers; the Alathon polymer used for these studies has a slightly lower density than the Marlex. Molecular ends may also play a role as defects, although one might expect it to be a different role than that of the branches. In addition, the adhesion to the substrate may be affected by the presence of low molecular weight material in the suspension.

The cracks in the type C polymers do not appear to follow crystallographic planes. Whether they do so on an unresolvable scale leading to a jagged crack edge is not known. The formation of these cracks without fibers may well depend on the molecular weight. Work currently in progress using fractionated polymer is expected to define the effects of these various factors in more detail.

The rotation of the lattice shown by the diffraction pattern and micrograph in Figure 10 has been observed clearly in only one other crystal. However, considerably more investigation is needed to determine its frequency. It can be explained by a $\{110\}$ twin boundary sweeping through the crystal; the rotation of the lattice during $\{110\}$ twinning is shown in Figure 12a. In Figure 12c a tracing of the diffraction pattern in Figure 10 is shown properly oriented to correspond to the lattice as shown here. The left hand side of Figure 12a corresponds to the initial lattice of the crystal, the right hand side to its orientation following twinning. The reflection labeled 110_I is the only remaining visible reflection of the initial lattice. Its orientation with respect to the new orthorhombic lattice (reflections labeled with subscript zero) indicates that it was $\{110\}$ twinning that occurred in this case and not $\{310\}$ which is also likely.[1,13]

One notes that along the twin boundary every other molecular segment has an indeterminate (in the diagram) position along the c axis. The filled circles on the diagram correspond to a CH_2 on, for instance, the basal plane of the cell and the nonfilled circles to CH_2 one-half a repeat distance above this plane. As the twin boundary moves to the left, there is apparently considerable segmental motion involved. One possibility is that the segments in the "indeterminate" position slip along their axis by one-half a repeat distance (or less likely rotate by 180°) and the entire (110) plane slips along the new ($1\bar{1}0$) plane toward the lower right. Another possibility is that all of the molecules undergo a rotation of about 90° and a considerably smaller translation.

The diffraction patterns from the drawn crystals, as previously pointed out, indicate the presence of a monoclinic unit cell in addition to the orthorhombic cell. We have never observed a crystal entirely in the new form, the diffraction spots from it containing at most about 50% of the total intensity. The effect of lattice tilt on these relative intensities is not known.

Figure 12b shows the monoclinic lattice properly oriented to agree with the diffraction pattern in Figure 12c. One notes that this transformation also involves rotations of about 90° and one-half repeat distance slips of the molecules if it follows the twinning. It is believed more likely, comparing the lattice before and after twinning with that after the transformation, that the transformation occurs in some regions in lieu of the twinning.

References

1. Geil, P. H., *Polymer Single Crystals*, Interscience (Wiley), New York, 1963.
2. Geil, P. H., *J. Polymer Sci.*, **A2**, 3835 (1964).
3. Geil, P. H., *J. Polymer Sci.*, **A2**, 3857 (1964).
4. Bassett, D. C., *Phil. Mag.*, **6**, 1053 (1961).
5. Schindler, A., unpublished data.
6. Burbank, R. D., *Bell System Tech. J.*, **39**, 1627 (1960).
7. Bassett, D. C., and A. Keller, *Phil. Mag.*, **7**, 1553 (1962).
8. Bunn, C. W., *Trans. Faraday Soc.*, **35**, 482 (1939).
9. Turner-Jones, A., *J. Polymer Sci.*, **62**, S56 (1962).
10. Tanaka, K., T. Seto, and T. Hara, *J. Phys. Soc. Japan*, **17**, 873 (1962).
11. Anderson, F. R., *J. Appl. Phys.*, **35**, 64 (1964).
12. Geil, P. H., F. R. Anderson, B. Wunderlich, and T. Arakawa, *J. Polymer Sci.*, **A2**, 3707 (1964).
13. Frank, F. C., A. Keller, and A. O'Connor, *Phil. Mag.*, **8**, 64 (1958).

Résumé

On a étudié les caractéristiques de déformation de cristaux de polyéthylène fixés sur un substrat en Mylar, et on a examiné l'effet du poids moléculaire moyen, de la distribution des poids moléculaires, des types de défauts et de plans de plissement, de l'orientation et de la présence de frontières des domaines de plissement différent. On suggère que la présence de défauts a un effet plus important que le poids moléculaire et sa distribution. Il est démontré que les surfaces plissés du type {100} se déforment d'une manière différente de celle du type {110}. Les domaines de séparation entre les surfaces plissées {100} et {110} sont particulièrement sensibles à la cassure, tandis que ceux entre les surfaces plissées voisines {110} ne le sont pas. Il est mis en évidence que la déformation se fait par un jumelage {110} et une transformation des cristaux. La déformation plastique, sans déroulement moléculaire ni cassure se manifeste dans beaucoup de cristaux de polyéthylène jusqu'à des élongations atteignant au moins 150%.

Zusammenfassung

Der Einfluss von Molekulargewichtsmittel und -verteilung, Art der Fehlstellen, Art und Orientierung der Faltungsebenen, sowie der Anwesenheit von Begrenzungsflächen zwischen den Faltungsbereichen auf die Deformationseigenschaften von auf einem Mylar-Substrat gereckten Polyäthylen-Einkristallen wurde untersucht. Der Einfluss des Fehlstellengehaltes ist grösser als derjenige von Molekulargewicht und Verteilung. Die Faltungsebenen vom {100}-Typ werden in anderer Weise deformiert als diejenigen vom {110}-Typ. Während an den Begrenzungsflächen zwischen {100}- und {110}-Faltungsbereichen der Bruchvorgang leicht einsetzt, ist dies an den Grenzen zwischen benachbarten {110}-Faltungsbereichen nicht der Fall. Die Deformation durch {110}-Zwillingsbildung und eine Kristallumwandlung wurden eindeutig nachgewiesen. In vielen Polyäthylenkristallen tritt bei Dehnung bis mindestens auf 150% plastische Deformation ohne Auffaltung der Moleküle oder Bruch auf.

Polymer Deformation. III. Annealing of Drawn Polyethylene Single Crystals and Fibers

P. H. GEIL,* *Camille Dreyfus Laboratory, Research Triangle Institute, Durham, North Carolina*

Synopsis

Polyethylene single crystals plastically deformed by drawing as much as 100% and fibers that occasionally form during this deformation have been annealed at 121 and 125°C. Striations with a spacing similar to that measured with small-angle x-ray diffraction are observed on the fibers in contact with a substrate. No readily apparent change occurs during the annealing of freely suspended fibers. Similar striations are observed along slip bands and other grossly deformed regions within the crystals. Recrystallization through an "ameboid" motion occurs in both drawn and undrawn crystals on Mylar substrates and results in an irregular crystal boundary. The more usual type of recrystallization involving an increase in fold period appears to occur more readily at a given temperature in undrawn crystals than in the plastically deformed ones. The **b** axis in drawn crystals was found to rotate during the annealing treatment so as to be nearly perpendicular to the draw direction. Any polymer in the monoclinic unit cell returns to the more stable orthorhombic unit cell.

Considerable research by electron microscopy and small-angle x-ray scattering has been done on the effect of annealing both single crystals and bulk polyethylene. (For a review, see Chapter V, ref. 1.) In general, the thickness of the lamellae increases with increasing temperature and annealing time. Similarly it has been found that the small angle x-ray diffraction long period from drawn polyethylene increases with time and temperature of annealing (see Chapter VII, ref. 1, this chapter corresponding to Part I of this series of papers).

Other than some unpublished work of Kobayashi,[2] we know of no reports of electron microscope studies of the effect of annealing drawn polyethylene. Kobayashi has shown that when a blown polyethylene film is fully drawn transverse to the machine direction and then annealed, the original fibrillar appearing structure is replaced by a lamellar type structure. These lamellae are oriented essentially normal to the original fiber direction[1,2] (see Fig. VII-59 in ref. 1). It was suggested that the molecules might retract (if originally fully elongated) and fold in a manner similar to that in single crystals in forming the lamellae. The work reported in the present

* Present address: Case Institute of Technology, Cleveland, Ohio.

paper was undertaken as part of a broad study of the deformation of poly-
mers.[1,3,4]   Of interest here is not only the effect of annealing plastically
deformed crystals resulting when polymer crystals are drawn on a Mylar
(E. I. du Pont de Nemours & Co., Inc.) substrate but also the effect of
annealing the "fully" drawn fibers extending across cracks that are occa-
sionally found in the drawn crystals.[1,3]

EXPERIMENTAL

The crystals used were listed as type E in the preceding paper in this
series.[3]   As in that work they were deposited on Mylar substrates and the
substrate drawn the desired amount at room temperature.   They were
then annealed in air in a test tube in a controlled temperature oil bath,
removed, and shadowed as previously described (Chapter I, ref. 1; and
ref. 3).

RESULTS

Annealing of the Undrawn Crystals

Annealing of undrawn crystals appears to give rise to at least two ef-
fects.[1]   When they are annealed on a glass substrate,[5] holes are formed
and the crystal increases in thickness.   Also, however, as found by Hirai
et al. for crystals annealed on a collodion substrate,[6] there can occur a
change in outline of the crystal with no apparent change in area before hole
formation occurs.   Hirai describes the change as resulting from an "ame-
boid" motion.

Both effects were found in the undrawn crystals used for this work when
annealed on Mylar.   Figure 1 shows crystals which were deposited on a
Mylar substrate previously drawn 50% (to determine if any epitaxial effect
occurred) and then annealed 1 hr. at 125°C.   The original linear edges
have been replaced by an irregular edge.   One notes that the thin layer of
material at the edge of the crystal has nearly the same contour as the
thicker portion.

The holes that developed are found to be oriented along specific direc-
tions in the $\{110\}$ fold domains.   This direction, which appears to be
essentially perpendicular to the growth faces, is probably $\langle 310 \rangle$.   In the
$\{100\}$ domains the situation is not as clear.   Usually the holes were more
rounded with an indication that they might be aligned along $\langle 100 \rangle$.   Al-
though Bassett et al.[7] found that the $\{100\}$ domains were considerably dif-
ferent in their annealing characteristics from the $\{110\}$ domains, holes
forming in the $\{100\}$ domains at a lower temperature, there appears to be
only a slight difference in these crystals.

As indicated previously (Chapter V, ref. 1), the holes formed during the
initial stages of the annealing of polymer crystals may have a crater like
structure.   In Figure 1b several holes are indicated by arrows which have
shadows on both sides.   Their appearance suggests, in this case, that
thickening has occurred on one side of the hole, the white area closest to
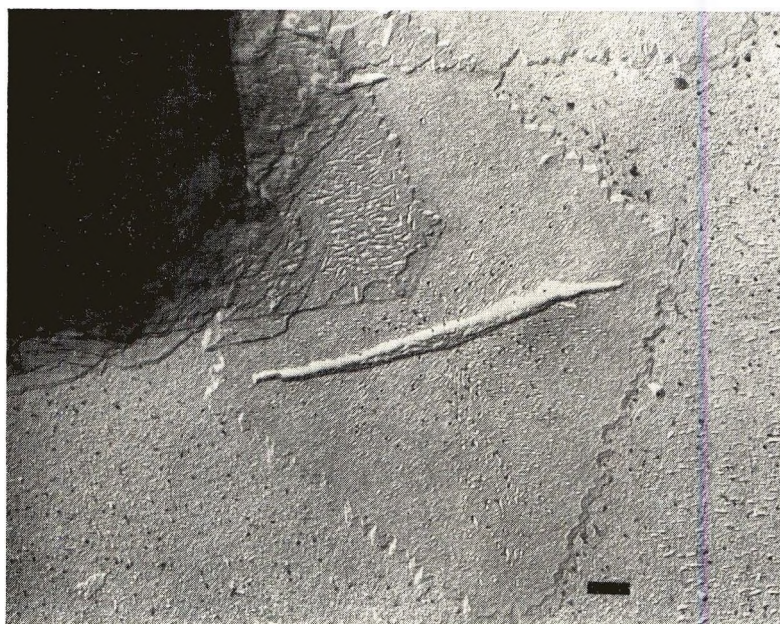
Fig. 1. (a) Polyethylene single crystals annealed on a Mylar substrate at 125°C. for 1 hr. The substrate but not the crystal had been drawn 50% perpendicular to the shadow direction. (b) Portion of (a) at higher magnification. The arrows indicate several regions in which the holes may have a craterlike structure (see text). The scale bar represents 0.5 μ on this and all subsequent micrographs. All samples were shadowed with Pt at $\tan^{-1} 2/8.5$.

the bottom of the micrograph corresponding to the hole and that on the other side of the dark line (toward the top of the figure) being a shadow behind the thickened portion. As previously discussed,[3] the round black spots are fibers of Mylar formed when the replica was stripped from the substrate.

An interesting effect is seen in the region in which the crystal on the left overlaps (or is overlapped by) the crystal in the center. Not only are the holes larger than in the region consisting of only a single lamella[1] but, in addition, their orientation seems to depend on an interaction between the two lamellae. Unfortunately, it is not known which lamella is on top; for discussion we will assume the left-hand one is. The holes in the (100) fold domain of the left-hand crystal are oriented parallel to those in the $(\overline{1}10)$ domain of the central crystal. Those in the $\{100\}$ domains of the left-hand crystal are in part oriented more or less normal to their corresponding growth faces (in the upper, (110) fold domain of left-hand crystal) and in part parallel to the $\{110\}$ growth face plane of the underneath lamellae (in the lower, $(1\overline{1}0)$ fold domain of left-hand crystal). In addition, the holes in that region of the (110) fold domain of the left-hand crystal which overlaps the $\{100\}$ domain of the underneath crystal are oriented parallel to the $\langle 100 \rangle$ direction of the underlying crystal. Detailed considerations of the interaction between the lamellae would require knowledge of which lamella was on top and thus are not possible at present. One also notes that the apparent original boundary of the left-hand crystal can still be seen in the overlapping region. If the central crystal were on top, this feature could possibly be explained in terms of low molecular weight material in the original thin edge or in terms of the deformation of the central crystal when it collapsed over the left-hand crystal. However, neither of these explanations appears too satisfactory.

Annealing of Fibers Drawn from the Crystals

As previously discussed,[1,3] when polyethylene crystals containing overgrowths are drawn on a Mylar substrate, wide cracks are frequently formed in the overgrowths. Fibers are found drawn across these cracks when they are not parallel to growth faces. The micrographs presented in this paper (Figs. 2–4) depict the effect of annealing these fibers as well as some formed inadvertently when a crystal-substrate preparation was accidentally rubbed between the time of stretching and replication. No difference has been observed in the structure of the fibers resulting from these two processes either before or after annealing. There was, however, a major difference in the appearance of fibers in contact with the substrate and those suspended in the air between the faces of the cracks.

Both before (Fig. 2 of ref. 3) and after annealing the suspended fibers appear to be structureless (Fig. 2). As indicated previously,[3] they appear to be excessively black in positive prints, scattering or absorbing more electrons than one would expect from their thickness.

In regions where the fibers were in contact with the Mylar substrate, however, a series of striations perpendicular to the fiber formed during the annealing.   These striations were found to have a spacing of 250–300 A. in most of the fibers, for all elongations of the substrate, annealing temperature of 121 or 125°C., and 1 hr. or 20 hr. annealing time at 125°C.   (The fiber to the lower left of Figure 2 is one of a few examples in which a considerably larger spacing was found.)   They resemble those pictured by Kobayashi in drawn, annealed film.[1,2]
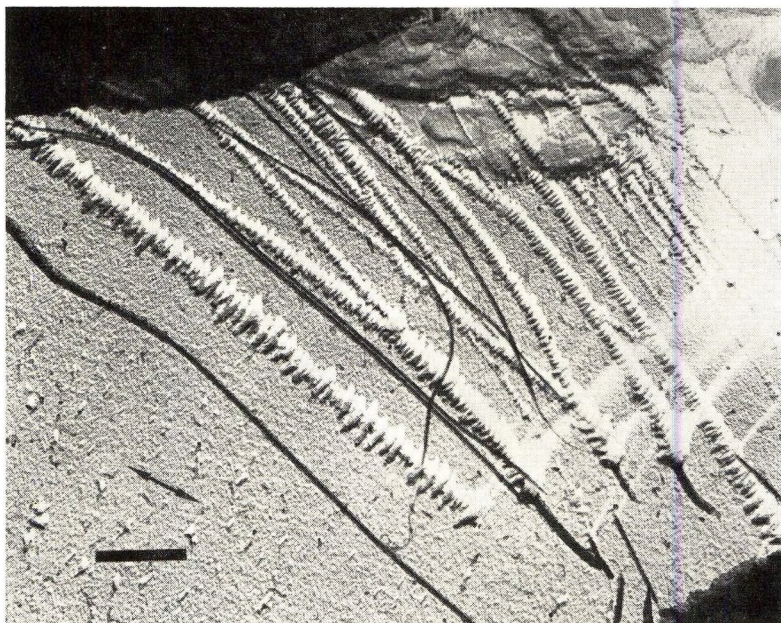

Fig. 2. Fibers drawn across a crack in a crystal overgrowth, annealed at 125°C. for 1 hr.   The three dark T-shaped structures at the lower right are the ends of fibers extending up from the substrate.   The substrate was drawn 50%.

At 125°C. the type of substrate does not appear to affect the result; the striations on the fibers lying on top of the polyethylene lamellae at the upper right of Figure 2 are similar to those on the fibers in contact with the Mylar.   At 121°C., however, there is a suggestion that the striations may not develop as easily on fibers in contact with polyethylene lamellae (Fig. 3).   In addition, striations often cannot be seen in the smallest diameter fibers at both temperatures but particularly so at the lower temperature.

The orientation of the striations is determined by that of the fibers and not that of the substrate.   In the sample which was rubbed (Fig. 4), fibers can be seen lying in two or more directions.   In the curved fiber at the center of Figure 4a higher magnification shows that the striations are everywhere nearly perpendicular to the fiber axis.   In the lower portion of Figure 4a and at higher magnification in Figure 4b can be seen a broad area containing a network of two intersecting sets of striations.   One corre-

sponds to the fibers running from left to right. The other is believed to result from portions of the fibers extending from the lower left toward the top of the figure. The sections of most of these fibers near the center of the picture are missing, either due to retraction during formation of the striations or as a result of the rubbing process itself. As mentioned above, the smallest fibers in many areas show no evidence of the striations. In other cases, as here. a few widely spaced bumps can be seen.


Fig. 3. Fibers drawn across an overgrowth crack and annealed at 121°C. for 1 hr. The substrate was drawn 100%.

Although, as indicated above, the suspended fibers are usually apparently structureless, there were a few indications in the sample annealed 20 hr. at 125°C. of the development of striations with an approximately 100 A. spacing. Although these may have resulted from astigmatism in the microscope, they are believed to be real.

Annealing of Drawn Crystals

Bright-field micrographs suggest that the interior of plastically deformed crystals is not affected by temperatures at which holes develop in undrawn crystals. In Figure 5, except along a few specific lines, one sees no evidence of recrystallization in the interior of the crystal. The irregular boundary discussed earlier has developed. It has been found on all crystals annealed on Mylar at 121 and 125°C., drawn and undrawn.

Some form of recrystallization has occurred along lines corresponding to cracks and "slip bands" in the unannealed crystal.[3] Whereas in the unannealed crystal the slip bands have more of the appearance of being a crack
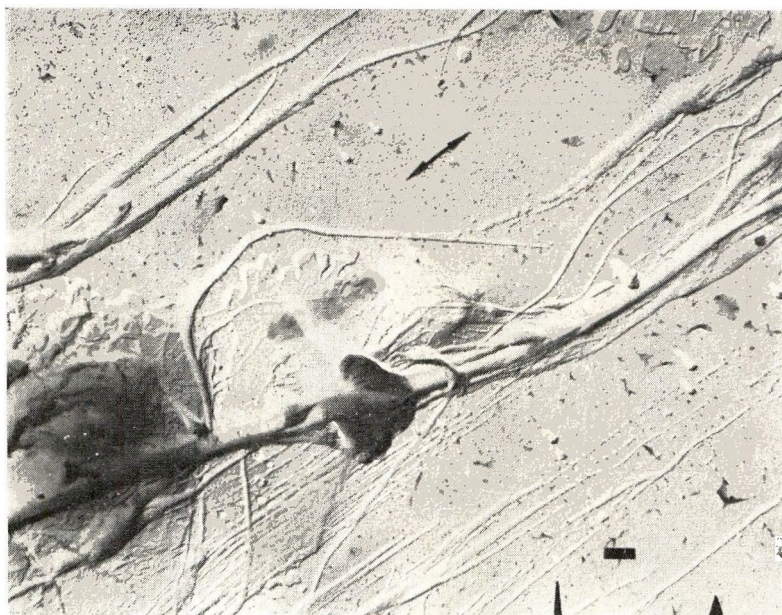
(a)

b

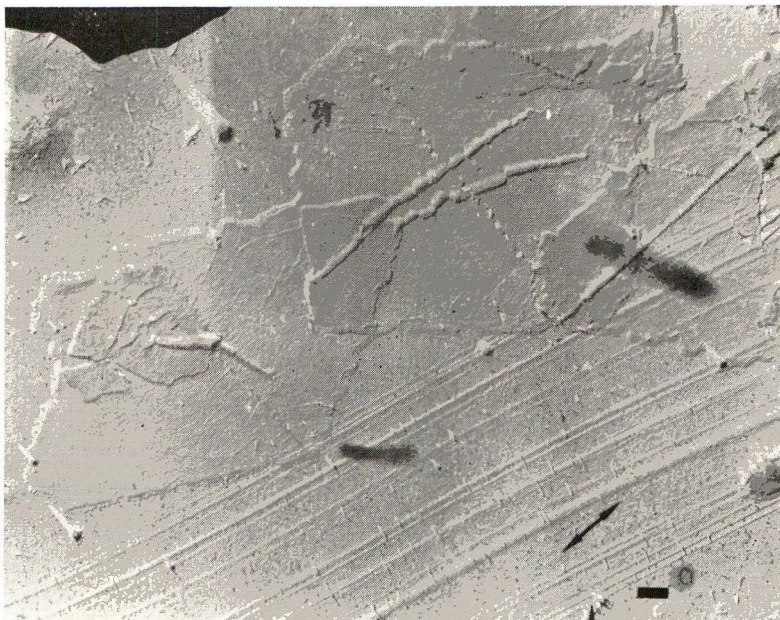Fig. 4. (a) Fibers formed by inadvertently rubbing a crystal-substrate preparation before annealing it at 125°C. for 1 hr. The substrate had been drawn 25%. (b) Higher magnification of the lower left of (a) showing a region containing crossed fibers.

(a)

in the crystal (Fig. 7 of ref. 3), after annealing they appear as ridges. Even more obvious is the formation of striations similar to those forming when the drawn fibers are annealed. The angle between the striations and the slip band varies between about 90°, as in Figure 5, and about 60° (see, for instance, Fig. 6). Following annealing, slip bands are frequently found in the {110} fold domains as well as in the {100} domains to which they are usually restricted before annealing. They can be seen in the upper-most {110} domains of both crystals in Figure 5, for instance.

Some form of recrystallization is apparent in the {110} {100} phase boundaries along which cracks formed during the elongation.[3] Again the annealed fiber type of striations are found, this time more or less parallel to the boundary and probably arising from the recrystallization of fibers drawn across the cracks.

In the unannealed crystal the {110} fold domain boundaries usually appear to deform uniformly with the rest of the crystal (II). In Figure 5c one notes that single annealed-fiber type striations have developed along this boundary. This type of structure, occurring when the boundary is nearly perpendicular to the draw direction, is more frequent than would be expected on the basis of the frequency of cracks or obvious deformation along the boundary in unannealed crystals.

One notes in Figure 5 a thin film of granular material partially covering the crystals. It is particularly obvious on the crystal at the lower left of Figure 5a because of its boundary (Fig. 5c) whereas it nearly completely covers the crystal at the upper right of Figure 5a. We suggest that this is low molecular weight material precipitated from solution as the solvent
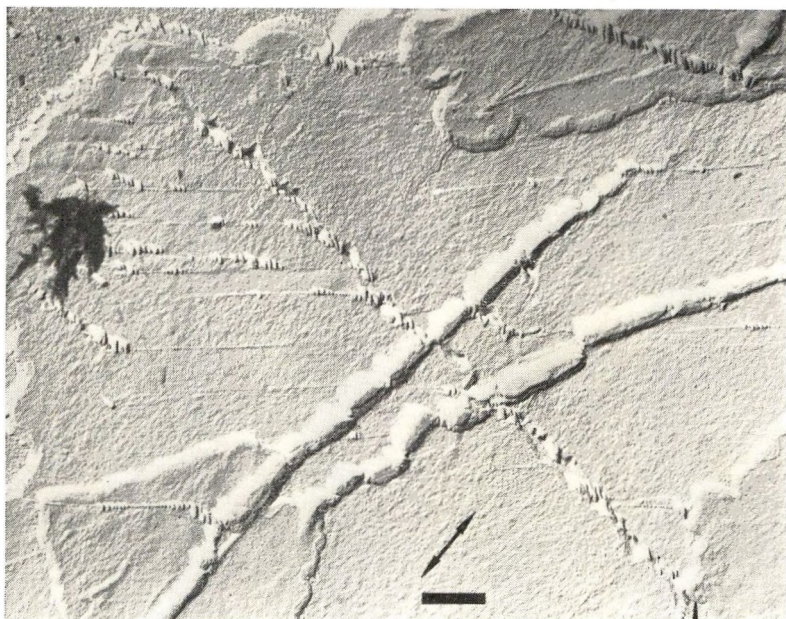
(b)
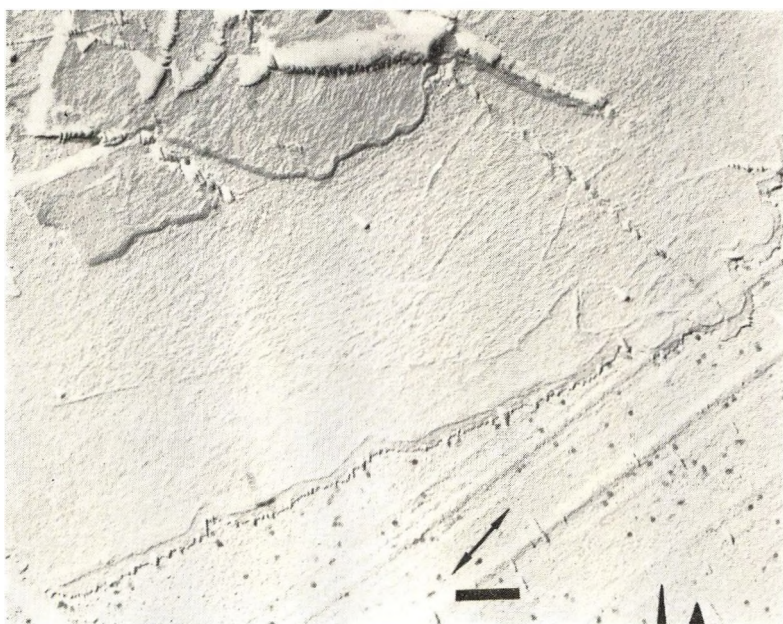
(c)

Fig. 5. (a) Single crystals drawn 25% and annealed at 125°C for 1 hr.   (b), (c) Higher magnifications of portions of (a).

evaporated. It probably melted and recrystallized during the annealing process. One also notes that there are annealed-fiber-type striations along the edge of the crystals as well as a few scattered ones on the sub-
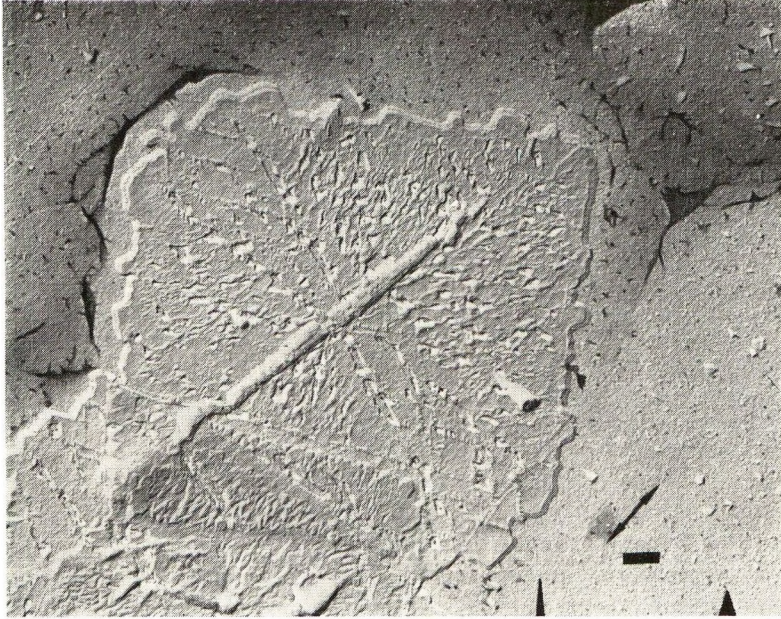
(a)

(b)

Fig. 6. (a) Single crystal from the same sample as those in Fig. 5. Sheets of Mylar are attached to the replica along the top of the micrograph. (b) Higher magnification of a {100} fold domain and portions of the neighboring {110} domains of the crystal in (a).

strate itself.   On the substrate they are frequently found associated with scratches in the Mylar (i.e., the ridges in Fig. 5a) and are oriented normal to the scratch.   The scratches, however, have been in the draw direction making it difficult to determine the cause of the orientation.   We again attribute this material to low molecular weight polymer, the striations probably corresponding to paraffin crystal lamellae oriented normal to the substrate (see also discussion section).

In the preparation of crystals drawn 25% and annealed at 125°C. for 1 hr., as in Figure 5, a few crystals were found in which obvious recrystallization had occurred throughout the $\{110\}$ fold domains (Fig. 6).   Numerous large holes have formed, oriented in each $\{110\}$ domain, as in the undrawn crystal, almost perpendicular to its growth face.   There is some evidence that the holes are not present along a region near the edge of the crystal.   A similar region can be found on the undrawn crystals in which the "ameboid" recrystallization takes place (Fig. 1).

Although in undrawn crystals $\{100\}$ fold domains are apparently more susceptible to annealing[7] or at least, as in this paper, as susceptible, they are less affected following deformation.   In Figure 6b it can be seen that the major portion of this domain has few or no holes.   Annealed-fiber-type striations are seen along the slip bands and phase boundary cracks.   This apparent difference in stability between different fold domains was also seen in other crystals.   Often $\{100\}$ was less affected than $\{110\}$.   In other cases pairs of opposite $\{100\}$ domains would be affected differently (see Fig. 9).   This feature is probably related to previously described[1,3] differences in their structure before annealing, ripples forming, for instance, in one pair of opposite $\{110\}$ domains and not the other.

When annealed for 20 hr. instead of 1 hr. at 125°C., holes are found throughout the single lamella crystals (Fig. 7).   In regions two lamellae thick the holes are larger than in regions only one lamella thick.   In other regions of this sample gross changes in shape of the crystal occurred, all resemblance to a truncated diamond disappearing.   The striations in the fibers on the substrate at lower left (in the region in the shadow of the overgrowth) appear more widely separated from each other, but of about the same thickness, than in samples annealed for a shorter time.   Further investigation of this is needed.   Because the annealing was done in air, degradation may have occurred.

At elongations of 25 and 50% and 1 hr. annealing time only slight differences were observed between crystals annealed at 121 and those annealed at 125°C.   Further observations with crystals annealed at other temperatures are in progress.   At 121°C. holes were found in only a very few crystals whereas at 125°C. approximately $\frac{1}{4}$ of the crystals developed holes (usually smaller and more widely spaced than in Fig. 6).   As indicated in Figure 8, however, annealed-fiber-type striations developed along slip bands, phase boundaries, and domain boundaries during the annealing at 121°C. as well as at 125°C.   In addition, the edges of the crystal changed shape.

In comparing crystals drawn 25% and 50% and annealed at 125 °C. it appeared that holes were found more frequently in those drawn 50% (Fig. 9). In addition, annealed-fiber-type striations were found intermixed with the holes throughout the various fold domains. Although holes were only infrequently found in the crystals drawn 25% and 50% and annealed at 121 °C., holes were found in most of the crystals drawn 100% (Fig. 10).
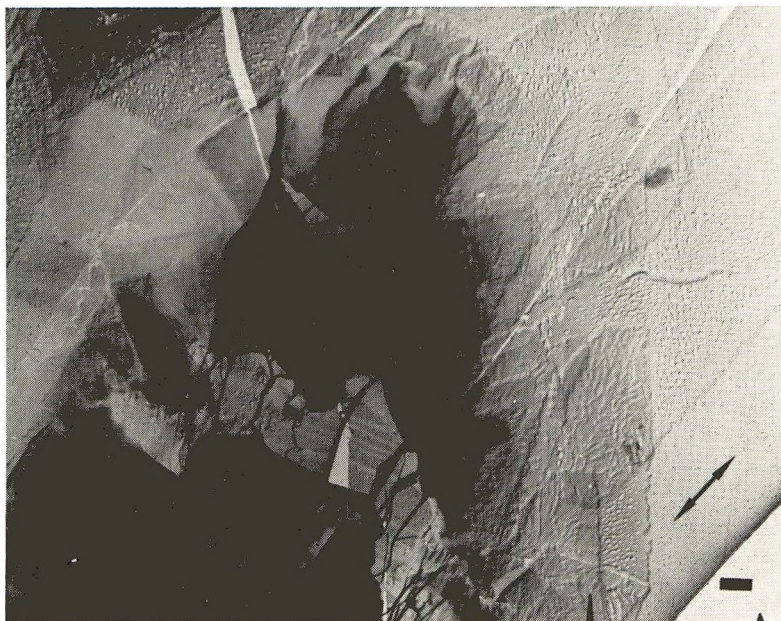

Fig. 7. Crystals drawn 50% and annealed at 125°C. for 20 hr. Fibers drawn across a crack in overgrowths can also be seen.

In the portions of the crystals in Figure 10 which overlap and in which the growth faces are nearly parallel a fine grained hole structure or granulation has developed (as at left center and top left of Fig. 10b). When the growth faces of the overlapping crystals are at an angle to each other (top center of Fig. 10b) the holes that develop are larger than in the single lamella regions of the crystal. A similar effect was observed in the case of the overgrowth on the central crystal of Figure 10a.

It was apparent from dark-field micrographs and diffraction patterns that even when no obvious effect of the annealing, except for the change in shape of the crystal's edge, could be seen in bright field, a recrystallization was taking place in the crystal. In the diffraction patterns no evidence of the triclinic unit cell reflections[1,3] was found for the annealed crystals. The diffraction patterns that were found consisted of a number of more or less randomly arranged {110}, {200}, and {020} reflections of the ortho-rhombic unit cell (Fig. 11). Frequently one of the {110} reflections or an {020} reflection was considerably more intense than the remainder. In those crystals in which the {020} reflection was both prominent and local-

ized (Fig. 11) it was found that the **b** axis was almost normal to the draw direction. (In unannealed crystals the **b** axis tends to be in the draw direction.[3] Reflections other than $hk0$ reflections also are present in the diffraction patterns from the annealed crystals (Fig. 11a).

In dark field, using reflections on the {110} and {200} rings, only a few small regions of the crystal are bright. In Figure 11c these regions are near the center of the crystal; their position varies from crystal to crystal. Considerably more intensity is contributed to these reflections from regions containing overgrowths or overlapping crystals. Unfortunately, in obtaining the micrograph in Figure 11a a portion of the {110}, {200} ring was included in the aperture along with the 020 reflection. By comparison with other patterns and micrographs it is believed that the single layer crystal in the micrograph is primarily contributing to the 020 reflection with the overgrowths contribution more to the {110} and {200} reflections. The single lamella crystal in Figure 11a has an overall low brightness that is, however, somewhat greater than the bulk of the crystal in Figure 11c, suggesting that most of the crystal is contributing to the 020 reflection.

DISCUSSION

We are unable at this time to give any conclusion concerning the reason why polyethylene crystals annealed on a polymer substrate (Mylar as here, or collodion as in the work of Hirai et al.[6]) change shape during annealing. Surface energies probably play an important role. In our experience[8] annealing on carbon substrates produces effects similar to that obtained during annealing on glass. Further work on a number of different substrates and with various annealing treatments is needed.

The regions along the boundaries of these crystals in which holes do not occur presumably are those in which the molecular motion has given rise to the change in shape. If Hirai et al.[6] are correct that no change in area occurs during this process, then the fold period must remain constant with any changes in thickness being due only to changes in molecular tilt. With the annealing treatment used in this work the thickness of the major portion of the rest of the crystal also appears to remain about the same. Some increase in thickness occurs in the vicinity of each hole. We have previously attributed a similar effect in crystals annealed a short time at relatively low temperatures on glass to recrystallization occurring in the vicinity of defects.[1]

Other than for the fact that the Mylar substrate permits a change in shape of the crystal during annealing, it does not appear to affect the recrystallization process. There is no evidence for the orientation of the substrate, for instance, affecting the formation or alignment of the holes. On the other hand, the alignment of the holes apparently is affected by the interaction between overlapping polyethylene lamellae as pointed out with respect to Figure 1. Individual annealed-fiber-type striations, it was indicated, are found more or less randomly distributed over the surface of the
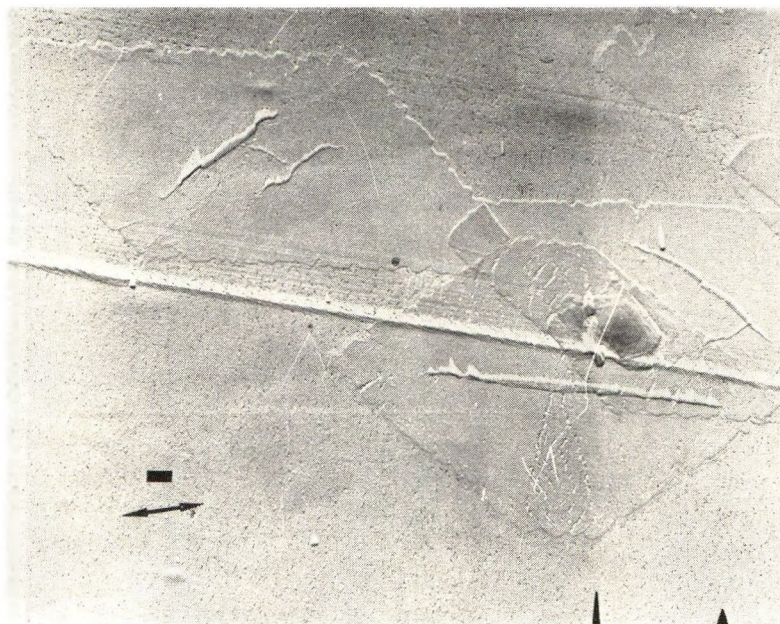
(a)

Mylar after the annealing of drawn crystals. These structures can also be observed in Figure 1. On the right-hand side of Figure 1a they are all aligned normal to some striations or scratch marks in the Mylar. They probably, as previously suggested, are paraffin crystal lamellae oriented normal to the substrate and, in this case at least aligned as a result of a form of epitaxial crystallization following melting during the annealing treatment.

Fischer and Schmidt report[9] that the small-angle x-ray diffraction long periods of fibers of polyethylene formed by drawing bulk polymer 16× at 70°C. increases from about 195 A. to about 270 A. if annealing is carried out for 1 hr. at 125°C. Annealing for 1 hr. at 121°C., according to their data, should result in a long period of about 250 A. Both of these figures are in the range of the 250–300 A. striation spacing we observe. Their data suggest that it is likely we would not, on a limited number of samples such as we used, observe a difference between the 121 and 125°C. annealing treatments. It is therefore tempting to relate the striations we observe to the long period measured by Fischer and Schmidt.

On the other hand, it must be recognized that similar striations were generally not observed on the annealed fibers suspended in the air but only on those in contact with either a polyethylene lamella or Mylar substrate. Only in the case of long annealing times was there a suggestion of striations in the suspended fibers, and then it was on the order of a 100 A. spacing. In addition, the original structure of these fibers may not be identical to those of Fischer and Schmidt, both because of the method and temperature of formation and their size. Regardless, however, it is believed that further study of the fibers described here at different annealing temperatures and times is highly desirable.
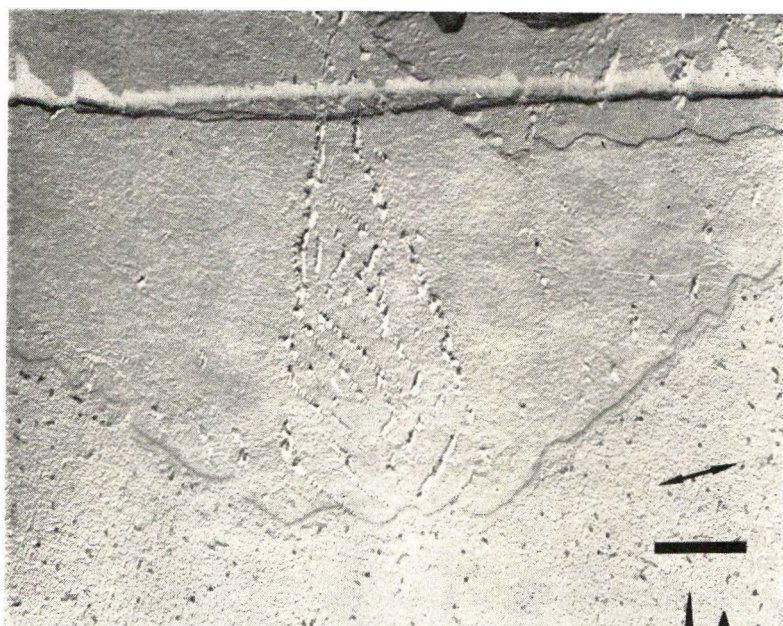
(b)
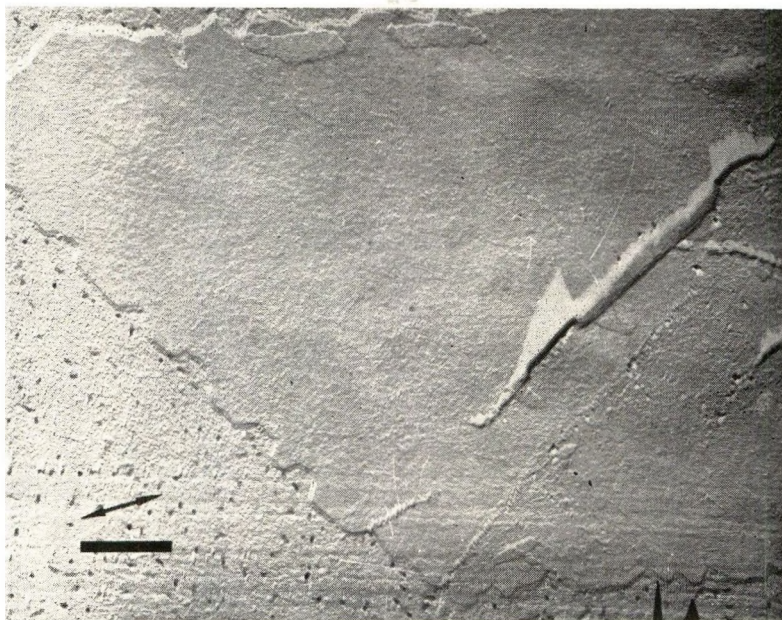
(c)

Fig. 8. (a) Single crystals drawn 50% and annealed at 121°C. for 1 hr.   (b), (c) Higher
magnifications of portions of (a).

Tentatively we suggest that the observed striations result from a re-
crystallization process in which the molecules retract and fold to form
lamellae oriented normal to the fiber axis.   We have not been able to date
to obtain diffraction patterns from the annealed fibers in order to confirm

the suggested molecular orientation. The presence of the substrate may change the surface energy sufficiently to permit its occurrence in those fibers in contact with the substrate at a lower temperature than when suspended. The surrounding fibrils in a macroscopic fiber or film might serve the same purpose. This suggestion of folding, it is recognized, is in contradiction to both of the currently postulated theories of polymer crystallization (for review, see Chapter VI, ref. 1) if it is assumed that the molecules are fully extended in the original fiber. It is possible, but we believe doubtful, that the striations are the result of epitaxial crystallization of low molecular weight polymer on the fibers similar to that observed on the edges of some crystals (Fig. 5c) and randomly scattered about the substrate. This would explain some of the substrate dependence observations. However, it is not believed that there is sufficient low molecular weight material available to explain all of the material in Figure 4, for instance, or in the cracks in the overgrowths.

Fig. 9. Single crystal drawn 50% and annealed at 125°C. for 1 hr.

It is suggested that the hole formation in the drawn crystals occurs in a manner similar to that in undrawn crystals, through an increase in fold period and accompanying lateral contraction, at the same time that polymer in the triclinic unit cell must be undergoing a transformation back to the more stable orthorhombic unit cell. Although it often appears that certain fold domains (i.e., those in which holes are not found, as in Fig. 9) are not undergoing recrystallization, the changes in the diffraction pattern indicate that even though an increase in fold period may not be taking place, a form of recrystallization is occurring that is resulting in a new lattice in the

(a)

(b)

Fig. 10. (a) Single crystals drawn 100% and annealed at 121°C. for 1 hr. Mylar fibers are present in most of the holes that developed in these crystals during annealing. (b) Higher magnification of a portion of (a) in which the crystals overlap.

crystal. Changes in molecular tilt and relaxation of any internal stress are undoubtedly also occurring.

(a)
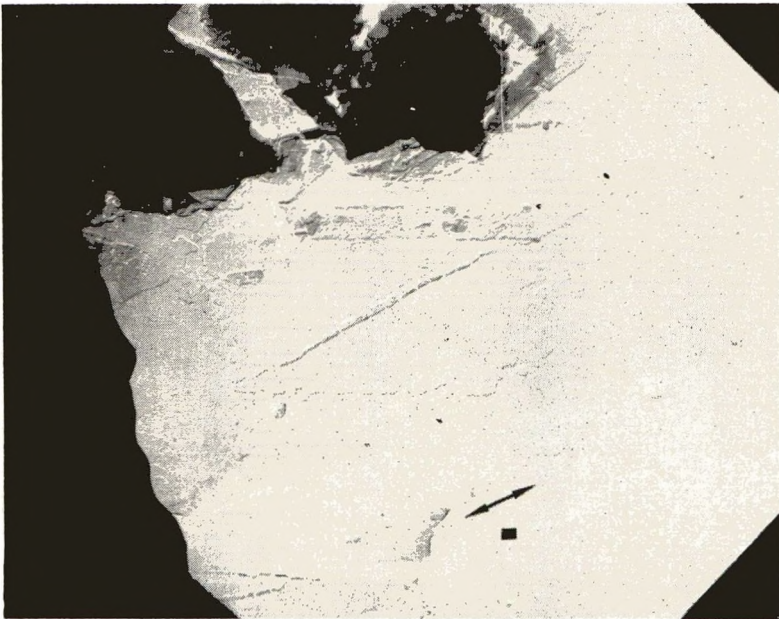
(b)

Fig. 11. (a) Diffraction pattern and dark-field micrograph from a crystal drawn 50%
and annealed at 125°C. for 1 hr.   The reflections included in the objective aperture in
producing the dark field image can be seen in the diffraction pattern, the plate being
exposed for the diffraction pattern both before and after the aperture was inserted.
(b) Bright-field micrograph of the crystal in (a).   Holes are present in two of the {110}
fold domains and in the overlapping lamellae.   (c) Diffraction pattern and dark-field
micrograph of a crystal drawn 50% and annealed at 125°C. for 1 hr.   The position of the

(c)
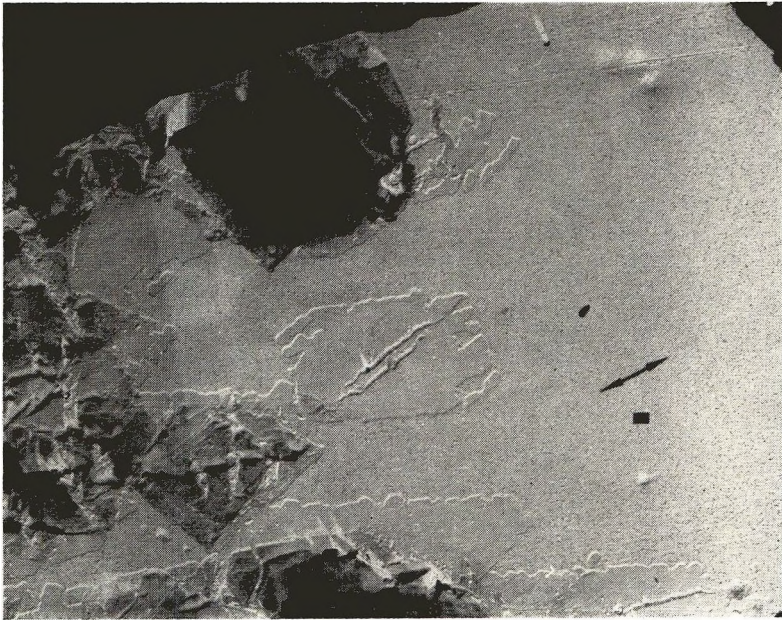
(d)

objective aperture is again visible in the diffraction pattern. The diffraction pattern is from the central crystal in the dark field micrograph; the selected area blades were opened to outer limits of the micrograph following 30 sec. of the 2 min. exposure.   (d) Bright field micrograph of the crystal in (c).   In both (a) and (c) the diffraction pattern should be rotated about 15° counterclockwise to be properly oriented with respect to the micrographs.

It is believed that most, perhaps all, of the annealed-fiber-type striations observed along slip bands and interior domain boundaries, as well as scattered throughout the domain as in Figure 9, result from the annealing of fiberlike structures formed in these regions during the original deformation. Thus one might expect, since the fold plane crosses the slip band, that when one side of the band slips with respect to the other, fibers are drawn out more or less parallel to the slip band. The orientation of the striations, normal to the fiber axis, would thus be more or less normal to the slip band. Likewise the striations would be nearly parallel to cracks oriented perpendicular to the draw direction, as at domain or phase boundaries, across which fibers are drawn. Whether the striations may develop in regions in which the deformation has not resulted in true fibers but, perhaps, only in highly tilted sheets of molecules is not known.

In the previous paper in this series clear indication of a rotation of the lattice during draw by a twinning mechanism was given. The diffraction pattern was rotated with respect to the faces of the crystal. Likewise, following annealing, the orientation of the diffraction patterns in Figure 11, for instance, does not agree with that of the crystal. It was found[3] that the **b** axis became aligned in the draw direction. In Figure 11 the **b** axis is nearly perpendicular to the draw direction. Whether or not twinning and/or a crystal transition occurred during the initial deformation is, of course, not known, since diffraction patterns could not be obtained from the same crystal before and after annealing. Further investigation of numerous crystals of known orientation may help decide this point. Likewise a tilting stage is needed to define the orientation of the **a** and **c** axes in the annealed crystals.

It is known (see review in Chapter VII, ref. 1) that the annealing of drawn polyethylene results in the rotation of the molecular axis away from the draw direction. Using branched polyethylene, Belbeoch and Guinier,[10] for instance, find the **b** axis to be oriented normal to the draw direction with **a** and **c** randomly rotated about it. In addition, orientation of the **a** axis parallel to the original draw direction is obtained when lightly crosslinked polyethylene is drawn less than 250% above the melting point and then allowed to crystallize while constrained.[11] Both of these results suggest a tendency for **b** to become aligned normal to the draw direction. As in the case of the initial drawing of the crystals in which **b** becomes aligned parallel to the draw direction,[3] there appears to be a relationship between the deformation characteristics of polyethylene lamellae on a Mylar substrate and the bulk polymer. This relationship should aid in investigating the deformation properties of bulk polyethylene.

References

1. Geil, P. H., *Polymer Single Crystals*, Interscience (Wiley), New York, 1963.
2. Kobayashi, K., unpublished data.

3. Geil, P. H., *J. Polymer Sci.*, **A2**, 3813 (1964).
4. Geil, P. H., *J. Polymer Sci.*, **A2**, 3857 (1964).
5. Statton, W. O., and P. H. Geil, *J. Appl. Polymer Sci.*, **3**, 357 (1960).
6. Hirai, N., T. Mitsuhata, and Y. Yamashita, *Kobunshi Kagaku*, **18**, 33 (1961).
7. Bassett, D. C., F. C. Frank, and A. Keller, *Nature*, **184**, 810 (1959).
8. Geil, P. H., unpublished data.
9. Fischer, E. W., and G. Schmidt, *Angew. Chem.*, **74**, 551 (1962).
10. Belbeoch, B., and A. Guiner, *Makromol. Chem.*, **31**, 1 (1959).
11. Judge, J. T., and R. S. Stein, *J. Appl. Phys.*, **32**, 2357 (1961).

Résumé

Des mono-cristaux de polyéthylène déformés par étirement à 100% et des fibres qui sont formées occasionnellement pendant cette déformation ont été recuits à 121 et 125°C. Des stries possédant un espacement semblable à celui mesuré par diffraction des rayons-X a un petit angle ont été observées sur les fibres en contact avec un substrat. Il n'y a pas de changement apparent pendant le recuit des fibres suspendues librement. On observe des stries semblables le long des rubans lamellaires et d'autres régions très déformées dans les cristaux. La recristallisation par un mouvement 'amiboïde' se passe aussi bien dans les cristaux étirés que dans les cristaux non-étirés sur des substrats de Mylar et donne une jonction irrégulière des cristaux. La méthode la plus courante de recristallisation comprenant une augmentation de la période de plissement semble se passer plus facilement à une température donnée dans les cristaux non-étirés que dans ceux qui ont été déformés. On a trouvé que l'axe b dans les cristaux étirés tourne pendant le traitement de recuit de telle façon qu'il est presque perpendiculaire à la direction d'étirage. Chaque polymère du système monoclinique retourne dans le système orthorhombique qui est plus stable.

Zusammenfassung

Durch Reckung bis auf 100% plastisch verformte Polyäthyleneinkristalle und bei dieser Verformung gelegentlich gebildete Fasern wurden bei 121 und 125°C getempert. Auf den mit einem Substrat in Kontakt stehenden Fasern wurde die Bildung von Streifen beobachtet, deren Abstand den mittels Röntgenkleinwinkelstreuung gemessenen Werten ähnlich ist. Bei der Temperung von frei aufgehängten Fasern trat keine auf einfache Weise feststellbare Veränderung auf. Eine ähnliche Streifenbildung wurde längs Gleitbändern und anderen stark deformierten Bereichen im Kristall beobachtet. Sowohl in gereckten als auch in nicht gereckten Kristallen auf Mylar-Substraten tritt Rekristallisation durch eine "amöbenartige" Bewegung auf und führt zu unregelmässigen Kristallbegrenzungsflächen. Der übliche, mit einer Zunnahme der Faltungslänge verbundene Rekristallisationstyp tritt anscheinend bei einer gegebenen Temperatur in nicht gereckten Kristallen leichter als in plastisch deformierten Kristallen auf. Die b-Achse in gereckten Kristallen dreht sich während der Temperung in eine zur Ziehrichtung fast senkrechte Lage. Ein Polymeres mit monokliner Elementarzelle kehrt in die stabilere Struktur mit orthorhombischer Elementarzelle zurück.

Polymer Deformation. IV. Drawing of Nylon 6 and Polyoxymethylene Crystals

P. H. GEIL,* *Camille Dreyfus Laboratory, Research Triangle Institute, Durham, North Carolina*

Synopsis

Electron micrographs of nylon 6 and polyoxymethylene crystals drawn on a Mylar substrate at room temperature indicate that the deformation of these crystals occurs through a combination of plastic deformation and the formation of cracks. In nylon 6 cracks are formed preferentially between hydrogen-bonded planes but can also form so as to result in rupture of the hydrogen bonds. There was no evidence for twinning or a crystal transformation during the deformation of either polymer.

In previous papers of this series[1-3] we have discussed electron microscope and diffraction studies of the drawing of polyethylene single crystals and preliminary studies of the drawing of bulk polyethylene and polyoxymethylene.[1] We consider here our initial results concerning the drawing of nylon 6[1,4,5] and polyoxymethylene[1,6] single crystals at room temperature.

We have previously indicated that cracks parallel to the short axis of the crystal often develop when nylon 6 crystals are deposited on a substrate. Fibers are drawn across these cracks.[4] Similar cracks develop if the crystals are treated with ultrasonics.[5] The hydrogen bonds in the crystal are formed between neighboring molecular segments and are parallel to the short axis of the crystal.[4] The unit cell corresponds to that obtained by treatment of the nylon 6 with iodine–potassium iodide.[5,7]

EXPERIMENTAL

As in our previous work,[1-3] the crystals were drawn on a Mylar (E. I. du Pont de Nemours & Co., Inc.) substrate, elongations of more than 100% being attainable. The solvents in which the crystals were grown were removed by evaporation at about 90°C. in a vacuum oven. Heating of the Mylar appeared to reduce the maximum attainable elongation from the 200% that was possible in the case of the room temperature solvent evaporation used with polyethylene crystals.[2] Following elongation the crystals were treated in the same manner as described previously.[2]

The nylon 6 crystals used in this study were from the same preparation as those described previously;[4] they were grown by ambient cooling of a

glycerin solution. The polyoxymethylene crystals were grown from cyclohexanol and have also been previously described.[1,8] The majority of the crystals in this preparation are too large for suitable study, folding and crumpling during solvent removal. In addition, some work was done with crystals grown from bromobenzene. As indicated by Bassett,[9] these crystals are pyramidal. The nylon 6 crystals, as previously suggested,[1] are planar (see Fig. 4).

ELECTRON MICROSCOPE OBSERVATIONS

Nylon 6

Numerous cracks are formed in the nylon 6 crystals at elongations of as low as 5%. Within a given fold domain they usually have the same orientation, but the orientation may differ from that in neighboring domains. In crystals drawn 50% or less there is generally only one set of cracks in each domain; with higher elongations two or more sets of cracks may develop.

For elongations of 50% or less the cracks are parallel to the short axis when the direction of draw is within about 45° of the long axis (Figs. 1 and 2). As seen in Figure 2 they are not strictly linear but tend to have numerous jogs. As in the case of polyethylene,[1,2] the cracks in the overgrowths
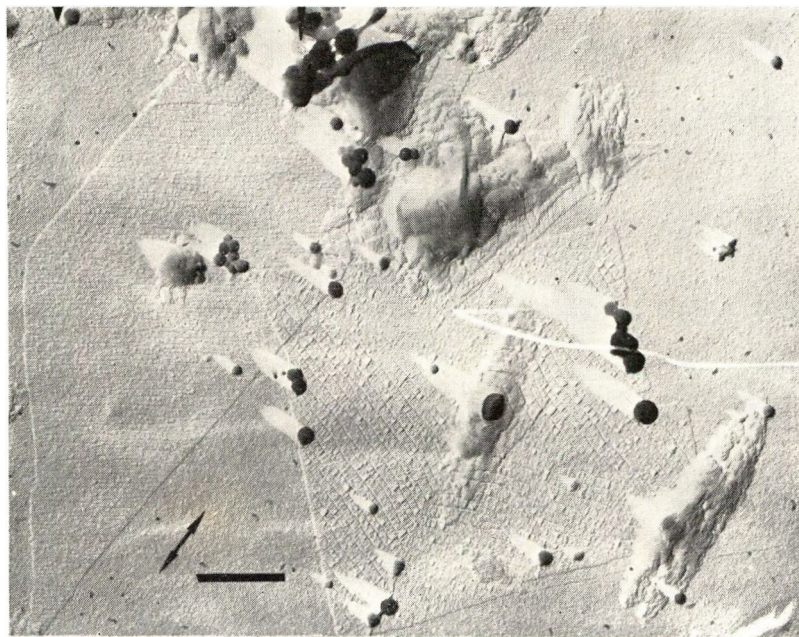

Fig. 1. Nylon 6 crystals drawn 25%. The round objects are globules of nylon 6;[1] the small black spots fibers of Mylar resulting from the sample preparation process.[2] At the lower right is a portion of a spherulite. In this and all subsequent micrographs the shadowing was with Pt at $\tan^{-1} 2/8.5$. The scale represents 1 μ in this figure and 0.2 μ in all subsequent figures.

Fig. 2. Portion of a nylon 6 crystal drawn 25%. Fibers can be seen in the cracks on the overgrowth.

are more widely separated and also are wider. Although fibers can easily be seen in the cracks on the overgrowths, we have not been able to observe them in the cracks in the single lamellae. This is probably due to the narrowness of the cracks.

In the only crystal observed which was drawn almost exactly parallel to its axis, two intersecting sets of cracks, making angles of about 30° and 135° (after the 25% elongation) with the short axis, were found. As discussed later, this may result from the lack of deformation by a type of slip along the hydrogen-bonded planes in this crystal, the material between the cracks in the other crystals slipping sideways during the elongation when the draw direction is at an angle to the long axis. In this crystal the slip occurred along two intersecting planes.

When the draw direction is nearly parallel to the short axis, the cracks which develop are formed at various angles. They vary from essentially parallel to the long axis (Fig. 3) to nearly parallel to the edges of the crystal. Although they are nearly parallel to each other in a given fold domain they may lie at different angles to the axes in neighboring domains. The fact that they intersect the fold domain boundaries indicates that the various angles observed is not a result of the change in shape of the crystal during the elongation. Fibers drawn across the cracks are seen in areas which are two or more lamellae thick, but they have not been clearly resolved in regions in which only a single lamella is present.

Considerable wrinkling of the surface occurs in those crystals drawn nearly parallel to the short axis (Fig. 4) whereas almost none is found in the
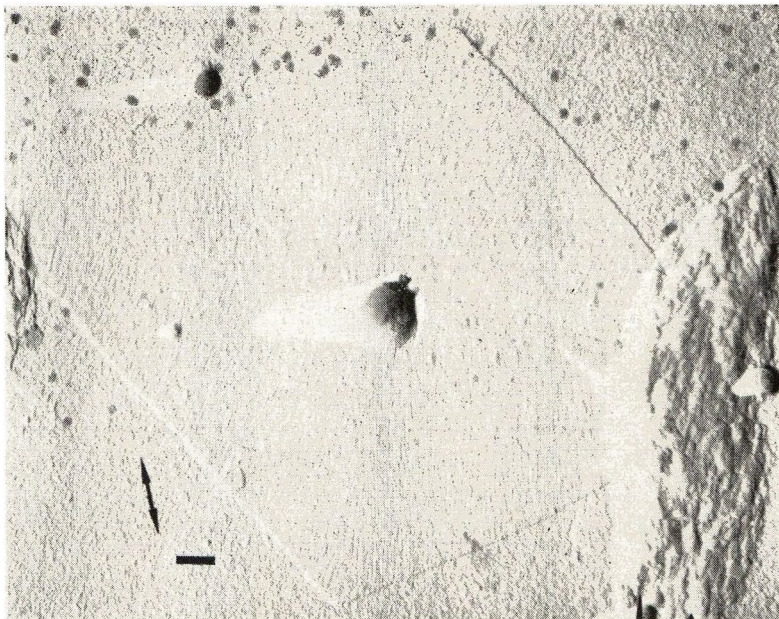
Fig. 3. Nylon 6 crystal drawn 5%. Cracks have formed in only two of the four fold domains. The striations seen here formed during solvent evaporation[4] and are not due to the elongation. Note the lamellar appearance of the nylon 6 globule at the center of the crystal. A portion of a spherulite is to the left of the crystal.
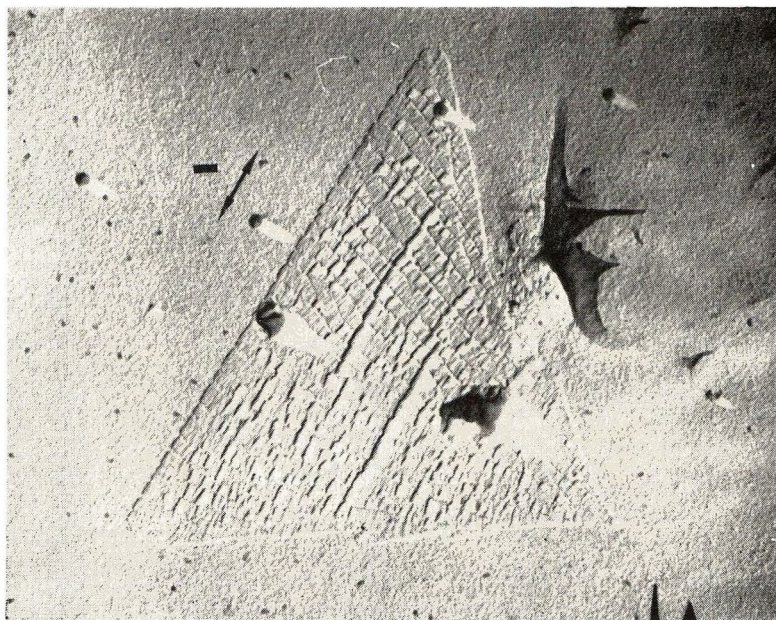
Fig. 4. Nylon 6 crystal which folded back on itself along its smaller axis and then was drawn 25%. Note that the fold is linear, indicating the crystal was planar. Fibers are present in the cracks. The large dark area just to the right of the crystal is an attached sheet of Mylar.

Fig. 5. Portion of a nylon 6 crystal drawn 100%. Two sets of cracks are present in the direction indicated by the single-headed arrows.

crystals drawn at an angle to this axis (Figs. 1 and 2). This wrinkling is believed to result from the lateral contraction of the Mylar exceeding that of the crystal during the drawing operation. In addition, the crystals drawn almost parallel to the short axis appear to decrease in thickness less than when drawn along the long axis. The cracks are also narrower in the latter crystals.

With increasing elongation, in the case of crystals drawn nearly parallel to the short axis, the cracks become wider and the wrinkling increases. When drawn at an angle to the short axis, however, secondary sets of cracks develop with elongations over 50% and wrinkles can be seen (Fig. 5). The surface of the Mylar itself takes on a granular appearance. In both cases, however, the total width of the cracks is insufficient to account for the observed elongation. Plastic deformation must also be occurring.

Diffraction patterns from the drawn nylon 6 crystals show that the spots spread into diffuse arcs with increasing draw (Fig. 6). The original spacings[4] of 4.0 and 4.1 A. remain, however, up to elongations of at least 100% indicating that under these conditions of draw a crystal transition does not take place. Dark-field micrographs suggest that most of the crystal (except for the wrinkles) is contributing to the diffraction pattern.

Spherulites, as well as the globules and single crystals, are formed during the crystallization of nylon 6 from glycerin. They consist of nylon 6 in the low temperature crystal modification and appear to be composed of twisted ribbons of irregular lamellae.[1,6] Widely spaced cracks, with

(a)
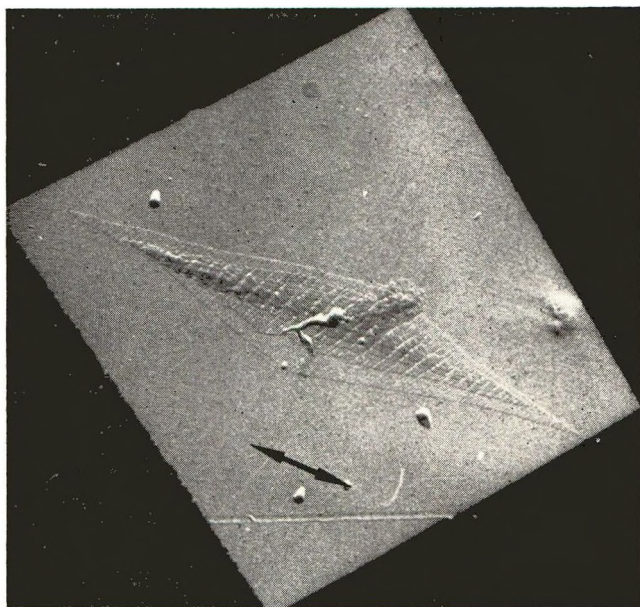
(b)

Fig. 6. Diffraction pattern: (a) from a nylon 6 crystal, (b) a crystal drawn 50%.

fibers, are formed during their elongation on Mylar (see Fig. 1, lower right). Their diffraction pattern, which before elongation consists of rings or arcs, does not undergo any apparent change.

The globules, as suggested by the one at the center of the crystal in Figure 3, are apparently lamellar. (This has been clearly shown in the case of polyoxymethylene.[10]) They do not appear to change shape during the elongation (Fig. 5, for instance), suggesting that only a small portion of their surface is in contact with the substrate.

Polyoxymethylene

Polyoxymethylene crystals also appear to be less susceptible to plastic deformation than polyethylene[1,2] and perhaps less than nylon 6. In the case of polyethylene all of the elongation up to at least 150%, at least in certain directions, can be accommodated by plastic deformation without the formation of cracks. In nylon 6 cracks are always found when the crystals are drawn at room temperature but some of the deformation, particularly when the draw direction is perpendicular to the hydrogen-bond directions, can also apparently occur plastically. In the case of polyoxymethylene numerous small cracks are found to develop perpendicular to the draw direction (Fig. 7). These cracks, although irregular and jogged, tend to be parallel or perpendicular to one of the hexagonal unit cell faces. Oftentimes intersecting sets of cracks are found. In the smaller crystals, at least, no wrinkles resulting from lateral contraction during elongation are found; the pleats or wrinkles observed being a result of crystal collapse during solvent removal. With the very large crystals the situation is not as clear; the wrinkles observed may be due to lateral contraction of the substrate.

Fig. 7. Portion of a small star-shaped[8] polyoxymethylene crystal drawn 25%. Two sets of cracks can be observed, as indicated by the single-headed arrows.

As in the case of the other polymers the cracks in superimposed lamellae are larger and more widely spaced than when only one lamella is present. Fibers can be seen drawn across these larger cracks but cannot be resolved in the smaller ones. With increasing elongation the entire crystal appears to break up in small pieces resulting in a granular appearance if the pieces are sufficiently small (Fig. 8). Electron diffraction patterns from the drawn

Fig. 8. Portion of a large polyoxymethylene crystal drawn 50%. The larger scale granulation corresponds to the crystal, the smaller to the Mylar. The crystal edges are indicated by the arrows.

crystals consist of diffuse arcs with some spottiness being retained when overgrowths are present. Dark-field micrographs suggest the majority of the crystal is contributing to the diffraction pattern.

Discussion

Nylon 6 and polyoxymethylene crystals develop cracks when they are drawn. In this respect they are similar to certain types of polyethylene crystals, i.e., those which are believed to incorporate low molecular weight polymer and/or fewer branches. They differ from the polyethylene crystals which undergo plastic deformation during elongation and are believed to incorporate defects such as branches.[2] Both nylon 6 and polyoxymethylene are linear polymers, suggesting that the defects play an important role in determining the ductility of the crystal. It was not possible in the present work, however, to investigate the effect of molecular weight average and distribution.

Polyoxymethylene crystallized slowly from the melt fractures rather than draws when stretched at room temperature. Drawing can occur at temperatures on the order of 100°C. In the initial stages of elongation fibrillar appearing material is observed extending across cracks in the lamellae.[1] The appearance resembles that of the cracks in the overgrowths on single crystals drawn at room temperature except that the fibers in the latter appear to be more independent; in the bulk material there appears to be some lateral cohesion between the fibers. Examination of single crystals and melt crystallized films drawn at temperatures above 100°C. should determine whether or not polyoxymethylene crystals can deform plastically or whether all elongation results from the development of cracks and the accompanying fibers resulting from, probably, molecular unfolding.

The observations of drawn nylon 6 crystals suggest that some plastic deformation can accompany crack formation, particularly so if the crystals are drawn at an angle to the hydrogen bonds. When the draw direction is within about 45° of the long axis of the crystal, the lateral contraction of the substrate is accommodated by a corresponding lateral contraction of the crystal. In contrast to polyethylene[2] there does not appear to be a decrease in thickness of the lamellae at elongations up to 100%. The lateral contraction, it is suggested, is accommodated by some form of slip. This would require breaking of hydrogen bonds. The maximum amount of molecular tilt, if any, and slip is apparently more limited than in the case of polyethylene, since additional sets of cracks as well as wrinkles develop as the elongation increases. Considerable further investigation of this type of deformation, in particular utilization of a tilting stage and dark-field microscopy, is needed. Some rotation of the lattice apparently occurs, as indicated by the spreading of the spots into diffuse arcs.

When the nylon 6 crystals are drawn close to parallel to the hydrogen–bond direction, and when polyoxymethylene crystals are drawn, there is apparently less plastic deformation. More of the elongation occurs through the development of cracks. In no case, in either nylon 6 or polyoxymethylene, was there any evidence of twinning.

References

1. Geil, P. H., *Polymer Single Crystals*, Interscience (Wiley), New York, 1963, Chap. VII.

2. Geil, P. H., *J. Polymer Sci.*, **A2**, 3813 (1964).

3. Geil, P. H., *J. Polymer Sci.*, **A2**, 3835 (1964).

4. Geil, P. H., *J. Polymer Sci.*, **44**, 449 (1960).

5. Ogawa, M., T. Ota, O. Yoshizaki, and E. Nagai, *J. Polymer Sci.*, **B1**, 57 (1963).

6. Geil, P. H., N. K. J. Symons, and R. G. Scott, *J. Appl. Phys.*, **30**, 1516 (1959).

7. Kinoshita, Y., *Makromol. Chem.*, **33**, 1, 21 (1959).

8. Reneker, D. K., and P. H. Geil, *J. Appl. Phys.*, **31**, 1916 (1960).

9. Bassett, D. C., personal communication.

10. Geil, P. H., in preparation.

Résumé

Des microphotographies électroniques de cristaux de nylon 6 et de polyoxyméthylène, mis sur un substrat de Mylar, à température ambiante, indiquent que la déformation de ces cristaux se fait par une combinaison de la déformation plastique et de la formation de fissures. Dans le nylon 6 les fissures se forment de préférence entre les plans liés par liens-H, mais peuvent se former aussi de façon à ce que les liaisons H se rompent. Il n'y a pas de preuve pour accepter le jumelage de ces effets ou pour une transformation du cristal.

Zusammenfassung

Elektronenmikroskopische Aufnahmen von bei Raumtemperatur auf einem Mylar-Substrat gereckten Nylon 6- und Polyoxymethylenkristallen zeigen, dass bei der Verformung dieser Kristalle plastische Deformation und Rissbildung zusammenwirken. In Nylon 6 tritt zwar die Rissbildung bevorzugt zwischen den durch H-Bindungen gebildeten Schichten ein, kann jedoch auch zur Spaltung der H-Bindungen führen. Es konnten weder Zwillingsbildung noch Kristallumwandlungen während der Deformation nachgewiesen werden.

Polyquinoxalines

J. K. STILLE and J. R. WILLIAMSON, *Department of Chemistry, University of Iowa, Iowa City, Iowa*

Synopsis

The reaction of stoichiometric amounts of 1,4-diglyoxalylbenzene with 3,3'-diaminobenzidine affords nearly quantitative yields of a polyquinoxaline. Reaction of the monomers in the absence of solvent and heating to 250°C. or reaction of the monomers in a solvent to form a prepolymer and heating of the prepolymer to 250°C. provides soluble polymer with nearly identical properties. Heating the polymer to 375°C. under reduced pressure increase the molecular weight. A study of model compounds and reactions indicates that the polymer is predominately poly[2,2'-(1,4-phenylene)-6,6'-diquinoxaline] instead of the 2,3'- or 3,3'-isomers. These polymers are stable in air to 500°C. and under nitrogen lose only 20% of their weight at 800°C.

INTRODUCTION

The preparation of a polymer containing a totally aromatic structure has been an object of prime interest, since such a polymer should exhibit excellent thermal stability.[1,2] One avenue to the synthesis of totally aromatic polymers is a cyclic condensation reaction which provides an aromatic or pseudoaromatic ring containing one or more heteroatom.[3-8] These polymers, particularly the benzimidazoles, have shown excellent thermal stability.

One reaction which should readily lend itself to the formation of an aromatic polymer is the formation of a quinoxaline by the reaction of a 1,2-dicarbonyl compound with an aromatic 1,2-diamine. The reaction is nearly quantitative in most cases and requires only mild conditions for the reaction.[9,10] A polymerization reaction utilizing this condensation reaction would require an aromatic tetramine, in which the amine functions are positioned in two *ortho* sets, and a tetracarbonyl compound in which the ketone or aldehyde groups are situated in two α-dicarbonyl sets joined by an aromatic nucleus. Such a requirement is met in the reaction of 1,4-diglyoxalylbenzene (I) with 3,3'-diaminobenzidine (II) to afford the polyquinoxaline (III).
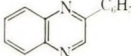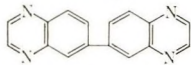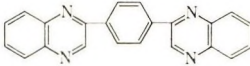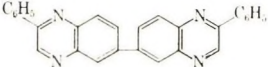
EXPERIMENTAL

Monomers

1,4-Diglyoxalylbenzene Dihydrate (I). To a solution of 22.2 g. (0.2 mole) of selenium dioxide in 100 ml. of dioxane and 4 ml. of water containing

nOHC—CO— ⟨benzene⟩ —CO—CHO·2H$_2$O + n [structure II with NH$_2$ groups] ⟶

II

[structure III] + 6nH$_2$O

III

3 drops of concentrated hydrochloric acid was added 15 g. (0.0925 mole) of 1,4-diacetylbenzene. The mixture was heated at the reflux temperature for 4 hr., during which time the selenium metal precipitated. The mixture was filtered and the filtrate was cooled to afford yellow crystals of crude 1,4-diglyoxalylbenzene. Alternate concentration of the solution under reduced pressure and cooling afforded 18 g. (80%) of product, which was recrystallized from water to obtain pure product, m.p. 140–150°C. (dec.), reported[11] 110–111°C.

ANAL. Calc'd. for C$_{10}$H$_{10}$O$_6$: C, 53.10%; H, 4.46%. Found: C, 53.19%; H, 4.57%.

The infrared spectrum (Nujol mull) showed maxima at 3360 (OH stretching) and 1700 cm.$^{-1}$ (C=O stretching).

3,3′-Diaminobenzidine(II).[8] This monomer was isolated from the tetrahydrochloride and purified just prior to use by adding, under nitrogen, a solution of oxygen-free 4% sodium hydroxide to a concentrated oxygen-free aqueous solution of the tetrahydrochloride. The precipitated free amine was removed by filtration under nitrogen, dried, and sublimed at 170°C./0.05 mm. Hg, m.p. 179–179.5°C., reported[8] 178–179°C.

Model Compounds

Quinoxaline (IV)[12] and 2-phenylquinoxaline (V)[13] were synthesized by known procedures. The ultraviolet spectra of the model compounds are reported in Table I.

6,6′-Diquinoxaline(VI). To a solution of 0.642 g. (0.003 mole) of 3,3′-diaminobenzidine in 30 ml. of deoxygenated water at 70°C. was added, under nitrogen, an aqueous solution of 1.596 g. (0.006 mole) of glyoxal bisulfite. The yellow precipitate which formed immediately was removed and recrystallized from 95% ethanol to afford 0.69 g. (90%) of light yellow crystals of 6,6′-diquinoxaline, m.p. 257–258.5°C.; reported[14] black crystals, no m.p.

ANAL. Calc'd. for C$_{16}$H$_{10}$N$_4$: C, 74.41%; H, 3.87%; N, 21.70%. Found: C, 74.65%; H, 4.23%; N, 21.70%.

1,4-Di(2-quinoxalyl)benzene(VII). To a solution of 0.54 g. (0.003 mole) of o-phenylenediamine dihydrochloride in 15 ml. of oxygen-free water was added, under nitrogen, 15 ml. of an aqueous oxygen-free solution of

TABLE I
Ultraviolet and Visible Spectra of Quinoxalines

Compound	Dioxane[a]		Sulfuric acid	
	λ, mμ	ε	λ, mμ	ε
IV	303	4,829	203	12,190
	316	5,370	250	21,690
			357	14,020
V	263	28,400	202	66,300
	333	12,250	280	32,000
			447	17,100
VI	262	56,300	203	61,000
	333	19,200	263	42,600
			381	29,000
VII	280	40,900	203	508,000
	353	39,200	280	101,000
			435	45,100
VIII$_a$	278	91,000	204	233,400
	373	58,500	303	68,000
			528	70,000
VIII$_b$				
VIII$_c$				
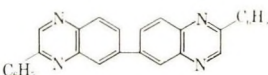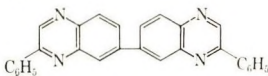
[a] No complete visible spectrum was taken in this solvent.

0.339 g. (0.0015 mole) of 1,4-diglyoxalylbenzene dihydrate. An immediate yellow precipitate formed. The reaction mixture was heated at the reflux temperature under nitrogen for 4 hr. The product was removed, dried under reduced pressure, and recrystallized from dioxane to give 5.0 g. (100%) of light yellow crystals, m.p. 272–274°C., reported[11] m.p. 262° C.

When the free amine was employed in a water solvent and in an ethanol–dioxane solvent mixture, 95% and 83% of product was obtained, respectively. A reaction of a mixture of o-phenylenediamine and 4,4'-diglyoxalylbenzene dihydrate at temperatures above the melting point of the free amine (>102°C.) afforded an 87% yield of product after one recrystallization.

2,2'-Diphenyl-6,6'-diquinoxaline(VIII). The reaction of 1.083 g. (0.003 mole) of 3,3'-diaminobenzidine tetrahydrochloride and 0.912 g. (0.006 mole) of phenylglyoxal hydrate was carried out in the usual manner in 60 ml. of water. The crude product was recrystallized from dioxane to afford 1.06 g. (86%) of yellow crystals, m.p. 314–315°C. No other compound was isolated.

ANAL. Calc'd. for $C_{28}H_{18}N_4$: C, 81.92%; H, 4.26%; N, 13.65%. Found: C, 81.54%; H, 4.26%; N, 13.56%.

In an N,N-dimethylaniline solvent, only a 17% yield was obtained. Reaction of the free amine with phenylglyoxal in a variety of solvents

TABLE II

Poly[2-(1,4-phenylene)quinoxaline]

Polymerization conditions[a]		Color	% soluble in		$[\eta]_{inh.}$, dl./g.[c]	Thermal gravimetric analyses	
			H_2SO_4	HMP[b]	HMP[b]	Nitrogen[d]	Air[e]
Melt	T_1	Red	100	55	0.67	800°C.	470°C.
	T_2	Dark red	71	10	1.28		
Dioxane, method A	T_1	Orange	100	55	0.40	800°C.	470°C.
	T_2	Brown	50	22	0.93		
Dioxane, method B	T_1	Orange	100	50	0.79	800°C.	460°C.
	T_2	Tan	45	20	1.27		
Amine hydrochloride, water		Yellow	100		0.40[f]	700°C.	450°C.
					0.48[g]		
Amine hydrochloride	T_1	Brown	100		0.64	700°C.	250°C.
Dioxane	T_2	Brown			1.46		

[a] T_1 and T_2 refer to the 250°C. and 350°C. heating cycles, respectively. Samples of polymer were withdrawn after the 250°C. cycle for solubility and viscosity measurements.
[b] Hexamethylphosphoramide.
[c] Inherent viscosities were obtained at 25°C. at concentrations of 0.04–0.31 g./100 ml. of solvent.
[d] Temperatures at which the polymer had lost 20% of its weight.
[e] Break temperature in the thermal gravimetric analysis curve.
[f] In formic acid.
[g] In trifluoroacetic acid.

afforded lower yields than that obtained with the amine hydrochloride in water: ethanol (46%), water (65%), N,N-dimethylaniline (32%).

Polymerizations

In all polymerization reactions the solvents used were deoxygenated by a prior reflux period with a nitrogen ebullator and distillation in a nitrogen atmosphere or under reduced pressure. In all reactions, the polymers were obtained in nearly quantitative yields. Results are given in Table II.

Melt Polymerization. To 2.0035 g. (0.00935 mole) of 3,3'-diamino-benzidine (II) was added 2.1144 g. (0.00935 mole) of 1,4-diglyoxalylben-zene dihydrate. The two solids were thoroughly mixed in a rotating flask and then heated to 180°C., at which temperature the mixture began to melt. The temperature was held at 180°C. for 1 hr. during which time the polymer became solid. The temperature was then raised to 250°C. and held there for 3 hr.

In a second heating cycle, the polymer was heated to 375°C. under 0.1 mm. for 3 hr. in a rotating flask containing 8 mm. diameter steel ball bearings to facilitate mixing.

In Dioxane; Method A. To a solution of 2.816 g. (0.0131 mole) of 3,3'-diaminobenzidine (II) in 50 ml. of purified dioxane heated to 95°C. was added with rapid stirring a solution of 2.972 g. (0.0131 mole) of 1,4-diglyoxalylbenzene dihydrate in 100 ml. of purified dioxane at 95°C. Immediately an orange precipitate formed, and the mixture was heated at the reflux temperature for 6 hr. The precipitated polymer was removed by filtration, and the nearly quantitative yield of polymer was heated in a rotating flask at 180°C. then to 250°C. and maintained at that temperature for 5 hr. The polymer did not melt during the heating.

ANAL. Calc'd. for $(C_{22}H_{12}N_4)_n$: C, 79.50%; H, 3.61%. Found: C, 78.86%; H, 4.63%.

In the second heating cycle, the polymer was treated at 375°C. under 0.1 mm. Hg for 1 hr. in a rotating flask with the steel bearings.

In Dioxane; Method B. The same procedure for the polymerization as described in method A was carried out, except that after the reflux period in dioxane, the dioxane was removed under reduced pressure leaving the total solids. This solid was treated to both heating cycles as described in method A.

Amine Hydrochloride In Water. To a solution of 0.587 g. (0.00163 mole) of 3,3'-diaminobenzidine tetrahydrochloride in 10 ml. of water in a Carius tube was added a hot solution of 0.3691 g. (0.00163 mole) of 1,4-diglyoxalyl-benzene. An immediate yellow precipitate was formed. The tube was alternately evacuated and filled with nitrogen three times and then sealed. The tube was slowly heated to 200°C. and held at that temperature for 8 hr. The water was removed under reduced pressure and the polymer residue was then heated at 200°C. for 3 hr.

Amine Hydrochloride in Dioxane. To a solution of 1.080 g. (0.003 mole) of 3,3'-diaminobenzidine tetrahydrochloride in 10 ml. of purified dioxane was added 0.678 g. (0.003 mole) of 1,4-diglyoxalylbenzene. The mixture was heated to the reflux temperature for 12 hr., and the solvent was removed under reduced pressure. The residue was heated to 250°C. under reduced
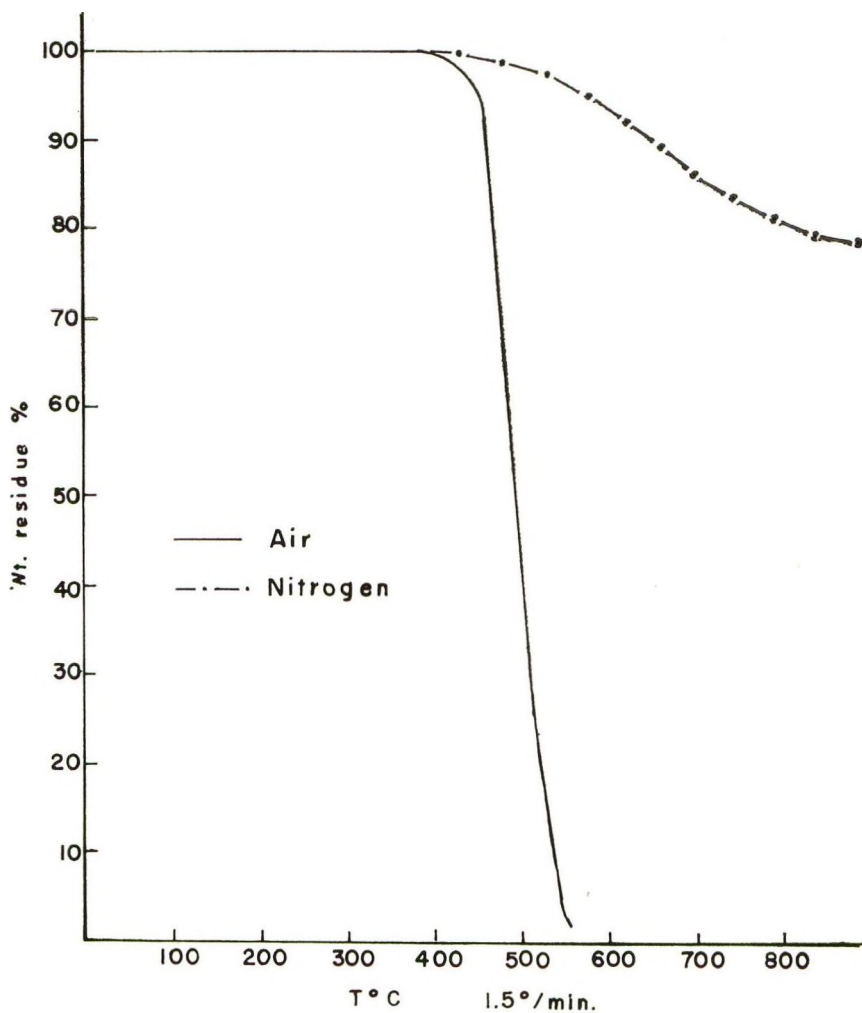

Fig. 1. Thermal gravimetric analysis on poly [2,2'-(1,4-phenylene)-6,6-diquinoxaline].

pressure (0.25 mm.) for 3 hr. The resulting polymer was slurried for 12 hr. in methanol containing ammonia in an attempt to remove bound hydrogen chloride. Analytical data on the polymer indicated that large amounts of hydrogen chloride were still present. A second heating cycle was carried out in the usual manner.

Thermal Gravimetric Analyses

Thermal gravimetric analyses in air and nitrogen were carried out at a heating rate of $1.5°/min$. The thermal gravimetric curves for all the polymer samples described were very similar. Figure 1 shows the curve for the polymer prepared by the melt polymerization.

DISCUSSION

In order to gain some information as to the conditions necessary for a quinoxaline forming polymerization reaction involving phenylglyoxal and 1,2-diaminobenzene type monomers, and in order to have compounds available for comparison with the polymer, a series of model quinoxalines were synthesized. In particular, the methods of formation of two quinoxalines, 1,4-di(2-quinoxalyl)benzene(VII) and 2,2'-diphenyl-6,6'-diquinoxaline-(VIII), were studied, since the syntheses of these two compounds separately utilized the monomers, 1,4-diglyoxalylbenzene(I) and 3,3'-diaminobenzidine(II) respectively, employed in the polymer synthesis.

Reactions of I with 1,2-diaminobenzene in solution or under melt conditions above the melting point of the diamine afforded in each case high yields of quinoxaline VII. Reaction of II with phenylglyoxal in a variety of solvents produced low yields of quinoxaline VIII. The highest yield of VIII was obtained when the tetrahydrochloride of amine II was tried.

There are three isomers (VIIIa–c) which may be formed from the reaction of 3,3'-diaminobenzidine with phenylglyoxal. Since only one compound was isolated in high yield in this reaction, a comparison of the ultraviolet spectra of this isomer with that of the other model compounds is helpful in assigning the structure of the isomer. Although band assignments in the quinoxaline system have not been made with certainty, it is not unreasonable to assign the higher wave length bands ($316–373$ mμ Table I) in dioxane to the ^1L_b (longitudinally polarized) band by analogy to the π-isoelectronic naphthalene system.[15] This is evidenced by the bathochromic and hyperchromic shifts from the substitution of a phenyl group in the 2-position (compounds IV and V).

If the isomer formed in the reaction of 3,3'-diaminobenzidine with phenylglyoxal were VIIIc, ^1L_b bands corresponding to those of either V or VI would be observed. No complete longitudinal polarization could occur in VIIIc, and it might be expected that the ^1L_b band would be in nearly the same position as that of V, with the exception that the extinction coefficient should be double, or nearly the same wave length and extinction coefficient as VI would be observed. This is clearly not the case. This leaves VIIIb and VIIIa as the two choices, but there is no compelling reason to believe that phenylglyoxal would react exclusively to put the phenyl group in the 2-position on one side of the diaminobenzidine molecule and always do the opposite on the other side of the molecule. Further, the length of the system for longitudinal polarization in VIIIb would be about the same as that of VII so that similar positions for the ^1L_b band would be expected. In

stead, a large bathochromic shift, which is double the shift in going from V or VI to VII (the intermediate system) is observed. We have assigned, therefore, the structure VIIIa to the reaction product. There is no reason to believe that a different reaction would occur in the polymerization of 3,3′-diaminobenzidine with 1,4-diglyoxalylbenzene, at least in 86% of the linkages, as represented by the yield of pure 2,2′-diphenyl-6,6′-diquinoxaline (VIII) obtained in the model reaction. Although the ultraviolet spectrum of the polymer was observed, band assignments of this type in the polymer were not readily made. On the basis of the model compound synthesis we have assigned the structure III to the polymer, although small amounts of 3-linkages may be present.

Reaction of 1,4-diglyoxalylbenzene (I) with 3,3′-diaminobenzidine afforded nearly quantitative yields of polymer III (Table II). Reaction of the two monomers in the absence of a solvent at 250°C. or reaction of the monomers in a solvent and heating the resulting polymer to 250°C. after the removal of the solvent produced polymer which was completely soluble in sulfuric acid and which had nearly the same molecular weight. Further heating of these polymer samples under reduced pressure to 375°C. substantially increased the molecular weight, but at no time during the heating cycle was any melting noticed. The low solubility of the polymer which has been treated in this way could be due to a crosslinking reaction, or a typical property of a high molecular weight polymer with such a rigid backbone.

In the polymerization reactions in the absence of solvent, small amounts of material sublimed from the reaction mixture as it became liquid near 180°C. Since this would evidently destroy monomer balance, the methods of prepolymerization in a solvent were carried out on the basis that oligomers formed would not sublime during the higher heating cycle, and higher molecular weights would be produced. No significant increases in the dilute solution viscosities were observed, however, from the prepolymer method.

No particular improvement in molecular weight or solubility was noted when the amine hydrochloride was tried. The resulting polymers could not be purged of bound hydrogen chloride, and this would tend to give abnormally high solution viscosities for the polymer. For the same polymer sample, a much higher solution viscosity is obtained in sulfuric acid than in hexamethylphosphoramide. In general, the polymer samples have much better solubilities in strong organic acids such as formic and trifluoroacetic than hexamethylphosphoramide, dimethylformamide, or dimethyl sulfoxide.

Thermal gravimetric analyses on the polymer samples (Table II, Fig. 1) show that the quinoxaline polymers (III) have thermal stabilities in air and nitrogen which are very similar to those obtained on the polybenzimidazoles.[3,8] In no instance during the heating under nitrogen was any melting observed.

References

1. Berlin, A. A., *J. Polymer Sci.*, **55**, 621 (1961).

2. Sorenson, W. R., papers presented at the 140th Meeting, American Chemical Society, Division of Polymer Chemistry, Chicago, September 1961; *Preprints*, p. 226.

3. Vogel, H., and C. S. Marvel, *J. Polymer Sci.*, **50**, 511 (1961).

4. Mulvaney, J. E., and C. S. Marvel, *J. Polymer Sci.*, **50**, 541 (1961).

5. Mulvaney, J. E., and C. S. Marvel, *J. Org. Chem.*, **26**, 95 (1961).

6. Abshire, C. J., and C. S. Marvel, *Makromol. Chem.*, **44–46**, 388 (1961).

7. Mulvaney, J. E., J. J. Bloomfield, and C. S. Marvel, *J. Polymer Sci.*, **62**, 59 (1962).

8. Vogel, H., and C. S. Marvel, *J. Polymer Sci.*, **A1**, 1531 (1963).

9. Pratt, Y. T., in *Heterocyclic Compounds*, Vol. VI, R. C. Elderfield, Ed., Wiley, New York, 1957, pp. 455–472.

10. Simpson, J. C. E., *Condensed Pyridazine and Pyrazine Rings*, Interscience, New York, 1953, p. 203.

11. Ruggli, P., and Gassenmeier, *Helv. Chim. Acta*, **22**, 496 (1939).

12. Jones, G., and K. C. McLaughlin, *Organic Synthesis*, **30**, 86 (1950).

13. Hindsberg, O., *Ann.*, **237**, 327 (1887); *ibid.*, **292**, 245 (1896).

14. Tiwari, L. D., and S. Dutt, *Proc. Natl. Acad. Sci. India*, **7**, 58 (1937).

15. Jaffe, H. H., and M. Orchin, *Theory and Applications of Ultraviolet Spectroscopy*, Wiley, New York, 1962.

Résumé

La réaction entre des quantités stoechiométriques de 1,4-diglyoxalylbenzène et de 3,3'-diaminobenzidine fournit de la polyquinoxaline pratiquement quantitativement. Que la réaction soit fait en absence de solvant à 250°C ou que l'on préparéd'abord dans un solvant un prépolymère que l'on chauffe ensuite à 250°C, on obtient des polymères solubles de propriétés quasi-identiques. Le poids moléculaire augmente par chauffage à 375°C sous pression réduite. Une étude de composés et de réactions 'modèles' indique que le polymère est principalement de la poly[2,2'(1-4-phénylène)-6,6'-diquinoxaline] et non pas les isomères 2,3'on 3,3'. Ces polymères sont stables à l'air à 500°C, chauffés sous azote ils perdent seulement 20% de leur poids à 800°C.

Zusammenfassung

Die Reaktion stöchiometrischer Anteile von 1,4-Diglyoxalbenzol und 3,3'-Diaminobenzidin liefert fast quantitative Ausbeuten eines Polychinoxalins. Die Reaktion die Monomeren ohne Lösungsmittel bei Erhitzen auf 250°C oder die Reaktion der Monomeren in einem Lösungsmittel zur Erzeugung eines Präpolymeren und Erhitzen des Präpolymeren auf 250°C ergibt ein lösliches Polymeres mit fast gleichen Eigenschaften. Erhitzen des Polymeren auf 375°C under vermindertem Druck vergrössert das Molekulargewicht. Eine Untersuchung von Modellverbindungen und -reaktionen zeigt, dass das Polymere hauptsächlich Poly[2,2'-(1,4-phenylen)-6,6'-dichinoxalin] anstelle der 2,3'- oder 3,3'-Isomeren ist. Diese Polymeren sind in Luft bis 500°C stabil und verlieren in Stickstoff bei 800°C nur 20% ihres Gewichts.

Polymerization in Liquid Sulfur Dioxide. Part XIX. Effects of Aniline and Its Derivatives on the Radical Polymerization of Acrylonitrile in Liquid Sulfur Dioxide

MINORU MATSUDA, SUSUMU ABE, and NIICHIRO TOKURA,
*The Chemical Research Institute of Non-aqueous Solutions, Tohoku University,
Sendai, Japan*

Synopsis

Radical polymerization of acrylonitrile in liquid sulfur dioxide was carried out at 50°C. with α,α'-azobisisobutylonitrile as an initiator. When aniline (An), dimethylaniline (DMA), dimethyl-o-toluidine (DMoT), and diethylaniline (DEA) were added to this system, it was found that each base acted as a retarder for the polymerization. When the chain transfer constant was calculated for each base, the values were 1.0 (An), 1.5 (DMA), 3.0 (DMoT), and 9.3 (DEA). The Alfrey-Price e_{tr} values calculated from these values were -2.79 (An), -3.14 (DMA), -3.72 (DMoT), and -4.66 (DEA). On plotting these values against pK_a of each base, a linear relationship was found.

INTRODUCTION

About ten years ago it was shown by Imoto and his collaborators[1-3] that redox polymerization of various vinyl monomers could be carried out with dimethylaniline as the oxidizing reagent in nonaqueous solvent such as benzene. In this case dimethylaniline promoted the decomposition of peroxides and accelerated the initial rate of the polymerization.

When a radical initiator which is free from induced decomposition, is used, dimethylaniline acts on elementary reactions other than initiation.[4] When acrylonitrile, having a comparatively large polarity, is used as the monomer, it acts as a retarder.

The polysulfone of acrylonitrile cannot be obtained by radical polymerization of acrylonitrile in liquid sulfur dioxide. This is because acrylonitrile has no donor-acceptor interaction of electrons with liquid sulfur dioxide.[5] On the other hand, the aniline derivatives, such as dimethylaniline, have such an interaction with liquid sulfur dioxide; there is a possibility that they give some effects different from those of aniline derivatives in benzene on each elementary reaction of the polymerization.

The effect of aniline derivatives on the radical polymerization of acrylonitrile in liquid sulfur dioxide have been examined, aniline, dimethylaniline,

dimethyl-*o*-toluidine, and diethylaniline being used as the aniline deriva-
tives.

EXPERIMENTAL

Acrylonitrile monomer (AN), liquid sulfur dioxide (liq. SO_2), and α,α'-
azobisisobutylonitrile (AIBN) were purified as has been reported prev-
iously.[5] Aniline (An), dimethylaniline (DMA), dimethyl-*o*-toluidine
(DMoT), and diethylaniline (DEA) were distilled in nitrogen atmosphere
under the reduced pressure into ampules, sealed, and then used.

The overall rate of the polymerization was determined by the gravi-
metric method. Namely, AN–AIBN solution of a definite concentration
was put into a pressure glass vessel (about 20 ml. capacity) which was
flushed with dry nitrogen several times under cooling (below about $-70°C$).
A definite amount of a solution of liquid sulfur dioxide and the aniline
derivatives solution (prepared by breaking a glass ampule containing a
known weight of aniline derivative in a known weight of liquid sulfur
dioxide) of known concentration was added to the AN–AIBN solution.

The initial concentrations of AN, liquid SO_2, and AIBN ($[AN]_0$, [liq.
$SO_2]_0$, and $[AIBN]_0$, respectively) were 7.54 mole/l. (50.0 vol.-%),
10.11 mole/l. (50.0 vol.-%), and 3.05×10^{-2} mole/l., respectively, in all
experiments. The polymerization temperature was 50.0°C.

Results and Discussion

Some results elementary analyses of acrylonitrile polymers obtained by
the radical polymerization in liquid sulfur dioxide are shown in Table I.

The results of qualitative analyses for sulfur in the polymers show that no
polysulfone is formed, irrespective of the kind of aniline derivative and its
concentration.

TABLE I
Results of Elementary Analysis of Polymers of Acrylonitrile obtained in Liquid
Sulfur Dioxide at 50.0°C.

Expt. no.	Added species	Concn., mole/l. $\times 10^2$	Conversion, wt.-%	N, %	S (qualitative analysis)
20	None	—	5.3	26.02	None
256	An	4.87	8.9	25.02	"
29	DMA	1.02	2.3	26.37	"
188	DMoT	4.79	5.7	25.33	"
230	DEA	5.05	4.1	25.93	"

With the radical polymerization of olefin in liquid sulfur dioxide, polysulfone
is usually obtained.[7,8] However, the radical polymerization of acryloni-
trile[5] and methyl methacrylate[6] does not give polysulfone.

It was found that sulfur-free polymers can be prepared even when a base
such as dimethylaniline is added, so liquid sulfur dioxide will be treated in
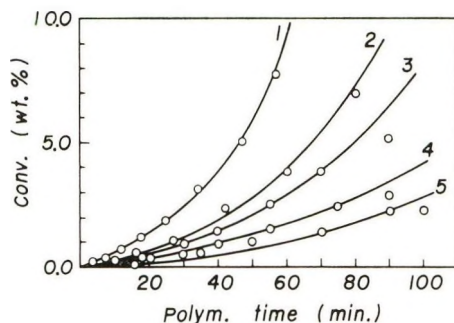
Fig. 1. Time–conversion curve obtained with the radical polymerization of acrylonitrile in liquid sulfur dioxide with added various concentrations of dimethylaniline: (1) 0.00; (2) 4.05×10^{-4} mole/l.; (3) 1.61×10^{-3} mole/l.; (4) 1.02×10^{-2} mole/l.; (5) 7.51×10^{-2} mole/l. $[AN]_0 = 7.54$ mole/l.; $[liq. SO_2]_0 = 10.11$ mole/l.; $[AIBN]_0 = 3.05 \times 10^{-2}$ mole/l.; polymerization temp. 50°C.
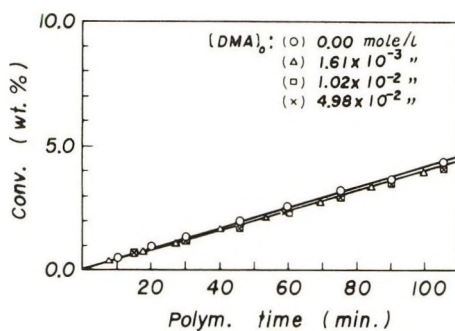

Fig. 2. Time–conversion curve obtained with the radical polymerization of styrene in liquid sulfur dioxide with added dimethylaniline at 50°C.

this discussion as a solvent in the polymerization of acrylonitrile instead of a comonomer.

The radical polymerization of acrylonitrile proceeds as a heterogeneous reaction in liquid sulfur dioxide.[5] Consequently, it is necessary to determine whether the heterogeneity of the system changes on addition of aniline or aniline derivatives. When the overall rate equation of the polymerization was experimentally determined at a constant initial concentration of dimethylaniline of 4.05×10^{-4} mole/l., the order of $[AIBN]_0$ was obtained as 0.85 ± 0.03. This value was the same as the value 0.87 obtained in the system containing no additive.[5] Consequently, may be considered that the heterogeneity of the system will not be changed from the kinetic point of view by the addition of aniline.

Figure 1 shows the time–conversion curve obtained with the radical polymerization of acrylonitrile in liquid sulfur dioxide system containing dimethylaniline. It is found from this figure that dimethylaniline acts as a retarder of the polymerization reaction. On the other hand, the time–conversion curve (Fig. 2) obtained with a similar polymerization system with
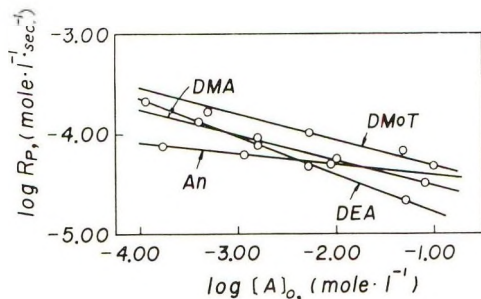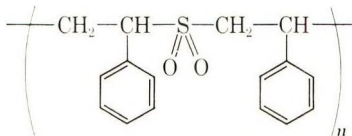
Fig. 3. Logarithmic plot of overall rate of polymerization of R_p vs. initial concentration of added aniline and aniline derivatives.

styrene indicates that the polymerization proceeds at a rate independent of the concentration of dimethylaniline. From the comparison of Figures 1 and 2, it is clearly shown that the retarding effect of dimethylaniline on acrylonitrile is exerted in elementary reactions other than initiation. Namely, the isobutylonitrile radical formed from the initiator does not react with dimethylaniline. In the case of styrene, no effect is exhibited by dimethylaniline, as is seen in Figure 2. This is due to the difference in the polarity of styrene from that of acrylonitrile. Alfrey-Price's e values of styrene and acrylonitrile are -0.8 and $+1.20$, respectively. This shows that acrylonitrile has the higher electron affinity. This difference in the e value is also seen with the polymer obtained in liquid sulfur dioxide. Styrene has some affinity for liquid sulfur dioxide and gives styrene polysulfone[6] as follows:

$$-\left(CH_2-CH-S-CH_2-CH\right)_n$$

The overall rate of polymerization at various concentrations of dimethylaniline was calculated from Figure 1. The relation between these values and the initial concentrations of dimethylaniline was plotted on a logarithmic scale. Figure 3 shows this relation together with corresponding values for aniline, dimethyl-o-toluidine, and diethylaniline. These results well satisfy a linear relationship, and the slope exactly corresponds to n in eq. (1), where the overall rate of polymerization is R_p, and where $[A]_0$ is the initial concentration of aniline derivative added. The values of n are given in Table II.

$$R_p = \text{const} \times [A]_0{}^n \tag{1}$$

n is thus negative for each aniline derivative. It is obvious that these bases retard the polymerization of acrylonitrile. With the change from aniline to diethylaniline, the value of n becomes more negative, showing
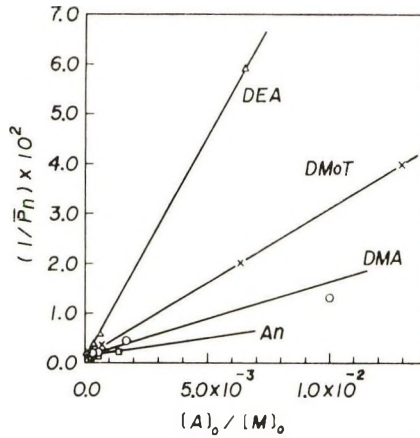
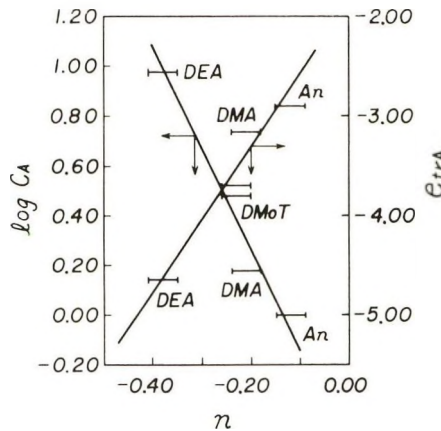Fig. 4. Plot of reciprocal degree of polymerization $(1/\bar{P}_n)$ vs. $[A]_0/[M]_0$.

Fig. 5. Plot of participation order n of aniline and its derivatives vs. chain transfer constant C_A and e_{tr}.

TABLE II
Values of n calculated from Eq. (1)

Added species	n
Aniline (An)	-0.12 ± 0.03
Dimethylaniline (DMA)	-0.21 ± 0.03
Dimethyl-o-toluidine (DMoT)	-0.23 ± 0.03
Diethylaniline (DEA)	-0.38 ± 0.03

that this effect becomes larger. This is related to the basicity of aniline derivatives as will be described below.

The degree of the polymerization of polymers $\bar{P}_n$ was calculated by using the viscosity formula of Houtz[10]

$$[\eta] = 1.75 \times 10^{-3} M_n^{0.66} \qquad (2)$$

where $|\eta|$ is the intrinsic viscosity in DMF at 60°C. The reciprocal of the degree of the polymerization can be expressed by Mayo's equation:[11]

$$1/\bar{P}_n = (1/\bar{P}_{n_0}) + (C_A[A]_0/[M]_0) \tag{3}$$

where $\bar{P}_{n_0}$ is the degree of the polymerization of a polymer obtained in a system containing no additive, C_A is the chain transfer constant to an aniline derivative ($\equiv k_{tr_A}/k_p$), and $[A]_0$ and $[M]_0$ are the initial concentrations of the aniline derivative and the monomer, respectively. Figure 4 is a schematic diagram of eq. (3). When each line is extrapolated to the $1/\bar{P}_n$ axis, all the lines not only coincide exactly with one another but also with the experimentally determined value of $1/\bar{P}_{n_0}$. The values of C_A are shown in Table III. The values of C_A are all large and show that these bases act as retarders. When the logarithm of C_A and the values of n are plotted, Figure 5 was obtained. This plot indicates that the radical of the aniline derivative formed as a result of chain transfer has lost the ability to polymerize acrylonitrile because of resonance stabilization and that the larger the effect on the overall rate of reaction (the larger the absolute value of n that is negative) the larger the retarding effect. The scheme of chain transfer of the end radical of the growing chain to an aniline derivative will be the same as that proposed by Imoto et al. for benzene.[4]

Such stabilization of the active end radical of acrylonitrile found in liquid sulfur dioxide was also recognized when various ammonium salts were added.[13]

The addition of a base thus decreases both the rate of reaction and the degree of polymerization. A base such as aniline has an electron donor-acceptor interaction with liquid sulfur dioxide, so the most reliable mechanism of the reaction cannot be obtained unless this interaction is taken into consideration.

TABLE III
Values of the Chain Transfer Constant C_A at 50.0°C.

Added species	C_A
An	1.0
DMA	1.5
DMoT	3.0
DEA	9.3

TABLE IV
e_{tr} and pK_a of Aniline Derivatives

Added species	e_{tr}	pK_a
An	−2.79	4.62
DMA	−3.14	5.06
DMoT	−3.72	5.86
DEA	−4.66	6.56

An aniline derivative such as dimethylaniline will be in the following equilibrium in liquid sulfur dioxide:[15]

$$\text{DMA} + \text{liq. SO}_2 \overset{k}{\rightleftharpoons} \text{DMA} \cdot \text{SO}_2 \qquad (4)$$
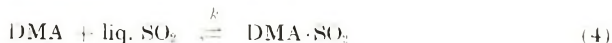
Qualitative evidence is supplied by the facts that the color of the mixture is yellowish red or reddish brown and that white powdery precipitate forms in the mixed solution when the temperature is lowered to about $-50°C$. However, the value of the equilibrium constant cannot be found in the literature and the discussion cannot be made in further detail. When the results are compared with those in benzene, there is no remarkable difference between the polymerization in benzene and that in liquid sulfur dioxide. A more detailed investigation is currently being made; results will be published later.
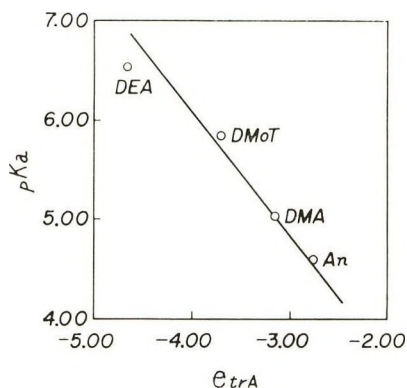

Fig. 6. Plot of e_{tr} vs. pK_a.

The value of C_A obtained with aniline derivatives can be related to the Q–e scheme of Alfrey-Price as in eq. (5): where Q_M and Q_{tr_A} are the mean

$$C_A = k_{tr_A}/k_p = (Q_{tr_A}/Q_M) \exp \left\{ -e_M \left(e_{tr_A} - e_M \right) \right\} \qquad (5)$$

reactivities of the monomer and the chain transfer agent, respectively. e_M and e_{tr_A} are the polar factors which are the electrostatic charge remaining in each reacting site. e_{tr} of aniline derivatives were calculated on the basis of a value of $Q = 5 \times 10^{-3}$ for dimethylaniline as calculated by Imoto et al.[4] and the values reported in the literature for Q_{AN} and e_{AN}. The values of e_{tr}, as well as those of pK_a, are shown in Table IV. The results shown in Table IV are schematically represented in Figure 6. There is a linear relationship between both these values. This fact indicates that factors e_{tr} and pK_a are essentially the same in character: namely, there is a linear relationship between the parameter e proposed by Alfrey-Price and pK_a, which is a measure of the basicity of the chain transfer agent. This relationship is equivalent to the relation between e and σ proposed by Hammett.[14] Reports will be made in the near future on the quantitative relationship between e and pK_a and its meaning.

References

1. Imoto, M., T. Otsu, and K. Kimura, *J. Polymer Sci.*, **15**, 475 (1955).

2. Imoto, M., and S. Choe, *J. Polymer Sci.*, **15**, 485 (1955).

3. Imoto, M., and K. Takemoto, *J. Polymer Sci.*, **18**, 377 (1955).

4. Imoto, M., T. Otsu, T. Ota, H. Takatsugi, and M. Matsuda, *J. Polymer Sci.*, **21**, 559 (1956).

5. Tokura, N., M. Matsuda, and F. Yazaki, *Makromol. Chem.*, **42**, 108 (1960).

6. Matsuda, M., M. Iino, and N. Tokura, *Makromol. Chem.*, **65**, 232 (1963).

7. Dainton, F. S., and K. J. Ivin, *Quart. Revs.*, **12**, 61 (1958).

8. Tokura, N., and M. Matsuda, *Kogyo Kagaku Zasshi*, **64**, 501 (1961).

9. Alfrey, T., and C. C. Price, *J. Polymer Sci.*, **2**, 101 (1947).

10. Houtz, R. C., *Textile Res. J.*, **20**, 786 (1950).

11. Mayo, F. R., *J. Am. Chem. Soc.*, **65**, 2324 (1943).

12. Tokura, N., M. Matsuda, and H. Kichiji, *Kogyo Kagaku Zasshi*, **65**, 1636 (1962).

13. Matsuda, M., *Makromol. Chem.*, **65**, 224 (1963).

14. Shen, M. C., *J. Polymer Sci.*, **B1**, 11 (1963).

15. Kashtanov, L. I., and N. V. Kazanakaya, *Zhur. Fiz. Khim.*, **28**, 1547 (1954).

Résumé

On a effectué la polymérisation radicalaire de l'acrylonitrile à 50°C dans l'anhydride sulfureux liquide en employant comme initiateur le α,α'-azobisisobutyronitrile. Lorsqu'on ajoute à ce système de l'aniline (An), de la diméthylaniline (DMA), de la diméthyl-o-toluidine (DMoT) et de la diéthylaniline (DEA), on trouve que chaque base est un rétardateur pour la polymérisation. On a calculé les constantes de transfert de chaîne pour chaque base, les valeurs sont: 1,5 (DMA), 3,0 (DMoT) et 9,3 (DEA). Les valeurs de e_{tr} de Alfrey-Price sont déduites de ces données: -2.79 (An), -3.14 (DMA), -3.72 (DMoT) et -4.62 (DEA). En mettant en graphique ces valeurs en fonction du pK_a de chaque base, on trouve une relation linéaire.

Zusammenfassung

Radikalische Polymerisation von Acrylnitril wurde in flüssigem Schwefeldioxyd bei 50°C unter Verwendung von α,α'-Azobiisobutyronitril als Starter durchgeführt. Bei Zusatz von Anilin (An), Dimethylanilin (DMA), Dimethyl-o-toluidin (DMoT) und Diäthylanilin (DEA) zu diesem System wirte jede Base als Verzögerer der Polymerisation. Die Kettenübertragungskonstanten für jede Base wurden berechnet und ergaben sich zu 1,0 (An), 1,5 (DMA), 3,0 (DMoT) und 9,3 (DEA). Die Werte von e_{tr} nach Alfrey-Price wurden aus diesen Werten berechnet: $-2,79$ (An), $-3,14$ (DMA), $-3,72$ (DMoT) und $-4,66$ (DEA). Wenn man diese Werte gegen pK_a jeder Base aufträgt, so ergibt sich eine lineare Beziehung.

Influence of Catalyst Depletion or Deactivation on Polymerization Kinetics[*]

HERBERT N. FRIEDLANDER, *Basic Research Department, Chemstrand Research Center, Inc., Durham, North Carolina*

Synopsis

Kinetic models based on the time dependence of the deactivation of catalyst sites have been fitted to data on reaction kinetics taken from the literature for polymerization of various olefins on a series of ionic and coordinate catalysts (both homogeneous and heterogeneous) for a variety of polymerization conditions. In clean coordinate polymerization systems where termination is unimportant, the propagation reaction plays a major role and is influenced by the number of active catalyst sites. The number of sites remains constant in some catalysts but varies in most. First-order deactivation of catalyst sites leads to dead-end kinetics similar to that described by Tobolsky for free-radical polymerization with catalyst depletion by first-order decomposition. Second-order deactivation leads to kinetics linear in the logarithm of time. In heterogeneous polymerization, it is difficult to find a physical model for interaction of isolated sites required for higher-order deactivation. The experimental data are fitted equally well by a mixed-order model assuming sites of different stability exhibiting first-order deactivation. At low conversions, the models are difficult to fit to experimental data in which monomer concentration is varing. Further experiments are required to test the models, obtain exact values for rates constants, and determine the influence of catalyst deactivation on molecular weight and molecular weight distribution.

INTRODUCTION

Interpretation of polymerization kinetics is often limited to the early stages of polymerization at low conversion owing to changes in catalyst concentration or activity. In 1958, Tobolsky[1] demonstrated that polymerization kinetics could be interpreted to high conversions in free-radical systems by taking into account the rate of decomposition of the catalyst, provided the termination reactions were not changed by viscosity retardation or other effects.[2] Tobolsky termed polymerization amenable to such kinetic interpretation as "dead-end polymerization" because the polymerization stops short of complete conversion owing to catalyst depletion. In extending studies to polymerization of styrene with 2,2'-azobisisobutyronitrile as initiator, he demonstrated that the ratio of the propagation to termination rate constants, $k_p/k_t^{1/2}$, can be readily determined.[3] Similarly, polymerization kinetics have been interpreted to high conversion for ethyl-

ene polymerization catalyzed by diethyl peroxydicarbonate[4] and for sty-
rene and vinyl chloride by redox catalysts.[5-7] Other redox systems should
be amenable to similar interpretation; for example, the conversion versus
time data of Welch[8] for the triethylberon–oxygen system show the trend
expected for dead-end polymerization.

Attempts have been made[9] to utilize similar kinetic approaches to explain
variations in polymerization caused by other factors influencing initiator
activity such as formation of solid phases during polymerization. How-
ever, no attempts have been made as yet to extend these concepts to the
general case of catalyst depletion of any kinetic order or to deactivation of
heterogeneous polymerization catalysts.

The importance of catalyst variation during polymerization in coordi-
nate complex or heterogeneous systems was first realized by Chien,[10] who
measured the number of active sites by termination with radioactive iodine.
He interpreted the changes in terms of modification of the termination re-
actions and was forced to apply a second-order termination reaction to fit
the kinetic data. However, it is difficult to give a good physical descrip-
tion to second-order interaction of catalyst sites in complex or heteroge-
neous systems. Recently[11] spectrophotometric and electron paramagnetic
techniques showed that Chien's catalyst undergoes reductive deactivation,
avoiding the second-order termination hypothesis.

A more elegant method for determining changes in number of active
catalyst sites was developed by Feldman and Perry,[12] utilizing tritiated
methanol for quenching of ethylene polymerization on Ziegler-type cata-
lysts. They conclude that the high value for the number of centers argues
against bimolecular termination. This technique was used for study of
propylene polymerization on a $TiCl_3$ catalyst by Bier et al.[13] and by Kohn
et al.,[14] who recognized the logarithmic first-order deactivation of catalyst
with a rate in the range from 2×10^{-3} to 14.4×10^{-3} min.$^{-1}$

Because of its importance in interpreting the mechanism for coordinate
complex or heterogeneous polymerization, calculations of reaction kinetics
are carried out taking into account deactivation of the catalyst with various
orders of decomposition as a possible model for these systems. This model
is especially applicable to coordinate polymerization or living polymer sys-
tems where termination reactions by dimerization and disproportionation
are not taking place. Instead, deactivation of initiator appears to limit the
reaction.

POLYMERIZATION KINETICS WITH CATALYST DEACTIVATION

The propagation reaction in polymerization with coordinate complex or
heterogeneous catalysts has been shown[15-18] to be, in general, a first-order
reaction in the number of active catalyst sites and in the monomer as shown
by eq. (1):

$$d[P]/dt = k_p [C^*] [M]$$

or

$$d[P]/[M] = k_p [C^*] dt \qquad (1)$$

where k_p is the rate of propagation and $[P]$, $[C^*]$, and $[M]$ are the concentration of polymer, catalyst, and monomer, respectively. Under special circumstances the overall polymerization reaction may be of more complex order in monomer.[15,19-21] However, many individual studies of olefin polymerization with heterogeneous catalysts are carried out at constant pressure and therefore at constant monomer concentration. We may, therefore, focus our attention on the change in catalyst concentration.

Monomer Concentration Held Constant

Certain catalysts, when applied in systems of high purity, maintain constant activity up to high conversion levels.[15,16] There is no termination or catalyst deactivation during the period studied. These kinds of catalyst systems are especially useful for block copolymerization.[22-24] At constant monomer concentration, $[M_c]$, eq. (1) integrates simply to give

$$X = [P]/[M_c] = k_p [C^*]t \qquad (2)$$

where X is the conversion to polymer in terms of the constant monomer concentration. Conversion is a linear function of time.

The first-order case is based on the reasonable assumption that active catalyst sites may undergo spontaneous first-order decomposition related to thermal dissociation of weak transition metal–carbon bonds, that is, to homolytic or heterolytic splitting of organometallic bonds. If the rate of disintegration is k_d, then

$$-d[C^*]/dt = k_d [C^*] \qquad (3)$$

which yields, on integration,

$$[C^*] = [C_0^*] \exp \{-k_d t\} \qquad (4)$$

where $[C_0^*]$ is the initial catalyst concentration. At constant monomer concentration and by substitution of $[C^*]$ from eq. (4) in eq. (1), the polymerization rate equation becomes:

$$d[P]/[M_c] = k_p[C_0^*] \exp \{-k_d t\} dt \qquad (5)$$

On integrating, typical dead-end polymerization kinetics are obtained:

$$X = (k_p/k_d) [C_0^*] (1 - \exp \{-k_d t\}) \qquad (6)$$

and the polymerization reaches a limiting conversion

$$X_\infty = (k_p/k_d) [C_0^*]$$

so that

$$X = X_\infty - X_\infty \exp \{-k_d t\}$$

or

$$\ln(X_\infty - X) = \ln X_\infty - k_d t \tag{7}$$

From eq. (7), k_d can be determined, and from the relation of X_∞ and $[C_0^*]$, k_p can be determined.

We may now consider the physically less probable case of second- or higher-order catalyst deactivation by migration and interaction of active sites where

$$-d[C^*]/dt = k_d[C^*]^n \tag{8}$$

where n is 2 or more. Integrating for $n = 2$, one obtains

$$[C^*] = [C_0^*]/(1 + [C_0^*]k_d t) \tag{9}$$

At constant monomer concentration and by substitution of $[C^*]$ from eq. (9) in eq. (1) the polymerization rate becomes

$$d[P]/[M_c] = k_p[C_0^*]dt/(1 + [C_0^*]k_d t) \tag{10}$$

On integrating, the fraction converted becomes proportional to the logarithm of the duration of polymerization:

$$X = (k_p/k_d)\ln(1 + [C_0^*]k_d t) \tag{11}$$

or

$$\exp\{(k_d/k_p)X\} = 1 + [C_0^*]k_d t$$

Many coordinate catalysts are made up of several components which interact. Thus, sites of one or more degree of stability may be present at the same time.[25,26] A common situation involves the simultaneous occurrence of stable sites $[C_s^*]$ and those undergoing first-order deactivation according to eq. (4). The polymerization rate equation is:

$$d[P]/[M_c] = k_p[C_s^*]dt + k_p'[C_0^*]\exp\{-k_d t\}dt \tag{12}$$

On integrating, one obtains

$$X = k_p[C_s^*]t + (k_p'/k_d)[C_0^*](1 - \exp\{-k_d t\}) \tag{13}$$

Initially, at short times,

$$X \simeq (k_p[C_s^*] + k_p'[C_0^*])t$$

A plot of X versus t defines a straight line through the origin. As time increases, the line becomes curved with a decrease in slope. Finally, at long times the line again becomes straight with a smaller slope corresponding to $k_p[C_s^*]$. The intercept on the conversion axis of the line at long time is a measure of $(k_p'/k_d)[C_0^*]$.

Table I summarizes the integrated kinetic expressions assuming no termination for various orders of catalyst deactivation with monomer concentration held constant.

TABLE I
Integrated Kinetic Expressions Assuming No Termination

Catalyst deactivation	Monomer concentration constant, $X = [P]/[M_c]$
None	$X = k_p[C^*]t$ [eq. (2)]
First-order	$X = (k_p/k_d)[C_0^*](1 - \exp\{-k_d t\})$ [eq. (6)] or $\ln(X_\infty - X) = \ln X_\infty - k_d t$ where $X_\infty = (k_p/k_d)[C_0^*]$ [eq. (7)]
Second-order	$X = (k_p/k_d)\ln(1 + [C_0^*]k_d t)$ [eq. (11)]
Mixed	$X = k_p[C_s^*]t + (k_p'/k_d)[C_0^*](1 - \exp\{-k_d t\})$ [eq. (13)]

Monomer Concentration Varies

One may also consider corresponding cases of catalyst deactivation under conditions when the monomer concentration is not held constant. Both first and second order utilization of monomer may be considered. The right-hand side of eqs. (1), (5), (10), and (12) remains unchanged. The left-hand side becomes $d[P]/[M]^n$ or $-d[M]/[M]^n$, where n is 1 or 2, which on integration and evaluation of the integration constant under the initial conditions yields $-\ln(1 - X)$ for $n = 1$ and $\{X/(1 - X)[M_0]\}$ for $n = 2$, where X now has the usual meaning of conversion in terms of the initial monomer concentration $[M_0]$:

$$X = ([M_0] - [M])/[M_0] = [P]/[M_0]$$

The integrated kinetic equations assuming no termination are summarized in Table II for the various orders of monomer consumption and catalyst deactivation.

When the monomer concentration is allowed to vary with conversion, its influence* on catalyst deactivation may be observable, and eq. (3) becomes

$$-d[C^*]/dt = k_d[C^*] + k_d'[C^*][M]^n \tag{3a}$$

* The author is indebted to a referee for pointing out this possibility. At present, there is no direct evidence in the literature to support the concept of deactivation by monomers. Such evidence can be obtained by studies of changes in the number of active sites as a function of monomer concentration and by the influence of monomer concentration on the types of end-groups and the width of the molecular weight distribution.

TABLE II
Integrated Kinetic Expressions Assuming No Termination

Catalyst deactivation	Monomer concentration varies, $X = [P]/[M_0] = ([M_0] - [M])/[M_0]$	
	First-order decrease	Second-order decrease
None	$-\ln(1 - X) = k_p[C^*]t$ [eq. (14)]	$X/(1 - X) = k_p[M_0][C^*]t$ [eq. (18)]
First-order	$-\ln(1 - X) = (k_p/k_d)[C_0^*]$ $\times (1 - \exp\{-k_d t\})$ or $\ln\left[\ln\left(\dfrac{1 - X}{1 - X_\infty}\right)\right]$ $= \ln\left(\dfrac{k_p}{k_d}[C_0^*]\right) - k_d t$ where $-\ln(1 - X_\infty)$ $= (k_p/k_d)[C_0^*]$ [eq. (15)]	$X/(1 - X) = (k_p/k_d)[M_0][C_0^*]$ $\times (1 - \exp\{-k_d t\})$ or $\ln\left(\dfrac{X_\infty}{1 - X_\infty} - \dfrac{X}{1 - X}\right)$ $= \ln\left(\dfrac{k_p}{k_d}[C_0^*][M_0]\right) - k_d t$ where $X_\infty/(1 - X_\infty)$ $= (k_p/k_d)[M_0][C_0^*]$ [eq. (19)]
Second-order	$-\ln(1 - X)$ $= (k_p/k_d)\ln(1 + [C_0^*]k_d t)$ [eq. (16)]	$X/(1 - X)[M_0]$ $= (k_p/k_d)\ln(1 + [C_0^*]k_d t)$ [eq. (20)]
Mixed	$-\ln(1 - X) = k_p[C_s^*]t$ $+ \dfrac{k_p'}{k_d}[C_0^*](1 - \exp\{-k_d t\})$ [eq. (17)]	$\dfrac{X}{(1 - X)[M_0]} = k_p[C_s^*]t$ $+ \dfrac{k_p'}{k_d}[C_0^*](1 - \exp\{-k_d t\})$ [eq. (21)]

At low conversions, the deactivation is more rapid than at higher conversions when monomer concentration becomes lower. Thus the rate of conversion would be expected to decrease with time approaching a linear condition similar to that predicted by the mixed-order deactivation case. Monomer deactivation of catalyst sites would have an effect on polymerization kinetics similar to second-order deactivation or termination.

INTERPRETATION OF EXPERIMENTAL DATA

A number of kinetic studies have been made of polymerization with coordinate complex or heterogeneous catalysts of various types. From the conversion versus time data given in the literature, the various kinetic expressions can be tested. Often the data given are not sufficient to determine the rate constants but the shape of the curve can be fitted. Most of the experimental data are given for systems at constant pressure so that the monomer concentration is fixed. These cases will be treated first.

The fit to the kinetic equations is made in the following manner: conversion X where given (or a number proportional to X) is plotted versus t. A straight line indicates no catalyst deactivation [eq. (2)]. A curved line

indicates one of the cases of catalyst deactivation. A curve which becomes linear at longer times of reaction indicates mixed deactivation [eq. (13)]. If the line approaches an asymptote of zero slope, first-order deactivation [eq. (7)] is indicated. This can be tested by determining X_∞ and plotting $\ln [(X_\infty - X)/X_\infty]$ versus t. The slope of the line gives k_d. Finally, by plotting X versus $\ln t$ [eq. (11)], second-order deactivation can be tested. A straight line is obtained for higher values of t when $[C_0^*]k_d t$ is large with respect to 1.

Monomer Concentration Held Constant

The sources of the existing data of interest to interpret, in which $[M]$ was held constant, are given in Table III along with the type of monomer polymerized and the catalyst system utilized. A wide range of systems has been investigated.

TABLE III
Polymerization Kinetics at Constant Monomer Concentration

System	Monomer	Catalyst	Reaction medium	Temp., °C.	Pressure, atm.	Reference
A	C_2H_4	$MoO_3 \cdot Al_2O_3 \cdot Na$	Benzene	250	65	15
B	C_3H_6	$TiCl_3 \cdot AlEt_2Cl$	n-Heptane	50	1.3	16
C	C_2H_4	$TiCl_4 \cdot AlEt_2Cl$	Petroleum ether	20	1	27
D	C_2H_4–C_3H_6	$VOCl_3 \cdot AlEt_2Cl$	—	—	—	22
E	C_2H_4–C_3H_6	$VOCl_3 \cdot AlEt_2Cl$	—	—	—	22
F	C_2H_4	$TiCl_4 \cdot AlR_3$	Decalin	100	~1.5	18
G	C_2H_4	$SiO_2 \cdot Al_2O_3 \cdot TiO_2 \cdot AlEt_3$	Decalin	60	1	28
H	C_3H_6	$TiCl_3 \cdot AlEt_3$	n-Heptane	70	1.9	29
I	C_2H_4	$(C_5H_5)_2TiCl_2 \cdot AlMe_2Cl$	Toluene	15	1.3	10
J	C_2H_4	$TiCl_4 \cdot Al$	n-Heptane	150	68	30
K	C_2H_4	$TiCl_4 \cdot Al$	n-Heptane	150	49	39
L	C_3H_6	$TiCl_3 \cdot AlEt_2Cl$	Hexane	50	1.8	14

Two experiments in which the rate of polymerization remains constant are illustrated in Figure 1. System A shows a 1-hr. induction period, after which constant activity is observed. These systems correspond to eq. (2). The ethylene polymerization system A has a higher slope and higher rate of polymerization, k_p, than the propylene polymerization system B.

Six experiments in which the rate of polymerization shows mixed order are illustrated in Figures 2 and 3.* In each case the initial linear reaction de-

* *Note added in proof.* After the drafting of this paper, the interesting work of W. E. Smith and Ralph G. Zelmer, *J. Polymer Sci.*, **A1**, 2587 (1963), came to our attention. Smith and Zelmer interpret ethylene polymerization on alkyl-promoted transition-metal catalysts in terms of second-order deactivation. Although derived in a different manner, their eq. (7) is identical to eq. (11) of this paper. However their data presented in their Figure 1 could be fitted as well by the two straight lines—initial and final—required by the mixed-order deactivation as it is by the log time relation expressed in their Figure 6 without the trial-and-error solution for $k_d[C_0^*]$.

creases in activity through a curved zone and finally reaches a new linear rate as expected from eq. (13). Systems C, D, and E (Fig. 2) reach about the same final rate. This relatively low final rate may be related to the
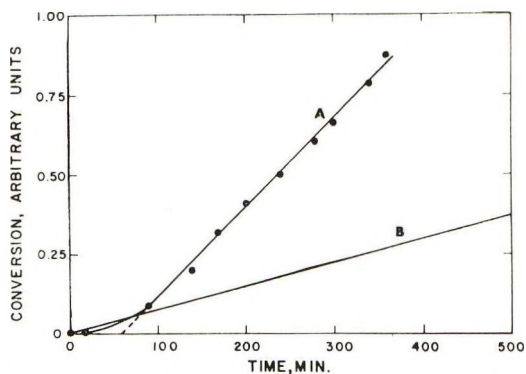

Fig. 1. Polymerization reactions at constant monomer concentration and constant activity applying eq. (2). System A shows a 1-hr. induction period.
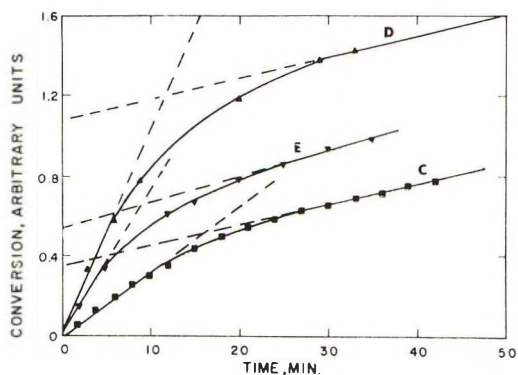

Fig. 2. Reactions at constant monomer concentration applying mixed-order deactivation of catalyst according to eq. (13).
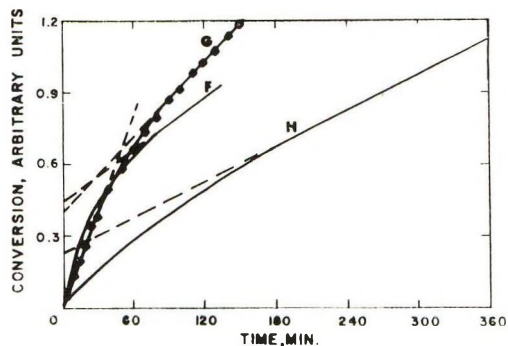

Fig. 3. Reactions at constant monomer concentration applying mixed-order deactivation of catalyst according to eq. (13).
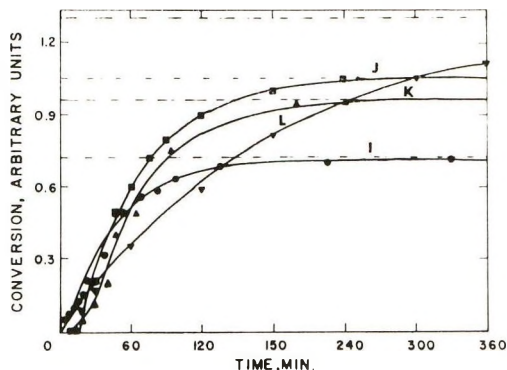
Fig. 4. Reactions at constant monomer concentration applying first-order deactivation according to eq. (7). Systems I, J, and K, show short induction periods. The asymptotes are indicated by dashed lines.
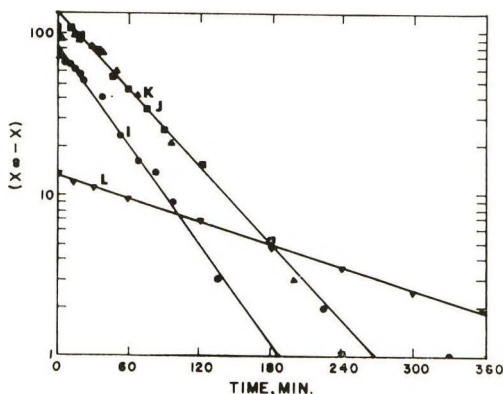

Fig. 5. Reactions at constant monomer concentration applying first-order deactivation according to the logarithmic form of eq. (7).

action of the $AlEt_2Cl$ which was used as the cocatalyst in each of these systems. On the other hand, systems F, G, and H (Fig. 3) reach higher final rates, which may relate to the more active AlR_3 used as cocatalyst in these systems and, further, in these cases, the initially active sites, which become deactivated, are of less importance. The wide variation in intercepts indicates that different numbers of catalytically active sites of varying stability are present. Systems F and G appear similar in activity and in rate of change of activity. System H shows again the lower overall activity associated with a propylene polymerization system.

Four experiments, showing first-order catalyst deactivation, corresponding to eq. (7), are illustrated in Figure 4. Following short induction periods, the initial rapid reaction slows, and finally a limiting conversion X_∞ is reached. When the difference between the actual and limiting conversion is plotted on a logarithmic scale against the time (Fig. 5), a straight line is obtained. The slope of the line is a measure of k_d. Values of k_d estimated
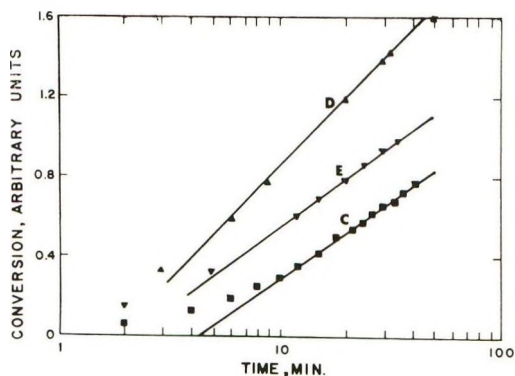
Fig. 6. Reactions at constant monomer concentration applying second-order deactivation according to eq. (11).
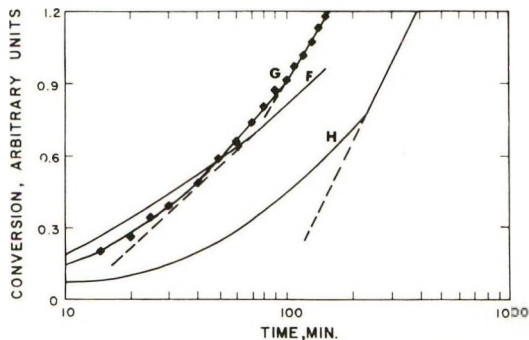

Fig. 7. Reactions at constant monomer concentration applying second-order deactivation according to eq. (11).

for systems I, J, K, and L from Figure 5 are given in Table IV. The value of k_d is about the same for the three systems I, J, and K involving ethylene polymerization on Ti–Al catalysts but is smaller for system L involving propylene. In this case, the usual slower reaction is observed.

It is of interest to compare the fit of various kinetic data to the second-order deactivation eq. (11). The data showing clear-cut zero- or first-order deactivation (systems A, B, I, J, K, and L) give distinctly curved lines when X is plotted versus log time. However, the data showing mixed-order (systems C, D, E, F, G, and H) do not give such a clear-cut distinction. Indeed systems C, D, and E when plotted in this manner (Fig. 6) show reasonably straight lines at higher times, whereas systems F, G and H show distinct curvature (Fig. 7). Second-order deactivation in heterogeneous systems is a process for which it is difficult to find a suitable physical model. The fit of systems C, D, and E may result from the fact that the duration of polymerization studied was relatively short. It may be that had polymerization been carried out for as long as systems F, G, and H, more curvature in the log time plot could have been expected.

TABLE IV
First-Order Decomposition Rates

System	Half-life for decomposition, min.	k_d, min.$^{-1}$
I	30	0.0231
J	35	0.0198
K	35	0.0198
L	130	0.00533

Monomer Concentration Varies

Two kinetic studies suitable for this type of interpretation have been carried out in which the monomer concentration is changing along with catalyst deactivation. The particulars of these systems (both with diene monomers) are given in Table V. To assess the order of monomer uptake,

TABLE V
Polymerization Kinetics with Variable Monomer Concentration

System	Monomer	Catalyst	Reaction medium	Temp., °C.	Pressure, atm.	Reference
M	C_4H_6	$TiCl_4 \cdot AlR_3$	n-Heptane	25	~0.15	21
N	C_5H_8	$TiCl_4 \cdot Al(i\text{-}Bu)_3$	"	10	(1 mole/l.)	19

first-order plots $-\log (1 - X)$ versus time (Fig. 8), and second-order plots $X/(1 - X)$ versus time (Fig. 9), were made. If no catalyst deactivation is occurring, straight lines should be observed according to eqs. (14) or (18), depending on the order of monomer uptake.

It is obvious, however, that the simple kinetics expressed by these equations is not adequate. First-order catalyst deactivation can be eliminated because no asymptote is reached. The possibility of second-order deacti-

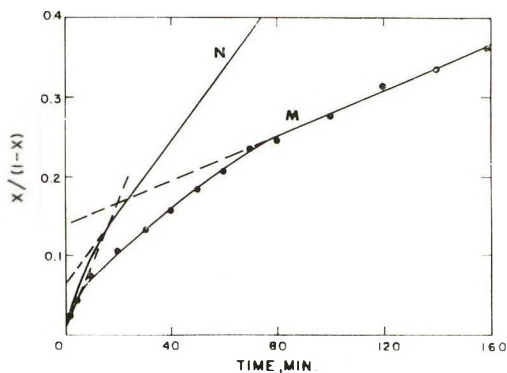Fig. 8. Reactions first-order in monomer applying mixed-order deactivation according to eq. (17).
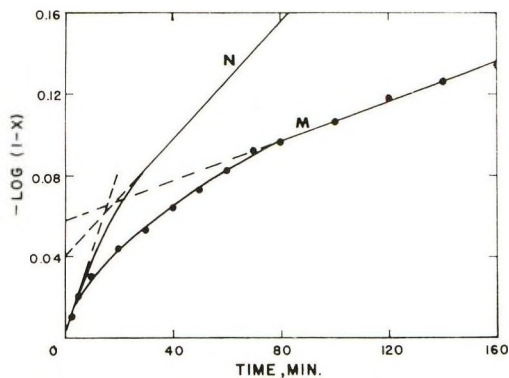
Fig. 9. Reactions second-order in monomer applying mixed-order deactivation according to eq. (21).
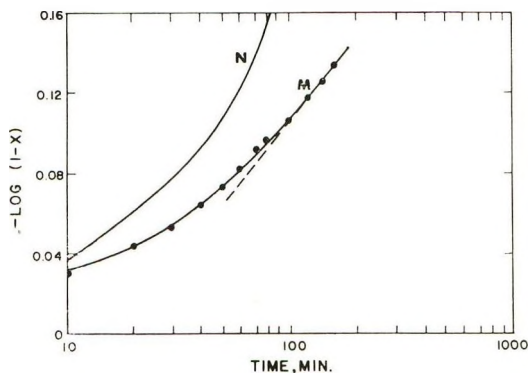

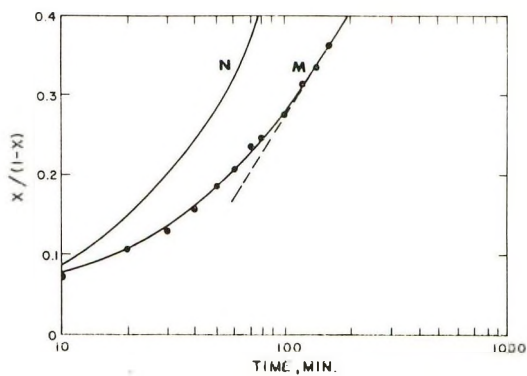Fig. 10. Reactions first-order in monomer applying second-order deactivation according to eq. (16).

Fig. 11. Reactions second-order in monomer applying second-order deactivation according to eq. (20).

vation according to eq. (16) or (20) was tested by making log time plots. In Figure 10, the curvature at higher times indicates that the data do not adequately fit eq. (16) with first-order kinetics with respect to monomer and second-order catalyst deactivation. In Figure 11, eq. (20) with second-order monomer kinetics and second-order catalyst deactivation is not fitted any better.

However, the best interpretation of the data is given by eq. (17) or (21) in terms of a mixed-order deactivation. The initial rapid polymerization (in either Fig. 8 or 9) decays to a slower linear reaction. The choice between the fit to first- or second-order monomer kinetics is difficult. Perhaps the fit is slightly better to eq. (17) for first-order monomer kinetics shown in Figure 8. It is interesting to note that the initial rapid uptake appears to be about the same for both systems M and N and may be related to the fact that the catalyst used in both systems is the same. However, after decay of the unstable catalyst sites, the butadiene system M is somewhat slower than the isoprene system N.

DISCUSSION

Interpretation of rate data in terms of catalyst depletion or active site deactivation allows a simple physical picture for the kinetics of coordinate and heterogeneous catalyzed polymerization. The common form of deactivation is a first-order decay which can be associated with dissociation of a weak chemical bond in the catalyst. The transition metal–carbon bond is just such an easily dissociated bond. In heterogeneous catalysts such organometallic bonds may be in different environments and have different stabilities. This situation leads to mixed-order deactivation reactions.

It is difficult to distinguish experimentally between such mixed-order reactions and higher-order deactivation because the inaccuracies of measuring rates mask the slight differences in the shape of the kinetic curves. At low conversion levels the distinction between the kinetic orders of deactivation is small. Data at high conversions are needed for clear-cut distinctions. These distinctions are even more difficult to determine when monomer concentration is also changing.

Because of these difficulties, rate data for coordinate heterogeneous reactions have often been interpreted in terms of kinetic models taken from homogeneous free-radical catalysis. These models, generally involving second-order termination, are not easily interpreted in terms of heterogeneous catalysts with isolated reactive sites. In order to establish mechanisms of reaction, kinetic data must be interpreted in terms of reasonable chemistry supported by evidence of reaction energetics and normal chemical bonding situations.

The model given here—a system of catalyst sites deactivated by bond breaking—is of interest because it is consistent with kinetic data from a wide variety of sources. It also appears to have physical validity in terms of the ease in breaking transition metal–carbon bonds. However, the data

given here do not eliminate such other explanations for changes in catalyst activity as control by monomer or polymer diffusion, transfer of active center from a site of one activity to a site of another, or accidental introduction of impurities along with the reactants.

The model given here also involves the assumption that the addition of the first monomer unit to the active site has the same rate as the addition of subsequent monomer units. Thus, the initiation step merges with the propagation reaction. Further, the assumption is made that inactivation of growing polymer sites by bond breaking is kinetically equivalent to loss of initiator. These are reasonable assumptions in interpretation of polymerization kinetics but may have an influence on interpretation of molecular weight distributions.

CONCLUSION

In those free radical-catalyzed polymerizations where the termination reactions play a minor role or are relatively constant, study of the depletion of catalyst has led to reasonable interpretation of polymerization rate data to high conversion levels. Similar interpretations of coordinate or heterogeneous catalyzed polymerization can be made in terms of catalyst site deactivation. This type of interpretation is especially useful in these systems because no clear cut kinetic termination reactions of importance are known besides the "killing" of sites by impurities. The value of such interpretations can be seen in the large number of systems of various monomers and catalysts that can be reasonably explained.

The catalyst deactivation model needs to be checked by careful measurement of a favorable system from which the rate constants can be accurately determined. Through studies at various initiator and monomer concentrations levels, rate constants for propagation and catalyst deactivation can be measured. By study of the influence of temperature on the deactivation process, the energies of activation of the propagation and deactivation processes can be separated. The ability of the model to predict polymer molecular weight and molecular weight distribution also needs to be checked.

References

1. Tobolsky, A. V., *J. Am. Chem. Soc.*, **80**, 5927 (1958).

2. Tromsdorff, E., H. Kohle, and P. Lagally, *Makromol. Chem.*, **1**, 169 (1948); R. G. W. Norrish and R. R. Smith, *Nature*, **150**, 336 (1942).

3. Tobolsky, A. V., C. E. Rogers, and R. D. Brickman. *J. Am. Chem. Soc.*, **82**, 1277 (1960).

4. Friedlander, H. N., *J. Polymer Sci.*, **58**, 455 (1962).

5. O'Driscoll, K. F., and S. McArdle, *J. Polymer Sci.*, **40**, 557 (1959); K. F. O'Driscoll and J. Schmidt, *J. Polymer Sci.*, **45**, 189 (1960).

6. Pavlov, B. V., and G. V. Korolev, *Vysokomol. Soedin.*, **1**, 869 (1959); *Polymer Sci. USSR*, **1**, 295 (1960).

7. O'Driscoll. K. F., *J. Polymer Sci.*, **61**, 84 (1962).

8. Welch, F. J., *J. Polymer Sci.*, **61**, 243 (1962).

9. Lyubetskiĭ, S. G., and V. V. Mazurek, *Vysokomol. Soedin.*, **4**, 1027 (1962).

10. Chien, J. C. W., *J. Am. Chem. Soc.*, **81**, 86 (1959).

11. Stepovik, L. P., A. K. Shilova, and A. E. Shilov, *Dokl. Akad. Nauk S.S.S.R.*, **148**, 122 (1963).

12. Feldman, C. F., and E. Perry, *J. Polymer Sci.*, **46**, 217 (1960).

13. Bier, G., W. Hoffmann, G. Lehmann, and G. Seydel, *Makromol. Chem.*, **58**, 1 (1962).

14. Kohn, E., H. J. L. Schuurmans, J. V. Cavender, and R. A. Mendelson, *J. Polymer Sci.*, **58**, 681 (1962).

15. Friedlander, H. N., *J. Polymer Sci.*, **38**, 91 (1959).

16. Chien, J. C. W., *J. Polymer Sci.*, **A1**, 425 (1963).

17. Natta, G., I. Pasquon, and E. Giachetti, *Angew. Chem.*, **69**, 213 (1957); *Makromol. Chem.*, **24**, 258 (1957).

18. Ludlum, D. B., A. W. Anderson, and C. E. Ashby, *J. Am. Chem. Soc.*, **80**, 1380 (1958).

19. Saltman, W. M., W. E. Gibbs, and J. Lal, *J. Am. Chem. Soc.*, **80**, 5615 (1958); *J. Polymer Sci.*, **46**, 375 (1960).

20. Gilchrist, A., *J. Polymer Sci.*, **34**, 49 (1959).

21. Gaylord, N. G., T.-K. Kwei, and H. F. Mark, *J. Polymer Sci.*, **42**, 417 (1960).

22. Bier, G., *Angew. Chem.*, **73**, 186 (1961).

23. Bier, G., A. Gumboldt, and G. Schleitzer, *Makromol. Chem.*, **58**, 43 (1962).

24. Bier, G., A. Gumboldt, and G. Lehman, *Plastics Inst. (London) Trans. J.*, **28**, 98 (1960).

25. Junghanns, E., A. Gumboldt, and G. Bier, *Makromol. Chem.*, **58**, 18 (1962).

26. Boor, J., Jr., *J. Polymer Sci.*, **C1**, 257 (1963).

27. Simon, A., and G. Ghymes, *J. Polymer Sci.*, **53**, 327 (1961).

28. Furukawa, J., T. Saegusa, T. Tsuruta, S. Anzai, T. Narumiya, and A. Kawasaki, *Makromol. Chem.*, **41**, 17 (1960).

29. Natta, G., I. Pasquon, and E. Giachetti, *Chim. Ind. (Milan)*, **39**, 1002 (1957).

30. Fukui, K., T. Shimidzu, T. Yagi, S. Fukumoto, T. Kagiya, and S. Yuasa, *J. Polymer Sci.*, **55**, 321 (1961).

Résumé

Des modèles cinétiques basés sur la dépendance vis-à-vis du temps de la désactivation des sites catalyseurs ont été appliqués aux cinétiques qu'on trouve dans la littérature sur la polymérisation de différentes oléfines avec une série de catalyseurs de coördination ou ionique hétérogènes et homogènes et pour une variété de conditions de polymérisations. Pour la polymérisation purement coordinative où la terminaison ne joue pas un grand rôle, la propagation joue un rôle important et est influencée par le nombre des centres catalytiques actifs. Le nombre de centres actifs reste constant dans certains catalyseurs mais varie dans la plupart. La désactivation de premier ordre des centres catalytiques donne lieu à une cinétique de polymère à groupes terminaux inertes, semblable à celle décrite par Tobolsky pour la polymérisation par radical libre avec épuisement du catalyseur par décomposition de premier ordre. La désactivation de deuxième ordre donne lieu à une cinétique linéaire par rapport au logarithme du temps. Pour la polymérisation hétérogène, il est difficile de trouver un modèle physique pour l'interaction de centres actifs isolés, nécessaire pour la désactivation d'un ordre plus élevé. On peut également très bien interpréter les données expérimentales en utilisant un modèle d'ordre mélangé en supposant que les centres actifs de différentes stabilités subissent une désactivation de premier ordre. Pour de faibles conversions, il est difficile de faire concorder les modèles avec les données expérimentales dans lesquelles on fait varier la concentration du monomère. Il faut encore d'autres expériences pour tester les modèles, pour obtenir des valeurs exactes des constantes de vitesse, et pour déterminer l'influence de la désactivation du catalyseur sur le poids moléculaire et sur la distribution du poids moléculaire.

Zusammenfassung

Ein auf der Zeitabhängigkeit der Desaktivierung der katalytischen Stellen beruhendes kinetisches Modell wurde reaktionskinetischen Literaturangaben für die Polymerisation verschiedener Olefine mit einer Reihe von ionischen und Koordinationskatalysatoren (sowohl homogen als auch heterogen) für eine Reihe von Polymerisationsbedingungen zugrunde gelegt. In reinen Koordinationspolymerisationssystemen, wo die Abbruchsreaktion unwesentlich ist, spielt die Wachstumsreaktion eine Hauptrolle und wird von der Zahl der aktiven Katalysatorstellen beeinflusst. Die Anzahl der Stellen bleibt bei manchen Katalysatoren konstant, variiert jedoch bei den meisten. Desaktivierung erster Ordnung der Katalysatorstellen führt zu einer Deadendkinetik ähnlich wie sie von Tobolsky für die radikalische Polymerisation mit Katalysatorverbrauch durch eine Zersetzung erster Art beschrieben wurde. Desaktivierung nach zweiter Ordnung führt zu einer im Logarithmus der Zeit linearen Kinetik. Bei heterogener Polymerisation ist es schwierig, ein physikalisches Modell für die Wechselwirkung der isolierten Stellen zu finden, wie es Desaktivierung höherer Ordnung benötigt. Die experimentellen Daten werden gleich gut durch ein Modell gemischter Ordnung unter der Annahme von Stellen verschiedener Stabilität mit Desaktivierung erster Ordnung wiedergegeben. Bei niedrigem Umsatz können die Modelle nur schwer den experimentellen Daten bei variierter Monomerkonzentration angepasst werden. Weitere Versuche müssen ausgeführt werden, um diese Modelle zu überprüfen, um genaue Werte der Geschwindigkeitskonstanten zu erhalten und um den Einfluss der Katalysatordesaktivierung auf Molekargewicht und Molekulargewichtsverteilung zu bestimmen.

# Polymerization of the Carbon–Nitrogen Double Bond in Carbodiimides

G. C. ROBINSON, *Ethyl Corporation, Baton Rouge, Louisiana*

Synopsis

Polymerization of one of the carbon-nitrogen double bonds in carbodiimides has been effected with *n*-butyllithium catalyst in hydrocarbon solvents at 25°C. Monomers converted to polymer include diethylcarbodiimide, di-*n*-butylcarbodiimide, di-*n*-hexylcarbodiimide, diphenylcarbodiimide, diallylcarbodiimide, and methylisopropylcarbodiimide. Monomers which failed to polymerize were dicyclohexylcarbodiimide, diisopropylcarbodiimide, and methyl-*tert*-butylcarbodiimide. Thermal polymerization and depolymerization of diethylcarbodiimide was investigated and the polymers were characterized. Polymers with an inherent viscosity of 0.1–0.4 (formic acid solvent) were obtained in this work. The steric limitations on the nature of the substituents at the backbone nitrogen and the pendant nitrogen of the polymer chain were elucidated. The *cis–trans* isomerism possible at the pendant nitrogen is discussed. The failure of a solution of polydiethylcarbodiimide in aqueous acetic acid (presumably a polyelectrolyte) to behave on dilution as a polyelectrolyte is tentatively attributed to the stiff polymer backbone. Depolymerization of these polymers appears to be an unzipping.

INTRODUCTION

In 1959 Shashoua disclosed that isocyanates could be polymerized to 1-nylons by a variety of anionic catalysts at low temperatures.[1] This was the first unequivocal demonstration of the polymerization of the carbon–nitrogen double bond. We wish to report success in the polymerization of the carbon–nitrogen double bond in carbodiimides. Carbodiimides contain only carbon, hydrogen, and nitrogen, and have the structure:

$$R_1—N=C=N—R_2$$
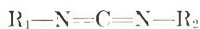
Carbodiimides can be easily synthesized in a variety of ways from the corresponding amines. They are probably optically active but have not yet been resolved.[2] Trimers, dimers, and "polymers" of these reactive substances have been frequently reported. The polymers, however, have never been characterized.

In the experimental section are described the preparation and purities of the carbodiimide monomers for which polymerization has been studied. This section also describes the polymerization technique found most useful, as well as experiments on the thermal polymerization and depolymerization of diethylcarbodiimide.

EXPERIMENTAL

Thioureas

The symmetrical N,N'-disubstituted thioureas were commercial materials or were prepared from the corresponding amine and carbon disulfide by the method of Zetzsche and Friedrich.[3] The unsymmetrical thioureas, 1-methyl-3-isopropylthiourea and 1-methyl-3-*tert*-butylthiourea, were prepared from methylisothiocyanate and the corresponding amine in toluene solution.

Carbodiimide Synthesis

Several of the procedures described for preparation of carbodiimides from mercuric oxide and the corresponding thiourea were tested. The general procedure of Sheehan[4] was adopted as most convenient. Preparation of diethylcarbodiimide is described in detail to illustrate the procedure actually used.

Into a 500-ml. three-necked flask fitted with a paddle stirrer, a water condenser, and a stopper were put 52.8 g. (0.40 mole) of diethylthiourea and 200 ml. of acetone. The mixture was heated to reflux and 43.4 g. (0.2 mole) of yellow mercuric oxide was added four times during a 3-hr. period. The solids were then separated by filtration through a medium porosity glass filter and washed thoroughly with ether. The combined filtrate and washings were diluted with water and the organic layer was repeatedly washed with water. The organic phase was separated and dried over sodium sulfate. Ether was removed through a Vigreux column by heating in a water bath. The product was distilled through a five-tray Oldershaw column at 44–46°C./35 mm. and weighed 22.5 g. (55%).

The carbodiimides made in this way were of variable purity. The purity of the crude product was established by vapor-phase chromatography (VPC) on a silicone column, 155°C., 60 cc./min. He. Where required, the monomers were purified by distillation through a spinning band column. The monomer properties are summarized in Table I.

TABLE I
Properties of Carbodiimide Monomers

Carbodiimide monomer	Boiling point, °C.	Pressure, mm. Hg	Purity, % (by VPC)
Diethyl	44–46	35	96
Diisopropyl	80	72	99
Diallyl	80.5–81[a]	35	—
Di-n-butyl	76	5.5[b]	99
Di-n-hexyl	89–90	0.55	96
Diphenyl	78–82[c]	0.03	—
Methylisopropyl	54	72	99
Methyl-*tert*-butyl	59	72	98

[a] Reported[6] b.p. 58–59°C./10 mm.

[b] Pressure not reliable.

[c] M.p. 9°C.; reported[6] b.p. 163–165°C./11 mm.

Catalyzed Polymerization

Catalyzed polymerizations were conducted in Erlenmeyer flasks of 10, 25, or 50 ml. capacity, depending on the scale of the experiment. The flask was heated to remove adsorbed water, capped with a rubber serum cap, and flushed with dry nitrogen through hypodermic needles. Weighed amounts of solvent and monomer were injected into the flask, followed by the desired volume of a $2.3M$ solution of n-butyllithium in n-hexane (Foote Mineral Co.). Successful polymerizations evolved heat, and usually a visible separation of polymer was noted. The feasibility of effecting the catalyzed polymerization in a solvent afforded a convenient means of controlling the heat evolution. On completion of polymerization, methanol dilution destroyed the catalyst and served to precipitate the polymer. The polymer was separated by filtration, thoroughly washed with methanol, dried, and weighed. Representative analytical data on the polymers are given in Table II.

TABLE II
Polymer Analyses

Polymeric carbodiimide	Calculated			Found		
	C, %	H, %	N, %	C, %	H, %	N, %
Diethyl	61.18	10.27	28.55	60.67, 60.84	10.36, 10.36	27.2
Di-n-butyl	70.07	11.76	18.17	70.08, 70.28	11.75, 11.75	17.7
Diphenyl	80.38	5.19	14.43	80.34, 80.20	5.76, 5.54	—
Methylisopropyl	61.18	10.27	28.55	—	—	28.1

Depolymerization of Polydiethylcarbodiimide

A sample of polydiethylcarbodiimide was heated in a 10-ml. distilling flask at 150–175°C./30 mm. The pyrolyzate was compared with the original monomer by vapor-phase chromatography on an Apiezon L column. The original monomer was 96% pure with two impurity peaks. The pyrolyzate showed the same impurities but the degree of purity was 99%.

Thermal Polymerization of Diethylcarbodiimide

A 6.5-g. sample of diethylcarbodiimide was heated in a sealed ampule at 100°C. for 8 hrs. Solid polymer occupied about 5% of the liquid volume. The tube was then heated at 150°C. for 8 hr. Under these conditions no liquid was visible in the tube after heating, but filtration showed the presence of 1 g. of polymer and 5 g. of monomer. The recovered monomer was heated at 115–125°C. for 30 hr. These conditions gave 50% conversion to polymer.

RESULTS AND CONCLUSIONS

Catalyst Screening

Various potential catalysts were screened for their ability to polymerize diphenylcarbodiimide, diethylcarbodiimide, and dicyclohexylcarbodiimide. The conditions tested are given in Table III. The inability to effect poly-

TABLE III
Catalyst Screening Results

Monomer	Solvent	Catalyst	Solvent/ monomer volume ratio	Monomer/ catalyst mole ratio	Temp., °C.	Polymer
$(C_6H_5N)_2C$	DMF	Na/DMF[a]	6	—	−40	No
$(C_6H_5N)_2C$	DMF	Na/DMF	8	—	−20	No
$(C_6H_{11}N)_2C$	Xylene	n-BuLi	6	15	−40	No
$(C_6H_{11}N)_2C$	DMF	n-BuLi	10	19	25	No
$(C_6H_{11}N)_2C$	Xylene	CH_3I	1.7	11	25	No
$(C_6H_{11}N)_2C$	Toluene	$AlBr_3$	20	100	−80	No
$(C_2H_5N)_2C$	DMF	Na/DMF	6	—	25	No
$(C_2H_5N)_2C$	Toluene	$AlBr_3$	12	400	25	Trace
$(C_2H_5N)_2C$	Toluene	$AlBr_3$	12	136	25	No
$(C_2H_5N)_2C$	Toluene	Brosyl Cl	12	52	25	No
$(C_2H_5N)_2C$	Toluene	n-BuLi	10	14	25	Yes
$(C_2H_5N)_2C$	Toluene	n-BuLi	10	43	0	Yes[b]
$(C_2H_5N)_2C$	Toluene	n-BuLi	10	43	25	Yes
$(C_2H_5N)_2C$	Toluene	n-BuLi	2	144	25	Yes
$(C_2H_5N)_2C$	Toluene	n-BuLi	1	270	0	Yes
$(C_2H_5N)_2C$	Toluene	n-BuLi	12	33	25	Yes
$(C_2H_5N)_2C$	None	Heat	—	—	120	Yes

[a] Cf. Shashoua.[1]

[b] Polymer separation after 2 hr.

merization of dicyclohexylcarbodiimide is ascribed to properties of the monomer rather than the catalysts, as discussed later.

Initial experiments used the sodium dispersion–dimethylformamide (DMF) catalyst of Shashoua. This catalyst failed to polymerize diphenyl or diethylcarbodiimide. The activity of the catalyst was proven by successful polymerization of phenyl isocyanate. The Lewis acid catalyst, anhydrous aluminum bromide, was also tested. This material failed to give polymer, with the possible exception of one experiment with diethylcarbodiimide where a trace of very impure polymer was obtained. It was considered that p-bromobenzenesulfonyl chloride (brosyl Cl) might serve as a mild cationic catalyst by converting the carbodiimide to a salt:

$$p\text{-}BrC_6H_4SO_2Cl + R-N=C=N-R \rightarrow p\text{-}BrC_6H_4SO_2-\overset{\overset{\displaystyle R}{|}}{N}-\overset{\oplus}{C}=N-R + Cl^\ominus$$

This salt was expected to serve as a cationic catalyst, but no polymer was obtained.

The use of n-butyllithium as catalyst proved successful. No crucial solvent/monomer or monomer/catalyst ratio was found for this catalyst. The rate of polymerization was a strong function of temperature. Conditions which gave instant polymerization at 25°C. required 2 hr. at 0°C. The polymerization conditions described are not general to all carbon–nitrogen double bonds since benzalaniline did not polymerize on treatment with n-butyllithium.

During this work the solid polymers formed in diethylcarbodiimide on

standing were investigated and found to be true polymers. For diethyl-carbodiimide a temperature of 120°C. was sufficient for substantial conversion to polymer in a short time.

Scope

Application of the n-butyllithium catalyst to a variety of carbodiimides was tested. The successful polymerizations are summarized in Table IV. From the examples studied it is clear that all di-n-alkylcarbodiimides can probably be polymerized. Examples are available from ethyl to n-hexyl. Aromatic carbodiimides should also be easily polymerized since diphenyl-carbodiimide polymerizes. Diallycarbodiimide polymerizes readily.

TABLE IV
Representative Polymerization Runs
(n-BuLi Catalyst, 25°C.)

Carbodiimide	Monomer wt., g.	Solvent	Solvent volume, ml.	Monomer/ catalyst, molar ratio	η_{inh}[a]	Polymer yield, %
Diethyl[b]	4.4	Toluene	5	270	0.41	37
Diethyl	0.85	Toluene	12	33	0.20	62
Diethyl[c]	—	—	—	—	0.22	—
Diphenyl	1	Toluene	5	17	0.11	60
Diallyl	1.05	Toluene	5	37	0.13	92
Di-n-butyl	1.70	n-Heptane	5	15	0.15	96
Di-n-hexyl	1.71	n-Heptane	5	15	0.12[d]	90
Methylisopropyl	1.7	n-Heptane	5	38	0.14	95

[a] Viscosities in formic acid at 30.0°C.

[b] Polymerization initiated at 25°C., conducted at 0°C.

[c] Thermal polymerization.

[d] $\eta_{inh} = 0.098$ in n-heptane.

Difficulties, probably of steric origin, appear with secondary alkyl groups. Neither dicyclohexylcarbodiimide nor diisopropylcarbodiimide will polymerize under the standard conditions. It will be noted that methyliso-propylcarbodiimide does polymerize. This shows that one secondary alkyl group will not necessarily prevent polymerization. On the other hand, methyl-*tert*-butylcarbodiimide failed to polymerize, indicating that tertiary alkyl groups are incompatible with polymer formation.

Properties

These polymers are all of relatively low molecular weight (η_{inh} 0.1–0.4) by viscosity measurements (see Table IV). Therefore, determination of crystallinity and similar properties useful in characterizing high polymers was not judged worthwhile. The polymers were snow-white solids except for the diallylcarbodiimide polymer, which was faintly yellow. The melting or decomposition points and solubilities are given in Table V. From the solubility data it is clear that these polymers are moderately strong

TABLE V

Polymer Properties

Carbodiimide	Melting point, °C.	Soluble in
Diethyl	164–168[a]	Formic acid, aqueous acids
Diallyl	163–180[b]	Formic acid
Di-n-butyl	132–140	Formic acid
Di-n-hexyl	130–147	Formic acid, n-heptane
Diphenyl	153–180	Formic acid
Methylisopropyl	184–188[a]	Formic acid

[a] Depolymerizes.

[b] Polymer a faint yellow, giving a red melt.

bases. This would be expected since the monomeric unit is an amidine. The polydiethylcarbodiimide can be dissolved in aqueous hydrochloric acid and precipitated with sodium hydroxide. The recovered polymer gives the same carbon/hydrogen analysis as the original polymer.

On treatment of poly(diethylcarbodiimide) with hot acetic anhydride no obvious change occurred, and the inherent viscosity was not changed. However, the depolymerization temperature increased to 215–225°C., suggesting protection of reactive chain ends by acetyl groups.

A study was made of the variation of the specific viscosity of a sample of polydiethylcarbodiimide with concentration in aqueous acetic acid.* A plot of η_{sp}/c versus c (range of c was 0.2–4.0 g./100 cc.) was essentially linear. This linearity was somewhat surprising since polyelectrolytes normally show a pronounced upward trend at low concentrations on such a plot.[7] The absence of this trend in carbodiimide polymers may, perhaps, be due to a relatively stiff polymer backbone.

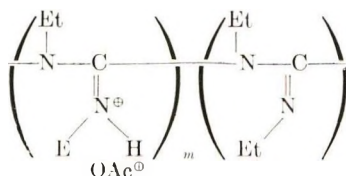## Polymer Structure

The polymer structure is presumed to be:
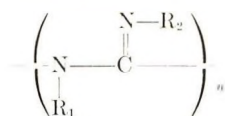
This is the simplest way in which the monomer can polymerize, and the structure is supported by infrared data. The infrared spectrum of the

* The species dissolved in aqueous acetic acid is presumably a polyelectrolyte having the structure:

polymers shows a carbon–nitrogen double bond stretch at 1640 ± 10 cm.$^{-1}$ and a doublet due to the nitrogen in the polymer backbone near 1360 and 1250 cm.$^{-1}$

In polymethylisopropylcarbodiimide it is uncertain *a priori* whether the isopropyl group is found only on the backbone nitrogen, only on the pendant nitrogen, or is randomly at both. Since diisopropylcarbodiimide and methyl-*tert*-butylcarbodiimide fail to polymerize, there must be some steric resistance to polymerization. One would guess then that the more demanding isopropyl group would be bonded to the pendant nitrogen rather than on the backbone of the chain. It is significant that Shashoua and coworkers were unable to make isopropyl 1-nylon. The presence of a methyl–nitrogen stretch bond at 1067 cm.$^{-1}$ is consistent with the methyl group being bonded to the backbone nitrogen.

It is of theoretical interest that these polymers may show *cis–trans* isomerism at the pendant nitrogen atom. Adjacent monomeric units may conceivably be *trans-trans* or *trans-cis*.

The structure of the polymer can be all *trans-trans*, all *trans-cis*, or a random mixture. No evidence bearing on this point is available except that the failure of methyl-*tert*-butylcarbodiimide to polymerize indicates that substituents at the pendant nitrogen are subject to some steric restraints. This would indicate that a *trans-cis* relationship is unlikely except for very small substituents.

Thermal Polymerization and Depolymerization

The way in which thermal polymerization of carbodiimides is initiated is not known. It is clear, however, from the work done with diethylcarbodiimide that the initiation step is of high activation energy. Polymerization is slow at 25°C. and even at 100°C. only about 1% of a sample of diethylcarbodiimide was converted to polymer during 8 hr. Heating at 115–125°C. for 30 hr. did give 50% conversion to polymer. At 150°C. polymerization was less complete, reflecting possibly a competition between depolymerization and polymerization. It was observed that at 30 mm. and 150°C. depolymerization proceeded at an appreciable rate. The polymer is rapidly depolymerized at 164°C.

The depolymerization appears to be an unzipping, since no molecular fragments other than monomer were detected in the pyrolyzate from polydiethylcarbodiimide and pyrolysis was complete. The facile polymerization and depolymerization of this monomer offers a convenient way to purify and store monomer for future use.

References

1. Shashoua, V. E., *J. Am. Chem. Soc.*, **81**, 3156 (1959); V. E. Shashoua, W. Sweeny, and R. F. Tietz, *J. Am. Chem. Soc.*, **82**, 866 (1960).

2. Khorana, H. G., *Chem. Revs.*, **53**, 145 (1953).

3. Zetzsche, F., and A. Friedrich, *Ber.*, **73**, 1114 (1940).

4. Sheehan, J. C., and V. V. Hlavka, *J. Org. Chem.*, **21**, 439 (1956).

5. Schmidt, E., F. Hitzler, and E. Lahde, *Ber.*, **71**, 1933 (1938).

6. Hunig, S., H. Lehmann, and G. Grimmer, *Ann.*, **579**, 77 (1953).

7. Schaefgen, J. R., and C. F. Trivisonno, *J. Am. Chem. Soc.*, **73**, 4580 (1951).

Résumé

La polymérisation d'une des double liaisons carbone-azote dans les carbodiimides a été effectuée à 25°C dans des solvants hydrocarbonés avec le *n*-butyllithium comme catalyseur. Les monomères transformés en polymere comprennent la diéthylcarbodiimide, la di-*n*-butylcarbodiimide, la di-*n*-hexylcarbodiimide, la diphénylcarbodiimide, la diallylcarbodiimide et la méthylisopropylcarbodiimide. Les monomères qui ne peuvent pas polymériser sont la dicyclohexylcarbodiimide, la diisopropylcarbodiimide, et la méthyl-*tert*-butylcarbodiimide. On a étudié la polymérisation thermique et la dépolymérisation de la diéthylcarbodiimide et les polymères obtenus ont été caractérisés. Des polymères possédant une viscosité de 0.1 a 0.4 (solvant acide formique) ont été obtenus dans ce travail. Les empêchements stériques à la nature des substituants sur l'azote de la chaîne principale et sur l'azote des ramifications de la chaîne polymérique ont été élucidés. On discute de l'isomérisme *cis-trans* possible à l'azote des ramifications. Le fait qu'une solution de poly(diéthylcarbodiimide) dans l'acide acétique aqueux (vraisemblablement un polyélectrolyte) ne se comporte pas par dilution comme un polyélectrolyte, est attribué à la rigidité de la chaîne polymérique principale. La dépolymérisation de ces polymères semble se faire par un procédé de proche en proche.

Zusammenfassung

Die Polymerisation einer der Kohlen-Stickstoffdoppelbindungen in Carbodiimiden wurde mit Hilfe eines *n*-Butyllithiumkatalysators in Kohlenwasserstofflösung bei 25°C bewirkt. Zu den in Polymere umgewandelten Monomeren gehören Diäthylcarbodiimid, Di-*n*-butylcarbodiimid, Di-*n*-hexylcarbodiimid, Diphenylcarbodiimid, Diallylcarbodiimid und Methylisopropylcarbodiimid. Nicht polymerisierbare Monomere waren Dicyclohexylcarbodiimid, Diisopropylcarbodiimid und Methyl-*tert*-butylcarbodiimid. Thermische Polymerisation und Depolymerisation von Diäthylcarbodiimid wurde untersucht, und die Polymeren wurden charakterisiert. Bei diesen Versuchen wurden Polymeren mit einer Viscositätszahl von 0,1 bis 0,4 (Ameisensaure als Lösungsmittel) erhalten. Die sterischen Grenzen in bezug auf die Natur der Substituenten des Hauptkettenstickstoffs und des Seitenkettenstickstoffs wurden untersucht. Die beim Seitenkettenstickstoff mögliche *Cis-Trans*isomerie wird diskutiert. Der Umstand, dass sich eine Lösung von Polydiäthylcarbodiimid in wässriger Essigsäure (wahrscheinlich ein Polyelektrolyt) bei der Verdünnung nicht wie ein Polyelektrolyt verhält, wird versuchsweise der steifen Polymerhauptkette zugeschrieben. Depolymerisation dieser Polymere scheint einem Zippmechanismus zu gehorchen.

Homopolymerization of N-Allylacetamide and N-Allylstearamide*

EDMUND F. JORDAN, JR., and ARTHUR N. WRIGLEY, *Eastern Regional Research Laboratory, Eastern Utilization Research and Development Division, Agricultural Research Service, U. S. Department of Agriculture, Philadelphia, Pennsylvania*

Synopsis

When benzoyl peroxide was decomposed at 90°C. in N-allylacetamide and in N-allyl-stearamide, $d[M]/d[P]$ was about 2 and $\overline{DP}$ was between 9 and 10, because of a wastage of benzoyloxy radicals. These radicals formed benzoic acid and benzene as a consequence of hydrogen abstraction from the amide, and the resulting amide radicals became substituted with ester and phenyl groups from the initiator. N-butylstearamide, a saturated model for N-allylstearamide, gave corresponding products. Rates of peroxide decomposition indicated strong induced effects, decreasing in the order: N-allylacetamide, N-allylstearamide, N-butylstearamide. Slopes of the linear plots of the four products (in moles per kilogram) against initiator (in equivalents per kilogram) in the three amides in the above order were: benzoic 0.521, 0.570, 0.575; benzene 0.027, 0.086, 0.168; amide substituted by benzoate 0.459, 0.320, 0.106; amide substituted by phenyl 0.087, 0.087, 0.142. Transfer, compared to substitution, increased with chain length and decrease in unsaturation, and induced peroxide decomposition was correspondingly lowered. Thus, kinetic chain decreased with acyl chain length and decrease in unsaturation. A mechanism that postulates polar species in the transition state when amides were solvents accounted for both transfer and aromatic substitution and helped explain the difference in behavior of N-allylamides and allyl esters. Plots of amide entering polymer (in moles per kilogram) against initiator concentration (in equivalents per kilogram) were curves; plots of log $(a - x)$ for amide disappearance against the same coordinate were linear. Slopes were: N-allylacetamide -0.0742; N-allylstearamide -0.1771.

Although the homopolymerization of allyl esters has been extensively studied,[1] few publications have described that of N-allylamides. The information available[2] suggested that N-allylamides were unpolymerizable, although polymers of unspecified conversion have been prepared from methallylamides.[2,3] Diallyl cyanamide[4,5] and certain allyl phosphonamides[6] failed to homopolymerize, suggesting that a nitrogen atom, existing in certain relationships to allylic functionality, might be rate-retarding. The possibility also existed that N-allylamides might resemble the difficultly polymerizable allyl bromide[7] and allyl alcohol,[7–10] the latter found to polymerize only when very large amounts of initiator were used.[8–10] However,

even the most difficultly polymerizable allylic monomers,[1,4,11-23] including
N-allylamides,[24-26] have been copolymerized readily with many vinyl mono-
mers.   This suggested that N-allylamides could also be homopolymerized
if proper initiator concentrations were used.

A large consumption of initiator is one of the characteristics of the poly-
merization of allyl monomers.[1,7,27-36]   In accordance with the mechanism
of degradative chain transfer, the ratio of the rate of propagation to the rate
of allylic hydrogen transfer is low (14–25 for allyl acetate[27,32]), and this
effects a corresponding reduction in $d[\text{M}]/d[\text{P}]$ (14–50 for allyl acetate[27,32])
compared with normal vinyl polymerization. Preliminary experiments
showed that the polymerization behavior of N-allylamides differed from
that of most allyl esters in one important respect.   Massive amounts of
benzoyl peroxide had to be used to effect appreciable polymerization ($d[\text{M}]/$
$d[\text{P}]$ ca. 2), even though the molecular weights of the polymers were similar
to those found for many allyl esters ($\overline{\text{DP}}$ ca. 10^{31}), which suggested that
chain termination was still degradative.   It could therefore be concluded
that a considerable wastage of benzoyloxy radicals must have occurred to
form low molecular weight reaction products.

This investigation was undertaken primarily to determine the path of
attack on N-allylamides by the radicals formed as a result of the thermal
fission of the peroxide.   N-Allylacetamide and N-allylstearamide were
selected as homolog extremes, and the saturated N-butylstearamide was
chosen as an approximate model for the long-chain N-allylamide. Benzoyl
peroxide, the initiator most extensively investigated in allyl ester polymeri-
zation, was used in this study.   Since long-chain amides melt at about
85°C., the polymerizations were carried out at 90°C. Emphasis was
placed on the quantitative determination of the products of peroxide de-
composition, while kinetic studies were used to support the analytical
evidence obtained.   The results obtained for N-allylamides were compared
with those reported for allyl acetate and other allyl esters, and a mecha-
nism was proposed rationalizing the differences observed.

PROCEDURE

Benzoyl peroxide was decomposed in small portions in the amide, main-
tained in a closed system at 90°C. under nitrogen for at least two lifetimes
of the peroxide; the volatiles were trapped and the other reaction products
determined by chemical means.   The volatiles consisted of benzene (ob-
tained uncontaminated in a cold trap and identified by infrared spectrum)
and carbon dioxide, determined gravimetrically on ascarite.   The balance
of the reaction mixture consisted of essentially five products: (1) benzoic
acid, determined by acid number and, after semiquantitative isolation,
identified by a mixed melting point; (2) a benzoate ester of the amide, de-
termined by ester number and identified in the infrared; (3) a nonpolymeric
phenyl derivative of the amide; (4) polymer, determined by decrease in
total unsaturation; and (5) unreacted amide.   The amount of the phenyl
derivative was determined indirectly as the difference between benzene and

carbon dioxide found, since both phenyl substitution and benzene formation are accompanied by the evolution of a mole of carbon dioxide from a benzoyloxy radical. Volatile, nonacidic, purely aromatic compounds, such as phenyl benzoate and diphenyl, usually found when benzoyl peroxide is decomposed in solvents,[35,37] were not found in any of the reaction products by gas-liquid chromatography. Thus, all aryl substitution was considered to be on the amide substrate. The foregoing analyses were independently verified by column chromatography of selected crude reaction products of two of the amides studied, *N*-allylstearamide and *N*-butylstearamide. By this means isolation of the pure phenyl and aryl substitution products was sought and fractionation of poly-*N*-allylstearamide attempted. Kinetic studies were used to indicate the relative rate enhancement, caused by any induced decomposition reaction, over normal rates of benzoyl peroxide decomposition in "slow" solvents.[37]

RESULTS AND DISCUSSION

Composition, Kinetics, and Reaction Path

The crude reaction product compositions of the three amides studied are listed in Table I, and the overall results are plotted in Figures 1–3. The most striking feature of these results is the unusually large proportion of benzoic acid and of nonpolymeric substitution products relative to polymer formed. $\overline{DP}$ values of about 10 for the polymer, together with the extremely low $d[\mathrm{M}]/d[\mathrm{P}]$ ratio of about 2, indicate that much of the peroxide must have formed nonpolymeric substitution products. The proportion of products varied with the amide "solvent" employed. For any given amide, formation of each nonpolymeric compound was a linear function of the benzoyl peroxide concentration. Polymer formation decreased with in-
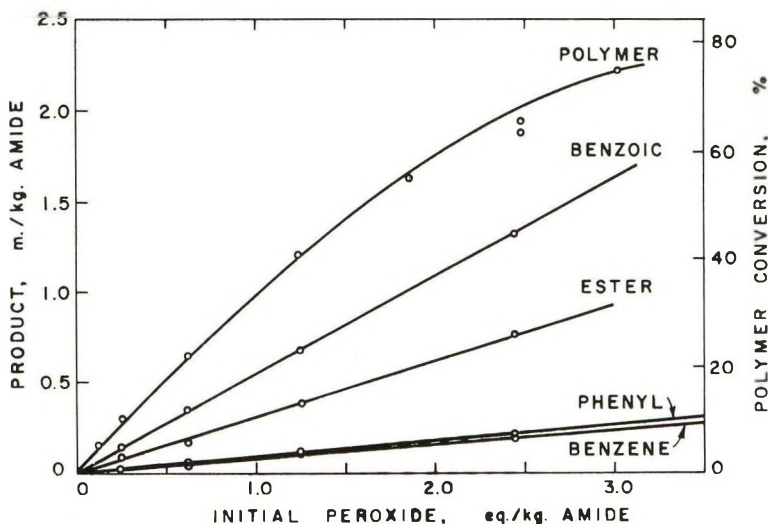

Fig. 1. Decomposition of benzoyl peroxide in *N*-allylstearamide at 90°C.

TABLE I

Products of the Decomposition of Benzoyl Peroxide in N-Allylamides and in N-Butylstearamide at 90°C.

Product	Product concentration, moles/kg. amide, at various initial peroxide concentrations[a,b]								
	N-Allylstearamide				N-Allylacetamide			N-Butylstearamide	
	0.247 equiv./kg.	0.617 equiv./kg.	1.249 equiv./kg.	2.438 equiv./kg.	1.953 equiv./kg.	4.122 equiv./kg.	6.035 equiv./kg.	1.168 equiv./kg.	2.344 equiv./kg.
Benzoic acid	0.140	0.348	0.683	1.333	1.082	2.202	3.192	0.690	1.375
Benzene	0.020	0.050	0.108	0.207	0.050	0.102	0.160	0.243	0.440
Benzoate-substituted amide	0.077	0.173	0.388	0.769	0.804	1.653	2.669	0.098	0.222
Phenyl-substituted amide	0.024	0.054	0.109	0.214	0.156	0.378	0.508	0.116	0.284
Total	0.261	0.625	1.289	2.523	2.091	4.335	6.528	1.156	2.321
Amide entering polymer[c]	0.300	0.674	1.035	1.881	2.766	4.781	6.428	—	—
$d[M]/d[P]$	2.43	2.18	1.66	1.54	2.79	2.32	2.13	—	—
$\overline{DP}$	10.17	9.05	9.12	9.66	7.86				

[a] Initial benzoyl peroxide concentration equalled one half these concentrations.

[b] Approximate mole-% peroxide concentrations, based on amide, corresponding to the values in the table are: N-Allylstearamide; 4, 10, 20, 40; N-allylacetamide, 10, 20, 30; N-butylstearamide, 20, 40.

[c] Based on total reduction in unsaturation. Other values, experimentally determined for N-allylstearamide and reported in Figs. 1 and 4 and not listed above are for initial peroxide and amide in polymer respectively: 0.1236 equiv./kg., 0.1613 mole/kg., 0.6180 equiv./kg., 0.6447 mole/kg., 1.2360 equiv./kg., 1.2017 mole/kg.; 1.8538 equiv./kg., 1.6260 mole/kg., 2.4718 equiv./kg., 1.9484 mole/kg.; 3.0920 equiv./kg., 2.2367 mole/kg.
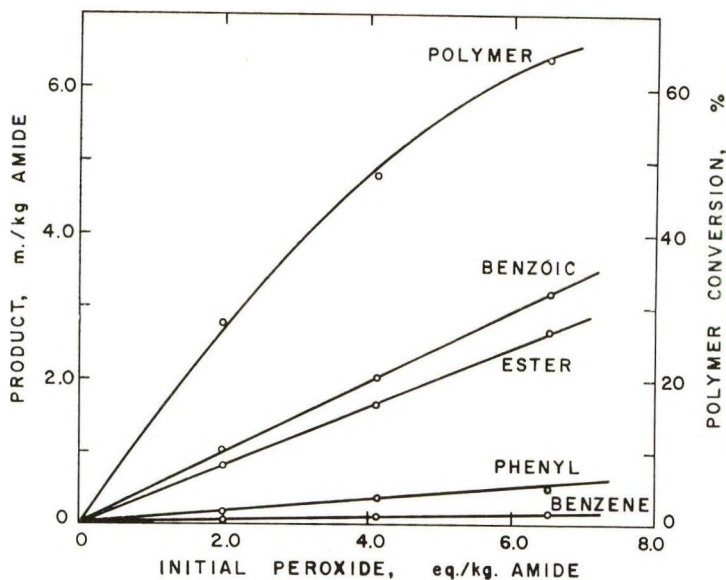
Fig. 2. Decomposition of benzoyl peroxide in N-allylacetamide at 90°C.
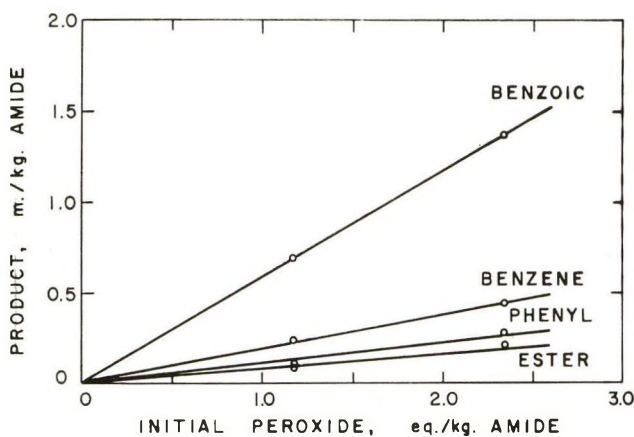
Fig. 3. Decomposition of benzoyl peroxide in N-butylstearamide at 90°C.

crease in initiator concentration in the polymerizable amides. However, log $(a - x)$ for both N-allylamides depended linearly on initiator concentration, as seen in Figure 4 for N-allylstearamide. The slopes, calculated as log mole fraction amide surviving versus initiator concentration (in equivalents/kilogram) were: N-allylstearamide -0.1771; N-allylacetamide -0.0742.

First-order benzoyl peroxide decomposition rates in the three amides at 90°C. are listed in Table II. The values shown may be subject to some uncertainty, since solution rates approached reaction rates in the N-allylamides. The rate data could be obtained only after considerable peroxide had already been destroyed, so that extrapolation of the relationship to

Fig. 4. Polymerization of N-allylstearamide at 90°C.

TABLE II

Rates of Decomposition of Benzoyl Peroxide
in Certain Amides and Other Solvents at 90°C.

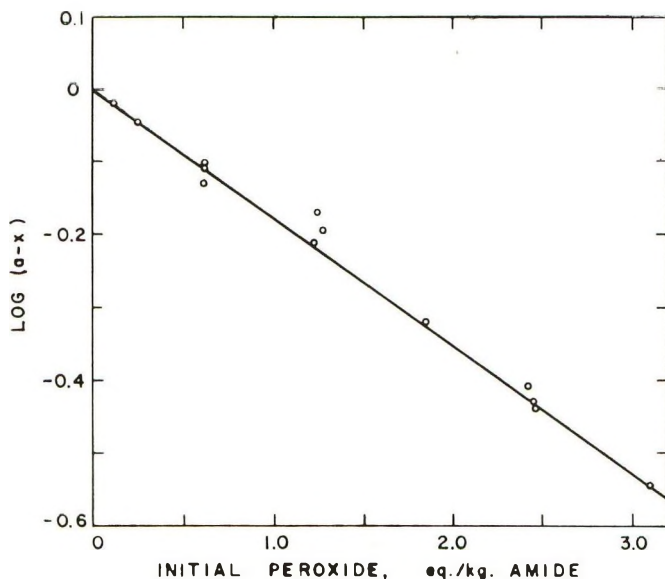| Solvent	Peroxide, mole/kg.	$k_1 \times 10^2$, min.$^{-1}$
N-Allylacetamide	1.0101	Immeasurably fast[a]
N-Allylstearamide	0.6491	9.07 ± 0.023
N-Butylstearamide	0.6182	3.24 ± 0.002
Allyl acetate	0.413	0.78[b]
Benzene	0.5861	0.776[b]

[a] At 70°C.

[b] Estimated as $2 \times k_{80}{}^\circ$ from data of Bartlett and Altschul[27] and Barnett and Vaughan.[46]

initial amide concentration might be subject to error. In addition, precision was adversely affected by the high frequency of sampling required. However, since relative reaction rates are probably adequately expressed by these rate constants, investigation of decomposition kinetics at different concentrations and temperatures was considered unnecessary. Because of the experimental difficulties, amide monomer disappearance was not determined as a function of time,[1,27-33] and only overall $d[M]/d[P]$ values were reported in Table I.

In Table II, the 90°C. rate constants for allyl acetate and benzene are estimated as 0.78×10^{-2} min.$^{-1}$ from literature values determined at 80°C. at concentrations in the range of the present investigation.[27] At 90°C. a concentration-dependent increase in induced decomposition

of benzoyl peroxide in allyl acetate has been noted by Litt and Eirich.[32] By extrapolation of these data a value of 3.5×10^{-2} min.$^{-1}$ may be estimated for an initial peroxide concentration of 0.6 mole/kg., similar to that used in this study.   However, the absolute value, independent of induced effects, was found by these authors to be 0.62×10^{-2} min.$^{-1}$ Thus the overall results illustrate the marked effect of induced decomposition on rate in the three amides.   The same reaction order and similar rates were found when benzoyl peroxide was decomposed in dimethylformamide,[38] n-butyl ether,[39] and n-butyl alcohol,[39] solvent classes which exert abnormally high induced effects on benzoyl peroxide and give rise to similar reaction products.

These results are in harmony with the reaction eqs. (1)–(13).

$$PhCOOCPh \rightarrow 2\ PhCO\cdot \tag{1}$$

$$PhCO\cdot + SH \rightarrow PhCOH + S\cdot \tag{2}$$

$$PhCO\cdot + SH \rightarrow PhH + S\cdot + CO_2 \tag{3}$$

$$S\cdot + PhCOOCPh \xrightarrow{k_{ind}} PhCOS + PhCO\cdot \tag{4}$$

$$S\cdot + PhCOOCPh \xrightarrow{k_{ind}} PhS + CO_2 + PhCO\cdot \tag{5}$$

$$PhC-O\cdot + M \rightarrow PhC-OM\cdot \text{ or } PhM\cdot + CO_2 \tag{6}$$

$$AM\cdot + M \rightarrow AM{\sim}M\cdot \tag{7}$$

$$AM{\sim}M\cdot + SH \rightarrow AM{\sim}MH + S\cdot \tag{8}$$

$$AM{\sim}M\cdot + PhCOOCPh \rightarrow AM{\sim}MOCPh + PhCO\cdot \tag{9}$$

$$AM{\sim}M\cdot + PhCOOCPh \rightarrow AM{\sim}MPh + CO_2 + PhCO\cdot \tag{10}$$

$$PhCO\cdot + S\cdot \rightarrow PhCOS \tag{11}$$

$$PhCO\cdot + S\cdot \rightarrow PhS + CO_2 \tag{12}$$

$$S\cdot + S\cdot \rightarrow S-S \tag{13}$$
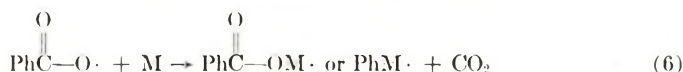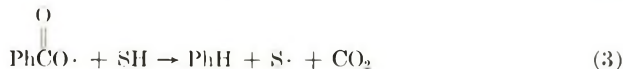
where SH is amide functioning as solvent; S·, the solvent radical; M, N-allylamide functioning as monomer; M·, the vinyl radical; and A, aromatic end group.

Reactions (2) and (3), involving transfer of a hydrogen atom from the amide solvent to form either benzene or benzoic acid, may be classified as transfer reactions.   Reactions (4), (5), (11), and (12) are aromatic-substitu-

tion reactions, forming the corresponding ester or phenyl substitution product, depending on whether or not carbon dioxide is expelled. Reaction (13) is the dimer-forming reaction, while reactions (6)–(10) produce polymer. Of special interest are the reactions of induced decomposition, eqs. (4), (5), (9), and (10). Also pertinent is the fact that dimer and substitution products are monomers capable of entering reaction (7).

Relative Proportion of Products Formed

In Table III slopes of the lines formed in Figures 1, 2, and 3 compare the relative proportions of the individual transfer and substitution reactions. Ratios of transfer (T) and substitution (S), together with ratios of ester formation (E) to phenyl substitution (P) are also compared. The relationship $T - S = D$ represents the slope for excess amide radical $(S\cdot)$ which terminated, presumably, as dimer [reaction (13)] but does not include dimer formed as a consequence of reaction (8). Total transfer relative to total substitution (T/S) increased in the order N-allylacetamide $< N$-allylstearamide $< N$-butylstearamide,[40] the reverse of the order of induced decomposition of peroxide (Table II), as would be expected. The lower the T/S ratio the longer was the kinetic chain and the larger the observed rate constant. As can be seen from the equations, the kinetic chain includes polymer formation in the case of the two polymerizable amides.

The N-butylstearamide radical was apparently terminated to a large extent by dimerization, or by other means discussed later. Evidence for this is seen (Table III) in its high D/S ratio, compared to the two polymerizable amides. Analytically about one third of the benzoyloxy radicals formed substitution products in this solvent. Aryl substitution receives additional support from the magnitude of the corresponding peroxide decomposition rate (Table II).

TABLE III

Slopes and Ratio of Slopes for the Products of Decomposition of Benzoyl Peroxide in N-Allyl- and N-Butylamides at 90°C.

Product formed	Formed by equation number	Ratio of slopes[a]	Slope m^b		
			N-Allyl-acetamide	N-Allyl-stearamide	N-Butyl-stearamide
Benzoic acid	(2)	—	0.521	0.570	0.575
Benzene	(3)	—	0.027	0.086	0.168
Amide substituted by benzoate	(4) + (11)	—	0.459	0.320	0.106
Amide substituted by phenyl	(5) + (12)	—	0.087	0.087	0.142
		T/S	1.00	1.61	2.99
		D/S	0.0003	0.614	1.99
		E/P	5.26	3.67	0.745

[a] $m_{benzoic\ acid} + m_{benzene} = T;$ $m_{ester\ formation} = E;$ $m_{phenyl\ substitution} = P;$ $E + P = S;$ $T - S = D,$ slope for formation of amide radicals that either terminated by dimerization or entered chains by effective chain transfer.

[b] $m = $ [Product]/[Peroxide equivalents], calculated by least squares method.

Two additional points emerge from the data of Table III. In N-allyl-acetamide, the equal occurrence of transfer and substitution limits termi-nation to the union of a solvent radical and a benzoyloxy or phenyl radical. This suggests that first-order kinetics apply to peroxide decomposition in this amide as well as in the other two (see Table II). When union of a solvent radical and an initiator radical is the only mode of termination, unimolecular kinetics are always observed.[37,38] The second point of interest is the decline in the ratio of ester to phenyl substitution (E/P) in going from N-allylacetamide to N-butylstearamide (Table III), which parallels the decline in the magnitude of the respective rate constants (Table II). Ap-parently, decrease in the induced reactions favored longer-lived benzoyloxy radicals, and thus promoted carbon dioxide evolution.[37]

Comparison with Allyl Acetate Polymerization

The ratio of consumption of allylamide in forming polymer to the total amount consumed in forming nonpolymeric aromatic substitution prod-ucts decreased from 4.2 to 2.4 for N-allylstearamide and from 3.5 to 2.5 for N-allylacetamide with increase in peroxide concentration. (The calcu-lation assumes one aromatic endgroup). These values compare with a ratio of >100 found when benzoyl peroxide was decomposed in allyl acetate.[27] In view of the predominance of hydrogen transfer found, the N-allylamides were either more labile than allyl esters toward abstraction of allylic hydrogen or significantly less reactive as monomers toward addition of initiator radicals. The latter situation seemed very unlikely, because Q and e values of N-allylamides[26] were similar to those of allyl acetate. With N-allylamides, transition-state stabilization through reso-nance, by the formation of polar structures such as I and II

$$
\begin{array}{cc}
\overset{O}{\overset{\|}{R\overset{\oplus}{C}NH}=CHCH=CH_2} & \overset{O}{\overset{\|}{R\overset{\oplus}{C}NH}=CHCH=CH_2} \\
\oplus \quad H\cdot & \oplus \quad \cdot OCOPh \\
PhCO\bar{O}: & PhCO\bar{O}: \\
I & II
\end{array}
$$

first proposed by Bamford for the decomposition of benzoyl peroxide in di-methylformamide[38], would provide a mechanism accounting for both trans-fer and aromatic substitution. Greater electron release by nitrogen than by oxygen should make such polar contributions more important in amides than in esters. Polymerization, then, would be the consequence of a competition for initiator radicals between addition and aromatic substitu-tion. Polymer chain termination via attack on the peroxide by the very active vinyl radicals[41] [reactions(9) and (10)] would continue the kinetic chain and account partly for the greater induced decomposition found in N-allylstearamide than in N-butylstearamide.

If reactions (9) and (10) had predominated, there should have been two aromatic endgroups per polymer chain. To check this point, the polymer benzoate ester groups were determined. The results are listed in Table IV together with two sets of calculated values. Both calculations assume the

same E/P ratio for the polymer as was found for the whole system (Table III). Calculation I assumes that esterified monomer was not copolymerized, while calculation II assumes that it was copolymerized to the extent available. Since there was opportunity for other reactions, these calculated values are only approximate. Although the results are not conclusive, they do support a polymer chain termination via reactions (9) and (10), which would account for the higher induced decomposition found in N-allylamides than in N-butylstearamide.

TABLE IV
Mole Ratio of Ester to Polymer[a]

Polyamide	Ester/polymer at various initial benzoyl peroxide concentrations[b]			
	10 mole-%	20 mole-%	30 mole-%	40 mole-%
N-Allylacetamide				
Found	2.21	2.40	1.60	—
Calculation I	1.68	1.63	1.68	—
Calculation II	2.01	2.49	3.26	—
N-Allylstearamide				
Found	—	1.35	—	1.53
Calculation I	—	1.56	—	1.57
Calculation II	—	2.21	—	3.10

[a] Calculated values based on $\overline{DP} = 10$.
[b] Based on weight of amide.

Results of Column Chromatography

Selected crude reaction products, obtained when benzoyl peroxide was decomposed in both N-butylstearamide and in N-allylstearamide, were chromatographed on a Florisil column, and fraction purity was monitored by thin-layer chromatography. Results for N-allylstearamide are listed in Table V and compared with results calculated from the data of Table I. Agreement is fairly good in view of the uncertainties involved in the calcu-

TABLE V
Comparison of Composition Results by Column
Chromatography and by Calculation from the Data in Table I

| Fate of initial amide after radical attack	Initial benzoyl peroxide, equiv./kg. amide	Composition, mole-%	
		By column chromatography	Calculated from data of Table I
In polymer[a]	1.249	36.14	44.58[b]
" "	2.438	60.10	70.36[b]
As aromatic-substituted monomer	1.249	12.04	9.60
"	2.438	18.23	10.56
As unreacted amide	1.249	52.26	45.80
" " "	2.438	21.77	19.08

[a] Includes aromatic-substituted polymer.
[b] Includes all dimer amide.

lations, which assume proportional copolymerization of the nonpolymeric aromatic substitution products and that all of the dimerized amide entered the polymer fraction. The latter assumption was made because no dimer was separated from the polymer fraction by chromatography.

Chromatography separated the reaction mixture into three main fractions, two of which, the unreacted amide and the polymer fraction, were obtained in a pure form. The middle fraction was a mixture of essentially two nonpolymeric compounds, which, on the basis of infrared spectra, were assigned the structures III and IV where R is either n-propyl or vinyl.

RCHNHCOR

III

RCHNHCOR
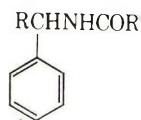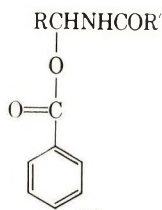
IV

These were the phenyl and ester derivatives formed as a result of reactions (4), (5), (11), and (12), and reported in Table I. No substitution on nitrogen was observed. From N-butylstearamide, III was obtained in almost pure form, as judged by thin-layer chromatography, m.p. 106–107°C.; from N-allylstearamide, IV was obtained in 90% purity as indicated by thin-layer chromatography and infrared examination of a single small fraction. Compound IV is similar to the ester formed when benzoyl peroxide was decomposed in dimethylformamide.[38]

The fractionation of poly-N-allylstearamide on Florisil is reported in Table VI. No dimer was found in spite of the prediction of the D/S ratio in Table III. Either the column was unable to separate dimer from higher molecular weight species, or hydrogen abstraction from the acyl portion

TABLE VI
Molecular Weight Distribution of Poly-N-allylstearamide

Fraction number	Initial benzoyl peroxide = 1.249 equiv./kg. amide			Initial benzoyl peroxide = 2.438 equiv./kg. amide		
	w_i	$\bar{M}_n$	Ester number	w_i	$\bar{M}_n$	Ester number
1	0.43	2703	29.2	0.10	1647	39.4
2	0.13	3340	25.0	0.22	2182	31.4
3	0.10	3076	⎫	0.29	3000	23.0
4	0.10	3455	⎬ 19.1	0.15	3691	21.0
5	0.14	4093	⎭	0.14	4771	18.2
6	0.07	4523	⎫ 15.0	0.05	4425	—
7	0.33	2561	⎭	—	—	—
Whole polymer	—	3292[a]	23.5[b]	—	2927[a]	29.4[b]

[a] $\sum w_i \bar{M}_n.$
[b] $\sum w_i$ (ester no.).

had generated radicals that were consumed in initiating polymers via effective chain transfer.[31]

Column chromatography of N-butylstearamide yielded about one third of the amount of products predicted by Table I, even though the unreacted amide fraction was separated in a pure state, as shown by thin-layer chromatography and melting point. Again, no dimer was isolated in a pure form, in spite of the large amount that was predicted by the results in Table III. In addition to the aromatic substitution products already discussed, about 35–45% of the reacted amide was polymer of unknown composition; the molecular weights, which were between 900 and 3000, increased with the peroxide content of the system. Even when the proportion of reacted amide was corrected for two transfers per amide unit, as required for polymer, only 50% of the predicted reacted amide was accounted for. It may be that a considerable portion of the polymer found was formed by radical attack on aromatic residues as has been observed in certain unreactive solvents.[42] However, infrared spectra of the polymer showed amide peaks.

EXPERIMENTAL

Preparation of Amides

N-Allylacetamide, N-allylstearamide, and N-butylstearamide were prepared by ester aminolysis at 30°C.,[43] and the long-chain amides were purified by the reference procedure. The preparation of N-allylacetamide was modified by the use of a ratio of amine to ester of 1.1/1 and a 24-hr. reaction time. After two precipitations in benzene (4 ml./ml. reaction product) to remove unused catalyst, and evaporation of the aromatic solvent from each filtrate, the crude N-allylacetamide was distilled (b.p. 104–104.5°C./10 mm.) to give the amide in 76% yield. The three amides were 99% pure by elementary analysis and by gas-liquid chromatography.

Benzoyl Peroxide

Benzoyl peroxide was Eastman Kodak White Label and was 99% pure by peroxide determination.[44] The peroxide value was checked frequently during this investigation.

Reaction Procedure

Weights of amide were taken in the range of 10–100 g. so that the initial weight of benzoyl peroxide did not fall below 2.9 g. nor exceed 6.0 g. in any experiment involving the long-chain amides. When N-allylacetamide was used, the peroxide weight range was between 4.8 and 7.3 g. for an amide weight range of 10–20 g. To the amide, in a flask containing a gas inlet, placed in a thermostatted bath at 90 ± 0.1°C., the benzoyl peroxide was added in small increments (0.2–0.4 g.), over a period of 30–90 min., by means of a small tube connected by rubber tubing to a neck of the reaction flask. The small tube was removed to receive the next increment, without opening the system to the outside, by clamping off the rubber tubing before

disconnecting. Gaseous reaction products were carried by Ascarite-treated nitrogen through a small Vigreux column, over solid anhydrous calcium sulfate, to an analytically tared Dry-Ice trap and then through two Ascarite tubes connected in series. Reaction was always continued for 3 hrs. after the addition of the last increment of initiator. The application of moderate vacuum for 1 hr. at 90°C. was necessary in those N-allylstearamide experiments in which 4 and 10 mole-% of initial benzoyl peroxide were used, in order to remove all of the benzene from the crude reaction mixture; vacuum applied in the other experiments removed no additional benzene. From the results of acid number, saponification number (0.2N alcoholic KOH, 1 hr. reflux), Wijs iodine number, and a peroxide number (the last was always zero), the data in Table I were calculated. The saponification did not hydrolyze any of the amides used; the blank titration was obtained when each of the amides was treated alone.

Kinetic Procedure

The peroxide was added and dissolved as described in the proceeding section except that the addition was done as quickly as possible. Addition and solution times were 30 min. for N-butylstearamide, 15 min. for N-allylstearamide, and 14 min. for N-allylacetamide, the last at 70°C. It was qualitatively observed that the accumulation of aromatic products shortened solution time. Initial samples were removed after 5 min. from N-butylstearamide, after 1 min. from N-allylstearamide (by quickly immersing and withdrawing short pieces of glass tubing, which were tared with the analytical flask), and after 15 sec. from N-allylacetamide (by use of a pipet). Because solution rates approached reaction rates, the first sample withdrawn showed that peroxide was destroyed in the three amides to the following extents: 36.8% in N-butylstearamide, 86.7% in N-allylstearamide, and 100% in N-allylacetamide. The balance of each decomposition followed good first-order kinetics. Benzoyl peroxide was only slightly soluble in N-allylacetamide at 60°C., so that a lower-temperature kinetic study was not practical.

Benzoic Acid

The reaction mixtures used to obtain the data in columns 3, 4, 8, and 9 of Table I were dissolved in benzene (10–20 ml./g.) washed with three equal volumes of 10% sodium carbonate solution at 30–40°C., washed free of alkali, washed once with 10% HCl solution, and freed of acid. The aqueous layers were extracted twice with ethyl ether (equal volumes) and the ether evaporated. Mixed melting points showed that the residue was pure benzoic acid, and recovery was 86–96% of that calculated from acid number.

Column Chromatography

The crude reaction mixture, after benzoic acid removal, was chromatographed from benzene solution on a Florisil column. Unreacted amide was eluted with pure benzene and 10% chloroform, the aromatic fraction

with 20–50% chloroform; the polymer was fractionated (Table VI) with 2–20% ethanol. The polymer found when N-butylstearamide was the reaction solvent required 5% acetic acid (followed by Florisil removal) for complete elution. Overall recovery was 93–96%. Thin-layer chromatography of selected fractions from column chromatography was used to monitor the column separations. Thin-layer results and melting points showed that the unreacted amide was very pure.

The aromatic fractions were shown by thin-layer chromatography to be a complex mixture in which two compounds, one high melting and one low melting, predominated. The low melting compound (isolated from one fraction of N-allylstearamide in 90% purity) had distinct infrared absorption peaks (carbon tetrachloride) at 1275 and 1117 cm.$^{-1}$, characteristic of benzoate C—O stretching modes and at 1720 cm.$^{-1}$, reflecting C=O stretching. The high melting compounds (melting range, 100–110°C.) showed distinct phenyl adsorptions at 1640–1650 cm.$^{-1}$, ascribed to phenyl shifted to higher wave number from the normal 1600 cm.$^{-1}$ region by proximity to the —CONH— grouping. The typical secondary amide NH stretching adsorptions at 3460–3500 cm.$^{-1}$, present in the pure amides, were retained and the maxima intensified in all of the products obtained, including the polymer, although the peak was shifted to as low as 3300 cm.$^{-1}$ in some of the polymer fractions. The amide II bands at 1500 cm.$^{-1}$, present in the pure amides, were generally broadened and shortened with increase in aromatic substitution. Since this was especially pronounced with the phenyl substitution product, in which interaction with the amide group is possible, the allylic carbon was considered the site of the major amount of aromatic substitution, although substitution at acyl carbon atoms may have contributed to the complexity of products. Qualitative agreement was obtained between the intensity of infrared maxima and the amounts of products shown by thin-layer chromatography.

Amide Polymers

Poly-N-allylstearamide was obtained from column chromatography as described above; poly-N-allylacetamide was isolated from the crude reaction mixtures as the residue from repeated aqueous extractions at room temperature. All molecular weights were found by a thermistor method.[45] The molecular weights of poly-N-allylstearamide samples were determined in carbon tetrachloride, in which the correct value was found for the monomer. Those of poly-N-allylacetamide were measured in chloroform, since this polymer was insoluble in carbon tetrachloride; a single sample checked in methyl ethyl ketone gave the same result. Micro acid and saponification determinations were made on the polymer and reported in Table VI as ester numbers. Unsaturation (Wijs iodine number) was low in poly-N-allylacetamide (ca. 0.5 double bond per chain) but higher in poly-N-allylstearamide (ca. 2 double bonds per chain), in which amide dimer could have copolymerized, because $T/S > 1$, (Table III). Poly-N-allylacetamide was a viscous semisolid at room temperature; poly-N-allylstearamide a soft wax melting at 70–80°C.

References

1. Laible, R. C., *Chem. Revs.*, **58,** 807 (1958).
2. Roe, E. T., J. M. Stutzman, and D. Swern, *J. Am. Chem. Soc.*, **73,** 3642 (1951).
3. Ballard, S. A., R. C. Morris, and V. W. Buls, U. S. Pat. 2,687,403 (1954).
4. Drechsel, E. K., and J. J. Padbury, U. S. Pat. 2,550,652 (1951).
5. Mullier, M., and G. Smets, *Bull. Soc. Chim. Belg.*, **62,** 491 (1953).
6. Toy, A. D. F., and R. S. Cooper, *J. Am. Chem. Soc.*, **76,** 2191 (1954).
7. Gaylord, N. G., and F. R. Eirich, *J. Am. Chem. Soc.*, **73,** 4981 (1951).
8. Dannenberg, H., and D. E. Adelson, Brit. Pat. 566,344 (1944).
9. Boyer-Kavenoki, F., *Bull. Soc. Chim. France*, **1959,** 624.
10. Adelson, D. E., and H. F. Gray, Jr., U. S. Pat. 2,555,775 (1951).
11. Kowolik, E. J., and J. W. Fisher, Brit. Pat. 757,203 (1956).
12. Kodak-Pathé, Fr. Pat. 1,104,541 (1955).
13. Hanede, T., M. Ishihara, and Y. Yamane, Japan. Pat. 14,145 (1961).
14. Levis, D. A., and P. A. Small, Ger. Pat. 1,106,500 (1961).
15. Csuros, Z., M. Gara, and I. Gyurkovics, *Acta Chim. Acad. Sci. Hung.*, **29,** 207 (1961).
16. Zonsveld, J. J., U. S. Pat. 3,013,999 (1961).
17. Chapin, E. C., and R. F. Smith, U. S. Pat. 2,894,938 (1959).
18. Reinhard, R. H., U. S. Pat. 2,891,037 (1959).
19. Tawney, P. O., Can. Pat. 575,985 (1959).
20. Matsumoto, M., M. Maeda, and T. Osugi, U. S. Pat. 2,909,502 (1959).
21. Shokal, E. C., and P. A. Devlin, Ger. Pat. 1,059,665 (1959).
22. Gumboldt, A., Ger. Pat. 949,648 (1956).
23. Takahashi, G., and I. Sakurada, *Kobunshi Kagaku*, **13,** 449 (1956).
24. Caldwell, J. R., U. S. Pat. 2,596,650 (1952).
25. Amagasa, M., and I. Yamaguchi, Japan. Pat. 8837 (1959).
26. Jordan, E. F., and A. N. Wrigley, *J. Appl. Polymer Sci.*, **8,** 527 (1964).
27. Bartlett, P. D., and R. Altschul, *J. Am. Chem. Soc.*, **67,** 816 (1945).
28. Bartlett, P. D., and K. Nozaki, *J. Polymer Sci.*, **3,** 216 (1948).
29. Gaylord, N. G., and F. R. Eirich, *J. Am. Chem. Soc.*, **74,** 334 (1952).
30. Gaylord, N. G., and F. R. Eirich, *J. Am. Chem. Soc.*, **74,** 337 (1962).
31. Gaylord, N. G., *J. Polymer Sci.*, **22,** 71 (1956).
32. Litt, M., and F. R. Eirich, *J. Polymer Sci.*, **45,** 379 (1960).
33. Bartlett, P. D., and F. A. Tate, *J. Am. Chem. Soc.*, **75,** 91 (1953).
34. Brown, A. C. R., and D. G. L. James, *Can. J. Chem.*, **40,** 796 (1962).
35. Bartlett, P. D., and R. Altschul, *J. Am. Chem. Soc.*, **67,** 812 (1945).
36. Sakurada, I., and G. Takahashi, *Kobunshi Kagaku*, **11,** 255 (1954).
37. Walling, C., *Free Radicals in Solution*, Wiley, New York, 1957, pp. 474–491.
38. Bamford, C. H., and E. F. T. White, *J. Chem. Soc.*, **1959,** 1860.
39. Bartlett, P. D., and K. Nozaki, *J. Am. Chem. Soc.*, **69,** 2299 (1947).
40. Buselli, A. J., M. K. Lindemann, and C. E. Blades, *J. Polymer Sci.*, **28,** 485 (1958).
41. Flory, P. J., *Principles of Polymer Chemistry*, Cornell Univ. Press, Ithaca, N. Y., 1953, pp. 155–158.
42. Lynch, B. M., and K. H. Pausacker, *Austral. J. Chem.*, **10,** 40 (1957).
43. Jordan, E. F., Jr., and W. S. Port, *J. Am. Oil Chemists' Soc.*, **38,** 600 (1961).
44. Lundberg, W. D., *Autoxidation and Antioxidants*, Vol. I, Interscience, New York, 1961, p. 37.

45. Filipic, V. J., J. A. Connelly, and C. L. Ogg, in *Proceedings 1961 International Symposium on Microchemical Techniques*, Interscience, New York, 1962, pp. 1039–1051.

46. Barnett, B., and W. E. Vaughan, *J. Phys. Colloid Chem.*, **51**, 926 (1947).

Résumé

Lorsque le peroxyde de benzoyle est décomposé à 90°C dans le *N*-allylacétamide et le *N*-allylstéaramide, $d[M]/d[P]$ est environ égal à 2 et DP se situe entre 9 et 10, à cause d'une perte en radicaux oxybenzoyles. Ces radicaux forment de l'acide benzoique et du benzène par arrachement d'hydrogène de l'amide, et les radicaux amides qui en résultent deviennent substitués avec les groupes esters et phényles à partir de l'initiateur. Le *N*-butylstéaramide, modèle saturé du *N*-allylstéaramide, fournit les produits correspondants. Les vitesses de décomposition du peroxyde montrent d'importants effets d'induction, dans l'ordre décroissant: *N*-allylacétamide, *N*-allylstéaramide, *N*-butylstéaramide. Les pentes des droites dans le graphique des quatre produits (en môles par kilo) en fonction de l'initia teur (en équivalents par kilo) dans les trois amides dans l'ordre ci-dessus sont: benzoïque 0.521, 0.570, 0.575; benzène 0.027, 0.086, 0.168; amide substitué par le benzoate 0,459, 0,320, 0.106; amide substitué par le phényle 0.087, 0.087, 0.142. Le transfert, comparé a la substitution, augmente avec la longueur de la chaîne et une diminution d'insaturation, et la décomposition induite du peroxyde est abaissée d'une valeur correspondante. Donc, la chaîne cinétique diminue avec la longueur de la chaîne acyle et une diminution d'inaturation. Un mécanisme faisant appel à des espèces polaires dans l'état de transition lorsque les amides jouent le rôle de solvants tient compte du transfert et de la substitution aromatique et aide à expliquer la différence dans le comportement des *N*-allylamides et des esters allyliques. Le graphique représentant l'amide engagée dans le polymère (en môles par kilo) en fonction de la concentration en initiateur (en équivalents par kilo) sont des courbes. Les graphiques de log $(a - x)$ pour la disparition de l'amide en fonction de la même coordinée sont linéaires. Les pentes sont: *N*-allylacétamide −0.0742: *N*-allylstéaramide −0.1771.

Zusammenfassung

Bei der Zersetzung von Benzoylperoxyd bei 90°C in *N*-Allylacetamid und *N*-Allylstearamid betrug wegen Nebenreaktioner der Benzoyloxyradikale $d[M]/a[P]$ etwe 2 und DP lag zwischen 9 und 10. Die Benzoyloxyradikale bildeten durch Wasserstoffabspaltung aus dem Amid Benzoesäure und Benzol, und die entstehenden Amidradikale erhielten Ester- und Phenylgruppen des Starters als Substituenten. *N*-Butylstearamid, ein gesattigtes Modell für *N*-Allylstearamid, lieferte analoge Produkte. Die Geschwindigkeit der Peroxydzersetzung liess starke induzierte Effekte erkennen, die in der Reihenfolge: *N*-Allylacetamid, *N*-Allylstearamid, *N*-Butylstearamid abnahmen. Die Neigung der linearen Abhängigkeit der vier Produkte (in Molen pro Kilogramm) vom Starter (in Aquivalenten pro Kilogramm) bei den drei Amiden in der angegebenen Reihenfolge betrug: Benzoesäure 0,521, 0,570, 0,575: Benzol 0,027, 0,086, 0,168; benzoatsubstituiertes Amid 0,459, 0,320, 0,106; phenylsubstituiertes Amid 0,087, 0,087, 0,142. Die Übertragung nahm im Vergleich zur Substitution mit der Kettenlänge und mit abnehmender Unsättigung zu. Ein Mechanismus mit polarem Übergangszustand bei Amidlösungsmitteln konnte Übertragung und aromatische Substitution erklären und liess auch den Unterschied im Verhalten von *N*-Allylamiden und Allylestern verstehen. Beim Auftragen des polymergebundenen Amids (in Molen pro Kilogramm) gegen die Starterkonzentration (in Äquivalenten pro Kilogramm) ergaben sich Kurven; das Diagramm von log $(a - x)$ für den Amidumsatz gegen die gleiche Grösse war linear. Die Neigungen betruge für *N*-Allylacetamid −0,0742 und für *N*-Allylstearamid −0,1771.

Diffusivities and Solubilities of Methane in Linear Polyethylene Melts*

J. L. LUNDBERG, *Bell Telephone Laboratories, Incorporated, Murray Hill, New Jersey*

Synopsis

Diffusion coefficients of methane in linear polyethylene melts measured by simple sorption experiments are from 1.5×10^{-5} to 3.6×10^{-5} cm.^{2}/sec. between 140.0 and 188.3°C. These diffusion coefficients are one-third to one-half those of methane in branched polyethylene melts at these temperatures. Solubilities of methane in branched and linear polyethylene melts are similar, approximately three molecules of methane per one hundred methylene units at 250 atm. partial pressure methane between 140.0 and 188.3°C. Temperature coefficients of solubilities of methane in branched and linear polyethylenes differ in that the solubility of methane in linear polyethylene melt appears to go through a minimum with temperature between 140.0 and 162.8°C. These differences in diffusion coefficients and temperature coefficients of solubilities are consistent with the presence of greater order in linear polyethylene melt than in branched polyethylene melt.

A simple sorption experiment can yield both diffusion coefficients and solubilities if the sorbent geometry is fixed, concentration is measured as a function of elapsed time, and the necessary approximations to the appropriate solution of the diffusion equation are amenable to analysis. We have described such an experiment together with data analyses.[1,2] In this study, molten linear polyethylene (Phillips Petroleum Company Marlex 6050), constrained in cylindrical shape in sintered stainless steel, was contacted with methane (Matheson Company C. P. grade, 99+ mole-% pure) in a closed, thermostatted system.[2] Gas was added in increments by quickly increasing pressure in the system once daily.[1] Pressure, elapsed time, and temperature were recorded by means of a data logging system.[2] The measured pressures were converted to moles of gas external to the polyethylene, and the mole–elapsed time data were fitted to two close approximations to the solution of Fourier's differential equation for radial diffusion (or heat conduction) in an infinite cylinder[3] to give diffusion coefficients and solubilities.[1] Solubilities were determined from the moles of gas, external to the polymer, extrapolated to zero elapsed time (one of the parameters deduced in fitting data to the diffusion equation) minus the moles of gas external to the polymer at long times when sorption was complete. The

latter was calculated from pressure measurements at long times; the former is best estimated by emphasizing data taken at short elapsed times. Therefore, solubilities were estimated by using only data taken from 5 to 30 (or 60) sec. elapsed time.[1,2] Diffusion coefficients are best estimated for the polyethylenes by emphasizing data taken during the latter parts of sorption runs when pressure-induced volume relaxations and concentration-dependent changes in the diffusion coefficients are largely complete. This procedure has been described in detail.[1]

Results

The solubilities of methane in linear polyethylene melts at 140.04, 162.78, and 188.31°C. are quite small, approximately three molecules of methane per 100 methylene units in polyethylene at 250 atm. partial pressure of methane (Table I). These solubilities are almost identical in magnitude to solubilities of methane in branched polyethylene melts.[1] The

TABLE I
Solubilities of Methane in Linear Polyethylene Melts

Temperature, °C.	Final pressure, atm. (gage)	Solubility, cc. (NPT)/g.
140.04	45.5	11.68 ± 0.10
	64.3	16.31 ± 0.13
	115.1	27.13 ± 0.16
	197.7	40.63 ± 0.22
	231.2	46.98 ± 0.24
	282.9	55.66 ± 0.30
	302.5	59.49 ± 0.31
	25.2	5.74 ± 0.06
	50.6	13.09 ± 0.09
	82.9	20.30 ± 0.11
	116.8	27.05 ± 0.13
	152.0	34.43 ± 0.18
	195.5	42.19 ± 0.22
	247.3	51.16 ± 0.22
	292.1	58.31 ± 0.25
	328.1	63.19 ± 0.25
162.78	20.9	5.00 ± 0.06
	49.8	10.59 ± 0.07
	93.3	17.88 ± 0.08
	158.4	30.45 ± 0.09
	221.2	41.35 ± 0.12
	279.9	51.19 ± 0.13
	317.4	56.78 ± 0.14
188.31	24.2	5.48 ± 0.06
	59.8	12.72 ± 0.07
	103.0	21.93 ± 0.11
	156.1	31.38 ± 0.14
	201.0	39.60 ± 0.18
	253.3	47.83 ± 0.20

only obvious difference between the solubilities in linear and branched polyethylenes is that in branched polyethylene methane solubility increases with temperature over the temperature range 125.4–227.6°C. while in linear polyethylene melt the solubility at 140.04°C. is greater than the solubility at 188.31°C. which in turn is greater than the solubility at 162.78°C. The solubility of methane in linear polyethylene melt goes through an apparent minimum with temperature somewhere between 140.04 and 162.78°C. The solubilities of methane in branched and linear polyethylenes at 188.43 and 188.31°C., respectively, are identical, within experimental error.

The diffusion coefficients of methane in linear polyethylene melts are smaller by factors of two to three than those in branched polyethylene melts (Table II). In the polyethylene melts at substantially constant pressure, diffusion coefficients of methane in linear polyethylene increase somewhat as sorption proceeds, while those in branched polyethylene are essentially constant, independent of concentration. This is demonstrated by comparing best-fit diffusion coefficients for data late in the diffusion runs (taken at long elapsed times) and those for all data over the entire diffusion runs. In the 140–188°C. region the ratios of diffusion coefficients at long elapsed times to those over all elapsed times extrapolated to 1 atm. pressure are 1.26 ± 0.05 for linear polyethylene and 1.021 ± 0.012 for branched polyethylene.

At 140.04°C. in linear polyethylene melt, the increase in diffusion coefficient with increasing methane concentration is almost exactly compensated by the expected decrease in diffusion coefficient with increasing pressure. This is shown by the lack of any discernible dependence of diffusion coefficient upon pressure among the sixteen determinations of diffusion coefficient made in two series of sorption runs at increasing increments of pres-

TABLE II
Diffusion Coefficients of Methane in
Linear and Branched Polyethylene Melts[a]

Temperature, °C.	$D \times 10^5$ at atmospheric pressure, cm.^{2}/sec.	
	Linear polyethylene	Branched polyethylene
140.04	1.46 ± 0.29	3.51 ± 0.47[b]
162.78	1.66 ± 0.18	4.77 ± 0.34[b]
188.31	3.56 ± 0.57	5.53 ± 0.17

Pressure dependence of diffusion coefficients in linear polyethylene

140.04   (D is approximately independent of pressure):
162.78 $\ln D = -11.002 \pm 0.075 - (5.3 \pm 3.8) \times 10^{-4} P$[a]
188.31 $\ln D = -10.240 \pm 0.099 - (2.28 \pm 0.64) \times 10^{-3} P$[a]

[a] P = pressure atmospheres (gage).

[b] Interpolated from diffusion coefficients measured at 125.4, 155.4, and 188.4°C. as reported previously.[1]

sure from 25.2 to 328.1 atm.   An average of these sixteen diffusion coefficients is $(1.46 \pm 0.29) \times 10^{-5}$ cm.^{2} sec., where the error cited is the standard deviation in a single measurement.   (The standard deviation of the mean is $\pm 0.07 \times 10^{-5}$ cm.^{2}/sec.)

Diffusion coefficients of methane in linear polyethylene melts at 162.78°C., $(1.66 \pm 0.18) \times 10^{-5}$ cm.^{2}/sec., and at 188.31°C., $(3.56 \pm 0.57) \times 10^{-5}$ cm.^{2}/sec., are extrapolated to atmospheric pressure by least-squares fitting of data (seven and six points respectively) to the equation

$$\ln D = (\ln D)_{P=0} + \text{constant} \times P_{\text{final}} \text{ (atm. gage).} \qquad (1)$$

Standard deviations cited are standard deviations in the intercepts of eq. (1).   The effect of pressure tending to decrease the diffusion coefficients of methane in linear polyethylene outweighs the tendency of diffusion coefficients to increase with increasing methane concentration.   Thus, the diffusion coefficients decrease slightly with increasing pressure (and increasing concentration of methane) at 162.78°C. where the slope of eq. (1) is $-(5.3 \pm 3.8) \times 10^{-4}$ atm.$^{-1}$ and decrease about four times as rapidly with pressure at 188.31°C., where the slope of eq. (1) is $-(2.28 \pm 0.64) \times 10^{-3}$ atm.$^{-1}$ (Table II).

Between 140.04 and 162.78°C. (and at atmospheric pressure) the diffusion coefficients of methane in linear polyethylene melts increase rather little, from $(1.46 \pm 0.29) \times 10^{-5}$ to $(1.66 \pm 0.18) \times 10^{-5}$ cm.^{2}/sec., corresponding to an apparent activation energy of approximately 2 kcal./mole.   The diffusion coefficient at 188.31°C. and atmospheric pressure is $(3.56 \pm 0.57) \times 10^{-5}$ cm.^{2}/sec.   The increase from 162.78 to 188.31°C. corresponds to an apparent activation energy of 12 kcal./mole.   This apparent change in the temperature coefficient of the diffusion coefficient, increasing as temperature increases over at least a portion of the 140–188°C. temperature interval probably is real and not an artifact of the experiment.   The changes in diffusion coefficients with temperature are greater than reasonable estimates of experimental error.

Discussion

Salient features of this study of the sorption of methane by linear polyethylene melts and the earlier study of the same in branched polyethylene melts[1] are as follows.   (1) The solubilities of methane in branched and linear polyethylene melts are almost identical in magnitude, within experimental error, at similar temperatures and methane pressures.   (2) The solubility of methane in linear polyethylene melt apparently goes through a minimum with temperature between 140.04 and 162.78°C. (3) The diffusion coefficients of methane in branched polyethylene melts are twice to thrice greater than those in linear polyethylene melts at the same temperatures.   (4) The diffusion coefficients of methane in linear polyethylene melts increase more slowly with temperature between 140.04 and 162.78°C. than between 162.78 and 188.31°C.   (5) At substantially con-

stant methane pressure, the diffusion coefficients of methane in linear poly-
ethylene melt increase with increasing methane concentration while those
in branched polyethylene melt are almost independent of methane con-
centration.

These sorption properties may be explained upon the supposition that
branched polyethylene melt is less ordered than is linear polyethylene melt.
This is to say that once a polymer is frozen, order persists in the melt over
the time scale of these experiments (i.e., several days), particularly at
temperatures close to the melting points of the polymers.

First, the magnitudes of the solubilities may be expected to be quite
insensitive to differences in order and small differences in unoccupied
volume in a polymeric liquid. The difference in unoccupied volume in
linear and branched polyethylene melts probably is small judging from the
similar specific volumes of linear and branched polyethylene melts.[4]
Further, solubility probably is little influenced by the amount of unoccupied
volume present in a liquid as compared to effects upon the entropy gain
associated with the joint occupation of volume by two different molecules
(or portions of molecules). Polyethylene is usually insufficiently branched
to decrease appreciably the number of possible configurations a polyethyl-
ene molecule may assume. Therefore, the entropies of mixing of methane
with linear and branched polyethylene melts might be expected to be quite
similar.

Second, the only differences in solubilities are in the temperature coeffi-
cients. The fact that a solubility minimum for methane in linear poly-
ethylene melt between 140.04 and 162.78 °C. was observed while none was
found for branched polyethylene melt above 125.4 °C. indicates that a simi-
lar minimum in solubility with temperature might be found if measurements
were made closer to the melting point of branched polyethylene. The per-
sistence of order upon melting for periods of time of the order of these ex-
periments would mean that the properties of a polymer melt formed by
melting a partially crystalline polymer may be determined in part by pre-
vious thermal and stress history. Consequently, measurement of proper-
ties of the polymer characteristic of an equilibrium condition of the melt
might be extremely difficult near the melting point. Certainly, whether it
be a kinetic or equilibrium effect, rather small changes in order of a liquid
may affect the partial molal heats of solution enough to change the sign of
those quantities particularly if the heats are close to zero as is the case here.

Third, to a first approximation, diffusion may be regarded as a thermal
jump process (perhaps resembling a random flight). Such a process should
be strongly dependent upon order in the medium in which jumps take place.
The presence of relatively few branches on a polymeric chain may be ex-
pected to decrease order in the polymeric liquid without there being enough
side chains to interfere appreciably with thermal jumps. In such a system
the diffusion coefficients of additives might be larger than in the linear poly-
mer. Such appears to be the case in branched polyethylene melt as com-
pared to linear polyethylene melt. The order present in the crystalline

polymer appears to persist into the liquid such that diffusion coefficients reflect this order.

Fourth, the temperature dependence of the diffusion coefficient of methane in linear polyethylene apparently increases with temperature. This and the solubility minimum with temperature may be associated with long-term persistence of order, particularly close to the melting point. These temperature coefficients are influenced by second-order effects and might be strongly dependent on structural differences in the mixtures insofar as they influence energies of interaction of gas and polymer molecules.

Fifth, methane appears to plasticize linear polyethylene melt and to have little or no effect on branched polyethylene melt, as reflected by increase in diffusion coefficient with concentration of methane at substantially constant pressure. The branches of branched polyethylene probably serve as plasticizer molecules in the melt. This is to say that these branches introduce disorder and facilitate transport processes. Addition of a hydrocarbon plasticizer such as methane should have little or no effect in the already structurally plasticized branched polyethylene melt as compared to linear polyethylene melt containing almost no plasticizing branches.

These diffusion coefficients appear to be sensitive to order of insufficient perfection and repeat length to give coherent diffraction patterns with x-rays. Thus, sorption and permeation studies under carefully controlled conditions, particularly on stressed and oriented polymer specimens, may give qualitative information about ordering in the range of distances between those resolvable in x-ray scattering and x-ray diffraction experiments.

References

1. Lundberg, J. L., M. B. Wilk, and M. J. Huyett, *J. Polymer Sci.*, **57**, 275 (1962).
2. Lundberg, J. L., M. B. Wilk, and M. J. Huyett, *Ind. Eng. Chem., Fundamentals*, **2**, 37 (1963).
3. Fourier, J., *The Analytical Theory of Heat* (1822), translation reprinted by Dover, Englewood, New Jersey, 1955.
4. Matsuoka, S., *J. Polymer Sci.*, **57**, 569 (1962).

Résumé

Les coefficients de diffusion du méthane dans le polyéthylène linéaire à l'état fondu mesurés par de simples méthodes de sorption varient de 1.5×10^{-5} à 3.6×10^{-5} cm^2. sec.$^{-1}$ dans la région de température de 140.0 à 188.3°C. Les coefficients de diffusion varient du tiers à la moitié des valeurs, trouvées dans les masses-fondues de polyéthylène ramifié aux mêmes températures. Les solubilités du méthane dans les masses fondues de polyéthylène linéaure et ramifié sont égales, à peu près trois molécules de méthane pour cent unités méthyléniques à une pression partielle de méthane de 250 atmosphères entre 140.0 et 188.3°C. Les coefficients de température pour les solubilités du méthane dans les polyéthylènes linéaire et ramifié diffèrent en ce que la solubilité du méthane dans la masse fondue du polyéthylène linéaire passe par un minimum pour des tem-

pératures de 140,0 à 162,8°C. Ces différences dans les coefficients de diffusion et les coefficients de température pour les solubilités sont en accord avec la présence d'une plus grande régularité dans les masses fondues du polyéthylène linéaire que dans les masses-fondues de polyéthylène ramifié.

Zusammenfassung

Die mittels einfachen Sorptionsversuchen in linearen Polyäthylenschmelzen gemessenen Diffusionskoeffizienten von Methan erstreckten sich im Temperaturbereich zwischen 140,0° und 188,3°C von $1,5 \times 10^{-5}$ bis $3,6 \times 10^{-5}$ cm² sec^{-1}. Die Diffusionskoeffizienten betragen ein Drittel bis die Hälfte derjenigen von Methan in verzweigten Polyäthylenschmelzen bei diesen Temperaturen. Die Löslichkeit von Methan in verzweigten und linearen Polyäthylenschmelzen ist ähnlich, ungefähr drei Methanmoleküle pro hundert Methyleneinheiten bei 250 Atmosphären Methanpartialdruck zwischen 140,0° und 188,3°C. Die Temperaturkoeffizienten der Löslichkeit von Methan in verzweigtem und linearem Polyäthylen unterschieden sich in der Weise, dass die Löslichkeit von Methan in einer linearen Polyäthylenschmelze bei Temperaturen zwischen 140,0°C und 162,8°C in Abhängigkeit von der Temperatur durch ein Minimum zu gehen scheint. Diese Unterschiede zwischen den Diffusionskoeffizienten und den Temperaturkoeffizienten der Löslichkeit hängen mit der grässeren Ordnung in linearen Polyäthylenschmelzen im Vergleich zu verzweigten Polyäthylenschmelzen zusammen.

Effect of Chemical Reagents on the Fine Structure of Cellulose. Part I. Action of Diazomethane

H. SPEDDING and J. O. WARWICKER, *The Shirley Institute, Didsbury, Manchester, England*

Synopsis

An infrared and x-ray study of the action of diazomethane on the fine structure of ramie and regenerated cellulose (fiber and film) has been made. It has been found that the methylation process affects the disordered regions, and also parts of the structure that are sufficiently highly ordered to be detected by x-ray methods but whose hydrogen-bond order is too low to be detected by the infrared-deuteration technique. The effect of partial methylation on the hydrogen bonding in the noncrystalline regions is described and discussed. The conclusion drawn from the results is that diazomethane can react in the noncrystalline and the imperfectly crystalline regions, but not in the highly ordered crystalline regions.

INTRODUCTION

The primary object of this work was to study the fine structure of cellulose and changes in it brought about by the use of chemical reagents. Two reagents were chosen for a preliminary study, diazomethane and acetyl chloride, but only the action of diazomethane will be described in the present paper.

The interest in diazomethane arises from the suggestion by Reeves and Sisson[1] and later by Sitch[2] that the amount of methylation is related to the proportion of the noncrystalline material because the reaction does not affect the crystalline regions to any appreciable extent. It would therefore seem that because diazomethane is a small molecule it might be a means of studying the noncrystalline regions and also provide data on the role these regions play in the reactivity of cellulose.

Two methods of study were used, x-ray diffraction and infrared spectroscopy. In the former the diffraction envelope measured by a micro-densitometer along the equator of the x-ray fiber diagrams was studied. For the infrared work, the spectrum in the 2150–3650 cm.$^{-1}$ region was studied before and after deuteration.

EXPERIMENTAL

Materials and Their Purification

Ramie, Fortisan, and regenerated cellulose film were used in this work. The ramie was supplied as bleached sliver which was extracted for 6 hr.

with methylene dichloride and 6 hr. with methanol, and then washed in water for 16 hr. and dried in air. The Fortisan was supplied in yarns whose individual filaments were about 0.26 den. (275 den./1080 fil. and 45 den./170 fil.) and these were purified in a similar manner to that described for ramie. Secondary cellulose acetate film, either commercial Clarifoil or film cast from acetone on a glass plate, was saponified in 2% potassium hydroxide in 50/50 vol. of methanol/water, and washed free from the reagents with water. The films used for infrared measurements were all cast from acetone and were about 5 μ thick, the actual thickness being later determined.

Methylation

The ethereal solution of diazomethane was prepared by the method of De Boer and Backer[3] from N-methyl-N-nitroso-p-toluenesulfonamide (Diazald). The fibers were methylated according to Head's procedure,[4] in which dry fibers were immersed in ethereal diazomethane solution saturated with water. The films were first swollen in water and then methylated in ethereal diazomethane. Methoxyl contents were determined by the Zeisel method. The samples investigated had methoxyl contents of 4.3% (D.S. = 0.23) and 7.9% (D.S. = 0.43) for ramie, 12.5% (D.S. = 0.69) for Fortisan, 8.75% (D.S. = 0.47), 12.27% (D.S. = 0.65), and 13.55% (D.S. = 0.75) for the films.

X-Ray Measurements

The fibres were cut into 1 in. lengths and made into standard 25 mg. bundles. Copper Kα radiation monochromatized by reflection from a pentaerythritol crystal and collimated by a round brass collimator of aperture 0.5 mm. was used. Photographs were taken with a semicylindrical camera of radius $R = 5.73$ cm. and a flat-plate camera with a film–specimen distance of 5.1 cm. In the former, a piece of aluminum sheet was inserted in the main beam between the specimen and the film, so that the main beam could be registered on the film as a measure of the total exposure time. On all the films a step wedge was subsequently registered with a rotating sector-wheel on a portion of the film blanked-off during the main exposure.

A microdensitometer trace was made along the equator of the photographs from the semicylindrical camera, and also along the step wedge. Ultimate intensities were therefore recorded in terms of x-ray exposure and put on a comparative scale by reference to the height of the peak recorded for the main beam. Correction for changes in orientation were also applied wherever necessary.

The flat-plate photographs were measured azimuthally around the main equatorial arcs and also along the calibration step wedges. In a few experiments equatorial traces were also recorded from the flat-plate photographs, but only if corresponding photographs taken with the semicylindrical camera were not available.

It was not found possible to make accurate standard specimens from the small amount of sheet available. However, since the films were isotropic, small cylindrical specimens could be prepared which were then mounted on the geniometer head of a single-crystal camera. After alignment of the cylinders on the rotation axis of the goniometer they were rotated during exposure. Photographs with a cylindrical camera of radius 3 cm. were taken with crystal-reflected copper $K\alpha$ radiation collimated by a round collimator of aperture 0.5 mm. A step wedge was also recorded.

Microdensitometer traces along the equator of these photographs and along the step wedge were measured.

Since the information required in this work was comparative, it was not necessary to correct the results for Lorentz and polarization factors.

Infrared Measurements

The infrared results in this paper were all obtained from films cast on glass plates, the preparation of which has already been given.

The cell used consisted essentially of a demountable sample chamber with external connections to admit and withdraw D_2O vapor. The body of the cell was made from Perspex, and the windows one of which could be removed to allow the insertion of the sample were of calcium fluoride. The seal between the body of the cell and the window was made via an O-ring so that on evacuation the window adhered by air pressure only and could be rotated through 90° without breaking the vacuum in the cell. The window carried a pin that engaged the sample holder so that by the rotation of the window the sample could be rotated during the determination to test for any dichroism of the sample.

The cell was mounted in the Unicam SP 100 infrared spectrometer, which was evacuated. The cell walls of the instrument were freed from water vapor and carbon dioxide by placing in them, trays of B.D.H. molecular seive, type 5A.

Deuteration of Materials

Deuteration exchange was carried out with D_2O (99.7 g. $D_2O/100$ g. liquid). The sample to be deuterated was fixed in a brass holder and placed in the deuteration cell, which was then closed as described. The cell was placed in position in the spectrometer and evacuated for $1/2$ hr., after which time the vacuum line was closed and the tap to the D_2O supply opened. Deuteration was followed spectroscopically at the temperature of the instrument ($\approx 25°C$.), and when deuteration had reached the required stage (see below), the cell was then pumped out over P_2O_5 through a cold trap immersed in liquid nitrogen. The removal of D_2O, plus small amount of H_2O and HOD formed during the reaction, was again followed spectroscopically. Any rehydrogenation that occurred in this process as a result of leaks in the apparatus could be allowed for by noting the variation in the OH band intensity during the course of the evacuation. The same correction was applied to the final OH and OD intensities, since the

ratio of α_{OH}/α_{OD} was sufficiently close to unity for the small differences involved.

To simplify the recognition of the appearance of discrete OD peaks, due to the deuteration of the crystalline regions,[5] superimposed on the relatively intense, smooth, OD absorption band of the noncrystalline regions, use was made of a difference technique. In this, a piece of film of the same material as the sample film, contained in a similar cell, was placed in the reference beam when "crystalline" deuteration in the sample was suspected. The reference film was then deuterated for successive short periods (of the order of seconds) and the difference spectrum recorded after each deuteration, until virtually all the absorption due to deuterated noncrystalline regions in the sample was cancelled out, thus revealing clearly the presence of any peaks from deuterated crystalline material. To avoid the possibility of deuteration of crystalline regions in the reference film, which would have defeated the object of this difference technique, the reference film was made thicker than the sample, and this is why the time required for deuteration of the reference was so short. Care had to be exercised in choosing the reference film in order that the baselines of reference and sample spectra were approximately the same. Minor adjustments could be made by means of a rocksalt plate in the appropriate beam.

When the difference spectrum showed peaks at 2580 and 2561 cm.$^{-1}$ characteristic of "crystalline" OD absorption[1], the reference cell was removed from the spectrometer in readiness for drying and recording the spectrum of the deuterated noncrystalline regions of the sample film. Such drying took ca. 10 min. and was judged complete when the decrease in absorption at the OD maximum—initially rapid while the D_2O was being removed—became very slow. The spectrum of the deuterated noncrystalline regions was then recorded, and the intensity of the hydroxyl band at 3447 cm.$^{-1}$ (measured from a baseline drawn from 3650 cm.$^{-1}$ to the absorption trough between the OH and CH bands) taken as the measure of the undeuterated hydroxyl groups. This is permissible, according to Mann and Marrinan,[6] only if the orientation of (101) planes parallel to the film surface is either absent or present to a constant extent. X-ray measurements showed that this condition was fulfilled in the samples investigated here.

The extent of the deuteration of the crystalline regions was determined by subsequently rehydrogenating the film deuterated in the noncrystalline regions until the absorbance of the residual OD doublet was constant within experimental accuracy. Rehydrogenation was originally effected by merely exposing the films to atmospheric moisture but, in order to speed up the process, saturated H_2O vapor was later used with each film in another cell similar to that used for deuteration.

Measurement of Film Thickness

It is difficult to make accurate measurements of the thickness of films like those used here (ca. 4 μ). Moreover, if the thickness varies, it is the

"effective" thickness over the absorbing area that is required. For this reason it was decided to use a β-ray gauge for the measurements, as this is an absorption method that "samples" an area and does not rely on point-by-point measurements. Difficulties still remained however; for example, the true sample area in these spectroscopic measurements varied because automatic slit programming, by which the slit width was varied continuously with frequency, was employed. (Later, to minimize the effect of such difficulties, the films were masked so that in area of 3 mm. $\times$ 10 mm. was defined for both infrared and β-gauge measurements.) The relation between β-gauge reading and thickness was determined separately by using some unmethylated films that were sufficiently large and uniform for the thickness to be determined from weight, density, and area measurements. It was assumed that the relation between gauge reading and thickness was the same for the methylated and unmethylated films.

It should be mentioned here that although these thickness measurements were difficult and tedious they were necessary because there was no reliable internal standard available. A CH absorption band (e.g., that at ca. 2900 cm.$^{-1}$) could not be used as a measure of sample thickness without involving doubtful assumptions as to the (varying) extent of the contribution by the substituent methyl groups to the total CH intensity.

RESULTS AND DISCUSSION

X-Ray Results from Ramie (Cellulose I) and Fortisan (Cellulose II)

Figure 1 gives the comparison of the equatorial scans for methylated ramie with a methoxyl content of 4.3% and untreated ramie. These results were derived from a flat-plate photograph and have been standardized by making the intensities of the 002 peak agree. The justification for such a standardization is that the interest lies in a change in shape of the diffraction envelope which will be emphasized if the envelopes are made to agree at one point.

It will be readily seen that within the limits of the experimental error no marked change has been brought about by the methylating ramie to a methoxyl content of 4.3%.

Figure 2 gives similar results from the semicylindrical camera for methylated ramie with a methoxyl content of 7.9% and untreated ramie. The curve for untreated ramie is the mean of two determinations that agreed well with each other when standardized via the main-beam calibration spot. The two curves shown have been standardized via the main-beam calibration spot, but have not been further corrected for orientation because the orientation measurements on the corresponding flat-plate photographs showed that the change in orientation was within the experimental error [mean half-angle at half-height = 7.4° (treated), 7.0° (untreated ramie)]. The most significant difference between the curves is that the apparent positions of the peaks have all changed slightly. To check that these shifts were genuine and not attributable to some experimental factor, the x-ray
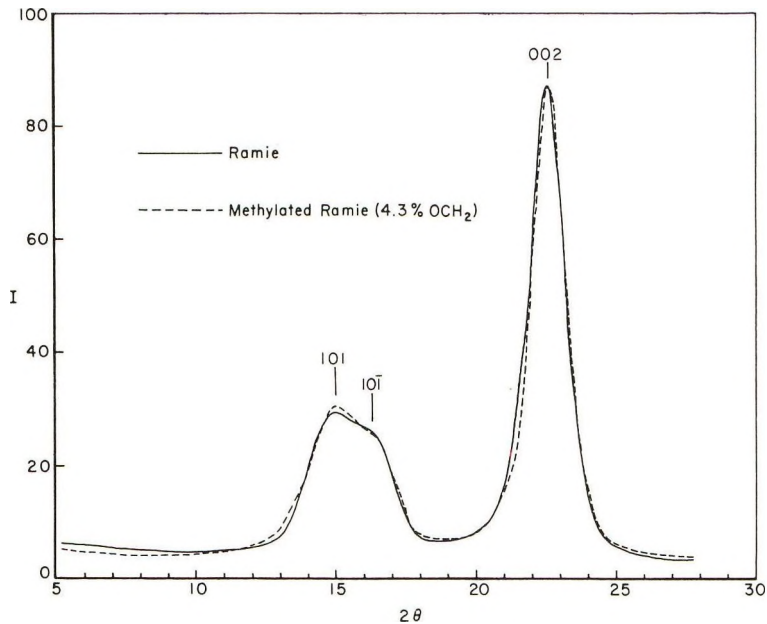
Fig. 1. Equatorial scans from the x-ray diagrams of (———) ramie and (- -) methylated ramie with a methoxyl content of 4.3%. (Flat-plate camera, F = 5.1 cm.)
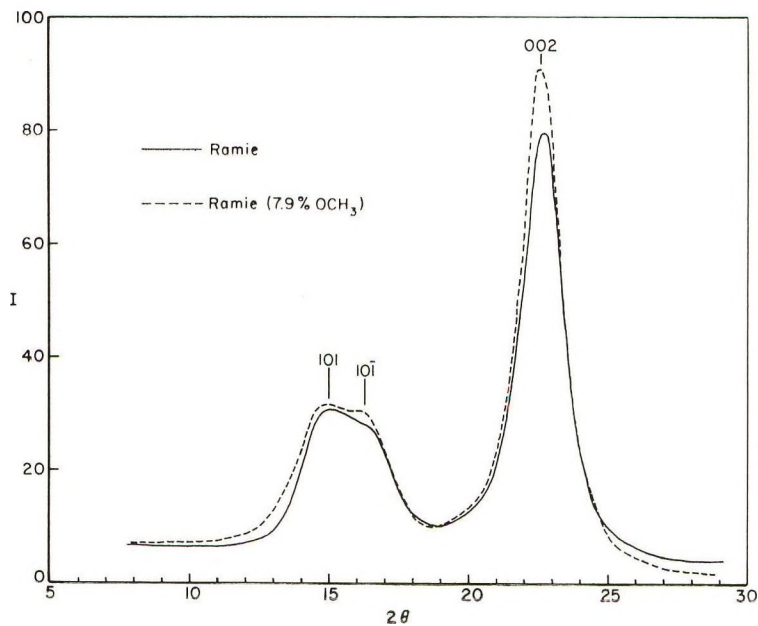

Fig. 2. Equatorial scans from the x-ray diagrams of (———) ramie and (- -) methylated ramie with a methoxyl content of 7.9%. (Semicylindrical camera, R = 5.73 cm.)
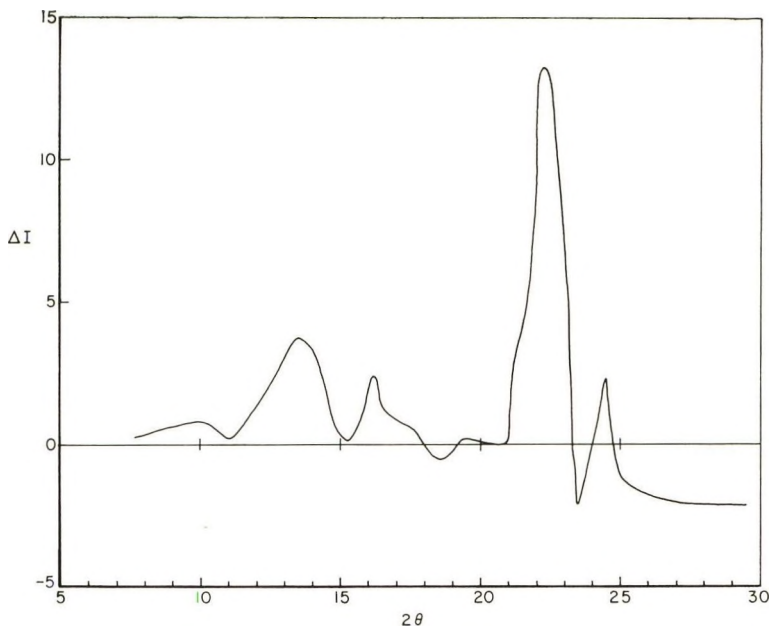
Fig. 3. Residual intensity after subtraction of the equatorial scan for ramie from that for methylated ramie with a methoxyl content of 7.9%.

photographs were retaken with sodium fluoride powder dusted onto the bundles to act as a calibration standard. When reference was made to the sodium fluoride lines superimposed on the photographs it was still found that the curve for the treated sample had slight shifts in the peak positions relative to the curve produced from the blank. It was therefore concluded that the shifts shown are genuine.

To bring out the essential differences of these curves, the difference in intensity at different 2θ values has been plotted versus 2θ (Fig. 3). Although a shift in the curves relative to each other along the 2θ axis can cause peaks and troughs to appear on such a difference curve, the peaks that appear do not have appreciable troughs associated with them, and must, therefore, have additional causes for their appearance. The conclusion is made plausible by reference to the original curves. These peaks appear in the ranges 11–$15.3°$ (max. at $13.5°$), 15.3–$18°$ (max. at $16.2°$), and 21–$23.3°$ (max. at $22.3°$) in 2θ. It is evident that they are associated with alterations in the 101 ($14.7°$), $10\bar{1}$ ($16.3°$), and 002 ($22.6°$) peaks and there is no evidence of an additional peak developing at $2\theta = 20°$, which might be attributed to scatter from amorphous material.

It would appear from this evidence that up to a methoxyl content of 4.3% very little detectable difference is found. However, in the light of the later evidence a tendency for changes in the 101 region of the curve is present, but not great enough to be positively attributed to structural changes. At a methoxyl content of 7.9%, changes consistent with the formation of

crystallites with large interplanar spaces than normal are beginning to develop; no doubt most of the crystalline regions are still unaffected, but the diffraction envelope is the sum total of the diffraction from both the unchanged and changed crystalline regions.

There is no evidence that a single peak at about $2\theta = 20°$ is developing preferentially to the rest of the pattern. Such a peak might be expected if the cellulose contained regions in which chains took all possible directions[7] (so-called amorphous regions), and methylation was taken place randomly
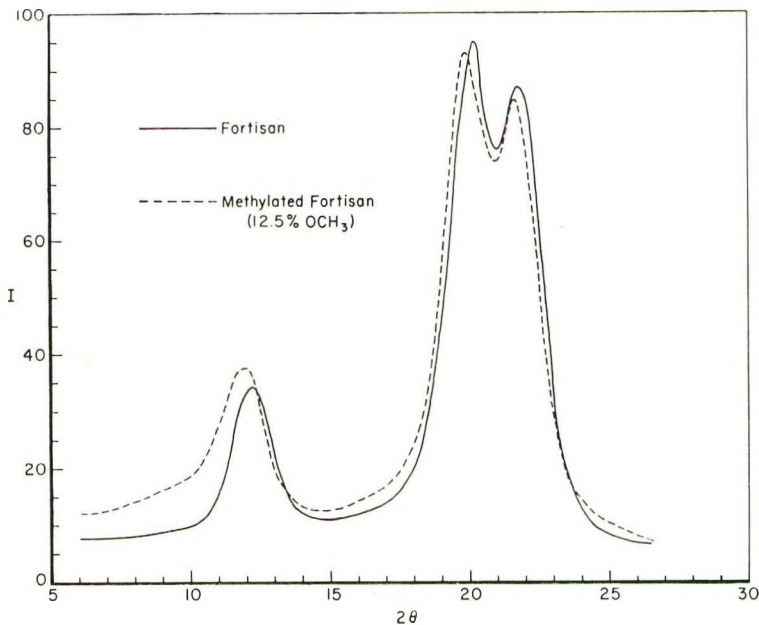

Fig. 4. Equatorial scans from the x-ray diagrams of (———) Fortisan and (- -) methylated Fortisan with a methoxyl content of 12.5%. (Semicylindrical camera, $R = 5.73$ cm.)

in such regions. Nor is there any suggestion that such regions are developed as a result of partial methylation in the fringe of the crystalline regions.

It thus became desirable to compare these results with those for the methylation reaction of ethereal diazomethane on a sample of cellulosic rayon, and for this purpose Fortisan was chosen, since it gives an excellent x-ray diagram. Figure 4 gives the equatorial scans for this fiber before and after methylation to a methoxyl content of 12.5%. These scans have been scaled in accordance with the main-beam calibration spot, but again orientation differences were within the experimental error (50% half-angle = 6.5 and 6.7 for the untreated and the treated Fortisan, respectively), and correction for orientation was thus unnecessary. Figure 5 gives the corresponding difference curve.

It is evident again that there is a shift of all the main peaks to smaller 2θ values, that is, there is evidence for greater interplanar spacings in the crystalline regions. The greatest effect is seen to be at right angles to the 101 planes, that is, in a direction that causes an increase in the interplanar spacing of these planes. The peaks in the difference curve for $2\theta > 18°$ can be mainly accounted for by the shift in the curves that can be seen in Figure 4. However, there is evidence that peaks are developing in the regions $2\theta = 6-12°$ and $13-18.5°$. Part of the peak in the region of $2\theta = 6-17°$ is due to the increase in height and shift in position of the 101 peak of the cellulose, but there still remains evidence of peak developing around 2θ
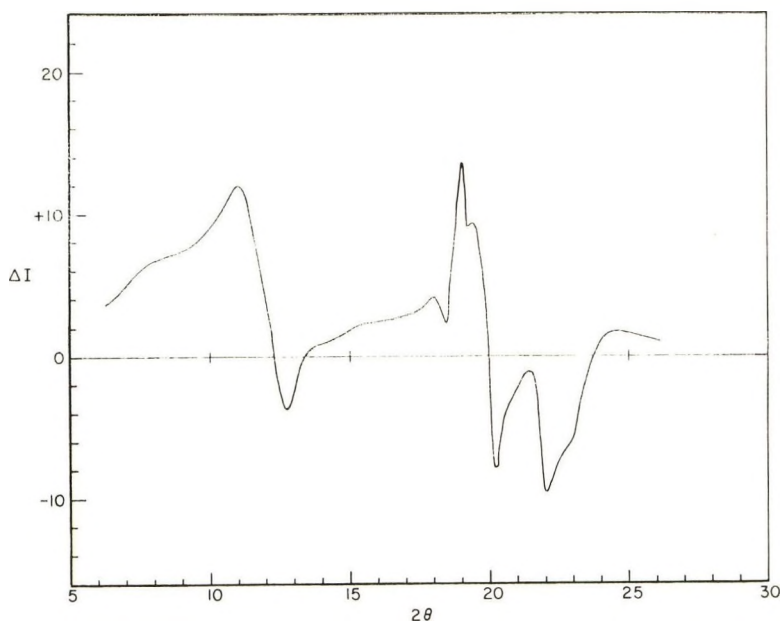

Fig. 5. Residual intensity after subtraction of the equatorial scan for Fortisan from that of methylated Fortisan with a methoxyl content of 12.5%.

$= 8°$. Although part of the peak in the difference curve in the region $2\theta = 13-18.5°$ can be attributed to a shift of the $10\bar{1}$ peak to lower 2θ values, again there remains a broad residual peak $2\theta = 16-17°$ that seems to be additional to the main pattern. Further discussion of these features will be given after a consideration of the results for the regenerated cellulose film that add support to these data.

Results from Regenerated Sheet (Cellulose II)

X-ray results from the regenerated sheet are not so detailed as with Fortisan because these sheets were isotropic. Furthermore it was not easy to standardize the exposure and therefore for purposes of comparison, the curves (Fig. 6) were made to coincide on the $(021 + 10\bar{1} + 002)$ peak.

TABLE I
Measurements on Films Deuterated in the Noncrystalline Regions

Sample	D.S.	$A_{crystalline}/$ thickness (in μ)	Peak frequency of OD band, cm.$^{-1}$	Half-band width of OD band, cm.$^{-1}$
Unethylated	0	0.050	2458	165
cellulose	0.47	0.055	2557	130
	0.68	0.060	2559	130
Methylated	0.75[a]	0.050	2559	125
celluloses	0.75[a]	0.055	2559	125
	0.75[a]	0.060[b]	2560	128

[a] Three different portions of the same methylated cellulose deuterated separately.
[b] Film masked for infrared and β-gauge measurements.

The general observations are similar to those with Fortisan; there is some evidence for a shift of the $10\bar{1}$ peak, but the evidence is confused with regard to the 002 peak. However, the curves clearly are altered the most in the region of $2\theta = 7$–$13°$ and to a smaller extent in the large $2\theta = 13$–$20°$. Furthermore, these alterations become progressively more marked as the degree of methylation is increased, and there is thus no doubt that they are
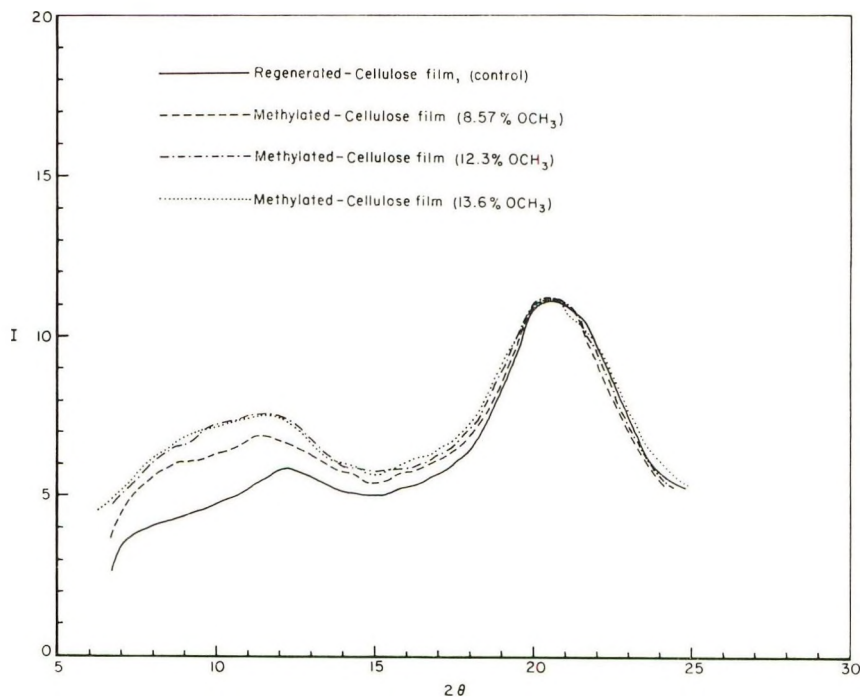

Fig. 6. Equatorial scans from the x-ray diagrams of (———) regenerated cellulose film and methylated regenerated cellulose films with various methoxyl contents: (- -) 8.6; (—·—) 12.3; (···) 13.6%. (Cylindrical camera, $R = 3$ cm.)
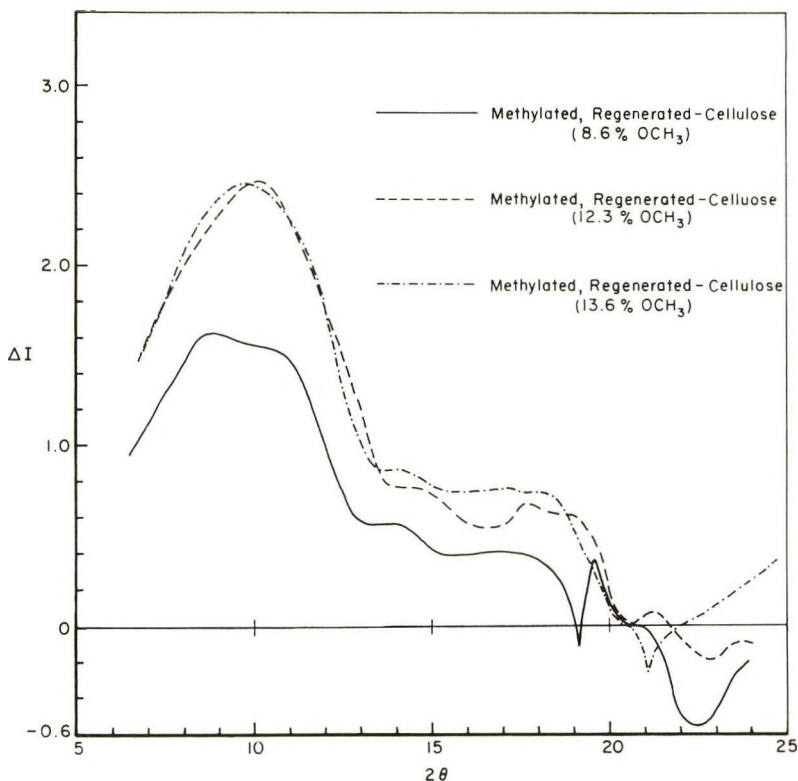
Fig. 7. Residual intensities after subtraction of the equatorial scan for regenerated celulose film from those of methylated regenerated films with various methoxyl contents: (1———) 8.6%; (- -) 12.3%; (—·—) 13.6%.

due to the methoxyl content of the samples. The difference curves (Fig. 7) necessarily agree at the $(021 + 10\bar{1} + 002)$ peak, because of the method of scaling applied to the intensity curves, and consequently little information about change in the region of this composite peak is available.

The infrared results are relevant to this section and can be used to elucidate further the type of reaction taking place. Any methylation of crystalline regions would be expected to diminish the intensity of the hydroxyl absorption bands remaining after deuteration of the noncrystalline regions.

As far as can be judged from the results given in Table I there is no evidence that the crystalline regions have been attacked during methylation, although the accuracy of the measurements is not sufficient to rule out the possibility that up to ca. 10% of the crystallite hydroxyl groups have been replaced. (This figure is estimated from the variation in the $A_{OH(crystalline)}$ thickness values for the film DS = 0.75 and the accuracy of the β-gage thickness measurements.) Thus there is definite experimental evidence that the chemical reaction occurs mainly in the noncrystalline regions, and, as expected, the intensities of the noncrystalline OD bands of the methyl-
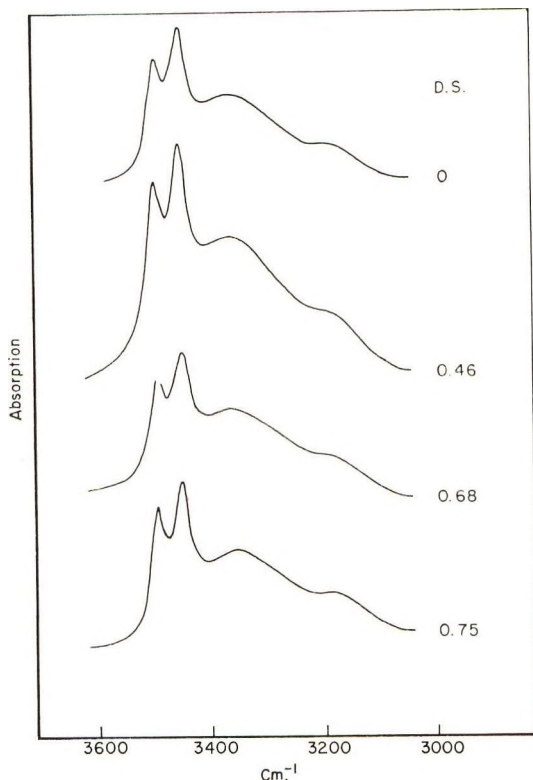
Fig. 8. Hydroxyl absorption bands in films deuterated in the noncrystalline regions

ated samples are lower than those of the untreated sample. For reasons given below, however, a quantitative measure of the extent of this attack in noncrystalline regions is not obtainable from the OD band intensities.

Quite apart from the intensity considerations discussed above, the absence of attack on crystalline regions is strongly suggested by the constancy of shape of the absorption bands of the undeuterated hydroxyl groups (see Fig. 8). There is a possible alternative, namely, that methylation has occurred in the crystalline regions without changing the nature of the unmethylated crystalline portion, but this possibility is rejected on the grounds that formation of methyl groups in crystalline regions would produce distortion of the neighboring unmethylated portions of the original crystallites. Such distortions would be expected to change the hydrogen-bonding system of the hydroxyl groups of these neighboring regions without being sufficient to render all of these same hydroxyl groups accessible to deuteration. Therefore, this should lead to a change in the shape of the hydroxyl bands in the deuterated spectra, whereas no such change is indicated in Figure 8.

Figure 9 shows the OD band in the spectra of noncrystalline deuterated films of both the original and the methylated celluloses. (The absorbance

Fig. 9. OD absorption bands in films deuterated in the noncrystalline regions.

of each OD band has been scaled to give the same peak absorbance through-
out.) The change on methylation is quite obvious (see also Table I) and
precludes the use of intensity measurements on this band to determine the
number of OD groups relative to the unmodified cellulose, since the change
is almost certainly accompanied by a change in the absorption intensity
per OD group.

This change is taken as evidence that methylation has affected the hydro-
gen-bonding system of the OH groups left in the noncrystalline regions after
methylation. For reasons given above this view is to be preferred to the
alternative one that the changes in the OD band are due to the formation,
in regions originally crystalline, of OH groups accessible to D_2O vapor.

The change is virtually complete in the film with the lowest D.S. investigated (0.46), and the three methylated celluloses have very similar OD bands. (The similarity may be even greater than Figure 9 suggests, for the low-frequency "tail" is slightly doubtful in the film with D.S. = 0.68.) The main difference from the unmethylated film is on the low frequency side of the band, where the absorbance of the methylated films is lowered appreciably more than on the high frequency side. (It must be remembered that the peak absorbances have been scaled to give the same reading, and that the intensity across the entire 2200–2700 cm.$^{-1}$ region of the spectrum decreases on methylation; what we are discussing here are the relative decreases.) This means that the hydroxyl groups left in the noncrystalline region after methylation are less strongly hydrogen-bonded on the whole than those in the noncrystalline regions of the original cellulose, and that the range of hydrogen-bond strengths is narrower in the methylated samples. The former effect was to be expected and can be accounted for quite simply by the steric effect of the methyl groups. The latter effect, however, could not have been predicted. It means that methylation has not affected the hydrogen-bonding system of the noncrystalline hydroxyl groups uniformly throughout the region in which they occur, otherwise the band-shape would be unaltered and merely shifted in frequency.

GENERAL DISCUSSION OF RESULTS

It has been shown above that both for samples of cellulose I and cellulose II the x-ray results show a distinct change in the x-ray diagrams after methylation of the samples. Such a change could be interpreted as evidence for attack on the crystalline regions, but for cellulose II samples infrared evidence fails to find such attack, and therefore some reconciliation between the two results for cellulose II is required.

It is convenient to discuss the evidence for cellulose I separately from that for cellulose II because it is believed that the fine structures of these two forms of cellulose are basically different.

For samples of cellulose I it has been shown from a study of the difference curves that there is little or no evidence for randomly arranged chains, so that changes found can be attributed to lattice changes. The question then arises whether any methylcellulose crystallites are being formed simultaneously with the breakdown of the cellulose lattice.

Two forms of methyl cellulose reported by Hess et al.[9-11] are relevant to the discussion: the "halbmethyl-cellulose" of Hess and his co-workers, with strong equatorial reflections at θ = 9.36–9.0° and 19.66–19.5°, and trimethylcellulose with strong equatorial reflections at 2θ = 8.1° and 20.24°; (there are weaker reflections at 2θ = 20.4° and 16.1° respectively but these are less likely to be detected). Both forms have meridional reflections with 2θ = 19.5° and 17.1° respectively, that might contribute to the equatorial x-ray diagrams of isotropic sheet.

If these values of 2θ are compared with the observed difference peaks for

samples of ramie it will be seen that there is no evidence for the presence of either of these methylcellulose lattices. The results can be explained without postulating the existence of another form of methyl cellulose. The data show the mode of reaction with ethereal diazomethane where the experimental conditions cause a minimum disturbance of the original fine structure. The simplest interpretation is that the main attack is on the hydroxyl groups that are approximately at right angles to the 101 plane. (In this work the simple cell of Meyer and Misch[8] is found convenient for description purposes but this must not be taken to imply that this is the correct cell for cellulose.) Such an attack must cause an expansion of the lattice to accommodate the new methoxyl groups, and according to how these groups lie in relation to the chains will the relative intensities of the reflections of the x-ray diagram be changed.

Since the smallest changes in lattice spacing seems to be the $(10\bar{1})$ and (002) planes the methoxyl groups must lie in or near these planes, causing the greatest change in the spacing of the 101 plane, as found. The data are therefore consistent with a lattice that in expanding approximately at right angles to the (101) plane, and this would mainly presuppose the formation of a new peak at lower 2θ values than that for the (101) plane, which is observed. At this stage of the reaction probably no stable methyl cellulose structure has been formed. What is remarkable is that such lattice changes are evident for such a low methoxyl content at 7.9%.

In explanation of these facts it is suggested that up to a methoxyl content of 4.3% the accessible internal surfaces are methylated, and above this methoxyl content the crystalline regions are being attacked already, but owing to the rigidity of the system it is impossible for the chains to take up the positions for a true methylcellulose crystal structure. Such a picture is more consistent with the methylation of fibrils in which the fibrillar surfaces are first methylated followed later by the methylation of the more accessible near-crystalline regions in the fibrils, rather than methylation in a crystalline–amorphous network of the type generally attributed to cellulose. It is of interest to note that even after the treatment of cellulose successively six times with diazomethane Head[4] did not achieve a methoxyl content higher than 14.9%. This suggests that diazomethane has extreme difficulty in penetrating the crystalline lattice of cellulose, and by inference such a crystalline structure must be extensive. However, it is also true, as shown by the present investigation, that diazomethane can penetrate some imperfectly crystalline regions and hence cannot be used as a measure of the proportion of noncrystalline material.

On the other hand, with cellulose II samples the additional peaks revealed by the difference curve could be attributed to a form of methylcellulose, although there is in addition a broad region between 15–20° (2θ) that cannot easily be attributed to a methyl derivative.

In the cellulose II films the infrared evidence seems to suggest that all the attack has taken place in the noncrystalline regions whereas the x-ray evidence suggests that attack on the crystallites has also taken place. This

apparent contradiction is due to the fact that the two techniques do not de-
tect and measure completely identical regions of the cellulose. Recently,
for instance, Dr. R. Jeffries of these laboratories has shown that it is possi-
ble to prepare material that is found to be at least 98% (and probably
100%) noncrystalline by the infrared-deuteration technique, yet x-ray
analysis detected the presence of crystalline regions. Clearly chains that
react with deuterium oxide can be sufficiently close to neighboring chains
to give the diffraction effects of imperfect crystalline regions. In view
of this, it is suggested that the cellulose II samples contain imperfectly
crystalline regions that diffract x-rays but appear to be noncrystalline (i.e.,
accessible) to the infrared-deuteration technique.

Thus it is suggested that in cellulose II methylation initially proceeds on
to the accessible internal surfaces that can be either single chains or groups
of chains. Further reaction then takes place in the imperfectly crystalline
material, resulting in methoxyl groups occupying positions in the unit cell
approximately between the (101) planes and causing a lattice expansion in
these regions mainly in the direction of the normal to these planes. Such
an expansion and position of the methoxyl groups will affect the (10$\bar{1}$) and
(002) planes as well, according to the actual positions occupied by the
groups, thus accounting for the shifts in the main peaks observed. It is
probable that it is this regions that is detectable by x-rays but indetectable
by infrared techniques. Furthermore, this methylated region is the most
likely one to be reoriented to form an imperfect methylcellulose crystalline
regions, and thus further contribute to the x-ray diffraction pattern. It
should be understood that the highly ordered crystalline regions will still
contribute to the x-ray pattern in the same way throughout, the apparent
shifts of peaks being due to the superimposition of the diffraction pattern
from the rest of the material, which on methylation has altered, on to the
original pattern. It is the differentiation of these highly-ordered regions
from the rest of the material that is studied by the infrared technique and
accounts for the fact that this technique finds no attack on the crystalline
regions due to methylation.

There remains the region in the range $2\theta = 15-20°$ that cannot be
directly accounted for by simple changes in lattice dimensions. This
region is thought to be due to diffraction from regions of lower order than
crystalline regions that would give an equatorial streak that would become
more intense as methylation of these regions took place. Such regions seem
to be present in Fortisan but not in ramie. Thus the fine structure picture
emerges from this study that in Fortisan there are regions of different de-
grees of order, some of which could be classified as noncrystalline in that the
chains may still be approximately parallel but have no set relation with
each other. Whether a true amorphous region exists, i.e., one in which
there is zero order in all directions, is doubtful; its absence is difficult to
prove, however, since Mann and his co-workers[12] have obtained indications
of such a region in a weak, diffuse halo found on x-ray diagrams of Fortisan.

The situation in regenerated cellulose films is very similar to that in

Fortisan, but owing to the use of isotropic films the evidence is not quite so clear. Further discussion of these results is therefore unnecessary.

Thus with cellulose II, although there is more evidence for the formation of a methylcellulose crystal structure than with cellulose I, there are no marked reflections of methylcellulose such as were found for a sample of methylated mercerized ramie of similar methoxyl content by Hess et al.[9,10] The mode of reaction of ethereal diazomethane is thus different from that of dimethyl sulfate in the presence of caustic soda. This is perhaps not surprising, since in the ethereal diazomethane reaction the cellulose structure is not highly swollen, and in consequence it is less likely that segments of methylated cellulose chains can rearrange easily to form the correct spatial arrangement for crystalline forms of methyl cellulose.

These results are quite consistent with those obtained by Sitch,[2] who for other reasons thought that treatment with diazomethane caused the methylated samples to be more accessible to acid hydrolysis. It has been shown here that at a certain stage of the reaction there is evidence of a disturbance of the imperfectly crystalline regions, even in the dry state. It might therefore be inferred that more material would be accessible to acid attack, as was found by Sitch, and such an attack would be further aided by the fact that weaker hydrogen bonding would be possible in the nonordered regions.

References

1. Reeves, R. E., and W. A. Sisson, *Contrib. Boyce Thompson Inst.*, **13**, 11 (1943).

2. Sitch, D. A., *Shirley Inst. Mem.*, **26**, 89 (1952); *J. Textile Inst.*, **44**, T407 (1953).

3. De Boer, Th. D., and H. J. Backer, *Rec. Trav. Chim.*, **73**, 229 (1954).

4. Head, F. S. H., *Shirley Inst. Mem.*, **25**, 209 (1951); *J. Textile Inst.*, **43**, T1 (1952).

5. Marrinan, H. J., and J. Mann, *J. Appl. Chem.*, **4**, 204 (1954).

6. Mann, J., and H. J. Marrinan, *Trans. Faraday Soc.*, **52**, 492 (1956).

7. Ellefsen, Ø., E. W. Lund, B. A. Tønneson, and K. Øien, Meddelelse NR. 87 Fra Papirindustriens Forskninginstitutt, Oslo, 1957.

8. Meyer, K., and L. Misch, *Helv. Chim. Acta*, **20**, 232 (1937).

9. Hess, K., and C. Trogus, *Z. Phys. Chem.*, **B15**, 157 (1931).

10. Hess, K., C. Trogus, W. Eveking, and E. Garthe, *Ann.* **506**, 760 (1933).

11. Trogus, C., and K. Hess, *Z. Phys. Chem.*, **B4**, 321 (1929).

12. Mann, J., *Proceedings Wood Chemistry Symposium, Montreal* **1961**, Butterworth, London, 1962; K. J. Heritage, J. Mann, and L. Roldan Gonzalez, *J. Polymer Sci.*, **A1**, 671 (1963).

Résumé

Une étude par infra-rouge et rayons X de l'action du diazométhane sur la structure fine de la ramie et de la cellulose régénérée (fibre et film) a été effectuée. On a trouvé que le processus de méthylation affecte les régions désordonnées, et aussi les parties de la structure qui sont suffisamment ordonnées pour être dectetées par les méthodes aux rayons-X mais dont l'ordre de liaison-hydrogène est trop bas pour être detecté par la technique infra-rouge au deutérium. L'effet de la méthylation partielle sur la liaison hydrogène dans les régions non-cristallines est décrit et discuté. Les résultats

nous permettent de conclure que le diazométhane peut réagir dans les régions non-
cristallines et les régions imparfaitement cristallines mais non dans les régions de cri-
tallinité élevée.

Zusammenfassung

Eine Infrarot- und Röntgenstrahlenuntersuchung der Wirkung von Diazomethan
auf die Feinstruktur von Ramie und regenerierte Zellulose (Faser und Film) wurde
angestellt. Es wurde gefunden, dass der Methylierungsprozess die ungeordneten
Bereiche beeinflusst sowie auch Teile der Struktur, die eine für Röntgenmethoden aus-
reichend hohe Ordnung besitzen um entdeckt zu können deren Wasserstoffbindungsord-
nung aber nicht für die entdeckung durch das Infrarot-Deuterioerungsverfahren ausreicht.
Die Wirkung der partiellen Methylierung auf die Wasserstoffbindung der nichtkris-
tallinen Bereiche wird beschrieben und diskutiert. Aus den Ergebnissen wird gesch-
lossen, dass Diazomethan im nichtkristallinen Bereich und im unvollkommen kristallinen
Bereich reagieren kann, nicht dagegen im kristallinen Bereich hoher Ordnung.

Inadequacies in Time–Temperature Equivalence

N. G. McCRUM,* *Plastics Department, Du Pont Experimental Station, E. I. du Pont de Nemours & Company, Inc., Wilmington, Delaware*

Synopsis

The activation energy of the low temperature relaxation in polytetrafluoroethylene is obtained from creep experiments by using the analytical procedure known as time–temperature superposition. The activation energy obtained is 25 kcal./mole which is rejected in favor of the value determined in internal friction experiments, 18 kcal./mole. The discrepancy is attributed to temperature variation of the limiting compliances which cause the value obtained using time–temperature superposition to be too high. Comparable discrepancies are anticipated for relaxations in crystalline polymers and amorphous polymers at temperatures below the glass transition.

INTRODUCTION

Before applying the superposition analysis to the glass–rubber relaxation of amorphous polymers it is the practice to correct the measurements for temperature-induced changes in the relaxed compliance, J_R.[1,2] The validity of the analysis is due to J_R being approximately three orders of magnitude greater than J_U, the unrelaxed compliance. Consequently, after the initiation of relaxation[3] the elastic strain is a minute fraction of the rubber-elastic and may be neglected for all practical purposes.

However for the secondary relaxations which occur at temperatures below the glass transition and for relaxations in crystalline polymers the relaxation strengths are considerably smaller. There is therefore good reason to require that when using the superposition analysis for these relaxations corrections should be made for temperature induced changes in both J_R and J_U. The only alternative is to show that the corrections are smaller than the experimental error, since there can be no doubt that both limiting compliances vary with temperature.

The simplest way of doing this, in principle, is to determine directly the temperature dependence of J_R and J_U. An alternative procedure, adopted in the experiment described below, is to determine the activation energy ΔH_c for a particular mechanism by the superposition of uncorrected creep curves and to compare it with a reference value. In this instance the reference value is the activation energy ΔH_{if} determined from the frequency shift of the temperature of the internal friction peak.

* Present address: Engineering Laboratory, Parks Road, Oxford, England.

Choice of Experiment

In order to test the superposition analysis in the way outlined in the last paragraph, it is necessary to choose a relaxation with the following properties. (*1*) The relaxation must be linear. (*2*) The relaxation must not be overlapped to any significant extent by neighboring relaxations of different origin. (*3*) The specimen must not suffer an irreversible change, such as crystallite melting, while the experiments are in progress. (*4*) A reliable value of the activation energy must be known from internal friction experiments. (*5*) All parts of the distribution of relaxation times should possess the same activation energy.

The low temperature relaxation of polytetrafluoroethylene is known to possess properties (*1*) to (*4*).[4-9] The log $f - 1/T$ plot is linear over 7 decades (f is the frequency at which the internal friction is a maximum at temperature T) and gives a value $\Delta H_{if} = 18$ kcal./mole. Since the relaxation is governed by a distribution of relaxation times,[8] it is clear that at least in the region of the maximum of the distribution the activation energy is equal to 18 kcal./mole. However nothing is known of the activation energy of the wings of the distribution. It is therefore assumed, in the absence of evidence to the contrary, that the value of 18 kcal./mole holds for all parts of the distribution. This value of the activation energy is found for small relaxations as well as large ones, i.e., for specimens of high as well as low density.

Experimental

The specimen of polytetrafluoroethylene was molded from Teflon 7 (du Pont registered trade mark) fluorocarbon resin and cooled at 3°C./min. from the sintering temperature, 375°C.

The creep apparatus was in most essentials similar to that of Ke and Ross,[10] except that the coil producing the torque was mounted above the specimen after the manner of Morrison, Zapas, and DeWitt.[11] The specimen was a flat strip of size $3 \times 0.5 \times 0.060$ in. Torque was produced by current drawn from a storage battery or for oscillating experiments, from a sine wave generator. The rotation of the coil was observed by the deflection of two light beams reflected from a concave mirror attached to the coil. The deflection was observed with a kymograph for times of 0.3–30 sec. and simultaneously, by use of the other light beam, by eye and scale for 10–180 sec. The current was measured by recording the deflection of a high speed galvanometer in the kymograph.

The maximum strain was of the order of 10^{-3}. The shape of the specimen leads to a strain which varies across the specimen but this is not significant so long as the relationship between stress and strain is linear. Linearity was frequently checked by measuring the dependence of compliance on stress. Departures from linearity at all stresses used in the experiments were less than the experimental error.

The coil constant (torque per unit current) was determined as follows.

The dynamic compliance and logarithmic decrement for the specimen were measured at 23°C. with a torsion pendulum. The specimen was then mounted in the creep apparatus, also at 23°C., and an oscillating current passed through the coil at a frequency equal to that of the torsion pendulum. The coil constant was calculated from the film trace of the galvo and coil deflections using the compliance and logarithmic decrement determined with the torsion pendulum.

Temperature control at low temperatures was maintained by monitoring the flow of cooling gas by use of a cryostat similar to that described elsewhere.[12]   Before measurement, the temperature was maintained constant until equilibrium was reached.   Each experiment lasted for 180 sec., and in this time the temperature drift was always considerably below 1°C.

Results

The creep experiments were made with the same specimen at successively lower temperatures between −70.4°C. and −153.1°C.   The results are shown in Figure 1, in which the logarithm of the creep compliance, log $J(t)$, is plotted against log t.

The location and magnitude of the relaxation in the creep curves correlates with the results of internal friction experiments.   At constant temperature
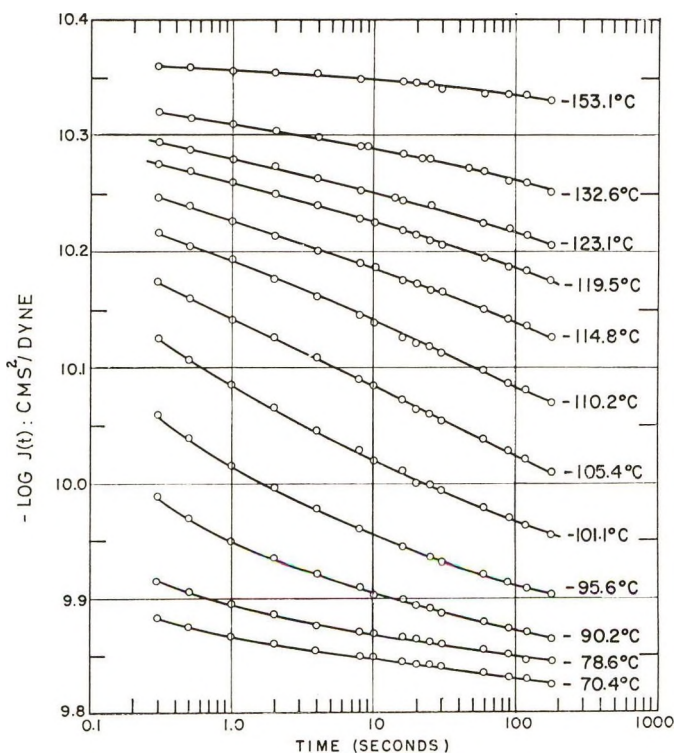

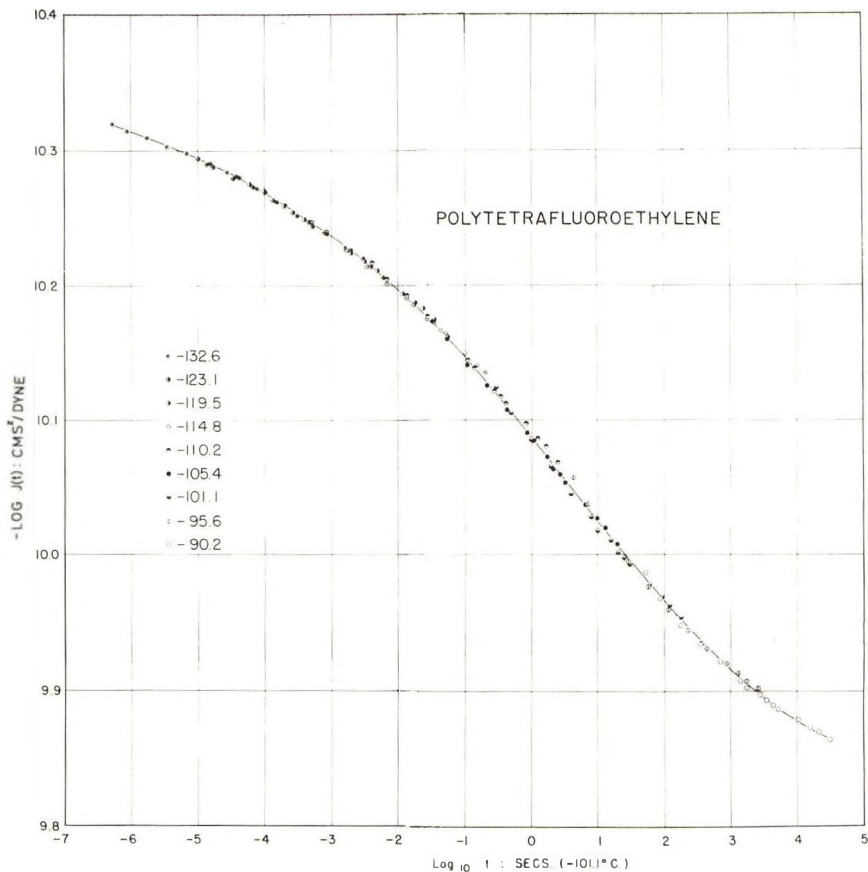Fig. 1. Creep compliance as a function of time.

Fig. 2. Compliance curves shown in Fig. 1, superposed by horizontal shifts with respect to the curve at −101.1°C.

the approximate relation between compliance and logarithmic decrement $\delta(\nu)$ at frequency ν is given[13] as:

$$\delta(\nu) = \frac{\pi^2}{2}\left(\frac{d \log J(t)}{d \log t}\right)_{t = 1/8\nu} \tag{1}$$

The peak in the logarithmic decrement of this specimen occurs at −100°C. (1 cycle/sec.) and is of height 36×10^{-2}. At −101.1°C. we note that according to eq. (1), $d \log J(t)/d \log t$ should be of maximum slope in the region below 1 sec., as is indeed the case in Figure 1. The maximum value of $d \log J(t)/d \log t$ predicts a peak of 38×10^{-2} in reasonable agreement with the measured value.

The creep curves shown in Figure 1 were superimposed by translations along the time axis (Fig. 2). The theory of superposition[1,2,14] yields the result that if the temperature dependence of J_U and J_R be neglected, each
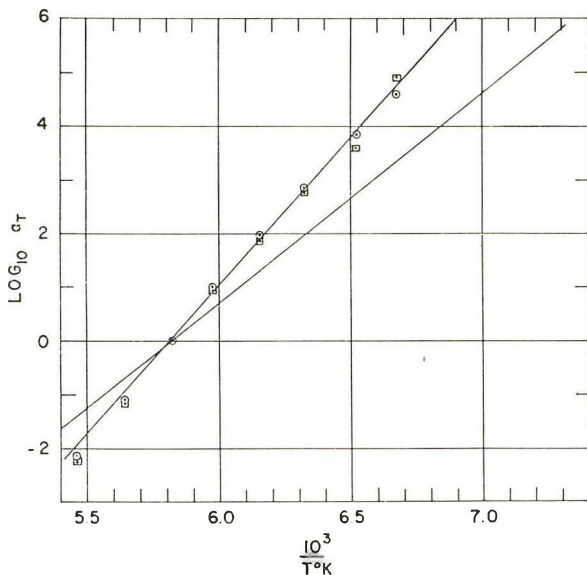
Fig. 3. Logarithm of the shift factor a_T as a function of $10^3/T°$K. Two independent superpositions are recorded by the circles and squares. The activation energy according to eq. (2) is 25 kcal./mole. The line without points has a slope which would yield an activation energy of 18 kcal./mole by eq. (2).

creep curve at T when shifted an amount log a_T with respect to the curve at T_0 ($T_0 = -101.1°C.$) superimposes to form a smooth master curve.

$$\log a_T = \frac{\Delta H_c}{2.30R}\left(\frac{1}{T} - \frac{1}{T_0}\right) \qquad (2)$$

The variation of log a_T with $10^3 T$ (where T is absolute temperature) is shown in Figure 3. In order to obtain an estimate of the subjective error, two separate superpositions were performed, and the two sets of log a_T are plotted in Figure 3. A reasonable fit to all the points was obtained by a straight line yielding a value of $\Delta H_c = 25$ kcal./mole by eq. (2). The second straight line in Figure 3 has a slope which would yield an activation energy of 18 kcal./mole. It is quite clear that ΔH_c obtained from the superposition of the creep curves is higher than ΔH_{if} by an amount well outside the experimental error.

Only the creep curves in the centre of the relaxation region were used to obtain ΔH_c. There are several reasons for this selection, the most important being that in making the comparison between ΔH_c and ΔH_{if} it seemed best to exclude as much as possible the effects of the wings of the distribution of relaxation times. Another reason, purely experimental, is that shift factors can be measured more accurately the greater the slope of the creep curve. The creep curves used to obtain ΔH_c are those measured at approximately 5°C. intervals between -90.2 and $-123.1°C.$

It turns out that the log a_T points for the creep curves at -78.6 and $-70.4°$ C. would fall directly on the 25 kcal. line of Figure 3. This is not true for the log a_T points for $-132.6°$C. and $-153.1°$C. which if used would cause the log a_T–$1/T$ plot to bend over concave to the $1/T$ axis. The obvious explanation is that the activation energy decreases at temperatures below $-123°$C. Verification of this hypothesis is outside the scope of this paper and would require the measurement of creep curves at more closely spaced temperatures below $-120°$C.

Discussion

If the creep curves are shifted by amounts log a_T calculated from eq. (1) with $\Delta H_c = 18$ kcal./mole, then the curves do not fall on a single curve (Fig. 4). The creep curve at any particular temperature lies below the
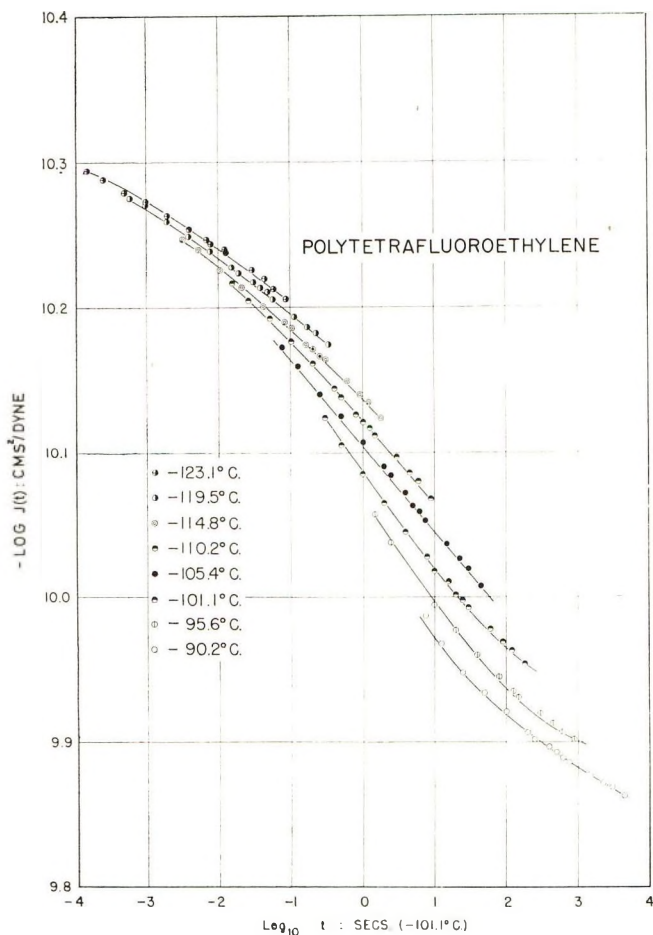

Fig. 4. Compliance curves shown in Fig. 1 shifted horizontally according to an activation energy of 18 kcal./mole.

curve at the next lower temperature. The most reasonable explanation of this is that the displacements are due to the temperature dependence of J_U and J_R. This hypothesis is supported by the following argument.

Experimental values of Young's modulus E, for polytetrafluoroethylene, have been determined by Baccaredda and Butta[7,15] at low temperatures at ca. 2×10^4 cycles/sec. We assume that at these frequencies in the region $-123°C.$ to $-90°C.$ the rate of decrease of E is caused by temperature variation of E_U alone; that is, relaxation is negligible. If Poisson's ratio is constant, then this rate of decrease, which varies from 0.1 to 0.7%/°C., is also that of G_U. This implies that the rate of increase of J_U between $-123°C.$ and $-90°C.$ varies from 0.1 to 0.7%/°C.

It is clear from the work of Baccaredda and Butta that there is no large difference between the temperature coefficients of J_U and J_R. Consequently we assume that they are equal and write:[16]

$$(J_R{}^T - J_U{}^T) = b_T(J_R{}^{T_0} - J_U{}^{T_0}) \qquad (3)$$

$J_R{}^T$ and $J_U{}^T$ are the value of the limiting compliances at T and $J_R{}^{T_0}$ and $J_U{}^{T_0}$ the values at T_0. The parameter b_T depends on T and T_0 and is of the order of unity. With the usual assumptions it follows that

$$\log b_T = \log J^T(t) - \log J^{T_0}\left(\frac{t}{a_T}\right)$$

The parameter b_T can therefore be determined from the vertical displacements of the creep curves in Figure 4. The value of b_T so obtained predicts a temperature dependence of J_U of between 0.4 and 1.1%/°C., in reasonable agreement with the high frequency measurements.

The preceding argument depends on the validity of eq. (3), which will be discussed in greater detail elsewhere.[17] Equation (3) is used here as a plausible hypothesis to show that ΔH_c derived from superposition is too high because of the temperature dependence of the limiting compliances. A similar discrepancy between ΔH_c and ΔH_{tf} for the β-relaxation in poly(methyl methacrylate) has also been shown to be due to the temperature dependence of the limiting compliances.[18] This temperature dependence, which cannot be caused by structural changes in the several senses described by Catsiff, Tobolsky, and Offenbach[19] and Nagamatsu,[20] is probably a consequence of the thermal expansion of the solid. There is every reason, therefore, to believe that for crystalline polymers and amorphous polymers in the glassy state correct values of ΔH_c will be obtained from superposition only after elimination of the effects due to temperature dependence of the limiting compliances.

References

1. Tobolsky, A. V., *Properties and Structure of Polymers*, Wiley, New York, 1960.
2. Ferry, J. D., *Viscoelastic Properties of Polymers*, Wiley, New York, 1961.
3. Ferry, J. D., and E. R. Fitzgerald, *J. Colloid Sci.*, **8**, 224 (1953).
4. Wolf, K., and K. Schmieder, *Ricerca Sci. (Suppl.)*, **25A**, 732 (1955).

5. Sauer, J. A., and D. E. Kline, *J. Polymer Sci.*, **118**, 491 (1955).

6. Kabin, S. P., *Sov. Phys. Tech. Phys.* **1**, 2542 (1957).

7. Baccaredda, M., and E. Butta, *J. Polymer Sci.*, **31**, 189 (1958).

8. McCrum, N. G., *J. Polymer Sci.*, **27**, 555 (1958).

9. Illers, K. H., and E. Jenckel, *Kolloid-Z.*, **160**, 97 (1958).

10. Ke, T. S., and M. Ross, *Rev. Sci. Instr.*, **20**, 795 (1949).

11. Morrison, T. E., L. J. Zapas, and T. W. DeWitt, *Rev. Sci. Instr.*, **26**, 357 (1955).

12. McCrum, N. G., *J. Polymer Sci.*, **34**, 355 (1959).

13. Zener, C., *Elasticity and Anelasticity of Metals*, Univ. Chicago Press, Chicago, 1956.

14. Alfrey, T., *Mechanical Behavior of High Polymers*, Interscience, New York, 1948, p. 132.

15. Baccaredda, M., and E. Butta, *Ann. Chim. (Rome)*, **49**, 559 (1959).

16. McCrum, N. G., and E. L. Morris, *Phil. Mag.*, **7**, 2115 (1962).

17. Morris, E. L., and N. G. McCrum, to be published.

18. Morris, E. L., and N. G. McCrum, *J. Polymer Sci.*, **B1**, 393 (1963).

19. Catsiff, E., A. V. Tobolsky, and J. Offenbach, *J. Colloid Sci.*, **11**, 989 (1956).

20. Nagamatsu, K., *Progr. Theor. Phys. Suppl.*, No. 10, 73 (1959).

Résumé

On obtient l'énergie d'activation de la relaxation à basse température de polytétrafluoroéthylène au départ d'expérience de fluage en utilisant le procédé analytique appelé superposition temps–température. L'énergie d'activation obtenue est de 25 kcal/mole; elle est toutefois rejetée en faveur de la valeur déterminée par des expériences de friction interne, 18 kcal/mole. Cette différence est attribuée à la variation de température des effets limitatifs, avec comme conséquence que les valeurs obtenues en utilisant la superposition temps–température sont trop élevées. Des différences comparables sont prévus pour la relaxation de polymères cristallins et des polymères amorphes à des températures inférieures à la transition vitreuse.

Zusammenfassung

Die Aktivierungsengergie der Tieftemperaturrelaxation von Polytetrafluoroäthylen wird aus Kriechversuchen unter Verwendung der als Zeit–Temperatursuperposition bekannten analytischen Methode gewonnen. Die erhaltene Aktivierungsenergie beträgt 25 kcal/Mol; dieser Wert wird jedoch zugunsten des in Versuchen über die innere Reibung bestimmten Wertes von 18 kcal/Mol verworfen. Die Unstimmigkeit wird der Temperaturabhängigkeit der Grenznachgiebigkeit zugeschrieben, die zu einem zu hohen Wert nach dem Verfahren der Zeit–Temperatursuperposition führt. Vergleichbare Unstimmigkeiten werden für die Relaxation bei kristallinen und amorphen Polymeren bei Temperaturen unterhalb der Glasumwandlung angenommen.

Studies in Condensed Phosphates. Part VI. Paper Chromatographic Studies of Condensed Phosphates

R. C. MEHROTRA* and V. S. GUPTA,† *Chemical Laboratories, University of Gorakhpur, Gorakhpur, India*

Synopsis

Paper chromatographic analysis of the complex polymetaphosphates, i.e., $(Na_x-M_{(1-x)/2}PO_3)_n$, where M is Ca, Ba, or Cu and $x = 1/3$ reveals that the observed values of R_f and R_g for the above derivatives are similar to those for the simple sodium polymetaphosphate $(NaPO_3)_n$, but are different from those of the phosphate anions viz., orthophosphate, pyrophosphate and trimetaphosphates.

INTRODUCTION

Paper chromatography has in recent years proved useful in the separation of phosphate mixtures. A number of studies have been made by several workers.[1-4] Morey[5] in 1952 described the preparation of $Na_4Ca(PO_3)_6$, which was later shown to be a trimetaphosphate derivative $Na_4Ca(P_3O_9)_2$ by Ohashi and Van Wazer.[6] Derivatives corresponding to the $Na_4Ca(PO_3)_6$ composition, among many others, have also been synthesized as described in earlier publications.[7-9] Their properties resemble those of sodium polymetaphosphate, as is evident from a study of such properties as conductivity. Hence it was considered worthwhile to carry out a chromatographic study of these derivatives.

EXPERIMENTAL

A rectangular chromatographic tank (2 ft. × 1.5 ft. × 9 in.), micropipet of 1.0 cc. capacity graduated to 0.01 cc., an ultraviolet source, Whatman special paper No. 1, and a spray bottle were employed.

Reagents

The chromatographic medium was made up from *tert*-butyl alcohol (80 cc.), water (20 cc.), and formic acid (5 cc.).

Ebel's chromatographic solvent[11,12] was made up in two forms: the

---

* Present address: Chemistry Department, University of Rajasthan, Jaipur, India.

† Present address: Planning & Development Division, Fertilizer Corporation of India Ltd., Sindri, Dist. Dhanbad, India.

acidic solvent consisted of isopropyl alcohol (750 cc.), a solution of 50 g. of trichloroacetic acid in water (to total volume of 250 cc.), and concentrated ammonia (2.5 cc.); the *basic solvent* comprised isopropyl alcohol (400 cc.), isobutyl alcohol (200 cc.), water (390 cc.), and concentrated ammonia (10 cc.).

The alcohols were distilled, and reagents were made by mixing and shaking the different solutions in a separatory funnel.

The reagent used to develop the chromatograms was made by moderate heating (i.e., 80°C.) of a solution of 0.4% (w/v) of ammonium molybdate in 8% HNO_3 for 5–10 minutes as described by Block and co-workers.[10]

Preparation of Sample

The sodium polymetaphosphate, complex polymetaphosphates, sodium trimetaphosphate, and sodium calcium trimetaphosphate were prepared as described previously.[13] Tetrasodium pyrophosphate was prepared by dehydrating disodium hydrogen orthophosphate (B.D.H. analytical reagent) at 500°C. for 5–6 hr.[14]

General Technique

Aqueous solutions of each sample, i.e., Graham's salt, sodium trimetaphosphate, tetrasodium pyrophosphate, sodium calcium trimetaphosphate, etc., were prepared by direct weighing (0.025%), and different solutions were spotted separately on the chromatogram (on the straight line) with a micropipet. Each addition of 0.01 cc. solution was followed by drying in order to avoid spreading. After preparing the chromatogram, it was hung from a trough in the tank which was previously saturated with the requisite solvent vapors, care being taken to hang the paper straight. Now the requisite solvent was added in the trough from one side and finally the tank was covered. A duplicate chromatogram was always allowed to run for each solvent in order to confirm the consistency of the experiment. The temperature was 30 ± 2°C. and the time for each run was recorded.

After 20–24 hr. the chromatograms were taken out, dried, sprayed with molybdate reagent, and then again dried. Precautions were taken to avoid excessive wetting with spraying agent. The chromatogram was then exposed to an ultraviolet source; a blue spot develops for each phosphate.

The same procedure was followed for each solvent. A two-dimensional technique was applied only for the derivatives of the type $(Na_{2/3}Ca_{1/6}PO_3)_n$. First the chromatogram was made with Ebel's acidic solvent and then, after drying, basic solvent was used; the rest of the procedure was the same as described before.

RESULTS AND DISCUSSION

The following conclusions may be drawn from the data given in Table I. (*1*) The R_f and R_g values of simple and complex sodium polymetaphosphates are very close to each other and are definitely lower than the corresponding values for the other ring and chain phosphates.

TABLE I

R_f and R_g Values of Various Phosphate Anions on Chromatography with tert-Butyl Alcohol–Water–Formic Acid and Ebel's Acidic Solvent

Phosphate species	tert-Butanol–Water–Formic Acid								Ebel's acidic reagent	
	Run I		Run II		Run III		Run IV			
	R_f	R_g	R_f	R_g	R_f	R_g	R_f	R_g	R_f	R_g
Orthophosphate	0.54	—	0.60	—	0.50	—	0.51	—	—	—
Pyrophosphate	0.40	0.74	0.37	0.60	0.32	0.65	—	—	—	0.79
Trimetaphosphate	0.39	0.71	—	—	0.245	0.50	0.30	0.58	—	0.55
$(NaPO_3)_n$	0.094	0.18	0.08	0.13	0.07	0.16	0.085	0.17	—	0.14
$(Na_{2/3}Ca_{1/6}PO_3)_n$	0.094	0.18	—	—	0.05	0.10	—	—	—	0.14
$(Na_{2/3}Ba_{1/6}PO_3)_n$	—	—	—	—	—	—	0.11	0.21	—	—
$(Na_{2/3}Cu_{1/6}PO_3)_n$	—	—	—	—	0.05	0.10	—	—	—	—
$NaCaP_3O_9$	—	—	—	—	—	—	0.27	0.54	—	—

(2) One more spot equivalent to $P_3O_9{}^{-3}$ was found in each chromatogram for simple and complex sodium metaphosphates. The presence of ring phosphates on breaking of long chain phosphates in solution has also been reported by Thilo et al.[15] It was also noticed in the case of each simple phosphate as well as in complex derivatives that the spots were slightly spread, forming a track. However, there was little variation in the value when the uppermost position of the trail was used to calculate the value of R_g.

(3) The R_f and R_g values for mixed sodium calcium trimetaphosphate are almost the same as those for sodium trimetaphosphate.

The two-dimensional chromatogram for $(Na_{2/3}Ca_{1/6}PO_3)_n$ did not show any point for lower molecular weight phosphates. On correlating the chromatographic results with other properties described in earlier publications[7-9] for complex derivatives, it can be concluded that these derivatives are polymeric in character, similar to sodium polymetaphosphate.

References

1. Ebel, J. P., *Compt. Rend.*, **234**, 621, 732 (1951).

2. Grunze, H., and Thilo, E., *Sitz. Ber. Deut. Akad. Wiss. Berlin, Kl. Math. Allgem. Naturwiss.*, **1953**, No. 5, 26.

3. Van Wazer, J. R., and E. Karl-Kroupa, *J. Am. Chem. Soc.*, **78**, 1772 (1956).

4. Westman, A. E. R., and A. E. Scott, *Nature*, **168**, 740 (1951).

5. Morey, G. W., *J. Am. Chem. Soc.*, **74**, 5783 (1952).

6. Ohashi, S., and J. R. Van Wazer, *J. Am. Chem. Soc.*, **81**, 830 (1959).

7. Mehrotra, R. C., and V. S. Gupta, *J. Polymer Sci.*, **54**, 613 (1961).

8. Mehrotra, R. C., and V. S. Gupta, *J. Polymer Sci.*, **55**, 81 (1961).

9. Mehrotra, R. C., and V. S. Gupta, *J. Polymer Sci.*, **58**, 501 (1962).

10. Block, R. J., E. L. Durrum, and G. Zweig, *A Manual of Paper Chromatography and Paper Electrophoresis*, Academic Press, New York, p. 427.

11. Ebel, J. P., *Bull. Soc. Chim.*, France, **20**, 991, 998, 1085, 1096 (1953).

12. Ebel, J. P., *Mikrochim. Acta*, **1954**, 679.

13. Gupta, V. S., Ph.D. Thesis, Gorakhpur University, India, 1962.

14. Bell, R. N., in *Inorganic Synthesis*, Vol. III, L. F. Audrieth, Ed., McGraw-Hill, New York, 1950, pp. 100-115.

15. Thilo, E., G. Schulz, and E. M. Wichmann, *Z. Anorg. Chem.*, **272**, 182 (1953).

Résumé

L'analyse chromatographique sur papier du complexe de polymétaphosphates, à savoir $(Na_xM_{(1-x)/2}PO_3)_n$ où M est Ca, Ba ou Cu et $x = {}^1/_3$ montre que les valeurs observees pour R_f et R_g pour les dérivés ci-dessus sont presque semblables à celles du polymétaphosphate de sodium ordinaire $(NaPO_3)_n$ mais sont différentes à partir des anions phosphates, à savoir, ortho-, pyro- et trimeta-phosphates.

Zusammenfassung

Die papierchromatographische Analyse von komplexen Polymetaphosphaten, namlich $(Na_xM_{(1-x)/2}PO_3)_n$, wo M Ca, Ba oder Cu und $x = {}^1/_3$ ist, zeigt, dass die beobachteten Werte von R_f und R_g für die oben angeführten Derivate denen des einfachen Natriumpolymetaphosphat $(NaPO)_{3n}$ fast gleich sind, jedoch verschieden von den Phosphatanionen, nämlich Ortho-, Pyro- und Trimetaphosphaten.

Studies in Condensed Phosphates.   Part VII.
Metachromatic Reactions of Sodium
Polymetaphosphate and Its Derivatives

R. C. MEHROTRA* and V. S. GUPTA,† *Chemical Laboratories,
University of Gorakhpur, Gorakhpur, India*

Synopsis

Metachromatic behavior of the complex metaphosphates is almost identical to that of Graham's salt and is quite different from that of either simple or mixed trimeta- or other lower phosphates. With toluidine blue, the wavelength of maximum absorption shifts from 630 to 530 mμ in all the above cases. Addition of calcium or barium chlorides did not show any change in the optical density or wavelength of maximum absorption except at $4.0 \times 10^{-4}M$ barium chloride concentration.

INTRODUCTION

In previous studies of sodium polymetaphosphate and its derivatives, viscosity, conductivity, and chromatography have been investigated.[1-5] The present paper deals with the metachromatic properties of these materials.

Metachromasy is a property of certain dye-stuffs which do not obey Beer's Law. It is generally agreed that such deviations are due to a reversible polymerization of the dye molecules, the polymer exhibiting an absorption spectrum different from that of the monomer. The dyestuffs are adsorbed by stainable substrates in two different shades of color, designated as the normal and the metachromatic color; for example, a toluidine blue gives normally blue color in aqueous solution but it gives metachromatic purple color in sodium polymetaphosphate. Wiame[6] studied the metachromatic effect of sodium hexametaphosphate on toluidine blue. According to this author, a dilute solution of the dye in water gives maximum absorption at 630 mμ, but this maximum shifts to a lower value (530 mμ) in the presence of hexametaphosphate. The change in color from blue to purple is clearly visible.   It was shown by Wiame that a 0.1% solution of hexametaphosphate forms a precipitate if an excess of dye is added.   It was also concluded from his study that orthophosphate, pyrophosphate, and tripolyphosphate derivatives did not exhibit any meta-

* Present address: Chemistry Department, University of Rajasthan, Saipur, India.
† Present address: Planning & Development Department, Fertilizer Corporation of India Ltd., Sindri, Dist. Dhanbad, India.
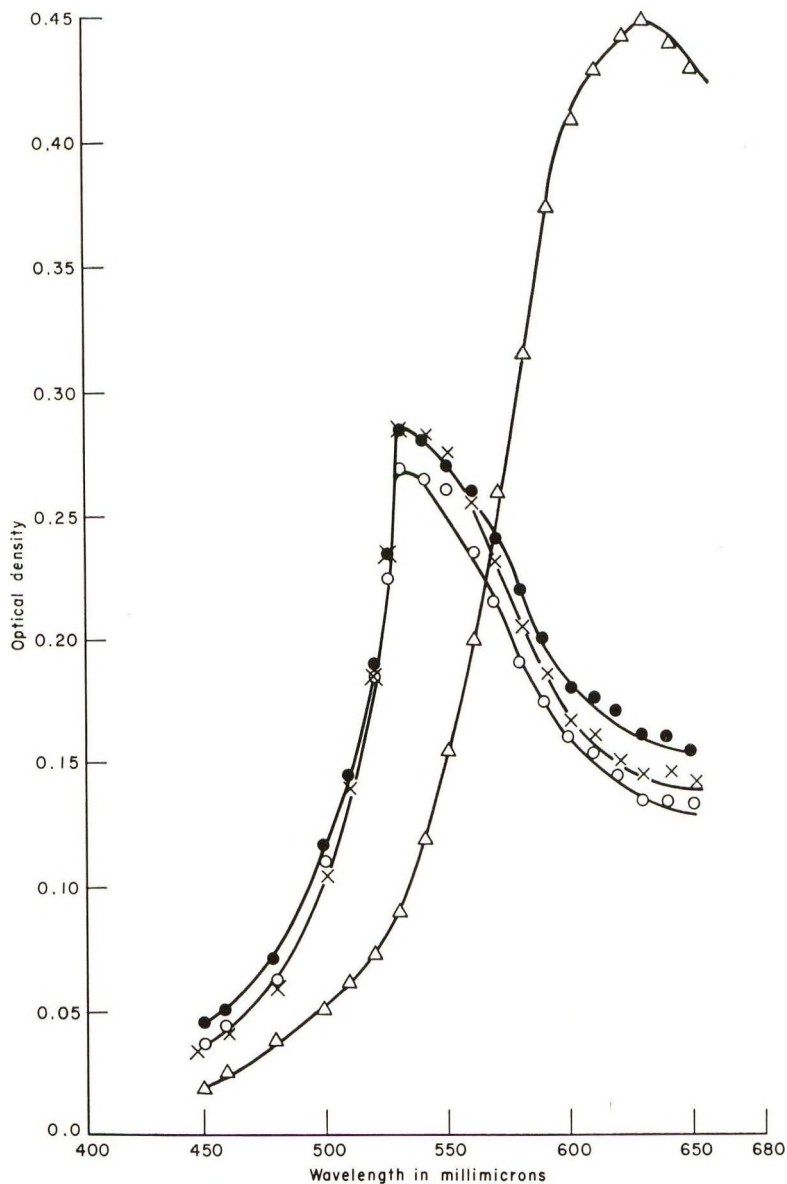
Fig. 1. Effect of concentration of $(NaPO_3)_n$ on toluidine blue spectrum. ($\triangle$) toluidine blue; $(NaPO_3)_n$, Mn = 4400: (O) 6.0 × 10^{-4}f, (×) 12.0 × 10^{-4}f, (●) 24.0 × 10^{-4}f.

chromatic effects.   Damle and Krishnan[7] have reported recently that metachromasy is inhibited by univalent metal and ammonium salts.

As the study of Wiame[6] was based on the now incorrect concept of "hexameric" nature of Graham's salt, it was thought that the metachromatic effect might throw some light on the degree of polymerization of sodium polymetaphosphate and its derivatives.   The main purpose of the
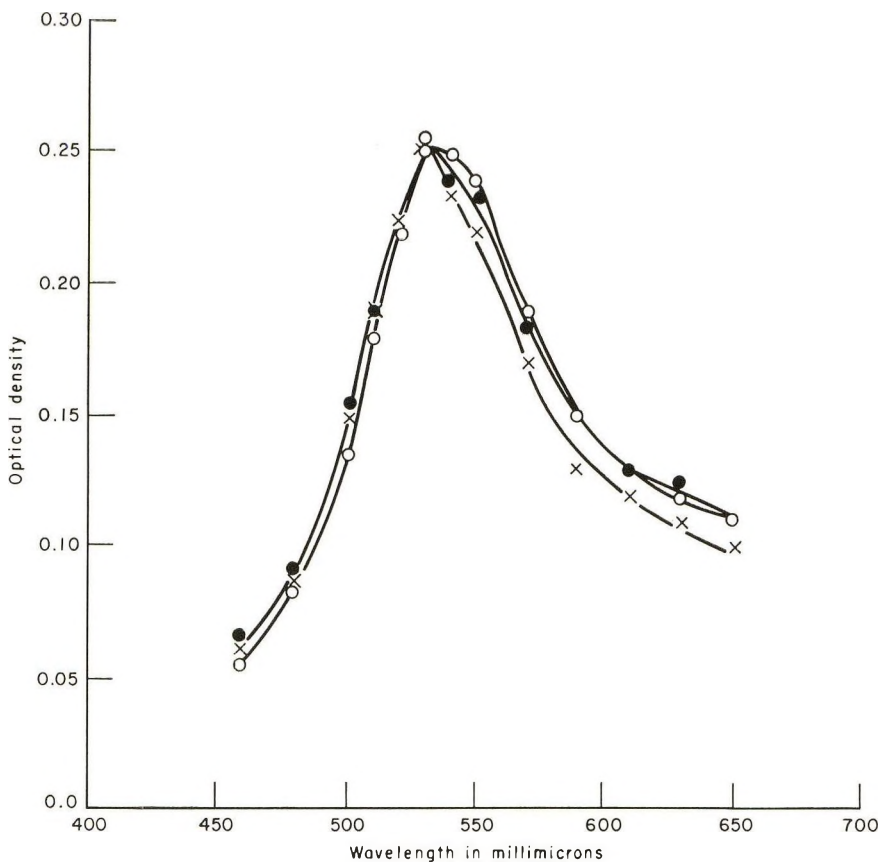
Fig. 2. Effect of concentration of $(Na_{2/3}Ba_{1/6}PO_3)_n$ in toluidine blue spectrum. $(Na_{2/3}$-$Ba_{1/6}PO_3)_n$, Mn = 5500: (O) $6.0 \times 10^{-4}f$, ($\times$) $12.0 \times 10^{-4}f$, ($\bullet$) $24.0 \times 10^{-4}f$.

study was to compare the effects of the simple and complex polymetaphosphates on the observed maximum of absorption as well as the extinction coefficient in this region.

EXPERIMENTAL

Samples of sodium polymetaphosphate with $\bar{M}_n$ values 7200, 6700, and 4400; $(Na_{2/3}Ca_{1/6}PO_3)_n$ having $\bar{M}_n$ values of 5300 and 4500; and $(Na_{2/3}Ba_{1/6}$-$PO_3)_n$ with $\bar{M}_n$ 5500 were studied. The synthesis of the phosphates and determination of molecular weights have already been reported.[1,2] Solutions $f/83.33$ in concentration* were prepared for each sample in distilled water. Toluidine blue dye (Judex L.R.) was used, and its concentration $(0.34 \times 10^{-3}$ g. in a total volume of 50 cc.) was kept constant throughout the study. Three concentrations viz., $6.0 \times 10^{-4}f$, $12.0 \times 10^{-4}f$, and $24.0 \times 10^{-4}f$ were taken for each sample of the polymetaphosphate. The

* f denotes formula weight. The formula weights for $(NaPO_3)_n$, $(Na_{2/3}Ca_{1/6}PO_3)_n$ and $(Na_{2/3}Ba_{1/6}PO_3)_n$ are taken as 102.0, 101.0, and 117.23, respectively.
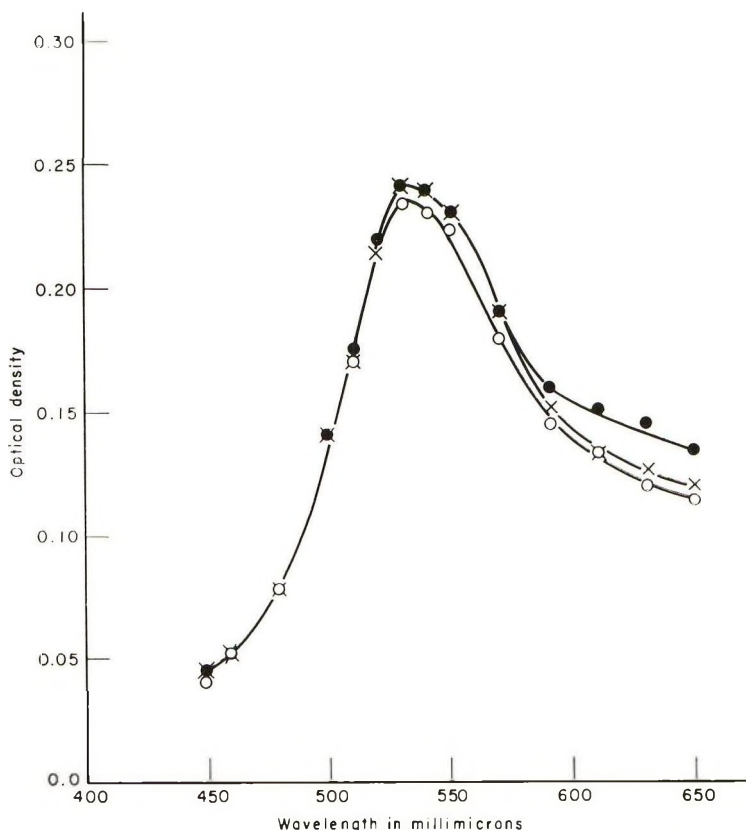
Fig. 3. Curves showing the effect of concentration of calcium chloride on Graham's salt (12.0 × 10^{-4}f) solution in the presence of toluidine blue. CaCl$_2$: (O) 1.0 × 10^{-4}M, (×) 2.0 × 10^{-4}M, (●) 4.0 × 10^{-4}M.

effect of addition of calcium and barium chloride solutions (1.0 × 10^{-4}, 2.0 × 10^{-4} and 4.0 × 10^{-4}M) with fixed concentrations of sodium poly-metaphosphate (M_n = 6700) and the dye (e.g., 12.0 × 10^{-4}f and 0.34 × 10^{-3} g., respectively) was studied. A Carl Zeiss PMQ II spectrophotom-eter was employed for measuring the optical densities. The optical densi-ties were plotted directly in different figures for samples of each molecular weight for simplicity. Only two representative diagrams have been given, i.e., those for with sodium metaphosphate and for (Na$_{2/3}$Ba$_{1/6}$PO$_3$)$_n$.

DISCUSSION

The following conclusions have been drawn on the basis of the results obtained which are shown in Figures 1 and 2.

(1) Toluidine blue solution shows a maximum optical density at 630 mμ.

(2) In the presence of all concentrations of Graham's salt as well as of the complex polymetaphosphate derivatives, the maximum shifts to 530 mμ.
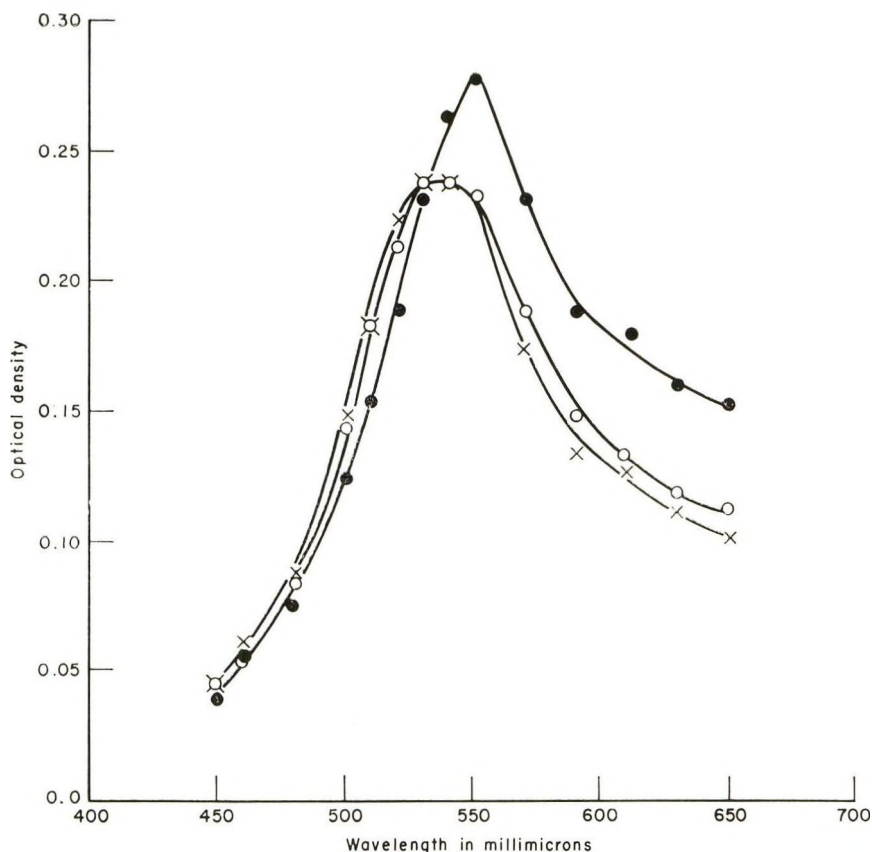
Fig. 4. Curves showing the effect of concentration of barium chloride on Graham's salt ($12.0 \times 10^{-4}f$) solution in the presence of toluidine blue. $BaCl_2$: (O) $1.0 \times 10^{-4}M$, ($\times$) $2.0 \times 10^{-4}M$, ($\bullet$) $4.0 \times 10^{-4}M$.

(3) If metachromasy, i.e., $\epsilon f_{530\ m\mu}/\epsilon f_{630\ m\mu}$ is calculated at each concentration of various samples, it is seen that the maximum value is in the region of $12.0 \times 10^{-4}f$.

Wiame[6] and Krishnan and Damle[7] reported that metachromasy is inhibited by monovalent metal and ammonium salts; our study reveals (Figs. 3 and 4) that calcium and barium chlorides do not show any marked effect except at $4.0 \times 10^{-4}M$ concentration of barium chloride.   In this case, the maximum has been found to shift from 530 mμ to 550 mμ, although the nature of the curve remains the same (Fig. 4).

The mechanism of metachromatic reactions with agar and Graham's salt was explained by Michaelis and Granick[8] and Wiame[6] on the basis of the change in the degree of polymerization of the dye.   Walton and Ricketts,[9] however, found that the above explanation does not hold in the cases of sulfonated dextrans and showed that the reactive groups on the dextrans are responsible for metachromasy.

Damle and Krishnan[7] had shown in an earlier publication that the metachromatic effects of low molecular weight sodium polyphosphates are dependent on the degree of polymerization. In a latter publication,[10] however, Tiwari and Krishnan concluded that for the sodium polyphosphates having molecular weights in the range 3,600–20,000, the metachromatic effect is independent of polymerization and is the same for different samples on an equal weight basis. This latter conclusion has been fully confirmed in the present studies also. A conclusion of greater interest to us is that that the metachromatic effects of the complex metaphosphates, $(Na_{2/3}Ca_{1/6}PO_3)_n$ and $(Na_{2/3}Ba_{1/6}PO_3)_n$ are almost similar to those of simple sodium metaphosphate, $(NaPO_3)_n$ solutions. These observations again confirm the similarity in the polymeric nature and in the reactivity of the endgroups in the cases of the simple Graham's salt and the complex derivatives described during the course of the present investigations.

References

1. Mehrotra, R. C., and V. S. Gupta, *J. Polymer Sci.*, **54**, 613 (1961).
2. Mehrotra, R. C., and V. S. Gupta, *J. Polymer Sci.*, **55**, 81 (1961).
3. Mehrotra, R. C., and V. S. Gupta, *J. Polymer Sci.*, **58**, 501 (1962).
4. Gupta, V. S., Ph.D. Thesis, Gorakhpur University, Gorakhpur, India, 1962.
5. Mehrotra, R. C., and V. S. Gupta, *J. Polymer Sci.*, **A2**, 3959 (1964).
6. Wiame, J. M., *J. Am. Chem. Soc.*, **69**, 3146 (1947).
7. Damle, S. P., and P. S. Krishnan, *Arch. Biochem. Biophys.*, **49**, 58 (1954).
8. Michaelis, L., and S. Granick, *J. Am. Chem. Soc.*, **67**, 1212 (1945).
9. Walton, K. W., and C. R. Ricketts, *Brit. J. Exptl. Pathol.*, **35**, 227 (1954).
10. Tiwari, K. K., and P. S. Krishnan, *Arch. Biochem. Biophys.*, **82**, 99 (1959).

Résumé

Le comportement méthachromatique des méthaphosphates complexes sont en général identiques à celui du sel de Graham et tout-à-fait différent de celui des triméthaphosphates soit simples, soit mélangés, ou d'autres phosphates. Avec le bleu de toluidine la longueur d'onde d'absorption maximale se déplace de 630 à 530 mμ dans tous les cas considérés. L'addition du chlorure de calcium ou de baryum ne changent rien à la densité optique ou à la longueur d'onde du maximum d'absorption, sauf à une concentration en chlorure de baryum de $4.0 \times 10^{-4} M$.

Zusammenfassung

Das metachromatische Verhalten der komplexen Metaphosphate ist dem von Grahamsalz fast gleich und ziemlich verschieden von dem einfacher oder gemischter Trimeta- oder anderer niedrigerer Phosphate. Mit Toluidinblau verschiebt sich die Wellenlänge des Absorptionsmaximums von 630 nach 530 mμ in allen oben angeführten Fällen. Zusatz von Calzium- oder Bariumchlorid ergab keine Änderung der optischen Dichte oder der Wellenlänge des Absorptionsmaximums ausser bei $4,0 \times 10^{-4} M$ Bariumchloridkonzentration.

Cyclo- and Cyclized Diene Polymers.   I.
Polymerization of Conjugated Dienes to Ladder Cyclo-Polymers with Complex Catalysts*

N. G. GAYLORD, *Gaylord Associates, Inc., Newark, New Jersey,* and I. KÖSSLER, M. ŠTOLKA, and J. VODEHNAL, *Institute of Physical Chemistry, Czechoslovak Academy of Sciences, Prague, Czechoslovakia*

Synopsis

Polymerization of isoprene, butadiene, and chloroprene with complex catalysts consisting of alkyl or arylmagnesium bromide or triethylaluminum and excess TiCl₄ leads to the formation of powdery, insoluble, probably crosslinked polymers with high density and high heat resistance (>370°C.). The structure of these polymers differs from that of those prepared at higher molar ratios of organometallic compound to titanium tetrachloride. The infrared analysis of the powdery polymers and comparisons with the spectra of cyclized 3,4-polyisoprene and cyclized 1,4-*cis*-polyisoprene indicate that the polymer chain consists of fused six-membered saturated rings in the form of a linear ladder or spiral ladder structure. The residual linear segments with 1,4 units, present in the predominantly cyclic polymers, may be isomerized to a cyclic form by the action of H_2SO_4. Removing the linear segments from the polymer chain further improves the heat resistance. It is proposed that the cyclic structure is formed during the polymerization from 1,2-polymer and not as a result of the action of catalyst components on primarily formed linear chains. The cyclic structure may be ascribed to all three investigated polymers.

I. INTRODUCTION

Stereospecific polymerization of dienes in the presence of complex catalysts to yield rubbery polymers has been studied by numerous authors. In many reports on diene polymerization with Ziegler-type catalysts the authors noted that under certain conditions, insoluble polymer powders were formed from butadiene and isoprene.[1–6] Polyisoprenes prepared with an $Al(i\text{-}C_4H_9)_3$–$TiCl_4$ catalyst system at low Al/Ti molar ratios were reported to be powders with a softening point of 160°C. and with predominantly 1,4 structure.[1] Saltman, Gibbs, and Lal[2] have reported that the plot of polyisoprene yield versus molar ratio of $Al(i\text{-}C_4H_9)_3$ to $TiCl_4$ indicates two maxima of conversion, the first at 0.3 and the second at 1.0. Insoluble, powdery polymer is formed in the region of the first maximum. No other details have been presented concerning the structure of the poly-

mer except for a comment on the similarity to some polymers prepared by Richardson.[7] A similar dependence on the molar ratio of the catalyst components has been found by Adams and co-workers.[6] Kropacheva et al.[3] have studied the polymerization of isoprene with a sodium alkyl-titanium tetrachloride catalyst system and proposed that $TiCl_4$ in excess, or other catalyst components, may induce isomerization of 1,2- or 3,4-polyisoprene to the cyclic form. In most of these publications, the 1,4 enchainment is assigned to insoluble powdery polymers from dienes, and only in a few of them is the possibility of other structures considered.[3,7−9] Mention of "unusual" structures of diene polymers has appeared also in some discussions of polymer analysis.[10]

In all of these examples, a striking disagreement was observed between total unsaturation and the determination of 1,4 and 1,2 (3,4) structures. A lower content of double bonds in diene polymers may be accounted for by the formation of internal cyclic structures.

In the present investigation, the results of diene polymerization with Ziegler-Natta type catalysts under conditions favoring the formation of insoluble, powdery (cyclic) polymers has been studied.

II. EXPERIMENTAL

Materials

Monomers. Isoprene of 99.5% purity was used in all experiments. Butadiene was C. P. or instrument grade (Matheson Co.) or the purified product from treatment of a 90% material in the usual manner through complexing with univalent copper. Chloroprene was purified by distillation and the fraction of 99% purity was utilized.

Catalyst. Titanium tetrachloride was purified grade from J. T. Baker Co., or technical grade, refluxed several hours in the presence of copper powder and distilled *in vacuo*. Grignard reagents, phenyl or *n*-butylmagnesium bromide, were prepared in the usual manner in ether. Ether, free and bound, was removed from the mixture by heating at higher temperatures. In the experiments with isoprene and chloroprene, a solution of phenylmagnesium bromide in xylene was used. Phenylmagnesium bromide was prepared in the absence of ether in xylene by the direct synthesis from magnesium and bromobenzene, as described by Bryce-Smith and Cox.[11] The triethylaluminum used was reported to contain about 5% ethoxy groups.

Solvents. Benzene and *n*-heptane were refluxed for 4 hr. over a fresh suspension of sodium and distilled in a nitrogen atmosphere. Toluene used in cyclization reactions was treated successively with H_2SO_4, a solution of Na_2CO_3, and distilled water.

Polymerization

All polymerizations with complex catalysts were carried out in an atmosphere of dry nitrogen and care was taken to avoid air and moisture. Sol-
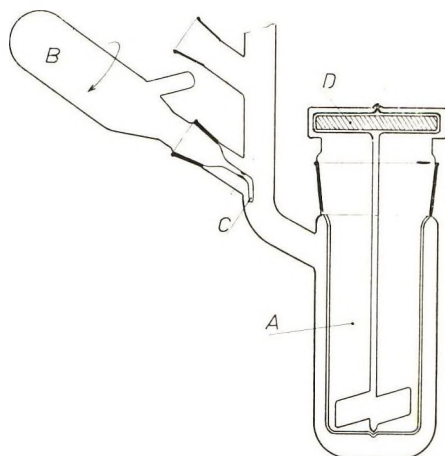
Fig. 1. Polymerization apparatus: (A) reaction vessel (100 ml.); (B) sealed ampule with solvent, monomer, etc.; (C) breakable end; (D) magnetic stirrer.

vents, monomer, and catalyst components were injected into a 100 ml. flask under stirring, by means of graduated syringes. In some experiments the components were added separately from glass ampules in the device described in Figure 1. Monomer and solvent, free of water and dissolved gases, were distilled under vacuum into ampules provided with a breakable end. Similar ampules were used for the catalyst components. The ampules containing all components were joined to the reaction flask. The flask was flushed with nitrogen and evacuated, the breakable ends were broken by turning, and the components admitted in desired order into the reaction vessel provided with a magnetic stirrer. The polymerization was stopped by the addition of methyl alcohol containing phenyl-β-naphthylamine.

Isoprene was polymerized in benzene at 20°C.; concentration of the monomer, 140 g./l., $TiCl_4$, 20 mmole/l. The molar ratio of phenyl and n-butylmagnesium bromide to titanium tetrachloride varied from 0.5 to 8.

Butadiene-1,3 was bubbled into n-heptane or benzene at 5–87°C. at such a rate that the mixture was at all times saturated with monomer. The catalyst concentration was the same as in the case of isoprene.

Chloroprene was polymerized in benzene with $Al(C_2H_5)_3/TiCl_4$ catalyst (Al/Ti molar ratio 0.33) or in n-heptane with phenylmagnesium bromide/$TiCl_4$ catalyst (molar ratio 0.5) under the same conditions as isoprene.

Cyclization

In order to cyclize residual linear structures in powdery cyclopolyisoprene, cyclopolybutadiene, and cyclopolychloroprene, the polymers were treated with H_2SO_4 in toluene suspension at 20°C. for 20 hr. These samples were compared with cyclized natural rubber, balata, and synthetic 3,4-polyisoprene.[12]

An attempt was made to cyclize polyisoprene (deproteinized natural rubber and synthetic 3,4-polyisoprene) by the action of the components of the polymerization catalyst under the conditions used in the polymerizations. A 3% solution of polyisoprene in toluene was treated with $TiCl_4$ (20 mmole/l.) or phenylmagnesium bromide (10 mmole/l.) or with the fresh reaction product of both components, all at 20°C. for 3 hr.

Determination of Density and Temperature of Decomposition

The density of polymer powders was determined by the method described by Daneš, Polák, and Krivánek.[13] The temperature of decomposition was determined in air in a capillary tube. The powdery character disappeared at a definite temperature and a clear liquid meniscus could be observed. The transition from solid to liquid states was not reversible.

Infrared Analysis

Infrared spectra were taken partly on a Perkin-Elmer 21 instrument in the range of 600–4000 cm.$^{-1}$, and partly on a UR-10 spectrophotometer (Carl Zeiss, Jena) in the 400–4000 cm.$^{-1}$ range. The potassium bromide pellet technique was used for all samples. The measurements were made using the baseline method or the differences between the optical densities of two wavelengths.[14]

III. RESULTS

Isoprene

The yield of isoprene polymer depends upon the molar ratio of phenylmagnesium bromide to titanium tetrachloride. The conversion curves
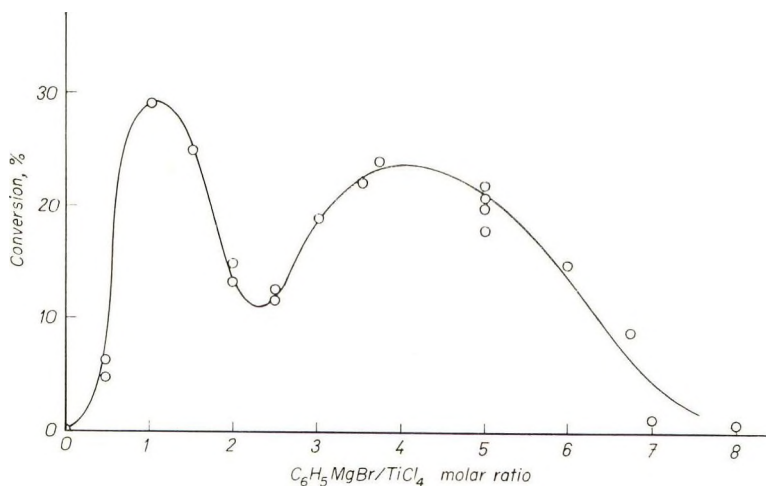

Fig. 2. Yield of polyisoprene as a function of the molar ratio of catalyst components. Temperature 20°C.; reaction time, 3 hr.
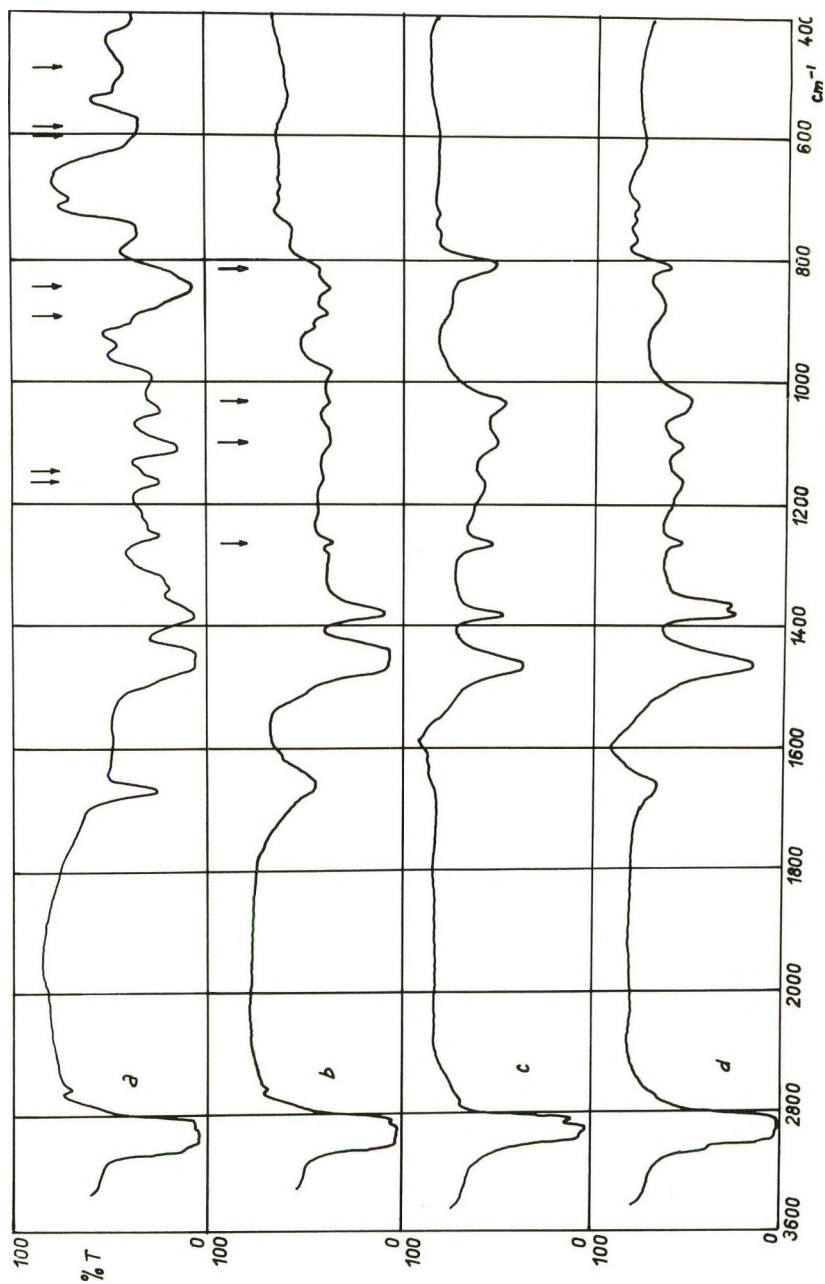
Fig. 3. Infrared spectra of polyisoprenes: (*a*) sample obtained at high Mg/Ti molar ratios (second maximum, see Fig. 2); (*b*) sample obtained at low Mg/Ti molar ratios (first maximum); (*c*) sample (*b*) cyclized by H₂SO₄; (*d*) cyclized 3,4-polyisoprene.

show two maxima (Fig. 2). As expected, neither $TiCl_4$ nor phenylmagnesium bromide alone is catalytically effective. $TiCl_4$ with traces of water as a cocatalyst was also ineffective in initiating polymerization with reasonable rate. In all cases, polymerization was initiated by the reaction product of titanium tetrachloride and organometallic compound. Polymer formed in the range of the second maximum of the yield (at RMgX/ $TiCl_4 \sim 3$ which corresponds to $AlR_3/TiCl_4$ about 1) was predominantly 1,4-polyisoprene (see Fig. 3a). Near the first maximum at RMgX/$TiCl_4$ ~ 1, a powdery polymer was formed. The polymer contained some soluble portion which could be extracted by the usual solvents. The extract was rich in 1,4 units. The residue, after the extraction, was insoluble in all common organic solvents, and had a relatively high density and high temperature of decomposition. The typical infrared spectrum of the insoluble cyclopolymer is shown in Figure 3b.

On lowering the ratio of Mg/Ti, the content of 1,4 structure decreased. This is evident from low intensities of absorption bands at 475 (1,4), 572 (1,4-*cis*), 600 (1,4-*trans*), 840–845 (1,4), 1130 (1,4-*cis*), 1150 (1,4-*trans*), and 1665 (C=C) cm.$^{-1}$. Simultaneously, new bands appeared at 820, 1040, 1090, and 1265 cm.$^{-1}$. The width of the band at 1665 cm.$^{-1}$ increased.

Butadiene

The yield of butadiene polymer is also dependent upon the catalyst composition and on temperature. The yield dependence on the molar ratio phenylmagnesium bromide/titanium tetrachloride is shown in Table I, which represents the data in the region of the first maximum. The temperature dependence is presented in Table II. As in the case of isoprene, at molar ratios Grignard reagent/$TiCl_4$ of about 5 or $AlR_3/TiCl_4 \sim 1$, which represents the region of the second maximum, most of the polymer contained 1,4 addition units (Fig. 4a). At low molar ratios, powdery insoluble cyclopolybutadienes were formed. Infrared spectra of these powders (Fig. 4b) differ greatly from those of 1,4 or 1,2-polybutadienes.[15,16] The intensity of absorption bands at 670–740 cm.$^{-1}$ assigned to *cis*-1,4 structures, as well as 910 (1,2), 965 (1,4-*trans*) and 1639 (C=C) cm.$^{-1}$ de-

TABLE I
Polymerization of Butadiene (1 hr., 20°C.)

Molar ratio, $C_6H_5MgBr/TiCl_4$	Yield, g.
2.0	0.05
1.1	0.1
0.6	0.4
0.4	0.3
0.3	0.6
0.22	0.7
0.15	0.5
0.075	0.4

TABLE II

Effect of Temperature on Polymerization of Butadiene with
C_6H_5MgBr–$TiCl_4$ Catalyst (Conversions after 1 hr.)

Molar ratio, $C_6H_5MgBr/TiCl_4$	Temperature, °C.	Yield, g.	trans-1,4 configuration, %
0.3	54	0.05	7
	41	0.04	11
	27	0.10	15
	15	0.14	17
	5	0.16	26
2.0	87	2.7	
	75	0.6	
	66	0.5	
	27	0.15	

creased, and new absorption bands appeared near 805, 1020, 1265, and 1378 cm.$^{-1}$. The width of the band of C=C groups increased.

Besides polymerization with complex catalysts, the cationic polymerization of butadiene with $TiCl_4$ and traces of water was carried out. Infrared analysis of the resulting polymers indicate that samples contain both linear structures and structures present in the powdery cyclopolymers obtained with the aid of complex catalysts. No polymerization was observed with $TiCl_4$ without traces of water under the mild conditions used.

Chloroprene

As in the case of isoprene and butadiene, chloroprene polymerized to powdery insoluble cyclopolymers with the aid of complex catalysts at low molar ratios of organometallic compound to titanium tetrachloride. Infrared analyses indicate the formation of new structures, not present in emulsion polychloroprene (Fig. 5). Absorption bands at 602, 667 (C–Cl), 826 (1,4), and 1002 cm.$^{-1}$ are very weak. The intensities of the bands at 882 (3,4) and 910 (1,2) cm.$^{-1}$ are relatively low. New bands appeared at 700, 805, 1020, 1090, and 1265 cm.$^{-1}$. The intensity of absorption bands at 1378, 1495, 2865, and 3020 (CH$_3$ groups) cm.$^{-1}$ markedly increased. The width of the band of C=C increased.

Cyclization

The powdery cyclopolymers still containing some amount of linear structures were completely cyclized by the action of H_2SO_4 in toluene suspension. The absorption bands assigned to the linear forms disappeared (Figs. 3c, 4c). The infrared analyses indicate that attempts to cyclize 1,4-cis and all-3,4-polyisoprenes by the action of the components of the polymerization catalyst failed under the conditions used for the preparation of the powdery cyclopolymers.
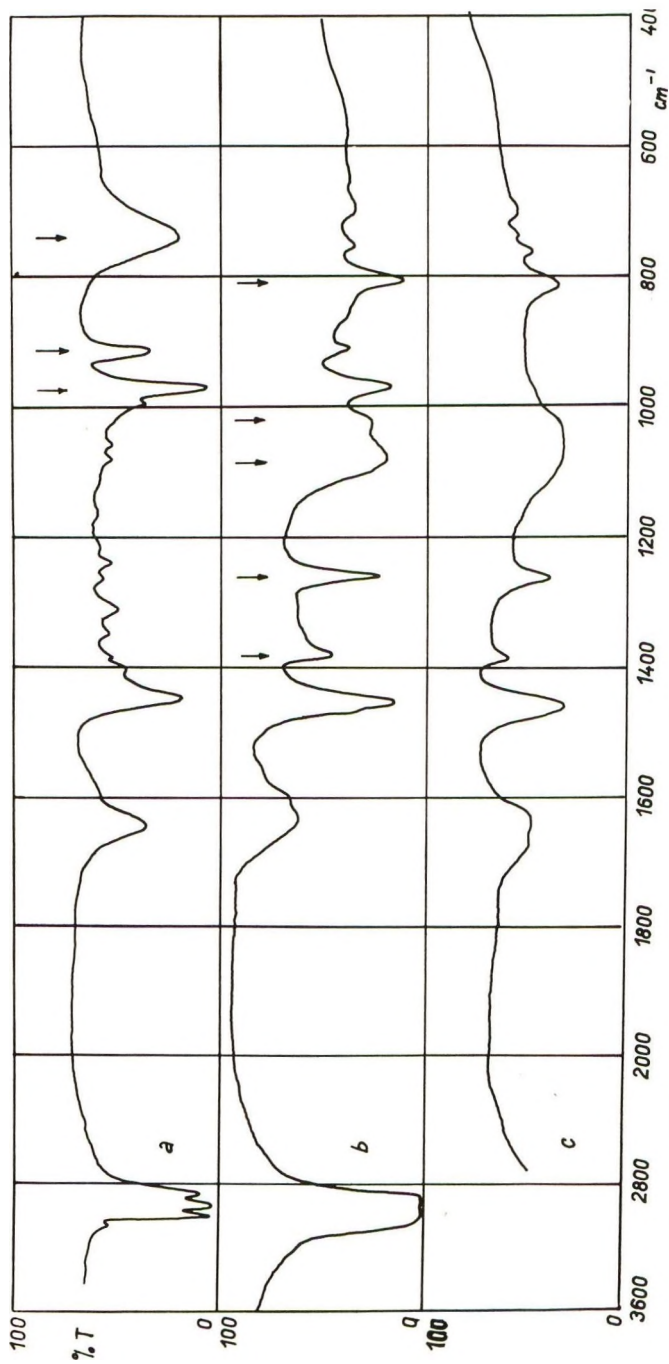
Fig. 4. Infrared spectra of polybutadienes: (a) sample obtained at the molar ratio Mg/Ti = 5; (b) sample obtained at the molar ratio Mg/Ti = 0.5; (c) sample (b) cyclized by H_2SO_4.
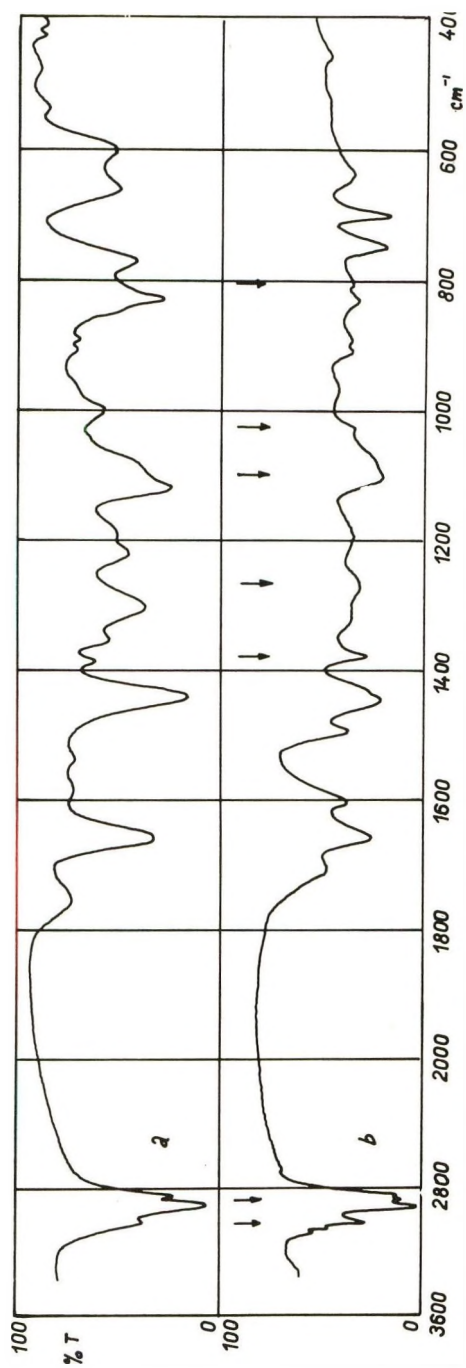
Fig. 5. Infrared spectra of polychloroprenes: (a) emulsion polychloroprene (Svitpren K); (b) sample obtained at the molar ratio Mg/Ti = 0.5.

Properties of Cyclopolymers

By analysis of the infrared spectra of the polymers prepared directly during the polymerization and determination of the 1,4-unit content, it is apparent that cyclopolyisoprene contains at least 70% cyclic structure, cyclopolybutadiene contains at least 85% cyclic structure, and cyclopolychloroprene contains more than 60% cyclic structure.

The most notable characteristic of these cyclopolymers is their thermal stability. When they are heated in air in a capillary tube, there is no visible change until a sudden "melting" or decomposition occurs from the solid to the liquid state. This is an irreversible change since the material remains liquid after cooling to room temperature. As shown in Table III, the decomposition temperatures are 370°C. for cyclopolyisoprene, 405°C. for cyclopolybutadiene, and 422°C. for cyclopolychloroprene.

TABLE III
Properties of Diene and Cyclopolymers

Polymer	Decomposition point, °C.	Density, g./cm.³
Hevea rubber		0.92 (25°C.)[a]
Cyclized Hevea	95–130 (softening pt.)[b]	0.98–1.016 (20°C.)[b]
Cyclopolyisoprene $(C_6H_5MgBr/TiCl_4 = 0.5)$	370	1.082 (25°C.)
Completely cyclized cyclopolyisoprene	388	—
Polybutadiene	—	0.90 (25°C.)[c]
Cyclized polybutadiene	—	1.07 (25°C.)[c]
Cyclopolybutadiene, $(C_6H_5MgBr/TiCl_4 = 0.5)$	405	0.966 (25°C.)
Completely cyclized cyclopolybutadiene	413	—
Cyclopolychloroprene $(C_6H_5MgBr/TiCl_4 = 0.5)$	422	—

[a] Data of D'Ianni et al.[20]

[b] Data of various workers summarized by Gordon.[21]

[c] Data of Shelton and Lee.[22]

Upon further cyclization with sulfuric acid, which probably involves the cyclization of residual 1,4-structures, the temperature of decomposition is raised further. Softening temperatures of 370 and 420°C. have been reported[3] for polyisoprene and polybutadiene, respectively, prepared under the influence or alkylaluminum dichloride and titanium tetrachloride, although no supporting data for a cyclic structure have been given. The softening point in the region of 95–130°C., reported by various authors for cyclized Hevea attests to the probable difference in structure between the cyclopolymer obtained from the monomer and that obtained by cyclization of the linear polymer.

In contrast to the 370°C. decomposition temperature for cyclopolyiso-prene, cyclized 3,4-polyisoprene softened, with gas evolution, at 140–170°C.

The thermal and oxidative dehydrochlorination of both cyclopolychloro-prene and polychloroprene prepared by free radical initiated polymerization in benzene solution, was followed by conductivity measurements of a standard sodium hydroxide solution in which the liberated hydrogen chlo-ride was trapped.   In a nitrogen atmosphere, in both cases a two-stage de-hydrochlorination occurred.   During the first stage 3–5% of the total chlorine content was liberated.   Thereafter a very slow dehydrochlorina-tion occurred.   This second-stage reaction was very temperature-depend-ent in the case of radical-polymerized polychloroprene, i.e., apparent activation energy 11 kcal./mole, as compared to 3–4 kcal./mole for cyclo-polychloroprene.

TABLE IV
Dehydrochlorination of Chloroprene Polymers

	HCl liberated at 100°C., mole/g. × 10⁴			
	After 1 hr.		After 2 hr.	
	In N_2	In O_2	In N_2	In O_2
Cyclopolychloroprene	2.3	3.0	2.7	4.2
Radical-initiated polychloroprene	—	12.8	—	26.0

Oxidative dehydrochlorination curves showed a marked difference be-tween the cyclopolychloroprene and the radical-polymerized polychloro-prene.   The latter exhibited the usual short induction period followed by a rapid rate increase.   The cyclopolychloroprene showed no induction period, i.e. initially, as in the case of the nitrogen atmosphere, a small amount of HCl was liberated.   Thereafter the rate decreased continually, i.e., the total HCl liberated increased very slowly.   This is markedly dem-onstrated in Table IV.

IV. DISCUSSION

Saltman, Gibbs, and Lal[2] suggested that the insoluble polymer powder from isoprene is a crosslinked material, with infrared characteristics similar to those reported by Richardson,[7] who analyzed polybutadienes and poly-isoprenes prepared by means of Friedel-Crafts catalysts.   Richardson de-termined the relative content of each type of addition (cis and trans-1,4 and 3,4) independently and compared the percentage of all structures with found values and showed the striking disagreement between both values.   He presumed that some isomerization (or cyclization) might occur, but he gave no further evidence.   Marconi et al.[5] proposed that polymer prepared with a catalyst from an alkyl derivative of a group IIb metal and excess $TiCl_3$ is all trans-1,4-polyisoprene.   The view of trans-1,4-enchainment in polymer powders is supported by many authors.

The fact that the character of polymers prepared at low molar ratios of organometallic compound to titanium tetrachloride differs greatly from the character of polymers formed in the region of high ratios and the appearance of two maxima in the yield dependence on the catalyst composition support the idea of different polymerization mechanisms. The molar ratio of catalyst components favoring the formation of powdery cyclopolyisoprene corresponds to that when powdery cyclopolybutadiene is formed (Fig. 2 and Table I).
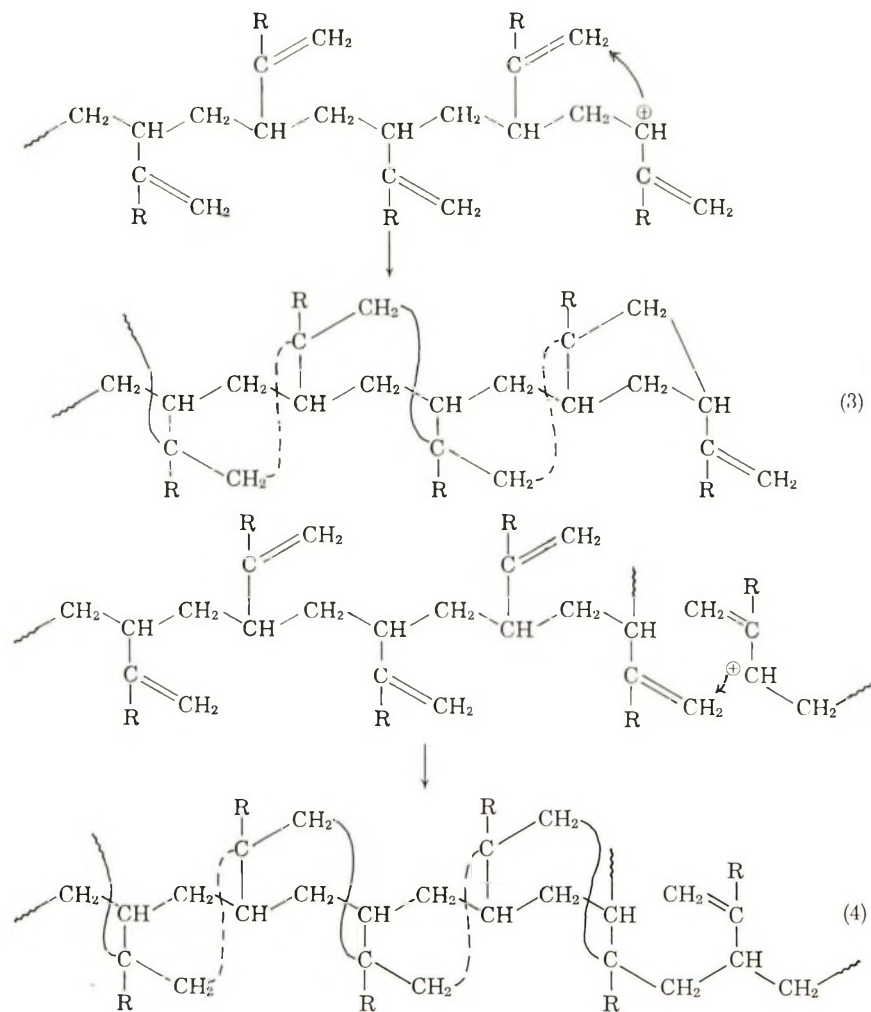
The temperature dependence of the yield of butadiene polymer is remarkable. In the range of the first maximum of the conversion it decreases with increase in temperature. Entering the region of the second maximum of conversion (where linear polymer is formed) it increases with an increase in temperature (Table II). This may be caused by different polymerization mechanisms.

If we consider that the monomer is adsorbed on the catalyst surface and that there is an adsorption–desorption equilibrium, as the temperature is raised, less monomer remains adsorbed due to the low complexing activity of the catalytic sites formed at the low catalyst ratios. However, that polymer which is formed at higher temperatures contains less of the linear *trans*-1,4 configuration than polymer formed at lower temperatures, and is of the insoluble powdery type. The desorption of polymer from the catalyst surface may also be a factor since the polymer formed at lower temperatures contains more linear structures and may have a higher solubility than that found at higher temperatures. However, this is probably more of a factor at higher catalyst ratios where the polymer structure is virtually completely linear and the polymer will be desorbed at higher temperatures to a greater extent, permitting the absorption of additional monomer on vacated catalytic sites with the resultant increased yield with temperature.

As indicated previously, infrared analysis proves that the structure of the powdery cyclopolymers is very different from that of the linear *trans*- or *cis*-1,4 polymers. Infrared spectra of the insoluble polymers from all three investigated dienes (isoprene, butadiene, and chloroprene) are very similar to each other and also similar to that of the spectrum of cyclized 3,4-polyisoprene[12] (Figs. 3b–d, 4b, c and 5b). It is probable that all of these polymers have basically the same cyclic structure. The content of remaining linear forms can be determined from the intensity of absorption bands assigned to the usual structural forms of diene polymers. Due to the insolubility of the cyclopolymers, chemical methods for the determination of residual unsaturation were unreproducible.

Although a 1:1 Al/Ti mole ratio in an aluminum alkyl–titanium tetrachloride catalyst system yields all-*trans*-1,4-polybutadiene and all-*cis*-1,4-polyisoprene, this difference only exists in the region of this ratio. At constant temperature, with Al/Ti mole ratios of less than 1, both isoprene and butadiene polymers show a decrease in *cis*-1,4 content from that obtained at a mole ratio of 1. At a constant Al/Ti ratio, the effect of lower

temperatures of polymerization is to decrease the *cis*-1,4 content of both polyisoprene and polybutadiene. From this analogous behavior, coupled with the recent proposal that both isoprene and butadiene monomers, and in fact almost all 2-substituted butadienes, possess the same *trans* configuration,[17] it is reasonable to propose that the cyclopolymerization encountered in this and other investigations, involves all of the dienes in the *trans* configuration.

Two alternative mechanisms can be advanced to account for the cyclopolymerization of conjugated diene monomers to ladder polymers. In both cases, the initial stage of polymerization involves the 1,2-isotactic or 1,2-syndiotactic polymerization (3,4-isotactic or 3,4-syndiotactic in the case of isoprene and chloroprene) of *trans* monomer. Since the metal halide is present in considerable excess, the polymerization can be considered as cationic. A reversal of the direction of polymerization involving an intramolecular cyclopolymerization would yield, after the formation of the initial five-membered ring, a sequence of fused six-membered saturated rings [eqs. (1) and (3)].

Alternatively, the cyclization reaction may be initiated by the copolymerization of a monomer unit or a growing chain with the pendant double bonds [eqs. (2) and (4)]. The failure of the catalyst components individually or together to cyclize either 3,4-polyisoprene or *cis*-1,4-polyisoprene is consistent with both suggested paths.

(1)

(2)

$$(3)$$

$$(4)$$

In the case of an isotactic sequence, the structure of the cyclopolymer is essentially that of a linear ladder polymer containing fused cyclohexane rings [eqs. (1) and (2)]. In the case of the syndiotactic sequence, the structure of the cyclopolymer is essentially that of a spiral ladder polymer containing fused cyclohexane rings, in which one chain spirals around the backbone but is connected thereto at every third carbon atom [eqs. (3) and (4).]

Since the ring-forming reaction can continue through the pendant 1,2 (3,4) groups of neighboring polymer chains, the ladder polymers are insoluble, probably highly crosslinked, products.

A fused ring structure analogous to that shown in eqs. (1) and (2) has been proposed[3] without any substantiating evidence and with the further proposal that the cyclization results from the action of catalyst components on preformed, presumably 1,4, polymer. This is not supported by the re-

sults in the present investigation. The fused ring structure has been obtained by cyclization of 3,4-polyisoprene by BF_3,[18] $POCl_3$[18], and sulfuric acid.[12]

The low thermal stability of cyclized 3,4-polyisoprene (softening point less than 200°C.) and the excellent temperature resistance of the bridgehead chlorine atoms in cyclopolychloroprene point to the spiral ladder structure rather than the linear ladder structure for the cyclopolymers. However, it is recognized that the proposed reaction paths can lead to a number of different cyclopolymers. Cyclization of isotactic sequences [eqs. (1) and (2)] can lead to a product in which all 1,3-junctures are *cis* or diaxial and all 1,2-junctures are *trans* or axial-equatorial or to a product in which all 1,2-junctures are *cis*. Cyclization of syndiotactic sequences [eqs. (3) and (4)] can lead to 1,3-*trans*–1,2-*cis* or to 1,3-*trans*–1,2-*trans* products. Since both *cis* and *trans* structures are possible at the 1,2-junctures, the failure to remove the bridgehead chlorine atoms by *trans*-elimination involving α-hydrogen *cis* to the chlorine is insufficient evidence for structural differentiation.

If we consider that the catalyst operates as a typical Ziegler-Natta type catalyst, then the monomer units entering the chain would do so by a concerted mechanism involving insertion into the chain at the site of the catalytic species and there would be a counterion derived from the catalyst located at that site. In the system discussed herein the ion pairs might have the compositions $(RTiCl_4)^-(MgBr)^+$ and $(RTiCl_4)^-(AlR_2)^+$. The length of the cyclized sequence is dependent upon the number of syndiotactic or isotactic units in sequence and will be interrupted by the presence of the alternative 1,2 or a *cis*- or *trans*-1,4 unit. The cyclopolymers are, therefore, block copolymers containing sequences of cyclic units having a ladder structure and linear, probably *trans*-1,4, units, with the possibility of a small amount of uncyclized 1,2 units.

This block character is confirmed by the fact that the infrared spectra of the liquids obtained at high temperatures from the solid cyclopolymers are the same as those of their solid precursors except that the 1,4 units are absent in the former. Apparently when the polymer softens at high temperatures the sensitive 1,4 units are susceptible to oxidation and cleave to yield liquid polymers having the cyclic structure which existed between the 1,4 units. Further work is being carried out to determine the average length of the fused sequences.

It is known that Friedel-Crafts catalysts initiate polymerization of butadiene and isoprene to polymers with "unusual" structures.[4] It is possible that even in this case the polymers have a similar cyclic structure as the polymers prepared with the aid of complex catalysts. For example, the infrared spectrum of cationic polybutadiene polymerized with $TiCl_4$ as a catalyst and traces of water as cocatalyst, $(TiCl_4OH)^-H^+$, is very similar to that of the spectrum of cyclopolybutadiene with a relatively high content of linear segments. It appears probable that the complex catalyst with $TiCl_4$ in excess acts in a similar manner to a Friedel-Crafts catalyst.

Linear segments in cyclopolyisoprene and cyclopolybutadiene may be cyclized by the action of H_2SO_4. Completely cyclized polymers in which no absorption bands characteristic of linear structures were identified can be prepared in such a way (Figs. 2c and 3c). The temperature resistance of powdery cyclopolymers increases by the additional cyclization (Table III).

The acid-catalyzed cyclization of 1,4 units probably results in a different overall structure.[14] The great difference in the decomposition temperature of cyclopolyisoprene and that of cyclized 1,4-polyisoprene or 3,4-polyisoprene may be indicative of this structure difference.

The only major difference in the infrared spectra of cyclopolyisoprene and cyclized 3,4-polyisoprene is the presence of a dimethyl substituted carbon atom in the latter. This can be accounted for by a difference in the cyclization mechanism.[14] Alternatively, the presence of the *gem*-dimethyl absorption may indicate that the cyclized 3,4-polyisoprene is lightly fused, i.e., about 2–5 fused rings/block, while the cyclopolyisoprene is more highly fused, i.e., >5 rings/block.[19] It is apparent that at this time, there is insufficient data to permit an infrared differentiation between the linear ladder and spiral ladder structures.

References

1. Phillips Petroleum Co., Belg. Pat. 551,851 (October 17, 1956).

2. Saltman, W. M., W. E. Gibbs, and J. Lal, *J. Am. Chem. Soc.*, **80**, 5615 (1958).

3. Kropacheva, E. N., B. A. Dolgoplosk, V. F. Otten, and K. G. Golodova, *Zh. Obschei Khim.*, **29**, 1853 (1959).

4. Gaylord, N. G., T.-K. Kwei, and H. F. Mark, *J. Polymer Sci.*, **42**, 417 (1960).

5. Marconi, W., A. Mazzei, S. Cucinella, and M. DeMalde, *Chim. Ind. (Milan)*, **44**, 121 (1962).

6. Adams, H. E., R. S. Stearns, W. A. Smith, and J. L. Binder, *Ind. Eng. Chem.*, **50**, 1507 (1958).

7. Richardson, W. S., *J. Polymer Sci.*, **13**, 325 (1954).

8. Dolgoplosk, B. A., presented at International Symposium on Macromolecular Chemistry, Moscow, 1960; B. A. Dolgoplosk, G. P. Belonovskaja, I. I. Boldyseva, E. N. Kropacheva, K. V. Nelson, Ja. M. Rosinoer, and J. D. Chernova, *J. Polymer Sci.*, **53**, 209 (1961).

9. Dolgoplosk, B. A., B. L. Erussalimskiĭ, E. N. Kropacheva, and E. I. Tinyakova, *J. Polymer Sci.*, **58**, 1333 (1962).

10. Binder, J. L., *Anal. Chem.*, **26**, 1877 (1954).

11. Bryce-Smith, D., and G. F. Cox, *J. Chem. Soc.*, **1958**, 1050.

12. Stolka, M., J. Vodehnal, and I. Kössler, *J. Polymer Sci.*, **A2**, 3987 (1964).

13. Daneš, V., R. Polák, and M. Krivánek, *Chem. Listy*, **55**, 987 (1961).

14. Vodehnal, J., and I. Kössler, *Collection Czech. Chem. Communs.*, in press.

15. Golub, M. A., *J. Am. Chem. Soc.*, **80**, 1794 (1958).

16. Natta, G., *SPE J.*, **15**, 373 (1959).

17. Gresser, J., A. Rajbenbach, and M. Szwarc, *J. Am. Chem. Soc.*, **82**, 5820 (1960).

18. Angelo, R. J., *Polymer Preprints*, **4**, No. 1, 32 (1963); paper presented at 144th American Chemical Society Meeting, Los Angeles, April 1963.

19. Suggestion of the referee.

20. D'Ianni, J. D., F. J. Naples, J. W. Marsh, and J. L. Zarney, *Ind. Eng. Chem.*, **38**, 1171 (1946).

21. Gordon, M., *Ind. Eng. Chem.*, **43**, 386 (1951).

22. Shelton, J. R., and L.-H. Lee, *Rubber Chem. Technol.*, **31**, 415 (1958).

Résumé

La polymérisation de l'isoprène, du butadiène et du chloroprène avec des catalyseurs complexes constitués par des bromures d'alkyle-ou d'arylmagnésium ou du triéthyl-aluminium et avec un excès de TiCl$_4$, conduit à la formation d'un polymère poudreux insoluble, probablement ponté à haute densité et résistance élevée à la chaleur (>370°C). La structure de ces polymères diffère de celle correspondant à des polymères préparés au dépens de rapports molaires élevés de composés organométalliques et de tétrachlorure de titane. Les analyses infra-rouges d'un polymère poudreux et la comparaison avec les spectres de 3,4-polyisoprène cyclisé et de 1,4-*cis*-polyisoprène cyclisé indiquent que la chaîne polymérique est constituée de cycles fusionnés saturés à 6 membres ayant la structure d'une échelle linéaire ou d'une échelle en spirale. Les segments linéaires ré-siduels avec les unités 1,4, présents principalement dans les polymères cycliques, peuvent être isomérisés sous forme cyclique par l'addition de H$_2$SO$_4$. On améliore la résistance à la chaleur en enlevant les segments linéaires de la chaîne polymérique. On propose que la structure cyclique est formée au cours de la polymérisation du polymère 1,2 et ne résulte pas de l'action des composants du catalyseurs sur les chaînes linéaires formées préliminairement. La structure cyclique peut être attribuée aux trois polymères étudiés.

Zusammenfassung

Polymerisation von Isopren, Butadien und Chloropren mit aus Alkyl-oder Aryl-magnesiumbromid oder Aluminiumtriäthyl und überschüssigem TiCl$_4$ bestehenden komplexen Katalysatoren ergibt ein pulverförmiges, unlösliches, möglicherweise ver-netztes Polymeres mit hoher Dichte und grosser Hitzebeständigkeit (>370°C). Die Struktur dieser Polymeren unterscheidet sich von der mit höherem Molverhältnis von organometallischen Verbindungen zu Titantetrachlorid hergestellten. Infrarotanalyse des pulverförmigen Polymeren und ein Vergleich von zyklisiertem 3,4-Polyisopren und zyklisiertem 1,4-*cis*-Polyisopren ergab, dass die Polymerkette aus kondensierten sechs-gliedrigen gesättigten Ringen in der Form einer linearen oder spiraligen Leiterstruktur besteht. Die restlichen linearen Segmente mit 1,4-Einheiten, die in den hauptsächlich zyklischen Polymeren vorhanden sind, können durch H$_2$SO$_4$ zu einer zyklischen Form ionisiert werden. Die Hitzebeständigkeit wird durch Entfernen der linearen Segmente aus der Polymerkette weiter verbessert. Es wird angenommen, dass die zyklische Struk-tur während der Polymerisation von 1,2-Polymeren und nicht als ein Ergebnis des Ein-flusses der Katalysatorkomponenten auf die zuerst gebildeten linearen Ketten gebildet wird. Allen drei untersuchten Polymeren kann eine zyklische Struktur zugeschrieben werden.

Cyclo- and Cyclized Diene Polymers.   II. Infrared Study of the Cyclization of *cis*-1,4, *trans*-1,4, and 3,4-Polyisoprenes

M. ŠTOLKA, J. VODEHNAL, and I. KÖSSLER, *Institute of Physical Chemistry, Czechoslovak Academy of Sciences, Prague, Czechoslovakia*

Synopsis

Cyclization of *cis*-1,4, *trans*-1,4-, and 3,4-polyisoprene was carried out in toluene solution with sulfuric acid.   With 1% H_2SO_4, calculated on polymer, a stationary state of cyclization was reached in which 33% of the original unsaturation and about 50% of the total unsaturation remained in cyclized *trans*-1,4- and 3,4-polyisoprene.   The rate of cyclization of *cis*-1,4-polyisoprene was very small, and the limiting value was not reached even after 100 hr. at 80°C.   Infrared spectra of cyclized polymers show decreased absorption intensity of the bands characteristic of groups in the linear polymer.   With 10% H_2SO_4 calculated on polymer (a heterogeneous mixture), all three polyisoprenes cyclize to give polymer with none of the original unsaturation in the chain.   Infrared spectra of cyclized *trans*-1,4-and *cis*-1,4-polyisoprene are identical.   The spectrum of cyclized 3,4-polyisoprene differs only by two peaks, at 1385 and 1370 cm.$^{-1}$.   The spectra of all three cyclized isomers show new bands in infrared spectrum at 2870, 1265, 1200, 1040, and 810 cm.$^{-1}$.   A comparison has been made of the infrared spectra of cyclopolymers of isoprene, butadiene, and chloroprene prepared from monomers by use of Ziegler-Natta catalysts with spectra of cyclized polyisoprene.   The spectra are very similar, which indicates that both types of polymer have the same polycyclic structure.

I. INTRODUCTION

In the stereospecific polymerization of butadiene, isoprene, and chloroprene, by Ziegler-type catalysts at low molar ratios of the organometallic compound to a transition metal salt, insoluble powdery polymers, probably of cyclic structure, are formed.[1]   The aim of the present work was to study the cyclization of three isomers of polyisoprene: *cis*-1,4-polyisoprene (Hevea rubber), *trans*-1,4-polyisoprene (balata), and synthetic 3,4-polyisoprene with less than 3% of 1,4 and 1,2 addition, and to compare infrared spectra of the cyclized polymers with infrared spectra of cyclopolymers prepared directly from monomer by stereospecific polymerization.

The intramolecular cyclization of polyisoprene caused by various acids or Friedel-Crafts catalysts has been the subject of investigation of many authors.[2-8]   Some investigators proposed that a fused six-membered condensed ring structure is formed,[4] while others support the idea of monocyclic[5] or bicyclic[6] structures.

II. EXPERIMENTAL

Materials

cis-1,4-**Polyisoprene.** Deproteinized Hevea rubber was reprecipitated from 1% toluene solution by methanol and dried at 40°C. *in vacuo.*

trans-1,4-**Polyisoprene.** Balata was twice precipitated by methanol from 1% solution in toluene and dried *in vacuo* at 40°C.

3,4-Polyisoprene. This polymer was synthesized by ionic polymerization in xylene with phenylmagnesium bromide as a catalyst.[9] The residual fraction, after extraction by acetone to free it of low molecular weight polymer, was used in the cyclization. Toluene was purified by shaking 3 hr. with sulfuric acid, then with water and dried over $CaCl_2$.

Sulfuric acid was reagent grade, 96%.

Cyclization

All three polymers were cyclized by means of H_2SO_4 in toluene solution. To a 2% solution of polyisoprene 1 wt.-% of sulfuric acid, calculated on the weight of polymer, was added and the mixture heated to 80°C. The samples of cyclized polymer were isolated by pouring the mixture into methanol, filtered, carefully washed with methanol and dried *in vacuo* at 40°C. Under these conditions of cyclization all the sulfuric acid was dissolved in toluene and the cyclization was in a homogeneous system.

In other experiments, 10 wt.-%, calculated on the weight of polymer, of H_2SO_4 was added while stirring to a 2% solution of polyisoprene in toluene. The reaction, now heterogeneous, was carried out at 20°C. After 20 hr. of cyclization the temperature was raised to 80°C. Samples taken during cyclization were treated in the manner described above.

Infrared Spectra

Infrared spectra were obtained using the KBr pellet technique on a Zeiss UR-10 instrument. The range of wave numbers from 400 cm.$^{-1}$ to 4000 cm.$^{-1}$ was studied. The concentration of polymer in the KBr disk was approximately 3.5 mg./0.5 g. KBr, the disk being 13 mm. in diameter. The relative concentrations of some groups were determined from differences in optical densities. For example, the content of $CH_2=C(CH_3)$ groups in 3,4-polyisoprene determined from the absorption at 888 cm.$^{-1}$ (C_{888}) was estimated by measuring the transmission of the band at 888 cm.$^{-1}$ (I_{888}) and the transmission near 650 cm.$^{-1}$(I_{650}), where there is no specific absorption.

The value D_1 is proportional to the concentration of isopropenyl groups in the polymer:

$$D_1 = \log I_{650}/\log I_{888} = k_1 C'_{888} C'_p$$

where C_p denotes the polymer concentration in the KBr disk and k_1 is the absorptivity of the isopropenyl group at 888 cm.$^{-1}$. If the absorptivity of the —CH_2— group at 1450 cm.$^{-1}$ was to a first approximation, the same

both in linear polymer and in cyclized polymer and if there was no specific absorption at 1600 cm.$^{-1}$, it would be possible to check the polymer concentration in the disk by the determination of the value

$$D_2 = \log I_{1600}/\log I_{1450} = k_2 C_p$$

The value of the ratio $D = D_1/D_2$ was considered to be proportional to the concentration of isopropenyl groups. The spectra in which D_2 differed greatly from the average value were not used for the quantitative analysis. In the case of the band at 840 cm.$^{-1}$ the base line method was also used.

III. RESULTS

Immediately after the addition of H_2SO_4 to the polymer solution a decrease in viscosity was observed. When the cyclization was carried out with 10% H_2SO_4 the polymers isolated were less soluble, and lost their rubbery character, and became resinous. The infrared spectra of all samples changed substantially with cyclization.

Hevea

With 1% H_2SO_4 the intensity of the absorption at 572 cm.$^{-1}$ was lowered to about 80% of the original value. With 10% H_2SO_4 it totally disappeared, as did the band at 838 cm.$^{-1}$. The intensity of the bands at 1315 cm.$^{-1}$, assigned by Binder[10] to $=$C$-$H vibration connected with $-$C(CH$_3$)$=$CH$-$ groups in cis form, and 1130 cm.$^{-1}$ assigned to the same group, decreased in 1% H_2SO_4 and disappeared in concentrated H_2SO_4. The band near 1095 cm.$^{-1}$, originally present in Hevea, disappeared in concentrated H_2SO_4. A shift of peaks from 1665 to 1670 cm.$^{-1}$ then increasing in width and finally covering the range between 1670 and 1650 cm.$^{-1}$ was observed. Simultaneously the intensity decreased. The absorption of $-$CH$_2-$ groups near 1455 cm.$^{-1}$ shifted to 1465 cm.$^{-1}$.

When concentrated H_2SO_4 was used, new bands appeared at 885 cm.$^{-1}$ and soon after at 696 and 732 cm.$^{-1}$. These bands disappeared when the cyclization was complete, and a very broad and strong band appeared at 1175 cm.$^{-1}$. In completely cyclized polymer new peaks remained at 810, 885, 1040, 1175 and 1265 cm.$^{-1}$, together with a very weak band at 1200 cm.$^{-1}$.

In the range of C$-$H stretching vibrations around 3000 cm.$^{-1}$ the absorption intensity at 2750 and 3040 cm.$^{-1}$, decreased and new very weak bands appeared at 2685 and 3060 cm.$^{-1}$. The $-$CH$_2-$ symmetric vibration peak[11] shifted to 2870 cm.$^{-1}$.

Infrared spectra of cyclized cis-1,4 polyisoprene are presented in Figure 1. The arrows indicate typical bands.

Balata

After 100 hr. of reaction with 1% H_2SO_4, calculated on polymer, the intensities of peaks at 600 and 473 cm.$^{-1}$ decreased to about 30% of the original values. These bands also disappeared in concentrated H_2SO_4.
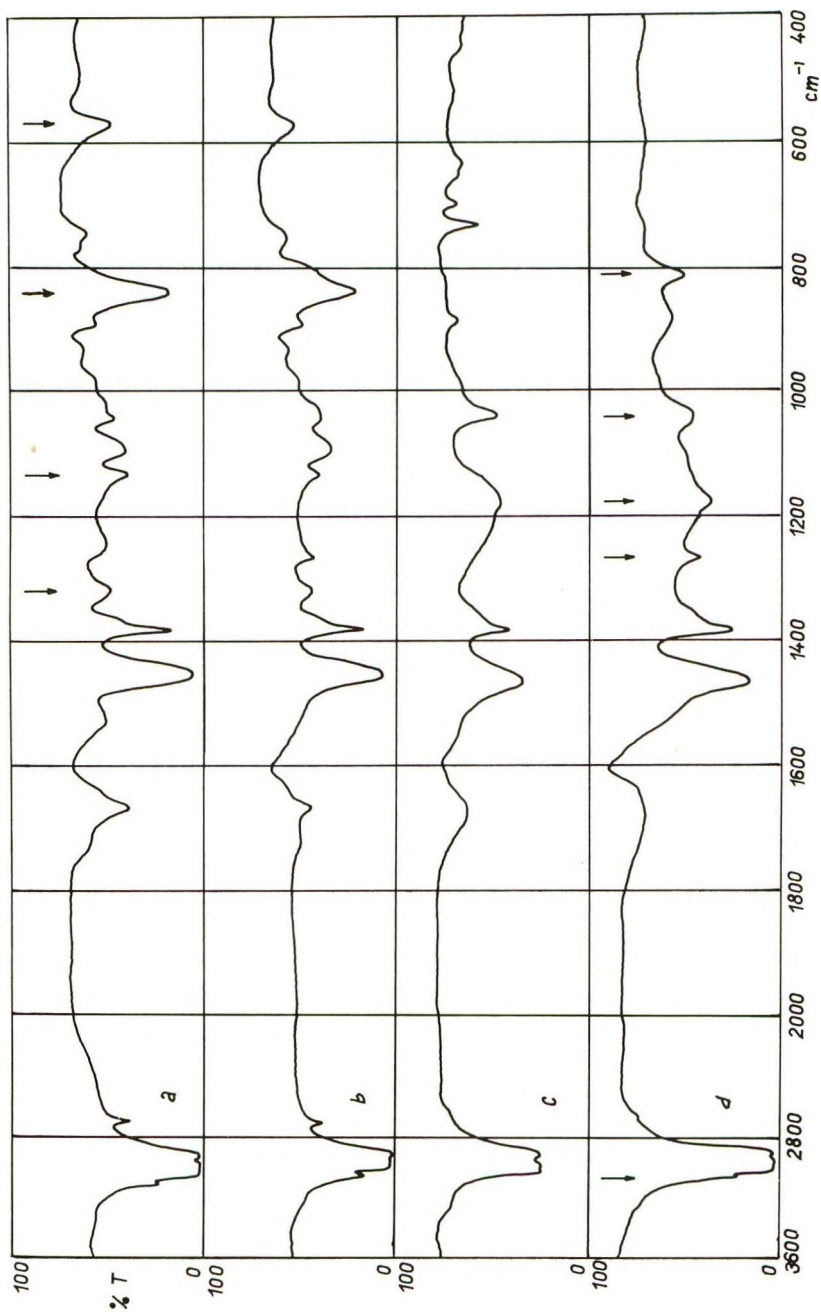
Fig. 1. Infrared spectra of cyclized cis-1,4-polyisoprene: (a) Hevea rubber, untreated; (b) cyclized with 1% H₂SO₄ (calc. on rubber), 105 hr. at 80°C.; (c) cyclized with 10% H₂SO₄ (in heterogeneous mixture), 8 hr. at 20°C.; (d) cyclized with 10% H₂SO₄, 100 hr. at 80°C.
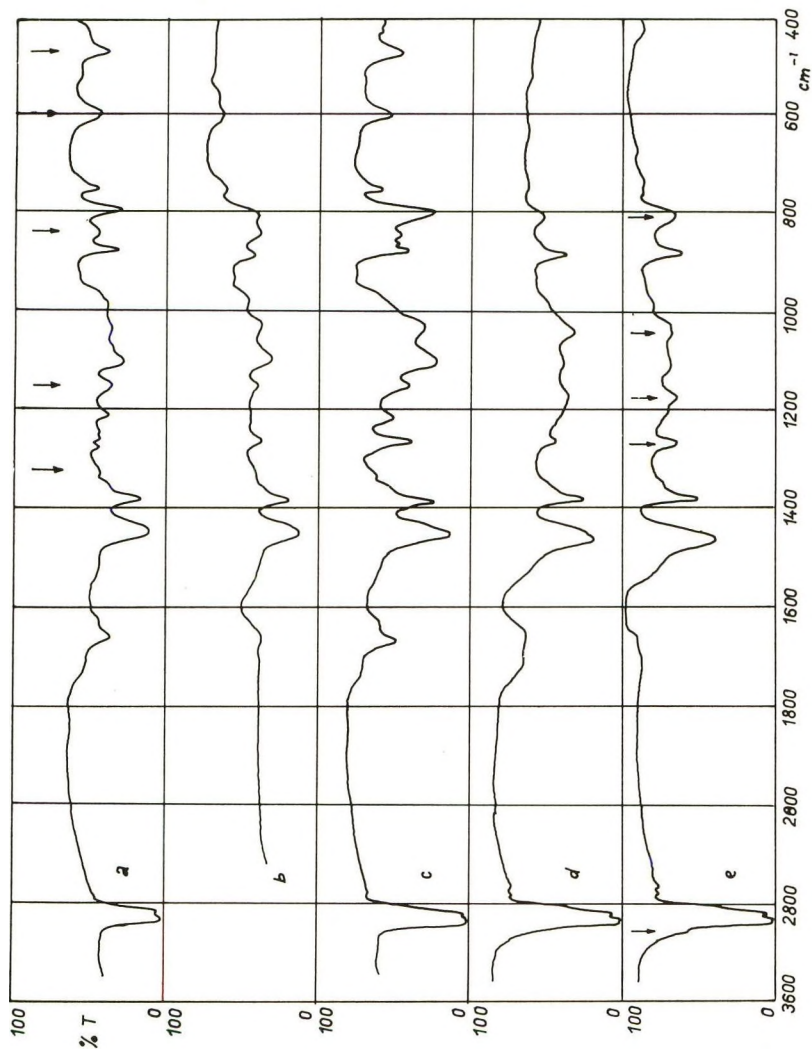
Fig. 2. Infrared spectra of cyclized *trans*-1,4-polyisoprene: (*a*) balata, untreated; (*b*) cyclized with 1% H$_2$SO$_4$, 105 hr. at 80°C.; (*c*) cyclized with 10% H$_2$SO$_4$, 0.5 hr. at 20°C.; (*d*) cyclized with 10% H$_2$SO$_4$, 7.5 hr. at 80°C.; (*e*) cyclized with 10% H$_2$SO$_4$, 100 hr. at 80°C.
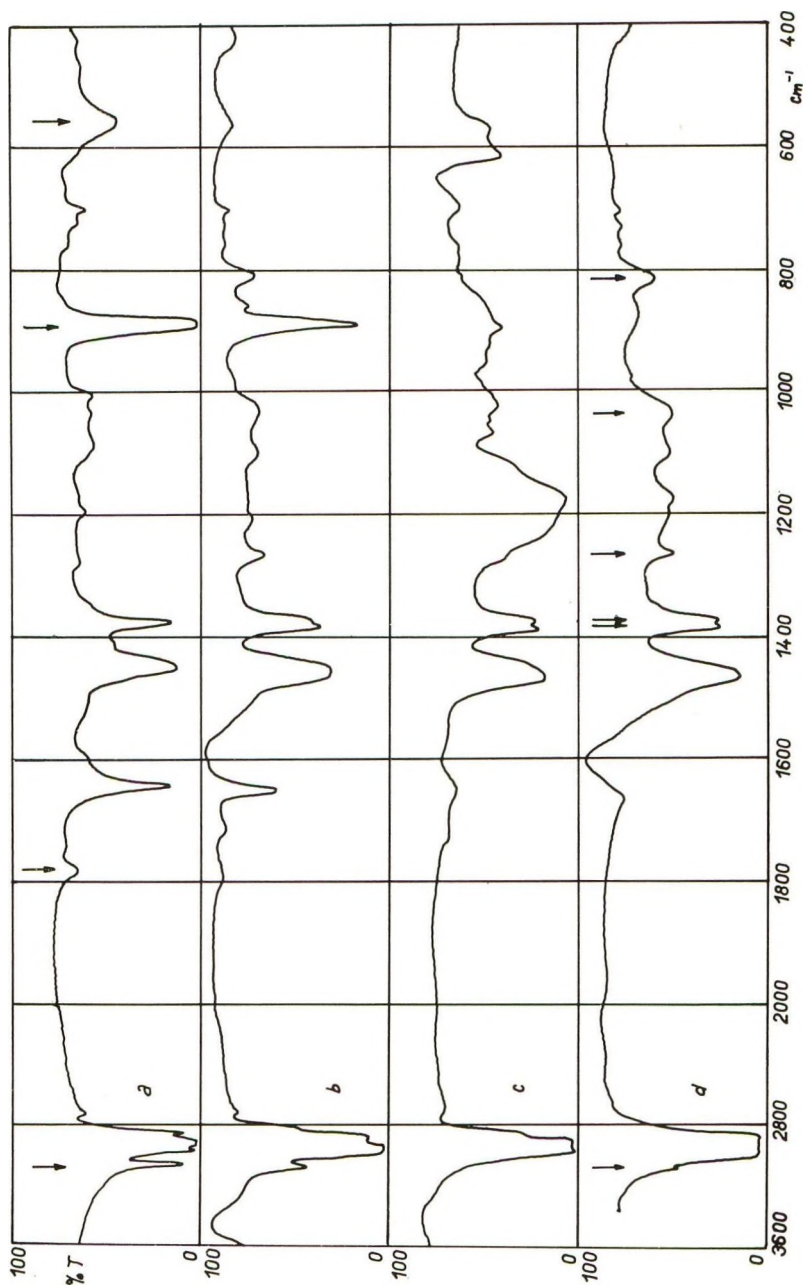
Fig. 3. Infrared spectra of cyclized 3,4-polyisoprene: (a) untreated polymer; (b) cyclized with 1% H₂SO₄, 105 hr. at 80°C.; (c) cyclized with 10% H₂SO₄, 0.5 hr. at 20°C.; (d) cyclized with 10% H₂SO₄, 100 hr. at 80°C.

Uncyclized balata shows bands at 789, 845, and 878 cm.$^{-1}$ when the KBr pellet technique is used.   In carbon disulfide solution only the band at 845 cm.$^{-1}$ is present.   All three absorption bands changed their intensity on treatment with dilute acid.   The intensity of bands at 878 and 789 cm.$^{-1}$ decreased first; the latter shifted to 810 cm.$^{-1}$ as the intensity of the band at 845 cm.$^{-1}$ diminished.   All three bands disappeared on cyclization with 10% H_2SO_4 but new absorption arose at 882 cm.$^{-1}$.   Characteristic bands of *trans*-1,4-polyisoprene at 1330[10] and 1150 cm.$^{-1}$ and the absorption at 1105 cm.$^{-1}$ were not present in the cyclized polymer.   As in cyclized Hevea, new absorption arose at 1175 cm.$^{-1}$ and the same shift of peaks of —C=C stretching vibrations were observed.   The —CH$_2$— band at 1455 cm.$^{-1}$ changed its position to 1465 cm.$^{-1}$ and the band of —CH$_3$ symmetric vibrations at 1384 cm.$^{-1}$ shifted to 1378 cm.$^{-1}$.

In the region of 3000 cm.$^{-1}$ the following changes were observed: decrease in intensity of the band at 3049 cm.$^{-1}$, appearance of new very weak bands at 2685 and 3060 cm.$^{-1}$, and the shift of the band at 2850 to 2870 cm.$^{-1}$.

A peak at 1265 cm.$^{-1}$ appeared in the early stages of the cyclization and later new absorption appeared at 1040 cm.$^{-1}$.   Cyclized *trans*-1,4-polyisoprene showed the same new absorption bands as *cis*-1,4-polyisoprene.

Infrared spectra of cyclized balata are presented in Fig 2.

3,4-Polyisoprene

The intensity of absorption bands at 566, 888, 1784, and 3077 cm.$^{-1}$, typical for this polymer, decrease very rapidly in the presence of concentrated H_2SO_4.   With 1% H_2SO_4 their intensity decreased to about 30% of the original values.   The absorption of the —C=C— stretching vibration shifts from 1643 to 1650 cm.$^{-1}$ and in the final stages to 1665 cm.$^{-1}$. Its intensity measured at the maximum of absorption drops to about 50% using 1% H_2SO_4, to less than 10% using concentrated H_2SO_4.   A shift of the peak at 566 cm.$^{-1}$ to 580 cm.$^{-1}$ and later to 590 cm.$^{-1}$ was also noted.
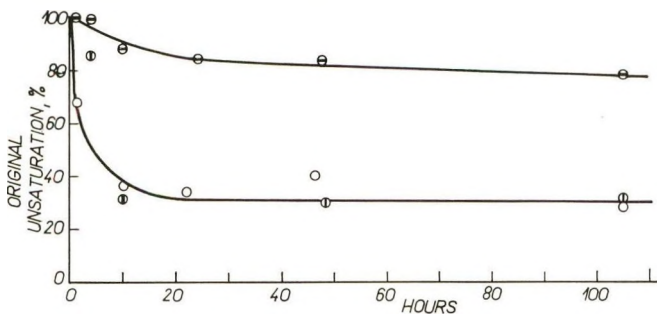

Fig. 4. Content of linear unsaturation in the polymer cyclized with 1% H_2SO_4 as determined from the decrease in intensity of the absorption bands: ($\ominus$) *cis*-1,4-polyisoprene, 572 cm.$^{-1}$; ($\oplus$) *trans*-1,4-polyisoprene, 600 and 473 cm.$^{-1}$; ($\bigcirc$) 3,4-polyisoprene, 566 and 888 cm.$^{-1}$.
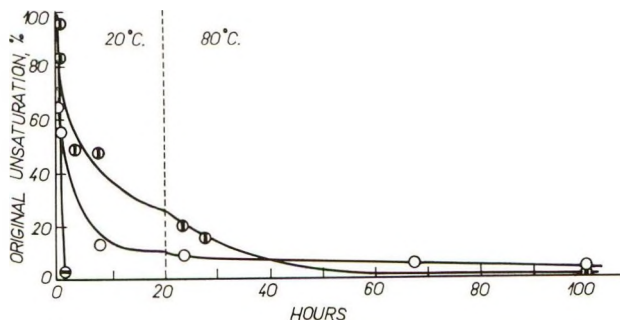
Fig. 5. Content of linear unsaturation in the polymer cyclized with 10% H_2SO_4. Cyclization carried out at 80°C., after 20 hr. at 20°C. The symbols are the same as in Fig. 4.

The absorption band at 1378 cm.$^{-1}$, characteristic of the CH_3 group, splits in cyclized polymer to two peaks, one at 1385 cm.$^{-1}$, the second at 1370 cm.$^{-1}$.

New bands appeared at 1175 cm.$^{-1}$ only with 10% H_2SO_4 and was weak in completely cyclized polymer. With the dilute (1%) H_2SO_4, the infrared spectra showed additional changes: a shift of absorption from 1085 to 1100 cm.$^{-1}$, a slight increase in intensity of absorption at 1033 cm.$^{-1}$, and appearance of new bands at 1265, 1015, and 1070 cm.$^{-1}$. With 10% H_2SO_4 the spectrum underwent these changes: new bands appeared at 1245 and 618 cm.$^{-1}$ (indicating formation of intermediates, since they disappear in the final stages of cyclization), the peak at 775 cm.$^{-1}$ shifted to 760 cm.$^{-1}$, characteristic absorption of $-CH_2-$ groups shifted from 1450 to 1465 cm.$^{-1}$, and a new peak appeared at 1040 cm.$^{-1}$.

In the region of C—H stretching vibrations these changes were observed: decrease of the intensity at 3077 cm.$^{-1}$, shift of the absorption at 2852 cm.$^{-1}$ to 2870 cm.$^{-1}$, and appearance of a new very weak band at 3060 cm.$^{-1}$.

Infrared spectra of cyclized 3,4-polyisoprene are presented in Figure 3.

The absorptions at 572 cm.$^{-1}$ in cis-1,4-polyisoprene, 600 cm.$^{-1}$ and 473 cm.$^{-1}$ in $trans$-1,4-polyisoprene, and 888 cm.$^{-1}$ or 566 cm.$^{-1}$ in 3,4-polyisoprene, were used for the determination of original unsaturation (see Figs. 4 and 5).

IV. DISCUSSION

It is difficult to decide whether monocyclic, bicyclic, or polycyclic structures are formed simply on the basis of the determination of $-C=C-$ double bonds because of the unreliability of chemical methods of analysis and very meager data on absorptivities of $-C=C$ stretching vibrations in infrared analysis.

Based on the results of cyclization of polyisoprenes by H_2SO_4 it appears that the type of cyclic structures formed depends upon reaction conditions

and the character of the solvent.[4] The formation of cyclized polymer (white, insoluble powder) with no characteristic absorption indicating the presence of residual linear unsaturation, points up differences from soluble cyclized polymers which are considered to be mono- or bicyclic. Most authors have studied only the soluble cyclization products. Infrared spectra presented in Figures 1b, 1d, 2b, and 2e, 3b, and 3d show the differences between soluble and insoluble cyclic polymers.

The possibility of crosslinking by the action of oxygen can be ruled out because there was no sign of gelation during cyclization.

cis and trans-1,4-Polyisoprene

The cyclization mechanism involves first the protonation of the double bond in the chain, eq. (1):

$$(1)$$
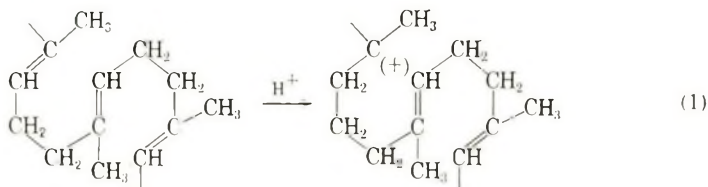
The addition of the proton probably proceeds in the Markownikoff sense to give an intermediate to which two or at least one hydrogen atom is attached, and the positive charge is localized on the carbon with no hydrogen. The adjoining double bond in the chain is then polarized and a new bond, closing the ring, is formed. The positive charge then transfers to the carbon atom on this next double bond.

$$(2)$$
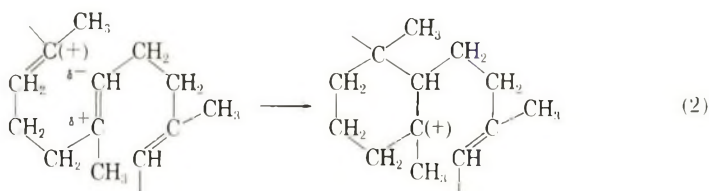
The possibility of isomerization, eq. (3),
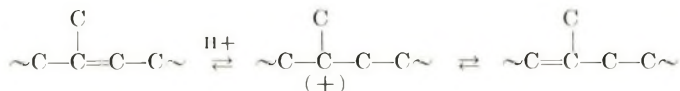
must be taken into account. This type of isomerization should lead to a reversal of the direction of cyclization and may cause the linking of two cyclic segments when two terminal unsaturations come together in space.

Three possible modes of deprotonation are shown in eqs. (4).

$$(4)$$

Gordon[5] proposed only formation of monocycles with Flory's distribution[12] of original double bonds. According to Golub and Heller,[6] the propagation of cyclization stops after a bicyclic structure has been reached. These workers found that the ratio of meth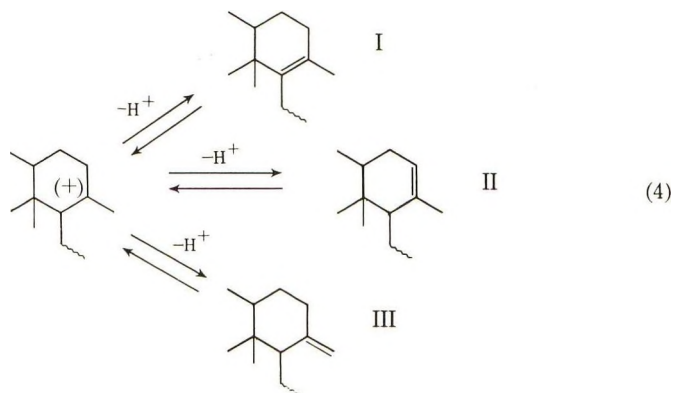yl groups adjacent to saturated carbons to those on doubly bonded carbon is about $2:1$, which, under the assumption of only bicyclic structures should mean that no original double bonds remain in the cyclized polymer. The formation of one bicyclic structure requires three double bonds in the linear chain. If no double bond is preferentially protonized and monocycles are improbable, then less than three double bonds may be left between two bicycles. These two or one "linear" double bonds are unable to close the ring and should remain unreacted. Their characteristics should be found in the infrared spectrum.

From the results of the experiments with H_2SO_4, it follows that polyisoprene may be cyclized to such a degree that no linear double bonds remain in the chain. There is good evidence from infrared spectra for this situation. It may be presumed that in higher concentrations of acid, the rate of deprotonation is relatively slower and the reverse protonation of "terminal" double bond easier and therefore a higher number than three of linear double bonds react to form fused ring structures. The formation of polycyclic structures is also indicated in the work of Wallenberger.[15]

The degree of cyclization and the formation of mono-, bi-, or polycyclic structures can be only roughly estimated from the decrease in intensity of absorption bands characteristic of the original double bonds and from the decrease of the total amount of unsaturation accompanied by shifts of peaks indicating the formation of new double bonds.

Use of the absorption band near 840 cm.$^{-1}$, assigned to the out-of-plane vibration of the C—H group in —C(CH$_3$)=CH—, leads to some errors in the determination of double bonds in the linear chain. The intensity of this absorption band is very dependent on the way the samples were prepared for infrared investigation. The optical density of this band is higher if the sample is in solution and lower in a KBr disk or as film. Furthermore, balata with the KBr technique shows new absorptions between 780 and 900 cm.$^{-1}$ which are known in gutta-percha film. It is evident that ab-

sorption is greatly influenced by environment. It appears that not only crystallization but also the presence of various "hard" substituents such as the cyclic structures influence the intensity and the position of the peak near 840 cm.$^{-1}$. The content of linear unsaturation was determined by means of the bands at 572 cm.$^{-1}$ in *cis*-1,4-polyisoprene, and 600 and 473 cm.$^{-1}$ in *trans*-1,4-polyisoprene; these bands are also in some way connected with —C(CH$_3$)=CH— group, but are unaffected by the method of preparation of the samples.

Using 1% H$_2$SO$_4$, calculated on *trans*-1,4-polyisoprene, some stationary state exists in the cyclization reaction where about 33% of the original unsaturation and about 50% of all double bonds remain (see Fig. 4). If the formation of bicycles is assumed, where three linear double bonds are consumed and one new double bond is formed in each bicyclic structure, then based on our results 1.5 original double bonds, on the average, remain per bicycle. If the formation of monocyclic structures is assumed, where two linear double bonds are consumed and a new one formed per monocycle, 85% of the original double bonds, on the average, remains per ring while about 30% should remain according to Flory's calculation.

In our case, presuming monocyclic structure, the ratio of methyl groups adjacent to saturated carbon atoms to methyl groups on double bonded carbon atoms is about 0.5:1. If bicycles are formed, this ratio should be 0.8:1. Golub and Heller, using a nuclear magnetic resonance method, found this ratio to be about 2:1.[6]

It seems very probable that the stationary state and thus the number of rings in the cyclic structure and the ratio of the number of cyclic segments to remaining double bonds in the chain depends on reaction conditions.

The unsaturation value cannot be confirmed by other analytical methods because of their unreliability. The concept of the dependence of the intensity of the band at 840 cm.$^{-1}$ on neighboring substituents and orientation is supported by the results with 10% H$_2$SO$_4$. In one sample of cyclized *trans*-1,4-polyisoprene where about 30% of the original double bonds, as determined from the peaks at 600 and 473 cm.$^{-1}$ were still present, the band at 845 cm.$^{-1}$ was already absent.

The linear unsaturation disappeared completely with the use of 10% H$_2$SO$_4$, after a short reaction period. This is shown by the disappearance of the bands below 700 cm.$^{-1}$, typical peaks at 1130 or 1150 cm.$^{-1}$, and 1315 or 1325 cm.$^{-1}$, respectively, and the bands at 1105 cm.$^{-1}$ in balata, and 1095 cm.$^{-1}$ in Hevea, indicating the presence of —CH$_2$— groups adjacent to a —C(CH$_3$)=CH— group, *trans* or *cis*, in the linear polymer.

During the cyclization, methylene groups in linear chains became methylene groups in cyclic rings, a change which is accompanied by the shift of absorption from 1455 cm.$^{-1}$ to 1465 cm.$^{-1}$ and from 2850 cm.$^{-1}$ in *trans*-1,4-polyisoprene and 2857 cm.$^{-1}$ in *cis*-1,4-polyisoprene to 2870 cm.$^{-1}$. The shift of the symmetric deformation vibration of CH$_3$ group from 1384 cm.$^{-1}$ in *trans*-1,4-polyisoprene to 1378 cm.$^{-1}$ in the cyclized polymer is probably due to the new position of the CH$_3$ group on saturated carbon.

The substitution on —C=C— changes with cyclization and these changes are accompanied by the shift of the band at 1665 cm.$^{-1}$, first to 1670 cm.$^{-1}$ characterizing intermediate structures (probably structure I with its slow rate of reverse protonation), and then to the band with an increased width of absorption.

During the cyclization of Hevea and balata, when the original unsaturation disappeared, a new strong peak appeared near 1175 cm.$^{-1}$. This band was not present in polymer cyclized with 1% H_2SO_4 where the original double bonds remain between cyclic segments. In cyclopolymers,[1] where we propose polycyclic structure with long cyclic segments and long linear segments, this band is relatively weak and becomes more intense only when the double bonds in linear segments are cyclized by the action of H_2SO_4. Therefore it is connected with the relative number of cyclic segments in a polymer molecule or with "terminal" rings adjacent to saturated fragments between cyclic segments (IV).

IV
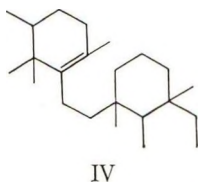
Hevea is more readily cyclized with concentrated H_2SO_4 than balata, but with 1% H_2SO_4 the order is reversed (see Figs. 4 and 5). The final products of cyclization of both polymers show no difference in infrared spectra (Figs. 1d and 2c); cis-1,4-polyisoprene and trans-1,4-polyisoprene yield the same cyclic polymer. This is possible only if the cyclization goes according to the scheme shown in eq. (5):

$$cis \searrow \qquad \nearrow I$$
$$(LH)^+ \rightarrow (CH)^+ \rightleftarrows II \qquad (5)$$
$$trans \nearrow \qquad \searrow III$$
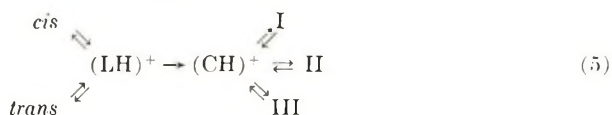
where $(LH)^+$ is the linear ion, $(CH)^+$ denotes the cyclic ion, and I, II, and III are the structures previously shown. The structure with tetrasubstituted double bond predominates.[6]

Different rates of cyclization of Hevea and balata are due to different rate constants of protonation and cyclization; the vicinal double bond to be cyclized requires a suitable steric arrangement. In one of the polymers the arrangement is suitable for cyclization and in the other the arrangement requires a higher activation energy.

This scheme does not rule out cis–trans isomerization.

3,4-Polyisoprene

Initiation of isomerization may be represented as shown in eq. (6).

$$(6)$$
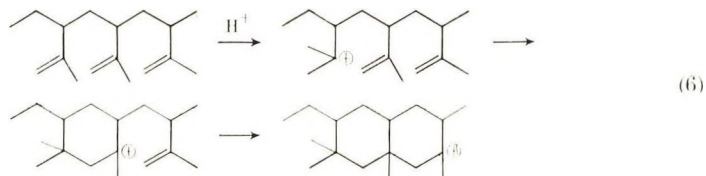
That a new tetrahedral $\diagup$ C(CH$_3$)$_2$ group appears in the first ring is shown by the splitting of the band at 1378 cm.$^{-1}$ to two bands at 1385 and 1372 cm.$^{-1}$.

Three routes of deprotonation are possible, as in the case of 1,4-polymers, eqs. (7):

$$(7)$$
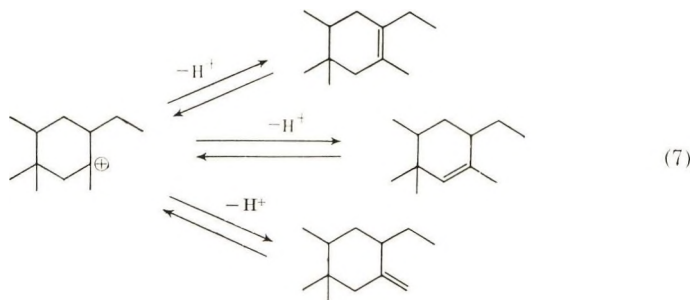
When 1% H$_2$SO$_4$ is used at 80°C. the same stationary state was reached as in balata.   With 10% H$_2$SO$_4$ almost all isopropenyl unsaturation disappeared, which is indicated by the decrease in intensity of the bands at 3077, 1784, 888, and 566 cm.$^{-1}$. [9]

All three cyclized polyisoprenes exhibit the same new absorption peaks at 3060, 2870, and 1265 cm.$^{-1}$, and very weak bands near 1200, 1175, 1040, and 810 cm.$^{-1}$.   The bands connected with the original double bonds in the polymer disappear completely.

Comparison with Cyclopolymers (Prepared from Monomer)

All infrared spectra of cyclized polymers and cyclopolymers are very simple;   the number of peaks is very small in comparison with that in cyclized isoprene dimers[13] and polymers cyclized to a low degree with 1% H$_2$SO$_4$.

No difference between the infrared spectra of cyclized balata and Hevea was found in the whole range from 400 to 4000 cm.$^{-1}$.   The infrared spectrum of 3,4-polyisoprene differs only by the presence of two peaks at 1370 and 1385 cm.$^{-1}$ and small peaks near 725 and 760 cm.$^{-1}$.

Absorption bands at 1040 cm.$^{-1}$ and near 1200 cm.$^{-1}$ belong to —C—C— stretching vibrations.   The band at 1040 cm.$^{-1}$ was found by Morero, et al.[14] in the spectrum of 1,4-polybutadiene and is present also in 3,4-polyisoprene.[9]   Morero assigned this band to
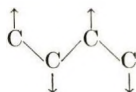
vibrations. The band at 1213 cm.$^{-1}$ was also described as characteristic for the vibration of the type

$$C \rightarrow C \rightarrow$$
$$\diagdown \diagup \diagdown$$
$$\leftarrow C \leftarrow C$$
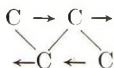
A similar band was found in 3,4-polyisoprene at 1197 cm.$^{-1}$.[9] The bands at 1040 cm.$^{-1}$ and near 1200 cm.$^{-1}$ in cyclized polymers are probably of the same origin.

Practically no differences exist between the infrared spectra of cyclopolymers prepared from monomer and cyclized polyisoprenes prepared by cyclization of linear *trans*-1,4-, *cis*-1,4-, and 3,4-polyisoprenes. The relatively low intensity of the band at 1175 cm.$^{-1}$ in cyclopolymers is due to the low content of "terminal" double bonds. The presence of very weak absorption bands between 760 and 700 cm.$^{-1}$ indicates that the structure of cyclopolymer from isoprene is close to that of cyclized 3,4-polyisoprene. However, the similarity in infrared spectrum is not convincing and requires more evidence.

The spectra of cyclopolybutadienes[1] have the same characteristics as those of cyclopolyisoprenes and cyclized polyisoprenes. The peak near 1380 cm.$^{-1}$ indicates the presence of CH_3 groups. Its intensity is a function of the length and the number of cyclic segments in the molecule. The infrared spectrum of cyclopolychloroprene[1] is very similar to those of cyclopolyisoprene and cyclopolybutadiene. Also in this case some CH_3 groups are present and the spectra contain all peaks characteristic of cyclic structures plus a new peak at 2960 cm.$^{-1}$.

New absorption peaks at 2870, 1265, 1200, 1040, and 810 cm.$^{-1}$ are common to all cyclized polyisoprenes and to cyclopolymers from isoprene. Cyclopolybutadiene and cyclopolychloroprene also appear to have the same structure in the cyclic polymer chain.

References

1. Gaylord, N. G., I. Kössler, M. Stolka, and J. Vodehnal, *J. Am. Chem. Soc.*, **85**, 641 (1963); *J. Polymer Sci.*, **A2**, 3969 (1964).

2. Staudinger, H., and W. Widmer, *Helv. Chim. Acta*, **9**, 529 (1926).

3. D'Ianni, J. D., F. J. Naples, J. W. Marsh, and J. L. Zarney, *Ind. Eng. Chem.*, **38**, 1171 (1946).

4. Van Veersen, G. J., *Rubber Chem. Technol.*, **24**, 957 (1951).

5. Gordon, M., *Ind. Eng. Chem.*, **43**, 386 (1951).

6. Golub, M. A., and J. Heller, *Can. J. Chem.*, **41**, 937 (1963).

7. Rao, N. V. C., *Makromol. Chem.*, **16**, 1198 (1955).

8. Ramakrishnan, C. S., S. Dagupta, and N. V. C. Rao, *Makromol. Chem.*, **20**, 46 (1956).

9. Stolka, M., J. Vodehnal, and I. Kössler, *Collection Czech. Chem. Communs.*, **28**, 1535 (1963).

10. Binder, J. L., *J. Polymer Sci.*, **A1**, 37 (1963).

11. Ciampelli, F., and I. Manoviciu, *Gazz. Chim. Ital.*, **91**, 1045 (1961).

12. Flory, P. J., *J. Am. Chem. Soc.*, **61**, 1518 (1939).

13. Binder, J. L., K. C. Eberly, and G. E. P. Smith, Jr., *J. Polymer Sci.*, **38**, 229 (1959).

14. Morero, D., E. Mantica, and L. Porri, *Nuovo Cimento, Suppl.*, **15**, Ser. 10, 136 (1960).

15. Wallenberger, F. T., *Makromol. Chem.*, **93**, 74 (1962).

Résumé

On a fait la cyclisation du *cis* 1,4- et *trans* 3,4-polyisoprène en solution dans le toluène au moyen d'acide sulfurique. Avec 1% H_2SO_4, calculé par rapport au polymère, on atteint un état stationnaire de cyclisation dans lequel 33% de l'insaturation originale et environ 50% de l'insaturation totale restent dans le *trans*-1,4- et 3,4-polyisoprène cyclisé. La vitesse de cyclisation du *cis*-1,4-polyisoprène est très petite et la valeur limite n'est même pas atteinte après 100 hrs à 80°C. Les spectres infrarouges des polymères cyclisés montrent une diminution de l'intensité d'absorption des bandes caractéristiques des groupes dans le polymère linéaire. Avec 10% H_2SO_4, calculé sur le polymère (un mélange hétérogène), tous les trois polyisoprènes cyclisent pour donner un polymère n'ayant plus aucune insaturation originale dans la chaîne. Les spectres infrarouges du *trans*-1,4 et *cis*-1,4-polyisoprène cyclisé sont identiques. Les spectres du 3,4-polyisoprène cyclisé diffèrent seulement par deux pics à 1385^{-1} et 1370 cm^{-1}. Les spectres des trois isomères cyclisés montrent de nouvelles bandes dans le spectre infrarouge à 2870, 1265, 1200, 1040 et 810 cm^{-1}. On a fait une comparaison des spectres infrarouges du cyclopolymères de l'isoprènes du butadiène et du chloroprène préparés à partir de monomères en employant des catalyseurs du type Ziegler-Natta avec les spectres du polyisoprène cyclisés. Les spectres sont très similaires, ce qui indique que les deux types de polymères ont la même structure cyclique.

Zusammenfassung

Die Zyklisierung von *Cis*-1,4-, *Trans*-1,4- und 3,4-Polyisopren wurde in Toluollösung mit Schwefelsäure ausgeführt. Mit 1% H_2SO_4, bezogen auf das Polymere, wurde ein stationärer Zyklisierungszustand erreicht, bei welchem 33% der ursprünglichen Ungesättigtheit und etwa 50% der totalen Ungesättigtheit im zyklisierten *Trans*-1,4- und 3,4-Polyisopren verblieb. Die Zyklisierungsgeschwindigkeit von *Cis*-1,4-Polyisopren war sehr gering, und der Grenzwert wurde nicht einmal nach hundert Stunden bei 80°C erreicht. Infrarotspektren der zyklisierten Polymeren zeigen eine verminderte Absorptionsintensität der für die Gruppen in linearen Polymeren charakteristischen Banden. Mit 10% H_2SO_4, bezogen auf das Polymere (eine heterogene Mischung), zyklisierten alle drei Polyisoprene unter Bildung eines Polymeren ohne jede ursprüngliche Ungesättigtheit. Infrarotspektren des zyklisierten *Trans*-1,4- und *Cis*-1,4-Polyisopren sind identisch. Das Spektrum des zyklisierten 3,4-Polyisopren unterscheidet sich nur durch zwei Maxima bei 1385 cm^{-1} und 1370 cm^{-1}. Die Spektren aller drei zyklisierten Isomere zeigen neue Banden im Infrarotspektrum bei 2870, 1265, 1200, 1040 und 810 cm^{-1}. Ein Vergleich der Infrarotspektren, der mit Ziegler-Natta-Katalysatoren dargestellten Zyklopolymeren von Isopren, Butadien und Chloropren mit Spektren von zyklisiertem Polyisopren wurde durchgeführt. Die Spektren sind recht ähnlich, was dafür spricht, dass beide Polymertypen die gleiche polyzyklische Struktur besitzen.

A Contribution to the Preparation of Phenolic Polynuclear Compounds with Sulfonyl Bridges

H. KÄMMERER and M. HARRIS,* *Institute for Organic Chemistry, University of Mainz/Rhein, Germany*

Synopsis

For the preparation of phenolic di- and tricyclic compounds with sulfonyl bridges the Fries rearrangement is suitable, and for the corresponding products with three and four benzene rings the Friedel-Crafts reaction may be used.   The exchange of sulfonyl bridges for methylene bridges produces a marked increase in the melting point.

INTRODUCTION

Oligomeric compounds possess properties which are partly similar both to the usual organic compounds and also to macromolecular products. To clarify the connection between structure and reaction behavior of polymeric substances, it is of special interest to prepare and investigate the oligomeric compounds.   Phenolic polynuclear compounds with sulfonyl bridges are, for example, used as synthetic tanning agents.   However, little is known of their preparation and properties.   Continuation of earlier investigations[1] have indicated that two methods are generally suitable for the preparation of structurally uniform phenolic polynuclear compounds with sulfonyl bridges, namely, the Fries rearrangement and the Friedel-Crafts reaction.

DISCUSSION

Syntheses for Structurally Uniform Phenolic Polynuclear Compounds with Sulfonyl Bridges

Starting Materials.   In addition to the esters, which were prepared in the usual manner, the sulfonyl chlorides were also necessary for the Friedel-Crafts condensation reaction.   The introduction of sulfochloride groups in the binuclear sulfones can be easily achieved by treatment with chlorosulfonic acid.   Typical examples are the sulfonyl chlorides I, II, and III.

Fries Rearrangement.   This reaction is not only applicable for the preparation of sulfones (IV and V), but can also be used to obtain the three nuclear compounds with two sulfonyl bridges (VI).

* Present address: Eastman Research AG, Zürich, Switzerland.
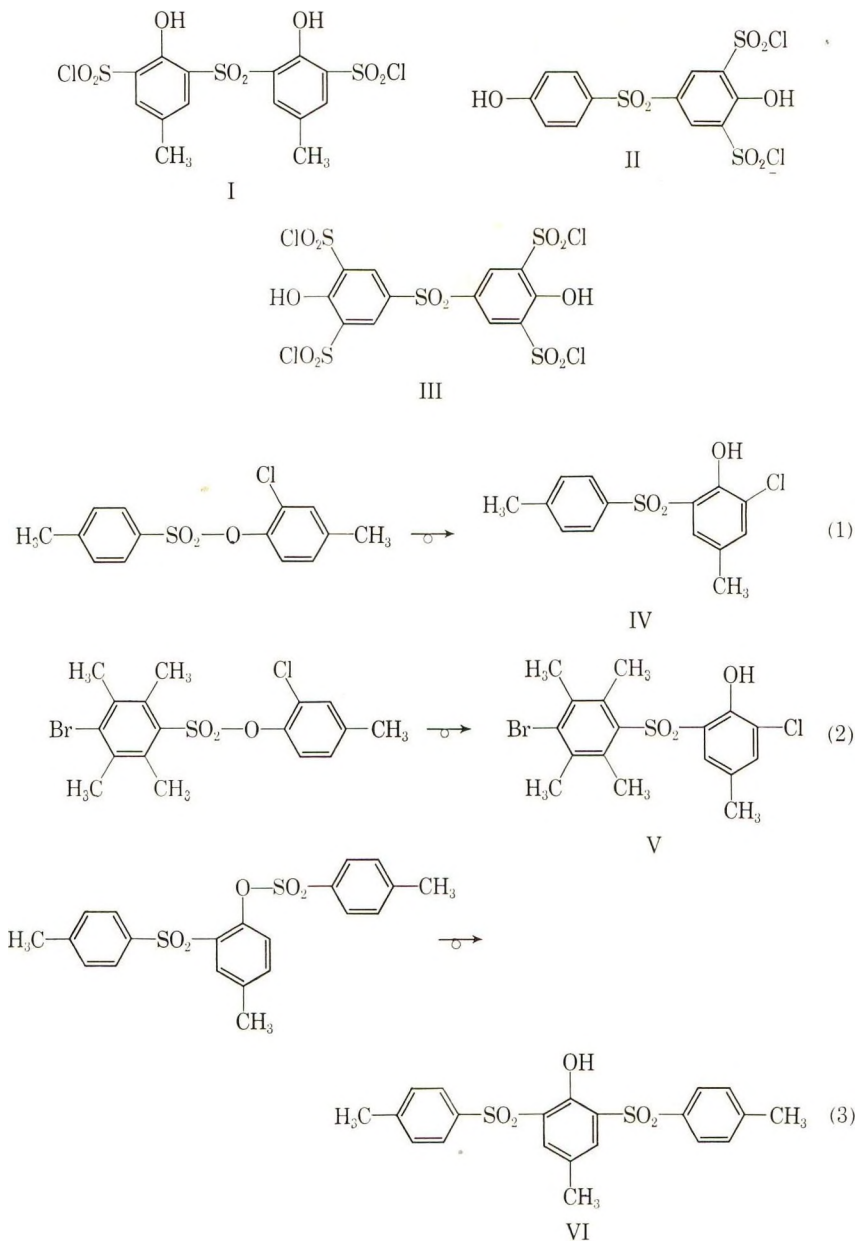
The scheme indicating the preparation of bi- and trinuclear compounds with sulfonyl groups by means of the Fries rearrangement is shown in eqs. (1)–(3).

Friedel-Crafts Condensation. In order to avoid undesirable side reactions the sulfonyl chlorides were reacted with methylated reactants, stannic chloride being used as catalyst. By this method it was not only possible to

prepare the trinuclear but also the tetranuclear compound with sulfonyl bridges, as shown in eq. (4).

$$(4)$$
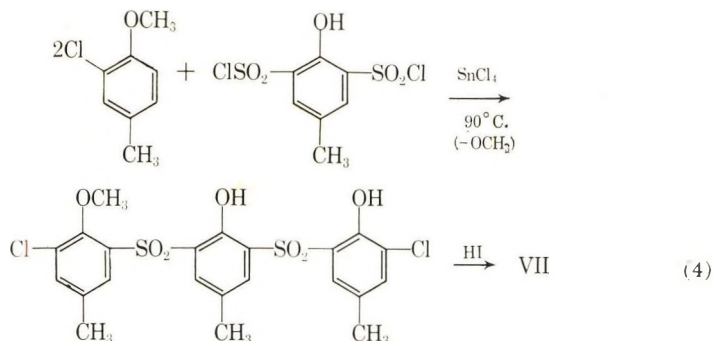
The acetylation and elemental analysis together with the determination of the number of acetyl groups present in the reaction product indicated that during the condensation a methoxy group had been cleaved. The reaction product was treated with hydrogen iodide producing the trinuclear compound (VII) containing three phenolic hydroxy groups per molecule [eq. (4)].

$$(5)$$
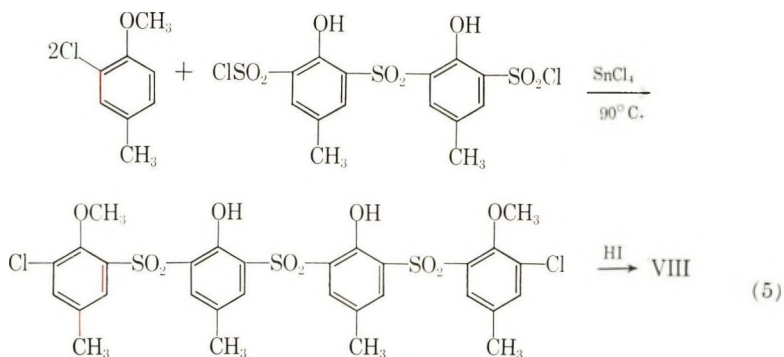
The reaction of I with 3-chloro-4-methoxy-1-methylbenzene and subsequent treatment of the reaction product with hydrogen iodide yielded the tetranuclear compound VIII with four free phenolic groups per molecule [eq. (5)].

Molecular weight determination of the prepared polynuclear compounds by the usual methods is difficult. However it is possible to ascertain from the chlorine value the lowest molecular weight From the method of synthesis a factor is obtained which has to be multiplied by the lowest molecular weight. Therefore, for compounds I, II and III the determined molecular weights are: 475 (calcd. 475), 448 (calcd. 447) and 635 (calcd. 644). With compounds VII and VIII the chlorine atoms possess the character of endgroups; thus the determined molecular weights are: 524 (calcd. 517) and 713 (calcd. 688).

Comparison of Melting Points of Phenolic Polynuclear Compounds with Methylene and Sulfonyl Bridges

As the corresponding structurally defined phenolic polynuclear compounds possessing methylene instead of sulfonyl bridges are known,[1,2] it was possible to show the influence of the sulfonyl bridge on the melting points. As expected, the melting points of the polynuclear compounds with sulfonyl bridges are markedly higher. (Table I.)

TABLE I

Comparison of Melting Points of Phenolic Polynuclear Compounds with Methylene or Sulfonyl Bridges

(Q = Bridge)

Structure	Q	Melting point, °C.	Difference Δ, °C.
	$-CH_2-$ $-SO_2-$	160 179	19
	$-CH_2-$ $-SO_2-$	168 238– 240	71
	$-CH_2-$ $-SO_2-$	208 246– 252	41

EXPERIMENTAL

Preparation of the Sulfonyl Chlorides

Sulfonyl Chloride I. A 1.67-g portion (6 mmole) of 6,6′-dihydroxy-3,3′-dimethyldiphenylsulfone was dissolved in 15 ml. chlorosulfonic acid at room temperature and then heated for 1 hr. at 40–50°C. After standing for 24 hr. at room temperature the reaction mixture was added dropwise to ice. After filtering and drying over concentrated sulfuric acid the product was recrystallized from petroleum ether; yield 2 g. (70%); m.p. 184–187°C.

ANAL. Calcd. for $C_{14}H_{12}Cl_2O_8S_3$ (475.4): C, 35.38%; H, 2.54%; Cl, 14.92%; Found: C, 35.88%; H, 2.66%; Cl, 14.91%.

Sulfonyl Chloride II. 4,4′-Dihydroxydiphenylsulfone (2.5 g., 0.01 mole) was added in small portions with stirring to 40 ml. chlorosulfonic acid and heated for 45 min. at 50°C. After 48 hr. the reaction mixture was decomposed with ice, yielding a white precipitate which was dried over concen-

trated sulfuric acid and recrystallized from dioxane. Colorless crystals melting at 201–203°C. were obtained in a yield of 89%.

ANAL. Calcd. for $C_{12}H_8Cl_2O_8S_3$ (447.3): C, 32.21%; H, 1.80%; Cl, 15.86%. Found: C, 32.40%; H, 1.99%; Cl, 15.88%.

The infrared spectrum of phenol-trisulfochloride exhibits a strong substitution band at 11.46 μ. With compounds II and III substitution bands were also evident at 11.46 μ and 11.35 μ, respectively. Thompson and co-workers[3] who carried out a detailed study on the infrared spectra of phenol–formaldehyde condensates, assigned the 1,2,3,5-tetrasubstitution band, to the 11.37–11.76 μ region. The 1,2,4-trisubstitution band (12.20–12.50 μ) was not present in the above spectra. If the structure is that as indicated above, a 1,4-disubstitution band should be present. This was actually the case, the band being at 11.95 μ. As the result of infrared spectral studies, compound II is shown to contain two sulfonyl chloride groups in one of the two benzene rings.

Sulfonyl Chloride III. A 3-g. (12 mmole) portion of 4,4′-dihydroxy-diphenylsulfone was added with stirring to 50 ml. chlorosulfonic acid and heated at 130–140°C. for 3–4 hr. After standing overnight white crystals, 1.5 g. (20%) separated out, which on being recrystallized from dioxane melted at 230–240°C. (dec.).

ANAL. Calcd. for $C_{12}H_6Cl_4O_{12}S_5$ (644.3): C, 22.37%; H, 0.94%; Cl, 22.00%; S, 24.85%. Found: C, 23.08%; H, 1.16%; Cl, 21.67%; S, 24.72%.

The product gave a red color with ethanolic ferric chloride. The sulfonyl chloride III dissolves readily in water, methanol, ethanol, and acetone, less readily in dioxane, and is insoluble in petroleum ether.

Preparation of Bi- and Tri-nuclear Sulfones by Means of the Fries Rearrangement

Sulfone IV. (a) 1-Methyl-benzene-4-sulfonic acid 2-chloro-3-methyl-phenyl ester was prepared by shaking vigorously a mixture of 19 g. (0.1 mole) p-toluenesulfonyl chloride in 45 ml. acetone and 16.5 g. (0.1 mole) sodium salt of 3-chloro-4-hydroxy-1-methylbenzene. The reaction mixture was poured into 200 ml. water, and the crystals collected. After drying, the ester, which was obtained in almost a 100% yield, was recrystallized from ethanol and melted at 101–102°C. The ferric chloride test was negative.

ANAL. Calcd. for $C_{14}H_{13}ClO_3S$ (296.8): C, 56.68%; H, 4.42%; S, 10.81%. Found: C, 56.92%; H, 4.55%; S, 10.61%.

(b) A 5-g. portion (17 mmole) of the prepared ester (a) was mixed thoroughly with 0.03 mole $AlCl_3$ and treated at 100–110°C. for $1^1/_2$ hr. and again for the same time at 150°C. The cooled reaction product was decomposed with HCl–ice and stirred for about 1 hr. After filtering the solid was dissolved in 10% KOH and on acidification the sulfone was precipitated. After recrystallization from alcohol, the product was obtained

in 74% yield and melted at 146–147.5 °C. The infrared spectrum showed a band at 3 μ (–OH).

ANAL. Calcd. for $C_{14}H_{13}ClO_3S$ (296.8): C, 56.68%; H, 4.42%; S, 10.81. Found C, 56.64%; H, 4.63%; S, 10.49%.

Sulfone V. (a) 4-Bromo-2,3,5,6-tetramethylbenzenesulfonyl chloride (6 g., 19 mmole) was dissolved in 40 ml. acetone; after mixing and shaking with 3.3 g. (20 mmole) of the sodium salt of 3-chloro-4-hydroxy-1-methyl-benzene in 30 ml. water a crystalline product was precipitated. The reaction mixture was poured into 150 ml. water. After filtration and drying the ester was recrystallized from ethanol, giving a product which melted at 93–95°C. in 95% yield.

ANAL. Calcd. for $C_{17}H_{18}BrClO_3S$ (417.8): C, 48.89%; H, 4.34%. Found: C, 48.86%; H, 4.31%.

(b) To 2.1 g. (5 mmole) of the foregoing prepared ester was added well with 1.5 g. AlCl$_3$ (10 mmole) and the mixture slowly heated to 120°C. and kept at this temperature for a few hours. The darkly colored reaction product was decomposed with HCl–ice and dissolved in 10% KOH. On acidifying, a brown product was obtained. An ethanolic solution of the product was treated with active charcoal, and on standing crystals separated out which melted at 152–153°C.; yield 55%. The infrared spectrum showed a strong band at 3 μ (–OH).

ANAL. Calcd. for $C_{17}H_{18}BrClO_3S$ (417.8): C, 48.89%; H, 4.34%; S, 7.68%. Found: C, 49.01%; H, 4.57%; S, 7.63%.

Sulfone VI. (a) A 2.8 g. portion (10 mmole) of the sodium salt of 4-methylbenzene-(6-hydroxy-3-methylbenzene)sulfone in 10 ml. water was mixed with 1.9 g. (10 mmole) p-toluenesulfonyl chloride and shaken vigorously for about 20–30 min. The reaction mixture was poured into 75 ml. water, filtered, and the white solid product dried. The ester was obtained in 60% yield and crystallizes from ethanol in leaflets which melt at 142–144°C.

ANAL. Calcd. for $C_{21}H_{20}O_5S_2$ (416.5): C, 60.59%; H, 4.84%; S, 15.40%. Found: C, 60.62%; H, 5.03%; S, 15.13%.

(b) A 1.5-g. portion (3.6 mmole) of the foregoing sulfonic ester was mixed thoroughly with 1.3 g. AlCl$_3$ (10 mmole) and heated slowly to 125–130°C. and kept at this temperature for 1 hr. The temperature was increased slowly to 140–145°C. (reaction time: 5 hr.). After cooling, the darkly colored reaction product was pulverized and decomposed with HCl–ice. After working up in the usual manner the sulfone after recrystallization from chloroform–petroleum ether melted at 221–223°C.; yield 40–50%. A strong band was present at 3 μ (–OH) in the infrared spectrum.

ANAL. Calcd. for $C_{21}H_{20}O_5S_2$ (416.5): C, 60.59%; H, 4.84%; S, 15.40%. Found: C, 60.70%; H, 5.10%; S, 15.03%.

Preparation of Tri- and Tetranuclear Sulfones by Means of the Friedel-Crafts Reaction

Sulfone VII. 4-Hydroxy-1-methylbenzene-1,3-disulfonyl chloride (3.1 g., 10 mmole), 15 ml. 3-chloro-4-methoxy-1-methylbenzene, and 6 ml. $SnCl_4$ were heated at 90°C. for 70 hr. The reaction mixture was poured into water, and the brown organic layer was collected. This was steam-distilled to remove the excess methyl ether, leaving a brown solid residue which on boiling with a little methanol produced a white product which was demethylated with hydrogen iodide. The sulfone was recrystallized from benzene and melted at 238–240°C.; it is easily soluble in alcohol, acetic acid, ethyl acetate, and isopropyl alcohol. The ferric chloride test gave a red-brown color.

ANAL. Calcd. for $C_{21}H_{18}Cl_2O_7S_2$ (517.4): C, 48.78%; Cl, 13.70%; S, 12.39%. Found: C, 48.91%; Cl, 13.52%; S, 12.05%.

The acetylated product was obtained by refluxing the sulfone in acetic anhydride for 3 hr. The cooled reaction mixture was poured with stirring into water, and the precipitated acetate which was obtained in a nearly theoretical yield was recrystallized from alcohol and melted at 267°C.

ANAL. Calcd. for $C_{27}H_{24}Cl_2O_{10}S_2$ (643.5): C, 50.40%; Cl, 11.02%; S, 9.97%. Found: C, 50.24%; Cl, 10.90%; S, 9.97%.

A further sample of the sulfone was dissolved in alkali to which was added with stirring a 10% excess of ethyl chlorocarbonate. The precipitate after crystallization from alcohol melted at 237–238°C.; yield 90%.

ANAL. Calcd. for $C_{30}H_{30}Cl_2O_{13}S_2$ (733.6): Cl, 9.67%; S, 8.74%. Found: Cl, 9.59%; S, 8.57%.

Sulfone VIII. A mixture of 4.75g. (0.01 mole) sulfonyl chloride I, 15 ml. 3-chloro-4-methoxy-1-methylbenzene, and 6 ml. $SnCl_4$ was heated at 90°C. (oil-bath) for 75 hr. After pouring the reaction mixture into water, the organic layer was separated, and the excess methyl ether was removed by steam distillation. The residue was demethylated with hydriodic acid and purified by reprecipitating the sulfone from a benzene solution with petroleum ether and finally crystallization from acetic acid–water; m.p. 246–252°C.; yield 50–55%. The infrared spectra of VIII and VII were identical.

ANAL. Calcd. for $C_{28}H_{24}Cl_2O_{10}S_3$ (687.6): C, 48.93%; Cl, 10.32%; S, 13.99%. Found: C, 49.03%; Cl, 9.94%; S, 13.94%.

The acetate derivative was prepared as described for sulfone VII and melted after recrystallization from acetic acid–water at 270–272°C.

ANAL. Calcd. for $C_{36}H_{32}Cl_2O_{14}S_3$ (855.8): C, 50.55%; Cl, 8.29%; S, 11.24%. Found C, 50.46%; Cl, 8.12%; S, 11.39%.

References

1. Kämmerer, H., and M. Harris, *Makromol. Chem.*, **62**, 18 (1963).

2. Kämmerer, H., W. Rausch, and H. Schweikert, *Makromol. Chem.*, **56**, 123 (1962).

3. Thompson, H. W., and P. Torkington, *Trans. Faraday Soc.*, **41**, 246 (1945); H. W. Thompson, *J. Chem. Soc.*, **1947**, 289, 1960.

Résumé

Des composés phénoliques à deux ou trois noyaux benzéniques reliés par des ponts sulfoniques ont été préparés par transposition de Fries; de même des composés analogues à trois ou quatre noyaux ont été préparés par la méthode de Friedel et Crafts. L'échange d'un groupe méthylénique par un groupe sulfonique entraîne une élévation appréciable du point de fusion.

Zusammenfassung

Zur Herstellung phenolischer Zwei- und Dreikernverbindungen mit Sulfonbrücken ist die Friessche Verschiebung, zur Herstellung entsprechender Drei- und Vierkernverbindungen die Friedel-CraftsKondensation geeignet. Der Austausch einer Methylenbrücke gegen eine Sulfongruppe bewirkt eine beträchtliche Schmelzpunktserhöhung.

Polymerization of Chlorinated Diphenylsiloxanes

JAMES B. GANCI* and FREDERICK A. BETTELHEIM, *Chemistry Department, Adelphi University, Garden City, New York*

Synopsis

Chlorinated diphenylsiloxanes were prepared by acid- and base-catalyzed polymerization of the corresponding diols in polar organic solvents. Under mild conditions, cyclic tetramers were isolated. More forcing conditions in the presence of base yielded resins containing largely cyclic species which showed extensive cleavage of the phenyl groups. The order of the phenyl group cleavage among the polymers indicated that the inductive effect of the substituent halogen plays a dominant role.

INTRODUCTION

Polysiloxanes have desirable properties with respect to temperature coefficient of viscosity, resistance to oxidation at elevated temperatures, and retention of elastic properties at low temperatures. While much attention has been focused on methyl silicones by industry, relatively little has been done with phenyl silicones chiefly because of their brittle, resinous nature and consequent limited range of applicability. Phenyl silicones are, however, highly resistant to air oxidation and have good thermal stability. It has been reported that chlorinated phenyl silicones resist air oxidation and are thermally stable up to at least 450°C. The introduction of chlorine atoms onto the phenyl nuclei renders the polymer less flammable.[1]

The purpose of this investigation was to study the polymerization of diphenyl- and chlorinated diphenylsiloxanes in polar organic solvents.

EXPERIMENTAL

Preparation of Monomers

Bis-*p*-chlorophenyldichlorosilane. This compound was prepared according to Schott and Berge.[2] The Grignard reagent of *p*-bromochlorobenzene (405 g.) was added to 138 g. silicon tetrachloride. Distillation yielded 118 g. of bis(*p*-chlorophenyl)dichlorosilane, b.p. 168–171°C./1 mm. Hg (reported[2] 178–181°C./1.5 mm.).

Bis(3,4-dichlorophenyl)dichlorosilane.   1-Bromo-3,4-dichlorobenzene was prepared by the action of bromine on *o*-dichlorobenzene in the presence of iron filings in 55–60% yield; b.p. 237–240°C. (Lit.[3] 237°C.). The

experimental procedure is identical with that of the previous preparation of bis(p-chlorophenyl)dichlorosilane.

1-Bromo-3,4-dichlorobenzene (414 g.), dissolved in 800 ml. ether, was added to 48.9 g. magnesium covered with 200 ml. ether. The Grignard solution was added to 131 g. $SiCl_4$ chilled with ice. The reaction of the Grignard reagent with the $SiCl_4$ did not proceed readily in the cold but rather took place as the mixture was allowed to warm to room temperature. Before distillation, the solution was filtered, removing the magnesium salt. Filtration was done under N_2 pressure to exclude moisture.

Distillation yielded 90 g. (41% of theoretical based on $SiCl_4$) of colorless, supercooled liquid which crystallized on standing, b.p. 203–206°C./0.4 mm.

ANAL. Calcd. for $C_{12}H_6Cl_6Si$: C, 36.86%; H, 1.55%; Cl, 54.41%; Si, 7.18%. Found: C, 36.98%; H, 1.75%; Cl, 54.27%; Si, 7.15%.

Hydrolysis Products of Diphenyldichlorosilanes

Diphenylsilanediol. Technical grade diphenyldichlorosilane (General Electric Co.) was redistilled under vacuum. The fraction boiling from 102–103°C./1 mm. was collected (Lit.[4] 116°C./2 mm.).

The silane was hydrolyzed by dissolving it in ether and pouring the ether solution on an ice-cooled water–$NaHCO_3$ solution.[1,5] The evolution of CO_2 (frothing) subsided after approximately 20–30 min. After washing the ether layer with water, evaporation left a white solid which was recrystallized in poor yield (40%) from ethyl acetate. The white, crystalline product melted at 162–164°C. (Lit.[6–8] 130–160°C.).

Hydrolysis Product of Bis(p-chlorophenyl)dichlorosilane. The hydrolysis of bis(p-chlorophenyl)dichlorosilane according to a method by Schott was attempted in order to prepare the diol.[2] The silane (118 g.) was dissolved in dry ether (1 liter) and added to approximately $1^1/_2$ liters of ice–water mixture with stirring over a period of 1 hr. The product was recrystallized from ethyl acetate–cyclohexane, yielding 72 g. of white product; m.p. 143.5–145°C. Molecular weight by endgroup analysis yielded a value of 370 (theoretical mol. wt. for diol = 285). (Schott reported a yield of pure diol with m.p. 117.5°C.)

Hydrolysis Product of Bis(3,4-dichlorophenyl)dichlorosilane. The hydrolysis of the silane was carried out according to Schott's method in an attempt to obtain the corresponding diol. The silane (123 g.), was hydrolyzed, and the resulting crude hydrolysis product was recrystallized, yielding three fractions: (1) from cyclohexane, 27 g., m.p. 77–90°C.; (2) from ligroin–cyclohexane–ethyl acetate, 40 g., m.p. 117–135°C.; (3) from ligroin–ethyl acetate, 12 g., m.p. 120–140°C. The combined product totaled 79 g., which was 80% of theoretical yield of diol. The combined fractions yielded molecular weight by endgroup analysis of 485 (theoretical diol = 354).

Polymerization

The polymerization of the diols was performed under a variety of conditions. The different solvents used were dimethylformamide and mixtures of dimethylformamide, ethanol and dioxane. The catalysts used

were KOH in varying Si/KOH molar ratios from 75 to 11,000, and HCl and H_2SO_4 in varying Si/H^+ molar ratios from 20 to 1500. The time of polymerization varied from 1 to 24 hr., while the temperatures of polymerization were the boiling points of the solutions (105–150°C.).

Molecular Weight Determination

Two methods were used to estimate the molecular weight of the polymers. The first was an endgroup determination according to Damm and Noll[9] utilizing the reaction of silanol with phenyl isocyanate.

The second method was based on colligative properties, the vapor pressure lowering of the polymer solutions being measured in a Mechrolab vapor pressure osmometer, model 301 A. Viscosity measurements were also performed in a Cannon-Fenske-Ostwald capillary viscometer.

RESULTS

The results of the polymerization of the diols can be summarized as follows.

At high Si/OH^- ratio and at relatively low temperatures the cyclic tetramers are formed first. Polymerization of the diphenylsilanediol at 150°C. in dimethylformamide at a Si/OH^- ratio of 11,000 yielded a crystalline product with a melting point of 198–201°C. which could be identified with octaphenylcyclotetrasiloxane reported in the literature.[10]

Bis(3,4-dichlorophenyl)silanediol in dimethylformamide (15 ml.)–dioxane (35 ml.)–ethanol (0.2 ml.) at 109°C. at a Si/OH^- ratio of 1200 polymerized to form cyclic tetramer with a melting point of 216–218°C. Elementary analysis gave the results shown in Table I. The molecular weight of the tetramer was found to be 1360 ± 40 (theoretical 1344).

Since this compound, octakis(3,4-dichlorophenyl)cyclotetrasiloxane, is not reported in the literature as yet, the interatomic distances and the x-ray diffraction intensities, as obtained from a powder diagram with CuKα source, are given in Table II.

The same cyclic tetramer was obtained with acid catalysis with the use of either aqueous HCl or H_2SO_4 in 20–1500 Si/H^+ ratios from dimethylformamide–dioxane mixtures as solvents. The melting point and the x-ray diffraction pattern of the acid-catalyzed tetramer were identical with those of the base-catalyzed one and a mixed melting point of the two gave no melting point depression.

The cyclic tetramer of the bis(p-chlorophenyl)silanediol polymerization was not isolated in crystalline form but as a resinous compound (which might have been largely tetramer) with 1100 molecular weight. The resin was obtained by polymerization in a mixture of 140 ml. dimethyl-

TABLE I

	C, %	H, %	Cl, %	Si, %
Found	42.55	1.75	42.44	8.36
Calculated for $(C_{12}H_6Cl_4SiO)_n$	42.88	1.80	42.20	8.36

TABLE II
d Spacings Obtained from Diffraction Pattern of Octakis(3,4-dichlorophenyl)cyclotetrasiloxane

d, A.	Intensity[a]
10.35	s
6.67	w
5.77	w
5.18	s
4.35	m
3.98	m
3.59	s
3.36	m
3.22	w
3.03	m
2.78	m
2.61	vw
2.47	vw
2.37	vw

[a] s = strong, w = weak, m = medium, vw = very weak.

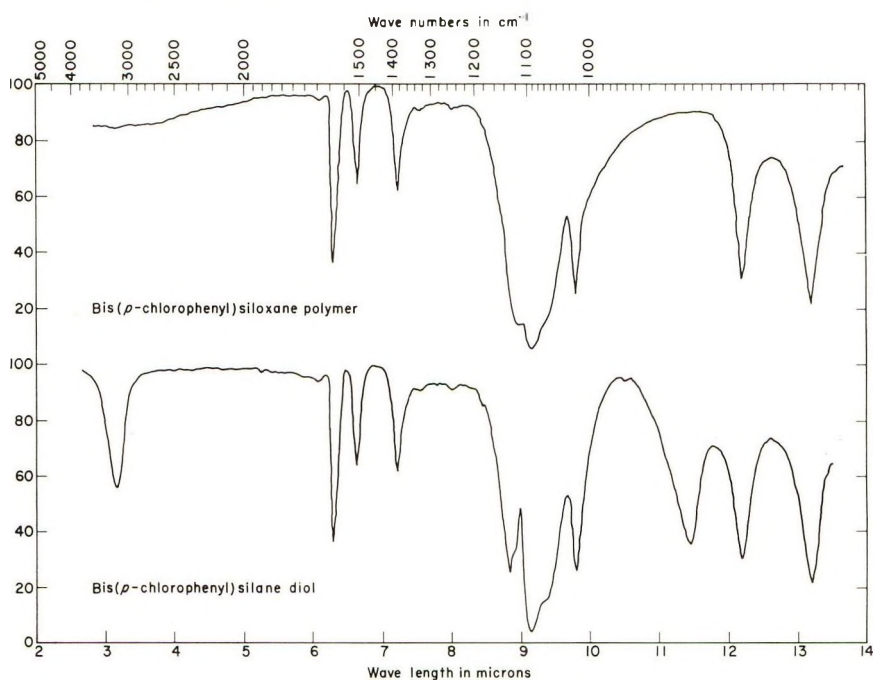Fig. 1. Infrared spectra of bis(p-chlorophenyl)silanediol and bis(p-chlorophenyl)-siloxane.

formamide, 60 ml. dioxane, and 8 ml. of ethanol at 120°C. for 1 hr. with a Si/OH⁻ ratio of 120. The infrared spectrum of this tetramer or mixtures of oligomers also indicated cyclic compounds (Fig. 1) since the characteristic OH absorption bands at 3200 and 875 cm.$^{-1}$ were missing, as compared to the spectrum of the diol.

At low Si/OH⁻ ratio and high temperatures, further polymerization occurs, with opening of the ring structures and simultaneous cleavage of the phenyl side chains. The new resinous compounds are also partly cyclic in nature as can be seen from (a) discrepancy between the molecular weights obtained by endgroup determination and from the colligative property measurements (60,000 vs. 1500) (b) the infrared spectra (similar to those in Fig. 1), where the OH bands are missing for the resinous compounds.

There is also a definite trend for the phenyl cleavage to become more extensive with decreasing Si/OH⁻ ratio. Furthermore, the inductive effect of the halide on the benzene ring is evident. Under identical polymerization conditions, 12% of the phenyl groups, 25% of the chlorophenyl groups, and about 40% of the dichlorophenyl groups were cleaved.

DISCUSSION

It has been shown that the cyclic diphenylsiloxanes show greater thermodynamic stability than their methyl counterparts and greater lability of organic side groups towards basic polymerization catalysts. However, it is surprising to note the complete indifference of the chlorinated tetramer octakis(3,4-dichlorophenyl)cyclotetrasiloxane towards acid catalysis. When subjected to reflux for 1 hr. at 107°C. with molar ratio Si/H⁺ of 10, the starting material is recovered unchanged with no evidence of phenyl cleavage having taken place.

Instances of phenyl group cleavage of acids are frequent in the literature, and the process is believed to proceed by an electrophilic aromatic substitution mechanism.[11] On the other hand, less is mentioned about the extent of cleavage by bases of the silicon-phenyl bond which would involve nucleophilic attack at silicon.[12]

Results of the polymerization reactions showed that the chlorophenyl and dichlorophenyl groups were cleaved extensively by the base catalyst (KOH) under the conditions of the reactions (100–150°C., 10^{-3}–$10^{-4}M$ KOH). Even the phenyl group, under similar conditions, was cleaved. The order of reactivity noted for the cleavage reaction was in decreasing order of susceptibility: dichlorophenyl > chlorophenyl > phenyl. This order of reactivity is to be expected if one considers the electron withdrawing effect of the chloro group in the phenyl nucleus.

Endgroup analysis of the polymer yielded high molecular weights (20,000–60,000). The polymers obtained were actually low molecular weight ($\sim$1500) species in the light of viscosity and vapor pressure-lowering measurements.

Cyclic species behave, in endgroup analysis, like polymers of infinite molecular weight. Thus if cyclic species comprise a considerable percentage of the polymer, one would expect deceivingly high results from thi method. An infrared examination of bis(p-chlorophenyl)silanediol and its corresponding polymer shows bands at 3200 and 875 cm.⁻¹ in the diol spectrum which are clearly missing from the polymer spectrum. These bands have been assigned to the stretching (hydrogen-bonded) and defor-

mation modes, respectively, of the —OH group.[13]   This supports assignment of a cyclic structure to the polymer.

The question now remains as to the nature of the cyclic siloxane in the resinous polymer.   The cyclic tetramers are crystalline materials with sharp melting points.   The polymers, on the other hand, are amorphous as viewed by x-rays.   The tetramers have only limited solubilities in common solvents, such as benzene and acetone, whereas the resins dissolve readily. The conclusion is therefore that the cyclic species present predominantly in the resin are higher molecular weight cyclics.   A mixture of cyclic species would account for the lack of crystallinity of the polymers.   No higher cyclic species than the tetramer has been reported and characterized in the literature in the cases of diphenylsiloxanes.   On the other hand, cyclic dimethylsiloxanes containing up to nine repeating units (18-membered rings) have been isolated.[14]

References

1. Rochow, E. G., U. S. Pat. 2,258,219 (1939/41).
2. Schott, G., and H. Berge, *Z. Anorg. Allgem. Chem.*, **297**, 32 (1958).
3. Hurtley, W. H., *J. Chem. Soc.*, **79**, 1297 (1901).
4. Kerr, R. W., and D. C. Hobbs, *Ind. Eng. Chem.*, **45**, 2542 (1955).
5. Rochow, E. G., U. S. Pat. 2,258,218 (1939/41).
6. Kipping, F. S., and R. Robison, *J. Chem. Soc.*, **105**, 484 (1914).
7. Kilthey, W., and F. Eduardoff, *Ber.*, **37**, 1139 (1904).
8. Burkhard, C. A., *J. Am. Chem. Soc.*, **67**, 2173 (1945).
9. Damm, K., and W. Noll, *Kolloid-Z.*, **158**, 97 (1958).
10. Hyde, J. F., and R. C. de Long, *J. Am. Chem. Soc.*, **63**, 1194 (1941).
11. Eaborn, E., *Organosilicon Compounds*, Academic Press, New York, 1960, p. 31.
12. Beck, E. W., W. H. Daudt, H. J. Fletcher, M. J. Hunter, and A. J. Barry, *J. Am. Chem. Soc.*, **81**, 1256 (1959).
13. Richards, R. E., and H. W. Thompson, *J. Chem. Soc.*, **1949**, 124.
14. Rochow, E. G., *The Chemistry of the Silicones*, Wiley, New York, 1946, pp. 60–80.

Résumé

On a préparé des diphénylsiloxanes chlorés à partir des diols correspondants.   La réaction a été catalysée soit par un acide soit par une base.   En travaillant dans des conditions relativement douces, on isole des tétramères cycliques.   En travaillant dans des conditions moins douces en présence de base, on obtient des résines contenant des cycles plus larges mais dans lesquelles le groupe phényle est largement dégradé.   La rupture du groupement phényle, qui se produit intensivement, montre que l'effet inductif du substituant halogéné joue un rôle majeur.

Zusammenfassung

Chlorierte Diphenylsiloxane wurden durch Säure- und Basen-katalysierte Polymerisation aus den entsprechenden Diolen in polaren organischen Lösungsmitteln hergestellt. Unter milden Bedingungen wurden zyklische Tetramere isoliert.   Stärkere Bedingungen ergaben in Gegenwart einer Base Harze mit einem Gehalt an hauptsächlich zyklischen Gruppen, die eine ausgedehnte Spaltung der Phenylgruppen zeigen.   Die Reihenfolge der Phenylgruppenspaltbarkeit bei den Polymeren deutet eine Hauptrolle des induktiven Effekts der Halogensubstituenten an.

Degradation of
Poly-3,3-bis(chloromethyl)oxacyclobutane (Penton)

J. H. GOLDEN and E. A. HAZELL, *Explosives Research and Development Establishment, Ministry of Aviation, Waltham Abbey, Essex, England*

Synopsis

The degradation of Penton [poly-3,3-bis(chloromethyl)oxacyclobutane] by electron irradiation in vacuum has been investigated. Viscometric measurements on the irradiated material showed that the polymer underwent random chain scission without crosslinking. The chemical changes responsible for the fairly rapid breakdown of the polymer were examined by infrared analysis and by analysis of the gases, predominantly hydrogen, hydrogen chloride, and carbon monoxide, evolved during irradiation. The chain scission of Penton is accompanied by formation of terminal unsaturation and allylic chlorine groups. The effects of radiation on the flexural and tensile properties of Penton were examined, and it was shown that the pattern of behavior in flexure was closely similar to that in tension. The form of the tensile strength curves obtained for irradiated Penton at various rates of straining was examined and related to that of hypothetical brittle strength curves. Some effects of radiation, rate of testing and temperature on the brittle strength of the polymer have been determined. The viscometric and tensile results obtained were compared with those obtained for the structurally related polyoxymethylene (Delrin) which was much less resistant to radiation.

INTRODUCTION

Although little is known of the effects of ionizing radiation on polyethers, recent work on polyformaldehyde (e.g., Delrin)[1-3] and on poly-3,3-bis-(chloromethyl) oxacyclobutane (Penton)[3] has suggested the occurrence of chain scission accompanied by fairly rapid loss of mechanical strength. Following our study[4] of the radiation-induced scission of polycarbonate an examination of the effects of radiation on these polyethers was therefore of interest. The scission of Penton and the accompanying changes in mechanical properties have been studied in some detail. The ductile–brittle transition induced by radiation has been examined and an attempt made to relate this transition to those induced by speed and temperature. Chemical changes have been studied by infrared and ultraviolet spectroscopy and by analysis of the gases evolved during irradiation.

Some results on the breakdown of Delrin (polyformaldehyde) have been included for comparison.

EXPERIMENTAL

Preparation of Specimens

The polyethers used were poly-3,3-bis(chloromethyl)oxacyclobutane (Penton, Hercules Powder Co.) and polyoxymethylene (Delrin, General Electric Co.).

Granules of Penton were dried at 60°C./12 mm. for 8 weeks over calcium chloride, placed in glass ampules equipped with break-seals and, after rigorous degassing (60°C./10^{-6} mm.) for 6 hours the ampoules were sealed. After irradiation the gases evolved were analyzed and the polymer used for ultraviolet light absorption measurements.

A thin film of Penton was cast from cyclohexanone on to a rock-salt plate and rigorously degassed. The infrared absorption of the film was determined before and after irradiation.

Injection-molded dumbbells were dried in vacuum for 8 weeks before irradiation and subsequently used for measurement of tensile and flexural properties and for viscosity determinations.

Irradiation

Specimens were irradiated by using a linear accelerator electron beam (4 m.e.v.) at a dose rate of 1 Mrad./min. by the techniques previously described.[4]

Test Methods

Specimens were tested not less than two weeks after irradiation. During this period dumbbells were kept in vacuum, and ampules were not opened. Unless otherwise stated the temperature of testing was 20 ± 1°C.

Viscosity Measurements. The intrinsic viscosity of Penton specimens was obtained in cyclohexanone at 103.4°C. and that of Delrin specimens in m-cresol at 144.5°C.; a modified dilution viscometer[5] adapted for use at elevated temperatures essentially as described by Harness[6] was used.

Tensile Properties. These were determined using special dumbbells[4] at various strain rates with the equipment previously described.[4,7] Tensile strength refers to maximum yield strength for specimens which yielded and to fracture strength for brittle specimens.

Flexural Properties. Flexural properties were measured in general accordance with ASTM D790-58T except that the strain rate was 0.375 in./in./min. and the span:depth ratio was 8:1. The exceptions were mainly determined by the form of test piece used.

Flexural modulus, maximum yield strength, or breaking strength in the absence of yield, and the appropriate deflections were determined.

Light Absorption of Penton. The infrared spectrum of a film cast onto a rock-salt plate was determined before and after irradiation in vacuum. The ultraviolet spectrum of the irradiated polymer in chloroform was determined using a Unicam S.P. 500 spectrophotometer.

Gas Evolution from Penton. Hydrogen chloride was estimated gravi-
metrically as silver chloride. Other gases were determined by mass spec-
troscopy.

RESULTS AND DISCUSSION

Viscosity

On irradiation Penton evolved gases and its softening point (148°C. on a
Kofler hot-stage microscope) was reduced to 125–126°C. after 100 Mrad
and to 89–90°C. after 200 Mrad. The polymer became soluble in many
organic solvents including chloroform, tetrahydrofuran, xylene and methyl-
isobutyl ketone.

The intrinsic viscosity $[\eta]$ of Penton in cyclohexanone at 103.4°C. is
shown in Figure 1 as a function of radiation dose R. Up to a dose of 100
Mrad the results could be expressed by the equation:

$$([\eta]_0/[\eta]) - 1 = 0.084R + 0.25 \qquad (1)$$

A similar relationship has been taken as evidence of random fracture by
Jellinek.[8,9]
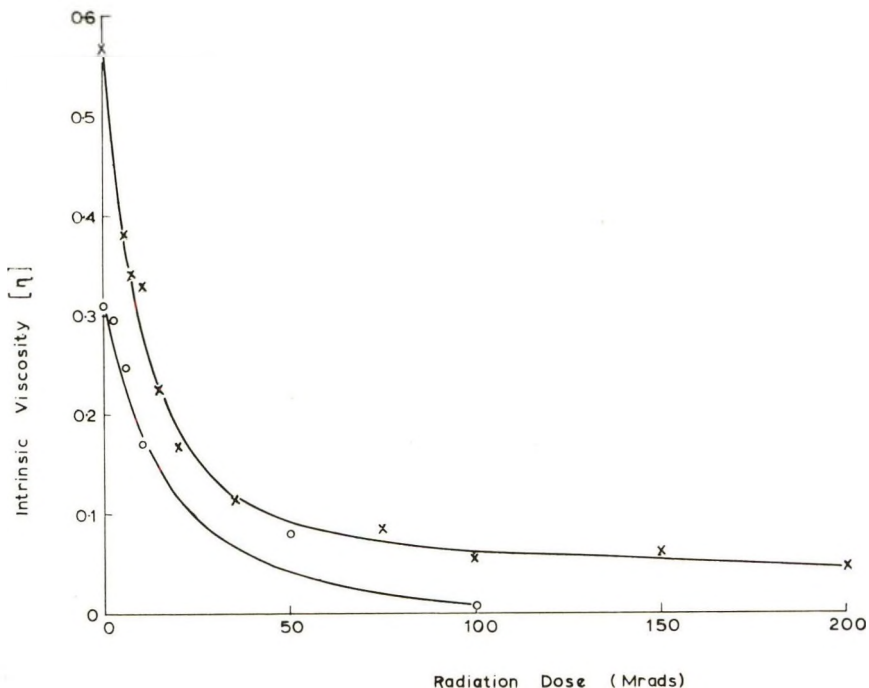
Fig. 1. Changes in intrinsic viscosity $[\eta]$ of Penton and Delrin with radiation dose R:
(×) Penton in cyclohexanone at 103.4°C.; (O) Delrin in m-cresol at 144.5°C.
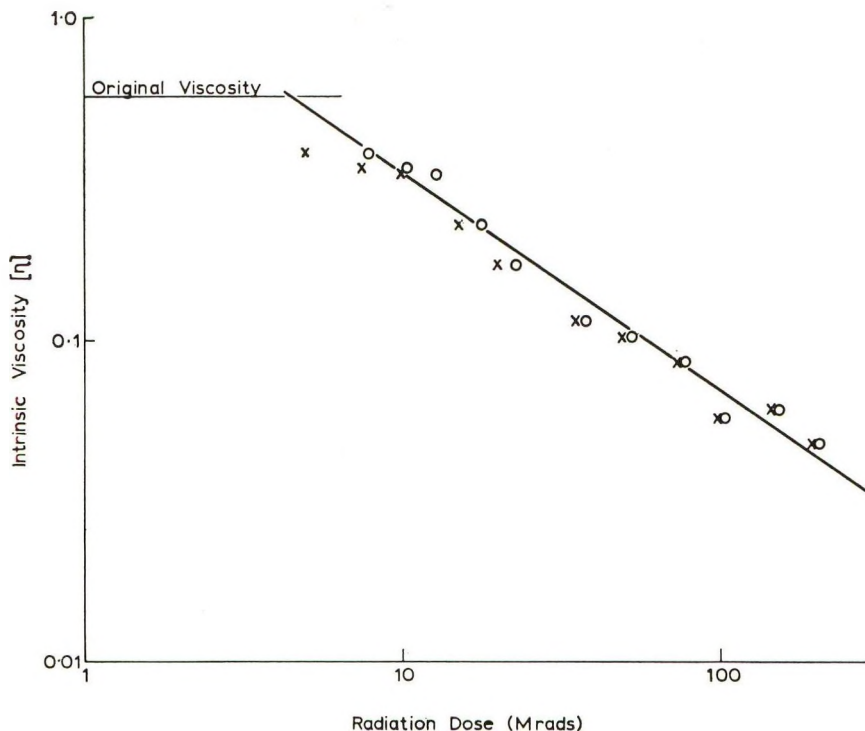
Fig. 2. Changes in intrinsic viscosity $[\eta]$ of Penton with radiation dose R: ($\times$) R; (O) $R + R_0$. Linear relationship $\log [\eta] = -0.68 \log (R + R_0) + \log 1.575$ shown.

Charlesby[10] showed that for random fracture:

$$\log [\eta] = -\alpha \log (R + R_0) + C \qquad (2)$$

where α is a constant of the Mark-Houwink equation $[\eta] = K \bar{M}_v{}^\alpha$ and R_0 is the "virtual" radiation dose needed to fracture a molecule of infinite molecular weight sufficiently for the resultant to have the same number-average molecular weight $\bar{M}_n$ as the initial polymer studied. R_0 (2.95 Mrad) was obtained from eq. (1) and a plot of $[\eta]$ against $(R + R_0)$ on a log-log scale gave a straight line (statistical correlation coefficient 0.99) (Fig. 2),

$$\log [\eta] = -0.68 \log (R + R_0) + \log 1.575 \qquad (3)$$

whence $\alpha = 0.68$. This relationship establishes that the polymer degrades by random chain scission.

The intrinsic viscosity of Delrin in m-cresol is also shown in Figure 1 as a function of radiation dose and again the results indicate random scission of the polymer.

Mechanical Properties

In previous investigations the physical damage to high polymers caused by irradiation has usually been assessed by measurements of the changes in
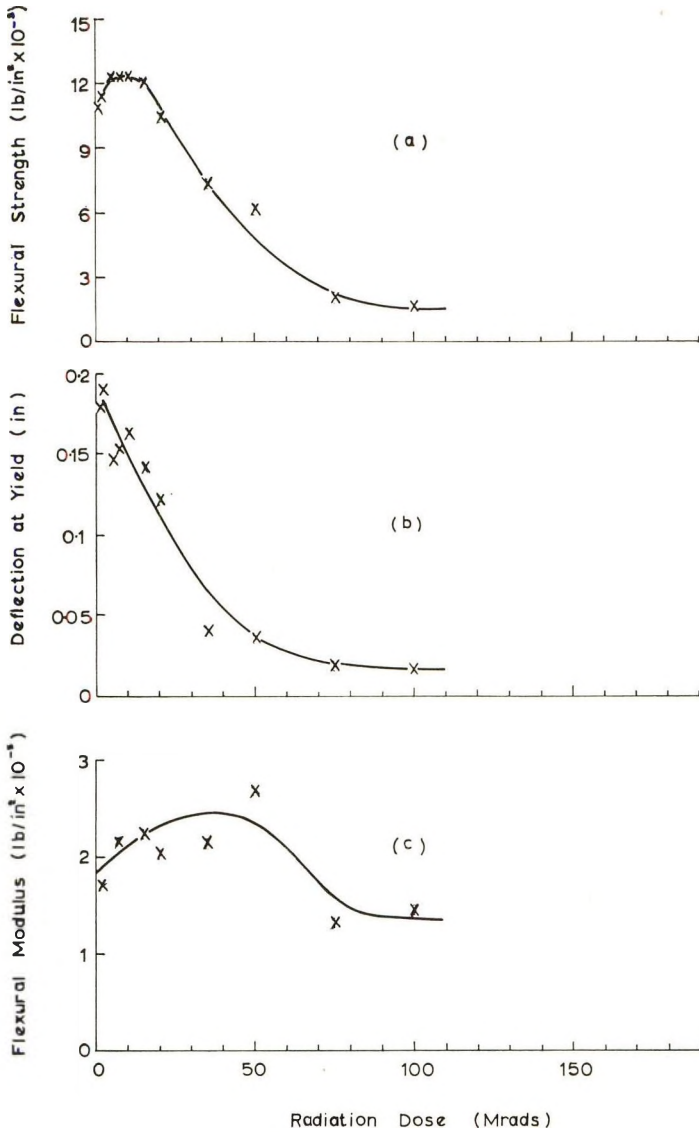
Fig. 3. Changes in flexural properties of Penton, tested at 0.5 in./min., with radiation dose R: (a) flexural strength; (b) deflection at yield; (c) flexural modulus.

tensile properties.   Determination of these properties became increasingly difficult as the material became brittle as sharp stress concentrations occur in the grips and slight misalignment can affect the results.   This suggests that the maximum brittle strength is not always attained and the progressive change in strength through the ductile–brittle transition is therefore difficult to follow.   These difficulties and those attending accurate measurement of modulus would be largely overcome if the mechanical properties were measured in flexure.   Accordingly, specimens were tested by both
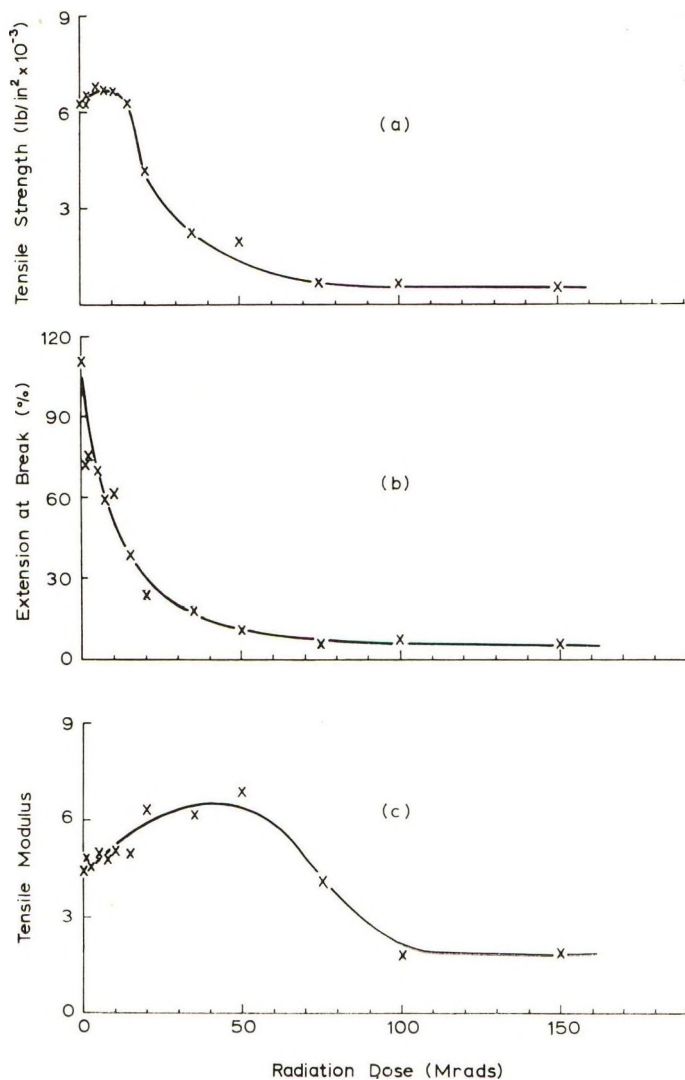
Fig. 4. Changes in tensile properties of Penton, tested at 0.1 in./min., with radiation dose R: (a) tensile strength; (b) extension at break; (c) tensile modulus (arbitrary units).

methods for comparison and in fact a similar pattern of behavior was obtained in flexure to that in tension (Figs. 3 and 4), and the flexural method possessed the advantages of greater consistency and reliability.

The maximum yield strength (Figs. 3a and 4a) increased up to a radiation dose of approximately 10 Mrad and then fell rapidly to a very low value at about 80 Mrad. This initial increase is of considerable interest as the molecular weight (Figure 1) decreases steadily over this range of dose; this is discussed in detail in the next section.
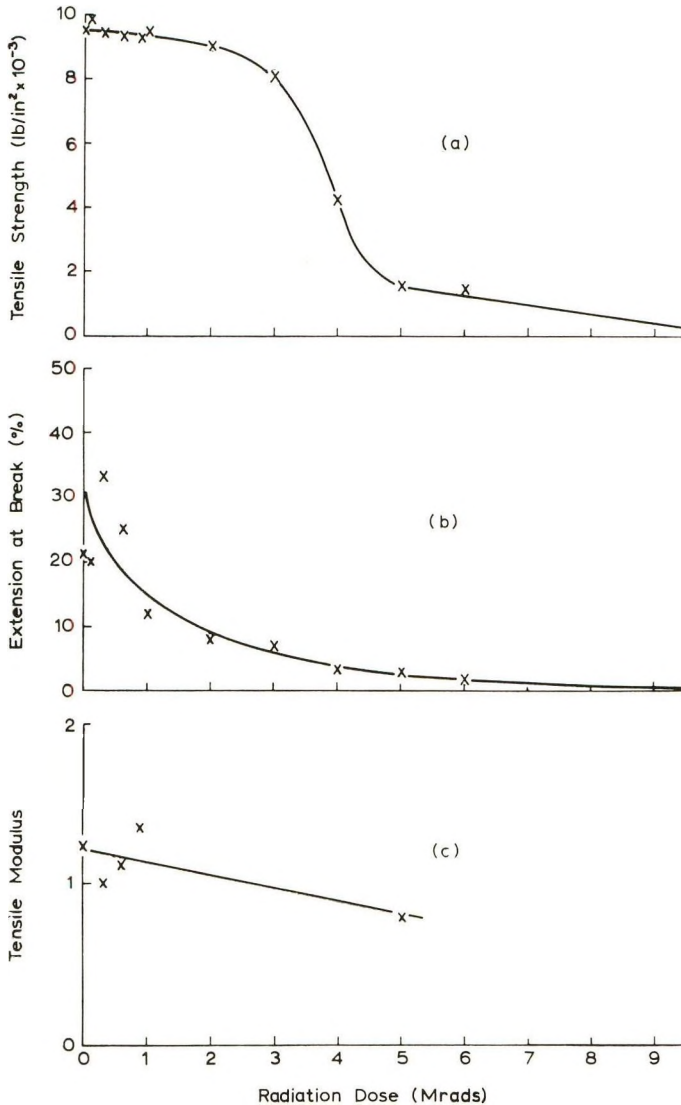
Fig. 5. Changes in tensile properties of Delrin, tested at 0.1 in./min., with radiation dose R: (a) tensile strength; (b) extension at break; (c) tensile modulus (arbitrary units).

Both tensile extension at break and flexural deflection at yield decrease with dose (Figs. 4b and 3b), although the former falls more rapidly, as would be expected for this ultimate property in which greater overall strains are imposed on the specimen.

The tensile modulus curve shown in Figure 4c, although on an arbitrary scale, shows considerable similarity to the flexural modulus curve (Fig. 3c). The increase in flexural modulus from about 1.8×10^5 lb./in.^{2} at zero dose

to 2.6×10^5 lb./in.^{2} at 50 Mrad is followed by a small decrease at higher doses.

For comparison the deterioration of the tensile properties of Delrin with increasing radiation dose was examined, and it was found that although the behavior was similar (Figs. 4 and 5), Delrin was much less resistant to radiation than Penton. Figures 4a and 5a show that the most rapid decrease in maximum yield strength occurs at approximately 20 Mrad for Penton and 4 Mrad for Delrin. A measure of the resistance to radiation of polymers undergoing chain scission can conveniently be obtained by comparison of the doses required to reduce their initial strengths by one half; for Delrin, Penton, and a polycarbonate (Lexan)[4] these values are 4, 27, and 150 Mrad. If elongations at break are considered similarly, then the corresponding doses required to reduce the initial elongation of these polymers by half are 1, 10, and 60 Mrad.

Ductile–Brittle Transition

Relationships between the maximum tensile yield strength of Penton and radiation dose at various straining rates are given in Figure 6. The curves all appear to follow the same pattern as that obtained at the conventional straining rate (0.1 in./min.), with an initial maximum in yield strength followed by a continuous decline. Similar maxima in the graphs of strength versus radiation dose have been recorded[11] for various thermoplastic films after ultraviolet irradiation and an enhancement of the strength of a poly-
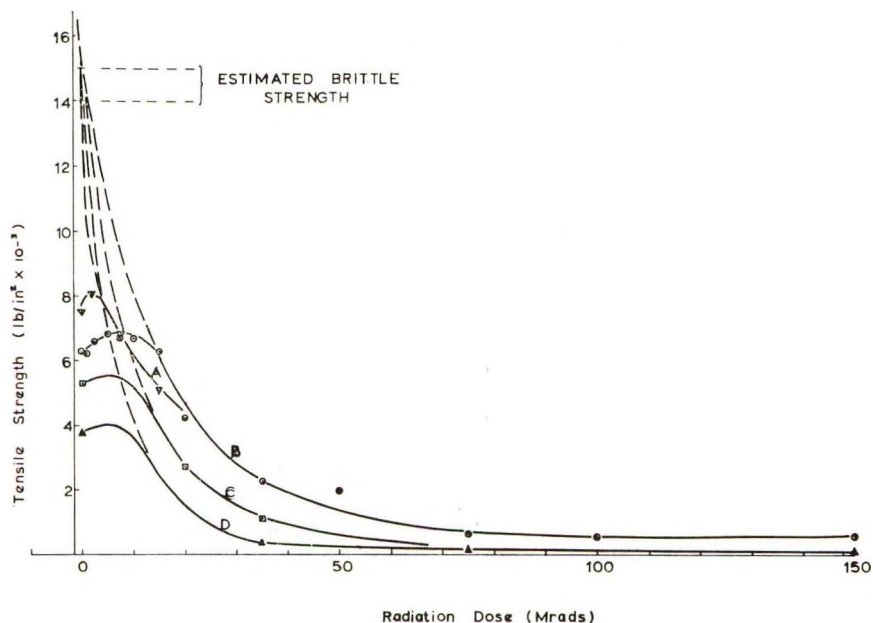
Fig. 6. Changes in tensile strength measured at various rates: with radiation dose R: (A) 10.0 in./min.; (B) 0.1 in./min.; (C) 0.01 in./min.; (D) 0.0005 in./min.
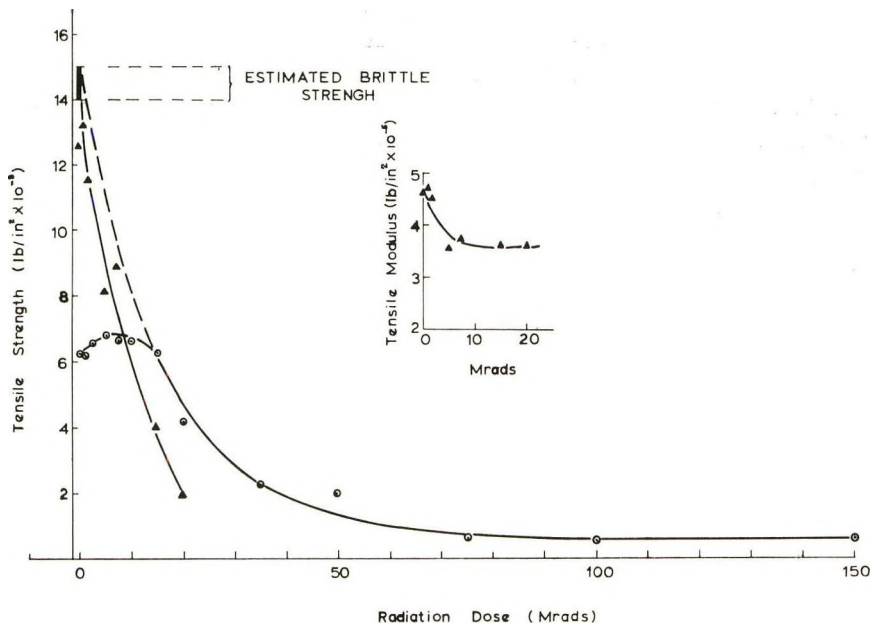
Fig. 7. Changes in tensile strength of Penton, tested at 0.1 in./min. with radiation dose R: (O) room temperature (20°C.); (Δ) − 196°C. Inset: change in tensile modulus with radiation dose at − 196°C.

carbonate [from 2,2-(4,4′-dihydroxy-3,3′,5,5′-tetrachlorodiphenyl)propane] film after a low dose of high energy radiation has been the subject of a recent patent.[12] The occurrence of such maxima has not hitherto been explained, and the reason is not immediately obvious. In the present investigation the complete absence of crosslinking and the steady reduction in molecular weight suggest that this phenomenon is physical (possibly associated with specimen geometry) rather than chemical in nature.

The initial rise in the maximum yield strength curve (0–10 Mrad) is characterized by ductile fractures; after the transition from ductile to brittle behavior at about 20 Mrad the subsequent continuous reduction in strength is characterized by brittle fractures. The initial increase in strength may be due to the reduced freedom of the specimen to yield. The strength recorded at low doses would have been greater had yielding not occurred, and extrapolation of that part of the curve characterized by brittle fractures (Fig. 6) towards low doses indicates the ideal behavior were yielding to be suppressed. From the strength values for unirradiated Penton at various straining rates published elsewhere[7] it was deduced that the maximum brittle strength of material of this molecular weight lies between 14,000 and 15,000 lb./in.². All the extrapolated curves shown should therefore pass through this range of strength at zero dose. At this stage it is of interest to note that our results show that the radiation dose R_0 needed to fracture a molecule of infinite molecular weight sufficiently for

the resultant to have the same viscosity-average molecular weight as the unirradiated polymer was 2.95 Mrad.   Hence, by implication, the theoretical maximum strength of Penton, to which value all the curves obtained at different straining rates (Fig. 6) should extrapolate (2,000,000 lb./in.^{2} has been quoted[13] for rupture of the primary valence bonds of a polymer chain), must lie on the -2.95 Mrad ordinate.

Further evidence for the shape of the hypothetical brittle strength curve was provided by a series of tensile tests at $-196°C.$, a temperature low enough to ensure that all the specimens exhibited brittle behavior. The glass transition temperature[14] of Penton is $5°C$.   The results (Fig. 7) show a curve of the expected form with a maximum recorded brittle strength of 13,800 lb./in.^{2} for unirradiated material.   The brittle nature of these failures is characterized by Hookean behavior up to failure, and Young's modulus calculated therefrom is substantially constant after an initial fall (Fig. 7, inset).

It is significant that the brittle strength of a specimen is greater at higher temperatures than at lower temperatures.   This effect may be associated with differences in ease of crack propagation, as the possibility of stress concentration at the apex of a crack will decrease with increase of temperature.

Light Absorption

The color of Penton specimens irradiated in vacuum changes progressively from a pale straw through amber to a brownish-black with increase in dose.   The irradiated material in chloroform exhibited an intense absorption band at 306 mμ ($E_{1\ cm.}^{1\%}$ 3.39 after a dose of 200 Mrad) with a long tail into the visible region.

The infrared spectrum of irradiated Penton film showed a series of new absorption bands which are given in Table I together with possible assignments.

TABLE I
Absorption Bands formed by Irradiation of Penton Film

Band, cm.$^{-1}$	Intensity	Possible assignment
3436	m	OH stretch
1786	vw	$=CH_2$, oxygenated grouping
1646	w	Nonconjugated $CR_2=CH_2$
1410–1460		Increased absorption due to unsaturation
980	w	$=CH_2$
730	w	(CH_2)

A slight shift of the C-O absorption from 1075 to 1078 cm.$^{-1}$ was also noted. An overall loss of sharpness in absorption, together with an increase in the band at 1027 cm.$^{-1}$ and a decrease in that at 897 cm.$^{-1}$ may be due to loss of crystallinity.[15]

The results show the formation of hydroxyl groups and also the development of unconjugated terminal unsaturation which may be responsible for the ultraviolet absorption at 306 mμ.

Gas Evolution

Krasnansky et al.[3] found that hydrogen, carbon dioxide, methyl chloride, butene, and pentene were evolved when poly-3,3-bis(chloromethyl)oxacyclobutane was exposed to Co^{60} γ-radiation. In the present work some-

TABLE II
Gas Evolution from Penton Irradiated in Vacuum to a
Dose of 200 Mrad

Gas evolved	Quantity, ml./g.
Hydrogen	2.16
Carbon monoxide	1.47
Carbon dioxide	0.11
Methyl chloride	0.074
Methane	0.016
Oxygen	0.0096
Hydrogen chloride[a]	2.72

[a] Determined argentometrically.
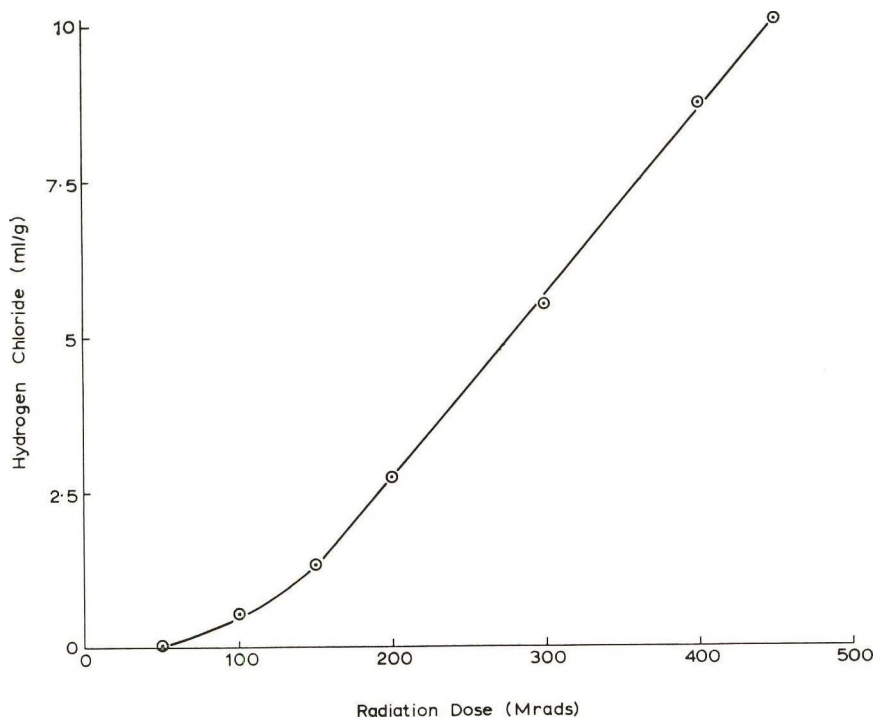
Fig. 8. Rate of evolution of hydrogen chloride from Penton with radiation dose R

what different results were obtained, and the mass spectrographic analysis of the gases evolved when Penton was exposed in vacuum to a dose of 200 Mrad is shown in Table II.

The products are thus similar to those found on thermal degradation of the polymer.[16]

The hydrogen chloride evolved, although not detected by mass spectroscopy, was identified by its infrared spectrum in the 3.25–3.75 μ region, and estimated as silver chloride. The quantity Q evolved, shown as a function of radiation dose in Figure 8, rapidly became directly proportional to radiation dose R, according to the equation

$$Q = 0.030R - 3.17 \qquad (4)$$

whence G (moles of hydrogen chloride evolved per 100 e.v.) is 1.27.

Effect of Radiation on Chemical Structure

The occurrence of random chain scission and absence of crosslinking on exposure of poly-3,3-bis(chloromethyl)oxacyclobutane to radiation are indicated by the changes in viscosity and by the complete solubility of the irradiated specimens at all doses examined (up to 500 Mrad).

Mechanisms proposed to account for the radiation-induced degradation of polymers which undergo chain scission without crosslinking have been reviewed by Chapiro[17] with particular reference to polyisobutylene and poly(methyl methacrylate), both of which contain quaternary carbon atoms and bear a structural resemblance to poly-3,3-bis(chloromethyl)-oxacyclobutane. Although in this case some conclusions can be drawn, in the absence of detailed quantitative analyses of unsaturation and chain scission, it is not possible to specify a complete mechanism. Spectroscopic measurements reveal the formation of hydroxyl groups and of terminal ethylenic unsaturation which suggest scission of the chain both at the ether linkage and adjacent to the quaternary carbon atom.

The relatively low carbon–chlorine bond strength favors scission of the chlorine atoms of the chloromethyl groups as in simple aliphatic halides.[18] Evolution of hydrogen chloride and the absence of chlorine suggest that, in the present case, facile abstraction of hydrogen occurs. In the alkyl halides loss of hydrogen by the resultant alkyl radicals and formation of alkenes has been postulated,[18] and a similar process is probable in this case, as appreciable amounts of hydrogen are formed in addition to terminal unsaturation. The formation of C=C—CH$_2$Cl groupings during irradiation is likely as solutions of irradiated polymer show the presence of considerable labile chlorine which is probably allylic rather than vinylic in character.

The relatively small quantity of methyl chloride found suggests that scission of chloromethyl groups occurs to only a limited extent. The carbon monoxide must arise from breakdown of the ether linkage but probably involves extensive radical rearrangement.

It is apparent from the structure of the polymer that scission at any point, unless followed by recombination or radical abstraction, must lead to

chain scission by rearrangement thus explaining the rapid breakdown of the polymer by irradiation.

References

1. Harrington, R., *Rubber Age*, **85**, 973 (1959).

2. Sasakura, H., N. Takuchi, and T. Mizuno, *J. Phys. Soc. Japan*, **17**, 572 (1962).

3. Krasnansky, V. J., B. G. Achhammer, and N. S. Parker, *SPE Trans.*, **1**, 133 (July 1961).

4. Golden, J. H., and E. A. Hazell, *J. Polymer Sci.*, **A1**, 1671 (1963).

5. Harding, G. W., *J. Polymer Sci.*, **55**, S27 (1961).

6. Harness, A. A., *J. Polymer Sci.*, **19**, 591 (1956).

7. Hall, H. W., and E. A. Hazell, S.C.I. Monograph No. 17, *Techniques of Polymer Science*, Society of Chemical Industry, London, 1963, p. 226.

8. Jellinek, H. H. G., *Can. J. Chem.*, **39**, 2056 (1961).

9. Jellinek, H. H. G., *Pure Appl. Chem.*, **4**, 419 (1962).

10. Charlesby, A., *J. Polymer Sci.*, **15**, 263 (1955).

11. Stephenson, C. V., B. C. Moses, and W. S. Wilcox, *J. Polymer Sci.*, **55**, 451 (1961).

12. Schnell, H., and U. Veiel, Ger. Pat., 880,628 (1961).

13. Haward, R. N., in *The Strength of Plastics and Glass*, Cleaver-Hume, London, 1949, p. 10.

14. Dainton, F. S., D. M. Evans, F. E. Hoare, and T. P. Melia, *Polymer*, **3**, 271 (1962).

15. Hatano, M., and S. Kambara, *J. Appl. Polymer Sci.*, **6**, 232 (1962).

16. Hatano, M., *Kogyo Kagaku Zasshi*, **64**, 728 (1961).

17. Chapiro, A., *Radiation Chemistry of Polymeric Systems*, Interscience, New York–London, 1962.

18. Swallow, A. J., *Radiation Chemistry of Organic Compounds*, Pergamon Press, Oxford, 1960, p. 94.

Résumé

On a étudié la dégradation du Penton [poly(3,3-bis(chlorométhyl)oxacyclobutane)] par irradiation électronique dans le vide. Des mesures viscosimétriques effectuées sur le matériel irradié, montrent que le polymère subit une scission statistique de la chaîne sans pontage subséquent. On a examiné, par analyse infra-rouge et par analyse des gaz, les changements de la structure chimique qui sont responsables, de la dégradation particulièrement rapide du polymère. Les gaz qui se dégagent durant l'irradiation sont surtout de l'hydrogène, du gaz chlorhydrique et de l'oxyde de carbone. On a étudié également l'effet de l'irradiation sur les propriétés mécaniques du Penton en extension et en flexion, et on les a reliées à des courbes hypothétiques de force de rupture cassante. On a déterminé certains effets de l'irradiation, de la vitesse de l'essai et de la température sur la force de rupture cassante du polymère. On a comparé les résultats des mesures viscosimétriques et des mesures des propriétés mécaniques en tension à des études similaires effectuées sur un polymère de structure voisine, le poly(oxyméthylène) (Delrin) qui est beaucoup moins résistant aux irradiations.

Zusammenfassung

Der Abbau von Penton (Poly[3,3-bis(chloromethyl)oxacyclobutan]) durch Elektronenbestrahlung im Vakuum wurde untersucht. Viskositätsmessungen am bestrahlten

Material liessen eine statistische Kettenspaltung des Polymeren ohne Vernetzung erkennen. Die für den ziemlich raschen Abbau des Polymeren verantwortlichen chemischen Änderungen wurden mit Infrarotanalyse und Analyse der vorwiegenden, während der Bestrahlung entwickelten Gase, Wasserstoff, Chlorwasserstoff und Kohlenmonoxyd untersucht. Die Kettenspaltung von Penton wird von einer Bildung von endständigen ungesättigten Gruppen und Allylchlorgruppen begleitet. Der Einfluss der Strahlung auf die Biege- und Zugeigenschaften von Penton wurde untersucht und es wurde die grosse Ähnlichkeit des Verhaltens bei Biegung und Dehnung gezeigt. Die Gestalt der für bestrahltes Penton erhaltenen Zugfestigkeitskurven bei verschiedenen Streckgeschwindigkeiten wurde untersucht und mit den hypothetischen Bruchfestigkeitskurven in Beziehung gebracht. Einige Strahlungseffekte, die Testgeschwindigkeit und die Temperatur bei der Bruchfestigkeit des Polymeren wurden bestimmt. Die Viskositäts- und Spannungsergebnisse wurden mit denen für das strukturell ähnliche Poly(oxymethylen) (Delrin), das gegenüber Strahlung weniger widerstandsfähig war, verglichen.

Thermal Stability of the Copolymer of Sulfur Dioxide and *cis,cis*-1,5-Cyclooctadiene

A. H. FRAZER, *Pioneering Research Division, Textile Fibers Department, Experimental Station, E. I. du Pont de Nemours & Company, Inc., Wilmington, Delaware*

Synopsis

The copolymer of sulfur dioxide and *cis,cis*-1,5-cyclooctadiene has been synthesized under a variety of conditions and pyrolyzed. Degradation of this copolymer followed first-order kinetics to a first approximation at 220°C. or above. Random cleavage of the polymer chain accompanied the pyrolysis as it was carried out in these experiments. Pyrolysis of the copolymer up to 75% loss of weight yielded the monomers as cracking products and in the mole ratio of the copolymer composition.

INTRODUCTION

Copolymers formed from simple olefins and sulfur dioxide have been known for a number of years.[1-4] These products appear to be 1:1 copolymers regardless of the mole ratio of olefin to sulfur dioxide for the polymerization.[1-4] Another characteristic of these systems is the maximum temperature ("ceiling temperature") above which copolymerization will not take place. This is noted with various olefins and appears to be a value uniquely determined by the olefin in question.[5,6] It has been widely recognized that the olefin/SO_2 copolymers are thermally unstable at elevated temperatures, however, very little[7] quantitative data on the decomposition are recorded.

Recently we have reported[8] the copolymerization of sulfur dioxide with *cis,cis*-1,5-cyclooctadiene. This copolymer (I) is believed to possess a bicyclic sulfone structure.

I
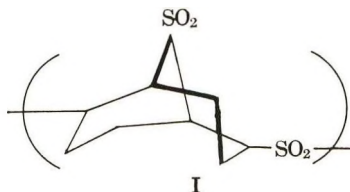
We were interested in studying the rates and products of the thermal degradation of this copolymer.

EXPERIMENTAL AND RESULTS

Copolymerization of Sulfur Dioxide with 1,5-Cyclooctadiene: General Method

All polymerizations were carried out in round-bottomed flasks fitted with a Dry Ice condenser, thermometer, and magnetic stirrer. Provisions were made so that the polymerization could be carried out under an inert atmosphere, open to the air, or with a gas bubbling through the reaction mixture.

After *cis,cis*-1,5-cyclooctadiene (b.p. 67–68/46 mm., +99.8% pure by vapor-phase chromatography), and the distilled solvents were added, the flask was chilled to −70°C. and anhydrous sulfur dioxide, as a liquid, was transferred under nitrogen to the flask. With the flask still at −70°C., the catalyst was added and the reaction mixture allowed to rise to the reflux temperature of the given mixture. The time of reaction noted in Table I refers to elapsed time from the addition of the catalyst to the precipitation of the reaction mixture. For those mixtures in which such polymer solvents as dimethyl sulfoxide and tetramethylene sulfone were used, the polymer remained in solution and was precipitated by the addition of methanol. For nonsolvent, polymer precipitated during the polymerization. In all cases, the isolated products were repeatedly washed with methanol to remove all traces of monomers and solvents.

TABLE I[a]

Reaction medium	Initiators[d]	Temp., °C.	Time, hr.	Atmosphere	Yield,[g] %	η_{inh}[h]	% S	First order $k \times 10^5$ (240°C.)
Diethyl ether	A	15	2	N_2	37	0.62	26.42	2.80
—	B	−5	10	N_2	23	0.90	26.93	2.75
DMSO[b]	A	22	8	N_2	84	0.21	26.51	2.70
TMS[c]	A	25	16	N_2	83	1.55	26.94	2.60
TMS[c]	A	25	16	Air[e]	89	1.95	26.85	2.65
TMS[c]	A	25	16	Air[f]	93	2.10	26.93	2.70
TMS[c]	—	25	16	Air[f]	50	1.20	26.84	2.82
DMSO[b]	C	22	16	N_2	88	0.21	26.43	2.61
TMS[c]	C	25	16	N_2	80	1.4	26.86	2.76
TMS[c]	C	25	16	Air[a]	98	2.2	26.76	2.68
TMS[c]	C	−4	2	N_2	15	1.13	26.87	2.85

[a] All reactions carried out with 10% wt. conc. of monomers; $M_{SO_2}/M_{C_8H_{12}} = 0.25/0.10$.

[b] DMSO, Dimethyl sulfoxide.

[c] TMS, Tetramethylene sulfone.

[d] A initiator, 5 drops of ascaridole and 5 drops of conc. HCl; B initiator, 1 drop of ascaridole and 400 cc. of HCl (gas); C initiator, 5 drops of methyl ethyl ketone peroxide

[e] Reaction mixture opened to air.

[f] Air bubbled through reaction mixture.

[g] Yield, per cent based on 1,5-cyclooctadiene.

[h] η_{inh}, inherent viscosity (ln η_{rel}/c) for 0.5 g. polymer/100 ml. dimethyl sulfoxide solution.

The dried polymer was analyzed for sulfur and the inherent viscosities determined in dimethyl sulfoxide. The preparation of copolymer under widely varied conditions, reaction media, etc., are summarized in Table I.

Inherent viscosity, η_{inh}, $(\ln \eta_{rel}/c)$ for 0.5 g. polymer/100 ml. of dimethyl sulfoxide solution was determined at 30°C. in an Ostwald-Fenske viscometer.

Measurement of Rates of Thermal Degradation of I

Rate curves for the decomposition of this copolymer were obtained using a thermogravimetric balance[9] under N_2 at temperatures in excess of 200°C. It was found that the degradation followed first-order kinetics to a first
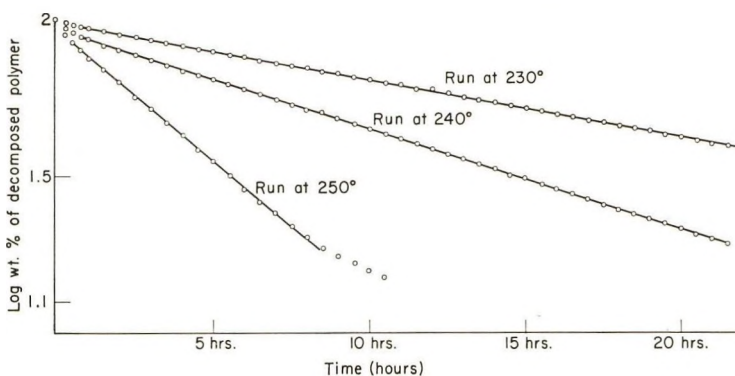
Fig. 1. First-order decomposition curves for I.
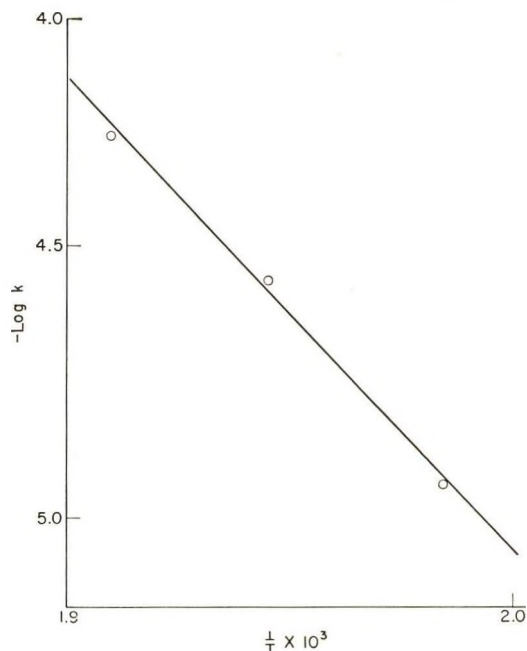
Fig. 2. Plot for E_a for decomposition of I.

approximation up to 75% loss of weight, particularly at temperatures of 220–250°C. Figure 1 illustrates the results from such studies at 230, 240, and 250°C. The specific velocity constants k for these temperatures were: 1.18×10^{-5} sec.$^{-1}$ (230°C.), 2.68×10^{-5} sec.$^{-1}$ (240°C.), and 5.43×10^{-5} sec.$^{-1}$ (250°C.). Figure 2 shows the activation energy E_a for this process to be 41 kcal/mole with a frequency factor of 5.2×10^{13} sec.$^{-1}$ on the basis of the above k values. In the degradation studies at temperatures of 200–220°C., the rates were extremely slow, and the scatter of data was such that no valid conclusions could be drawn.

Measurement of Change in Inherent Viscosity of I on Heating

Samples of I were heated at 230, 240, and 250°C. for various periods of time in glass tubes under N_2, and the inherent viscosity η_{inh} in dimethyl sulfoxide of these heated samples determined. Figure 3 illustrates these data.

Thermal Degradation Products of I

Although there are numerous references in the literature indicating that olefin/SO_2 copolymers and diene/SO_2 copolymers pyrolyze to the original monomers, there was only one instance[8] for the olefin/SO_2 copolymers and no instances for the diene/SO_2 copolymers where reasonable quantitative data were found.

We have studied the degradation of I under a nitrogen atmosphere at 250°C. The apparatus consisted of a flask heated at 250°C. and attached to a slow stream of nitrogen. The exit line was connected in series to two traps kept at −196°C., and the system protected with drying tubes. Four 100 g. samples of I were heated under these conditions until ca. 25%, 50%, 75%, and 85%, respectively, of original weight was lost. The trapped volatile products were separated and analyzed by VPC and infrared. The residue, after extraction, was carefully analyzed. Results are summarized in Table II.

The above data show that for runs 1, 2, and 3 where, based on the aforementioned kinetic data, the decomposition follows first-order kinetics, the

TABLE II
Thermal Degradation Products of I (250°C./1 atm./Nitrogen)

Run	Volatiles			Residue		
	Total wt., g.	Total H_2O, g.	C_8H_{12}/SO_2 molar ratio	Total wt., g.	η_{inh}	S, %[a]
1	24.5	6.0	2/1.1	72.1	0.12	26.6
2	43.5	6.3	2/1.1	52.4	0.11	26.6
3	72.3	6.3	2/1.1	23.4	0.11	26.3
4	80.5	9.8	2/0.8	10.2	0.10	25.5

[a] 27.1% sulfur is theory for copolymer containing 2 moles of SO_2 and 1 mole of 1,5-cyclooctadiene per polymer repeat unit.
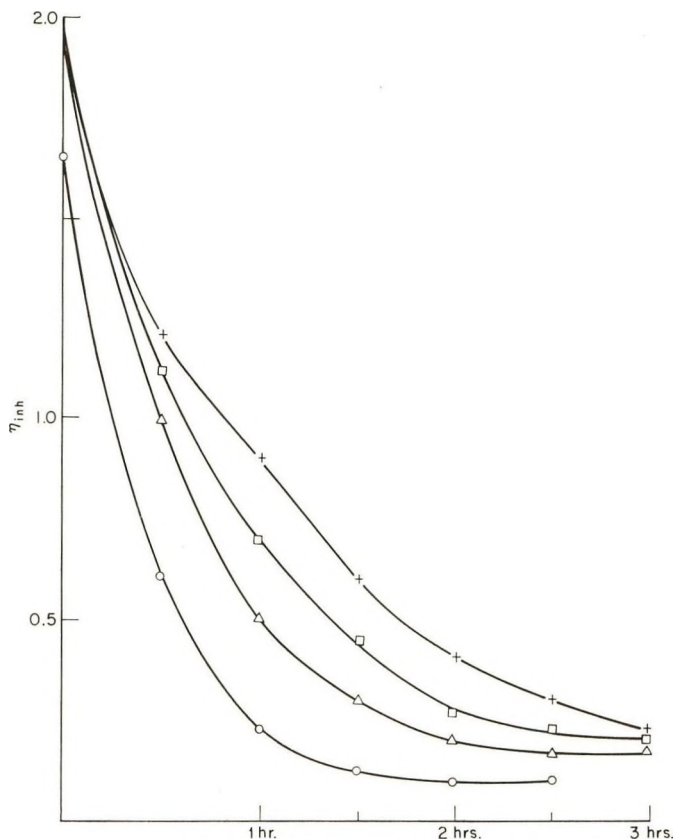
Fig. 3. Effect of thermal degradation on η_{inh} of I: ($+$) run at 230°C.; ($\square$) run at 240°C.; ($\triangle$) run at 250°C.; ($\bigcirc$) propylene/SO$_2$ copolymer, run at 230°C.

material balance is over 95%. For these runs, in the volatile fractions, the water obtained is slightly higher than that expected from the water absorption of the polymer (5.3 wt.-% based on film). The residues in these runs were tan solids which yielded no soluble products on extraction with ethyl acetate, benzene, dioxane, acetone, or ethanol and which appear to be low molecular weight copolymer. Analysis of these residues for residual double bond by infrared absorption in the 6.0 to 6.2 μ region (see Fig. 4) and catalytic hydrogenation in tetramethylene sulfone was negative. In run 4, where, based on kinetic data, first-order kinetics is not followed throughout, the material balance is 90.7%, and product water is ca. 50% greater than in the other runs. The residue in this run was brown, but the analysis for residual double bonds was negative.

DISCUSSION

It is difficult to determine the detailed mechanism of pyrolyses of the type described herein where reactions take place in an unfused solid. How-
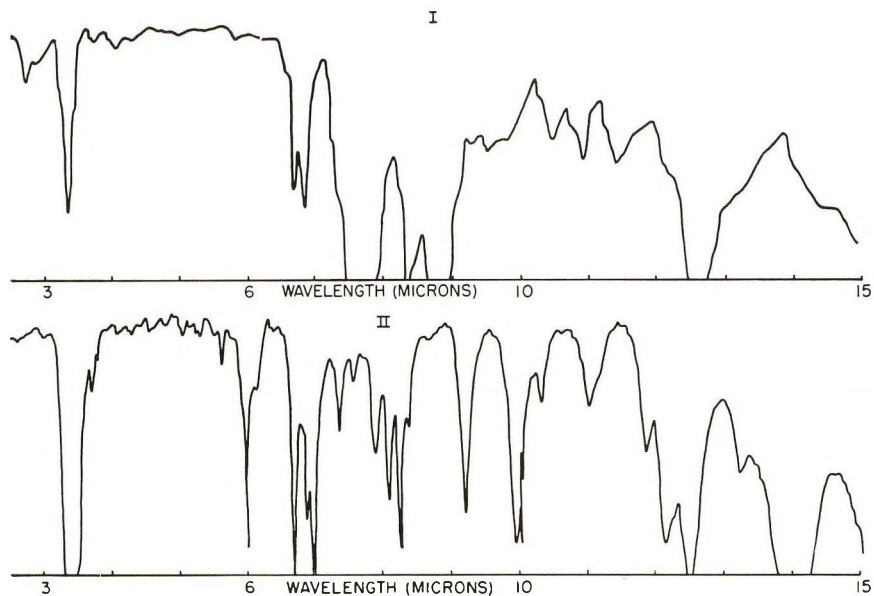
Fig. 4. Infrared spectra of (*I*) copolymer I and (*II*) *cis,cis*-1,5-cyclooctadiene.

ever, some observations and tentative conclusions can be drawn with regard to the thermal degradation of I and, also, as related to the degradation of other olefin/SO$_2$ and diene/SO$_2$ copolymers.

Earlier workers[3] suggested the possibility that weak links might account for the instability of olefin/SO$_2$ copolymers. An example was the sulfinic ester groups which might result from copolymerization through an S—O linkage rather than by exclusive formation of C—S bonds. Although this particular example might be argued against on the basis of the stability of olefin/SO$_2$ copolymers in strong acid solutions, it was felt that if weak linkages did exist, differences in activation energy for formation of these structures might lead to products of widely different stability if the polymer syntheses were carried out under widely different conditions. A comparison of the runs in Table I where I was prepared at different temperatures, in widely different reaction media, and with different polymerization initiators show this is apparently not the case for this copolymer of sulfur dioxide and *cis,cis*-1,5-cyclooctadiene. The relatively small difference in k values suggest no drastic changes in structure.

It is apparent from an inspection of Figure 1 that the initial parts of the degradation curves do not follow first-order kinetics exactly. In an attempt to determine if this deviation might be due to some particular chemical grouping, the thermal degradation was followed by the examination of the infrared spectra of these films of I (Fig. 4), after heating. Unfortunately, after less than 2 hr. heating, polymer degradation was so severe (see Fig. 3) that these films became embrittled, cracked, and opaque. However, up until this point was reached, the infrared spectra of the original

film and those of the heated films were identical. Thus, it would appear that if this deviation from first-order kinetics is due to a different type of linkage, these weak linkages are present in less than 1% concentration.

The degradation of I follows first-order kinetics to a first approximation at 220°C. or above, whereas it is reported[7] that the degradation of butadiene/SO_2 copolymer does not. It could be argued that this is not a valid comparison, since the butadiene/SO_2 copolymer contains a residual double bond per polymer repeat unit, and a different type of degradative behavior might be expected. A more valid comparison would be with the olefin/SO_2 copolymers. Indeed, in the case of the copolymers of sulfur dioxide with ethylene, propylene, butene-2, and isobutene, respectively, degradation of these copolymers is reported[7] to follow first-order kinetics at 200°C. or above. However, it is interesting that for the propylene/SO_2 copolymer[7] the k at 229°C. is ca. 100 times greater than the k for I at 230°C. Similarly, E_a for the propylene/SO_2 copolymer is 32 kcal./mole, whereas for I it is 41 kcal./mole. Thus it would appear that the bicyclic sulfone structure of I is inherently more stable than the linear α,β-sulfone structure of the olefin/SO_2 copolymers.

The heating of I which is illustrated in Figure 3 caused a precipitous drop in inherent viscosity with very little weight loss (Fig. 1). At 230°C. the inherent viscosity was reduced over 75% when the weight loss was only about 3%. This behavior suggests degradation by random chain scission or by splitting of weak links located randomly in the chain. This appears reasonable since the frequency factor of 5.2×10^{-13} sec.$^{-1}$ for this degradation process is in agreement with that found by Schaefgen[10] for a random chain cleavage process. Thus, in this respect, the decomposition I is similar to the pyrolysis of the olefin/SO_2 copolymers[7] and suggests that the differences in stability of I and these copolymers are of degree and not of kind.

This is borne out in the pyrolysis studies of I summarized in Table II. As in the case of the propylene/SO_2 copolymer,[7] the pyrolysis of I, under conditions where first-order kinetics were followed, yielded monomers (sulfur dioxide and cis,cis-1,5-cyclooctadiene) as cracking products and in approximately the mole ratio of the copolymer composition. In the one case where first-order kinetics was not followed (run 4, Table II) throughout the reaction, the increased water and decreased sulfur dioxide in the volatile products and low sulfur content of the residue suggest a possible oxidation-reduction reaction between sulfur dioxide and the hydrocarbon part of the polymer. If this is correct, this secondary reaction could explain the deviation from first-order kinetics above 75% reaction.

References

1. Mathews, F. E., and H. M. Elder, Brit. Pat. 11,635 (1915).
2. Fredrick, D. S., H. D. Cogan, and C. S. Marvel, *J. Am. Chem. Soc.*, **56**, 1815 (1934).
3. Hunt, M., and C. S. Marvel, *J. Am. Chem. Soc.*, **57**, 1691 (1935).

4. Staudinger, H., and B. Ritzenthaler, *Ber.*, **63**, 455 (1935).

5. Snow, R. D., and F. E. Frey, *J. Am. Chem. Soc.*, **65**, 2417 (1943).

6. Dainton, F. S., and K. J. Ivin, *Proc. Roy. Soc. (London)*, **A212**, 96 (1952); *Trans. Faraday Soc.*, **46**, 331 (1950).

7. Naylor, M. A., and A. W. Anderson, *J. Am. Chem. Soc.*, **76**, 3962 (1954).

8. Frazer, A. H., and W. P. O'Neill, *J. Am. Chem. Soc.*, **85**, 2613 (1963).

9. Peterson, H. H., *Instr. Automation*, **28**, 1104 (1955).

10. Schaefgen, J. R., *J. Polymer Sci.*, **41**, 133 (1959).

Résumé

Le copolymère anhydride sulfureux et *cis,cis*-1,5-cyclooctadiène a été synthetisé dans des conditions variées et pyrolysé. En première approximation, la dégradation de ce copolymère suit une cinétique du premier ordre, à 220°C ou au delà. Une rupture statistique de la chaîne polymérique accompagne la pyrolyse telle qu'on l'a effectuée dans nos expériences. La pyrolyse du copolymère jusqu'à perte de 75% de son poids fournit les monomères comme produit de (cracking) dans un rapport molaire qui correspond à la composition du copolymère.

Zusammenfassung

Das Copolymere aus Schwefeldioxyd und *Cis,cis*-1,5-Cyclooctadien werde unter einer Reihe von Bedingungen synthetisiert und pyrolysiert. Der Abbau dieses Copolymeren folgt bei 220°C oder darüber in erster Näherung einer Kinetik erster Ordnung. Die unter diesen Umständen ausgeführte Pyrolyse war von einer statistischen Spaltung der Polymerkette begleitet. Pyrolyse des Copolymeren lieferte bis zu einem Gewichtsverlust von 75% die Monomeren als Crackprodukte im Molverhältnis der Copolymerzusammensetzung.

Experimental Data on Dilute Polymer Solutions. Hydrodynamic Properties and Statistical Coil Dimensions of Poly(*n*-butyl Methacrylate). Part II

R. VAN LEEMPUT and R. STEIN,* *Laboratoire de Chimie Générale, Université Libre de Bruxelles, Brussels, Belgium*

Synopsis

Viscometric measurements were carried out on poly(*n*-butyl methacrylate) fractions in chloroform, benzene, toluene, and dioxane. Light-scattering and viscometric measurements on these fractions were carried out in isopropanol over a narrow range of temperatures. The Flory-Fox θ-temperature was obtained by graphical interpolation on a plot of the second virial coefficient versus the reciprocal of the absolute temperature. Values of Φ, calculated according to the Flory-Fox equation were found to be abnormally low, notwithstanding the application of heterodispersity corrections, a mean value of 1.62×10^{23} being found in isopropanol in the temperature range investigated. The dependence of $[\eta]$ on the mean radii of gyration is found to be less than that predicted by the Flory-Fox theory. The light-scattering dimensions systematically appear to be too large in the ideal solvent, a discrepancy that cannot be explained by accumulated experimental factors.

INTRODUCTION

In a preceding article,[1] the authors reported measurements carried out on this polymer in two solvents, acetone and methyl ethyl ketone. In the present paper, measurements have been carried out on poly(*n*-butyl methacrylate) (PBM) in isopropanol over a range of temperatures including the Flory θ-temperature as well as in four other solvents.

The experimental results are treated on the basis of the equations of Flory and Fox and Kurata et al.[2-4]

EXPERIMENTAL

Polymer fractions and experimental procedure have been described.[1] All light-scattering measurements were carried out by use of vertically polarized light of 436 mμ wavelength. Appropriate refractive index and Fresnel corrections were applied. The values of *dn/dc* for isopropanol are 0.1059, 0.1066, 0.1068, 0.1076, and 0.1097 at 20.0, 23.7, 25.0, 31.0, and 45.0°C., respectively.
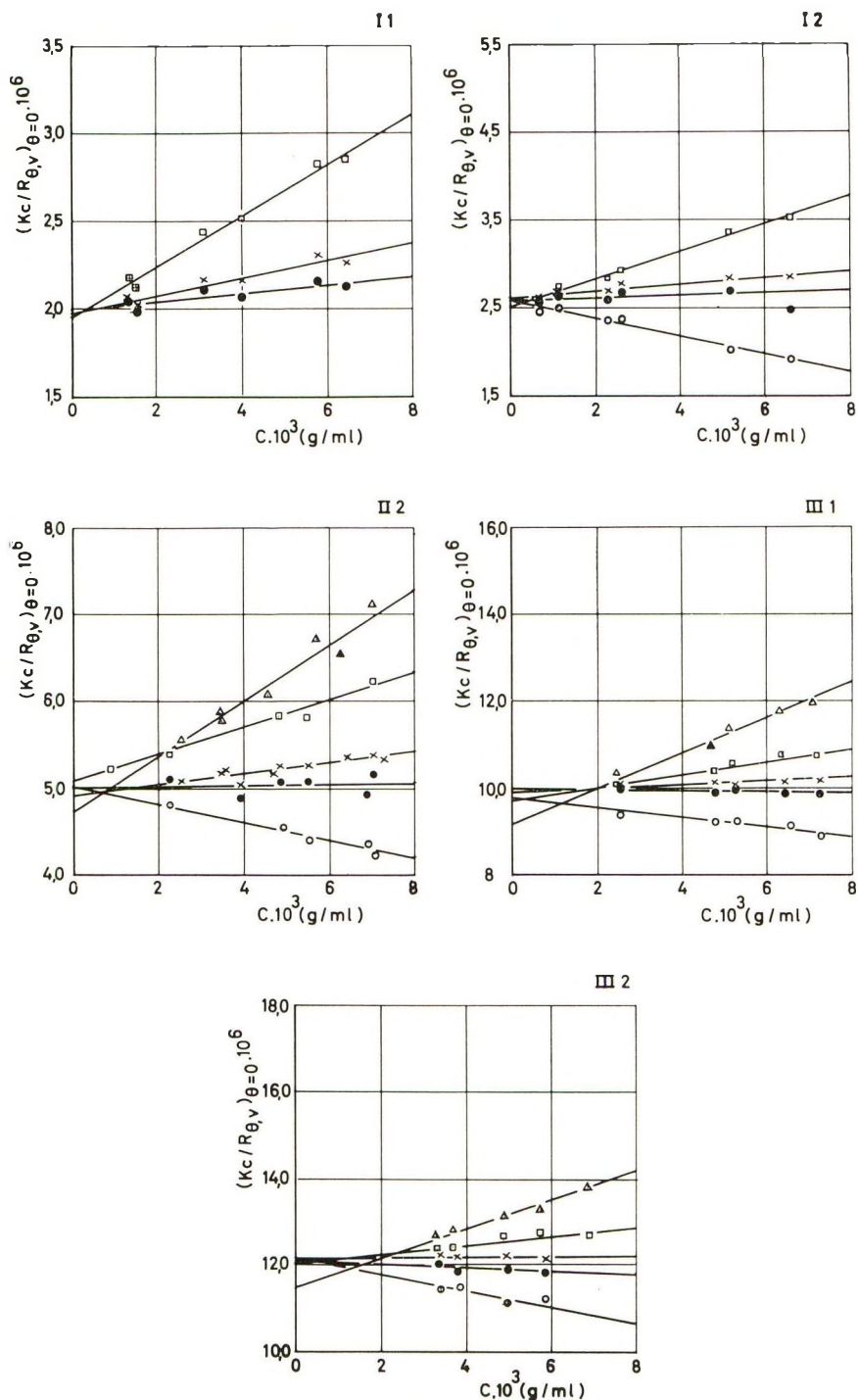
Fig. 1. Concentration dependence at zero angle of reduced scattered intensities at 436 mµ for five PBM fractions in isopropanol at various temperatures: (O) 20.0°C.; (●) 23.7°C.; (×) 25.0°C.; (□) 31.0°C.; (△) 45.0°C.

RESULTS AND DISCUSSION

The experimental results are collected in Tables I and II and Figure 1. The results of angular scattering intensities, measured in isopropanol at five temperatures, were treated by the Zimm method. Values obtained from these diagrams were calculated by the method of least squares. Figure 1 shows typical lines of the values $(Kc/R_{\theta,v})_{\theta = 0}$ plotted against the concentration c of PBM fractions in isopropanol. No third virial coefficient was taken into account. The weight-average molecular weight values $\bar{M}_w$ obtained from these measurements are seen to be 2–5% lower than those obtained in the previous work using acetone and MEK as solvents.

TABLE I
Light-Scattering and Viscometric Measurements on Poly(n-butyl
Methacrylate) Fractions in Isopropanol at Various Temperatures

| Temp., °C. | Fraction | Light scattering | | | $[\eta]$ | $M_w{}^a$ | b^a |
		$M_w \times 10^{-3}$	$A_2 \times 10^6$	$\langle \bar{S}^2 \rangle_{LS}{}^{1/2} \times 10^8$			
20.0	I–2	506	−39	179	21.71		
	II–2	260	−40	118	15.41		
	III–1	134	−42	98	12.09		
	III–2	108	−70	87	11.67		
23.7	I–1	650	10	211	27.39	640	10
	I–2	500	6	181	24.99	514	10
	II–2	258	2	131	19.46	269	6
	III–1	130	−3	98	13.19	136	5
	III–2	107	−15	106	12.19	117	12
25.0	I–1	653	20	229	31.43		
	I–2	492	14	201	29.74		
	II–2	263	24	150	19.97		
	III–1	129	7	110	15.52		
	III–2	107	3	113	13.91		
31.0	I–1	653	57	245	40.15		
	I–2	508	62	211	36.61		
	II–2	252	62	153	22.24		
	III–1	131	55	99	18.51		
	III–2	107	40	110	16.19		
45.0	II–2	262	128	168	—		
	III–1	134	165	104	—		
	III–2	109	138	116	—		

a Values previously published[1] and adopted in all calculations here.

This difference, falling, as it does, within the limits of experimental error, has been neglected, and the values of $\bar{M}_w$ previously reported[1] have been adopted in all subsequent calculations. They are shown in Table I, together with the values of b, the parameter which characterizes the width of the distribution.

Heterodispersity correction factors have been applied in all cases, as previously reported.[1]

TABLE II

Linear Expansion Coefficients Calculated According to Flory and
Kurata et al. for Poly(n-butyl Methacrylate) in Different Solvents at 25°C.

Solvent	Fraction	$[\eta]$, ml./g.	$\dfrac{[\eta]}{[\eta]_\theta}$	$\left(\dfrac{[\eta]}{[\eta]_\theta}\right)^{1/3} = \alpha$	$\left(\dfrac{[\eta]}{[\eta]_\theta}\right)^{1/2.4} = \alpha$
Isopropanol	I–1	31.43			
(Θ-solvent)	I–2	29.74			
	II–2	19.97			
	III–1	15.52			
	III–2	13.91			
Chloroform	I–2	105.5	3.55	1.53	1.70
	II–2	66.6	3.34	1.49	1.65
	III–1	40.3	2.60	1.38	1.49
	III–2	37.3	2.68	1.39	1.51
Benzene	I–2	96.7	3.25	1.48	1.63
	II–2	59.1	2.96	1.44	1.57
	III–1	35.1	2.26	1.31	1.40
Toluene	I–2	89.2	3.00	1.44	1.58
	II–2	56.1	2.81	1.41	1.54
	III–1	32.8	2.11	1.28	1.37
Methyl ethyl	I–1	91.8	2.92	1.43	1.56
ketone	I–2	77.2	2.60	1.38	1.49
	II–2	50.1	2.51	1.36	1.47
	III–1	31.6	2.04	1.27	1.35
	III–2	28.6	2.06	1.27	1.35
Dioxane	I–2	70.2	2.36	1.33	1.43
	II–2	46.3	2.32	1.32	1.42
	III–1	27.4	1.77	1.21	1.26
Acetone	I–1	73.4	2.34	1.33	1.43
	I–2	62.4	2.10	1.28	1.36
	II–2	43.4	2.17	1.29	1.38
	III–1	28.0	1.80	1.22	1.28
	III–2	24.8	1.78	1.21	1.26

Relations between M_w, $[\eta]$, and $\langle S^2 \rangle^{1/2}$

The constants in the relationships between the limiting viscosity number $[\eta]$, the mean-square weight-average radius of gyration $\langle \overline{S^2} \rangle_w$, and the weight-average molecular weight M_w

$$[\eta] = K \overline{M}_w^\varepsilon \tag{1}$$

$$\langle \overline{S^2} \rangle_w = C \overline{M}_w^{1+\beta} \tag{2}$$

are shown in Table III. Heterogeneity corrections have been applied, as previously described.[1]

It will be seen that the value of the mean-square radius of gyration appears to be a simple function of the molecular weight only in the vicinity of the Flory temperature (cf. the value of β, Table III). This result does not confirm those of Chinai et al.[5,6] for some substituted polymethacrylic esters.

TABLE III

Viscometric Constants for PBM in Various Solvents

Solvent	Temp., °C.	$K \times 10^3$	ϵ	β	$C \times 10^6$	$\Phi \times 10^{-23}$
Isopropanol	20.0	6.5	0.44	−0.05	1.16	1.66
	23.7	4.4	0.48	0.0	0.44	1.78
	25.0	4.2	0.50	0.0	0.54	1.38
	31.0	3.3	0.53	0.02	0.50	1.67
Benzene	25.0	0.48	0.75	0.17		
Toluene	25.0	0.48	0.75	0.17		
Chloroform	25.0	0.91	0.71	0.14		
Dioxane	25.0	0.99	0.67	0.11		

Average values of Φ in the Flory equation (corrected by a heterodispersity factor q)

$$|\eta|_{\text{measured}} = \Phi q 6^{1/2} \langle S^2 \rangle_{\text{LS}}^{3/2} / \bar{M}_w \tag{3}$$

will be found in Table III. These abnormally low values cannot be explained by experimental errors as this would imply errors of up to 40% in the values of $\langle S^2 \rangle_{\text{LS}}^{1/2}$. They indicate a too highly extended chain in the region of the θ-temperature; an explanation on the basis of a drainage parameter as discussed by Kurata and Yamakawa[2] is tempting, but would imply an unusual solvent effect.

Determination of the θ-Temperature

A plot of the second virial coefficient A_2 of PBM fraction in isopropanol against the reciprocal temperature gave curves cutting the $A_2 = 0$ line over a fairly narrow range. The temperatures equivalent of the limits of this range were 23.5 and 25.3°C. According to this plot and to the values of the exponents ϵ and β (Table III), the value of 25.0°C. was chosen as the actual θ-temperature. This result may be compared with the value of 23.7°C. reported by Chinai and Valles.[7]

The Expansion Coefficient α and the Unperturbed Dimensions

A test for Flory's relation of the type proposed by Krigbaum and Carpenter[8] and which consists of plotting $[\eta]\bar{M}_w/q$ against $\langle S^2 \rangle_{\text{LS}}^{1/2}$ on a log–log scale is again applied. Here q is the correction factor as it appears in eq. (3). Such tests were applied for the PBM fractions in isopropanol at 20.0, 23.7, 25.0, and 31.0°C. The slopes of the lines are, respectively, 2.93, 2.68, 2.84, and 2.68 and may be compared with the values of 2.83 and 2.87 previously obtained in MEK and acetone, respectively. The average value 2.80 falls between the value of 3 proposed by Flory and that of 2.43 proposed by Kurata et al.

Table II sets out the linear expansion coefficients calculated in all the solvents studied at 25.0°C. These coefficients have been calculated according to both the theories in question. It will be seen that the values

of α tend to increase with molecular weight as predicted by Flory[9] and as found in several poly(vinyl acetate)–solvent[10] and PBM–MEK[5] systems.

Table IV shows the various ratios obtained from the unperturbed root-mean-square radii of gyration $\langle \overline{S_0^2} \rangle^{1/2}$, as calculated by using the theoretical limiting value $\Phi = 2.87$ and $\langle \overline{S_0^2} \rangle_{\mathrm{LS}}^{1/2}$ as measured in the ideal solvent, and from the root-mean-square radius of gyration of a molecule with completely unhindered chain rotation $\langle \overline{S^2} \rangle_f^{1/2}$. These latter values were calculated by assuming a C—C bond length $l = 1.54$ A. and a bond angle $\theta = 109.5°$, with P being the degree of polymerization and the number of bonds $n = 2P$. A definite difference between the ratios $\langle \overline{S_0^2} \rangle_{\mathrm{LS}}^{1/2}/\langle \overline{S^2} \rangle_f^{1/2}$ and $\langle \overline{S_0^2} \rangle^{1/2}/\langle \overline{S^2} \rangle_f^{1/2}$ for PBM in the ideal solvent will be noticed. This is due to the repercussion of the abnormally low values of Φ on these ratios. The values of $\langle \overline{S_0^2} \rangle_{\mathrm{LS}}^{1/2}/\langle \overline{S^2} \rangle_f^{1/2}$ are much higher than those reported by Chinai.[5] A consequence of this anomaly lies in the fact that the ratios $\langle \overline{S_0^2} \rangle^{1/2}/\langle \overline{S^2} \rangle_f^{1/2}$ calculated on the basis of the theoretical value of Φ closely resemble those reported by Chinai. Moreover, the ratios shown in Table IV for PBM in methyl ethyl ketone are much lower than those reported by Chinai.

TABLE IV

Parameters Derived from Viscosity and Light-Scattering Data
on PBM Fractions at 25.0°C.[a]

| Fraction | Isopropanol | | MEK | Acetone |
	$\dfrac{\langle \overline{S_0^2} \rangle^{1/2}}{\langle S^2 \rangle_f^{1/2}}$	$\dfrac{\langle \overline{S^2} \rangle_{\mathrm{LS}}^{1/2}}{\langle S^2 \rangle_f^{1/2}}$	$\dfrac{\langle \overline{S^2} \rangle_{\mathrm{LS}}^{1/2}}{\langle S^2 \rangle_f^{1/2}}$	$\dfrac{\langle \overline{S^2} \rangle_{\mathrm{LS}}^{1/2}}{\langle S^2 \rangle_f^{1/2}}$
I–1	1.89	2.46	3.06	2.99
I–2	1.94	2.42	2.96	3.02
II–2	1.90	2.46	2.74	2.74
III–1	2.00	2.56	2.77	2.79
III–2	1.90	2.83	2.58	2.75

[a] $\langle \overline{S_0^2} \rangle$ is calculated from the equation $[\eta] = \Phi 6^{3/2} \langle \overline{S_0^2} \rangle^{3/2}/M_w$, using the theoretical limiting value of 2.87×10^{23} for Φ; $\langle \overline{S_0^2} \rangle_{\mathrm{LS}}$ is the value measured at 25.0°C. in isopropanol.

References

1. Van Leemput, R., and R. Stein, *J. Polymer Sci.*, **A1**, 985 (1963).
2. Kurata, M., H. Yamakawa, and E. Teramoto, *J. Chem. Phys.*, **28**, 785 (1958).
3. Kurata, M., and H. Yamakawa, *J. Chem. Phys.*, **29**, 311 (1958).
4. Kurata, M., W. H. Stockmayer, and A. Roig, *J. Chem. Phys.*, **33**, 151 (1960).
5. Chinai, S. N., and R. A. Guzzi, *J. Polymer Sci.*, **21**, 417 (1956).
6. Didot, F. E., S. N. Chinai, and D. W. Levi, *J. Polymer Sci.*, **43**, 557 (1960).

7. Chinai, S. N., and R. J. Valles, *J. Polymer Sci.*, **39**, 363 (1959).

8. Krigbaum, W. R., and D. K. Carpenter, *J. Phys. Chem.*, **59**, 1166 (1955).

9. Flory, P. J., *Principles of Polymer Chemistry*, Cornell Univ. Press, Ithaca, N. Y., 1953, Chap. 14.

10. Moore, W. R., and M. Murphy, Jr., *J. Polymer Sci.*, **56**, 519 (1962).

Résumé

On a déterminé les indices viscosimétriques limites de fractions de polyméthacrylate de butyle-*n* dans le chloroforme, le benzène, le toluène et le dioxanne. Des mesures de diffusion latérale de la lumière et de viscosité à différentes températures ont été effectuées dans l'isopropanol. La température Θ dans ce solvant a été déterminée par interpolation graphique du second coefficient du viriel en fonction de l'inverse de la température. Les valeurs de Φ, calculées suivant la relation de Fox-Flory et corrigées pour l'hétérodispersité, sont anormalement faibles; une valeur moyenne de 1,62 × 10²³ a été obtenue dans le domaine de température étudié. La variation de [η] en fonction du rayon de giration est moindre que celle prévue par la théorie de Fox-Flory. Les dimensions obtenues dans le solvant idéal semblent trop élevées.

Zusammenfassung

Viskositätsmessungen wurden für verschiedenen Poly(*n*-Butylmethacrylat) Fraktionen in Chloroform, Benzol, Toluol und Dioxan durchgeführt. Für diese Fraktionen wurden die Viskosität und Lichtstreuung über einem Schmalen Temperaturbereich in Isopropanol gemessen. Die Flory Θ-Temperatur ist mittels Interpolation in einem Diagramm des Zweiten Virialkoeffizients gegen die Reziprokaltemperatur erhalten worden. Die berechneten Φ-Werte aus der Flory-Fox Gleichung sind trotz Anbringung Heterodispersitätskorrektur ungewöhnlich gering ein Durchschnittswert von 1,62 × 10²³ ist innerhalb des untersuchten Temperaturbereichs gefunden worden. Die Abhängigkeit von [η] zum Trägheitsradius des Knäuels ist geringer als es nach der Flory Theorie zu erwarten war. Die Lichtstreuungsgrössen scheinen systematisch in dem idealem Lösungsmittel übertrieben zu sein. Solche Unterschiede können nicht durch gesammelte experimentelle Faktoren erklärt werden.

Density Gradient Centrifugation of a Graft Copolymer

H. A. ENDE, *Chemstrand Research Center, Inc., Durham, North Carolina,* and V. STANNETT, *Camille Dreyfus Laboratory, Research Triangle Institute, Durham, North Carolina*

Synopsis

A well-defined graft copolymer of polystyrene and cellulose acetate has been investigated using the density gradient ultracentrifugation method. The initial sample showed two peaks. These were found to be pure graft copolymer and polystyrene; the latter was easily removed by further extraction of the mixture with benzene. The composition of the graft copolymer was determined from the buoyant densities of the graft and the two homopolymers and found to be 49% polystyrene, 51% cellulose acetate compared with 44.1 and 55.9%, respectively, estimated from the weight loss after acid hydrolysis.

One of the chief difficulties in the field of graft copolymerization is the lack of a suitable method for estimating the amount actually grafted or checking that a given sample is free from one or both of the attendant homopolymers. The cellulose acetate–styrene system[1,2] provides graft copolymers which may be essentially freed from homopolymers because their solubility differences are so great. For example, secondary cellulose acetate is soluble in a 70:30 acetone–water mixture and quite insoluble in benzene, whereas polystyrene is soluble only in benzene and the graft polymers are insoluble in both solvents. Because the cellulose acetate may be hydrolyzed away by acid, the composition and the molecular weight of the side chains can also readily be determined.

The development of the density gradient centrifugation method for the investigation of copolymers[3,4] led us to investigate a well characterized sample of cellulose acetate–styrene graft copolymer by this technique.

EXPERIMENTAL

Cellulose Acetate–Styrene Graft Copolymer

The sample was prepared by irradiating a solution of cellulose acetate in a 50:50 styrene–pyridine mixture at 0.32 Mrad/hr. with γ-radiation from a Co[60] source to a total dose of 10 Mrad. The graft polymer was isolated by precipitating in a large excess of benzene followed by extraction with a 70:30 acetone–water mixture. The product was further extracted with benzene followed by freeze drying.

The composition was determined by dissolving the graft copolymer in a small quantity of dimethylformamide, diluting to about 2% with 6% sulfuric acid, and refluxing for 24 hr.; the residual polymer was isolated by dissolving in benzene and reprecipitating in methanol. Infrared examination showed the residue to be pure polystyrene. The viscosity-average molecular weight was found to be 119,000. The original cellulose acetate had a degree of substitution of 2.53 and a viscosity-average molecular weight of about 120,000. Separate studies have shown[2] that little degradation accompanies grafting under the conditions described.

Ultracentrifugation

A Spinco analytical ultracentrifuge Model E, equipped with schlieren optics was used. For some of the experiments reported here an aluminum double sector cell was used in order to obtain a base line representing the refractive index gradient in the density gradient solvent mixture and thus locate the actual position of the band maxima. All experiments were conducted at a speed of 50,740 rpm. A density gradient mixture consisting of 300 g. bromoform/l. in dimethylformamide was found to be suitable and located all the polymers at convenient levels in the cell.

RESULTS

The schlieren diagram of the graft copolymer, with base line, is given in Figure 1 and shows two bands, partly overlapping each other. A separate experiment with pure polystyrene showed that the polystyrene collected in exactly the same position as the left-hand polymer band in Figure 1. A simultaneous experiment was then conducted with the graft
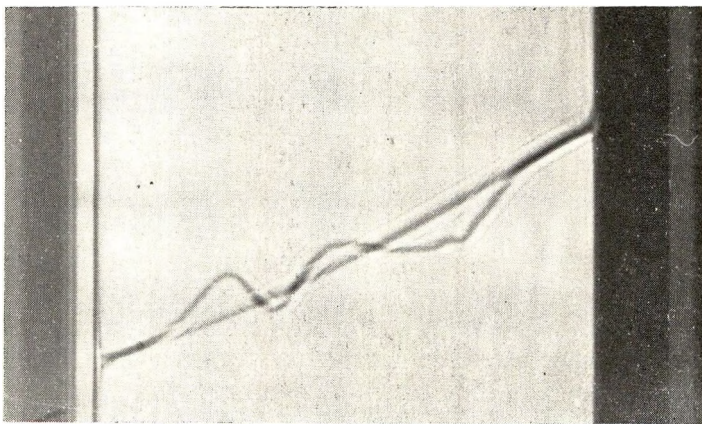
Fig. 1. Schlieren diagram of cellulose acetate polystyrene graft copolymer before extraction. An aluminum double sector centerpiece was used in order to provide the baseline. Phase angle 75°, speed 50, 740 rpm. Solvent: DMF, additive: bromoform. Additive concentration: 300 g./l. mixture.
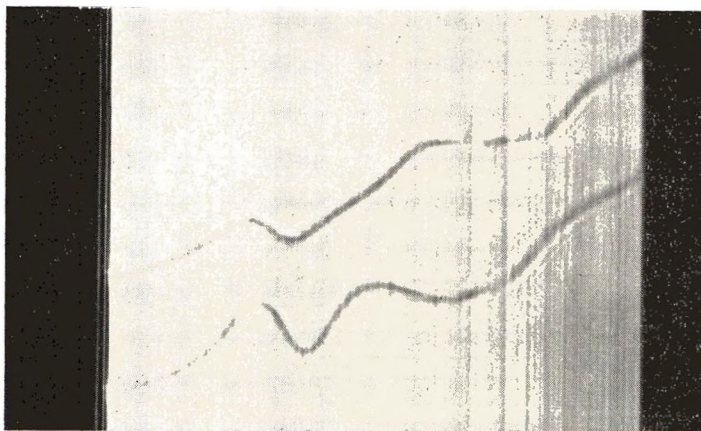
Fig. 2. Schlieren diagram of physical mixture of polystyrene and cellulose acetate (upper curve) and of the graft copolymer (lower curve). All other data as in text for Fig. 1 except that two single sector cells were used.
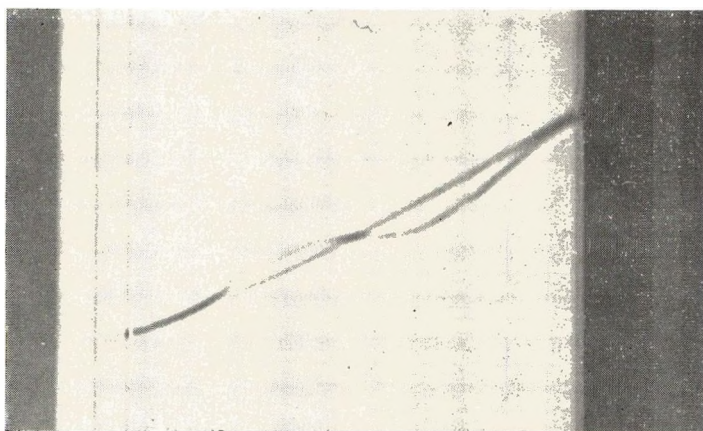
Fig. 3. Schlieren diagram of cellulose acetate–polystyrene graft copolymer after it has been extracted. All other data as in text of Fig. 1.

copolymer in one cell and a mixture of polystyrene and cellulose acetate containing about 10% polystyrene in the other, and the two schlieren diagrams obtained are shown in Figure 2. The polystyrene bands are quite clear, but the cellulose acetate is seen to collect at a different (more dense) position than the graft copolymer. The polystyrene used in this experiment was obtained by hydrolysis of a sample of the graft copolymer itself, and the cellulose acetate was recovered from the grafting solution by extraction with aqueous acetone in order to more closely simulate the actual components of the graft copolymer. Both polymers were checked for contamination by infrared analysis and were found free from the other compound.

In view of the evidence of apparent contamination of the graft with polystyrene, a finely divided (freeze-dried) sample was repeatedly extracted

with benzene until the extract gave a completely clear solution with meth-
anol. This sample was then run under similar conditions as before in the
ultracentrifuge; the resulting schlieren diagram is shown in Figure 3. It
can be seen that all the polystyrene was successfully removed by the
additional extractions with benzene.

The unsymmetric nature and broadness of the graft copolymer band,
also seen in Figure 3, indicate a wide composition distribution.

CALCULATION OF THE COPOLYMER COMPOSITION

The volume fractions at the band positions were calculated according to
equations developed by Hermans and Ende[5] and the corresponding densi-
ties calculated. The buoyant densities of the various polymers were then
taken as the densities of the bromoform–dimethylformamide solution at
the maximum concentration of the polymer bands. The following values
were obtained for the buoyant densities: ρ_P (polystyrene) 1.0809_9; ρ_{CA}
(cellulose acetate) 1.1820_5; ρ_G (graft copolymer) 1.1299_1.

Assuming additivity of the densities, the volume fraction of polystyrene
Φ_P in the graft copolymer is equal to

$$\Phi_P = (\rho_G - \rho_{CA})/(\rho_P - \rho_{CA})$$

Inserting the measured values of the densities, this leads to a weight
percentage of polystyrene component in the graft of about 49%.

The composition was also determined by acid hydrolysis of a weighted
sample as described in the experimental section. This led to a value of
44.1% of polystyrene, repeated in duplicate.

DISCUSSION AND CONCLUSIONS

It can be seen that the density gradient ultracentrifugation technique
is a powerful tool for determining the purity of graft copolymers. There
is, indeed, no other unequivocal method known to the authors at this time.
It is interesting to note that once the contamination with homopolymers is
known it is comparatively easy to devise methods to remove them. Four
cellulose acetate–styrene graft copolymer preparations were made, two
with long side chains and two with short. After the observations reported
above, all four were further extracted in the manner described. Both long
side chain (M.W. about 120,000) grafts contained about 10% of occluded
polystyrene, but the two short side chain (M.W. about 28,000) samples
were free of contamination. Presumably the longer chains are carried
down into the gel fraction when the graft copolymer is separated from
benzene solution. The homopolymer in this method of grafting is of very
similar molecular weight and molecular weight distribution as the grafted
side chains.

The composition of the graft copolymer determined from density gradient
measurements is somewhat different than that obtained by direct analysis.
This discrepancy must be seen in terms of the errors inherent in the meth-

ods used. With the density gradient method an error is introduced by taking the position of the maximum concentration of the somewhat skewed curve of the graft for the buoyant density. Preferential adsorption is another source of error.[5] In the graft both the cellulose acetate and the polystyrene portions are forced into an environment different from that of the homopolymers in which the preferential adsorption might be somewhat different. In this case the equations used will not hold rigorously. A small error might also be introduced in the direct hydrolysis method of analysis owing to the loss of low molecular weight fractions in the methanol.

The wide composition distribution is caused by the superimposition of the molecular polydispersity of the two component polymers. The heterogeneity of the graft copolymer as seen from the undulations in the band suggests a heterogeneous composition distribution rather than a continuous one. Cold alkaline hydrolysis of the sample has shown that about 47% of the side chains are attached to the cellulose acetate ester groups and 53% to the main cellulosic backbone. It is possible that the latter are, in fact, attached to broken ends of the cellulose chain ruptured by the radiolysis, i.e., the sample actually consists of a mixture of block and graft copolymers.

References

1. Yasuda, H., J. A. Wray, and V. Stannett, *J. Polymer Sci.*, **C2**, 287 (1963).
2. Stannett, V., U. S. A.E.C. publication T.I.D. 7643, pp. 259–267 (Nov. 1962).
3. Hermans, J. J., *J. Polymer Sci.*, **C1**, 179 (1963).
4. Hermans, J. J., and H. A. Ende, *J. Polymer Sci.*, **C4**, 519 (1964).
5. Hermans, J. J., and H. A. Ende, *J. Polymer Sci.*, **C1**, 161 (1963).

Résumé

On a examiné un polymère greffé bien défini du polystyrène et de l'acétate de cellulose, au moyen de la méthode du gradient de densité par ultracentrifugation. L'échantillon initial présentait deux pics, ceux-ci s'avérèrent être le copolymère greffé pur et le polystyrène, ce dernier étant aisément éliminable par extraction ultérieure au benzène. On a déterminé la composition du polymère greffé au départ des mesures de densité par déplacement du polymère greffé et des deux homopolymères; on a trouvé 49% de polystyrène pour 51% d'acétate de cellulose comparés aux 44.1% et 55.9% respectifs déterminés à partir de la perte de poids après hydrolyse acide.

Zusammenfassung

Ein gut definiertes Graftcopolymeres aus Polystyrol und Zelluloseacetat wurde unter Verwendung des Dichtegradient-Ultrazentrifugenverfahrens untersucht. Die ursprüngliche Probe wies zwei Maxima auf. Diese erwiesen sich als reines Graftcopolymeres und Polystyrol, welch letzteres durch weitere Extraktion mit Benzol leicht aus der Mischung entfernt werden konnte. Die Zusammensetzung des Graftcopolymeren wurde aus der Auftreibsdichte des Graft- und der zwei Homopolymeren bestimmt und ergab sich zu 49% Polystyrol und 51% Zelluloseacetat, verglichen mit 44,1% bzw. 55,9%, bestimmt aus den Gewichtsverlusten nach Säurehydrolyse.

Analysis of Copolymers by Means of Density Gradient Centrifugation. II. Comparison with Kinetic Requirements

H. A. ENDE and J. J. HERMANS, *Chemstrand Research Center, Inc., Research Triangle Park, Durham, North Carolina*

Synopsis

Four styrene–iodostyrene copolymers of uniform iodine content are examined in the density gradient centrifuge under conditions similar to those used in a previous study, in which the copolymer investigated showed compositional distribution. The results obtained determine the relation between the iodine content of a copolymer and its position in the density gradient. This enables one to compare the average square of the fluctuation in iodine content with that derived from the kinetic copolymer equation. The two results agree satisfactorily.

Introduction

In a previous paper,[1] data were presented concerning the density gradient centrifugation of a styrene–iodostyrene copolymer in 1-chloropentane, which contained 0.814 g. tetraethyllead/ml. mixture. The temperature at which the experiments were done was 12°C., which is very close to the theta temperature of the system studied. The copolymer was the product of high conversion (64%) and contained 24.0 wt.-% iodine (see Table I). Quantitative information concerning the fluctuations in molecular weight and buoyant density could be derived from the schlieren curve obtained. For any individual species, the buoyant density determines the position at which this species tends to collect, and the buoyant density may therefore be expressed in terms of the distance r between this position and the center of rotation. Likewise, fluctuations in buoyant density may be expressed in terms of the difference

$$w = r - \bar{r}$$

where $\bar{r}$ is an average value, the choice of which is arbitrary. For the sake of convenience, $\bar{r}$ was taken as the position where the refractive index gradient is zero. This has certain consequences for the relation between the averages $\langle w \rangle$, $\langle w^2 \rangle$ and the schlieren curve.[1] The analysis of this curve showed that for the sample investigated $\langle w \rangle = -0.032$ cm.; $\langle w^2 \rangle = 0.0046$ cm.^{2}.

However, the analysis was incomplete, in the sense that no comparison was made with $\langle w^2 \rangle$ estimated from the kinetic theory of copolymerization.

Moreover, $\langle w \rangle$ must be approximately equal to the difference between the position $\bar{r}$ and the position r_u which would have been observed with a sample that has a uniform iodine content of 24.0%.

To check these points, one must first determine the relation between the iodine content and the equilibrium position of the copolymer in the density gradient.

Experiments and Discussion

Dr. D. Braun (Deutsches Kunststoff Institut, Darmstadt, Germany) kindly put at the authors' disposal four additional samples, all obtained from a low conversion copolymerization run, so that the iodine content of the molecules in each individual sample is uniform. Iodine analysis gave

TABLE I

Sample	Degree of conversion, %	Iodine, wt.-%
1	8.43	17.94
2	10.68	20.60
3	11.43	24.04
4	11.63	26.55
5	64.0	24.0
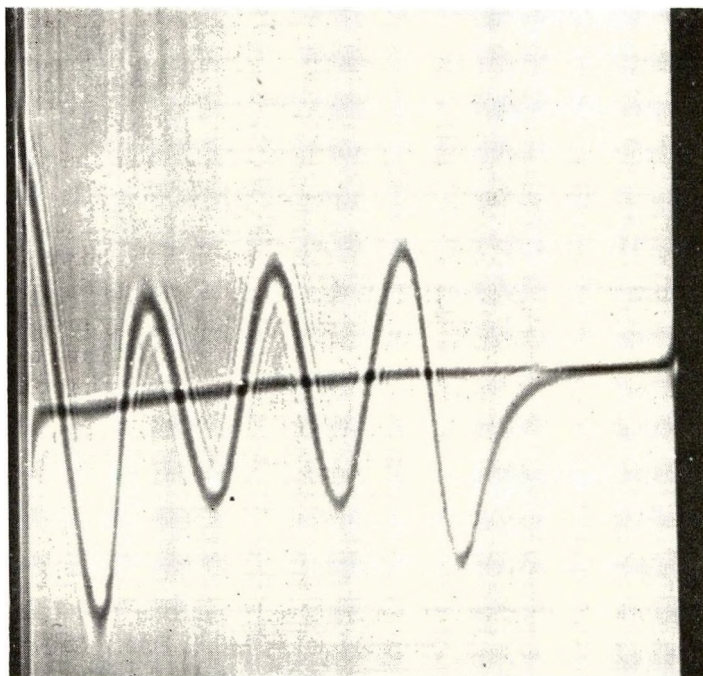
Fig. 1. Sedimentation equilibrium of a mixture of samples 1, 2, 3, and 4 at 25°C in 1-chloropentane–tetraethyllead.
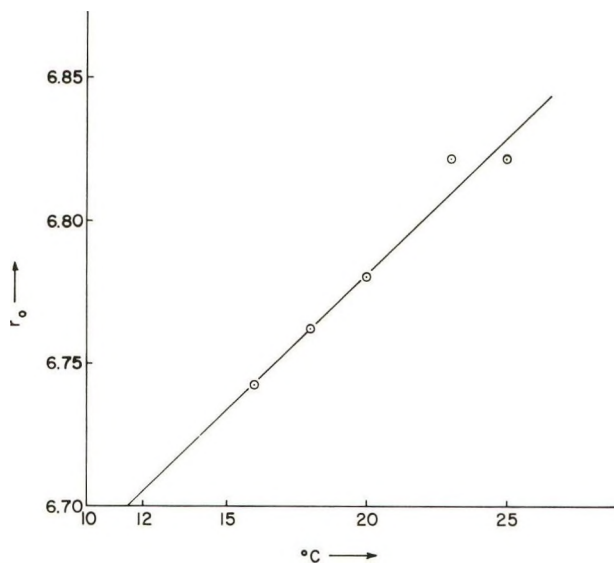
Fig. 2. Position of zero concentration gradient for sample 4 as a function of temperature.

the results shown in Table I where, for comparison, the high conversion sample used in the previous study has been added (sample 5).

Ultracentrifugation was carried out in a new type of cell which assures perfect equality of the column lengths in the two sectors.[2] By way of illustration, Figure 1 shows a mixture of all four samples 1, 2, 3, 4, at equilibrium. However, this run was made at 25°C. because sample 4 precipitates at 12°C. The individual peaks are not symmetrical because they overlap to some extent, but nevertheless a comparison with Figure 1 in the previous article[1] shows very clearly the large effect of the nonuniform density distribution in sample 5 as compared to samples 1–4. The position of zero concentration gradient for sample 4 was determined at 25, 23, 20, 18, and 16°C. These positions are plotted versus temperature in Figure 2, and extrapolated to 12°C. for comparison with the other samples. Samples 1, 2, and 3 were each run separately at 12°C., with the result shown in Figure 3, in which the extrapolated value for sample 4 has been added.

From Figure 3 one can read the position of zero concentration gradient which sample 5 would have if its iodine content were uniform. This is found to be $r = 6.55$ cm. The actual distance from the center of rotation was 6.60 cm., and the difference, -0.05 cm., is to be compared with the value $\langle w \rangle = -0.032$ cm. which was calculated from the schlieren curve (see Table I in the previous article[1]). The agreement is reasonably good.

Finally, one can use the relation between position w and per cent iodine, p, to calculate the standard deviation $\langle (p - \bar{p})^2 \rangle$ from the standard deviation Δ^2, which is $\langle w^2 \rangle - \langle w \rangle^2$, or 0.0035 cm.^{2} This gives

$$\langle (p - \bar{p})^2 \rangle^{1/2} = 1.0\%$$
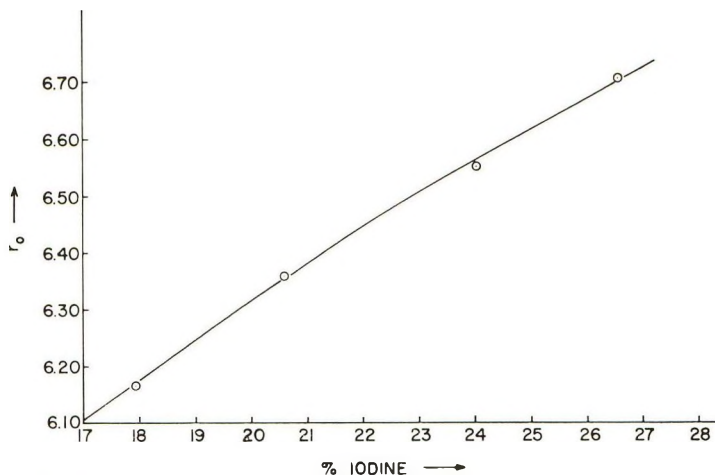
Fig. 3. Position of zero concentration gradient for samples 1, 2, 3, and 4 at 12°C.

On the other hand, this standard deviation may be estimated from the well-known copolymer equation[3]:

$$\frac{dM_1}{dM_2} = \frac{M_1}{M_2} \frac{r_1 M_1 + M_2}{M_1 + r_2 M_2}$$

where M_1 and M_2 represent the concentration of styrene and iodostyrene monomer, respectively. The reactivity ratios r_1 and r_2 are 0.62 and 1.25, respectively.[4] For a degree of conversion of 64%, this leads to a value of 1.2% for $\langle (p - \bar{p})^2 \rangle^{1/2}$, which compared well with the result derived from the schlieren curve.

References

1. Hermans, J. J., and H. A. Ende, J. Polymer Sci., C4, 519 (1963).

2. Ende, H. A., Makromol. Chem., in press.

3. Küchler, L., Polymerisationskinetik, Springer Verlag, Berlin-Göttingen-Heidelberg, 1951.

4. Walling, C., E. R. Briggs, K. B. Wolfstirn, and F. R. Mayo, J. Am. Chem. Soc., 70, 1537 (1948).

Résumé

On a étudié quatre copolymères de styrène-iodostyrène d'une teneur en iode uniforme au moyen d'une centrifugeuse à gradient de densité, dans des conditions semblables à celles des études antérieures, études dans lesquelles les copolymères montraient une distribution en fonction de leur composition. Les résultats obtenus déterminent la relation entre la teneur en iode d'un copolymère et sa position dans le gradient de densité. Ceci permet de comparer le carré moyen des fluctuations de teneur en iode avec celui dérivé d'une opération cinétique de copolymérisation. Ces deux résultats sont en accord suffisant.

Zusammenfassung

Vier Styrol-Jodstyrolcopolymere mit einheitlichem Jodgehalt wurden in der Dichte-gradient-Zentrifuge unter ähnlichen Bedingungen wie in einer vorhergehenden Studie, in der das untersuchte Copolymere eine Zusammensetzungsverteilung zeigte, untersucht. Die erhaltenen Ergebnisse bestimmen die Beziehung zwischen dem Jodgehalt eines Copolymeren und seiner Stellung im Dichtegradienten. Dies ermöglicht einen Vergleich des mittleren Schwankungsquadrates des Jodgehaltes mit dem aus der kinetischen Co-polymergleichung abgeleiteten. Beide Ergebnisse stimmen befriedigend überein.

The Effect of Simultaneously Occurring Processes on the Course of Polymer Crystallization

W. BANKS and A. SHARPLES, *Arthur D. Little Research Institute, Inveresk Gate, Musselburgh, Midlothian, Scotland*, and J. N. HAY, *Chemistry Department, University, Old Aberdeen, Scotland*

Synopsis

The possibility that simultaneously occurring processes may account for the anomalous fractional values of the Avrami exponent found in recent polymer crystallization experiments is considered, and, on balance, rejected. A more likely explanation is that one of the assumptions used in deriving the Avrami equation is at fault. This leads to the conclusion that the Avrami parameters cannot be used diagnostically to provide information on crystallization mechanism, as has been considered to be the case in the past.

Introduction

When a polymer crystallizes from its supercooled melt, the extent of crystallization is usually considered to be related to time through an equation developed by Avrami and others,[1-4] which may be expressed in the form

$$W_L/W_0 = \exp \{-zt^n\} \tag{1}$$

where W_L/W_0 is the weight fraction of the liquid phase remaining after time t, and z and n are constants. According to existing ideas,[2,4] n is required to be an integer with a value of 1, 2, 3, or 4, and in the past this parameter has been used diagnostically to provide information on the number of dimensions in which growth occurs, and also on the nature of the nucleation process. Thus, for example, a value of 4 has been taken to indicate spherulitic growth from sporadically formed nuclei. In fact, in order for such conclusions to be justifiable, several assumptions, usually made implicitly, must hold. These are (1) that the nuclei are randomly spaced; (2) that the time dependence of the nucleation process is of either zeroth or first-order; (3) that the linear dimensions of the growing bodies are related to some integral power of time (normally the first power); (4) finally that the density of the growing bodies is constant.

Several studies have been reported where the required integral values of n have been found, but more recently there has also been evidence to indicate that for some systems n can be fractional, and yet at the same time remain constant throughout the course of the crystallization.[5-7] One possible explanation to reconcile these apparently anomalous values of the Avrami

exponent with the current theory is the suggestion that two processes, with different, but integral, values of n, may be occurring simultaneously.[8,9]

In this paper consideration is given to this possibility in the light of recent experimental data.

Correct Form of the Avrami Equation

First, it should be noted that the various forms of the Avrami equation which exist are derived from one or other of two different basic approaches,[1,3] and that, ignoring various minor discrepancies, two correspondingly different types of expression result. The one is given in eq. (1) and arises from the Avrami treatment itself[1,2]; the other takes the form

$$V_L/V_t = \exp\{-z't^n\} \tag{2}$$

where V_L/V_t is the volume fraction of the liquid phase remaining after time t. This can be transformed to

$$W_L/W_0 = (\rho_0/\rho_t) \exp\{-z't\}^n \tag{3}$$

where ρ_0 and ρ_t are the densities of the crystallizing system at zero time and time t, respectively. This is the type of equation proposed by Evans[3] and adopted by Morgan[4] for the specific case of crystallizing polymers. It differs formally from eq. (1) by the factor ρ_0/ρ_t, which, for systems of practical interest (i.e., which decrease in volume during crystallization), is not constant. Calculations suggest that differences of up to 3% may occur in the apparent values of n obtained when eqs. (1) and (3) are applied to actual experimental data, and although such differences are not large, they may be significant in the subsequent discussion. Equation (3) is the one more likely to be at fault, as it is based on the treatment of expanding spheres and involves the assumption that the nuclei do not change their positions during crystallization. This is not justifiable in a contracting system, and so eq. (1) is used as the basis for calculations in this paper.

Analysis of Experimental Data

n is usually obtained by expressing eq. (1) in the form

$$\ln(-\ln W_L/W_0) = \ln z + n \ln t \tag{4}$$

and analyzing accordingly. Various experimental methods have been suggested for obtaining W_L/W_0, but the one used most frequently involves the determination of the volume of the system, V_t, as a function of time, when W_L/W_0 can be calculated from

$$W_L/W_0 = (V_\infty - V_t)/(V_\infty - V_0) \tag{5}$$

Such dilatometric measurements can be made extremely accurately, although errors in V_0, and in the determination of zero time, can lead to spurious conclusions, especially if fast rates of crystallization are involved. In systems where the Avrami process is succeeded by a stage of secondary
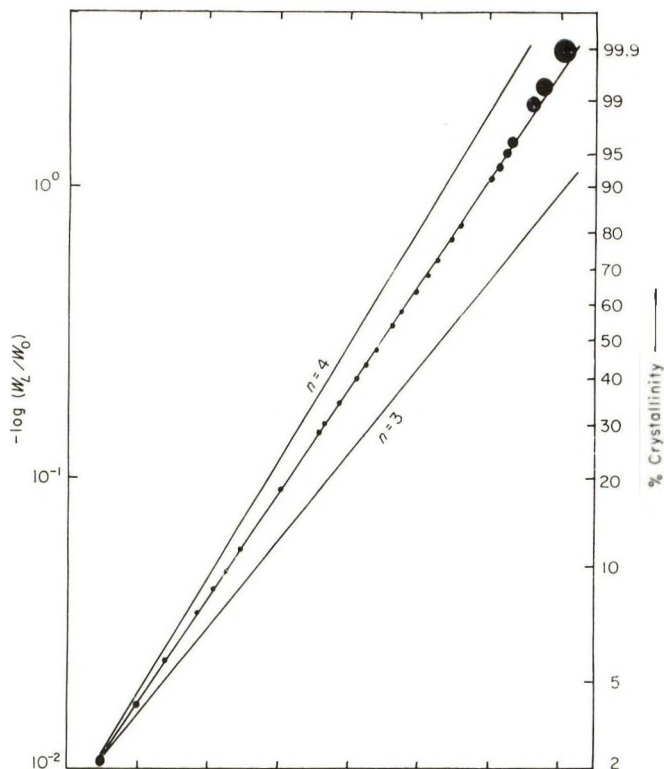
Fig. 1. Crystallization[6] of poly(decamethylene terephthalate) at 122.95°C., showing conformity with Avrami equation for a large extent of the process; $n = 3.587 \pm 0.008$.

crystallization, the selection of a suitable value of V_∞ in eq. (5) is also a problem.[7] However, it is the double logarithmic form of the plot [eq. (4)] which is most likely to lead to false conclusions; these can nevertheless be avoided by attaching the appropriate weight to data at the various stages of crystallization.

Figure 1 shows some dilatometric data for the crystallization of poly-(decamethylene terephthalate) where the absence of secondary crystalliza-tion[6] removes any ambiguity concerning the choice of V_∞. The results are plotted according to eq. (4), and a maximum error of 0.1 mm. is reasonably ascribed to the readings of dilatometer height (from which V_∞, V_0, and V_t are derived), for a total change of 142 mm. The distortion of the crystal-linity scale is immediately apparent, but nevertheless it is evident first that the data are adequately represented by eq. (4) for greater than 95% of the process, and secondly that the derived Avrami exponent is sig-nificantly different from either of the neighboring integral values. In fact, for the results between 2% and 97% crystallization there is no trend in n, and the mean value derived from the regression line is 3.587, with an as-sociated standard error of 0.008. There is thus no justification for one expedient which has been used in the past, namely, to assume that observed

fractional values of n can be approximated to the neighboring integer. Errors of up to 0.8 in n have been tolerated in previous studies,[10] and if allowance is made for this point, it is likely that the existence of true fractional values is more widespread than is generally considered to be the case.

Theoretical Expression for Two Simultaneously Occurring Processes

The possibility of explaining these observed fractional values of n on the assumption that two processes are occurring simultaneously is now given theoretical consideration. In order to demonstrate the likely effects most simply, a specific case is considered here initially rather than a general one; the example chosen is that of spherulitic growth occurring simultaneously from two types of nuclei originating instantaneously and sporadically. Following the development of the Avrami treatment used by Mandelkern,[2] an intermediate stage of crystallization is first considered, corresponding to time t, and the actual amount of the liquid phase converted (dW_s) in subsequent time dt is compared with the amount (dW'_s) which would be converted if there were no restrictions on growth due to the mutual impingement of the growing bodies. Then

$$dW_s/dW'_s = 1 - (W_s/W_0) \tag{6}$$

where W_s is the actual weight of material converted at time t. The hypothetical weight converted ignoring impingement (W'_s) derives contributions from instantaneously and sporadically formed nuclei growing at all times τ between $\tau = 0$ and $\tau = t$, so that

$$W'_s = \frac{4\pi\rho_s W_0 N_1 G_1{}^3 t^3}{3\rho_L} + \int_0^{\tau=t} \frac{4\pi\rho_s W_0 N_2 G_2{}^3 (t-\tau)^3 \, d\tau}{3\rho_L} \tag{7}$$

where ρ and ρ_L are the densities of the solid and liquid phases, and G_1 and G_2 are the radial growth rate constants. N_1 represents the number of instantaneous nuclei formed per unit volume, and N_2 the number of sporadic nuclei formed per unit volume in unit time.

Thus,

$$dW'_s = \left[\frac{4\pi\rho_s W_0 N_1 G_1{}^3 t^2}{\rho_L} + \frac{4\pi\rho_s W_0 N_2 G_2{}^3 t^3}{3\rho_L} \right] dt$$

and

$$\int_{W_0}^{W_s=W_s} \frac{dW_s}{1 - W_s/W_0} = \int_0^{t=t} \frac{4\pi\rho_s W_0}{\rho_L} \left[N_1 G_1{}^3 t^2 + \frac{N_2 G_2{}^3 t^3}{3} \right] dt$$

so that

$$1 - \frac{W_s}{W_0} = \frac{W_L}{W_0} = \exp -\left\{ \frac{4\pi\rho}{\rho_L} \left(\frac{N_1 G_1{}^3 t^3}{3} + \frac{N_2 G_2{}^3 t^4}{4} \right) \right\} \tag{8}$$

Equation (8) can be simplified to

$$W_L/W_0 = \exp - \{z_1 t^3 + z_2 t^4\} \tag{9}$$

to be comparable with eq. (1). The combination of several processes, each of the form $W_L/W_0 = \exp \{-z_i t^m\}$, leads to a similar expression containing the product of the exponentials, provided that the nuclei are randomly spaced, and that the densities of the various growing bodies are identical and constant throughout the course of the crystallization.

Equation (9) can be written

$$- \ln (W_L/W_0) = t^3(z_1 + z_2 t)$$

or

$$\ln[-\ln (W_L/W_0)] = 3 \ln t + \ln (z_1 + z_2 t) \tag{10}$$

from which it is evident that the conventional Avrami plot of $\ln [- \ln (W_L/W_0)]$ versus $\ln t$ will not yield a straight line. The same is true of any combination of processes, provided that the exponent in at least one case differs from that for the remainder.

However, although a straight line giving a constant, fractional value for n, is not predicted theoretically, the question now to be answered is whether such a condition might be approximated to within observed experimental error for a large part of the crystallization process.

Comparison of Experimental Data with Theoretical Expression

For the data given in Figure 1, the error associated with the regression line is extremely small; the value of n is 3.587 ± 0.008. If it is now assumed that this fractional value arises from the combination of two processes with $n = 3$ and $n = 4$, then eq. (9) can be used to obtain hypothetical values of t corresponding to the actual values of W_L/W_0 used in Figure 1. (The actual values are used in computing the mean figure for n and its associated standard error, in order to ensure that no bias results from incorrect weighting.) Only one adjustable parameter is relevant, namely, z_1/z_2, and various values were tested to discover which gave the closest approximation to the experimental data. The best fit was obtained with a figure of $z_1/z_2 = 7.7$, and a regression analysis was made using the actual values of W_L/W_0 in Figure 1 between 2 and 97%, and the hypothetical values of t calculated from eq. (9). The absolute values used for z_1 and z_2 were 10^{-4} and 1.3×10^{-5}. The result gave $n = 3.587$ with an associated standard error of 0.011, which is not significantly different from the standard error associated with the experimental data. Thus in this particular case, the postulate of simultaneously occurring processes would seem to be capable of accounting for the observed fractional and constant value of n.

However, calculations showed that when two processes with lower values of n are combined (with, for example, $n = 1$ and $n = 2$) the apparent constancy of n when calculated by using an analog of eq. (9) is no longer evi-
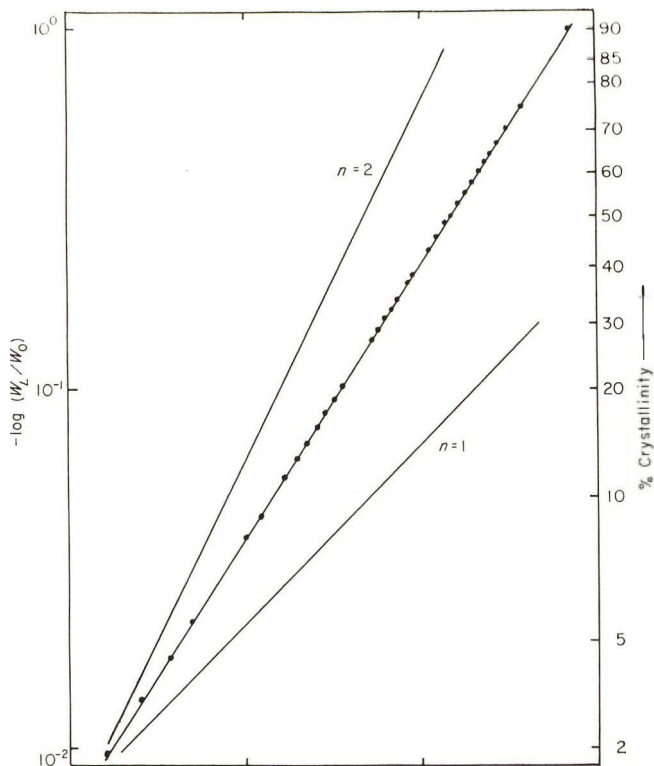
Fig. 2. Seeded crystallization[11] of polyethylene fractions 5902 at 128.14°C., from a seed crystallinity of 2%, showing conformity with Avrami equation; $n = 1.509 \pm 0.003$.

dent. A suitable experimental example to test this case arises in the seeded crystallization of polyethylene,[11] and an Avrami plot for a typical run is shown in Figure 2. Conformity to a straight line is again apparent, indicating a value of n which is constant throughout the process, the figure derived from a regression analysis being 1.509 ± 0.003. If it is now assumed that two concurrent processes are operative with $n = 1$ and $n = 2$ (corresponding, say, to rods growing from instantaneously and sporadically initiated nuclei[2,4]), then the values of z_1 and z_2 which give adequate agreement are 10^{-2} and 10^{-3}. As in the previous case, the regression analysis was made for the observed values of W_L/W_0 (given in Fig. 2) and the hypothetical values of t calculated by using the appropriate analog of eq. (9), i.e.,

$$W_L/W_0 = \exp - \{z_1 t + z_2 t^2\} \tag{11}$$

The result was a value of $n = 1.468$, which was sufficiently close to the experimental value of 1.509 for present purposes. (A closer fit could have been obtained by choosing z_1 and z_2 more carefully, but the calculations involved are excessively time-consuming, and unnecessary in view of the fact that precise agreement is not required.) The standard error, however,
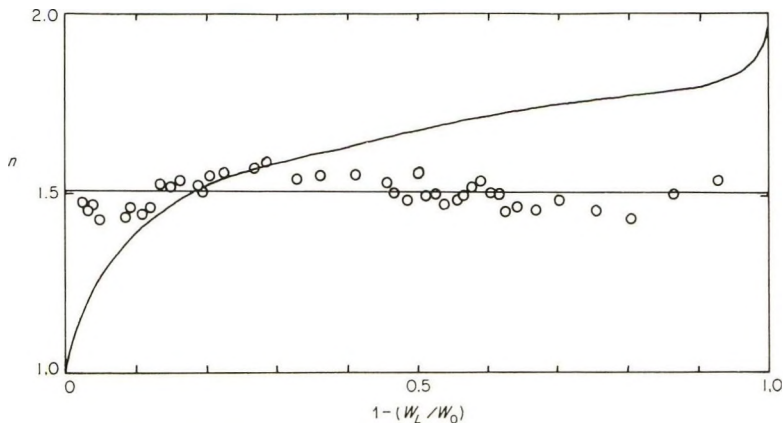
Fig. 3. Results from Fig. 2 expressed in the form of n vs. extent of crystallization $(1 - W_L/W_0)$. The curve is the hypothetical plot calculated from eq. (11) on the assumption of two concurrent processes, and the straight line corresponds to the mean value of $n = 1.509$ obtained for the experimental data.

was 0.019, which is so much greater than the error of 0.003 associated with the experimentally observed data that it must be concluded that the postulate of two simultaneously occurring processes is not capable of accounting for the results in this particular case.

The position can be seen more clearly if n is determined from successive pairs of readings by using eq. (11) and expressed as a function of extent of crystallization $(1 - W_L/W_0)$, although it should be realized that the errors in n resulting from such difference calculations are arbitrarily high, and dependent on the proximity of the pairs of readings chosen. The results from Figure 2 are expressed in this way in Figure 3, and it is now quite obvious that whereas the experimental values of n show no trend throughout the course of crystallization, the theoretical values calculated assuming two concurrent processes increase progressively to an extent which is well outside experimental error.

Discussion

As the theoretical expressions derived from the assumption of two simultaneously occurring processes fit the experimental data only under favorable circumstances (i.e., when the relative difference of the two contributing Avrami exponents is small), it is tempting to make the general conclusion that this is not the correct explanation to account for the fractional values of n which have been observed for several crystallizing polymer systems. Support for this conclusion derives from three sources. First, in polyethylene,[7] as molecular weight is decreased, n increases progressively from 2 to 4, and after passing through a maximum, decreases again to 2. The entire range of intermediate values of n is covered, and to account for such behavior, an extremely complicated combination of processes would

need to be postulated, with, for example, sporadically nucleated disks being required to change suddenly to instantaneously nucleated spheres as n passes through a value of 3. Secondly, and more positively, a clear case exists with poly(ethylene oxide),[12] where spherulitic growth from instantaneously formed nuclei (requiring $n = 3$) can readily be observed in the microscope, and yet where the experimentally determined result for n has the theoretically unacceptable value of 2.0. Finally, the postulate of concurrent processes cannot account for values of n which are less than 1.0, and such values have recently been observed in the seeded crystallization of polyethylene.[13]

In order to account for this situation it is of interest to note that in the large majority of systems n approaches but does not exceed 4, when such variables as temperature and molecular weight are changed. From this it is reasonable to assume that spherulitic growth from sporadically formed nuclei is usually present but that some additional factor is also operative to cause n to be less than its required value of 4. (The possibility of spherulitic growth from instantaneously formed nuclei is not excluded, but the corresponding value of $n = 3$ can no longer be considered to be unambiguous.) Of the assumptions listed in the introduction, the one which is most likely to be unacceptable is that which requires the growing bodies to be constant in density throughout the entire period of their formation. Spherulites are reasonably considered to grow through a process of branched fibrillation,[5,14] so that there is no reason to expect the degree of packing to remain constant as growth proceeds. This would suggest that in deriving the Avrami equation, the quantity ρ_s, representing the effective density of the transformed phase [cf. eq. (8) and ref. 2], instead of being considered as a constant parameter, should be replaced by a function which depends on the size of the growing bodies (and hence on time). A suitable function would lead to a modified Avrami equation of the form

$$W_L/W_0 = \exp\left\{(-yt^4)\,(At^{-m})\right\} \tag{12}$$

where y contains all the terms of the normal rate constant, z, except the density contribution; and At^{-m} represents the latter, and is now time-dependent. When $m = 0$, the normal Avrami equation with $n = 4$ is recovered, and when $m > 0$ reduced values of n are obtained, which in general are fractional. (A corresponding equation would also exist for the case of instantaneously nucleated spherulites, when the maximum value of n would be expected to be 3.)

Conclusions

On balance it is considered that the assumption of two or more simultaneously occurring processes cannot account for crystallization data which yield fractional values of the exponent n in the Avrami equation. Consequently the alternative explanation must be that one of the assumptions used in deriving the form of the Avrami equation normally applied to poly-

mer crystallization is wrong. The most likely one is that which requires the growing bodies to remain constant in density throughout the entire course of their development.

Two important consequences arise from this situation. First, the rate constant derived from the usual Avrami analysis is likely to contain more parameters than are usually postulated [cf. eq. (12)]. In support of this it has already been shown that for polyethylene crystallization[7] the temperature dependence of the rate constant is more satisfactorily accounted for if a contribution from n is included. Secondly, it is evident that conclusions concerning the nature of the growing bodies, and of the nucleation process, cannot be made from values of n whether these be fractional or integral.[12] In other words, it is not justifiable to use the Avrami exponent diagnostically to provide information on crystallization mechanism.

References

1. Avrami, M., *J. Chem. Phys.*, **7**, 1103 (1939).
2. Mandelkern, L., *Chem. Revs.*, **56**, 903 (1956).
3. Evans, U. R., *Trans. Faraday Soc.*, **41**, 365 (1945).
4. Morgan, L. B., *Phil. Trans. Roy. Soc. London*, **247**, 13 (1954).
5. Rohleder, J., and H. A. Stuart, *Makromol. Chem.*, **41**, 110 (1961).
6. Sharples, A., and F. L. Swinton, *Polymer*, **4**, 119 (1963).
7. Banks, W., M. Gordon, R.-J. Roe, and A. Sharples, *Polymer*, **4**, 61 (1963).
8. Rabasiaka, J., and A. J. Kovacs, *J. Applied Phys.*, **32**, 2314 (1961).
9. Parrini, P., and G. Corrieri, *Makromol. Chem.*, **62**, 83 (1963).
10. Hatano, M., and S. Kambara, *Polymer*, **2**, 1 (1961).
11. Banks, W., M. Gordon, and A. Sharples, *Polymer*, **4**, 289 (1963).
12. Banks, W., and A. Sharples, *Makromol. Chem.*, **59**, 233 (1963).
13. Banks, W., and A. Sharples, unpublished results.
14. Banks, W., J. N. Hay, A. Sharples, and G. Thomson, *Polymer*, **5**, 163 (1964).

Résumé

On a considéré la possibilité que des processus simultanés peuvent justifier les valeurs fractionnaires anormales de l'exposant d'Avrami, trouvées récemment dans des expériences de cristallisation de polymères; ce qui a été rejeté après étude. Une explication plus vraisemblable est qu'une des hypothèses utilisées en dérivant l'équation d'Avrami, tombe en défaut. On peut en conclure que les paramètres d'Avrami ne peuvent pas être utilisés avec sûreté pour donner une information sur le mécanisme de cristallisation, comme on le considérait auparavant.

Zusammenfassung

Die Möglichkeit, dass gleichzeitig auftretende Prozesse für die in neueren Polymer-kristallisationsversuchen gefundenen anomalen gebrochenen Werte des Avrami-Exponenten verantwortlich sind, wird erwogen und verworfen. Eine wahrscheinlichere Erklärung ist, dass eine der Annahmen bei der Ableitung der Avramigleichung fehlerhaft ist. Dies führt zu dem Schluss, dass die Avrami-Parameter nicht als Mittel zur Gewinnung eines Aufschlusses über den Kristallisationsmechanismus verwendet werden können, wie es früher in Betracht gezogen wurde.

Fracture Processes in Polymeric Materials. V. Dependence of the Ultimate Properties of Poly(methyl Methacrylate) on Molecular Weight

J. P. BERRY,* *General Electric Research Laboratory, Schenectady, New York*

Synopsis

The influence of molecular weight on the fracture surface energy, Young's modulus, tensile strength, and inherent flaw size in poly(methyl methacrylate) has been determined.   In common with other mechanical properties, the dependence of the fracture surface energy on molecular weight can be represented by $\gamma = A - (B/M)$, where M is the molecular weight, and A and B are arbitrary constants.   By extrapolation, the upper limiting value is 1.55×10^5 ergs/cm.^{2}, while the surface energy, and hence the tensile strength, should become zero for a polymer of molecular weight 25,000.   This value is in good agreement with that found directly from brittle strength measurements.

Introduction

There is now a considerable body of evidence to support the application of the classical flaw theories of tensile strength to the ultimate properties of glassy polymers.   According to the Griffith theory the tensile strength T is inversely related to the size of the flaw in the sample c by the equation[1]

$$T = K(E\gamma/c)^{1/2}$$

where K is a dimensionless geometrical factor, of the order of unity, E is the tensile modulus of elasticity, and γ is the fracture surface energy, i.e., that which is required for the formation of unit area of new surface as the initial flaw increases in size.   The form of the relation between tensile strength and flaw size has been verified for conventional poly(methyl methacrylate)[2] and polystyrene[3] at room temperature.   The results indicate that two factors are important in determining the tensile strength of these materials: (1) the fracture surface energy and (2) the size of the inherent (natural) flaw in the sample tested.   The experimental value of the fraction surface energy is much greater than that predicted from the molecular structure, a finding that has been attributed to a local ductile response of the material under the influence of the high stresses in the vicinity of the flaw.[2]   This response gives rise to a thin layer of material of modified structure at the surface which results in optical interference.   The

---

* Present address: Rubber and Plastics Research Association, Shawbury, Shrewsbury, Shropshire, England.

interference colors bear a specific relation to the surface features and their topography.[4]

The inherent flaw size appears to be related to the crazing behavior of the material,[3] but unfortunately this phenomenon is relatively poorly understood. However, recent work has resulted in the elucidation of some of the structural characteristics of the physical defects that are observed.[5-7]

The influence of the ambient experimental temperature and molecular structure (crosslinking) on these factors has also been determined, and the results give further support to the significance attributed to them.[8]

A further variable that merits attention is the molecular weight of the material. The effect of this variable on some of the fracture properties has already been described, in particular the appearance of the fracture surface.[9] In view of the presumed relation between the character of the surface and the fracture surface energy, some dependence of the latter parameter on the molecular weight of the material would be expected. Recent work has indicated the dependence of crazing of polystyrene, albeit in the presence of the solvent, on the molecular weight.[10] Consequently the value of the inherent flaw size of a glassy polymer might be expected to show a corresponding dependence.

Earlier work on the fracture properties of poly(methyl methacrylate) and polystyrene indicated that the values of the fracture surface energy and the inherent flaw size for these materials were significantly different.[2,3] However, the molecular weights of the materials were also significantly different; that of the poly(methyl methacrylate) was 3×10^6 and that of the polystyrene was 3.5×10^5. It is therefore necessary to establish whether the observed difference in properties is due to intrinsic differences in the materials or is merely a consequence of the difference in the molecular weight.

Experimental Materials and Methods

Samples of poly(methyl methacrylate) with viscosity-average molecular weights ranging from 9.8×10^4 to 6×10^6 were obtained through the courtesy and cooperation of the Rohm and Haas Company. They were supplied in sheets $3/16$ and $1/4$ in. in thickness.

Fracture surface energies were obtained by the cleavage method,[11] samples being cut from the plane of the sheet material $1\frac{1}{2}$ in. wide and 8–10 in. long. The thickness of the strip was reduced along the midline by using a circular saw with a blade 6×10^{-3} in. thick. Slots were cut to a depth of 0.050 in. in the $3/16$ in. sheet and to a depth of 0.080 in. in the $1/4$ in. sheet.

At the conclusion of a cleavage experiment, when the sample had been split along the median plane, the elastic modulus E of the separated halves was determined by a three point bending experiment. The half samples were then machined to a dumbbell configuration and the tensile strength T_0 was determined. From these data and the known value of the fracture

surface energy (γ), the value of the inherent flaw size c_0 was obtained by substitution in the equation

$$c_0 = 2E\gamma/\pi T_0^2$$

A crack was then introduced into the edge of the second half-sample by the method already described, and its length c measured with the travelling microscope.   From the tensile stress required to fracture this sample T an alternative, though less accurate value of the inherent flaw size c_0', or equivalently, the fracture surface energy was determined, for comparison with that obtained in the cleavage experiment.   The appropriate equation is

$$c_0' = T^2c/T_0^2$$

Results and Discussion

The cleavage technique has been fully described elsewhere.[11]   In all of the samples the relation between the applied force f, the resulting deflection δ and the length of the crack in the sample l could be described with a high degree of accuracy by the empirical relation $f = (ae^{-n})\delta$, where the arbitrary constant n had the value of ~ 2.68 instead of that (3) expected from simple beam theory.   The equilibrium condition of the cleavage sample held at fixed deflection is given by $(f\delta/w) = (4\gamma/n)l$, where γ is the fracture surface energy, w is the width of the fracture plane, and the other parameters have the significance already ascribed to them.   The fracture surface energy is then determined from the slope of the relation between the equilibrium values of $(f\delta/w)$ and l, by a least-squares analysis of the data.

In many of the samples the crack did not propagate smoothly, but rather in a stick-slip manner.   Under these conditions the graph of $(f\delta/w)$ versus l
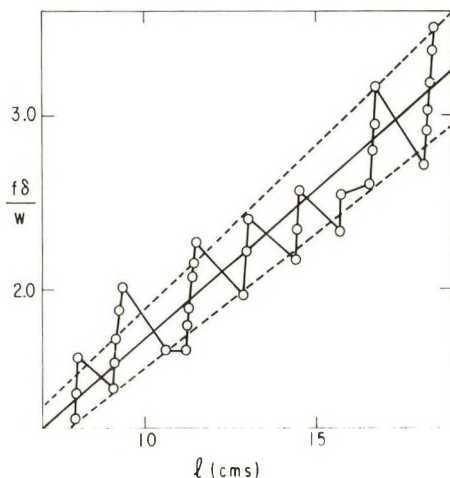
Fig. 1. Effect of stick-slip crack propagation on the determination of the fracture surface energy by the cleavage technique.
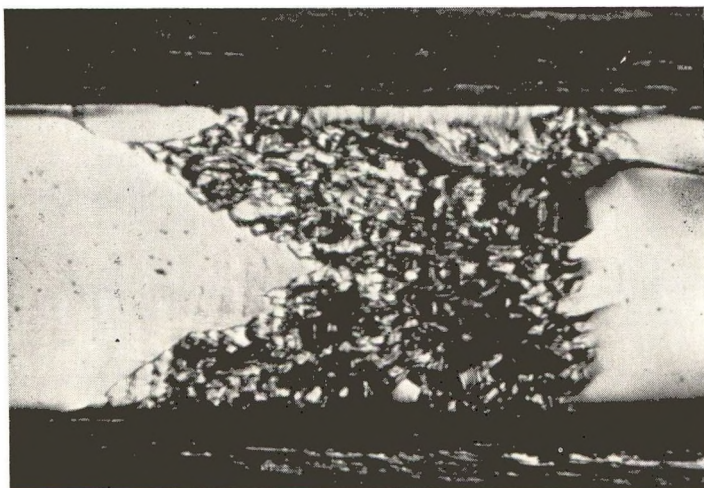
Fig. 2. Fracture surface in the "stick" phase. The crack propagated from left to right. Width of fracture plane 2.2 mm.
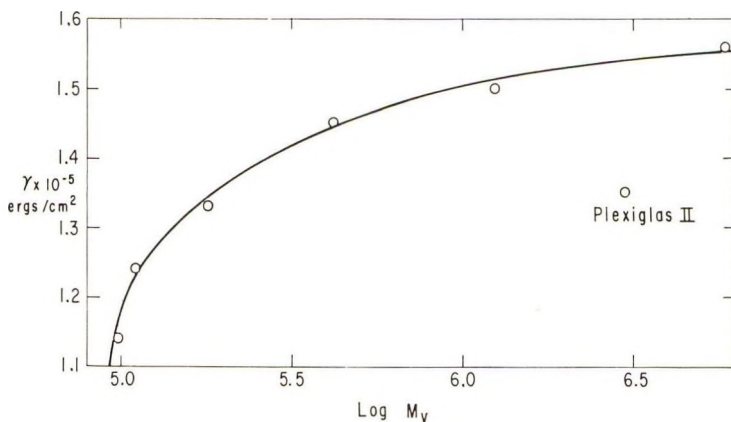
Fig. 3. Dependence of fracture surface energy on molecular weight.

showed a characteristic zigzag periodic fluctuation about the best line through the data points, as illustrated in Figure 1. The excursions represented a spread of about ±10% in the value of the fracture surface energy as obtained from the slope of the linear relation. This effect was most pronounced at the lower end of the molecular weight range, and it has also been reported in experiments on polystyrene,[12,13] poly(vinyl chloride),[14] and in poly(methyl methacrylate) of conventional molecular weight ($\sim 3 \times 10^6$) at low temperatures.[15] The influence of the stick slip behavior is also apparent in the characteristics of the fracture surface. Under conditions where the crack is moving quickly the surface is smooth, but as the velocity decreases and the crack begins to "stick" the surface becomes increasingly irregular (Fig. 2). One consequence of this response is that, because of the

surface irregularity in the "stick" phase, the true width of the fracture plane may be much greater than the distance w from one edge of the fracture plane to the other. Correction of the data for this effect would reduce the scatter of the points, though for lack of a satisfactory method of assessing the degree of surface irregularity such corrections have not been made. In all of the samples the fracture surfaces displayed the characteristic interference colors.

The stick-slip mode of crack propagation tends to reduce the precision of the experiment, but the reproducibility of the values of the fracture surface energy in duplicate experiments was good, usually within 5%, indicating that the accuracy of the cleavage technique is, in fact, greater than its precision. The dependence of the fracture surface energy on the viscosity-average molecular weight of the polymer is illustrated by the data summarized in Table I and by Figure 3.

TABLE I

$\bar{M}_r \times 10^{-5}$	$\gamma \times 10^{-5}$, ergs/cm.^{2}	$E \times 10^{-5}$, psi	T_0, psi	c_0, mm.	c'_0, mm.
0.98	1.14	3.33	9,880	0.036	0.029
1.1	1.24	3.56	9,260	0.047	0.039
1.8	1.33	3.58	10,490	0.040	0.026
4.2	1.45	3.67	10,810	0.042	0.036
12.5	1.50	4.25	10,160	0.058	0.048
30	1.35	4.44	10,120	0.056	0.042
60	1.56	4.24	10,010	0.061	0.050

For comparison, the fracture surface energy of polystyrene ($M_v = 3.5 \times 10^5$) is 7×10^5 ergs/cm.^{2} by the cleavage technique,[4] while the inherent flaw size is $\sim$1 mm.^{3}. It is clear from these data that the difference in the fracture properties of the two materials previously studied cannot be attributed only to differences in molecular weight.

In the present series of materials there is not a very strong dependence of the fracture surface energy on molecular weight until $M_v \sim 4 \times 10^5$, when the energy decreases rapidly as the molecular weight is further reduced. From the way in which it is defined, the fracture surface energy is directly proportional to the thickness of the yielded region that lies immediately ahead of the crack tip. Consequently the contribution which any particular molecule makes to the surface energy will be determined by the length that is contained within this region. A sufficiently long molecule will start in the unyielded region, pass through the yielded region, and terminate once again in the unyielded region. Under these conditions the contribution made by the molecule to the surface energy will be independent of its length. Correspondingly this energy should tend to a limiting value at high molecular weights, as the present experimental results indicate. If one or both ends of a polymer molecule are found within the yielded region, that molecule will not make a full contribution to the fracture sur-
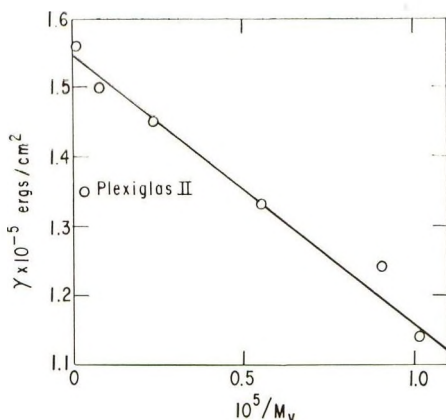
Fig. 4. Dependence of fracture surface energy on reciprocal molecular weight.

face energy. The polymer chains are believed to be in an extended configuration within the yielded region,[2] and hence the smallest molecule that can contribute fully to the surface energy will have its ends on the boundaries of the yielded region, on opposite sides of the fracture plane, and will be fully extended between these points. Assuming that the interference colors observed on the fracture surfaces are of first order, the total thickness of the yielded region is $\sim$5–6 $\times$ 10³ A. A fully extended molecule of poly-(methyl methacrylate) of this length has a molecular weight of $\sim$2–2.4 $\times$ 10⁵, and consequently the fracture surface energy must decrease for polymers of lower molecular weight. The present results show that the surface energy becomes markedly dependent on molecular weight when this is less than 4 $\times$ 10⁵. The agreement with the calculated value at which this effect would be expected to occur can be considered satisfactory in view of the crudity of the assumptions used in the calculation. In particular, the molecules are unlikely to be fully extended, and the limiting molecular weight would therefore be expected to be somewhat greater than the value obtained on that assumption.

The data for Plexiglas II UVA are included in Figure 3 for comparison with those for the materials that had been specially prepared. As shown in the figure, the fracture surface energy of the commercial polymer falls significantly below the smooth curve passing through the data points for the other materials. In view of the dependence of the fracture surface energy on molecular weight, this finding suggests that the differences in the method of preparation of the polymers resulted in differences in the molecular weight distribution.

The nature of the dependence of the fracture surface energy on molecular weight is similar to that observed for other mechanical properties, including the tensile strength.[16,17] The general relation can be represented by

$$P = A - (B/\bar{M}_n)$$

where P is the measured property, $\bar{M}_n$ is the number-average molecular weight, and A and B are constants. As illustrated in Figure 4, there is

reasonable agreement with a relation of this form when P is identified with the fracture surface energy, in terms of the viscosity-average molecular weight, $\bar{M}_v$. The constants A and B are then 1.55×10^5 ergs/cm.^{2} and 3.9×10^9 ergs/cm.^{2}/mass unit. It may be deduced from these figures that the upper limiting value of the fracture surface energy, for a sample of infinite molecular weight, should be $\sim 1.55 \times 10^5$ ergs/cm.^{2}. On the assumption that the linear relation can be extrapolated to lower molecular weights than those of the samples studied in the present investigation, the fracture surface energy (and hence the tensile strength) becomes zero for a sample with a molecular weight of 25,000.

The dependence of the other ultimate properties on molecular weight is indicated by the results summarized in Table I. The tensile modulus E increases with log $\bar{M}_v$ in approximately a linear fashion, but over the range studied the tensile strength is essentially independent of molecular weight, rather than varying linearly with its reciprocal, as discussed above. Vincent also has determined the dependence of the brittle strength of poly-(methyl methacrylate) on molecular weight, but over a wider range (2×10^4–10^6).[18] The samples were broken in flexure at $77°$K., and the results show a strong and essentially linear dependence on the reciprocal of the number-average molecular weight, particularly at values of $\bar{M}_n < 10^5$. The results obtained on samples with higher molecular weights, corresponding to those of the present samples, show a lesser dependence, and it is felt that the two sets of data are not inconsistent. It is interesting to note that according to Vincent's data, a polymer of molecular weight of 25,000 has essentially a zero brittle strength, in good agreement with the prediction based on the extrapolation of the fracture surface energy data. In view of the uncertain validity of that extrapolation, it would clearly be desirable to determine directly the fracture surface energy and other ultimate properties of samples with molecular weights extending down to the critical value.

The values of the inherent flaw size c_0 calculated from these data show only a slight dependence on molecular weight, increasing by about 70% for a change of a factor of 60 in molecular weight. This finding is perhaps surprising, in view of the much stronger molecular weight dependence of environmental stress cracking of polystyrene, as measured by the time to break under a standard (1000 psi) load.[10] The latter represents a more complex system, however, since the polymer was exposed to a butanol atmosphere, and a time variable rather than a stress variable failure point was used to characterize behavior. It is interesting to note that the values of c_0', obtained from the critical tensile stress for fracture of a sample containing a flaw of known size, fall consistently slightly below, but show the same variation with molecular weight as c_0. This finding indicates that the imprecision in the data is due to variations in the properties of the samples, rather than in the technique of determining c_0 (or c_0').

It was observed that the quality of the surface finish of the samples varied considerably and showed a marked improvement on going from the lowest to the highest molecular weight studied. It might have been expected

that the surface imperfections would have had some effect on the measured value of the inherent flaw size, but this factor did not appear to exert any significant influence on the results. Thus, in the determination of the tensile strength T_0, the samples did not show any particular preference for failure at an existing surface imperfection. This is consistent with earlier observations on polystyrene.[3]

References

1. Griffith, A. A., *Phil. Trans. Roy. Soc.*, **A222**, 180 (1921).
2. Berry, J. P., *J. Polymer Sci.*, **50**, 107 (1961).
3. Berry, J. P., *J. Polymer Sci.*, **50**, 313 (1961).
4. Berry, J. P., *J. Appl. Phys.*, **33**, 1741 (1962).
5. Bessonov, M. I., and E. V. Kuvshinskii, *Fiz. Tverd. Tela*, **1**, 1441 (1959); Engl. transl. *Soviet Phys. Solid State*, **1**, 1321 (1960).
6. Spurr, O. K., and W. D. Niegisch, *J. Appl. Polymer Sci.*, **6**, 585 (1962).
7. Kambour, R. P., *Nature*, **195**, 1299 (1962).
8. Berry, J. P., *J. Polymer Sci.*, **A1**, 993 (1963).
9. Newman, S. B., and I. Wolock, *J. Appl. Phys.*, **29**, 49 (1958).
10. Rudd, J. F., *J. Polymer Sci.*, **B1**, 1 (1963).
11. Berry, J. P., *J. Appl. Phys.*, **34**, 62 (1963).
12. Benbow, J. J., and F. C. Roesler, *Proc. Phys. Soc.*, **B70**, 201 (1957).
13. Svensson, N. L., *Proc. Phys. Soc.*, **78**, 876 (1961).
14. Shoulberg, R. H., private communication.
15. Broutman, L. J., D. Sc. Thesis, Massachusetts Institute of Technology, Cambridge, June 1963.
16. Sookne, A. M., and M. Harris, *Ind. Eng. Chem.*, **37**, 478 (1945).
17. Flory, P. J., *J. Am. Chem. Soc.*, **67**, 2048 (1945).
18. Vincent, P. I., *Polymer*, **1**, 425 (1960).

Résumé

On a déterminé l'influence des poids moléculaires sur l'énergie de surface à la cassure, le module de Young, la force de tension et l'importance de la crevasse dans le polyméthacrylate de méthyle. En commun avec d'autres propriétés mécaniques, la relation entre l'énergie de surface à la cassure et le poids moléculaire peut être représentée par gamma = $A - (B/M)$ où M est égal au poids moléculaire, et A et B des constantes arbitraires. Par extrapolation la valeur limite est égale à 1.55×10^5 ergs/cm² tandis que l'énergie de surface et la force de tension doivent être égales à zéro pour un polymère de poids moléculaire de 25.000. Cette valeur est en accord avec celle trouvée directement par des mesures de forces de cassure.

Zusammenfassung

Der Einfluss des Molekulargewichts auf die Bruchoberflächenergie, den Young-Modul, Zugfestigkeit und spezifische Fehlstellengrösse in Poly(methylmethacrylat) wurde bestimmt. In Übereinstimmung mit anderen mechanischen Eigenschaften kann die Abhängigkeit der Bruchoberflächenergie vom Molekulargewicht durch $\gamma = A - (B/M)$ dargestellt werden, wo M das Molekulargewicht und A und B willkürliche Konstanten sind. Durch Extrapolation ergibt sich der obere Grenzwert zu $1{,}55 \times 10^5$ erg sec/cm², während die Oberflächenenergie und folglich die Zugtestigkeit für ein Polymeres mit dem Molekulargewicht 25.000 Null werden sollte. Dieser Wert ist in guter Übereinstimmung mit dem direkt aus Bruchfestigkeitsmessungen gewonnen.

Radiation-Induced Polymerization of Acrylonitrile in Liquid Ethylene*

YONEHO TABATA, KIYOSHI HARA, and HIROSHI SOBUE,
Department of Nuclear Engineering and *Department of Industrial Chemistry,
University of Tokyo, Tokyo, Japan*

Synopsis

A mixed system of acrylonitrile and ethylene was irradiated with γ-rays from a Co^{60} source at $-78°C$. In the mixed system, ethylene did not polymerize, and only acrylonitrile polymerized. It was found that polymerizations due to both $C=C$ double bond and the $C\equiv N$ triple bond of acrylonitrile occurred in the mixed system. The ratio of one type of polymerization to the other varied continuously with concentration of the monomer; the polymerization of $C=C$ only occurs in bulk (100% monomer), as well known, but on the other hand, the polymerization of $C\equiv N$ occurs predominantly in a dilute solution of the monomer. The polymerization due to $C\equiv N$ triple bond would be by an ionic mechanism, probably an anionic. The experiments showed that the polymerization of acrylonitrile in the ethylene solution proceeds by a partial ionic mechanism at moderate concentrations of the monometer. The product obtained by the polymerization in such a mixed system is a mixture of polymers having the following structures:

$$CH_2=CH \xrightarrow{\sim\sim} -CH_2-CH-CH_2-CH-CH_2-CH-$$
$$\qquad | \qquad\qquad\quad | \qquad\quad | \qquad\quad |$$
$$\qquad C\equiv N \qquad\qquad C\equiv N \quad C\equiv N \quad C\equiv N$$

and

$$CH=CH \xrightarrow{\sim\sim} -C=N-C=N-C=N-C=N-$$
$$\quad | \qquad\qquad\qquad | \qquad | \qquad | \qquad |$$
$$\quad C\equiv N \qquad\qquad CH \quad CH \quad CH \quad CH$$
$$\qquad\qquad\qquad\qquad\; || \qquad || \qquad || \qquad ||$$
$$\qquad\qquad\qquad\qquad CH_2 \quad CH_2 \quad CH_2 \quad CH_2$$
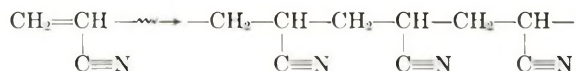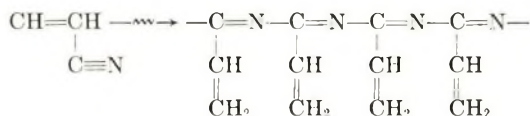
Introduction

Many studies have been carried out on the radiation-induced polymerization of acrylonitrile in bulk and in solution.[1-8] The polymerization proceeds by a radical mechanism in bulk and by an ionic mechanism in some amine solvents. On the other hand, the polymerization proceeds by a nonradical and nonionic mechanism, in the ordinary sense, in the solid state of the monomer at extremely low temperature.[9-11] The authors have proposed "Electronic Polymerization" for such solid state polymerizations.[12,13]

In this paper, the polymerization of acrylonitrile in a mixed system of acrylonitrile and ethylene is reported. Acrylonitrile and ethylene are very easy soluble in each other at $-78°C$.

Experimental

Acrylonitrile monomer was freed from inhibitors by distillation. Ethylene was purified by passage through 30% aqueous NaOH and 87% aqueous H_2SO_4 and was dried by passage through a trap at $-78°C$. Ethylene was condensed into an ampule containing solid acrylonitrile monomer at liquid nitrogen temperature. The ampule containing solid monomers was evacuated to 10^{-2} to 10^{-3} mm. Hg. Irradiation was carried out by γ-rays from a Co^{60} source at $-78°C$. The dependence of the dose rate and the influence of monomer concentration on the polymerization were investigated. The infrared spectra of the polymers obtained were measured. The solubility of the polymer obtained was also examined.

Results and Discussion

The relation between the polymerization yield and the irradiation dose for the polymerization of acrylonitrile in ethylene solution is shown in Figure 1. A relatively short induction period was observed, and the polymerization yield increased linearly with the irradiation dose. Neither homopolymerization nor copolymerization of ethylene was observed in the mixed system. It was found that only the polymerization of acrylonitrile is possible in the mixed system.

The relation between the conversion and the concentration of acrylonitrile in the ethylene solution at a dose rate of 7×10^4 r/hr. at $-78°C$. is shown in Figure 2. The figure shows that the rate of polymerization
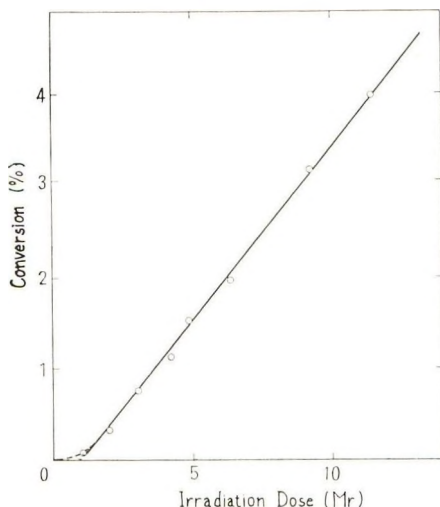
Fig. 1. Relation between conversion and the irradiation dose at a dose rate of 7×10^4 r/hr. at $-78°C$. The concentration of acrylonitrile was 50 vol.-%.
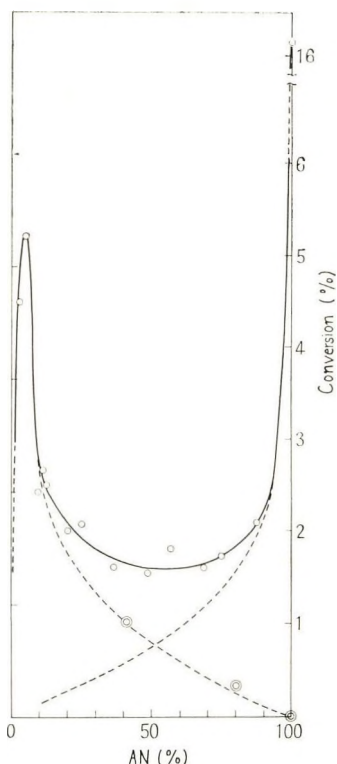
Fig. 2. Relation between conversion and the concentration of acrylonitrile in the monomer mixture at $-78°C$. The dose rate was 7×10^4 r/hr., the total dose was 6.4×10^6 r. The effect of pyrogallol on the polymerization is also shown, (O) presence of pyrogallol, 2.5 %-wt. for acrylonitrile.

decreases rapidly with decreasing concentration of acrylonitrile above an equal concentration (v/v) of acrylonitrile; on the other hand, at lower concentrations, the rate of polymerization increases rapidly with the concentration of ethylene.

The polymers obtained by polymerization in ethylene solution were colored products. The lower the monomer concentration, the deeper the color of the polymer obtained (yellow → red → brown → dark).

The infrared spectra of the polymers obtained are shown in Figure 3. It is obvious from the figure that the infrared spectrum of the polymer varies remarkably, depending on the concentration of acrylonitrile. The lower the concentration of acrylonitrile, the more intense the absorption observed at about 1660 cm.$^{-1}$, ν (C=N). On the other hand, the higher the acrylonitrile concentration, the more intense the absorption observed at 2240 cm.$^{-1}$, ν(C≡N). In the case of polymerization at a monomer concentration of 20 vol.-%, new absorption bands at 2180 and 810–820 cm.$^{-1}$ appeared.

These results suggest that polymerization involving the nitrile group C≡N may take place in the presence of ethylene.
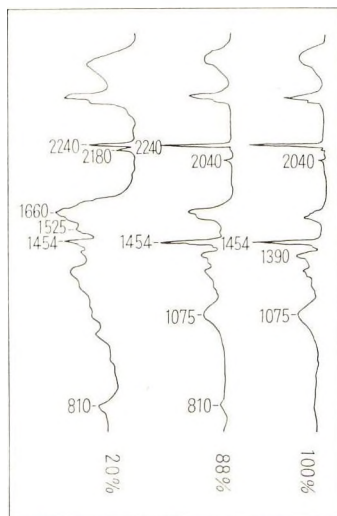
Fig. 3   Infrared spectra of the polymers obtained at various monomer concentrations.
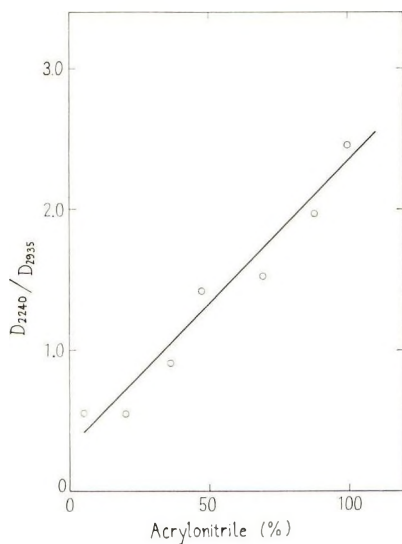
Fig. 4. Relation between the relative absorption intensity of nitrile, $\nu(C\equiv N)$, D_{2240}/D_{2935} and the monomer concentration in the ethylene solution. The polymers were obtained by irradiation with 6.4×10^6 r at dose rate of 7×10^4 r/hr.

The relation between the relative absorption intensity of the nitrile group, $\nu(C\equiv N)$ $(D_{\nu(C\equiv N)}/D_{\nu(CH)}$, where D is the absorption intensity) and the monomer concentration is shown in Figure 4. It is evident from the figure that the content of the nitrile group $C\equiv N$ in the polymer obtained decreases linearly with the ethylene concentration.
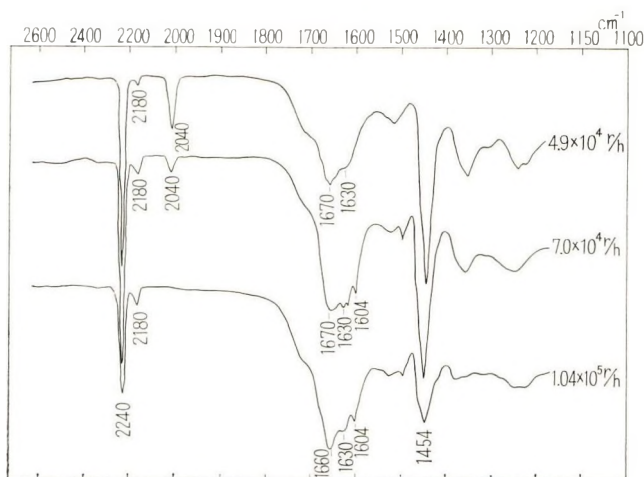
Fig. 5. Infrared spectra of the polymers obtained at various dose rates. Irradiation dose was 6.4×10^6 r and the acrylonitrile concentration was 50 vol.-%.

In another series of experiments, polymerizations were carried out at dose rates of 4.9×10^4, 7.0×10^4, and 1.04×10^5 r/hr. under same total doses of 6.5×10^6 r and at the same monomer concentration of 50 vol.-%. The results are shown in Figure 5 and Table I. These results show that the higher the dose rate, the more intense the absorption observed at about 1660 cm.$^{-1}$, $\nu(C=N)$. On the other hand, the absorption due to the ketene-imine structure decreased with the dose rate.

These results indicate that though the ordinary polymerization of acrylonitrile at the $C=C$ bond proceeds favorably at a lower dose rate, polymerization at the $C \equiv N$ triple bond proceeds more favorably at higher dose rates.

These dose rate dependencies suggest that the polymerization due to $C \equiv N$ triple bond would proceed by an ionic mechanism. The rate of polymerization is usually proportional to the dose rate in an homogeneous ionic polymerization while the rate is proportional to the square root of the dose rate in an homogeneous radical polymerization.

TABLE I
Dose Rate Dependence on the Structure of
Polyacrylonitrile Obtained

Dose rate, r/hr.	D_{2935}	D_{2240}	D_{1660}	D_{2240}/D_{2935}	D_{1660}/D_{2935}
4.9×10^4	0.208	0.321	0.132	1.54	0.64
7.0×10^4	0.272	0.387	0.251	1.42	0.92
1.04×10^5	0.178	0.084	0.258	0.89	1.47

TABLE II
Fusion Temperature of the Products

Concentration of acrylonitrile, vol.-%	Fusion point or range, °C.		
	First	Second	Decomposition
100	—	218	275 (darkens)
50	75–85	210	210–240 (darkens)
20	56–61	—	

The effect of a radical inhibitor, pyrogallol, on the polymerization is shown in Figure 2. It is obvious that the polymerization is inhibited at higher concentrations more than at lower concentrations of acrylonitrile. This suggests the polymerization proceeds by a radical mechanism at the higher concentration of the monomer and by an ionic mechanism in the lower concentration of the monomer. Therefore, the mechanism of the polymerization due to $C \equiv N$ in a dilute solution would be ionic.

The products obtained have two fusion temperatures, probably those of polyacrylonitrile and the other material, as shown in Table II.

The higher fusion temperature corresponds to that of ordinary polyacrylonitrile and the lower one to that of the other material.

On the other hand, the infrared spectrum of the product could be obtained by a superposition of the spectrum of polyacrylonitrile and the other material.

Therefore, the product is probably a mixture of two homopolymers, and the composition varies continuously with the monomer concentration.
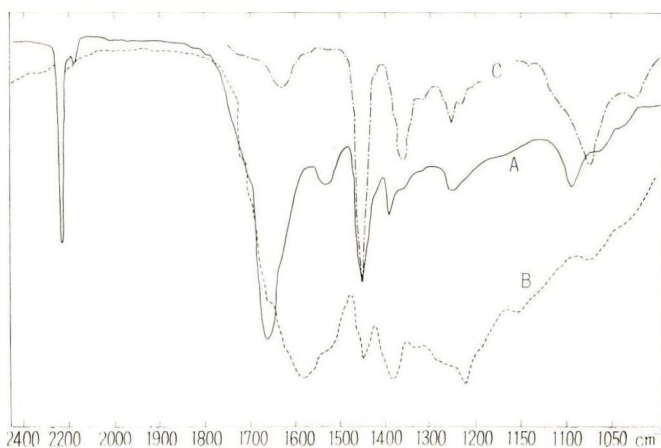
Fig. 6. Infrared spectra of polyacrylonitriles obtained by different methods: (A) polymerization of acrylonitrile in the ethylene solution (54 vol.-% acrylonitrile vat −78°C.); (B) the heat treatment (at 150°C. for 2 hr.) of polyacrylonitrile which was polymerized in solid state at −94°C.; (C) polymerization in bulk at 20°C.

The product obtained by polymerization in the ethylene–acrylonitrile system was not soluble in dimethylformamide, but the product was swelled by the same solvent, indicating a network structure. It seems likely that the polymer with conjugated double bonds ($-C{=}N-$) obtained would be crosslinked by the vinyl group by further irradiation.

Infrared spectra of three different polymers, A, B, and C are shown in Figure 6. The products were obtained by the polymerization in an ethylene solution (54 vol.-% acrylonitrile) at $-78°C.$, by heat treatment (at 150°C. for 2 hr.) of polyacrylonitrile which was obtained by solid-state polymerization at $-94°C.$, and by the polymerization of acrylonitrile at 20°C., respectively. It is evident from the figure that the spectrum of polymer A is quite different from spectrum of B. Previously, the authors reported that polymer B would be a high stereo-regular polyacrylonitrile (syndiotactic structure) in which a long sequence of intramolecular conjugated double bond could be formed by heat treatment.[14]

Generally, the absorption of $C{=}N$ stretching vibration in a conjugated cyclic system appears in the region of $1480-1660$ cm.$^{-1}$ and the absorption in an open chain system or a nonconjugated system appears in the region of $1640-1690$ cm.$^{-1}$. Figure 6 suggests that polymer A has mainly an open chain system of $-C{=}N-$ conjugated double bonds, on the other hand, B polymer has a long sequence of conjugated cyclic system of the type
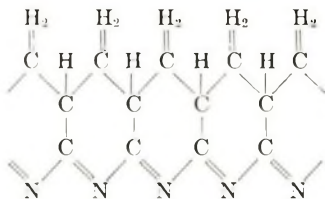
As experimental conditions of our study are quite different from those used by Tobin and Deichert,[15] it is not surprising that there are several differences between the infrared spectra obtained by the two research groups.

Ethylene did not polymerize in the ethylene–acrylonitrile mixed system, as described above. From these experiments, it was found that the ethylene retards the polymerization of $C{=}C$ double bond, while the same compound promotes the polymerization of the $C{\equiv}N$ triple bond.

It was concluded from these results that the polymerization in the mixed system proceeds by a partial ionic mechanism, depending on the monomer concentration; that is, an ionic polymerization of $C{\equiv}N$ in dilute solution and a radical polymerization of $C{=}C$ in concentrated solution.

The structure of the obtained polymers (I, II) would be presented, as an ideal form, as follows.

I

$$-C=N-C=N-C=N-C=N-$$

$$CH_2=CH \xrightarrow{\ C_2H_4\ } \begin{array}{cccc} \text{CH} & \text{CH} & \text{CH} & \text{CH} \\ \| & \| & \| & \| \\ \text{CH}_2 & \text{CH}_2 & \text{CH}_2 & \text{CH}_2 \end{array}$$
$$|$$
$$CN$$

II
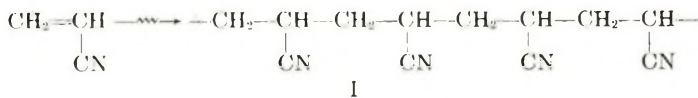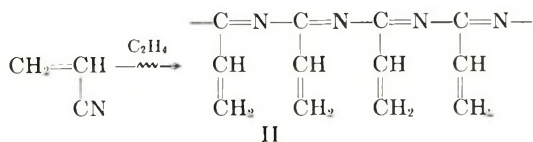
It is suggested from the insolubility of the polymer in dimethylformamide and the infrared spectrum of the product that the structure of the product would be a three-dimensional network (III) and most of the vinyl group would be consumed by the crosslinking.

III
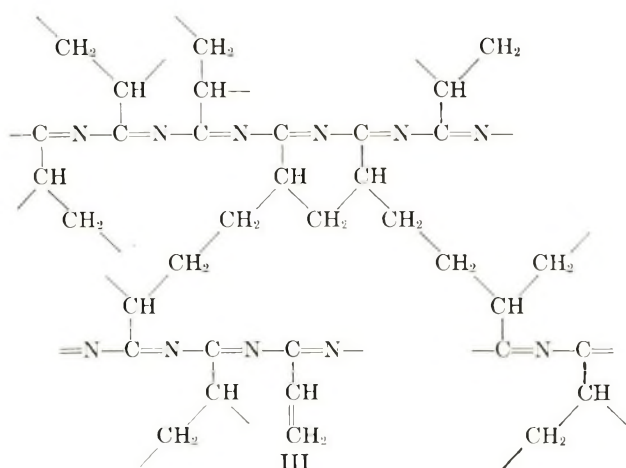
The polymerization mechanism in the mixed system would be as shown schematically in eqs. (1)–(4).

Ionization:

$$C_2H_4 \xrightarrow{\ \ } C_2H_4{}^+ + e \tag{1}$$

Excitation:

$$CH_2=CH-CN \xrightarrow{\ \ } CH_2=CH-CN^* \tag{2}$$

Energy Transfer:

$$CH_2=CH-CN^* + C_2H_4 \rightarrow CH_2=CH-CN + C_2H_4{}^* \tag{3}$$

Electron Capture:

$$CH_2=CH-CN + C_2H_4{}^+ + e \rightarrow CH_2=CH-CN^- + C_2H_4{}^+ \tag{4}$$
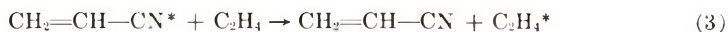
Though many kinds of excitation, ionization, and various energy transfer processes could contribute to the initiation process, the processes mentioned above would play a most important role in the polymerization of these mixed systems. The anionic polymerization of nitrile $C\equiv N$ would proceed via eqs. (1) and (4), and the radical polymerization of $C=C$ would be regarded by the processes of eqs. (2) and (3).

References

1. Bernstein, I. A., E. C. Farmer, W. G. Rothschild, and F. F. Spalding, *J. Chem. Phys.*, **21**, 1303 (1953).

2. Bernas, A., and J. Danon-Sebban, *J. Chim. Phys.*, **53**, 418 (1956).

3. Arthur, J. C. et al., *J. Phys. Chem.*, **63**, 1366 (1959).

4. Bensasson, R., et al., *J. Chim. Phys.*, **53**, 93 (1956); *J. Polymer Sci.*, **30**, 163 (1958).

5. Chapiro, A., M. Magat, and A. Prévot-Bernas, *J. Chim. Phys.*, **54**, 776 (1957).

6. Chen, C. S. H., N. Colthup, W. Deithert, and R. Y. Webb, *J. Polymer Sci.*, **45**, 247 (1960).

7. Prévot, A., and J. Sebban-Danon, *J. Chim. Phys.*, **53**, 418 (1956).

8. Bernas, A., and M. Bodard, *J. Polymer Sci.*, **48**, 167 (1960).

9. Sobue, H., and Y. Tabata, *J. Polymer Sci.*, **43**, 459 (1960).

10. Tabata, Y., and H. Sobue, *Doitai To Hoshasen*, **3**, 220 (1960).

11. Bensasson, R., and R. Marx, *J. Polymer Sci.*, **48**, 53 (1960).

12. Tabata, Y., H. Sobue, and K. Oshima, paper presented at 2nd International Congress of Radiation Research, August, 1962, Harrogate, England.

13. Sobue, H., Y. Tabata, M. Hiraoka, and K. Oshima, *J. Polymer Sci.*, C4, 943 (1964).

14. Tabata, Y., and H. Sobue, paper presented at 3rd Japanese Conference of Radio-isotopes, October, 1961.

15. Tobin and Deichert, *J. Polymer Sci.*, **54**, 160 (1961).

Résumé

Un mélange d'acrylonitrile et d'éthylène a été irradié avec des rayons-gamma de Co⁶⁰ à −78°C. Dans le mélange, l'éthylène ne polymérisait pas, tandis quel 'acrylonitrile uniquement polymérisait. On a trouvé que des polymérisations dues aux doubles liaisons —C=C— et aux triples liaisons C≡N de l'acrylonitrile se manifestaient dans le mélange. Le rapport de ces deux types de polymérisations changeait continuellement avec la concentration en monomère; la polymérisation de la liaison C=C se manifeste uniquement en bloc (100% de monomère), ce qui est bien connu; tandis que la polymérisation de la liaison —C≡N est prédominante dans une solution diluée de monomère. La polymérisation due à la triple liaison —C≡N se ferait par un mécanisme ionique, probablement anionique. Les expériences montrent que la polymérisation de l'acrylonitrile dans la solution d'éthylène se fait par un mécanism ionique partiel, pour des concentrations moyennes en monomère. Le produit obtenu par la polymérisation dans un mélange pareil est un mélange de polymères avec les structures suivantes:

$$CH_2{=}CH \longrightarrow -CH_2{-}CH{-}CH_2{-}CH{-}CH_2{-}CH-$$
$$\qquad | \qquad\qquad\qquad | \qquad\quad | \qquad\quad |$$
$$\quad C{\equiv}N \qquad\qquad C{\equiv}N \quad C{\equiv}N \quad C{\equiv}N$$

et

$$CH{=}CH \longrightarrow -C{=}N{-}C{=}N{-}C{=}N{-}C{=}N-$$
$$\qquad | \qquad\qquad\quad | \qquad\; | \qquad\; | \qquad\; |$$
$$\quad C{\equiv}N \qquad\qquad CH \quad CH \quad CH \quad CH$$
$$\qquad\qquad\qquad\qquad\quad \| \qquad\; \| \qquad\; \| \qquad\; \|$$
$$\qquad\qquad\qquad\qquad\; CH_2 \quad CH_2 \quad CH_2 \quad CH_2$$
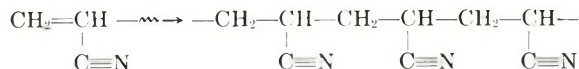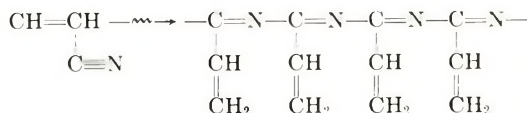
Zusammenfassung

Eine Mischung aus Acrylnitril und Äthylen wurde mit Gammastrahlen von Co⁶⁰ bei −78°C bestrahlt. In der Mischung polymerisierte zwar Acrylnitril, Äthylen dagegen nicht. Man fand, dass in der Mischung sowohl eine Polymerisation der C=C-Doppelbindung als auch der C≡N-Dreifachbindung von Acrylnitril auftrat. Das

Verhältnis der einen Polymerisationsart zur anderen zeigte eine stetige Variation mit der Monomerkonzentration; die $C=C$-Polymerisation tritt bekanntermassen nur in Substanz (100% Monomeres) auf, andrerseits aber tritt die $C\equiv N$-Polymerisation vorwiegend in einer verdünnten Monomerlösung auf. Die auf die $C\equiv N$-Dreifachbindung zurückzuführende Polymerisation könnte einen ionischen, wahrscheinlich einen anionischen Mechanismus besitzen. Das Experiment stellte klar, dass die Polymerisation von Acrylnitril in Äthylenlösung bei mittlerer Monomerkonzentration nach einem teilweise ionischen Mechanismus verläuft. Das bei der Polymerisation in solchem Mischsystem erhaltene Produkt ist eine Mischung von Polymeren mit folgender Struktur:
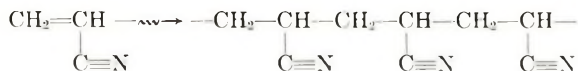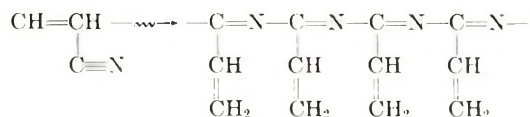
$$CH_2{=}CH \longrightarrow -CH_2-CH-CH_2-CH-CH_2-CH-$$
$$\phantom{CH_2{=}}\underset{C\equiv N}{|} \underset{C\equiv N}{|} \underset{C\equiv N}{|} \underset{C\equiv N}{|}$$

und

$$CH{=}CH \longrightarrow -C{=}N-C{=}N-C{=}N-C{=}N-$$
$$\phantom{CH{=}}\underset{C\equiv N}{|} \underset{\underset{CH_2}{\|}}{CH} \underset{\underset{CH_2}{\|}}{CH} \underset{\underset{CH_2}{\|}}{CH} \underset{\underset{CH_2}{\|}}{CH}$$

X-Ray-Induced Polymerization of Diphenylvinylphosphine Oxide

H. R. ALLCOCK, *Chemical Research Department, Central Research Division, American Cyanamid Company, Stamford, Connecticut*

Synopsis

Diphenylvinylphosphine oxide was polymerized in the molten state by x-irradiation to give polymers with molecular weights up to 10,000.   The results of variations in total radiation dose, dose rate, and temperature, are consistent with a free radical polymerization mechanism in which chain transfer is important.   Infrared spectra of the polymers provided evidence that phenyl groups are involved in the chain transfer processes.

INTRODUCTION

The polymerization of molten diphenylvinylphosphine oxide induced by x-rays at low dose rates was reported briefly by Tsetlin and co-workers,[1] who obtained a polymer of molecular weight, 30,000.   This behavior contrasted markedly with the free radical-catalyzed solution and bulk polymerization of this monomer which gave low molecular weight products[2–4] and with the organometallic-catalyzed polymerization which yielded polymer of molecular weight up to 10,000, and for which an anionic type mechanism was proposed.[5]   The present work constitutes an attempt to examine the x-ray-induced polymerization of diphenylvinylphosphine oxide at low and high dose rates and at different temperatures in an attempt to obtain information about the reaction mechanism.

EXPERIMENTAL

Materials

Diphenylvinylphosphine oxide (m.p., 117–117.5°C.) was prepared and purified as described previously.[3,5]   *N,N*-Dimethylformamide (Eastman, spectro grade) and absolute ethanol were used as received.   Toluene, tetrahydrofuran, and pyridine were purified as described previously[5] and were stored in a glass vacuum system.

Irradiation Technique

For bulk polymerizations at low dose rates, diphenylvinylphosphine oxide (3 g.) was degassed and sealed under vacuum in cylindrical Pyrex glass ampules, 25 mm. in diameter, 22 mm. deep, with the flat faces approxi-

mately 2 mm. thick. The monomer was then irradiated through the upper face, while the ampule was three-quarters immersed in an oil bath.

Bulk polymerizations at high dose rates were performed on monomer samples (1 g.), degassed and sealed under vacuum in 12 mm. diameter, 1 mm. wall Pyrex tubes. For irradiations at temperatures below the melting point, the monomer was melted and allowed to resolidify in order to present a uniform volume and surface area. The tubes were then irradiated at right angles to the long axis.

For solution reactions with dimethylformamide or ethanol, 5 ml. quantities of the solvents were added by syringe to monomer (1 g.) in constricted 18 mm. diameter, 1 mm. wall Pyrex tubes. The solutions were then degassed and the tubes were sealed. When toluene, tetrahydrofuran, or pyridine was used as a solvent, the tubes and monomer were degassed on a vacuum line and dry solvent was condensed in from a reservoir.

Temperature Control

Reactions at temperatures above 25°C. took place with the tubes or ampules partly immersed in an oil bath (or Dowtherm bath at 160°C.), which was regulated to within $\pm\frac{1}{2}$°C. Reactions at -78°C. were performed in tubes partly immersed in an acetone–Dry Ice bath.

X-Ray Sources

Irradiations at low dose rate were performed by use of a General Electric Maxitron x-ray source, 250 kvp, 30 ma. unfiltered, with the sample 13 cm. from the target. Under these conditions, the dose rate at the sample was measured as 0.26 Mrad/hr. by ferrous sulfate dosimetry.

Irradiations at high dose rate were carried out at 10 cm. below the water-cooled, $\frac{1}{8}$ in. thick gold target of a Van de Graaff accelerator, type KS (3 M.e.v./3 kw.), a 5-in. scan being used. The abbreviation 3 M.e.v. C.P. used in the text refers to 3 M.e.v. constant potential x-rays with a filtration of $\frac{1}{8}$ in. of gold (E_{max} = 3.0 M.e.v., E_{av} = 1.0 M.e.v., E_{peak} = 0.5 M.e.v., E_{min} = 0.3 M.e.v.). Contour maps of dose rates were determined at various horizontal levels below the target by ferrous sulfate dosimetry in 5 ml. beakers. The dose rate on the axis, at a distance of 10 cm. below the target, was 3 Mrad/hr.

Isolation of Polymer

After irradiation, the reaction products were dissolved in absolute ethanol (100 ml. for 3 g. reactions, 50 ml. for 1 g. reactions), and polymer was precipitated by the slow addition of water (100 ml. or 50 ml.). The precipitate was filtered off, was washed with 50 vol.-% aqueous ethanol (500 ml. or 250 ml.), and was then dried in a vacuum oven at 60°C. Polymer yields and conversions discussed in this work refer to products isolated in this manner. Evaporation of the aqueous ethanolic filtrates yielded oligomers and, in some cases, unchanged monomer. Only a partial separation of these soluble components could be effected by crystallization.

Characterization of the Polymer

The molecular weights of the polymers were in a region where both number-average and weight-average methods are least accurate. For this reason, the values obtained by each method were not always consistent. Molecular weights were determined by light-scattering measurements in dimethylformamide or by a vapor pressure thermistor technique in methanolic solutions. Reduced specific viscosity values were obtained for 1% solutions in dimethylformamide at 30°C. Glass transition temperatures were derived from differential thermal analysis curves. X-ray powder diffraction patterns were used to demonstrate the amorphous nature of the polymers. A typical product prepared after 8 hr. reaction at 130°C., 10 cm. below the target of the 3 M.e.v. C.P. x-ray source, gave analysis values of C, 74.05%; H, 5.60%; P, 13.45%. $C_{14}H_{13}PO$ requires C, 73.59%; H, 5.70%, P, 13.59%.

Infrared Spectra

The spectra of the polymeric products were determined as Nujol or halocarbon (mixed chlorinated and fluorinated hydrocarbon) mulls using a Perkin-Elmer, Model 21, sodium chloride prism spectrometer. The infrared absorption spectra showed bands for aliphatic and aromatic groups (3060, 2935, 1990, 1907, 1825, 1772, 1595, 1580, 1490, 1443, 1075, 1030, 1000, 980, 930, 845, 795, 745, 720, and 697 cm.$^{-1}$), P = 0 groups (1185 cm.$^{-1}$), P–phenyl (1122 cm.$^{-1}$), and C–phenyl (1500 and 1455 cm.$^{-1}$). (The aryl ring-stretch bands at 1595 and 1443 cm.$^{-1}$ are found well within five wave numbers of these positions for all diphenylalkyl and dialkylphenylphosphine oxides.) The semiquantitative estimates of C–phenyl ratios were made on the basis of the peak heights at 1605, 1500, and 1455 cm.$^{-1}$ relative to the P–phenyl peak heights at 1595, 1490, and 1443 cm.$^{-1}$. The polymers and related organophosphorus compounds, such as $(C_6H_5)_2P$-$(O)C_2H_5$, $(C_6H_5)_2P(O)CH_2C_6H_5$, $(C_6H_5)_2P(O)CH(C_6H_5)OCH_3$, and $(C_6H_5)_2P$-$(O)CH(C_6H_5)CH_3$, were examined as halocarbon mulls and as chloroform solutions. The peak heights of the solid samples and the optical densities of the solutions indicated that for radiation and peroxide induced polymer one C–phenyl group was present for each three or four diphenylphosphine oxide units.

RESULTS AND DISCUSSION

Properties of the Polymers

The highest polymers prepared by the x-ray method corresponded to a weight-average molecular weight of 10,000, and gave reduced specific viscosity values of 0.03 to 0.04. In this respect, the polymers were not of higher molecular weight than those prepared with the use of organometallic catalysts[5] and did not approach the 30,000 value reported by Tsetlin et al.[1] The glass transition temperature of poly(diphenylvinylphosphine oxide)

prepared in the present work was 75°C. compared to the 180°C. value reported by the latter authors.[1]   The polymers showed a strong tendency to form solid hydrates when exposed to the atmosphere, a property which was noted for poly(diphenylvinylphosphine oxides) prepared by other techniques.[2,5]   Polymers prepared by the x-ray irradiation method were considerably more soluble in solvents such as ethanol, methanol, benzene, and toluene than were polymers of similar molecular weight prepared by the use of organometallic catalysts.[5]   The solution viscosity–molecular weight relationship appeared to be similar to that of linear polymers prepared by ionic processes.[5]

Effect of Increases in the Total Radiation Dose

Bulk polymerizations of the molten monomer were carried out with 250 kvp x-rays.   The results are shown in Table I.

TABLE I
Effect of Increases in the Radiation Dose of 250 kvp X-Rays[a]

Reaction time, hr.	Total dose; Mrad	Polymer isolated, %	Molecular weight[b]	η_{sp}/C	T_y, °C.
5	1.3	34.6	6030	0.04	83
10	2.6	48.5[c]	4280	0.04	74–85
27.8	7.2	40.0	4311 (8500)[d]	0.03	73
50.0[e]	15.0	57.0	~10,000 (10,000)[d]	0.03	75

[a] Reaction temperature, 130°C.
[b] MW by vapor pressure thermistor.
[c] No residual monomer was present in the reaction mixture after this point.
[d] MW by light scattering.
[e] Comparable conditions to those used by Tsetlin et al.[1]

TABLE II
Effect of Increases in the Radiation Dose of 3 M.e.v. C.P. X-Rays; Reaction Temperature 130°C.

Reaction time, hr.	Total dose, Mrad	Polymer isolated, %	Molecular weight[a,b]
0.66	1.98	15.2	—
1.0	3.0	27.1	1400
1.5	4.5	42.2[c]	4300
2.0	6.0	42.9	3873
3.0	9.0	47.5	4500
4.0	12.0	48.0	4600
6.0	18.0	51.8	4700
8.0	24.0	48.6	5600

[a] MW by vapor pressure thermistor ($\bar{M}_n$).
[b] $\eta_{sp}/C = 0.03–0.05$.
[c] No residual monomer was present in the reaction mixture after this point.

No appreciable reaction was apparent after an x-ray dose of 2.6 Mrad, the point which coincided with solidification of the mixture and depletion of the monomer. The reaction products, other than those described, were low molecular weight oligomers.

Polymerizations of the molten monomer at 130 and 160°C. were also performed with the use of 3 M.e.v. (C.P.) x-rays, and the effects of increasing the total radiation dose under these conditions are shown in Tables II and III.

For these reactions, the polymerization appeared to have ceased essentially after 4.5 Mrad at 130°C. and after 3.0 Mrad at 160°C., at which points the mixtures were no longer liquid and no residual monomer was present. Further irradiation resulted in only minor increases in the amount of polymer isolated. It was apparent that the reduced specific viscosities and the molecular weights of the polymers were not influenced appreciably by increases in the radiation dose. As a "blank" reaction, a sample of diphenylvinylphosphine oxide was heated at 160°C. for 8 hr. The monomer was recovered unchanged.

TABLE III

Effect of Increases in the Radiation Dose of 3 M.e.v. C.P. X-Rays; Reaction Temperature 160°C.

Reaction time, hr.	Total dose, Mrad	Polymer isolated, %	Molecular weight[a]
0.25	0.75	12.5	1360
0.5	1.5	27.0	2630
1.0	3.0	65.4[b]	1800
2.0	6.0	68.2	2060
4.0	12.0	67.8	1910
6.0	18.0	78.6	1320
8.0	24.0	77.5	1400

[a] MW by vapor pressure thermistor ($\bar{M}_n$).

[b] No residual monomer was present in the reaction mixture after this point.

TABLE IV

Effect of Radiation Dose Rate on the Polymerization of Molten Diphenylvinylphosphine Oxide at 130°C.

Dose rate, Mrad/hr.	Reaction time, hr.	Total dose, Mrad	Polymer yield, %	Molecular weight[a,b]
0.26	10	2.6	48.5	4280
0.37	8	2.96	41.8	3500
0.75	4	3.0	39.2	4100
1.50	2	3.0	33.1	4100
3.00	1	3.0	27.1	~1400

[a] MW by vapor pressure thermistor.

[b] Reduced specific viscosities, 0.03–0.04.

Effect of Increases in the Radiation Dose Rate

The data in Table IV show the effects of variations in the dose rate for reactions which received approximately the same total radiation dose.

Increases in the radiation dose rate brought about decreases in the polymer yield for a given total dose. The yield of polymer appeared to be approximately proportional to the square root of the dose rate, but the degree of polymerization was essentially unaffected by the dose-rate under these conditions.

Effect of Temperature Variations

The effect of temperature changes on the polymerization at high dose rates is shown in Table V.

TABLE V

Effect of Temperature Changes on the X-Ray-Induced Polymerization of Diphenyl-vinylphosphine Oxide[a]

Temperature, °C.	Polymer yield, %	MW	η_{sp}/C
−78	0		
60	0		
97	1.4		
130	48.6	5600	0.04
160	77.5	1400	0.03

[a] 3 M.e.v. C.P. x-rays; 8 hr. reaction time; total dose 24 Mrad.

Below the melting point of the monomer, at −90°C. and 60°C., no significant polymerization occurred in the solid state. Unchanged monomer and small amounts of oligomers were isolated from these reactions. At only 20°C. below the melting point of the monomer, the polymerization was extremely slow. Above the melting point the polymerization was accelerated markedly as the temperature was increased from 130°C. to 160°C. It is apparent from Tables II and III that the temperature increase resulted in higher yields of polymer isolated, but that lower molecular weight polymers were produced at 160°C. than at 130°C.

Solution Reactions

The solution polymerization of diphenylvinylphosphine oxide was also examined briefly at 70°C., with ethanol, tetrahydrofuran, dimethylformamide, and pyridine as solvents. After 8 hr. irradiation, at a dose rate of 3 Mrad/hr., only trace amounts of polymer were formed. The reaction products were low molecular weight oligomers and unchanged monomer.

Reaction Mechanism

The results obtained in this study are consistent with a free radical-type polymerization mechanism. The weight-average molecular weight
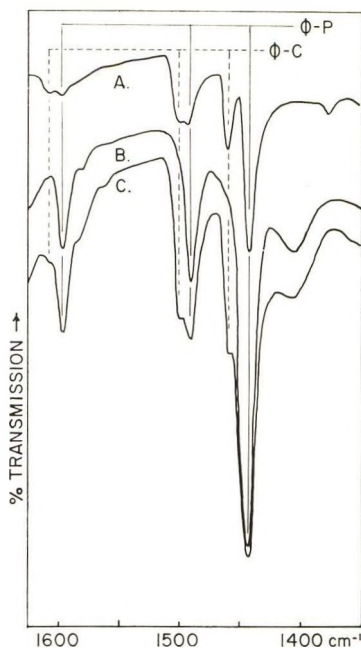
Fig. 1. Changes in infrared bands associated with α-phenyl substituents: (A) C_6H_5P-$(O)CH(C_6H_5)CH_3$; (B) poly(diphenylvinyl phosphine oxide) prepared with the use of n-butylmagnesium chloride as initiator[5]; (C) polymer prepared by x-irradiation.

value of 10,000 appears to be an approximate upper limit for polymers prepared and isolated by this process, a figure which corresponds to a degree of polymerization of about 40 monomer units. The molecular weights of the products were not affected appreciably by changes in dose rate or total radiation dose, and in this respect the reaction resembled free radical polymerizations described previously,[4] in which the chain length was independent of initiator concentration. Chain transfer undoubtedly plays a large part in limiting the molecular weight of poly(diphenylvinylphosphine oxide),[4] and the decrease in molecular weight which accompanies temperature increases in this reaction is consistent with this interpretation.

Polymerization was not accompanied by extensive decomposition. Small amounts of phosphinic vapors were evolved from products which had been subjected to prolonged irradiation at high dose rates, but carbon, hydrogen, and phosphorus analyses of precipitated and exhaustively dried polymers corresponded to the values expected for poly(diphenylvinylphosphine oxide). Furthermore, the x-ray-induced polymerization did not result in excessive crosslinking, since in no case was ethanol-insoluble polymer obtained. Infrared spectra were consistent with the structure of a vinyl addition polymer and showed no evidence of P–O–C units which would be expected if the polymerization involved phosphine oxide groups.

However, although the infrared spectra were identical with those of polymers prepared by standard free radical procedures,[4] they exhibited

minor differences from spectra of poly(diphenylvinylphosphine oxide) prepared by ionic catalysis.[5] These differences, shown in Figure 1, involved peaks at 1605, 1500, and 1455 cm.$^{-1}$ which were present in the radiation- and peroxide-initiated polymers but which were absent in the ionic-catalyzed material. Comparisons with the spectra of $(C_6H_5)_2P(O)CH(C_6H_5)$-OH, $(C_6H_5)_2P(O)CH(C_6H_5)OC_2H_5$, and $(C_6H_5)_2P(O)CH(C_6H_5)CH_3$ and similar derivatives, indicated that these peaks were due to the presence of carbon-phenyl units in the position α to the phosphine oxide group.*

The peak heights for a polymer of molecular weight 5000 indicated that at least one monomer unit in four contained phenyl substituents at the α positions. The 800 cm.$^{-1}$ region of the spectrum suggested that no disubstituted phenyl groups were present.

In view of the evidence available, it is reasonable to ascribe these results to chain transfer and termination reactions which involve abstraction of phenyl groups from monomer or polymer molecules by terminal polymer radicals. The detailed mechanism of this process has not been established, but a simple chain termination process by phenyl group abstraction does not provide an adequate explanation of the results. The α-carbon-phenyl content of the polymer was much higher than would be expected for one carbon-phenyl group as a terminal unit on each chain, although the carbon and hydrogen ratios were not increased. One explanation of this anomaly is that chain branching may occur through side group phosphorus atoms, but evidence for or against such a mechanism could not be obtained from infrared spectra, nuclear magnetic resonance data, or electron spin resonance spectra.

The polymers prepared in this work were of lower molecular weight than the product reported by Tsetlin et al.,[1] a result which may be due to different irradiation, isolation, or characterization techniques. The lower glass transition temperature of these polymers is probably due to the lower molecular weight, since the physical properties are probably influenced markedly by the chain length in this region. It is clear, however, that the presence of α-phenyl groups in polymers prepared by x-irradiation or by peroxide catalysis[4] provides an explanation for the marked physical property differences of these polymers compared with linear, ionic-initiated material of similar molecular weight.[5]

* The 1500 and 1455 cm.$^{-1}$ bands fall outside the region for dialkylphenylphosphine oxides, but are very characteristic for carbon-phenyl absorption. In $(C_6H_5)_2P(O)$-$CH(C_6H_5)CH_3$ the 1455 cm.$^{-1}$ band shows some interference due to the α-methyl absorption. However, the band is mainly due to the aromatic ring since similar compounds which lack an α-methyl group, such as $(C_6H_5)_2P(O)CH_2C_6H_5$, also show this peak.

References

1. Tsetlin, B. L., T. Ya. Medved, Yu. G. Chikishev, Yu. M. Polykarpov, S. R. Rafikov, and M. I. Kabachnik, *Vysokomol. Soedin.*, **3,** 1117 (1961).
2. Berlin, K. D., and G. B. Butler, *J. Org. Chem.*, **26,** 2537 (1961).
3. Rabinowitz, R., and J. Pellon, *J. Org. Chem.*, **26,** 4623 (1961).
4. Rabinowitz, R., R. Marcus, and J. Pellon, *J. Polymer Sci.*, **A2,** 1233 (1964).
5. Allcock, H. R., and R. L. Kugel, *J. Polymer Sci.*, **A1,** 3627 (1963).

Résumé

La polymérisation de l'oxyde de diphényl-vinylphosphine par irradiation aux rayons-X a fourni des polymères de poids moléculaire s'élévant jusqu'à 10000. Les résultats obtenus en faisant varier la dose totale de radiation, la vitesse de dose et la température, suggèrent un mécanisme radicalaire de polymérisation au cours duquel le transfert de chaîne est important. Les spectres infra-rouges des polymères fournissent la preuve que des groupements phényles sont impliqués dans le processus de transfert de chaîne.

Zusammenfassung

Diphenylvinylphosphinoxyd wurde im geschmolzenen Zustand durch Röntgenbestrahlung zu Polymerem mit Molekulargewicht bis zu 10.000 polymerisiert. Die Ergebnisse bei Variation der totalen Strahlungsdosis, der Dosisleistung und der Temperatur stimmen mit einem radikalischen Polymerisationsmechanismus, bei welchem die Kettenübertragung von Bedeutung ist, überein. Infrarotspektren der Polymeren zeigen, dass die Phenylgruppen an der Kettenübertragung teilnehmen.

Radiation-Induced Electrical Conductivities in Polyamide Copolymers

PÉTER HEDVIG, *Plastics Research Institute, Budapest, Hungary*

Synopsis

Radiation-induced conductivities as high as 10^{-12} ohm^{-1} cm.$^{-1}$ were measured in polyamide copolymers irradiated by x-rays and Co^{60} γ-rays at dose rates of 0.1–20 r/sec. No temperature dependence for the induced conductivities could be detected between 10 and 60°C., while dark conductivities followed the usual exponential rule with activation energies between 1 and 2 e.v. Preirradiation of the samples resulted in a decrease of the induced conductivities. This effect could be controlled by addition of benzophenone and hydroquinone. A phenomenological model is presented for a possible explanation of the results.

EXPERIMENTAL

Mixed polymers (copolymers) were prepared by polycondensation of hexamethylenediammonium adipate (15%), hexamethylenediammonium sebacate (40%), and caprolactam (35%). A sheet of this polymer was placed between platinum electrodes and evacuated at room temperature to 10^{-5} mm. Hg pressure via liquid air trap for drying.

The dark conductivity was measured continuously during the course of pumping, which was carried on till the dark current settled. This procedure lasted for 1–2 hrs. The sample holder was sealed then. Irradiations, preirradiations, and conductivity measurements were made *in vacuo*. The effect of ionized air was checked by replacing the polymer sheet by polyethylene which had several decades higher conductivity then the mixed polymers under study. Temperature was kept constant within to 0.1°C. Induced currents were measured by means of an electronic microammeter compensated for the dark currents. The applied voltage varied between 200 and 800 v. Polymer sheets 0.5–1 mm. in thickness were used. The conductivities appeared to be ohmic within this range.

Irradiations were made with a 200 kv. x-ray unit with a 0.1 mm. Cu filter. Some of the irradiations were made with an 500 c. Co^{60} source, with the β-rays filtered out. The induced currents appeared to be the same in each case at the same dose rates. This is illustrated in Figure 2, where data from Co^{60} measurements and those taken by the 200 k.v. x-ray unit are presented. Dose-rates were measured by the ferrous sulfate method.

RESULTS

Figure 1*A* shows a log–log plot of the radiation-induced currents in the mixed polymer as a function of the irradiation dose rate.

Radiation-induced conductivities usually[1] are expressed as

$$\sigma_r \sim I^{\nabla} \tag{1}$$

where I is the dose rate (in roentgens/second). From the curves of figure 1. A value of $\nabla = 0.6$ was obtained for the mixed polymer investigated.

No significant change in σ_r could be detected by changing the temperature up to 60°C.
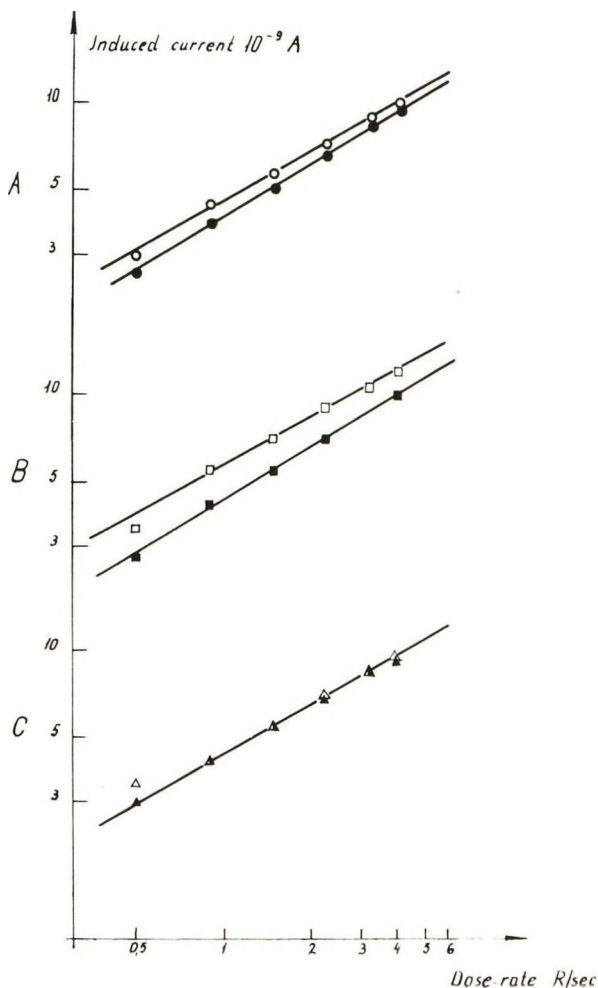
Fig. 1. Effect of preirradiation on the radiation-induced conductivities: (*A*) pure polymer; (*B*) polymer containing benzophenone; (*C*) polymer containing hydroquinone. Total dose 1.45 Mr; (●,■,▲) induced currents measured immediately after preirradiation.
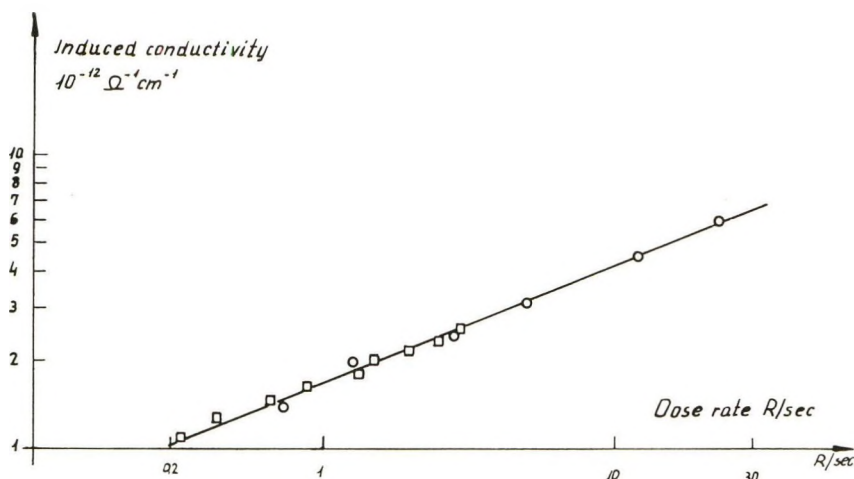
Fig. 2. Radiation-induced conductivity in a mixed polyamide containing such light-sensitizing agents as benzophenone, N,N'-methylene bisacrylamide, and hydroquinone: (□) 200 k.e.v. x-ray-induced conductivities; (O) Co^{60} γ-ray-induced conductivities.

Preirradiation by Co^{60} γ-rays (total dose 1.45 Mr) resulted in a decrease of the induced conductivity, while the ∇ value did not change appreciably (Fig. 1A). The time constants, i.e., the times required for the induced currents to reach equilibrium, were found to be very small (a few seconds for most of the samples investigated). On the other hand, several minutes were required for the dark currents to reach equilibrium.

Curves B and C of Figure 1 show the effect of preirradiation on samples containing benzophenone and hydroquinone. The changes caused by pre-irradiation are increased in samples containing benzophenone and they are practically eliminated by addition of hydroquinone. Figure 2 shows the $\sigma_r(I)$ curve of a mixed polyamide containing light-sensitizing agents, such as N,N'-methylene bisacrylamide, benzophenone, and hydroquinone.

DISCUSSION

According to the experimental results, the radiation-induced conductivities are decreased by increasing the preirradiation dose. This suggests, that some dose-dependent trapping centers are present on which electron and hole recombinations can occur. These centers should not appreciably depend on the dose rate however, since the character of the $\sigma_r(I)$ curves seem to be unaffected by preirradiation. Free radicals may obviously act as such centers.

During the course of preirradiation a certain radical concentration is formed, which depends on the preirradiation dose. This concentration remains fairly unchanged for weeks and is very little affected by the doses received during the course of the actual measurements.

The introduction of such radical trapping-centers leads to an extension

of the conductivity-scheme described by Vul.[2] The basic processes considered are the interactions of mobile electrons with holes, of mobile carriers with traps, and of mobile carriers with free radicals (Fig. 3).

Interaction of the Mobile Electrons with Holes

Electrons can recombine with holes through exciton states. The recombination probability is α_{EH}. Electrons can be pushed back into the mobile (conduction) state by thermal agitation, with a probability of β_{EH}. The exciton state–ground state transition probability is γ_H.

Interaction of the Mobile Carriers with Traps

A certain number of electrons and holes can be trapped by unspecified chemical or crystalline inhomogeneities (traps) with probabilities of α_{ET} and α_{HT}. The probabilities of release from the traps are β_{ET} and β_{HT} for electrons and holes, respectively. The energy distribution of the traps is considered to be uniform.

Interaction of the Mobile Carriers with Free Radicals

Electrons and holes can recombine with the free radicals formed by pre-irradiation. The recombination probabilities are α_{ER} and α_{HR}. Radicals can recombine by themselves with a probability of α_{RR}; this latter is however considered to be very small as compared with the other recombination processes. Following the phenomenological method of Vul,[2] on the basis of
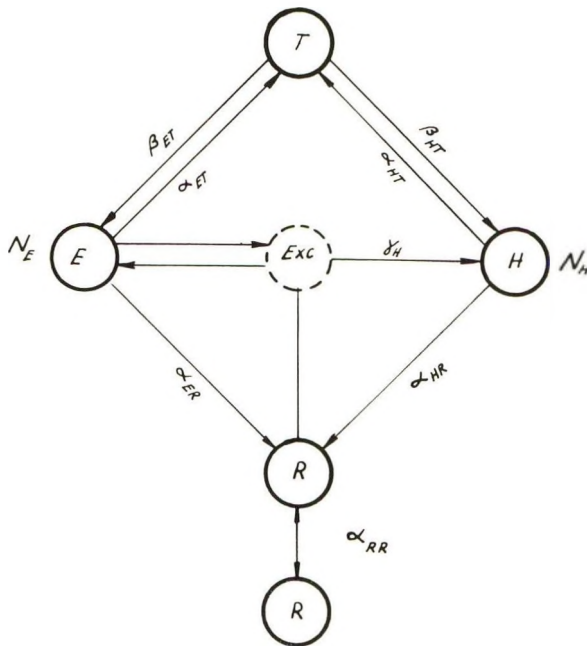
Fig. 3. Conductivity model.

the scheme illustrated in Figure 3, the following kinetic equations can be the derived:

$$N_E N_H + (\alpha_{ER}/\theta_H) N_E N_R - (\Gamma/\theta_H) = 0 \qquad (2)$$

$$N_E N_H + (\alpha_{HR}/\theta_H) N_H N_R - (\Gamma/\theta_H) = 0 \qquad (3)$$

where

$$\theta_H = \alpha_{EH} \gamma_H / \beta_{EH} + \gamma_H$$

Γ is the rate of formation of the electron-hole pairs, as induced by the irradiation. N_E, N_H, and N_R are the electron, hole, and radical concentrations, respectively. On the other hand, the trapping process is not the same for electrons as for holes. Traps are filled up to a certain extent, depending on the ratio of the α and β factors. This results in a difference in the equilibrium concentration of electrons and holes:

$$N_E - N_H = \delta N_T \qquad (4)$$

Introducing eq. (4) into eqs. (2) and (3) and solving them using the assumptions,

$$\frac{4\Gamma}{\theta_H [\delta N_T + (\alpha_{ER}/\theta_H) N_R]^2} \ll 1$$

$$\frac{4\Gamma}{\theta_H [\delta N_T - (\alpha_{HR}/\theta_H) N_R]^2} \ll 1$$

permits the total induced conductivity to be expressed as follows

$$\sigma_r = \frac{u_E \Gamma}{\theta_H \delta N_T + \alpha_{ER} N_R} + \frac{u_H \Gamma}{\theta_H \delta N_T - \alpha_{HR} N_R} + u_H \frac{\theta_H \delta N_T - \alpha_{HR} N_R}{2\theta_H} \qquad (5)$$

where u_E and u_H are the electron and hole mobilities, respectively. The last term in eq. (5) does not depend on the irradiation dose rate; it depends only on the total dose through N_R. It is however not a dark conductivity. Equation (5) is an equilibrium equation, where all the charge carriers are produced by the irradiation effects. In the absence of the radiation the carriers are released from the traps and diminish in nonequilibrium period a few seconds in duration. After that, only carriers responsible for the dark conductivity are present, which may have a quite different mechanism.

The appearance of a dose rate-independent term in the expression for σ_r can be interpreted by the difference in electron and hole trapping. This difference would decrease the rate of recombination between electrons and holes, resulting in a larger conductivity at the same irradiation dose-rate. According to eq. (5), $\sigma_r(I)$ follows eq. (6) instead of eq. (1):

$$\sigma(I) = \Sigma_0 I^\nabla + \sigma_0 \qquad (6)$$

Equation (5) would give $\nabla = 1$ in accordance with Fowler's results in the case of uniform distribution of traps. The same follows from the discussion

of Vul.[2] The difference is, that the absolute term σ_0 would shift the apparent ∇ values towards 0.5 even in the case of uniform trap distribution if ∇ is determined from the log–log plot of $\sigma_r(I)$, as usual. The "true" value should be evaluated by plotting $\ln(\sigma_r - \sigma_0)$ against I, where σ_0 can be determined from the linear plot by extrapolation to $I = 0$.

Since σ_0 is not negligible, apparent ∇ values may differ considerably from the true ones. In the present case, apparent ∇ values calculated from the $\ln \sigma_r - \ln I$ plot are close to 0.6, while the true values calculated from the $\ln(\sigma_r - \sigma_0)$–$\ln I$ plot are equal to about 0.9, indicating a fairly uniform distribution of traps. This can explain the small temperature dependence and small time constants observed, which are characteristic of the uniform distribution.

The numerical values of Σ_0, σ_0, and ∇ can be calculated by plotting σ_r against I and getting the first approximation of σ_0 by extrapolation. With the use of this value $\ln(\sigma_r - \sigma_0)$ is plotted against $\ln I$, and from the slope of the curve first approximation values for ∇ and Σ_0 are obtained. This procedure is repeated until a good fit with the experimental point is obtained. Some values of σ_0 and ∇ calculated this way are tabulated in Table I. As shown, preirradiation resulted in a significant decrease in

TABLE I

Additive	No preirradiation		Preirradiation, 1.45 Mr	
	∇	$\sigma_0 \times 10^{-13}$, cm.$^{-1}$	∇	$\sigma_0 \times 10^{-13}$, cm.$^{-1}$
None	0.9	1.1	0.9	0.8
Benzophenone, 1.3%	0.9	2.8	1	1.7
Hydroquinone, 3%	0.9	2.2	0.9	2.2

σ_0, leaving ∇ unchanged. The decrease in σ_0 can be caused by the increase of radical concentration N_R, as stated in eq. (5). Additives are believed to affect the preirradiation effects by controlling the radical concentration. Thus the strong radical acceptor, hydroquinone, practically eliminates the preirradiation effect, giving a rather irradiation-resistant product. Addition of benzophenone, on the other hand, increases the preirradiation effect, probably by producing extra radicals.

References

1. Fowler, I. F., *Proc. Roy. Soc. (London)*, **A236**, 464 (1956).
2. Vul, B. M., *Fiz. Tverd. Tela*, **3**, 2264 (1961).

Résumé

On a mesuré des conductivités induites par radiation aussi élevées que $10^{-12} \Omega$ cm^{-1} dans des mélanges de polymère et polyamide irradiés par les rayons X et les rayonne-

ments gamma du Co⁶⁰ à des vitesses de dose de 0,1 à 20 R/sec. On n'a pas remarqué de dépendance vis-à-vis de la température pour les conductivités induites entre 10° et 60°C, tandis que les conductivités sans irradiation suivent la loi exponentielle habituelle avec des énergies d'activation entre 1 et 2 eV. Une préirradiation des échantillons fait décroître les conductivités induites. Cet effet peut être controlé par l'addition de benzophénone et d'hydroquinone. On présente un modèle phénoménologique pour expliquer le mieux possible ces résultats.

Zusammenfassung

Strahlungsinduzierte Leitfähigkeit bis zu $10^{-12}\,\Omega^{-1}\,cm^{-1}$ wurde in mit Polyamid gemischten Polymeren, die mit Röntgen- und Co⁶⁰-Gammastrahlen bei Dosisleistungen von 0,1 bis 20 r/sec bestrahlt wurden, gemessen. Es konnte keine Temperaturabhängigkeit der induzierten Leitfähigkeit zwischen 10 und 60°C gefunden werden, während die Dunkelleitfähigkeit dem gewöhnlichen Exponentialgesetz mit Aktivierungsenergien zwischen 1 und 2 eV gehorchen würde. Vorgestrahlung der Proben ergab eine Abnahme der induzierten Leitfähigkeit. Dieser Effekt wurde durch Zusatz von Benzophenon und Hydrochinon unter Kontrolle gehalten. Ein phänomenologisches Modell zur Erklärung der Ergebnisse wird aufgestellt.

Free Radical Polymerization and Copolymerization of Bicyclo-(2.2.1)-hepta-(2.5)-diene (Norbornadiene)

JOSEPH PELLON, ROBERT L. KUGEL, RUTH MARCUS, and ROBERT RABINOWITZ, *Chemical Department, Central Research Division, American Cyanamid Company, Stamford, Connecticut*

Synopsis

A brief study of the homopolymerization of norbornadiene indicated that pre-gel polymer is limited to product having reduced viscosities below 0.2 dl./g. Pre-gel polymer of 17,000 molecular weight was isolated and characterized: pre-gel polynorbornadiene is soluble in benzene or chloroform, softens at 220–240°C., is thermosetting and shows poor molding characteristics. A cast rod of polynorbornadiene was found to have a heat distortion temperature of 186°C. and a flexural strength of 13,300 psi. Copolymer reactivity ratios of norbornadiene (M_1) determined with vinyl acetate were $r_1 = 1.3$ and $r_2 = 0.8$; with *p*-chlorostyrene, $r_1 \approx 0.01$ and $r_2 \approx 85$. Thermal behavior of several copolymers was determined.

INTRODUCTION

Free radical homopolymerization and copolymerization of norbornadiene was initially disclosed in publications by Kargin, Plate, and Dudnik,[1] and by Kolesnikov and co-workers.[2] The essential aspects of the free radical polymerization of norbornadiene have been outlined by the recent publications of Graham, Buhle, and Pappas,[3] Zutty,[4] and Wiley et al.[5] The purpose of the present paper is to present a further description of the homopolymerization, properties, and copolymerization reactivity of norbornadiene.

EXPERIMENTAL

Materials Used

Norbornadiene purchased from Shell Chemical Company was purified by fractional distillation in a Todd apparatus. A glass-helices column of intermediate size was used, and a heart cut isolated at a low take-off to reflux ratio (99:1–20:1). Purified monomer was stored under argon or purified nitrogen and used soon after it was distilled. Storage under an inert atmosphere was believed necessary, since the monomer formed a crystalline, nonpolymeric deposit on exposure to air. Other monomers used in copolymerization studies were purified by standard procedures.

Polymerization Procedures

Except for the runs used to prepare polymer for determination of its properties, all other polymerizations were carried out under carefully deaerated conditions in small polymerization tubes using carefully regulated constant temperature baths. Polymer was isolated as indicated in the scale-up procedure which follows.

Scale-up of Homopolymerization

A 250-ml. three-necked round-bottomed flask equipped with a reflux condenser, gas inlet, and outlet tube, and containing an oval Teflon-covered magnetic stirring bar was purged with nitrogen for 1 hr. A slurry of 0.1804 g. of azobisisobutyronitrile (AIBN, 0.1 mole-%) in 100 g. of norbornadiene was added under nitrogen, and the stirred mixture was purged for several minutes with N_2. Polymerization was carried on over a period of 6 hr. at 70°C.

The polymer was isolated by precipitating in hexane. Purification was achieved by twice dissolving in benzene and precipitating in hexane. The polymer was finally dissolved in benzene, filtered, and freeze-dried; yield 5.7 g.

RESULTS AND DISCUSSION

Homopolymerization

A brief study was made of the effect of varying the initiator, temperature, and initiator concentration on the free radical polymerization of norbornadiene. The results are summarized in Tables I and II.

Conversion after 24 hr. with various radical initiators is given in Table I. The temperature used for the different initiators was chosen so that all initiator half-lives would be of the order of 5 hr. Soft gel (Nos. 3 and 4) could be easily broken-up and extracted by boiling benzene. Hard clear plastic (Nos. 5 and 6) was cured and after several hours in boiling benzene was not swollen.

TABLE I
Free Radical Polymerization of Norbornadiene[a]

No.	Initiator	Temp., °C.	Appearance	Conversion, %
1	Thermal	70	Colorless liquid	0
2	Thermal	150	Colorless liquid	Trace
3	Azobisisobutyronitrile	70	Colorless gel	56[b]
4	Benzoyl peroxide	80	Light-yellow gel	36[b]
5	tert-Butyl perbenzoate	110	Light-yellow hard solid	—
6	Di-tert-butyl peroxide	130	Colorless hard solid	—

[a] Polymerization run in bulk for 24 hr. at 1 mole-% initiator.

[b] Represents insoluble polymer isolated after extraction with boiling benzene.

TABLE II
Effect of Reaction Conditions on Polymer Viscosities

Initiator	Initiator concn., mole-%	Temp., °C.	Time, hr.	Conversion, %	Reduced viscosity, dl./g.[a]
Di-*tert*-butyl peroxide	0.1	130	2	5	0.14
	0.01	130	2	3	0.14
	0.01	120	20	4.6	0.10
	0.01	110	48	3.8	0.15
Azobisisobutyronitrile	0.4	70	3	6.7	0.2
	0.01	70	7	4	0.14
	0.1	60	24	3.2	0.13
	0.01	60	48	1.7	0.14
	0.1	30	792	4	0.19[b]
Spontaneous[c]	Room temp.		—	0.8	0.11

[a] Reduced viscosity in benzene at 0.1%.

[b] Reduced viscosity in chloroform.

[c] Polymer was isolated from a sample of monomer which had been exposed several times to the air and then allowed to stand at room temperature.

In a search of conditions for obtaining soluble polymers of norbornadiene of maximum molecular weight, reaction temperature and initiator concentration were varied to alter the polymerization rate. Results are given in Table II.

The polymer molecular weights were found not to be sensitive to the rate of polymerization; reduced viscosities all were in the range of 0.1–0.2 dl./g.

Attempts at emulsion polymerization of norbornadiene also gave pre-gel polymers having intrinsic viscosities less than 0.1 dl./g. at low conversions and insoluble polymers at higher conversions.

It was of interest to compare the overall polymerization behavior of norbornadiene to other cyclic olefins. Results given in Table III show that ease of polymerization decreased in the order:

TABLE III
Relative Polymerizability of Cyclic Olefins

Initiator	Temp., °C.	Conversion, %[a]		
Azobisisobutyronitrile	70	0	1	Soft gel
tert-Butyl perbenzoate	110	0	2	Cured solid
Di-*tert*-butyl peroxide	130	0	12	Cured solid

[a] Conversion after 24 hr. with 1 mole-% initiator.

Homopolymer Properties

Table IV summarizes the properties of polynorbornadiene isolated at low conversions.

The free radical polymerization of norbornadiene is typified by the formation of soluble low molecular weight polymer at low conversions while higher conversion leads to cross linked polymer.

The essential features of the spectra (infrared and NMR) of the homopolymer prepared in this study are in accord with those recently reported by Wiley et al.[5] for the radiation-polymerized norbornadiene of 1500 molecular weight. These authors consider the ratio of nortricyclene (A) to norbornylene (B) units in their polymer (I) to be equal to 2/1.
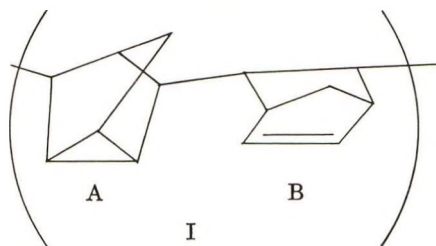
TABLE IV
Properties of Polynorbornadiene Obtained at Low Conversions[a]

Appearance	White powder
Conversion, %	6
Solubility	Soluble in benzene, tetrahydrofuran, CHCl$_3$, and CCl$_4$
Density, g./cc.	1.033
Crystallinity (x-ray)	Amorphous
Intrinsic viscosity, dl./g.[b]	0.20
Huggins' constant k'[c]	0.06
Molecular weight M_w[d]	17,000
Ratio of unsaturated protons to saturated protons[e]	1/17.5
Infrared[f]	Strong peaks at 710, 800 and 3050 cm.$^{-1}$
Thermal behavior on heating	Darkened at 225°C., softened at 238°C.; thermoset
Thermogravimetric analysis[g]	
In air $T'_i = 130$°C.	
$T_{10} = 322$°C.	
In N$_2$ $T_{10} = 348$°C.	

[a] Polymer prepared by polymerization for 6 hr. at 70°C. with 0.1 mole-% azobisisonitrile (see Experimental).

[b] In CHCl$_3$ at 30°C.

[c] Calculated from the formula $\eta_{sp}/c = [\eta] + k'[\eta]^2c$.

[d] Light scattering in benzene.

[e] Nuclear magnetic resonance in CDCl$_3$, ratio of area 3.90τ/7–10τ.

[f] Infrared in KBr pellet.

[g] T_i = temperature at which initial weight loss occurs; T_{10} = temperature at which 10% weight loss has occurred; heating rate is 10°C./min.

On the basis of the NMR data, homopolymer prepared in this study was found to have an A/B ratio of 3.6/1.

TABLE V
Mechanical Properties of Cast Polynorbornadiene[a]

	Polynorbornadiene	Poly(methyl methacrylate)
Heat distortion temp., °C.	186	76
Impact strength, ft./lb./in.^{2}	3.5	4.0
Flexural strength, psi	13,300	$17,000 \pm 600$
Flexural modulus, psi	0.38×10^6	0.49×10^6

[a] Rods 6 in. in length were machined and polished to $1/4$ in. diameter and used in determining physical properties.

TABLE VI
Determination of Reactivity Ratios for Norbornadiene (M_1)

Comonomer (M_2)	Molar feed ratio, $M_1/M_2{}^a$	Adjusted molar feed ratio, $M_1/M_2{}^b$	Conversion, %	Analysis, % carbon	Molar polymer ratio, M_1/M_2	Reactivity ratios[c] r_1	r_2
Vinyl acetate	0.2579	0.2550	10.4	64.76	0.3162		
	0.3767	0.3703	15.4	67.75	0.4752		
	0.4078	0.4030	11.0	68.15	0.4997		
	0.6476	0.6362	13.4	72.46	0.8286	1.28	0.82
	1.316	1.311	6.65	77.56	1.4851		
	3.116	3.100	5.9	84.10	3.6983		
	4.832	4.819	4.3	86.71	6.3946		
p-Chlorostyrene	2.0517	2.2212	6.5	69.49	0.0110		
	2.7243	2.9890	6.6	69.84	0.0358		
	3.9195	4.4451	6.9	70.08	0.0533	0.01	85
	5.4045	6.0317	4.9	70.82	0.1097		
	7.4568	8.3371	3.8	70.68	0.0987		

[a] Mixtures of 3–5 g. of monomer and about 15 mg. of azobisisobutyronitrile.
[b] Average of initial and final monomer ratios.
[c] Calculated on the basis of the Fineman-Ross equation.

TABLE VII
Copolymerization of Vinyl Acetate and Norbornadiene[a]

AIBN, g.[b]	Time, hr.	Conversion, %	Reduced viscosity, dl./g.[b]
0.0009	48	8.0	0.22
0.0030	$20^1/_4$	8.6	0.22
0.0028	48	Gel	—
0.0028	32	24.5	0.33

[a] Monomer feed 2.6 g. vinyl acetate and 1.8 g. norbornadiene.
[b] Measured at 0.5% concentration in benzene at 30°C.

TABLE VIII
Scale-Up Copolymerization Results[a]

| | Composition of feed | | | | | | | | Thermal behavior | | | |
Comonomer (M_2)	M_1, g.	M_2, g.	AIBN, g.	Molar ratio M_1/M_2	Time, hr.	Conversion, %	Intrinsic viscosity, dl./g.[b]	Polymer M_1/M_2	Softening temp., °C.[c]	Flow temp., °C.[c]	T_{10}, °C.[d] Air	T_{10}, °C.[d] N_2
Vinyl acetate	23.05	33.6	0.039	0.641	16	12.2	0.26	0.7195	70–100	110–160	328	325
Vinyl acetate	97.20	29.16	0.360	3.115	25.5	11.2	0.15	3.5106	80–135	240[e]	300	343
Methyl methacrylate	86.99	21.01	0.15	4.498	5	7.7	0.37	0.1191	80	140	335	335
Styrene	86.88	13.19	0.894[f]	7.4428	106[f]	7.6	0.12	No analysis	100–110	115–135	350	365
Acrylonitrile	28.6[g]	31.7	0.24	0.520	11.25	—	0.19[h]	0.467	100	135–160	383	384

[a] M_1 = norbornadiene, temperature = 60°C.
[b] In benzene at 30°C.
[c] Using a Fisher John's melting point apparatus.
[d] Temperature at which 10% weight loss occurs when a sample is heated at 10°C./min.
[e] Never free flowing.
[f] 0.385 g. added at 0 hr.; 0.214 g. added at 34 hr.; 0.295 g. added at 87 hr.
[g] Run in 75 ml. of butyrolactone.
[h] In acetone.

Properties of Polynorbornadiene Casting

Polynorbornadiene, described in Table IV, could not be molded to give test specimens suitable for determining physical properties. Standard procedures for preparing test specimens by cast polymerization proved inapplicable since adequate curing was obtained only at temperatures above the boiling point of the monomer (90–160°C.). However, rods of the polymer were successfully cast in sealed glass tubes using an aluminum liner to prevent crazing. Since the rods were not standard test specimens it was necessary to compare physical properties with those of a known plastic in the same form. Table V gives a comparison of the physical properties of cast polynorbornadiene with poly(methyl methacrylate).

Copolymerization

Reactivity ratios of norbornadiene with vinyl acetate and p-chlorostyrene were determined; data are presented in Table VI.

The reactivity ratios determined in this study and those given by Zutty[4] clearly define the reactivity of norbornadiene to be of a low order.

Copolymer Properties

Copolymerization of norbornadiene was generally in accord with behavior expected on the basis of data on the homopolymerization. In the copolymerization of norbornadiene with vinyl acetate, polymer viscosities were independent of initiator concentration but were directly related to conversion. The viscosity increased as the gel point was approached. In one of the examples tabulated in Table VII, copolymerization was carried to 24.5% conversion without gelation. It was observed, as expected, that as the percentage of norbornadiene in the monomer mixture decreased, the conversion before gelation increased.

As indicated by data given in Table VIII, the solubility and thermal behavior of the copolymers of norbornadiene were in most cases "averages" of the monomer pairs. A copolymer of vinyl acetate and norbornadiene containing 3 moles of norbornadiene to 10 of vinyl acetate started to soften and could be pressed to yield transparent spots at 50°C. Another copolymer containing 6.5 moles of norbornadiene to 1 mole of vinyl acetate did not soften with pressing until 230°C. and never melted. At 280°C. it became yellow and was later found to be insoluble in benzene.

References

1. Kargin, V. A., N. A. Plate, and L. A. Dudnik, *Vysokomol. Soedin.*, **1**, 420 (1959).
2. Kolesnikov, G. S., et al., *Vysokomol. Soedin.*, **2**, 451 (1960).
3. Graham, P. J., E. L. Buhle, and N. Pappas, *J. Org. Chem.*, **26**, 4658 (1961).
4. Zutty, N. L., *J. Polymer Sci.*, **A1**, 2231 (1963).
5. Wiley, R. H., W. H. Rivera, T. H. Crawford, and N. F. Bray, *J. Polymer Sci.*, **61**, 172 (1962).

Résumé

Une étude brève de l'homopolymérisation du noroborbornadiène indique qu'un polymère était obtenu présentant une viscosité réduite, inférieure à 0.2 dl/g. Un polymère pré-gel d'un poids moléculaire de 17.000 fut isolé et ses caractéristiques étudiées: le polynorbornadiène est soluble dans le benzène, ou le chloroforme, ramollit à 220–240°C, est thermostable et présente de pauvres caractéristiques de moulage. On trouve qu'une barre coulée de polynoroborbornadiène présente une température de distorsion à la chaleur de 186°C et une force de rupture à la flexion de 13.300 livres/pouce^2. Les paramètres de réactivité de la copolymérisation du norbornadiène (M_1) avec l'acétate de vinyle sont $r_1 = 1.3$ et $r_2 = 0.8$; avec le p-chlorostyrène on trouve $r_1 \approx 0.01$ et $r_2 \approx 85$. On a étudié le comportement thermique de plusieurs copolymères.

Zusammenfassung

Eine kurze Untersuchung der Homopolymerisation von Norbornadien zeigte, dass Prägelpolymeres auf ein Produkt bei reduzierten Viskositäten unter 0,2 dl/g beschränkt ist. Prägelpolymeres mit dem Molekulargewicht 17.000 wurde isoliert und charakterisiert: Prägelpolynorbornadien ist in Benzol oder Chloroform löslich, erweicht bei 220–240°, ist wärmehärtbar und zeigt schlechte Spritzgusscharakteristik. Ein Gussstab aus Polynorbornadien besitzt eine Wärmebeständigkeitsgrenze von 186°C und eine Biegebeständigkeitsgrenze von 186°C und eine Biegefestigkeit von 13.300 lb/in^2. Die mit Vinylacetate bestimmmten Copolymerreaktivitätsverhältnisse von Norbornadien (M_1) waren $r_1 = 1,3$ und $r_2 = 0,8$, mit p-Chlorstyrol $r_1 \approx 0,01$ und $r_2 \approx 85$. Das thermische Verhalten einiger Copolymerer wurde bestimmt.

Kinetic Study of the Polymerization of α-*d*-Styrene and/or Styrene by Homogeneous Catalysis.   Part I

C. G. OVERBERGER, F. S. DIACHKOVSKY,* and P. A. JAROVITZKY,† *Department of Chemistry, Polytechnic Institute of Brooklyn, Brooklyn, New York*

Synopsis

Increases in the rates of polymerization of α-*d*-styrene and/or styrene by homogeneous catalysis with the $(C_5H_5)_2TiCl_2$–$Al(C_2H_5)_2Cl$ catalyst system were shown to be directly proportional to the α-*d*-styrene monomer concentration.   These rate increases were explained by an increase in the concentration of active centers.   Polymer intrinsic viscosities were shown to be independent of the α-*d*-styrene monomer concentration. Changes in the polymerization rates were correlated with observed changes in the catalyst composition measured spectrophotometrically.   A scheme is suggested to explain the observed results.

INTRODUCTION

It has been shown earlier[1-4] that during the reaction of aluminum alkyls and $(C_5H_5)_2TiCl_2$, soluble species are produced which have the ability to catalyze the polymerization of some olefins.   It was shown that the ease of reduction of the $(C_5H_5)_2TiCl_2$ component is a function of the type of aluminum alkyl used; e.g., with $Al(C_2H_5)_3$, the reduction of titanium to a lower valence state occurs rapidly and results in the formation of a blue soluble complex designated as $(C_5H_5)_2TiCl·Al(C_2H_5)_2Cl$, which has been shown to have a very low catalytic activity.   This same reaction occurs with $Al(CH_3)_3$ to form $(C_5H_5)_2TiCH_3Cl·Al(CH_3)_2Cl$; its rate of reduction is very slow but can be accelerated by the addition of monomer, e.g., ethylene.   The rate of polymerization was shown to be proportional to the concentration of intermediate complexes formed during the reduction reaction of $(C_5H_5)_2TiCl_2$ with AlR_3.   Specifically,[4] it was shown that the rate of polymerization of ethylene was proportional to the concentration of an alkylated complex of titanium, e.g., $(C_5H_5)_2TiRCl·AlR_2Cl$.

---

* Present address: Institute of Chemical Physics of the Academy of Sciences of the U.S.S.R., Moscow, U.S.S.R.   Dr. F. S. Diachkovsky was at the Polytechnic Institute of Brooklyn from September to December 1962 under the terms of the exchange agreement between the Academy of Sciences, U.S.A., and the Academy of Sciences, U.S.S.R.

† This paper comprises a portion of a dissertation submitted by P. A. Jarovitzky in partial fulfillment of the requirements for the degree of Doctor of Philosophy in the Graduate School of the Polytechnic Institute of Brooklyn.

The use of α-d-styrene as a monomer in a heterogeneous system with TiCl$_4$ and Al(C$_2$H$_5$)$_3$ has been shown[5] to result in increasing rates of polymerization compared to those for styrene itself. The rate increases, as a function of α-d-styrene concentration, were suggested to be due to increasing concentrations of active centers. The suggested mechanism for the increased concentrations of active centers could not easily be proven, because of the instrumental limitations inherent in a heterogeneous system.

Based on the above, it was of interest to study the homopolymerization and copolymerizations of styrene and α-d-styrene, by homogeneous catalysis, e.g., with the use of (C$_5$H$_5$)$_2$TiCl$_2$ and Al(C$_2$H$_5$)$_2$Cl, in an effort to determine (a) the rate of polymerization and (b) the rate of reduction of Ti^{+4} to Ti^{+3}, both as a function of α,d-styrene concentration, so as to correlate these two effects. This particular catalytic system was previously studied in detail,[3,4,6-8] and a mechanism for the formation of the final, blue, and inactive complex of Ti^{+3} was suggested.[7]

EXPERIMENTAL

Preparation of α-d-Styrene

α-d-Styrene was prepared by the general procedure shown in eqs. (1) and (2). A detailed account of the preparation is given in an earlier paper.[5]

$$ (\geqq 85\%) \qquad (1) $$

$$ (\geqq 85\%) \qquad (2) $$
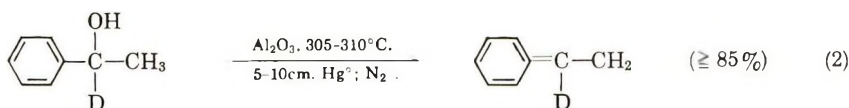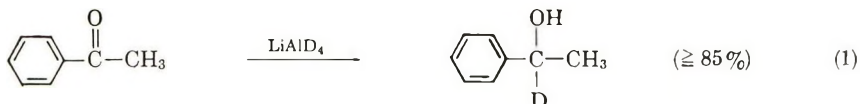
Determination of Reaction Rates

The experimental technique for the determination of rates of polymerization is that used and reported earlier for the heterogeneous Ziegler-Natta system.[5]

Determination of Rate of Change of Catalyst Components

The formation of the alkylated complex (C$_5$H$_5$)$_2$Ti(C$_2$H$_5$)Cl·Al(C$_2$H$_5$)Cl$_2$ (I) and its reduction to the final inactive form (C$_2$H$_5$)$_2$TiCl·Al(C$_2$H$_5$)Cl$_2$ (II), as per Long and Breslow[3] was followed by changes in the ultraviolet intensities at 520 and 750 mμ, respectively. The transition of I to II was followed (1) without the addition of monomer, (2) in the presence of styrene, and (3) in the presence of α-d-styrene.

All measurements were made on a Perkin-Elmer 350 spectrophotometer, with a reaction and solvent reference cell of 1 cm. width, and under the following reaction conditions: solvent benzene; temperature ca. 25°C.;

$[(C_5H_5)_2TiCl_2] = 4.6 \times 10^{-3}$ mole/l.; $[Al(C_2H_5)_2Cl] = 4.4 \times 10^{-1}$ mole/l.; total volume = 3.5 cm.³. Procedure for typical cell preparation is as follows. After the addition of 4.0×10^{-3} g. (1.6×10^{-5} mole) of $(C_5H_5)_2Ti-Cl_2$, the cell was repeatedly evacuated (at ≤ 0.5 mm.) and flushed with dry nitrogen through a rubber serum cap attached to the cell by means of a wide bore syringe needle. Monomer and solvent were next added volumetrically with a syringe in such amounts as to make the final volume 3.5 cm.³ after the addition of 2.0 cm.³ of 0.77 F $Al(C_2H_5)_2Cl$ solution in benzene. The latter is added via an especially designed catalyst delivery system devised and described in an earlier paper.[5]

Determination of Polymer Deuterium Content

The deuterium content of the polymers resulting from different feed concentrations of α-d-styrene monomer was estimated by infrared intensities measured at 2250–2260 cm.⁻¹ from films cast on salt plates from a chloroform solution. Measurements were made relative to the infrared spectrum of 100% pure α-d-styrene as analyzed by mass spectroscopy and nuclear magnetic resonance.

TOTAL MONOMER CONCENTRATION = CONSTANT = 0.41 MOLE/L

$[M_H]$ = STYRENE
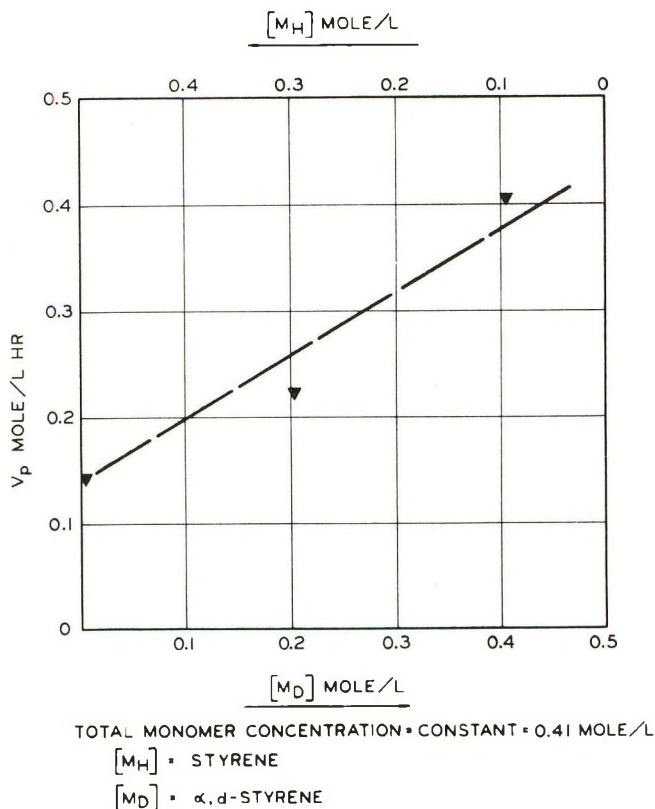
$[M_D]$ = α,d-STYRENE

Fig. 1. Homogeneous catalysis with $Al(C_2H_5)_2Cl + (C_5H_5)_2TiCl_2$. Effect of α-d-styrene concentration on initial reaction velocity.

Determination of Reaction Rates

A summary of rate data obtained is shown in Table I.   A plot of polymerization rates as a function of α-d-styrene concentration at a constant total monomer concentration of 0.41 mole/l. is shown in Figure 1.

TABLE I

Reaction Rates for Homopolymerization and/or Copolymerization of Styrene and/or α-d-Styrene by Homogeneous Catalysis with $Al(C_2H_5)_2Cl + (C_5H_5)_2TiCl_2$[a]

$[M_H]$, mole/l.	$[M_D]$, mole/l.	Temp. $+0.05$, °C.	Conversion, %	Initial rate, mole/l. hr.	$[\eta]_{C_6H_5Cl}^{29.3° C.}$
0.41	0	25.5	10	0.160	0.07
0.41	0	26.0	12	0.138	0.06
0.41	0	25.9	10	0.111	0.07
0.41	0	26.0	12	0.161	0.06
0.205	0.205	26.5	15	0.225	0.06
0	0.41	26.2	16	0.410	0.05

[a] $[Al(C_2H_5)_2Cl]$ = constant = 0.182 mole/l.; $[(C_5H_5)_2TiCl_2]$ = constant = 0.01 mole/l.; time = constant = 40 min.; average "standard" rate (100% styrene) = 0.143 ± 0.018; RMD = $\pm 12.6\%$; $[M_T]$ = constant = 0.41 mole/l. = total monomer concentration; $[M_H]$ = concentration of styrene; $[M_D]$ = concentration of α-d-styrene.
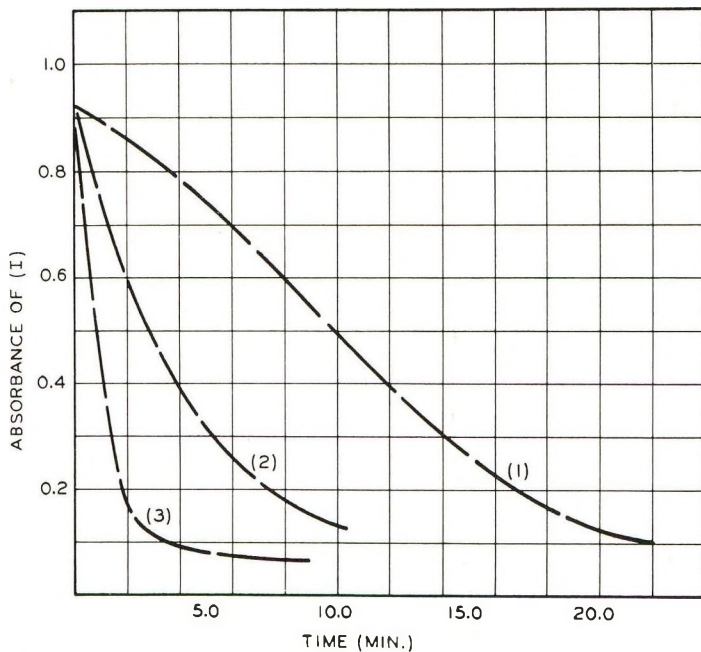
Fig. 2. Reduction of I as a function of time (measured at 520 mμ): (1) no monomer; (2) 0.62 mole/l. of styrene; (3) 0.62 mole/l. of α-d-styrene.

Determination of Rate of Change of Catalyst Components

Absorption values obtained for the disappearance of I in absolute units as a function of time are shown in Figure 2 for (a) no added monomer, (b) 0.62 mole/l. of styrene, and (c) 0.62 mole/l. of α-d-styrene.
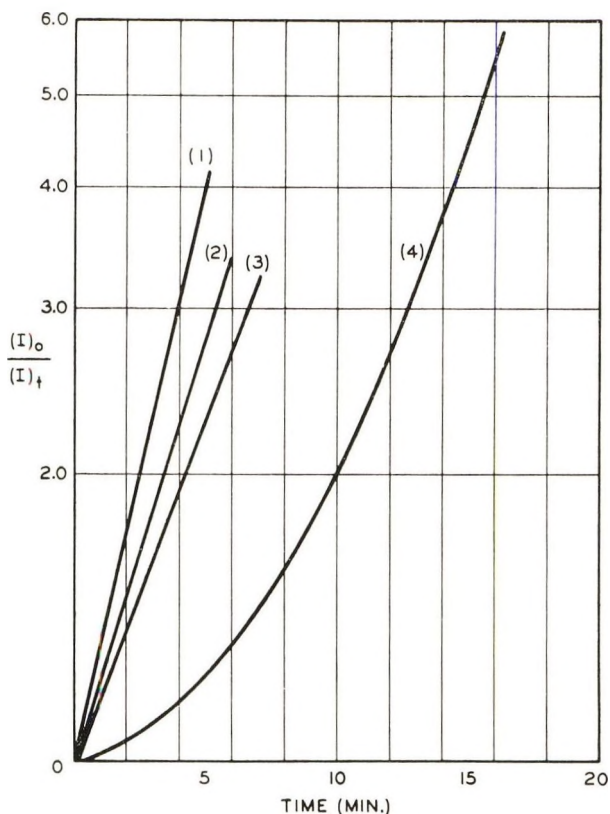
Fig. 3. First-order plots for reduction of I (measured at 520 mμ): (1) $[M_H]$ = 1.23 mole/l.; (2) $[M_H]$ = 0.62 mole/l.; (3) $[M_H]$ = 0.31 mole/l.; (4) no monomer.

Typical first-order plots for the rate of disappearance of I are shown in Figure 3 for (a) no added monomer and (b) styrene at different total monomer concentrations.

DISCUSSION

Data shown in Table I and plotted in Figure 1 indicate that the rate of polymerization increases with increasing α-d-styrene concentrations at a constant total monomer concentration. This rate increase is almost three-fold in the limit of 100% α-d-styrene compared to the rate of homo-polystyrene formation. The rate increase appears to be a linear function of α-d-styrene concentration, contrary to the effect noted for the hetero-

geneous Ziegler-Natta polymerization.[5] At low conversions the rate of polymerization can be approximated by the rate of propagation, e.g.,

$$V_{\text{Polymerization}} = V_{\text{Propagation}} = K_p[C^*][M_T]^r$$

where K_p is the propagation constant, $[C^*]$ is the concentration of active centers, $[M_T]$ is the total monomer concentration, and r is the order of reaction with respect to monomer.

At a constant total monomer concentration, increases in rate as a function of α-d-styrene concentration must then be explained either by ΔK_p or $\Delta[C^*]$, e.g., where:

$$\Delta K_p = (K_p)_D - (K_p)_H > 0$$

or

$$\Delta[C^*] = [C^*]_D - [C^*]_H > 0$$

where subscripts D and H refer to α-d-styrene and styrene, respectively.

Examination of final polymer films by infrared for this catalytic system indicate that here, as well as reported previously for the heterogeneous Ziegler-Natta system,[5] the deuterium content of the polymer is, within analytical errors, identical to the monomer feed, the conclusion being that in all probability, especially as measured at these low conversions, $(K_p)_D = (K_p)_H$.

The rate increases must then be explained in terms of $\Delta[C^*]$, analogous to the heterogeneous Ziegler-Natta catalyst system, reported earlier,[5] e.g., $\Delta V_p \propto \Delta[C^*]$.

Since this homogeneous catalyst system has been previously studied and defined in terms of the ultraviolet absorption spectra for two known components, it was of interest to study the rate of disappearance of I at 520 $m\mu$ and the rate of formation of II at 750 $m\mu$ as a function of (a) time only, without the addition of monomer, (b) α-d-styrene and styrene at the same monomer concentration and (c) styrene at varied total monomer concentrations.

Data plotted in Figure 2 indicate that:

$$(-d[I]/dt)_0 < (-d[I]/dt)_M$$

where $I = (C_5H_5)_2Ti(C_2H_5)Cl\cdot Al(C_2H_5)Cl_2$ and the subscripts 0 and M refer to the absence and presence of monomer, respectively; also,

$$(-d[I]/dt)_D > (d[I]/dt)_H$$

where the subscripts D and H refer to α-d-styrene and styrene, respectively, measured at the same monomer concentration of 0.62 mole/l.

Increasing monomer concentrations yield increasing values of $(-d[I]/dt)_M$. Typical rates of $(-d[I]/dt)_M$ for styrene at varied total monomer concentrations are shown in Figure 3 and indicate that the rate of disappearance of [I] is proportional to the first power of [I]. In the absence of

added monomer, $(-d[I]/dt)_0$ appears to be proportional to the square root of $[I]$.

It had previously been reported that $(-d[I]/dt)_0$ is proportional to the first power of $[I]$ by Long and Breslow[3] and to the square root of $[I]$ by Shilov et al.[6-8] The latter explained the square-root dependence by a dissociation of I to ionic species, which are said to be in equilibrium with $[I]$. Data indicate that these present findings support the work reported by Shilov. It is very likely that the addition of monomer to this catalyst system either destroys or shifts the equilibrium in such a way, that the square-root dependence is changed to a first-power dependence on $[I]$.

Measurements made at 520 and 750 mμ show the existence of an isosbestic point at 650 mμ. The nature of this isosbestic point is, within the experimental errors of these measurements, unaffected by the addition of either styrene or α-d-styrene monomer, but appears at constant values of wavelength and intensity of absorption for all tested experimental conditions. The existence of an isosbestic point by definition, means: $[I] + [II]$ = constant.

However, the increases in the rates of polymerization with increasing α-d-styrene concentrations indicate that the concentrations of active centers is increased. Perhaps more precisely, the concentration of active centers is decreased less with α-d-styrene than with styrene, since we are certainly not creating more growth sites than are potentially available from the catalyst itself. This suggests that a reaction at the α-carbon of styrene occurs which results in the destruction of C^* and thereby probably modifying the monomer as well as the catalyst. It is probable that the destruction of C^* is a reduction of Ti to a lower valence state (<4 or <3) which can no longer function as an active site for polymerization. The ability of a
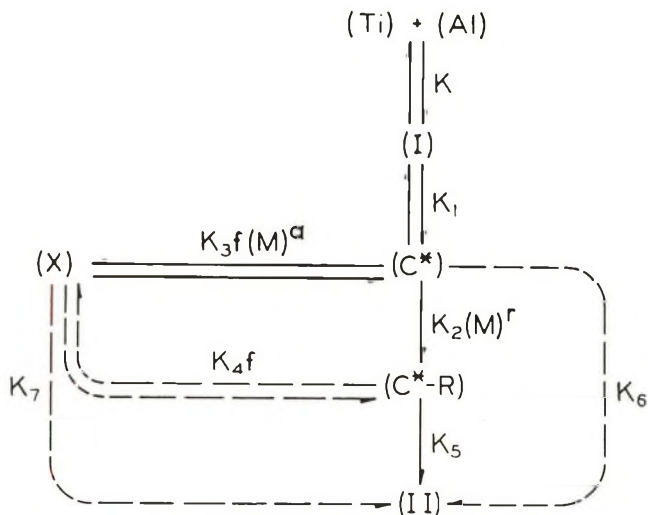
Fig. 4. Reaction scheme for homogeneous catalysis with $Al(C_2H_5)_2Cl + (C_5H_5)_2TiCl_2$.

monomer to destroy the potential catalyst sites in this catalytic system has been suggested earlier.[8]

If the formation of inactive C^* by monomer is presented as the formation of some new and unknown species (X), then the observed isosbestic point suggests: (a) [X] << [I] or [II]; (b) X yields an absorption identical to either I or II.

In addition to an accelerated rate of disappearance of [I], the rate of formation of inactive catalyst [II] was equally enhanced, and therefore in agreement with the observed constancy of the isosbestic point.

The acceleration of reduction of titanium in this system was rather surprising in view of the fact that α-d-styrene results in larger rates of propagation or larger effective concentrations of C^*.

In summary then: $3/1 \propto (V_p)_D/(V_p)_H \propto (d[I])_D/(d[I])_H \propto (d[II])_D/(d[II])_H \propto [C^*]_D/[C^*]_H$; with all subscripts as previously defined.

It is obvious then, that $C^* \neq$ I or II, but to an intermediate or transition state which accompanies the formation of II from I.

Schematically the overall process may be pictured as shown in Figure 4.

In the absence of monomer, K_2, K_4, and K_5 may be zero. However, K_3 may not be zero under any experimental conditions, as was indirectly implied by Long and Breslow,[3] thereby making K_7 a necessity in addition to K_6, based on the observed constancy of the isosbestic point, for the transformation of I to II, without and with added monomer. With the addition of monomer, it appears that $K_2 + K_5 > K_6 (+K_7)$, and that reactions indicated by dotted lines probably become negligible. Steps in the scheme containing the factor (f) indicate that a monomer isotope effect is operative; e.g., $f_D < f_H$, where the subscripts D and H refer to α-d-styrene and styrene, respectively. The scheme as shown is the simplest one possible which will explain all observed experimental data but is not suggested to be an absolute representation of the process. The monomer dependences associated with $K_3 f$ and K_2 shown as $[M]^a$ and $[M]^r$, respectively, in Figure 4 are at present not clearly understood. Based on data obtained for the Ziegler-Natta system[5] the power a may not be zero or equal to r. These factors will be further investigated.

Lastly, one must explain the constancy of intrinsic viscosities of polymers produced at much different rates of polymerization, e.g., $(DP)_H = (DP)_D$ and $(DP) = V_p/\sum V_t$; but $(V_p)_D >> (V_p)_H$, as shown in Table I.

Unless one wants to assume a negative isotope effect for the termination reaction of α-d-styrene, one must conclude that termination *does not* involve the α-carbon but the β-carbon of styrene, i.e., propagation occurs on the benzyl carbon of styrene as suggested for the heterogeneous Ziegler-Natta system reported earlier.[5] In that case one would not expect a change in the termination reactions for α-d-styrene based on the termination kinetics suggested for propylene,[9] and the DP would remain constant because it is independent of $[C^*]$. Therefore, although rate increases are a function of $\Delta[C^*]$, the latter are cancelled in the DP expression.

Additional evidence for the lack of dependence of the termination reac-

tions on the α-hydrogen or deuterium of styrene was obtained by collecting and analyzing a gas sample produced by the reaction of $(C_5H_5)_2TiCl_2$ + $Al(CH_3)_3$ and 100% α-d-styrene. The gas contained CH_4 and CH_3D in a ratio of ca. 100/1. This indicates that at this high termination rate (producing intrinsic viscosities in the range of 0.05–0.07), hydrogen from the β-carbon and not from the α-carbon is probably involved. It may be possible that the reactions governing the concentration of active centers involves both the α- and β-carbon of styrene. An effort will be made in the near future to check this possibility by conducting similar experiments but using β,β-d_2-styrene.

References

1. Breslow, D. S., and N. R. Newburg, *J. Am. Chem. Soc.*, **79**, 5072 (1957).
2. Chien, J. C. W., *J. Am. Chem. Soc.*, **81**, 86 (1959).
3. Long, W. P., and D. S. Breslow, *J. Am. Chem. Soc.*, **82**, 1953 (1960).
4. Stepovik, L. P., A. K. Shilova, and A. E. Shilov, *Dokl. Akad. Nauk SSSR*, **148**, 122 (1963).
5. Overberger, C. G., and P. A. Jarovitzky, *J. Polymer Sci.*, **C4**, 37 (1964).
6. Zefirov, A. K., N. N. Tichomirov, and A. E. Shilov, *Dokl. Akad. Nauk SSSR*, **132**, 1082 (1960).
7. Zefirov, A. K., and A. E. Shilov, *Dokl. Akad. Nauk SSSR*, **136**, 599 (1961).
8. Shilov, A. E., A. K. Shilova, and B. N. Bobkov, *Vysokomol. Soendin.*, **4**, 1688 (1962).
9. Natta, G., and L. Pasquon, in *Advances in Catalysis and Related Subjects*, Academic Press, New York, 1959.

Résumé

Il a été montré que l'accroissement des vitesses de polymérisation de l' α-d-styrolène et/ou du styrolène en utilisant le système de catalyse homogène formé par $(C_5H_5)_2TiCl_2$ et $Al(C_2H_5)_2Cl$ est directement proportionnel à la concentration du monomère α-d-styrolène. Cet accroissement de la vitesse s'explique par l'accroissement de la concentration des centres actifs. Les viscosités intrinsèques des polymères sont indépendantes de la concentration du monomère. Les variations des vitesses de polymérisation ont été comparées en fonction des variations de composition du catalyseur mesurées par spectrophotométrie. Un schéma a été proposé pour expliquer les résultats obtenus.

Zusammenfassung

Es konnte gezeigt werden, dass die Zunahme der Geschwindigkeit der Polymerisation von α-d-Styrol und/oder Styrol, katalysiert durch $(C_5H_5)_2TiCl_2$ und $Al(C_2H_5)_2Cl$, der Monomer-Konzentration an α-d-Styrol direkt proportional ist. Diese Geschwindigkeitserhöhungen wurden durch eine Zunahme der Konzentrationen an aktiven Zentren erklärt. Ausserdem wurde festgestellt, dass die Viskositäten der Polymeren von der α-d-Styrol Monomer-Konzentration unabhängig sind. Änderungen in den Polymerisationsgeschwindigkeiten wurden auf die spektrophotometrisch beobachteten Änderungen des Katalysatorsystems zurueckgeführt. Es wurde ein Schema vorgeschlagen, welches die beobachteten Ergebnisse erklärt.

Configuration and Hydrodynamic Properties of Fully Acetylated Guaran*

JOSEPH V. KOLESKE and SHELDON F. KURATH, *The Institute of Paper Chemistry, Appleton, Wisconsin*

Synopsis

Fully acetylated guaran, (guaran triacetate, GTA), was fractionated and the fractions in the weight-average degree of polymerization range of 171 to 12,400 were characterized by light scattering and viscometry. At high molecular weights, non-Newtonian flow was observed and after appropriate correction the intrinsic viscosity was found to be independent of shear gradient. Analysis of viscosity results according to the theory of Kurata and Yamakawa indicated that at high molecular weights the molecule is nondraining and that excluded volume effects are absent. Polymolecularity was estimated from ultracentrifuge and osmotic pressure measurements on certain key fractions and in the case of one fraction it was possible to determine the distribution of molecular weights and to demonstrate the validity of the Zimm-Schulz distribution. The ratio of the mean square radius of gyration to the molecular weight was found to decrease with increasing molecular weight indicating a non-Gaussian behavior that cannot be accounted for by the Porod-Kratky chain model. The dependence of radius of gyration on chain length is identical to that observed for hydroxyethyl cellulose and cellulose tricaproate indicating that the β-1,4-linked D-glucose chain of cellulose and the β-1,4-linked chain of GTA have similar configurations, in spite of chemical and structural differences between the anhydro sugar units. The α-1,6-linked D-galactose side groups on every other mannose unit of GTA do not appear to affect main chain configurations to any great extent. Equivalent bond lengths calculated from intrinsic viscosity and from light scattering indicate that it is necessary to distinguish between the hydrodynamic and light-scattering radius of gyration. The Flory coefficient calculated from the light-scattering radius of gyration was found to increase with increasing molecular weight. When the hydrodynamic radius of gyration was used in the calculation, agreement with the theoretical Flory constant was within experimental error.

INTRODUCTION

Guaran is the fraction that precipitates from a water dispersion of guar gum upon addition of a specified amount of ethanol.[1] The parent guar gum is a neutral polysaccharide obtained from the endosperm of the guar seed *(Cyamopsis tetragonalaba)*. From periodate oxidations,[2,3] methylation data,[4,5] partial hydrolyses,[6–8] and x-ray data,[9] the guar molecule has been shown to consist of a straight β-1,4-linked D-mannose main
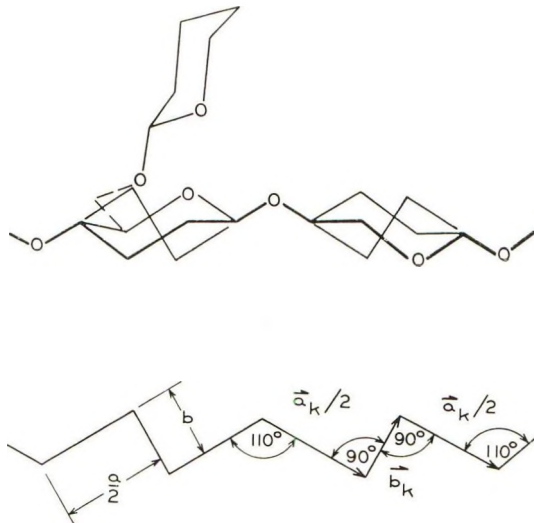
Fig. 1. The repeating unit of guaran and the corresponding bond and vector diagram.

chain with α-1,6-linked D-galactose side groups on every other mannose unit. Guaran may be fractionated without altering the ratio of galactose to mannose.

An examination of the molecule in terms of the eight possible strainless ring conformations[11] of the pyranose ring and utilization of the stereo-chemical convention of Greenwood and Rossotti[10] lead to the conclusion that both mannose and galactose units are probably in the Cl conformation. For the anhydromannose units this is substantiated by the fact that guaran has a fiber repeat distance of 10.3 A.,[9] a value identical to that obtained for cellulose.

Burchard[12] has indicated that the β-1,4-linked anhydroglucose units of cellulose are in the Cl conformation and has devised a statistical model based on this fact. A similar model can be constructed for the guaran molecule as shown in Figure 1. Except for the galactose side groups it is identical to that of cellulose, and hence values calculated for cellulose[12] of $a/2 = 2.67$ A. and $b = 1.43$ A. are applicable.

EXPERIMENTAL

Preparation of Guaran

The guar gum used in the present work was isolated by Haug[13] and is similar to that reported by Heyne and Whistler.[1] Guaran was obtained from a water dispersion of the gum by precipitation with ethanol. Upon addition of 25% ethanol by volume a precipitate representing 12.2% of the original gum was removed and discarded. The ethanol concentration was then increased to 40% by volume and the precipitated guaran was removed. The guaran represented 86% of the original gum, in agreement with the

86.5% value reported previously.[1] Approximately 2% of the guar gum remained soluble in 40% ethanol and was recovered by evaporation and later discarded.

Preparation of Guaran Triacetate

Guaran was acetylated at room temperature by the method of Carson and Maclay.[14] The acetyl content determined by the Eberstadt method[15] was 44.7%, indicating that full acetylation had been achieved (theoretical 44.8%). The melting point range was 226–227°C., in agreement with the literature value.[1]

For the remaining discussion the fully acetylated guaran will be referred to as guaran triacetate or GTA, with the understanding that this refers to a polymer with a repeat unit of 2,3,6-tri-O-acetyl-O-β-D-mannopyranosyl-$(1 \rightarrow 4)$-O-[2,3,4,6-tetra-O-acyl-α-D-galactopyranosyl-$(1 \rightarrow 6)$]-2,3-di-O-acyl-β-D-mannopyranosyl.

Fractionation

Guaran triacetate was first wet with a small amount of 95% ethanol and then dissolved in chloroform to yield a 0.1% solution. Fractions were obtained by slowly adding 95% ethanol to the agitated solution until turbidity was observed. After heating to 35°C. to effect solution, the system was allowed to cool slowly to 22.5°C., where it was maintained for a period of 24 hr. The precipitated polymer was recovered by centrifugation.

TABLE I
Light Scattering and Intrinsic Viscosity Results for GTA in Acetonitrile

Fraction	$\bar{M}_w \times 10^{-6}$	$\bar{N}_w^a$	$(\bar{S}_z^2)^{1/2}$, A.	$A_2 \times 10^4$, moles cm.^{3}/g.^{2}	$[\eta]$, dl./g.
2A	5.34	12,400	1303	0.38	9.45[b]
2B	4.84	11,200	1252	0.38	9.12[b]
3	3.30	7,640	1155	0.81	7.03[b]
4	2.68	6,200	1050	1.42	6.78[b]
2C	2.06	4,770	976	1.40	5.60[b]
5	0.85	1,970	680	2.90	3.87
6	0.33	764	356[c] 470[d]	2.48	1.79
7	0.23	532	336[c] 440[d]	3.91	1.16
8	0.074	171	197[c] 253[d]	4.70[e]	0.44

[a] Determined by using a monomer weight of 432.

[b] Obtained by extrapolation to zero shear stress.

[c] These values were obtained by using the dissymmetry method and a random coil model.

[d] These values were obtained by using the dissymmetry method and the rigid rod model.

[e] Obtained by plotting A_2 as a function of molecular weight and extrapolating.

With the exception of fraction 8, which was recovered by evaporation, this procedure was repeated for all of the fractions listed in Table I.

The first fraction was discarded, since it was very small and contained mostly dust that had been suspended in solution. Fraction 2 was very large and represented 46.3% of the original polymer. It was refractionated from a 0.1% solution to yield three fractions designated 2A, 2B, and 2C. The parent solution had a concentration of 0.054% when fraction 3 was precipitated, and the final fraction 8 was recovered by evaporation of a 0.004% solution. In the following discussions a distinction will be made between the fraction 2 sequence and the fraction 3 to 8 sequence.

Solvent Preparation

Acetonitrile was chosen as the solvent in the present work, since it was suitable for both light-scattering and ultracentrifuge investigations. Practical grade acetonitrile (Matheson, Coleman and Bell) was shaken for less than 1 min. with saturated aqueous potassium hydroxide and then stored over anhydrous sodium carbonate for at least 12 hr. Following this, the acetonitrile was twice distilled over phosphorus pentoxide. The middle fraction was retained each time, and the final product was then stored under nitrogen. Further details of the solvent purification are given elsewhere.[16]

LIGHT SCATTERING

Experimental Procedures

All light-scattering measurements were conducted at 22.5°C. at a wavelength of 4358 A. with a Brice-Phoenix light-scattering photometer (series 1937). A cylindrical cell (Brice-Phoenix C-101) was used in conjunction with the narrow slit system. The performance of the apparatus was checked by evaluating the Rayleigh ratio for benzene and toluene and the excess turbidity of a 0.5% solution of a Cornell standard polystyrene in toluene.

The high molecular weight fractions were clarified by centrifugation in special dust-exclusion cells[17] while the low molecular weight samples were clarified by repeated filtration under nitrogen pressure through solvent-resistant Polypore filters of 4500 A. pore size. Both methods provided adequate clarification without changing the solution concentration.

The refractive index gradient of GTA in acetonitrile was determined on a Baird Rayleigh interferometer and was found to be 0.1200 ± 0.0004 ml./g. at 546 mμ and 22.5°C. The Cabannes depolarization factor[18] corrections were found to average 0.89 ± 0.03 for all GTA fractions in acetonitrile.

For the higher molecular weight fractions values of Hc/τ were extrapolated as a function of $\sin^2(\theta/2) + kc$ and extrapolated to zero angle and zero concentration in the manner proposed by Zimm[19] as shown in Figure 2. The absolute turbidity, τ, and the optical constant, H, may be
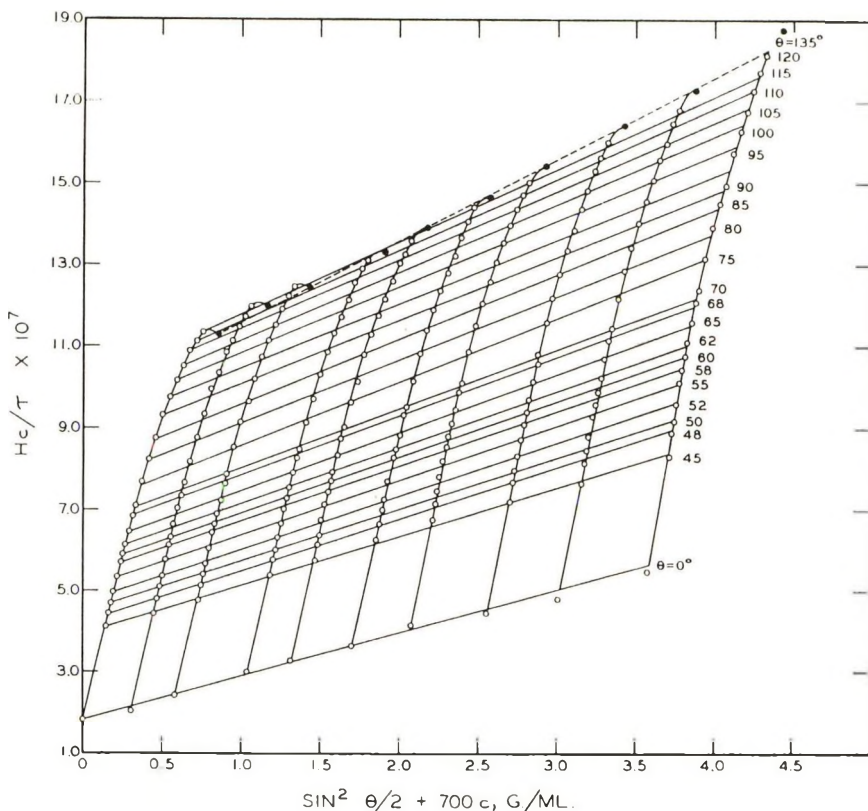
Fig. 2. Zimm plot for fraction 2B of guaran triacetate in acetonitrile at 22.5°C., λ = 4358 A.

obtained from expressions given elsewhere.[20] The variation of turbidity with scattering angle and concentration is given by

$$(Hc/\tau)_{\theta,c} = 1/\bar{M}_w P(\theta) + 2A_2 c \tag{1}$$

where $P(\theta)$ is the particle scattering factor, $\bar{M}_w$, is the weight average molecular weight, and A_2 is the second virial coefficient. At zero scattering angle, $\theta = 0$, $P(\theta) = 1$, and the intercept of the Zimm plot is

$$(Hc/\tau)_{\substack{\theta=0 \\ c=0}} = 1/\bar{M}_w \tag{2}$$

from which weight-average molecular weights were calculated. The second virial coefficient was obtained from the slope of the Zimm plot at zero scattering angle.

The root mean square radius of gyration is obtained from the initial slope and intercept of the zero concentration line according to the relation

$$(\bar{S}^2{}_z)^{1/2} = [(\lambda'/\pi)(3/16)]^{1/2}[\text{Slope/Intercept}]^{1/2} \tag{3}$$

where λ' is the wavelength of light in the solution. For the three lowest molecular weight fractions the angular variation of Hc/τ was subject to large errors, and the corresponding Zimm plots could not be made. For these fractions, $(\bar{S}^2_z)^{1/2}$ was determined by using the dissymmetry method[21] and dissymmetry tables.[22,23]

From the work of Holtzer et al.[24] on cellulose trinitrate the Gaussian chain model would appear to apply to a number average degree of polymerization as lo was 500. The GTA molecule, on the other hand, appears to be non-Gaussian over most of the molecular weight range covered in the present work. It is difficult, therefore, to decide on the molecular model to be used with the dissymmetry method. For this reason results based on both random coil and rigid rod models are included in Table I. Elsewhere, unless stated otherwise, analysis will be based on the random coil model.

Light-Scattering Results

The results of light-scattering measurements are summarized in Table I. The weight-average molecular weight, $\bar{M}_w$, weight-average degree of polymerization, $\bar{N}_w$, second virial coefficient, A_2, and the z-average root-mean-square radius of gyration, $(\bar{S}^2_z)^{1/2}$, are given. For the first six fractions, the root-mean-square radius of gyration was determined from Zimm plots. Dissymmetry measurements were used on the remaining fractions and results are reported for both coil and rod models.

VISCOSITY

Experimental Procedures

Viscosity measurements were conducted in a modified four-bulb Ubbelohde variable shear capillary viscometer at $25.00 \pm 0.02°C$. For those solutions exhibiting Newtonian flow, viscosities were determined from the efflux times in the customary manner on the basis of the Hagen-Poiseuille equation. Drainage and end-effect errors[25] were neglected, and only kinetic energy corrections were considered. The latter were calculated[26,27] to be less than 1% in all cases and were neglected.

For those fractions which did not exhibit shear dependence, the intrinsic viscosity was determined from plots of η_{sp}/c and of $(\ln \eta_{rel})/c$ versus c as shown in Figure 3.

The shear stress τ_R in dynes/cm.^{2} at the wall of the capillary of radius R and length L is given as:[28]

$$\tau_R = \bar{h}dgR/2L \qquad (4)$$

where d is the density of the fluid, and $\bar{h}$ is the mean hydrostatic head which can be obtained from Meissner's equation:[29]

$$\bar{h} = (m_1 - m_2)/\ln (m_1/m_2). \qquad (5)$$

Here m_1 and m_2 refer to the height of the hydrostatic head at the top and bottom of the bulb respectively.
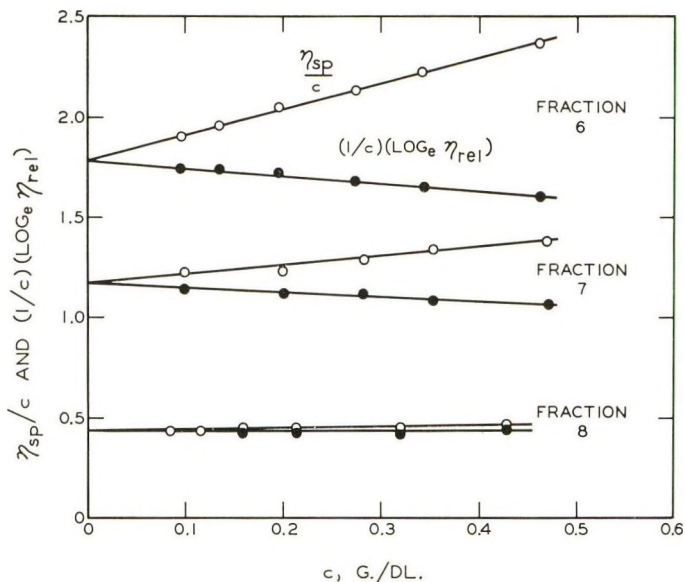
Fig. 3. Viscosity as a function of concentration for guaran triacetate in acetonitrile at 25°C.: (O) η_{sp}/c values; (●) (ln η_{rel})/c values.

For those fractions which exhibited shear dependent viscosities the apparent relative viscosity η^*_{rel} was plotted as a function of shear stress and extrapolated to zero at each concentration as shown in Figure 4. The zero stress intercepts were then used to calculate the apparent specific viscosity η^*_{sp}. Semilogarithmic plots of log (η^*_{sp}/c) versus c were then extrapolated to zero concentration as shown in Figure 5. The intercept at zero concentration was taken to be the intrinsic viscosity. The intrinsic viscosity values are recorded in Table I.

Results and Discussion

The intrinsic viscosity is shown as a function of molecular weight in Figure 6. Two distinct regions are apparent. In the low molecular weight region the data may be represented by the equation,

$$[\eta] = 2.62 \times 10^{-5}\bar{M}_w^{0.87} \tag{6}$$

and at high molecular weights by

$$[\eta] = 3.11 \times 10^{-3}\bar{M}_w^{0.52} \tag{7}$$

The standard error for each molecular weight exponent is ±0.03.

Two explanations for the transition from one limiting region to the other are considered. Either the transition is due to changes in the draining characteristics of the molecule[30-32] or the extrapolation procedure has not corrected viscosity data to zero rate of shear.

As indicated in Figure 6 all of the points in the high molecular weight region were subject to corrections for non-Newtonian flow. Since the vis-
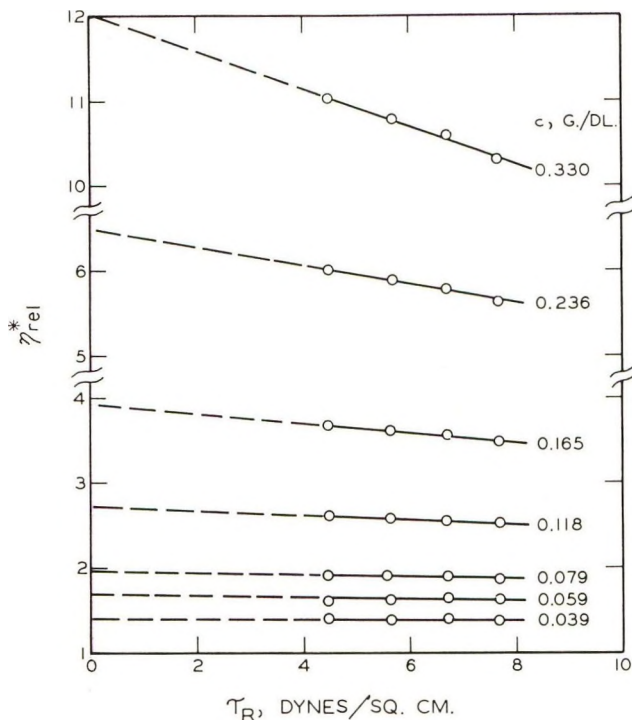
Fig. 4. Apparent relative viscosity as a function of shear stress for guaran triacetate fraction 2A in acetonitrile at 25°C. Data at selected concentrations have been omitted for reasons of clarity.

cosity of high molecular weight polymers decreases with increasing rate of shear, the transition in the intrinsic viscosity molecular weight behavior could possibly be due to inability to extrapolate to zero shear gradient.

In order to obtain an estimate of the effect of shear rate, intrinsic viscosity data for fraction 2A were subjected to the analysis suggested by Goldberg and Fuoss.[33]   For a Newtonian fluid the maximum shear gradient G_R at the wall of the capillary is given by,

$$G_R = hdgR/2L\eta_0\eta_{rel} = \tau_R/\eta \tag{8}$$

This expression is invalid for non-Newtonian flow and one must consider the parameter,

$$G_R = \tau_R\eta^*_{rel}/\eta_{rel} \tag{9}$$

where η^*_{rel} is the apparent relative viscosity calculated on the basis of the Hagen-Poiseuille equation.   The quantities without an asterisk are understood to refer to viscosities determined in the limit as the shear gradient approaches zero.

According to Goldberg and Fuoss, a plot of η^*_{sp}/c versus c at various constant G_R values calculated from eq. (9) should yield a family of curves with
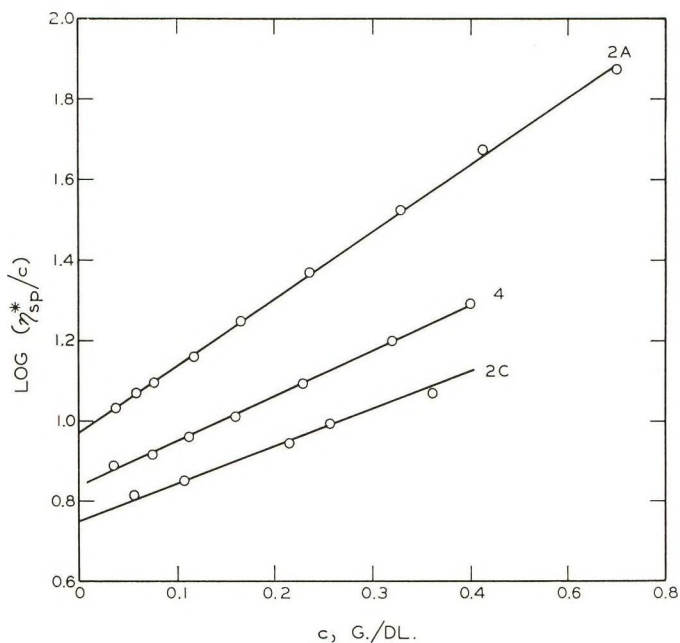
Fig. 5. Plot of log (η_{sp}/c) as a function of concentration for guaran triacetate in aceto-nitrile at 25°C. Data for Fractions 2B and 3 have been omitted for reasons of clarity.
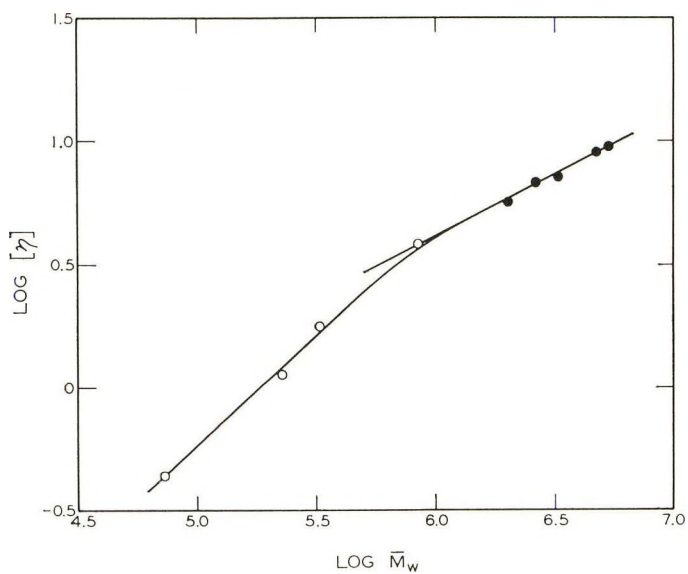
Fig. 6. Intrinsic viscosity as a function of molecular weight for guaran triacetate in acetonitrile at 25°C.: (●) those fractions for which corrections for non-Newtonian flow were required.
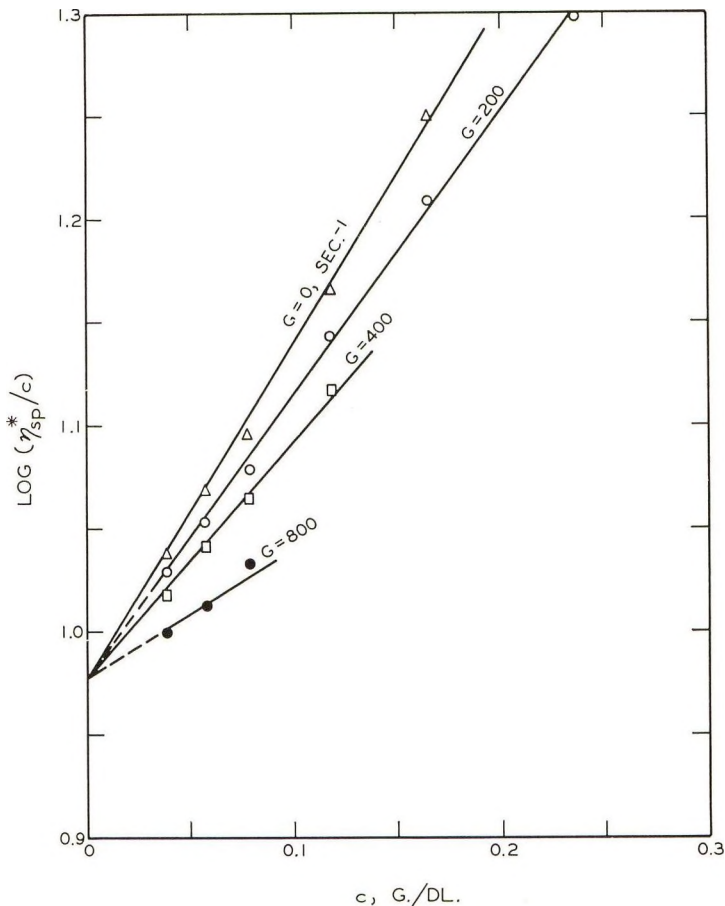
Fig. 7. Effect of shear rate on $\log (\eta_{sp}^*/c)$ as a function of concentration.

a common intercept if the intrinsic viscosity is independent of shear rate. The curves shown in Figure 7 represent such a plot. The log of η_{sp}^*/c has been plotted for ease of extrapolation.

The curves all have a common intercept, indicating that the intrinsic viscosity is independent of rate of shear. This is similar to the results observed for nitrocellulose in butyl acetate.[33] It should be pointed out that if η_{sp}/c is plotted versus c at constant values of τ_R or at constant values of G_R based on eq. (8) the opposite conclusion will be reached.[33-35]

Claesson and Lohmander[36] have examined the dependence of intrinsic viscosity of a high molecular weight cellulose nitrate, (D.P. about 10,000) and find that

$$[\eta]_G = [\eta]_0 (1 - 1.31 \times 10^{-4} G) \tag{10}$$

in the gradient range of 0.5–1600 sec.$^{-1}$. Here $[\eta]_G$ and $[\eta]_0$ are the intrinsic viscosities at the gradients G and zero respectively. Assuming

that this also holds for fraction 2B at a G of 200 sec.$^{-1}$, the intrinsic viscosities in Table I are estimated to be within 3% of the corresponding zero gradient values.

It appears, therefore, that the transition in the intrinsic viscosity molecular weight plot cannot be attributed to non-Newtonian flow effects. Rather, it appears to reflect a change in the draining characteristics of the molecule with molecular weight. This will be considered in greater detail in the hydrodynamic section of this paper.

POLYMOLECULARITY

In order to estimate the polymolecularity of the GTA fractions, osmotic pressure and ultracentrifuge experiments were conducted on certain key fractions. Fractions 2B and 3 were chosen as representative high molecular weight members of the two fractionation sequences. Fractions 6 and 8 had molecular weights low enough for osmotic pressure determinations.

Sedimentation Velocity Measurements

Sedimentation velocity experiments were conducted in acetonitrile at 25°C. in a Spinco Model E ultracentrifuge employing a standard An-D analytical head, a single sector boundary cell and schlieren optics. Centrifugations were conducted at 56,100 rpm, corresponding to a gravitational field of $229 \times 10^3 g$. Appreciable sedimentation occurred during acceleration, and speed–time data were obtained and used to calculate the equivalent sedimentation time.[37]

The apparent distribution function $g^*(S)$ which gives the relative amount of a molecular weight species with sedimentation coefficient S was determined from the customary relation:[38,39]

$$g^*(S) = (dn_c/dx)(\omega^2 t x^3)/(n_c^0 x_0^2) \tag{11}$$

where ω is the angular velocity, x is the distance from the center of the rotor, x_0 is the boundary position at zero time, and n_c^0 is the refractive index increment of the initial solution. The sedimentation coefficients were computed by the relation[38,39]

$$S = (1/\omega^2 t) \ln (x/x_0) \tag{12}$$

Apparent distribution functions were determined at several concentrations and the method of Gralen[38] was used to obtain the true distribution $g(S^0)$ at zero concentration. Corrections for boundary spreading by diffusion[38] were found to be unnecessary.

In order to make the appropriate transformations from distribution of sedimentation coefficient coordinates to distribution of molecular weight coordinates the limiting sedimentation coefficient was expressed as

$$S^0 = kM^a \tag{13}$$

since from the results of Yamakawa[40] one can show that for a nondraining polymer in the absence of excluded volume effects, $S^0 \sim [\eta] \sim M^a$. From eq. (7) it is apparent that $a = \frac{1}{2}$ within experimental error.

The transformation of $g(S^0)$ into the distribution of molecular weights $f(M)$ was accomplished by means of the relation[38]

$$f(M) = g(S^0)dS^0/dM \qquad (14)$$

When eqs. (13) and (14) are used in conjunction with the defining equations[38,41,42] for number-average, weight-average, and z-average molecular weights one finds that,

$$\bar{M}_n = k^{-2}/\int_0^\infty (S^0)^{-2}g(S^0)dS^0 \qquad (15)$$

$$\bar{M}_w = k^{-2}\int_0^\infty (S^0)^2 g(S^0)dS^0 \qquad (16)$$

and

$$\bar{M}_z = k^{-2}\int_0^\infty (S^0)^4 g(S^0)dS^0 / \int_0^\infty (S^0)^2 g(S^0)dS^0 \qquad (17)$$

The coefficient k was evaluated from eq. (16) by using the known values of $\bar{M}_w$ from light scattering. The number-average and z-average molecular weights were then calculated from eqs. (15) and (17).

Osmotic Pressure Measurements

Osmotic pressure measurements were conducted in acetonitrile at $30.000 \pm 0.001°C.$ in osmometers of the Zimm-Myerson[43] type. The cellulose membranes were of the dense type from Membran Gesellschaft, Göttingen, Germany, and were purchased from the Gelman Instrument Co., Chelsea, Michigan. Osmotic pressures were calculated from the difference in liquid levels between the osmometer capillary and the reference capillary at equilibrium. Plots of (π/c) versus c, where π is the osmotic pressure were extrapolated linearly to zero concentration, and the number-average molecular weights were calculated from the intercept.

Polymolecularity Results and Discussion

The results of the osmotic pressure and ultracentrifuge determinations are given in Table II.

In order to estimate polymolecularity it is customary to assume a generalized Zimm-Schulz[44,45] distribution of molecular weights in the form

$$f(M) = (y^{h+1}/h!)M^h \exp\{-yM\} \qquad (18)$$

where

$$y = h/\bar{M}_n = (h+1)/\bar{M}_w = (h+2)/\bar{M}_z \qquad (19)$$

TABLE II

Osmotic Pressure and Ultracentrifuge Results and Estimates of Polymolecularity

Fraction	$M_n \times 10^{-6}$	$M_z \times 10^{-6}$	$hM_w \times 10^{-7}$	h
2A	—	—	—	$(4.00)^a$
2B	3.96^b	5.93^b	—	4.00
3	2.48^b	4.12^b	1.00	3.03
4	—	—	—	(5.10)
2C	—	—	—	(4.00)
5	—	—	—	(12.4)
6	0.32^c	—	1.10	33.3
7	—	—	—	(45.7)
8	0.068^c	—	—	11.1

[a] Quantities in parentheses are estimated values (see text).
[b] Ultracentrifuge.
[c] Osmotic pressure.

The validity of this assumption has been verified in the case of fraction 2B. The distribution of sedimentation coefficients was transformed into a distribution of molecular weights by means of eqs. (13) and (14). The results are shown in Figure 8, where the open circles represent values calculated from ultracentrifuge data. The solid line represents values calculated from eq. (18) on the basis of a value of 4.00 for h and 1.03×10^{-6}
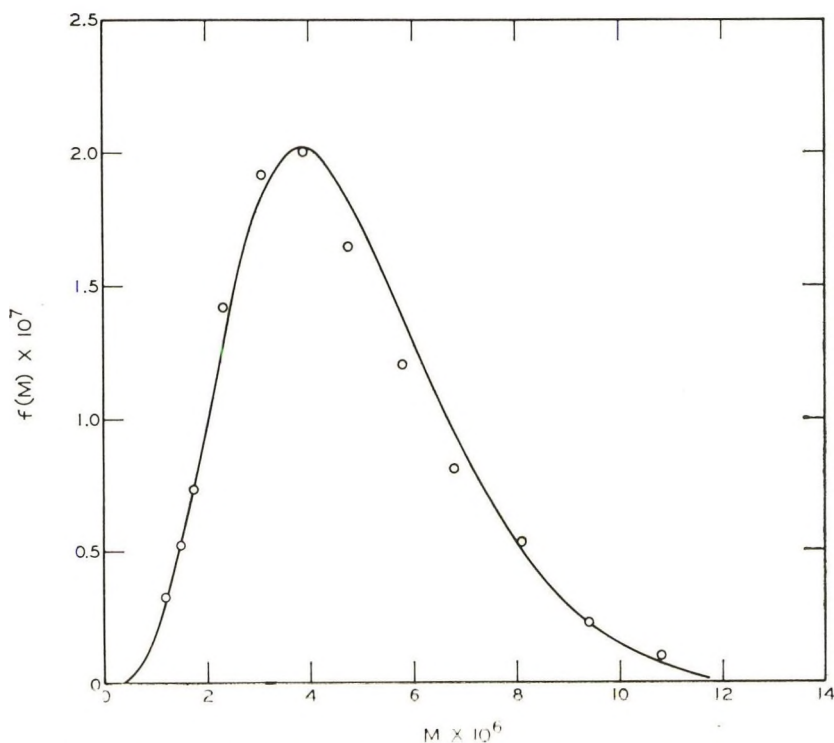
Fig. 8. Molecular weight distribution for guaran triacetate Fraction 2B.

for y.   The agreement between experimental and theoretical distributions is good.

The polymolecularity of the GTA fractions is expressed in terms of the Zimm-Schulz parameter h given in Table II.   The values of h reported for the fractions 2B, 3, 6, and 8 were calculated from experimental data. The values shown in parentheses are estimates obtained in the following manner.   Since fraction 2B is the middle fraction of the fraction 2 sequence, an average value of 4.00 for h has been assumed for both fractions 2A and 2C.   For fraction 3 the product of $h\bar{M}_w$ is 1.00×10^7 and for fraction 6 it is 1.10×10^7.   The values of h for fractions 4, 5, and 7 were calculated by assuming an average value of 1.05×10^7 for $h\bar{M}_w$ and employing the known values of $\bar{M}_w$ from light scattering.

MOLECULAR CONFIGURATION OF GUARAN TRIACETATE

Radius of Gyration and Molecular Weight

The variation of radius of gyration with molecular weight is shown in Figure 9.   The z-average molecular weights have been calculated on the basis of the information given in Table II and are summarized in Table III.
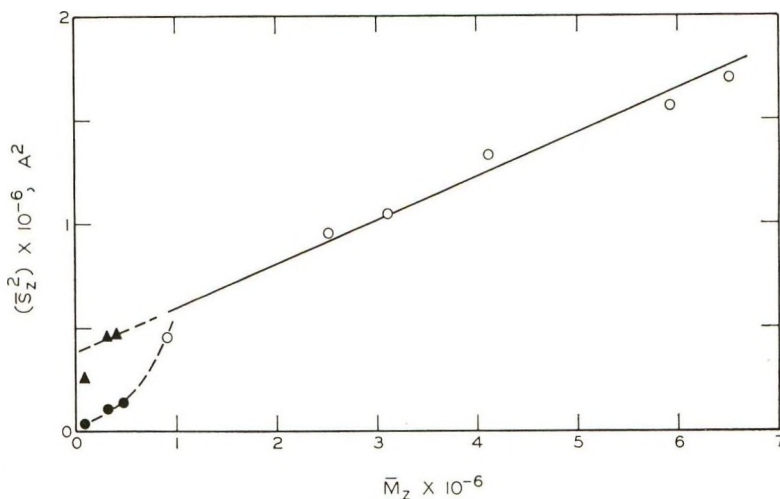
Fig. 9. Radius of gyration as a function of molecular weight for guaran triacetate in acetonitrile at 22.5°C.: (◯) data from Zimm plots; (▲) dissymmetry method, rod model; (●) dissymmetry method, coil model.

Above a molecular weight of 0.92×10^6, the plot of $\bar{S}_z{}^2$ versus $\bar{M}_z$ is seen to be linear and can be represented by the relation

$$\bar{S}_z{}^2 = 3.77 \times 10^5 + 0.210\ \bar{M}_z \tag{20}$$

At low molecular weights, where $\bar{S}_z{}^2$ is obtained from dissymmetry measurements, the curve depends upon the choice of the molecular model.

TABLE III
Configurational Parameters for Guaran Triacetate in Acetonitrile

Fraction	$M_z \times 10^{-6}$	α	$(\bar{S}_z^2)_0^{1/2}$, A.	$(\bar{S}_z^2)_0/M_z$, A.² mole/g.	$\dfrac{(\bar{S}_z^2)_0^{1/2}}{(r_{max})_z}$	Effective bond length b_0, A. From $(\bar{S}_w^2)_0^2$	Effective bond length b_0, A. From $[\eta]$
2A	6.51	1.02	1278	0.251	0.0164	25.4	23.4
2B	5.93	1.02	1228	0.254	0.0174	25.7	23.5
3	4.12	1.05	1100	0.294	0.0224	27.6	22.9
4	3.12	1.08	972	0.303	0.0261	28.2	23.5
2C	2.51	1.07	912	0.331	0.0292	29.3	23.0
5	0.92	1.10	618	0.417	0.0567	32.9	23.6
6[a]	0.34	1.06	336	0.332	0.0830	29.4	—
7[a]	0.24	1.13	297	0.376	0.106	31.3	—
8[a]	0.080	1.13	174	0.381	0.183	31.4	—

[a] Radius of gyration based on dissymmetry method and the random coil model.

For the rigid rod model the linear relation is preserved to low molecular weights. On the basis of the random coil model, however, there is a sharp decrease in radius of gyration at low molecular weight. This decrease is similar to that observed for cellulose trinitrate[46] in acetone, with the exception that in the case of cellulose trinitrate the linear portion of the curve extrapolates through the origin.

The Unperturbed Radius of Gyration

It is necessary to establish the radius of gyration in the absence of long-range interactions. Following Flory,[42] it is necessary to assume a uniform coil expansion expressed by the relation,

$$(\bar{S}_z^2)^{1/2} = \alpha(\bar{S}_z^2)_0^{1/2} \tag{21}$$

where $(\bar{S}_z^2)_0^{1/2}$ is the unperturbed root-mean-square radius of gyration obtained in the absence of long-range interaction and α is the expansion factor. The expansion factor may be estimated from the Flory-Krigbaum-Orofino[47] equation for the second virial coefficient given by,

$$A_2\bar{M}_w/[\eta] = 1.65 \log [1 - 4.50(\alpha^2 - 1)] \tag{22}$$

where the numerical coefficients are those suggested by Stockmayer.[48]

Values of $(\bar{S}_z^2)_0$ and α calculated from these equations are given in Table III. The expansion factors are close to unity and increase slightly with decreasing molecular weight. Values of α only slightly larger than unity appear to be characteristic of highly inflexible molecules[49] and have been observed for cellulose trinitrate,[49] cellulose tricaproate,[50] hydroxyethyl cellulose,[35] and cellulose in cadoxen.[51]

Configuration and Molecular Weight

The deviation from linearity shown in Figure 9 might be attributed to a transition from Gaussian to non-Gaussian behavior.[46] It is of interest, therefore, to examine the configurational behavior of GTA in light of the treatment of non-Gaussian chains as given by Benoit and Doty.[52] This analysis is based on the "wormlike" chain of Porod and Kratky.[53,54] The chain is described in terms of the persistence length q, which is the mean length of projection of an indefinitely long chain in the direction of its first link. The persistence length may be taken as a measure of relative chain stiffness. When q is large, the chain is very stiff and rodlike; when q is small, the chain is more flexible and coillike. Benoit and Doty[52] have obtained a relation between $(\bar{S}_z^2)_0$ and q which, after appropriate correction for heterogeneity,[49] becomes

$$(\bar{S}_z^2)_0 = q^2[\bar{x}_z/3 - 1 + (2/\bar{x}_w)(1 - 1/\bar{x}_n)] \tag{23}$$

where x is the number of Porod units in the molecule and is given by

$$x = r_{max}/q \tag{24}$$

where r_{max} is the length of the fully extended chain. For GTA this is given by $r_{max} = 5.15N$, where N is the degree of polymerization.[49]
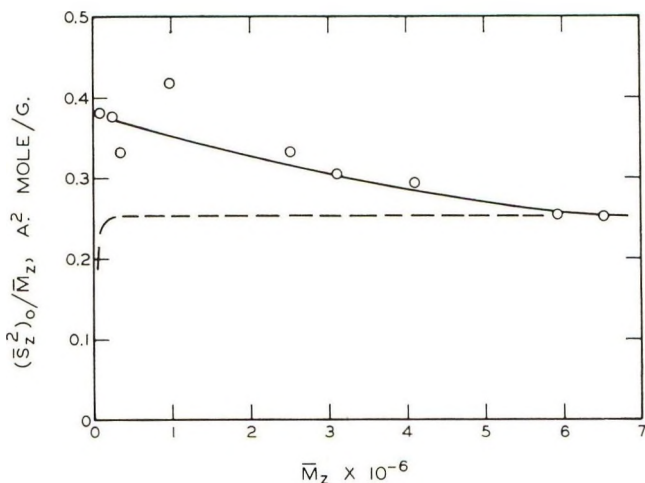
Fig. 10. Dependence of $(\bar{S}_z^2)_0/M_z$ on M_z for guaran triacetate in acetonitrile at 22.5°C.; (O) experimental values; (– –) values calculated from eq. (23) assuming a value for q of 64 A.

Values of persistence length computed from eq. (23) are found to decrease with increasing molecular weight and reach a limiting value of approximately 64 A. for the two highest molecular weight fractions. It is of interest, therefore, to examine the ratio $(\bar{S}_z^2)_0/\bar{M}_z$ as a function of molecular weight. Values of this ratio are given in Table III and are shown in Figure

10 as a function of molecular weight. The ratio decreases with increasing molecular weight and approaches a limiting value of 0.251.

If the persistence length of a polymer is known, eq. (23) can be used to calculate $(\bar{S}_z^2)_0$ and therefore values of the ratio $(\bar{S}_z^2)_0/\bar{M}_z$ as a function of molecular weight. The dashed line in Figure 10 is the result of such a calculation for GTA on the basis of a 64 A. persistence length. There is an appreciable difference at low molecular weights between the experimental values and the theoretically based curve. Similar deviations have been observed for hydroxyethyl cellulose,[35] cellulose tricaproate,[50] and amylose.[34] Cellulose trinitrate,[23,46,49] however, appears to follow the predicted curve.

In the Kuhn[55] equivalent chain model the polymer chain is assumed to be constructed of a series of rodlike segments joined to each other without valence angle restrictions. The chain is assumed to have the same contour length as the actual chain. The segment length, A_m, of the Kuhn equivalent chain[55] given by

$$A_m = 6(\bar{S}^2)/(r_{max}) = 2q \qquad (25)$$

is 128 A. The limiting Kuhn segment of the GTA molecule, therefore, consists of a rodlike sequence of 25 anhydromannose units.

The β-1,4-Polysaccharide Model of GTA

The Porod-Kratky persistence length, the Kuhn segment length, and the equivalent bond length are useful parameters for characterizing the polymer chain but have the disadvantage that they do not specifically take into account the skeletal parameters of the chain.

Skeletal models for the β-1,4-linked polysaccharide chain have been considered by Benoit,[56] Eliezer and Hayman,[57] and by Burchard,[12] who used the method of Lifson[58] to obtain the mean square radius of gyration. In the present discussion the results of Burchard will be used. According to Benoit[56] the cellulose chain can be simplified to the point where it can be represented by a series of perpendicular and parallel bonds as shown in Figure 1. Rotation is restricted to the ether linkages. The vectors $\mathbf{a}_k/2 + \mathbf{b}_k + \mathbf{a}_k/2$ associated with the $a/2$ and b distances of the kth anhydroglucose unit (anhydromannose for GTA) of the chain all lie in one plane. Values of $a/2 = 2.67$ A. and $b = 1.43$ A. are calculated by Burchard for cellulose. Internal rotation is described by the angle ϕ_r which may vary between the limits of $\pm \pi$ depending on the position of the vectors $\mathbf{a}_{k-1}/2 + \mathbf{b}_{k-1} + \mathbf{a}_{k-1}/2$ and $\mathbf{a}_{k+1}/2 + \mathbf{b}_{k+1} + \mathbf{a}_{k+1}/2$.

Hindered rotation may be described in terms of a rotation potential $V(\phi)$. For a single potential minimum one can use, following Debye,[59]

$$V(\phi)\begin{cases} 0 \text{ for } -\bar{\phi} \leqslant \phi \leqslant +\bar{\phi} \\ \infty \text{ for } \phi > +\bar{\phi} \text{ and } \phi < -\bar{\phi}. \end{cases} \qquad (26)$$

Burchard has pointed out that since every second sugar unit in the backbone of a β-1,4-linked polysaccharide is turned through 180° it may be

necessary to consider the existence of two potential minima, one at $\phi = 0°$ and the other at $\phi = 180°$.

For a single potential minimum Burchard[12] finds,

$$(\bar{S}^2)_0 = \left[\frac{N}{6} a^2 \left(\frac{1 + \cos\theta}{1 - \cos\theta}\right) + b^2\right]\left(\frac{1 + \overline{\cos\phi}}{1 - \overline{\cos\phi}}\right) \qquad (27)$$

and for two potential minima,

$$(\bar{S}^2)_0 = \left(\frac{N}{6}\right)\frac{1}{2}\left[a^2 \left(\frac{1 + \cos\theta}{1 - \cos\theta}\right) + b^2\right]\left[\frac{1 + \overline{\cos\phi}}{1 - \overline{\cos\phi}} + \frac{1 - \overline{\cos\phi}}{1 - \overline{\cos\phi}}\right] \qquad (28)$$

where θ is the supplement to the valence angle of the glycosidic oxygen $180° - \theta = 110°$.
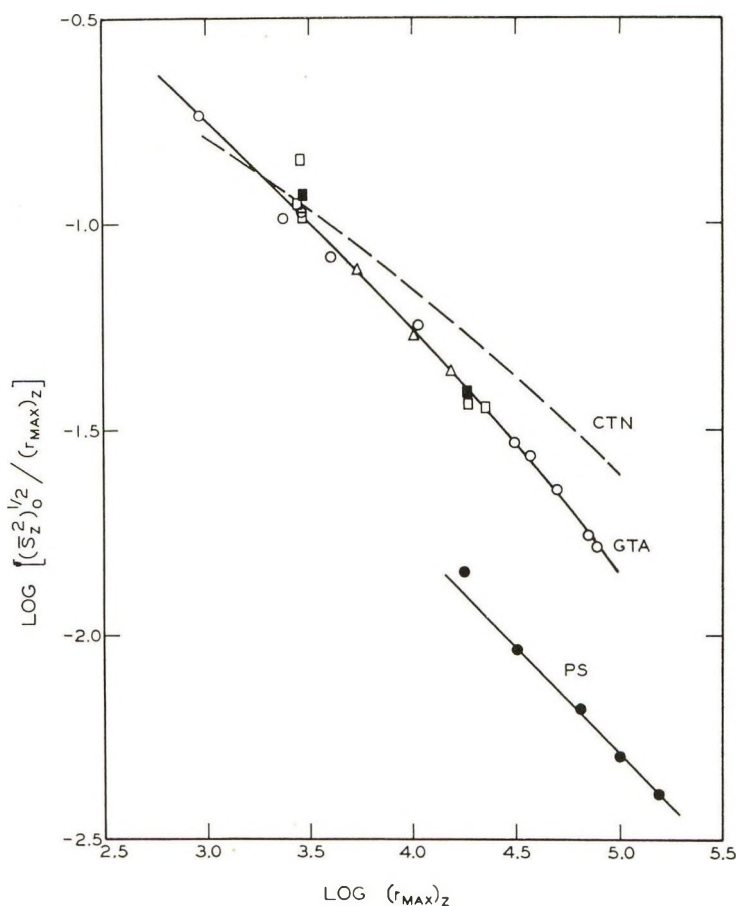
Fig. 11. Dependence of log $[(\bar{S}_z^2)_0^{1/2}/(r_{max})_z]$ on log $(r_{max})_z$ for: (O) guaran triacetate in acetonitrile; (□) cellulose tricaproate in dimethylformamide; (■) cellulose tricaproate in 1-chloronaphthalene; (△) hydroxyethyl cellulose in water; (●) polystyrene in cyclohexane; (– –) cellulose trinitrate in ethyl acetate.

Debye[59] has shown that for the potential represented by eq. (26),

$$\overline{\cos \phi} = \sin \overline{\phi}/\overline{\phi} \tag{29}$$

and since $\overline{\cos \phi}$ is easily obtained from eqs. (27) and (28), one can calculate $\overline{\phi}$. When this is done for the high molecular weight fractions in the region where $(\bar{S}_z^2)_0/\bar{M}_z$ reaches the limiting value of 0.251, the single potential model yields a value of $\overline{\cos \phi} = 0.832$ corresponding to $\overline{\phi} = 58.9°$ and for the double potential model $\overline{\cos \phi} = 0.913$ with $\overline{\phi} = 42.7°$. It is not possible, of course, to decide between a single or double potential model on the basis of evidence available at present.

The potential model of Debye is not particularly realistic and it is profitable to consider the more realistic single-fold potential,

$$V(\phi) = (V_m/2)(1 - \cos \phi) \tag{30}$$

which has been used by Taylor[60] who has tabulated values of $\overline{\cos \phi}$ as a function of V_m/RT. For $\overline{\cos \phi} = 0.832$ we find $V_m/RT = 6.65$, and at 25°C. one obtains a value of $V_m = 1,120$ cal./mole.

Configuration of GTA and Other Polymers

To compare the configuration of GTA with other polymers it is convenient to consider the variable $(\bar{S}_z^2)_0^{1/2}/(r_{max})_z$ as a function of $(r_{max})_z$ as suggested by Swenson and Thompson.[61] This is done in Figure 11 for GTA in acetonitrile at 22.5°C., cellulose trinitrate[46,49] in ethyl acetate at 25°C., cellulose tricaproate[50] in dimethylformamide at 41°C. and in 1-chloronaphthalene at 24°C., and hydroxyethyl cellulose[35] in water at 25°C. Polystyrene in cyclohexane at 34°C. is also shown.[62]

The similarity between hydroxyethyl cellulose, cellulose tricaproate, and GTA is quite striking and indicates that the molecules have a similar non-Gaussian behavior. In view of the size of the galactose group on the 6-carbon atom of every other anhydromannose unit of GTA one might expect galactose to have a marked influence on chain configuration. Actually, molecular models (Fisher-Taylor-Hirshfelder) indicate that the galactose side groups are too far removed to interfere with main chain configurations. It is of course realized that we may be dealing with a fortuitous choice of solvents and that in other solvents the similarity between GTA and these cellulose derivatives might be lost. This is certainly true for hydroxyethyl cellulose[63] in cadoxen, where the solvent forms a complex with the polymer.

At low $(r_{max})_z$ the $(\bar{S}_z^2)_0^{1/2}/(r_{max})_z$ ratios for cellulose trinitrate and GTA are approximately the same and are large enough so that the molecules are not expected to obey random flight statistics or to have spherical symmetry.[49] At higher $(r_{max})_z$ the ratio for cellulose trinitrate is higher and the molecule occupies a relatively larger molecular domain than GTA. The corresponding curve for polystyrene lies considerably below the polysaccharide curves, as would be expected of this flexible molecular chain.[61]

HYDRODYNAMIC PROPERTIES OF GUARAN TRIACETATE

Intrinsic Viscosity and Excluded Volume

According to the theory of Kurata and Yamakawa,[32] the intrinsic viscosity is given by

$$[\eta] = \pi^{3/2} N_A x F(x) [(\bar{S}^2)_0^{3/2}/M][1 + p(x)z] \tag{31}$$

where N_A is Avogadro's number, x is the draining parameter, and $xF(x)$ and $p(x)$ are tabulated functions of x. The quantity $(\bar{S}^2)_0$ can be written as

$$(\bar{S}^2)_0 = b_0^2 M/6M_0 \tag{32}$$

where M_0 is the molecular weight of the monomer unit and b_0 is the effective bond length. The draining parameter is given by,

$$x = \zeta M^{1/2}/[(6\pi^3)^{1/2}\eta_0 b_0 M_0^{1/2}] \tag{33}$$

where ζ is the friction coefficient of a monomer unit. Also z is the excluded volume parameter given by

$$z = (2\pi/3)^{3/2}(\beta M^{1/2})/(b_0^3 M_0^{1/2}) = q_e M^{1/2} \tag{34}$$

where β is a cluster integral.

On substituting eqs. (32) and (34) into eq. (31) and rearranging, one finds

$$[\eta]/M^{1/2} = \pi^{3/2} N_A (b_0^2/6M_0)^{3/2} xF(x)[1 + p(x)q_e M^{1/2}] \tag{35}$$

For large values of molecular weight, x will be large, and $xF(x)$ assumes a limiting value of 1.259 and $p(x)$ the value of 1.55 so that the equation becomes asymptotic to a straight line.[64]
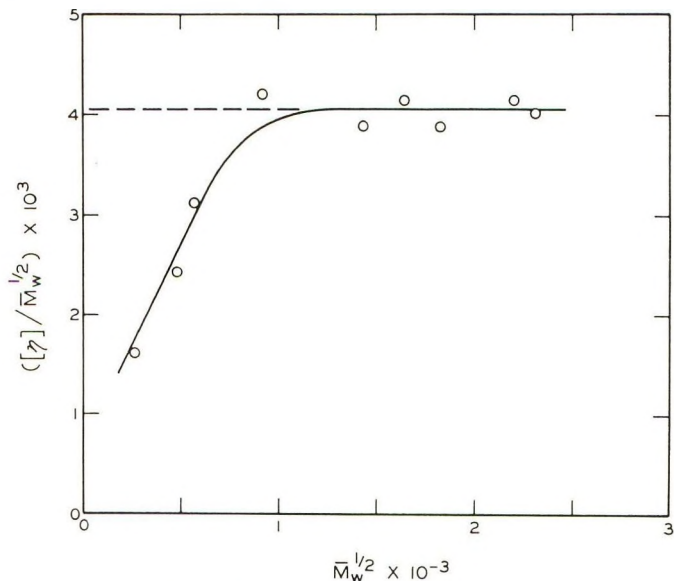
Fig. 12. Dependence of $[\eta]/M_w^{1/2}$ on $M_w^{1/2}$ for guaran triacetate in acetonitrile.

A test of this equation on GTA is shown in Figure 12, where a plot of $[\eta]/M^{1/2}$ versus $M^{1/2}$ is seen to be asymptotic to a straight line of zero slope. It is apparent that q_e is zero and that excluded volume effects are unimportant.

Upon rearranging eq. (35) and neglecting excluded volume effects, one obtains,

$$[\eta] = \pi^{1/2} N_A (b_0^2/6M_0)^{3/2} x F(x) M^{1/2} \tag{36}$$

Equation (36) is essentially the result of Kirkwood and Riseman.[31] The values for $xF(x)$ reported by Kirkwood and Riseman[31] and by Kirkwood, Zwanzig, and Plock[65] should be replaced by the revised values given by Kurata and Yamakawa[32] which are based on a simple scaling procedure and the asymptotic value for $xF(x)$ reported by Auer and Gardner.[66]

According to eq. (36), in the limit of high molecular weight where $xF(x)$ approaches a constant value, $[\eta] \sim M^{1/2}$. Within experimental error this is the limiting behavior shown in Figure 6. It should be pointed out that this limiting viscosity behavior was first predicted by Debye and Bueche[30] and later by Kirkwood and Riseman.[31]

This behavior is not observed for either cellulose tricaproate or hydroxyethyl cellulose which, according to Figure 11, have molecular conformations similar to GTA. These polymers are expected to have lower monomeric friction coefficients than GTA and apparently are still partially draining.

The Effective Bond Length

The effective bond length is the bond length of a hypothetical freely jointed chain with the same number of bonds as the actual polymer chain but having a greater contour length. It can be considered to be a measure of the "stiffness" of the molecule and can be calculated from light-scattering results through use of eq. (32) and from the intrinsic viscosity by means of eq. (36).

Effective bond lengths calculated from these equations are given in Table III and shown in Figure 13. The light-scattering effective bond lengths are seen to decrease with increasing molecular weight and at the highest molecular weight a value of 25.4 A. is obtained for b_0. Effective bond lengths from intrinsic viscosity measurements are independent of molecular weight and may be assigned a constant value for b_0 of 23.3 A.

It is apparent that there is an appreciable difference between the hydrodynamic and the light-scattering radius of gyration, and the hydrodynamic radius is always less than or equal to the light-scattering radius.

According to Kurata and Yamakawa[32] and Fixman,[67] chains with excluded volume effects cannot be Gaussian, and expansion of the coil is not uniform but occurs to a greater extent in the "skin" than in the "core" of the molecule. The net result is that the hydrodynamic radius varies less rapidly than the statistical radius as the molecular weight increases.

In the case of GTA, however, excluded volume effects are unimportant so that the details of the excluded volume theories do not apply in the pres-
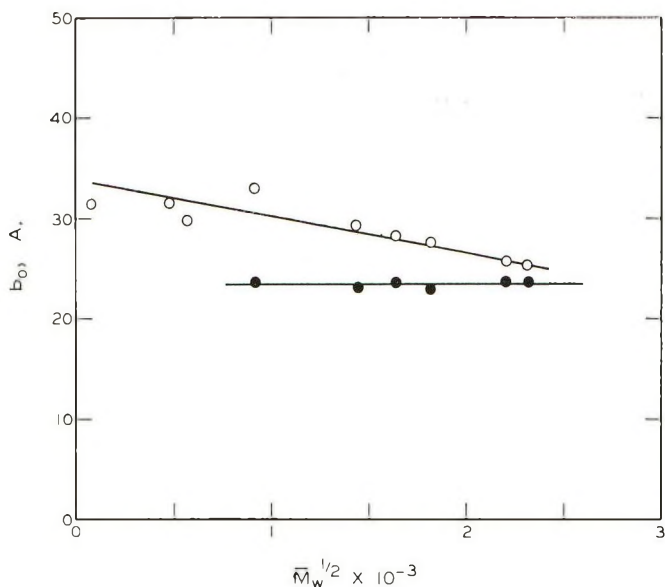
Fig. 13. Effective bond lengths for guaran triacetate in acetonitrile at 22.5°C.: (O) values from light scattering; (●) values from intrinsic viscosity.

ent case, although, of course, the hydrodynamic and statistical radii are different.

At the highest molecular weight the light-scattering equivalent bond length for GTA of 25.4 A. compares favorably with the value of 28 A. obtained for hydroxyethyl cellulose[35] in water and the value of 22–24 A. for cellulose tricaproate.[50] These are of course considerably lower than the 35 A. value found for cellulose trinitrate.[49]

The Flory Coefficient

According to Flory and Fox[68] the intrinsic viscosity may be expressed as,

$$[\eta] = \Phi(\bar{r}^2)^{3/2}/M \tag{37}$$

where $\bar{r}^2$ is the mean square end-to-end separation of the polymer chain and Φ is a constant for many flexible polymer systems. For this equation to be valid it is necessary for the molecule to coil sufficiently so as to approach spherical symmetry and for the internal hydrodynamic resistance to be great enough for Φ to approach its maximum asymptotic value.[69]

Guaran triacetate molecules do not always satisfy these conditions, so that the symbol $\{\Phi\}$ will be used to distinguish the Flory coefficient from its maximum asymptotic value Φ.

For a heterogeneous polymer, eq. (37) may be rearranged and written as

$$\Phi' = q_0 M_u[\eta]/(\bar{S}_z^2)^{3/2} \tag{38}$$
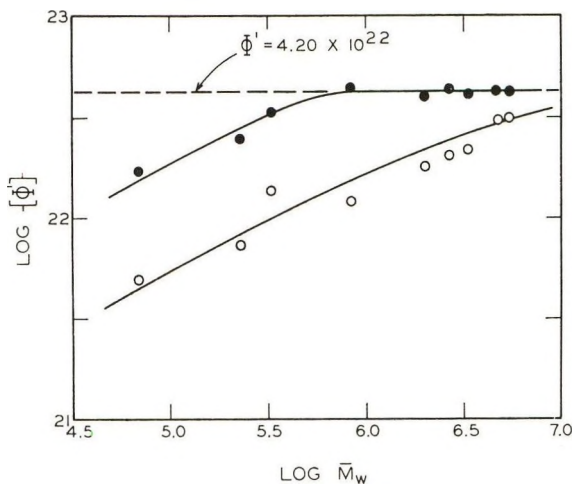
Fig. 14. Flory coefficient as a function of molecular weight for guaran triacetate in acetonitrile for values based on: (O) light-scattering radius of gyration; (●) hydrodynamic radius of gyration.

where $\Phi' = 6^{3/2}\Phi$. The term q_0 is a factor to correct for sample heterogeneity. For a distribution of the Zimm-Schulz type, eq. (18), q_0 is given by[50,70]

$$q_0 = [(h + 2)^{3/2}\Gamma(h + 2)/(h + 1)^2\Gamma(h + 1.5)] \tag{39}$$

Values of the Flory coefficient corrected for heterogeneity are given in Table IV and shown in Figure 14 as a function of molecular weight. The Flory coefficient has been calculated on the basis of both light-scattering and hydrodynamic radii of gyration.

When light-scattering values are used, the coefficient decreases rapidly with decreasing molecular weight. It is only at the highest molecular

TABLE IV
The Flory Coefficient for Guaran Triacetate in Acetonitrile

Fraction	Flory coefficient $\{\Phi'\} \times 10^{-22}$	
	Based on $(\bar{S}_z^2)$ from light scattering	Based on $(\bar{S}_z^2)$ from $[\eta]$
2A	3.09	4.24
2B	3.02	4.32
3	2.15	4.18
4	2.01	4.41
2C	1.68	4.09
5	1.19	4.43
6[a]	1.37	3.25
7[a]	0.72	2.51
8[a]	0.49	1.71

[a] Radius of gyration based on dissymmetry method and the random coil model.

weight that values of the coefficient approach the limiting theoretical value of $\Phi' = 6^{3/2}\Phi = (6^{3/2})(2.86 \times 10^{21}) = 4.20 \times 10^{22}$ reported by Ptitsyn and Eizner[71] and Kurata and Yamakawa.[32]

Values of the Flory coefficient based on the hydrodynamic radius of the molecule have been calculated assuming a constant equivalent bond length of 23.3 A. The results are somewhat surprising for when the hydrodynamic radius is used the asymptotic high molecular weight limit of the Flory coefficient is found to be $\{\Phi'\} = 4.28 \pm 0.67 \times 10^{22}$, which agrees with the recent theoretical value[32,71] within experimental error. At lower molecular weights $\{\Phi'\}$ is less than the asymptotic high molecular weight limit as a result of the draining effect.

CONCLUSIONS

The range in weight-average degree of polymerization of 171 to 12,400 found for GTA in this study is comparable in breadth and magnitude to similar studies conducted on cellulose trinitrate[46,49] and amylose.[34] The dependence of radius of gyration on chain length is identical to that observed for hydroxyethyl cellulose and cellulose tricaproate, indicating that the β-1,4-linked D-glucose chain of cellulose and β-1,4-linked D-mannose chain of GTA have similar configurations, in spite of chemical and structural differences between the anhydro sugar units. The α-1,6-linked D-galactose side groups on every other mannose unit of GTA do not appear to affect main chain configurations to any great extent.

Above a degree of polymerization of 1,970 the molecule is hydrodynamically nondraining. Intrinsic viscosity–molecular weight relations indicate that excluded volume effects are unimportant. Equivalent bond lengths calculated from intrinsic viscosity and from light scattering indicate that it is necessary to distinguish between the hydrodynamic and light-scattering radius of gyration.

The Flory coefficient calculated from the light-scattering radius of gyration was found to increase with increasing molecular weight. When the hydrodynamic radius of gyration was used in the calculation, agreement with the theoretical value of $\Phi' = 4.20 \times 10^{22}$ was obtained within experimental error. Corrections for polymolecularity were made on the basis of the Zimm-Schulz distribution, and reliable estimates were available for all molecular weight fractions.

References

1. Heyne, E., and R. L. Whistler, *J. Am. Chem. Soc.*, **70**, 2249 (1948).
2. Moe, O. A., S. E. Miller, and M. H. Iwen, *J. Am. Chem. Soc.*, **69**, 2621 (1947).
3. Whistler, R. L., T. K. Li, and W. Dvonch, *J. Am. Chem. Soc.*, **70**, 3144 (1948).
4. Swanson, J. W., *J. Am. Chem. Soc.*, **71**, 1510 (1949).
5. Ahmed, Z. F., and R. L. Whistler, *J. Am. Chem. Soc.*, **72**, 2524 (1950).
6. Whistler, R. L., and D. F. Durso, *J. Am. Chem. Soc.*, **73**, 4189 (1951).
7. Whistler, R. L., and D. F. Durso, *J. Am. Chem. Soc.*, **74**, 5140 (1952).
8. Whistler, R. L., and C. G. Smith, *J. Am. Chem. Soc.*, **74**, 3795 (1952).
9. Palmer, K. J., and M. Ballantyne, *J. Am. Chem. Soc.*, **72**, 736 (1950).
10. Greenwood, C. T., and H. Rossotti, *J. Polymer Sci.*, **27**, 481 (1958).
11. Reeves, R. E., *J. Am. Chem. Soc.*, **71**, 215 (1949).
12. Burchard, W., *Makromol. Chem.*, **42**, 151 (1960).
13. Haug, A. J., *Tappi*, **36**, 47 (1953).
14. Carson, J. F., and W. D. Maclay, *J. Am. Chem. Soc.*, **70**, 293 (1948).
15. Genung, L. B., and R. C. Mallatt, *Ind. Eng. Chem., Anal. Chem.*, **13**, 369 (1941).
16. Vermillion, F. J., Doctor's Dissertation, The Institute of Paper Chemistry, Appleton, Wis., 1963.
17. Swenson, H. A., A. J. Morak, and S. Kurath, *J. Polymer Sci.*, **51**, 231 (1961).
18. Cabannes, J., and Y. Rocard, *La diffusion moleculaire de la lumiere*, Presses Universitaires de Paris, Paris, 1929.
19. Zimm, B. H., *J. Chem. Phys.*, **16**, 1093 (1948).
20. Brice, B. A., M. Halwer, and R. Speiser, *J. Opt. Soc. Am.*, **40**, 768 (1950).
21. Debye, P., *J. Appl. Phys.*, **15**, 338 (1944).
22. Beattie, W. H., and C. Booth, *J. Polymer Sci.*, **44**, 81 (1960).
23. Beattie, W. H., and C. Booth, *J. Phys. Chem.*, **64**, 696 (1960).
24. Holtzer, A. M., H. Benoit, and P. Doty, *J. Phys. Chem.*, **58**, 624 (1954).
25. Hall, H. T., and R. M. Fuoss, *J. Am. Chem. Soc.*, **73**, 265 (1951).
26. Schulz, G. V., *Z. Elektrochem.*, **43**, 479 (1937).
27. Timell, T. E., *Svensk Papperstid.*, **57**, 777 (1954).
28. Cowie, J. M. G., *J. Polymer Sci.*, **49**, 455 (1961).
29. Schurz, J., and E. H. Immergut, *J. Polymer Sci.*, **9**, 279 (1952).
30. Debye, P., and A. M. Bueche, *J. Chem. Phys.*, **16**, 573 (1948).
31. Kirkwood, J. G., and J. Riseman, *J. Chem. Phys.*, **16**, 565 (1948).
32. Kurata, M., and H. Yamakawa, *J. Chem. Phys.*, **29**, 311 (1958).
33. Goldberg, P., and R. M. Fuoss, *J. Phys. Chem.*, **58**, 648 (1954).
34. Cowie, J. M. G., *Makromol. Chem.*, **42**, 230 (1961).
35. Brown, W., *Arkiv Kemi*, **18**, 227 (1961).
36. Claesson, S., and U. Lohmander, *Makromol. Chem.*, **44-46**, 461 (1961).
37. Van Holde, K. E., and R. L. Baldwin, *J. Phys. Chem.*, **62**, 734 (1958).
38. Fujita, H., *Mathematical Theory of Sedimentation Analysis*, Academic Press, New York, 1962.
39. Williams, J. W., K. E. Van Holde, and R. L. Baldwin, *Chem. Revs.*, **58**, 715 (1958).
40. Yamakawa, H., *J. Chem. Phys.*, **36**, 2995 (1962).
41. McCormick, H. W., *J. Polymer Sci.*, **36**, 341 (1959).
42. Flory, P. J., *Principles of Polymer Chemistry*, Cornell Univ. Press, Ithaca, N. Y., 1953.
43. Zimm, B. H., and I. Myerson, *J. Am. Chem. Soc.*, **68**, 911 (1946).
44. Zimm, B. H., *J. Chem. Phys.*, **16**, 1099 (1948).
45. Schulz, G. V., *Z. Phys. Chem.*, **B43**, 25 (1939).
46. Huque, M. M., D. A. I. Goring, and S. G. Mason, *Can. J. Chem.*, **36**, 952 (1958).
47. Orofino, T. A., and P. J. Flory, *J. Chem. Phys.*, **26**, 1067 (1957).
48. Stockmayer, W. H., *Makromol. Chem.*, **35**, 54 (1960).

49. Hunt, M. L., S. Newman, H. A. Scheraga, and P. J. Flory, *J. Phys. Chem.*, **60**, 1278 (1956).

50. Krigbaum, W. R., and L. H. Sperling, *J. Phys. Chem.*, **64**, 99 (1960).

51. Henley, D., *Arkiv Kemi*, **18**, 327 (1961).

52. Benoit, H., and P. Doty, *J. Phys. Chem.*, **57**, 958 (1953).

53. Porod, G., *Monatsh.*, **80**, 251 (1949).

54. Kratky, O., and G. Porod, *Rec. Trav. Chim.*, **68**, 1106 (1949).

55. Kuhn, W., and H. Kuhn, *Helv. Chim. Acta*, **26**, 1394 (1943).

56. Benoit, H., *J. Polymer Sci.*, **3**, 376 (1948).

57. Eliezer, I., and H. J. G. Hayman, *J. Polymer Sci.*, **23**, 387 (1957).

58. Lifson, S., *J. Chem. Phys.*, **29**, 89 (1958).

59. Debye, P., *Collected Papers*, Interscience, New York, 1954.

60. Taylor, W. J., *J. Chem. Phys.*, **16**, 257 (1948).

61. Swenson, H. A., and N. S. Thompson, personal communication.

62. Notley, N. T., and P. J. W. Debye, *J. Polymer Sci.*, **17**, 99 (1955).

63. Brown, W., D. Henley, and J. Öhman, *Makromol. Chem.*, **64**, 49 (1963).

64. Burchard, W., *Makromol. Chem.*, **50**, 20 (1961).

65. Kirkwood, J. G., R. W. Zwanzig, and R. J. Plock, *J. Chem. Phys.*, **23**, 213 (1955).

66. Auer, P. L., and C. S. Gardner, *J. Chem. Phys.*, **23**, 1546 (1955).

67. Fixman, M., *J. Chem. Phys.*, **23**, 1656 (1955).

68. Flory, P. J., and T. G. Fox, Jr., *J. Am. Chem. Soc.*, **73**, 1904 (1951).

69. Flory, P. J., and O. K. Spurr, Jr., *J. Polymer Sci.*, **27**, 231 (1958).

70. Krigbaum, W. R., and D. K. Carpenter, *J. Phys. Chem.*, **59**, 1166 (1955).

71. Ptitsyn, O. B., and Y. E. Eizner, *Soviet Phys.–Tech. Phys.*, **4**, 1020 (1959).

Résumé

On a fractionné une guarane totalement acétylée (guaran triacétate CTA) et on a caractérisé par diffusion lumineuse et par des mesures de viscosité les fractions dont les poids moléculaires s'étendent de 171 à 12.400. Pour des poids moléculaires élevés, on observe un résultat non-Newtonien et après une correction adéquate, on trouve que la viscosité intrinsèque est indépendante du gradient de cisaillement. L'analyse des données viscosimétriques en accord avec la théorie de Kurata et Yamakawa indique qu'aux poids moléculaires élevés la molécule ne s'écoule pas et que les effets du volume exclu sont absents. On a estimé la polymolécularité de certaines fractions par ultracentrifugation et par des mesures de pression osmotique et pour une fraction on a pu déterminer une distribution de poids moléculaire et montrer la validité de la distribution de Zimm-Schulz. On trouve que le rapport du carré moyen du rayon de gyration au poids moléculaire diminue pour une augmentation du poids moléculaire indiquant une distribution non-gaussienne qui ne peut pas être attribuée au modèle de chaîne Porod-Kratky. Cette dépendance du rayon de gyration vis-à-vis de la longueur de chaîne est identique à celle observée pour l'hydroxyéthylcellulose et le tricaproate de cellulose indiquant que la liaison bèta-1,4-glucosidique de la cellulose et la liaison bèta-1,4- de la chaîne de CTA ont la même configuration dans l'espace et les mêmes différences chimiques et structurales qu'entre les unités de sucres anhydres. Les groupements latéraux alpha-1,6-galactose attachés l'unité mannose du CTA ne semblent pas influencer considérablement la configuration de la chaîne principale. Les longueurs de liaison équivalente calculée au départ de la viscosité intrinsèque et de diffusion lumineuse indiquent qu'il faut distinguer entre le rayon de gyration hydrodynamique et celui déterminé par diffusion lumineuse. On trouve que le coefficient de Flory calculé à partir des rayons de gyration par diffusion lumineuse augmente avec l'augmentation du poids moléculaire. Lors des déterminations des rayons de gyration par des mesures hydrodynamiques, il y a accord avec la constante théorique de Flory compte tenu des erreurs expérimentales.

Zusammenfassung

Gänzlich acetyliertes Guaran (Guarantriacetat, GTA) wurde fraktioniert, und die Fraktionen im Gewichtsmittel-D.P.-Bereich von 171 bis 12,400 wurden durch Lichstreuung und Viskosimetrie charakterisiert. Bei hohen Molekulargewichten wurde nicht-Newtonsches Fliessverhalten beobachtet und nach geeigneter Korrektur wurde die Viskositätzahl als vom Scherungsgradienten unabhängig gefunden. Die Analyse der Viskositätsergebnisse nach der Theorie von Kurata und Yamakawa zeigt, dass bei höherem Molekulargewicht das Molekül nicht durchspült ist und Ausgeschlossene-Volumeffekte fehlen. Die Polymolekularität wurde aufgrund von Ultrazentrifugenmessungen und Bestimmungen des osmotischen Drucks von bestimmten Schlüsselfraktionen bestimmt, im Falle einer Fraktion war es möglich, die Molekulargewichtsverteilung zu bestimmen und damit die Gültigkeit der Zimm-Schulz-Verteilung zu zeigen. Das Verhältnis des mittleren Quadrates des Gyrationsradius zum Molekulargewicht nimmt mit zunehmendem Molekulargewicht ab und ziegt damit ein nicht-Gauss'sches Verhalten, das mit dem Porod-Kratky-Kettenmodell nicht erklärt werden kann. Die Abhängigkeit des Gyrationsradius von der Kettenlänge ist mit der für Hydroxyäthylzellulose und Zellulosetricaproat beobachteten identisch, was zeigt, dass die β-1,4-verknüpfte D-Glukosekette von Zellulose und die β-1,4-verknüpfte Kette von GTA trotz chemischer und Strukturunterschiede zwischen den Anhydrozuckereinheiten eine ähnliche Struktur besitzen. α-1,6-verknüpfte D-Galaktoseseitengruppen an jeder anderen Mannoseeinheit von GTA scheinen die Hauptkettenkonfiguration nicht in einem grösseren Ausmass zu beeinflussen. Aus der Viskositätszahl und Lichtstreuungsmessungen berechnete äquivalente Bindungslängen zeigen die Notwendigkeit einer Unterscheidung zwischen dem hydrodynamischen und dem Lichtstreuungsgy ationsradius. Der aus dem Lichtstreuungsgyrationsradius berechnete Flory-Koeffiziernt nahm mit wachsendem Molekulargewicht zu. Bei Benützung des hydrodynamischen Gyrationsradius zur Berechnung lag die Übereinstimmung mit der theoretischen Flory-Konstante innerhalb der Fehlergrenzen.

Kinetics of Ring-Scission Copolymerization*

O. C. DERMER and W. A. AMES,† *Department of Chemistry, Oklahoma State University, Stillwater, Oklahoma*

Synopsis

β-Propiolactone and propylene sulfide with triethylamine catalyst produced only polypropiolactone, but the lactone and DL-valine N-carboxy anhydride gave a copolymer of low molecular weight. Neither the classical copolymer equation nor the relationship pointed out by O'Driscoll applies to this copolymerization, but the valine N-carboxy anhydride was obviously the much more reactive. The rate of acid-catalyzed copolymerization of N-(2-hydroxyethyl)aziridine and N-(2-hydroxy-n-propyl)aziridine was essentially equal to the sum of the rates of the homopolymerizations of the two monomers, as was found by Shalitin and Katchalski for several pairs of N-carboxy-α-amino acid anhydrides. A mixture of propylene oxide and epichlorohydrin did not exhibit this ideal behavior and was polymerized very little more rapidly than propylene oxide alone.

INTRODUCTION

The ionic copolymerization of vinyl monomers differing much in structure is well known to be difficult because of the great disproportion in reactivities of monomers. While the same appears to be true for copolymerization by ring scission, only a very few cases have been studied. Several patents have claimed the production of useful copolymers from olefin oxides and olefin sulfides.[1,2] However, ethylene sulfide and ethylene oxide copolymerize appreciably only if the less reactive monomer (ethylene oxide) is in considerable excess.[3] Similarly, various aziridines and 1,2-epoxides yield only block copolymers or none at all.[4] β-Propiolactone and propylene oxide do not copolymerize; even when a mixture was treated with catalysts known to homopolymerize the epoxide, only polypropiolactone was obtained.[5]

Only a few measurements of the classical reactivity ratios, r_1 and r_2, for cyclic monomers have been reported: tetrahydrofuran 2.2 and ethylene oxide 0.08;[6] epichlorohydrin 1.8 ± 0.3 and propylene oxide 0.6 ± 0.5;[7] tetrahydrofuran 1.00 and 3,3-bis(chloromethyl)oxetane 0.82;[8] and α-pyrrolidone 5.0 and ε-caprolactam 0.85.[9]

Simplified forms of the classical copolymer equation have also been used recently. Shalitin and Katchalski[10] showed that for most pairs of N-car-

boxy-α-amino acid anhydrides (NCA's) tested, the relative reactivities of the monomers were identical with their absolute reactivities, i.e., the rate of copolymerization was essentially equal to the sum of the rates of homopolymerization. The relative reactivities were not determined by the usual competitive experiments, but are the ratios of the specific reaction rate constants of homopolymerization of the several monomers. Each such ratio is equivalent of the α value in Wall's copolymer equation.[11]

Bailey and France[12] and Dermer[3] obtained α values for some olefin sulfides, olefin oxides, and N-ethylaziridine by competitive experiments.

The present investigation was conducted to examine the behavior of other pairs of cyclic monomers. Some preparative experiments were made, and the applicability of the Shalitin-Katchalski relationship to monomers other than NCA's was studied.

EXPERIMENTAL

Preparative Work

β-**Propiolactone and Propylene Sulfide.** The lactone was distilled at reduced pressure before use. The propylene sulfide, b.p. 73°C./740 mm., was prepared by a published method.[3] A mixture of lactone (10.9 g.), sulfide (7.3 g.), freshly distilled N,N-dimethylformamide (180 ml.), and triethylamine catalyst (0.30 ml.) was stirred at room temperature. After 17 hr. a test portion poured into ether gave a white solid, softening point 74°C., corresponding in infrared spectrum to authentic polypropiolactone, softening point 86°C.[13] After 48 hr. the whole homogeneous reaction mixture was similarly worked up to give 6.4 g. (35%) of polypropiolactone, containing no more than traces of sulfur, and identified as before.

β-**Propiolactone and** DL-**Valine** N-**Carboxy Anhydride (Valine NCA).** The NCA was prepared according to the literature procedure,[14] and was recrystallized twice from ethyl acetate-petroleum ether before use. A mixture of β-propiolactone (42.8 g.), valine NCA (17 g.), anisole (150 ml.), benzene (100 ml.), and pyridine catalyst (0.28 g.) was heated at 70°C. for 68 hr. The resultant solution was poured into 3 l. of ligroine and the precipitated polymer collected, redissolved in acetone, and reprecipitated by pouring the solution into excess ethyl ether. The white powder (16.2 g., 27%) had softening point at 70°C. and λ_{max} 3.0, 5.75, 6.1, 6.5 μ (KBr pellet); these bands indicate the presence of both ester and amide groups. The powder contained 2.1% nitrogen. Its copolymeric nature was established by successive extractions with boiling acetone; the infrared spectrum of the residue after six extractions showed the presence of both ester (5.75 μ) and peptide (3.08, 6.12, 6.52 μ) groups, and the ratios of intensity of amide (6.12 μ) to ester bands after two and six extractions were 2.7 and 2.6, respectively. By contrast, a mechanical mixture of polyvaline and polypropiolactone, made to contain 2.1% nitrogen, after two and four similar extractions gave infrared spectra indicating the presence of only poly-

valine, the polyester having been completely removed. This technique of establishing the copolymeric nature of a product has been used before.[15,16]

The copolymer had intrinsic viscosity of 0.05 in N,N-dimethylformamide at 35°C. Titrations of its solution in chloroform–methanol with standard methanolic potassium hydroxide gave sharp (but fading) endpoints corresponding to number-average molecular weights of 1177, 1106, and 1177.

A copolymer was similarly made, but from a 50:1 mole ratio of lactone to NCA, in anisole with sodium methoxide catalyst, kept at room temperature for seven days. It had softening point 85°C.; η (in m-cresol at 35°C.) was 0.145; and molecular weight by titration was 3550.

Kinetic Studies

N-(2-Hydroxyethyl)aziridine (NHEA) and N-(2-hydroxy-n-propyl)aziridine (NHPA). Generous samples of NHEA and NHPA and a procedure for the determination of aziridine monomers were furnished by the Texas Division of The Dow Chemical Company. These samples were distilled at reduced pressure before use. The method for determination of the aziridines consisted of addition of an aliquot of the monomer solution to excess 20% $Na_2S_2O_3$, addition of sufficient $0.1N$ H_2SO_4 to the solution to maintain pH 4, and after a 30-min. period, back-titration of the excess acid with standard base to the potentiometric endpoint.

A 6-ml. portion (5.8375 g.) of NHEA and 29.00 ml. of distilled water in a 50-ml. volumetric flask were brought to 30.0°C. in a constant-temperature bath. Sulfuric acid (15.00 ml., $0.1069N$) was added as the stop watch was started. The change in concentration of NHEA was followed by withdrawing 3.00-ml. samples at known times and determining NHEA as
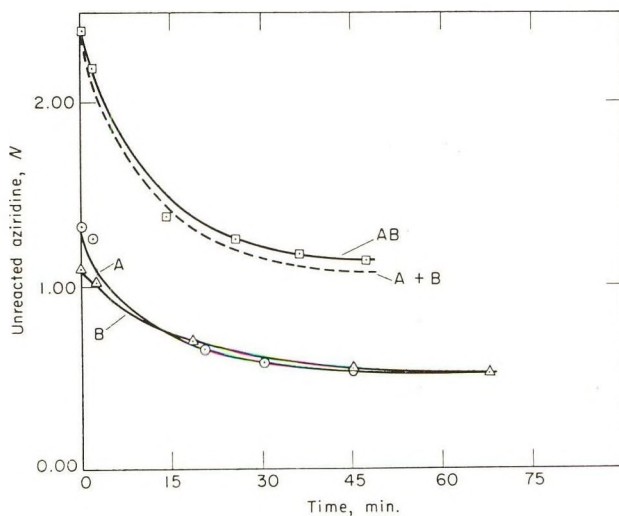
Fig. 1. Rates of acid-catalyzed polymerizations of aziridines: (A) homopolymerization of NHEA; (B) homopolymerization of NHPA; (A + B) sum of lines A and B; (AB) copolymerization of NHEA and NHPA.

already outlined. NHPA was homopolymerized like NHEA. Finally, NHEA (5.8324 g.) and NHPA (5.5236 g.) were copolymerized, the same amount of catalyst being used as in the homopolymerizations. The total volume of solution was 50.00 ml. The data are plotted in Figure 1.

Propylene Oxide and Epichlorohydrin. Propylene oxide was dried over pellet KOH. Both monomers were distilled before use. The cyclic ethers were determined by a procedure suitable for both water-soluble and water-insoluble epoxides.[17]

Propylene oxide (3.00 ml.) in a 200-ml. volumetric flask was placed in a constant-temperature bath at 27.0°C. and was diluted to volume with CH_2Cl_2. A 5.00-ml. aliquot was transferred into excess dioxane–HCl (15.00 ml.) for an initial titer. Methanol cocatalyst (1.00 ml., 1.48N) in CH_2Cl_2 was added to the volumetric flask, then BF_3 etherate (2.00 ml.,
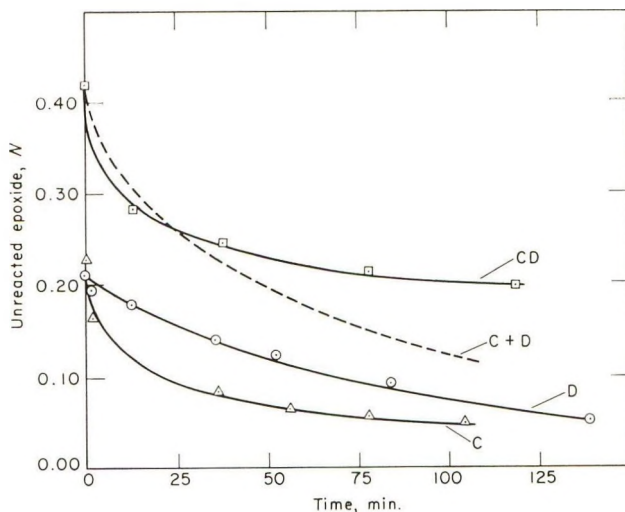
Fig. 2. Rates of acid-catalyzed polymerizations of epoxides in methylene chloride: (C) homopolymerization of propylene oxide; (D) homopolymerization of epichlorohydrin; ($C + D$) sum of lines C and D; (CD) copolymerization of the epoxides.

0.57N) in CH_2Cl_2, and the stop watch was started. Aliquots (5.00 ml.) were withdrawn at known times and were transferred to dioxane–HCl solution (15.00 ml.). After at least 15 min. the samples were diluted with neutralized ethanol containing cresol red indicator and titrated to the purple endpoint with standard methanolic NaOH. A blank containing an equivalent amount of catalyst was also analyzed. Next, epichlorohydrin (3.00 ml.) was homopolymerized just as described for propylene oxide. Finally, propylene oxide (3.00 ml.) and epichlorohydrin (3.00 ml.) were copolymerized with the use of the same amount of catalyst and the same total volume of solution as for the homopolymerizations of the individual epoxides. The data for the two homopolymerizations and the copolymerization are presented in Figure 2.

β-**Propiolactone and Valine NCA.** The weighed NCA was dissolved in 200 ml. of freshly distilled anisole and the resulting solution was filtered to remove traces of insoluble residue.   The required amount of β-propiolactone was added from a pipet, and the flask containing the solution was transferred to a constant-temperature bath at 35.0°C.   Triethylamine initiator was added after thermal equilibrium was established.

TABLE I

Copolymerization of β-Propiolactone and Valine NCA

NCA in monomer feed, mole-%	Conversion of feed to polymer, %	NCA units in polymer, mole-%[a]
5.3	1.9	60.7
12.3	9.8	84.8
20.0	11.2	89.6
35.1	6.9	93.1
63.9	9.0	94.4
80.0	10.4	98.1

[a] Calculation based on the observed value of 13.6% nitrogen in purified polyvaline rather than the theoretical value of 14.1%, which could not be reached by either micro-Kjeldahl or micro-Dumas procedures.   Others have also obtained low results (13.3% N) for polyvaline.[18]   Elemental analyses of polymers not infrequently give low results, probably owing in our case to obstinately trapped solvent or moisture.

The total monomer/initiator ratio for each experiment was approximately 200.   Polymerization was allowed to proceed to low conversion.   This was accomplished by frequently withdrawing 1.00-ml. aliquots and adding these to rapidly stirred ether.   As soon as solid precipitated in such a test, the reaction was stopped by adding the contents of the reaction flask to excess rapidly stirred ether.   The white product was isolated by filtration, washed by stirring with three 150-ml. portions of ether, isolated, and dried in a vacuum oven for 4 hr.   Each sample was analyzed for nitrogen by a micro-Kjeldahl procedure.   The results are recorded in Table I.

RESULTS AND DISCUSSION

The failure of propylene sulfide to enter into a copolymer with β-propiolactone was surprising but decisive.

Figure 1 indicates that the rate of copolymerization of NHEA and NHPA is, indeed, approximately equal to the sum of the rates of homopolymerization of the two monomers.   The ratio of rates, probably about 1, could not be calculated because the rate constants of homopolymerization could not be determined.   The homopolymerizations as performed were not simple pseudo first-order or second-order reactions.   The deviation from simple kinetics may be attributed to consumption of the catalyst by reaction with monomer and polymer as observed by Barb[19] in the homopolymerization of ethylenimine.

Figure 2 shows that the rate of copolymerization of propylene oxide and epichlorohydrin is only slightly greater than the rate of homopolymerization of propylene oxide. The homopolymerization of epichlorohydrin is first-order in monomer concentration, but the kinetics of polymerization of propylene oxide is more complex. The kinetics of polymerization of ethylene oxide catalyzed by BF_3 has been found to be quite involved.[20,21] In the present investigation, after an initial rapid reaction the rate of propylene oxide did approach first-order. This has been observed also with a ferric chloride–propylene oxide complex catalyst.[22] This change of rate was attributed to a change in the nature of the iron-containing catalyst.

The data of Table I when used to calculate monomer reactivity ratios for valine NCA and β-propiolactone by the Fineman-Ross procedure gave $r_1 = 11$, $r_2 = -0.16$. The negative value shows that the classical copolymer equation does not apply here, but it is apparent that the NCA is much more reactive than the lactone. A log-log plot of ratio of monomers in the feed versus ratio of monomer units in the polymer gave a line with slope about 0.8. This value is outside the range deduced by O'Driscoll,[23] who concluded that slopes between 1.0 and 2.0 represent extremes of behavior for monomers of very similar and very dissimilar polarities. It was not possible to test the applicability of the Shalitin-Katchalski relationship because polyvaline invariably precipitated during homopolymerization before the reaction had proceeded to sufficiently high conversion.

References

1. Gurgiolo, A. (to Dow Chemical Co.), U. S. Pat. 3,000,865 (1961).

2. Ballard, S. A., R. C. Morris, and J. L. Van Winkle (to Shell Development Co.), U. S. Pat. 2,484,370 (1949).

3. Dermer, O. C., WADC Technical Report TR 55-447 (1956), *Copolymers of Olefin Sulfides;* PB 121796.

4. Overberger, C. G., and M. Tobkes, paper presented at 145th Meeting American Chemical Society, New York, Sept. 1963; *Abstracts of Papers*, p. 29-U.

5. Inoue, S., Y. Tomoi, T. Tsuruta, and J. Furukawa, *Makromol. Chem.*, **48**, 229 (1961).

6. Murbach, W. J., and A. Adicoff, *Ind. Eng. Chem.*, **52**, 772 (1960).

7. Ishida, S., *Bull. Chem. Soc. Japan*, **33**, 731 (1960).

8. Saegusa, T., H. Imai, S. Hirai, and J. Furukawa, *Kogyo Kagaku Zasshi*, **65**, 699 (1962); T. Saegusa, H. Imai, and J. Furukawa, *Makromol. Chem.*, **56**, 55 (1962).

9. Kobayashi, F., and K. Matsuya, *J. Polymer Sci.*, **A1**, 111 (1963).

10. Shalitin, Y., and E. Katchalski, *J. Am. Chem. Soc.*, **82**, 1630 (1960).

11. Wall, F. T., *J. Am. Chem. Soc.*, **63**, 1862 (1941).

12. Bailey, F. E., Jr., and H. G. France, *J. Polymer Sci.*, **45**, 243 (1960).

13. Gresham, T. L., J. E. Jansen, and F. W. Shaver, *J. Am. Chem. Soc.*, **70**, 998 (1948).

14. Bailey, J. L., *J. Chem. Soc.*, **1950**, 3461.

15. Meerwein, H., D. Delfs, and H. Morschel, *Angew. Chem.*, **72**, 927 (1960).

16. Kuntz, I., *J. Polymer Sci.*, **54**, 569 (1961).

17. Jungnickel, J. L., E. D. Peters, A. Polgar, and F. T. Weiss, in *Organic Analysis* J. Mitchell et al., Eds., Vol. I, Interscience, New York, 1953, pp. 127–154.

18. Hanby, W. E., S. G. Waley, and J. Watson, *J. Chem. Soc.*, **1950**, 3009.

19. Barb, W. G., *J. Chem. Soc.*, **1955**, 2564.

20. Worsfold, D. J., and A. M. Eastham, *J. Am. Chem. Soc.*, **79,** 900 (1957).

21. Merrall, G. T., G. A. Latremouille, and A. M. Eastham, *Can. J. Chem.*, **38,** 1967 (1960).

22. Gee, G., W. C. E. Higginson, and J. B. Jackson, *Polymer*, **3,** 231 (1962).

23. O'Driscoll, K. F., *J. Polymer Sci.*, **57,** 721 (1962).

Résumé

Le bêta-propiolactone et le sulfure de propylène fournissent en présence de triéthyl-amine comme catalyseur uniquement de la polypropiolactone: par contre la lactone et le DL-valine-*N*-carboxy-anhydride donnent un copolymère de bas poids moléculaire. On ne peut appliquer ni l'équation classique de copolymérisation, ni celle d'O'Driscoll à cette copolymérisation. Mais le valine-*N*-carboxy-anhydride était le plus réactif. La vitesse de la copolymérisation catalysée par un acide de la *N*-(2-hydroxyéthyl)-aziridine et de la *N*-(2-hydroxy-*n*-propyl)-aziridine est essentiellement égale à la somme des vitesses des homopolymérisations des deux monomères comme ont trouvé Shalitin et Katchalski pour de différentes paires de *N*-carboxy-alpha-amino-anhydrides. Un mélange d'oxyde de propylène et d'épichlorhydrine ne montre pas le même comportement et polymérise beaucoup moins vite que l'oxyde de propylène tout seul.

Zusammenfassung

β-Propiolacton und Propylensulfid lieferten mit Triäthylamin als Katalysator nur Polypropiolacton, Lacton und DL-Valin-*N*-Carboxyanhydrid, jedoch gaben ein niedrigmolekulares Copolymers. Weder die klassische Copolymergleichung noch die von O'-Driscoll aufgestellte Beziehung wird dieser Copolymerisation gerecht; das Valin-*N*-Carboxyanhydrid war aber jedenfalls das bedeutend reaktionsfähigere. Die Geschwindigkeit der säurekatalysierten Copolymerisation von *N*-(2-Hydroxyäthyl)-Aziridin und *N*-(2-Hydroxy-n-propyl)-Aziridin war im wesentlichen der Summe der Homopolymerisationsgeschwindigkeiten der beiden Monomeren gleich, wie es schon von Shalitin und Katchalski für mehrere Paare von *N*-Carboxy-α-Aminosäureanhydrigen gefunden worden war. Eine Mischung von Propylenoxyd und Epichlorhydrin zeigte dieses ideale Verhalten nicht und polymerisierte nur wenig schneller als Propylenoxyd allein.

Refractive Indices and Compositions of Crazes in Several Glassy Polymers

ROGER P. KAMBOUR, *General Electric Research Laboratory, Schenectady, New York*

Synopsis

The void contents of crazes in four glassy polymers have now been determined from measurements of craze refractive indices. The void contents of poly(methyl methacrylate), polystyrene, polycarbonate, and styrene–acrylonitrile copolymer crazes are 40, 40, 45, and 60%, respectively. Available evidence suggests that craze void content does not depend on use of a crazing agent.

Crazes in transparent glassy polymers are known not to be true cracks at all. Rather they are sharply bounded regions of the polymer which contain a polymer filling which interconnects the bulk polymer on each side of the craze.[1-3] The craze is visible by virtue of the different optical properties of the filling from those of the bulk. We have previously reported that the refractive index of the craze can often be determined from a simple measurement of the critical angle for total light reflection at the craze–bulk polymer interface.[4,5] Furthermore, using the Lorenz-Lorentz equation, the composition of crazes can be calculated within 5% or so from such indices and various known parameters of the bulk polymer and the crazing liquid if such be contained in the craze.

Results reported previously have been for crazes in Lexan polycarbonate (General Electric Company) produced by immersion of stressed specimens in crazing liquids such as ethanol. Polycarbonate is most amenable to study because of the relative ease of producing large, properly thick, flat, well-spaced solvent crazes. Under these conditions the onset of total reflection is reasonably abrupt and the critical angle can be determined within a degree or two.

In view of the surprisingly large polycarbonate craze void content (45% void, everything in the craze beside polymer being considered void content for our purposes), it is of interest to know the composition of crazes in other systems. In materials such as polystyrene it is rather more difficult to produce "ideal" crazes. They tend to be more closely spaced, which sometimes obstructs viewing; in addition the craze is often somewhat curved, producing an apparent critical angle which varies from point to point; finally, many crazes are thin enough so that frustration of total reflection becomes quite noticeable. (Crazes as thin as 400 A. have been

observed, whereas frustration of reflection becomes important for crazes of thickness of the order of the wavelength of the light or less.[5]   With these crazes it is difficult to assign a value to the true critical angle.)

Polystyrene

The ability of a glassy polymer to sustain the growth of large crazes without fracturing depends, among other things, on molecular weight[6] and degree of orientation in the specimen under test, especially when no crazing agent is used.   Thus we have not been able to dry-craze injection-molded polystyrene tensile bars, even when well annealed.   Crazes were formed successfully, however, in specimens cut from compression-molded and well annealed $1/8$ in. thick sheets of Styron 666 polystyrene (Dow Chemical Company) ($\bar{M}_w = 375,000$, $\bar{M}_n = 230,000$).   Large crazes were produced by careful tensile loading.   At low stresses many fine crazes developed in the specimen surface, probably due to surface contamination; only when the stress was raised to 4000 psi did large crazes grow (e.g., 6 mm.^{2} in area). Polarized light reflected from the craze interface showed interference colors characteristic of crazes of thickness equal to or greater than the wavelength of light.   The craze "plane" tended to be slightly curved as evidenced by the fact that the critical angle ϕ_c changed in a regular manner from one side to the other.   The angle corresponding to critical reflection at the craze center was used (63° incident on the specimen surface).*   Thus the craze refractive index n_c is 1.33 as compared to 1.60 for that of the bulk polymer.   The craze void content is calculated to be 40%.

Styrene–Acrylonitrile Copolymer

Tyril 767 styrene–acrylonitrile copolymer (Dow Chemical Company) ($\bar{M}_w = 177,000$; acrylonitrile content 30 wt.-%) can be conveniently crazed by bending under liquid ethanol.   Injection-molded tensile bars were used without annealing.   The bulk polymer refractive index is 1.57 and the density is 1.07 g./cc. according to our measurements.   An average incident angle of 41.5° on the bar surface corresponds to the critical angle, and $n_c = 1.42$ for the ethanol-filled craze.   Assuming volume and polarization additivity, as before, the craze is calculated to contain 65% alcohol, 35% polymer by volume.   Drying out the craze under stress results in a critical angle so high that the wedge modification in the method of measurement must be used;[4,5] the dried craze nevertheless is calculated to be 60% void. This craze void content is higher than that for any other polymer yet studied.

---

* The relationship between the incident angle on the specimen surface i and that on the craze plane ϕ involves only Snell's Law, the bulk polymer index, and the orthogonality of the craze plane and the specimen surface, i.e., $\sin(90° - \phi) = \sin i / n_{polymer}$.

Poly(methyl Methacrylate)

It was not found possible to produce stable crazes in specimens injection-molded from Plexiglas (Rohm and Haas Company) poly(methyl meth-acrylate).   At all stress levels, temperatures, and conditions of annealing, with or without a crazing agent, only fracture occurred.   Stable crazes can be easily produced, however, in cast Plexiglas sheet with and without a crazing agent.   The difference is probably attributable to molecular weight difference (110,000 in the molding resin versus 10^6 in the cast sheet).

Solvent crazes were produced by bending under ethanol specimens cut from $1/8$ in. sheet.   Total reflection occurred at $33°$ average incident angle on the bar surface with the craze still full of solvent.   This leads to $n_c = 1.38$ and a craze alcohol content of 40% by volume.

Compared to polystyrene, poly(methyl methacrylate) is well known to be difficult to craze without a crazing agent.   Under optimum rates of linear loading we have found it possible to produce only small and thin, albeit flat and well-spaced, crazes in cast sheet under dry conditions.   As with small polystyrene crazes, the attainment of total reflection is a gradual process occurring over several degrees.   Reflection appears to begin at $\sim 44°$ incident angle on the bar surface and become complete at $55°$.   These angles, if used alternately for computation, lead to 30% and 50% void content in the craze, respectively.

An improved estimate of the critical angle can be made utilizing the fact that, under conditions of frustrated reflection, the angular spread and true critical angle are related indirectly for any given craze thickness and set of indices for craze and bulk polymer.   Curves of light transmission versus incident angle have been previously calculated for dried polycarbonate
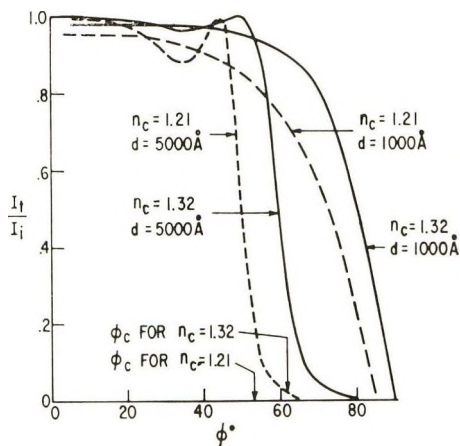
Fig. 1. Calculated relationships between light transmission fraction I_t/I_i and angle of incidence ϕ on the craze–bulk polymer interface for the two possible extreme values of craze refractive index n_c and for two values of craze thickness d. ϕ_c is the critical angle for total reflection

crazes of various thicknesses.[5] Similar curves calculated for hypothetical poly(methyl methacrylate) crazes of the two extremes in possible refractive index are shown in Figure 1. It can be observed that thin crazes (e.g., ~1000 A.) show a 30–40° range between 90% transmission and 10% transmission ($\Delta\phi_{90-10}$) with a critical angle ϕ_c rather close to the 90% transmission angle. For thicker crazes (~5000 A.), $\Delta\phi_{90-10}$ is 8–11° and ϕ_c is located in the middle of the spread. For 10,000 A. crazes, $\Delta\phi_{90-10} \sim 2°$ and ϕ_c is at the 90% angle. In short, the thicker the craze, the closer is ϕ_c to the extinction angle. This relationship is not very sensitive to differences in craze index. If it be assumed that the incident angles 44° and 55° reported above correspond respectively to ϕ_{90} and ϕ_{10} on the craze interface, then ϕ_{90} is 56°, ϕ_{10} is 62°, and ϕ_c is estimated as 60°. The void content of the polymethyl methacrylate dry craze is then calculated to be 40%.

Summary

In conclusion, crazes in the glassy polymers studied to date are 40–60% void. If the results for poly(methyl methacrylate) in particular are an accurate guide, the void content is the same regardless of whether a crazing agent is used.

Results are summarized in Table I.

TABLE I
Composition of Crazes in Glassy Polymers

Polymer	Crazing environment	Void in craze, %[a]
Poly (methyl methacrylate)	Liquid ethanol	40
Poly(methyl methacrylate)	Air	40
Polystyrene	Air	40
Polycarbonate	Liquid ethanol	45
Styrene–acrylonitrile copolymer	Liquid ethanol	60

[a] Per cent void for crazes still saturated with crazing agent refers to the volume occupied by the agent.

References

1. Bessonov, M. I., and E. V. Kuvshinskiĭ, *Plasticheskie Massy*, **5**, 57 (1961).
2. Lebedev, G. A., and E. V. Kuvshinskiĭ, *Soviet Phys. Solid State*, **3**, 1957 (1962).
3. Spurr, O. K., and W. D. Niegisch, *J. Appl. Polymer Sci.*, **6**, 585 (1962).
4. Kambour, R. P., *Nature*, **195**, 1299 (1962).
5. Kambour, R. P., *Polymer*, **5**, 107 (1964).
6. Rudd, J. F., *J. Polymer Sci.*, **B1**, 1 (1963).

Résumé

La teneur en cavités de craquelures dans 4 polymères vitreux a été déterminée à partir de mesures des indices de réfraction des craquelures. La teneur en cavités des craquelures de polyméthacrylate de méthyle, du polystyrène, du polycarbonate et du copolymère styrène–acrylonitrile s'évalue à 40, 40, 45 et 60% respectivement. Il semble que la teneur en cavités dans les craquelures ne dépend pas de l'emploi d'un agent provoquant ces craquelures.

Zusammenfassung

Der Leerraumgehalt von Rissen in vier glasartigen Polymeren wurde durch Messung des Rissbrechungsindex bestimmt. Der Leeraumgehalt von Polymethylmethacrylat-, Polystyrol-, Polycarbonat- und Styrolacrylnitril-Kopolymerrissen beträgt 40 bzw. 40 bzw. 45 bzw. 60%. Die vorhandenen Unterlagen zeigen, dass der Rissleerraumgehalt nicht von der Verwendung eines rissbildenden Stoffes abhängt.

Refractive Index and Composition of Poly(methyl Methacrylate) Fracture Surface Layers

ROGER P. KAMBOUR, *General Electric Research Laboratory, Schenectady, New York*

Synopsis

By using the phenomenon of total internal reflection of light the refractive index of the thin layer present on fresh poly(methyl methacrylate) fracture surfaces has been measured. The fracture surface refractive index, 1.32, is the same as that of the craze in the same polymer. The fracture surface layer is accordingly thought to be craze like in structure.

As measured by the Griffith criteria, the energy required to propagate a crack in glassy polymers such as poly(methyl methacrylate) and polystyrene is three orders of magnitude larger than that calculated on the basis of breaking a monolayer of carbon–carbon bonds (i.e., cleaving each length of polymer chain crossing the fracture plane once).[1] This large excess energy has been associated with a thin polymer layer differing in optical properties from the bulk. This layer has been inferred to exist on the fracture surface from the observation of interference colors thereon.[1,2] According to Berry, this layer might arise by a process of polymer elongation in a small region ahead of the growing crack. A knowledge of the optical properties and the thickness of the layer would help in assessing the structure of the layer, its cause, and its effect on the fracture propagation energy.

It has recently been found possible to measure the refractive index of crazes in glassy polymers by measurement of the critical angle for total reflection of light at the craze–bulk polymer interface.[3-5] Craze compositions can be calculated by using the Lorentz-Lorenz equation and crazes in PMMA appear to be 40% void.[4] The rough similarity of stress conditions for crazing and fracture leads one to suspect that PMMA fracture surface layers are at least qualitatively similar to crazes, i.e., expanded polymer structures with refractive indices substantially lower than that of the bulk.

The method for craze refractive index measurement depends on the craze being sandwiched between large regions of substantially higher refractive index, i.e., bulk polymer. This condition is half fulfilled for the fracture surface layer (assuming it to be crazelike) since it lies on the PMMA substrate (refractive index $n = 1.49$). It can be completely ful-

filled by placing the surface in contact with a liquid of high refractive index. Then if the layer were sufficiently planar and thick ($\sim$5000 A.), its refractive index could be measured in principle.

In practice it is somewhat difficult to produce large smooth planar areas on the fracture surface. This problem can be minimized by employing the proper sample configuration and stressing system.[6] A much greater problem is the lack of stability of these layers as made manifest by the disappearance of the interference colors. Organic agents or heat cause very rapid disappearance; liquid water at room temperature causes a noticeable change in less than $1/2$ hr. (Under normal atmospheric conditions, fading can be noticed in a day or two.)

Experimental

It has been found possible to bring aqueous salt solutions into contact with these surfaces for times in the range of a minute or so without producing any diminution in interference colors. Thus, saturated silver nitrate solution ($n = 1.49$ at 25°C.) is a suitable fluid.

Most of the fracture surfaces used have been produced by cleavage of polished disks $1/2$ in. thick and $1^1/2$ in. in diameter taken from Plexiglas II stock rod.[6] The cleavage set-up, shown in Figure 1, tends to produce fracture surfaces which are often fairly planar on a gross scale with the planes perpendicular to the disk faces. On these planes can be found suitably smooth areas. Both cleavage speed (which affects smoothness) and specimen temperature are easily varied. Cleavage at -195°C. produces only hazy rather than colored surfaces. Cleavage at 25 and 60°C. yields colored surfaces suitable for study.

The experimental set-up for optical measurements is shown in Figure 2. A small drop of silver nitrate is placed on a black horizontal table opposite the center of a vertical protractor attached to the table. A thin spacer is placed on the table in a suitable position, and the PMMA half disk placed
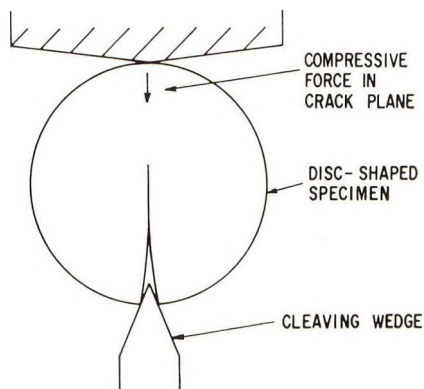
Fig. 1. Method for producing planar crack. Compressive force in crack plane prevents crack propagation from deviating away from desired plane.
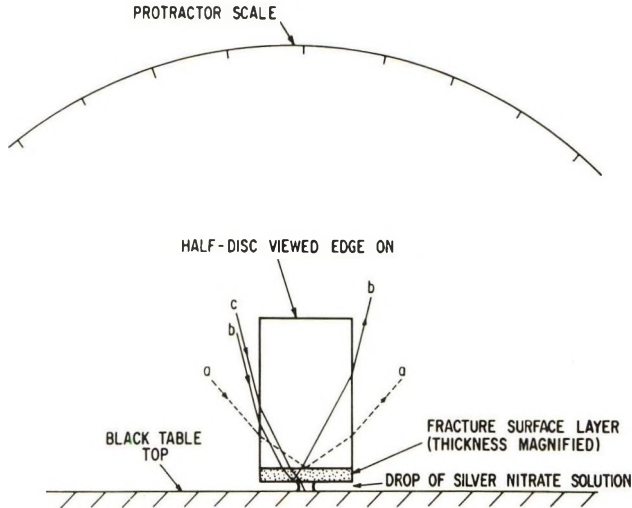
Fig. 2. Set-up for measurement of refractive index of fracture surface layer. Thin spacer holding fracture surface above table top is not shown. Beam *a* enters disk at low angle, hits interface at high angle and is totally reflected. Beam *b* enters at high angle and passes through surface layer but is totally reflected at air/layer interface. Beam *c* at same angle passes through layer and silver nitrate to become absorbed by black table top.

on it so that its faces are perpendicular to both the table and the plane of the protractor. When placed properly the desired area of the fracture surface contacts the drop without flattening it enough to produce interference colors in the liquid. The set-up is placed in diffuse light (e.g., on the window sill on a cloudy day) and the fracture surface is viewed through one of the faces of the half disk.

At high viewing angles the sharply bounded dark spot—the drop with the black background—is visible, surrounded by reflecting surface. As the viewing angle (i.e., reflection angle) is decreased, the drop becomes less visible and finally disappears, usually over a few degrees. If the area of the fracture surface covered by the drop is multiplanar, the disappearance occurs over a larger spread. The angle estimated to correspond to the critical angle is that at which the drop is just about to disappear. Its choice is aided by a sliding bar mounted on the protractor arc and used for visual alignment. The process takes a minute or so, and if the specimen is then removed, wiped dry, and inspected, there appears to be no change in interference colors in the area which had been in contact with the fluid.

Results

Some of the surfaces examined show a disappearance of the drop over a relatively wide angular spread (e.g., 10°). It is presumed that this spread is a consequence of surface nonplanarity in some cases and frustrated reflection effects caused by surface layers which are too thin in others.[4]

Those surfaces which show a fairly abrupt disappearance of the drop do so at angles which vary from 42° to 46° incident on the disk face. The refractive index of the surface layer is then calculated to be 1.32 ± 0.01. This value holds for samples fractured at 25 and 60°C.

As a check on the method of measurement, half of a fractured disk was annealed at 95°C. overnight to cause the layer to collapse. Upon removal of the disk from the oven the interference colors were gone, and when the disk was set up on the protractor table, the drop of silver nitrate solution could be seen at all angles of viewing.

The refractive index of the fracture surface layer can thus be as low as that of the craze in PMMA, and it is concluded that the surface layer, like the craze, is an expanded polymer structure with a void content as high as 40%. The expansion is seen to come about as a response to the hydrostatic tension which exists beyond the crack tip. The crazing process thus is not only associated with the Griffith flaw[7] but also with the Griffith energy for crack propagation.

The remaining structural questions concerning the layer are its thickness and the state of void dispersion. Since the onset of total reflection is not abrupt and indeed occurs over an appreciable angular spread on some areas of fracture surface, it may be speculated that the layer thickness varies from place to place in the range 5000–2000 A.

References

1. Berry, J. P., *J. Polymer Sci.*, **50**, 107 (1961).
2. Higuchi, M., *Repts. Res. Inst. Appl. Mech. Japan*, **6**, 173 (1958).
3. Kambour, R. P., *Nature*, **195**, 1299 (1962).
4. Kambour, R. P., *Polymer*, **5**, 107 (1964).
5. Kambour, R. P., *J. Polymer Sci.*, **A2**, 4161 (1964).
6. Berry, J. P., private communication.
7. Berry, J. P., *J. Polymer Sci.*, **50**, 313 (1961).

Résumé

En employant le phénomène de la réflection totale intrinsèque de la lumière, on a mesuré l'indice de refraction de la couche mince à la surface de brisure fraîche du polyméthacrylate de méthyle. L'indice de refraction de la surface de brisure 1.32 est le même que celui des craquelures du même polymère. La couche de la surface de brisure ést par conséquent supposée avoir la même structure que celle des craquelures.

Zusammenfassung

Unter Verwendung des Phänomens der totalen inneren Reflexion des Lichtes wurde der Brechungsindex der dünnen auf einer frischen Polymethylacrylatbruchoberfläche vorhandenen Schichte gemessen. Der Bruchoberflächenbrechungs index, 1,32, ist derselbe wie der eines Risses im gleichen Polymeren. Der Bruchoberflächenschichte wird daher rissähnliche Struktur zugeschrieben.

Generality of Product Probability Values in Unifying and Predicting Relationships Among Monomers in Copolymerization

GEORGE E. HAM, *Research Center, Spencer Chemical Company, Merriam, Kansas*

Synopsis

It is shown that a knowledge of the reactivity ratios for the binary systems A–B and B–C allows reactivity ratios for the copolymer system A–C to be calculated from the relationship: $P_{ab}P_{bc}P_{ca} = P_{ac}P_{cb}P_{ba} = \mathcal{P}$ (a constant). The various probabilities include the possibilities of adding A, B, or C monomers to any of the corresponding radicals and can be expressed in terms of binary reactivity ratios.   At equimolar concentrations it is shown that for systems of three conjugated or three unconjugated monomers $\mathcal{P}$ approximates 0.037. Similarly, for systems of two conjugated and one unconjugated monomers or two unconjugated and one conjugated monomers $\mathcal{P}$ approximates 0.006. Once the appropriateness of these constants is established, it is shown how the relationship may be used to assess the most probable values among widely varying reported reactivity ratios.   It is shown that the values of the constant $\mathcal{P}$ for different combinations of monomers allow the assessment of the reactivity of conjugated monomers compared with unconjugated monomers for conjugated or unconjugated radicals.   It develops that the reactivity of unconjugated monomers is between 5 and 10% of that of conjugated monomers for unconjugated radicals.   For more precise assessment of unknown reactivity ratios it is suggested that $\mathcal{P}$ is a product function of unique reactivity parameters characteristic of the individual monomers involved.

A recent paper[1] has presented a promising approach to the problem of predicting monomer reactivity in copolymerization.   The approach offers a more direct and possibly more precise means than the Q–e scheme and rests on a logical and easily discernible concept.   Simply stated, given reactivity ratios for systems A–B and B–C, the reactivity ratios for the copolymer system A–C may be calculated from the following relationship:

$$P_{ab}P_{bc}P_{ca} = P_{ac}P_{cb}P_{ba} = \mathcal{P} \text{ (a constant)} \tag{1}$$

Equimolar concentrations of monomers are assumed to simplify calculations.   The various probabilities include the possibilities of addition of A, B, and C to given radicals. $\mathcal{P}$ is undoubtedly influenced by the specific nature of the monomers involved and may be calculated by extensions of methods to be described below.   Unique parameters may be assigned to individual monomers and $\mathcal{P}$ assessed.   Fortunately, as will be shown herein the vast majority of copolymer systems can be treated in terms of

one of two unique values for $\mathcal{P}$.   When all of the three monomers involved
in the binary pairs have any appreciable amount of conjugation, that is,
are of the group of acrylates, methacrylates, acrylic acid, acrylonitrile,
methacrylonitrile, styrene and derivatives, vinylidene chloride, fumarates,
and the like, $\mathcal{P}$ is approximately 0.037. Values for reactivity ratios are
obtained which are in good agreement with experiment.

When two of the three monomers are of the group described above and
one is of low conjugation, that is, of the group of vinyl chloride, vinyl esters,
olefins, and the like, $\mathcal{P}$ is approximately 0.006, also in good agreement with
experiment.   It is estimated that 80% of the systems encountered by poly-
mer chemists are in the first two categories described, where $\mathcal{P}$ is 0.037 or
0.006.

The first category is straightforward in theory and description.   Assume
the hypothetical case wherein monomers of equal reactivity in copoly-
merization and terpolymerization and of equal concentration are allowed to
react with the various radicals.   Then the product of the individual
probabilities is

$$P_{ab}P_{bc}P_{ca} \;\;\; = P_{ac}P_{cb}P_{ba} \;\;\; = 0.037$$
$$(1/3)(1/3)(1/3) = (1/3)(1/3)(1/3) = 0.037 \tag{2}$$

The new theory generalizes the relationship so that in the event of alter-
nation tendencies or high reactivity of individual monomers in one or two
of the three binary systems leading to large individual probabilities the
third probability (likelihood of the remaining monomer adding to a specific
radical) must be small enough to yield the overall product probability of
0.037.

In the second category, comprising two conjugated monomers and a
single monomer of low conjugation, $\mathcal{P}$ is 0.006.   This value is the average of
a large number of systems with relatively little spread when obtained from
reliable data.

The hypothetical and highly specialized case may be considered where, in
binary and ternary copolymerizations involving equal proportions of two
conjugated monomers A and B and one unconjugated monomer C, $P_{ac} = P_{bc}$ and are individually small and $P_{ca} = P_{cb}$ and are large.   It is further
assumed that $r_{12} = r_{21} = 1$, $r_{32} = 1/r_{23}$, and $r_{31} = 1/r_{13}$.   We started with

$$P_{ab}P_{bc}P_{ca} = P_{ac}P_{cb}P_{ba} = 0.006 \tag{3}$$

Then x, the "general" reactivity of unconjugated monomers with con-
jugated radicals may be calculated if $x = 1/r_{13} = 1/r_{23} = r_{32} = r_{31}$, and the
"general" reactivity of conjugated monomers with conjugated radicals is
taken as 1:

$$\left[\frac{1/x}{(1/x) + 1(1/x) + 1}\right]\left[\frac{1}{1 + (1/x)1 + (1/x)}\right]\left[\frac{x}{x + (x)(x) + x}\right] = 0.006$$

$$\left[\frac{1}{1 + (1/x)1 + (1/x)}\right]\left[\frac{x}{x + (x)(x) + x}\right]\left[\frac{1/x}{(1/x) + (1/x)1 + 1}\right] = 0.006$$

$$\frac{x}{(2 + x)^3} = 0.006$$

Solution for x yields 0.052.

Since the product probabilities of such systems are almost always equal to 0.006, it may be accordingly generalized that the reactivity of most conjugated radicals with almost any unconjugated monomers is in the general range of 0.052 compared with a reactivity of 1 with most conjugated monomers, and the reactivity of most unconjugated radicals with conjugated monomers is 1/0.052 or 19.2 times their reactivity with unconjugated monomers. Admittedly this generalization is no better than the limiting assumptions; however, the value for general monomer reactivity of 0.052 for unconjugated monomers compared with 1 for conjugated monomers seems reasonable. It is interesting to note that although the two are but only remotely related, an average value of $Q = 0.03$ for ethylene (an unconjugated monomer) is obtained[2] based on styrene (a conjugated monomer) having a Q value = 1.

Entirely apart from the validity of the special case just treated, the generality of $P_{ab}P_{bc}P_{ca} = P_{ac}P_{cb}P_{ba} = 0.006$ requires that high values for one or two probabilities must be compensated by low values of remaining probabilities, so that the product probability may be 0.006.

It is inherent in the relationship $P_{ab}P_{bc}P_{ca} = P_{ac}P_{cb}P_{ba}$ that a direct relationship between monomer reactivity and radical reactivity is presented. Thus, for the probability of each monomer adding to a different radical the reverse situation is shown on the other side of the equation.

It is convenient and useful to employ equimolar proportions of monomers in utilizing the equality of product probabilities. Thus, for three "conjugated" monomers

$$P_{ab}P_{bc}P_{ca} = P_{ac}P_{cb}P_{ba} = 0.037 \tag{2}$$

although the equation is general for all monomer proportions. Thus, for equimolar monomer proportions

$$\left(\frac{r_{13}}{r_{13} + r_{12}r_{13} + r_{12}}\right)\left(\frac{r_{21}}{r_{21} + r_{23}r_{21} + r_{23}}\right)\left(\frac{r_{32}}{r_{32} + r_{32}r_{31} + r_{31}}\right) =$$

$$\left(\frac{r_{12}}{r_{12} + r_{13}r_{12} + r_{13}}\right)\left(\frac{r_{31}}{r_{31} + r_{31}r_{32} + r_{32}}\right)\left(\frac{r_{23}}{r_{23} + r_{23}r_{21} + r_{21}}\right) = 0.037 \tag{6}$$

However, the simpler derived expression (since the denominator products are equal)

$$r_{13}r_{21}r_{32} = r_{12}r_{31}r_{23} \tag{7}$$

is not so limited to equimolar concentrations.   Thus, it may be shown by substituting appropriate values for probabilities in the general relationship $P_{ab}P_{bc}P_{ca} = P_{ac}P_{cb}P_{ba}$ that

$$Br_{13}Cr_{21}Ar_{32} = Cr_{12}Br_{13}Ar_{23} \tag{8}$$

Dividing both sides by ABC yields

$$r_{13}r_{21}r_{32} = r_{12}r_{31}r_{23} \tag{7}$$

The main aim of our paper, however, is to show generalities about monomer reactivity in copolymerization.   Known values for reactivity ratios for systems of three related binary combinations, although much less rare today than a few years ago, do not always exhibit high accuracy in reported reactivity ratios in all combinations.   Examination of a large number of systems[3] shows that our generalizations are correct.   Reactivity ratios employed throughout this paper were taken from Young's compilation.

Styrene–Acrylonitrile–Acrylic Acid

In the binary systems comprising styrene–acrylonitrile–acrylic acid, reactivity ratios allow calculation at equimolar ratios of

$$P_{ab}P_{bc}P_{ca} = P_{ac}P_{cb}P_{ba}$$

$$(0.33)(0.228)(0.657) = (0.54)(0.0493)(0.745)$$

$$0.0491 = 0.0199$$

These results are based on reported values:[3] $r_{13} = 0.25$, $r_{21} = 0.04$, $r_{32} = 6$, $r_{12} = 0.41$, $r_{31} = 0.45$, $r_{23} = 0.13$.

Considering likely inaccuracies in the reactivity ratios involved, the agreement is satisfactory.   Assuming $P_{ac}P_{cb}P_{ba} = 0.37$,

$$\left(\frac{r_{12}}{r_{12} + r_{12}r_{13} + r_{13}}\right)\left(\frac{r_{31}}{r_{31} + r_{31}r_{32} + r_{32}}\right)\left(\frac{r_{23}}{r_{23} + r_{23}r_{21} + r_{21}}\right) = 0.037$$

and

$$r_{13}r_{21}r_{32} = r_{12}r_{31}r_{23} \tag{9}$$

r_{32} and r_{23} can be calculated.   The values obtained are quite good (Table I).

TABLE I

	Calculated	Reported	
r_{23}	3.15	6 ± 2	1.15
r_{23}	0.172	0.13 ± 0.02	0.35

Styrene–Methyl Acrylate–Acrylonitrile

This system styrene–methyl acrylate–acrylonitrile shows the problem of dealing with widely varying reported reactivity ratios.   For r_{32} and r_{23} reported values[3] are given in Table II.

TABLE II

r_{32}	r_{23}
0.15	1.05
1.5	0.84
0.67	1.26
1.4	0.95
0.84	0.83
0.50	0.71

The values used were $r_{23} = 0.95$, $r_{32} = 1.4$, $r_{12} = 0.75$, $r_{21} = 0.20$, $r_{13} = 0.41$, and $r_{31} = 0.04$.

$$P_{ab}P_{bc}P_{ca} = P_{ac}P_{cb}P_{ba}$$

$$(0.35)(0.15)(0.94) = (0.64)(0.0268)(0.71)$$

$$0.050 = 0.0122$$

It was decided to calculate r_{23} and r_{32}, since of all ratios needed they appeared to be known with the least accuracy. For $P_{ab}P_{bc}P_{ca} = 0.037$

$$r_{23} = 1.22 \text{ (calcd.)}$$

$$r_{32} = 0.443 \text{ (calcd.)}$$

These ratios are reasonable when compared with the scattered reported values shown above. These values also appear reasonable since repulsion of acrylonitrile monomer by acrylonitrile radical and better attraction between acrylonitrile radical and methyl acrylate monomer would lead to $r_{32} < 1$. Less selectivity by methyl acrylate radical between methyl acrylate and acrylonitrile would be expected.

Methyl Methacrylate–Methyl Acrylate–Vinyl Acetate

In the system methyl methacrylate–methyl acrylate–vinyl acetate:

$$P_{ab}P_{bc}P_{ca} = P_{ac}P_{cb}P_{ba}$$

$$(0.293)(0.0344)(0.86) = (0.0337)(0.128)(0.655)$$

$$0.0087 = 0.00282$$

These results are based on the reported values:[3] $r_{23} = 9.0$, $r_{32} = 0.1$, $r_{12} = 2.3$, $r_{21} = 0.47$, $r_{13} = 20$, $r_{31} = 0.015$. The value $r_{31}(0.015)$ of importance in calculating P_{cb} is probably too low, accounting for the low P_{cb} and product probability. Since this system contains a monomer of low conjugation

TABLE III

	Calculated	Experimental
r_{13}	22.5	20 ± 3
r_{31}	0.051	0.015 ± 0.015

$P_{ab}P_{bc}P_{ca}$ is assumed to be 0.006. Calculation of r_{13} and r_{31} yields the values of Table III.

Styrene–Methyl Acrylate–Vinyl Chloride

In considering the binary combinations which comprise the system styrene–methyl acrylate–vinyl chloride (single monomer of low conjugation), the following reported monomer reactivity ratios[3] were employed: $r_{13} = 35$, $r_{31} = 0.067$, $r_{12} = 0.75$, $r_{21} = 0.20$, $r_{23} = 9$, $r_{32} = 0.083$. Thus $P_{ab}P_{bc}P_{ca} = 0.00492$ and $P_{ac}P_{cb}P_{ba} = 0.00433$.[1] Assuming product probabilities equal to 0.006, r_{32} and r_{23} were calculated. The comparison with reported values was as given in Table IV.

TABLE IV

	Calculated	Reported
r_{32}	0.145	0.083
r_{23}	20.3	9.0

Ternary combinations employing ethylene as a single "unconjugated" monomer confirm product probabilities equal to approximately 0.006 and will be reported separately as means of predicting ethylene reactivity in copolymerization.

Methyl Methacrylate–Methyl Acrylate–Vinyl Chloride

The system methyl methacrylate-methyl acrylate-vinyl chloride allows the examination of yet another system with a single monomer of low conjugation (vinyl chloride).

Reactivity ratios from the literature[3] are: $r_{12} = 2.3$, $r_{21} = 0.47$, $r_{23} = 9.0$, $r_{32} = 0.083$, $r_{13} = 15$, $r_{31} = 0.02$.

Product properties are shown to be

$$P_{ab}P_{bc}P_{ca} = 0.00782$$
$$(0.290)(0.0343)(0.79)$$

and

$$P_{ac}P_{cb}P_{ba} = 0.0055$$
$$(0.0444)(0.19)(0.657)$$

It is apparent that calculation of r_{13}, r_{31}; r_{23}, r_{32}; or r_{12}, r_{21} assuming product probabilities $= 0.006$ would yield values in good agreement with those reported.

Acrylonitrile–Methyl Acrylate–Vinyl Chloride

Examination of the ternary system acrylonitrile–methyl acrylate–vinyl chloride allows us to check on the uncertain values reported for r_{12} in acrylonitrile–methyl acrylate copolymerization. Substitution in

$$r_{12}r_{23}r_{31} = r_{13}r_{32}r_{21}$$

for the reported values:[3] $r_{21} = 0.95$, $r_{32} = 0.083$, $r_{23} = 9$, $r_{13} = 3.7$, $r_{31} = 0.074$, and assuming the reported $r_{21} = 0.95$ (known with reasonable accuracy) a value for $r_{12} = 0.43$ results in good agreement with the value (0.443) predicted from the system styrene–methyl acrylate–acrylonitrile, where calculations were based on product probabilities $= 0.037$. In the system acrylonitrile–methyl acrylate–vinyl chloride with $r_{12} = 0.95$,

$$P_{ab}P_{bc}P_{ca} = P_{ac}P_{cb}P_{ba}$$

$$(0.647)(0.0513)(0.51) = (0.075)(0.46)(0.486)$$

$$0.0168 = 0.0167$$

Excellent agreement was obtained from the standpoint of equality, but not close enough to the desired 0.006 to give more than an approximation of predicted ratios.

Since the approach of product probabilities is independent of the Q–e scheme, we shall deal only briefly with the latter relationship. Since r_{12} and r_{21} may be calculated from the dependent reactivity ratios in the product probability scheme the following relationships arise from substitution in the Alfrey–Price equation:[4]

$$r_1 = r_{12} = r_{13}r_{32}r_{21}/r_{23}r_{31}$$
$$= (Q_1/Q_2) \exp\{-e_1(e_1 - e_2)\} \tag{10}$$

$$r_2 = r_{21} = r_{12}r_{23}r_{31}/r_{13}r_{32} = (Q_2/Q_1)\exp\{-e_2(e_2 - e_1)\} \tag{11}$$

With Zutty's simplified equation,[2] where the reference monomer is ethylene and its values are $Q_2 = 1$ and $e_2 = 0$, the relationship of eqs. (12) and (13) follow.

$$r_1 = r_{12} = r_{13}r_{32}r_{21}/r_{23}r_{32} = (Q_0)_1 \exp -\{e_0\}_1{}^2 \tag{12}$$

$$r_2 = r_{21} = r_{12}r_{23}r_{31}/r_{13}r_{32} = 1/(Q_0)_1 \tag{13}$$

Of course, in the approach of product probabilities monomer–radical interactions (a substantial contribution to e) are intrinsic to the relationship $P_{ab}P_{bc}P_{ca} = P_{ac}P_{cb}P_{ba} = \mathcal{P}$ leading to the likelihood of a unique monomer reactivity parameter for substitution in this relationship.

Vinyl Chloride–Vinyl Acetate–Acrylonitrile

There are a few instances in the literature where the related binary systems of three individual monomers, two of low conjugation, have been studied with fair precision. One of these is the system vinyl chloride–vinyl acetate–acrylonitrile.

Employing literature values[3,5] we have:

$$r_{12}r_{23}r_{31} = r_{13}r_{32}r_{21}$$

$$(1.8)(0.07)(3.7) = (0.074)(6.0)(0.6)$$

$$0.466 = 0.2664$$

This shows rather poor agreement. It was apparent from the literature that the most suspicious ratios were r_{23} and r_{32}. Another source[6] had reported $r_{32} = 6 \pm 2$ and $r_{23} = 0.02 \pm 0.02$. When these values were used, agreement was still uncertain.

$$r_{12}r_{23}r_{31} = r_{13}r_{32}r_{21}$$

$$(1.8)(0.02)(3.7) = (0.074)(6.0)(0.6)$$

$$0.133 = 0.266$$

A search of the literature showed that a detailed study of long-chain vinyl esters in copolymerization with acrylonitrile and methyl acrylate had been made.[7] Equivalence of behavior of these long-chain vinyl esters with vinyl acetate in copolymerization was shown (Table V).

TABLE V

	Vinyl stearate (M_1)		Vinyl acetate (M_1)		
	r_1	r_2	r_1	r_2	Ref.
Methyl acrylate	0.03	5.8	0.1	9	8
Acrylonitrile	0.03	4.3	0.061	4.05	8
			0.07	6	5

Analysis of vinyl stearate copolymers could be made with much greater accuracy because of the much greater weight of vinyl stearate at a given molar composition of the copolymers, so substitution of the vinyl stearate reactivity ratios for the vinyl acetate values was made.

$$r_{12}r_{23}r_{31} = r_{13}r_{32}r_{21}$$

$$(1.8)(0.03)(3.7) = (0.074)(4.3)(0.6)$$

$$0.2000 = 0.191$$

Excellent agreement resulted.

Similarly, product probabilities were very close:

$$P_{ab}P_{cb}P_{ca} = P_{ac}P_{cb}P_{ba}$$

$$(0.037)(0.925)(0.18) = (0.90)(0.155)(0.0464)$$

$$0.00615 = 0.00641$$

Vinyl Chloride–Vinyl Acetate–Methyl Acrylate

A study of the system vinyl chloride–vinyl acetate–methyl acrylate was similarly made, with substitution of ratios based on the more precise data:[7]

$$r_{12}r_{23}r_{31} = r_{13}r_{32}r_{21}$$

$$(1.8)(0.03)(0.9) = (0.083)(5.8)(0.6)$$

$$0.485 = 0.289$$

Product probabilities were

$$P_{ab}P_{bc}P_{ca} = P_{ac}P_{cb}P_{ba}$$

$$(0.0408)(0.925)(0.0865) = (0.885)(0.134)(0.0464)$$

$$0.00326 = 0.00552$$

Studies in ethylene binary copolymerizations with three monomers when two were of low conjugation (to be reported separately) have yielded product probabilities in the region of 0.0028.

It is seen that, based on much more limited and less reliable data (because of two very small and two large reactivity ratios involved) product probabilities in the range of 0.0028–0.0064 result in binary copolymerizations of monomers, two of low conjugation and one of moderate to high conjugation. The most accurate data point in the direction of an average $\mathcal{P} = 0.006$ for this type of system.

The case is considered in which two unconjugated monomers A and B are copolymerized in the three possible binary systems with a conjugated monomer C. The following very special assumptions are made for the purpose of calculating an alternate value for x, the general reactivity of unconjugated monomers with conjugated radicals:

$$x = 1/r_{32} = 1/r_{31} = r_{13} = r_{23}$$

and

$$r_{12} = r_{21} = 1$$

Substituting in $P_{ab}P_{bc}P_{ca} = P_{ac}P_{cb}P_{ba} = 0.006$ yields

$$\left[\frac{x}{x + (1)(x) + 1}\right]\left[\frac{1}{1 + (x)(1) + x}\right]\left[\frac{1/x}{1/x + (1/x)(1/x) + (1/x)}\right] =$$

$$\left[\frac{1}{1 + (x)(1) + x}\right]\left[\frac{1/x}{(1/x) + (1/x)(1/x) + 1/x}\right]\left[\frac{x}{x + (x)(1) + 1}\right] = 0.006$$

$$\left(\frac{x}{2x + 1}\right)\left(\frac{1}{1 + 2x}\right)\left(\frac{x}{2x + 1}\right) = \left(\frac{1}{1 + 2x}\right)\left(\frac{x}{2x + 1}\right)\left(\frac{x}{2x + 1}\right) = 0.006$$

$$x^2/(2x + 1)^3 = 0.006$$

Solution for x yields 0.10. This value for the general reactivity of unconjugated monomers with conjugated radicals is appreciably higher than the value (0.052) calculated earlier.

Without question, interactions are involved in actual practice that go beyond those allowed for in this hypothetical example.

The final combination to be considered is that involving three unconjugated monomers. As before, the special case of three monomers (now unconjugated) may be considered where equal monomer reactivity with all available radicals exists. Thus,

$$P_{ab}P_{bc}P_{ca} = P_{ac}P_{cb}P_{ba} = 0.037$$

(2)

$$(1/3)(1/3)(1/3) = (1/3)(1/3)(1/3) = 0.037$$

Two systems will serve to illustrate the utility of this relationship.

Vinyl Acetate–Vinyl Benzoate–N-Vinylpyrrolidone

Employing reported reactivity ratios[3] the following equality is shown:

$$r_{12}r_{23}r_{31} = r_{13}r_{32}r_{21}$$

$$(0.35)(0.44)(3.30) = (0.205)(2.45)(0.99)$$

$$0.508 = 0.498$$

Similarly, calculation of product probabilities shows:

$$P_{ab}P_{bc}P_{ca} = P_{ac}P_{cb}P_{ba}$$

$$(0.48)(0.53)(0.176) = (0.82)(0.238)(0.236)$$

$$0.0451 = 0.0461$$

The excellent agreement and similarity to the predicted product probability of 0.037 shows the usefulness of eq. (2) in predicting reactivity ratios in binary copolymerization in systems involving three unconjugated monomers.

Vinyl Chloride–Vinyl Acetate–Vinylene Carbonate

The following equality involving reactivity ratios is reasonably approached, considering the questionable reported ratios:

$$r_{12}r_{23}r_{31} = r_{13}r_{32}r_{21}$$

$$(1.8)(4.00)(0.09) = (5.2)(0.15)(0.6)$$

$$0.648 = 0.468$$

Product probabilities for this system are:

$$P_{ab}P_{bc}P_{ca} = P_{ac}P_{cb}P_{ba}$$

$$(0.318)(0.086)(0.59) = (0.11)(0.335)(0.57)$$

$$0.0162 = 0.0222$$

Although less than the theoretical value of 0.037, the similarity of product probabilities offers promise in predicting monomer reactivity in entirely unconjugated combinations of monomers.

A great measure of increased utility in predicting monomer reactivity ratios for a given untried binary system is attained by the choice of the third common monomer. The third monomer may be conjugated or un-

conjugated determining the value of $\mathcal{P}$. Moreover, certain ternary combinations of binary reactivity ratios are known with much greater precision than others as a close examination of the literature readily reveals. This fact is in evidence in advance of the untried copolymerization and is readily checked, once the new reactivity ratios are determined.

Acknowledgment is made of the great usefulness of the excellent compilation by Young[3] of reactivity ratios which were employed with selectivity in this work. Selections were based on attempts to assess the quality of the original work. In addition, selections were made in part on the basis of consistent agreement when applied in several ternary combinations as detailed above. Once chosen, reactivity ratios have been retained consistently from one ternary combination to another throughout this and a previous paper.[1] Added validity is given to conclusions drawn about a simplified approach to predicting terpolymer composition as outlined in the previous paper by the additional showings of the equality of $P_{ab}P_{bc}P_{ca} = P_{ac}P_{cb}P_{ba}$ contained in this paper.

References

1. Ham, G. E., *J. Polymer Sci.*, **A2**, 2735 (1964).
2. Burkhardt, R. D., and N. L. Zutty, *J. Polymer Sci.*, **A1**, 1137 (1963).
3. Young, L. J., *J. Polymer Sci.*, **54**, 411 (1961).
4. Alfrey, T., and C. C. Price, *J. Polymer Sci.*, **2**, 101 (1947).
5. Alfrey, T., J. Bohrer, H. Haas, and C. Lewis, *J. Polymer Sci.*, **5**, 719 (1950).
6. Fordyce, R. G., E. C. Chapin, and G. E. Ham, *J. Am. Chem. Soc.*, **70**, 2489 (1948).
7. Witnauer, L. P., N. Watkins, and W. S. Port, *J. Polymer Sci.*, **20**, 213 (1956).
8. Mayo, F. R., C. Walling, F. M. Lewis, and W. F. Hulse, *J. Am. Chem. Soc.*, **70**, 1523 (1948).

Résumé

Il a été montré que la connaissance des rapports de réactivité des systèmes binaires A-B et B-C petmet de calculer les rapports de réactivité des systèmes de copolymères A-C à partir de la relation: $P_{ab}P_{bc}P_{ac} = P_{ac}P_{cb}P_{ba} = \mathcal{P}$ (une constante). Les diverses probabilités incluent les possibilités d'addition de monomères A, B ou C à l'un quelconque des radicaux correspondants et peuvent être exprimées en termes de rapports de réactivité binaire. Il est démontré que pour les systèmes à concentrations équimolaires de trois monomères conjugués ou de trois monomères non-conjugués $\mathcal{P}$ est approximativement égal à 0.037. De même pour le système à deux monomères conjugués et un non-conjugué ou de deux non-conjugués et un conjugué, $\mathcal{P}$ est voisin de 0.006. Une fois la justésse de ces constantes établies, on peut démontrer comment la relation peut être utilisée pour établir les valeurs les plus probables pour les rapports de réactivité très variables décrits dans la littérature. Il est démontré que les valeurs de la constante $\mathcal{P}$ pour différentes combinaisons de monomères permet l'établissment de la réactivité pour des monomères conjugués comparés aux monomères non-conjugués avec des radicaux conjugués ou non. La réactivité de monomères non-conjugués serait entre 5 et 10% de celle de monomères conjugués pour des radicaux non-conjugués. Pour des évaluations plus précises de rapports de réactivité inconnus, il est suggéré que $\mathcal{P}$ est un produit fonction de paramètres uniques de réactivité caractéristiques de chacun des monomères entrant en réaction.

Zusammenfassung

Es wird gezeigt, dass die Kenntnis der Reaktivitätsverhältnisse für das binäre System A-B und B-C die Reaktivitätsverhältnisse für das Copolymersystem A-C aus der Beziehung $P_{ab}P_{bc}P_{ca} = P_{ac}P_{cb}P_{ba} = \varphi$ (eine Konstante) zu berechnen gestattet. Die verschiedenen Wahrscheinlichkeiten beinhalten die Möglichkeit, A, B, oder C-Monomere an jedes der entsprechenden Radikale zu addieren und können durch die binären Reaktivitätsverhältnisse ausgedrückt werden. Bei äquimolaren Konzentrationen nähert sich φ für Systeme von drei konjugierten oder drei unkonjugierten Monomeren 0,037. Analog nähert sich φ für Systeme mit zwei konjugierten und einem unkonjugiertem oder zwei unkonjugierten und einem konjugierten Monomeren 0,006. Sobald die Richtigkeit dieser Konstanten festgestellt ist, wird gezeigt, wie die Beziehung zur Ermittlung der wahrscheinlichsten Werte unter den in weiten Grenzen variierenden mitgeteilten Reaktivitätsverhältnissen verwendet werden kann. Die Werte der Konstanten φ für verschiedene Monomerkombinationen erlauben die Bestimmung der Reaktivität konjugierter Monomere im Vergleich mit unkonjugierten für konjugierte oder unkonjugierte Radikale. Daraus folgt, dass die Reaktivität unkonjugierter Monomere 5 bis 10% derjenigen konjugierter Monomere für unkonjugierte Radikale beträgt. Zur genaueren Bestimmung unbekannter Reaktivitätsverhältnisse wird angenommen, dass φ eine Produktfunktion einzelner für die einzelnen Monomeren charakteristischen Reaktivitätsparameter ist.

Calculation of Copolymerization Reactivity Parameters From Product Probabilities

GEORGE E. HAM, *Research Center, Spencer Chemical Company, Merriam, Kansas*

Synopsis

The premise is examined that there exists for each monomer in copolymerization a reactivity parameter p, such that a product probability $\mathcal{P}$ may be calculated for any combination of three monomers in binary or ternary polymerization, where $\mathcal{P} = P_{ab}P_{bc}P_{ca} = P_{ac}P_{cb}P_{ba}$. The consistency of this equation and its derived equation, $r_{12}r_{23}r_{31} = r_{13}r_{32}r_{21}$, with the Q–e scheme is demonstrated. Simplified equations are presented relating monomer and copolymer composition for any number of monomers: $a/b = P_{ba}/P_{ab}$, $a/c = P_{ca}/P_{ac}$, ..., up to $a/j = P_{ja}/P_{aj}$, where j is the final component in the copolymerization and each probability includes possibilities of reaction of a given radical with monomers a–j.

Two recent papers[1,2] have introduced the concept of product probabilities as a means of predicting monomer reactivity in copolymerization. Given reactivity ratios for the binary combination A–B and B–C, the reactivity ratios for the system A–C may be calculated from the following relationship:

$$P_{ab}P_{bc}P_{ca} = P_{ac}P_{cb}P_{ba} = \mathcal{P} \text{ (a constant)} \tag{1}$$

The various probabilities include the possibilities of addition of all three monomers, which are assumed to be present in equimolar proportions. Any of the individual probabilities can be expressed in terms of reactivity ratios, from which the power of the technique arises. Thus,

$$\left(\frac{r_{13}}{r_{13} + r_{13}r_{12} + r_{12}}\right) \cdot \left(\frac{r_{21}}{r_{21} + r_{21}r_{23} + r_{23}}\right) \cdot \left(\frac{r_{32}}{r_{32} + r_{32}r_{31} + r_{31}}\right) =$$

$$\left(\frac{r_{12}}{r_{12} + r_{12}r_{13} + r_{13}}\right) \cdot \left(\frac{r_{31}}{r_{31} + r_{31}r_{32} + r_{32}}\right) \cdot \left(\frac{r_{23}}{r_{23} + r_{23}r_{21} + r_{21}}\right) = \mathcal{P} \tag{2}$$

It is shown that predictions of reactivity ratios in good agreement with experiment result when for combinations of three conjugated monomers or three unconjugated monomers one employs

$$\mathcal{P} \simeq 0.037$$

and for combinations of two conjugated and one unconjugated monomers or two unconjugated and one conjugated monomers one employs

$$\mathcal{P} \simeq 0.006$$

There appears to be a theoretical basis for regarding $\mathcal{P}$ as the product of three copolymerization reactivity parameters p, characteristic of each of the individual monomers. More precisely, p for a given monomer may be regarded as the probability that it will add to a different radical in the presence of two unlike monomers. Of course, one of the three monomers present will be competing for its own radical. The range of possible values for p for conjugated monomers can not be large, since experience shows that the product of any three will be close to 0.037. However, for the time being we will concern ourselves with these differences, rather than the similarities, to ascertain what may be learned about individual monomer copolymerizability.

From the examination of all possible binary copolymerizations[3] involving the four monomers: x = styrene, y = acrylonitrile, z = methyl methacrylate, and w = methyl acrylate, we may calculate $\mathcal{P}$'s for all possible combinations of three monomers among the four concerned. Then we may write $\mathcal{P}$ as the product of three reactivity parameters:

$$xyz = 0.049 \tag{3}$$

$$yzw = 0.0279 \tag{4}$$

$$xzw = 0.0417 \tag{5}$$

$$xyw = 0.031 \tag{6}$$

Solution of the four equations in four unknowns yields the values:

$$x \text{ (styrene)} \qquad = 0.434$$

$$y \text{ (acrylonitrile)} \qquad = 0.291$$

$$z \text{ (MMA)} \qquad = 0.390$$

$$w \text{ (methyl acrylate)} = 0.248$$

Similarly, for the four monomers styrene, methyl methacrylate, acrylonitrile, and butadiene[3] taken in combinations of three, we may solve for individual reactivity parameters p:

$$xyw = 0.0472 \tag{7}$$

$$xzw = 0.0445 \tag{8}$$

$$yzw = 0.0263 \tag{9}$$

$$xyz = 0.049 \tag{10}$$

which yields:

$$x \text{ (styrene)} = 0.531$$
$$y \text{ (MMA)} = 0.313$$
$$z \text{ (acrylonitrile)} = 0.295$$
$$w \text{ (butadiene)} = 0.284$$

A variety of other systems of four monomers[3] were examined which allowed assessment of p's for styrene (St), methyl methacrylate (MMA), acrylonitrile (AN), methyl acrylate (MA), and butadiene. In addition, new parameters were determined for methacrylonitrile (MAN) and α-methylstyrene (α-MeSt). The various copolymerization reactivity parameters for the monomers are summarized in Table I. The combinations of four monomers employed in each assessment are shown in the vertical columns.

TABLE I
Reactivity Parameters

Monomers	Parameters					Arithmetic mean
St	0.531	0.497	0.398		0.434	0.465
MMA	0.313	0.302	0.495	0.453	0.390	0.391
AN	0.295		0.245	0.27	0.291	0.275
MA		0.27			0.248	0.259
MAN			0.298	0.299		0.299
α-MeSt				0.518		0.518
Butadiene	0.284	0.306				0.292

These new reactivity parameters must be used with caution. There is at present no way of relating them to Q and e values. However, it can be reasoned that to some extent, the higher the specific value (above 0.333), the more tendency toward alternation among the four monomers chosen in the specific calculation. (It is readily seen that a completely random terpolymerization of three monomers of equal reactivity in equimolar concentration would lead to $\wp = 0.037$ and to individual values of $p = 0.333$.) Furthermore, it is no accident that the combination of two highly electronegative monomers (styrene and butadiene) with two electropositive monomers such as MMA and AN or MMA and MA leads to a higher p for styrene than that derived from combinations of styrene with three electropositive monomers.

On the other hand, monomers associated with very low reactivity with their own radicals in the presence of other monomers, as for example acrylonitrile and methacrylonitrile, have p's less than 0.333, in spite of very high alternating tendency. Although they generally have a high affinity for radicals ending in other monomers, they too rapidly surrender

their sequences to a different monomer. Thus, it appears that for a high value of p, a happy compromise is necessary. High reactivity of the particular monomer with a wide variety of other conjugated radicals with a tendency to alternation (high probability of sequence initiation with the particular monomer but somewhat lower tendency to sequence termination) is needed. Styrene, α-methylstyrene, and methyl methacrylate appear to be almost ideal examples. The lower p value for methyl acrylate appears to be the consequence of lower resonance stabilization ($Q = 0.42$)[3] compared with that for methyl methacrylate ($Q = 0.74$),[3] and a generally lower reactivity with other radicals (cross-propagation).

Table I shows an interesting correlation between α-methyl substitution and increase in p. Thus, there is a Δp from methyl acrylate to methyl methacrylate of $+0.13$ from styrene to α-methylstyrene of $+0.053$; and from acrylonitrile to methacrylonitrile of $+0.024$.

Once a reasonable degree of confidence is established for the reactivity parameters of a group of monomers by the method described above, one may then more simply estimate values for new monomers for which more limited copolymerization data are available by simply calculating $\mathcal{P}$ from the reactivity ratios of three binary systems arising from the permutations of three monomers including the new monomer. Once $\mathcal{P}$ is established, if the p's for two of the monomers are known, that for the new monomer may be calculated as follows:

$$p_1 = \mathcal{P}/p_2 p_3 \tag{11}$$

By employing this technique, p for vinylidene chloride was calculated from the system styrene–methyl methacrylate–vinylidene chloride and styrene–acrylonitrile–vinylidene chloride, and values of 0.179 and 0.160, respectively, were obtained. These values compare favorably with a value of 0.214 obtained by the more involved solution of simultaneous equations described above for the four monomers styrene–methyl methacrylate–acrylonitrile–vinylidene chloride.

It is desirable to expand our study to the unconjugated monomers where $\mathcal{P} \simeq 0.006$ for the combination of two conjugated and one unconjugated monomers. It might be questioned whether the simple eq. (11) may be used, until we can show that equivalent results are obtained by the more complicated route described first. Employing the monomers styrene–methyl methacrylate–methyl acrylate–vinyl chloride, solution of the four simultaneous equations yields a reactivity parameter p for vinyl chloride (VCl) of 0.041. Using eq. (11) for the system St–MA–VCl and substituting appropriate p's for styrene and methyl acrylate and the calculated value of $\mathcal{P} = 0.00448$ one obtained a p value of 0.0372 for vinyl chloride. On the other hand, if one uses p values for styrene of 0.434 (rather than 0.465) and for methyl acrylate of 0.248 (rather than 0.259) obtained from more similar systems, a value of p of 0.0416 results. It is seen that quite good agreement compared with the more detailed calculation results in

either case. From the methyl methacrylate–methyl acrylate–vinyl chloride system a p value for vinyl chloride of 0.066 results.

For determination of p for certain unconjugated monomers, such as vinyl acetate, better data are available from combinations of two unconjugated monomers with a conjugated monomer. It is obvious that eq. (11) can not be applied directly because of the very low values of p involved for the two unconjugated monomers. However, it seems reasonable to use the modified eq. (12):

$$p_1 = (\mathcal{P}/p_2 p_3)\ (0.006/0.037) \tag{12}$$

The ratio 0.006/0.037 is simply $\mathcal{P}_3/\mathcal{P}_1$, where $\mathcal{P}_3$ is the observed probability product for a wide variety of combinations of two unconjugated monomers and one conjugated monomer and $\mathcal{P}_1$ is the corresponding value for three unconjugated monomers.

For determination of p for vinyl acetate the systems vinyl chloride–vinyl acetate–acrylonitrile and vinyl chloride–vinyl acetate–methyl acrylate were chosen. Values of approximately 0.05 and 0.04 were obtained with the modified eq. (12).

Because of the high accuracy of reactivity ratios obtainable, some means of treating combinations of three unconjugated monomers is desirable. It is not certain what form the equation should take, but the following equation seems reasonable and gives results consistent with the limited data available:

$$p_1 = (\mathcal{P}/p_2 p_3)(0.006/0.037)^3 \tag{13}$$

Presumably, it is simply a means of normalizing eq. (11). From the system vinyl chloride–vinyl acetate–vinylene carbonate a p value for vinylene carbonate of 0.026 results from eq. (13).

Table II summarizes in decreasing order the best values for p now obtainable for a limited number, but broad variety of monomers.

TABLE II

Monomer	p
α-Methylstyrene	0.518
Styrene	0.465
Methacrylic acid	0.391
Methyl methacrylate	0.391
Methyacrylonitrile	0.299
Butadiene	0.292
Acrylonitrile	0.275
Methyl acrylate	0.259
Vinylidene chloride	0.170
Vinyl chloride	0.054
N-Vinylpyrrolidone	0.053
Vinyl acetate	0.045
Vinyl benzoate	0.045
Vinylene carbonate	0.026

Whether values for p for given monomers are truly unique is open to real question. The data above show that the reactivity parameter is affected by the particular monomers involved in copolymerization. Actual electron transfer in the transition state may contribute to the problem. However, the data also show that useful estimates of reactivity ratios can be obtained from judicious applications of the reactivity parameter p. It is interesting to note that the p values of unconjugated monomers shown in Table II are approximately 10% of those of conjugated monomers, a result predicted in an earlier paper.[2]

Although the relationship, if any, between p values and Q and e values is not known, it is significant that the two basic equations, eqs. (21) and (20), which follow from the equality of product probabilities[1,2] are consistent with the Q–e scheme.

From the relationship[4]

$$K_{ij} = P_i Q_j \exp\{-e_i e_j\} \tag{14}$$

underlying the Q-concept the following equations result:

$$r_{13} = K^{11}/K^{13} = (Q_1/Q_3) \exp\{-e_1(e_1-e_3)\} \tag{15}$$

$$r_{32} = K^{33}/K^{32} = (Q_3/Q_2) \exp\{-e_3(e_3 - e_2)\} \tag{16}$$

$$r_{21} = K^{22}/K^{21} = (Q_2/Q_1) \exp\{-e_2(e_2 - e_1)\} \tag{17}$$

$$r_{13}r_{32}r_{21} = \exp\{-e_1{}^2 + e_1 e_3 - e_3{}^2 + e_2 e_3 - e_2{}^2 + e_1 e_2\} \tag{18}$$

In a similar way it may be shown that

$$r_{12}r_{23}r_{31} = \exp\{-e_1{}^2 + e_1 e_3 - e_3{}^2 + e_2 e_3 - e_2{}^2 + e_1 e_2\} \tag{19}$$

It follows that

$$r_{13}r_{32}r_{21} = r_{12}r_{23}r_{31} \tag{20}$$

Since both sides of eq. (21) possess a common denominator, it follows that eq. (2) is consistent with the Q–e concept. Equation (2) is the special case of

$$P_{ab}P_{bc}P_{ca} = P_{ac}P_{cb}P_{ba} \tag{21}$$

for equimolar monomer concentrations. The more general relationship for all monomer concentrations is also shown to be consistent with the Q–e scheme because it can also be shown to possess a common denominator:

$$\left(\frac{Br_{13}}{Br_{13} + Ar_{12}r_{13} + Cr_{12}}\right) \cdot \left(\frac{Cr_{21}}{Cr_{21} + Br_{23}r_{21} + Ar_{23}}\right) \cdot$$
$$\left(\frac{Ar_{32}}{Ar_{32} + Cr_{31}r_{32} + Br_{31}}\right) = \left(\frac{Cr_{12}}{Cr_{12} + Ar_{13}r_{12} + Br_{13}}\right) \cdot$$
$$\left(\frac{Br_{31}}{Br_{31} + Cr_{31}r_{32} + Ar_{32}}\right) \cdot \left(\frac{Ar_{23}}{Ar_{23} + Br_{21}r_{23} + Cr_{21}}\right) \tag{22}$$

Division by ABC yields eq. (20).   This consistency must not be regarded as a proof of the Q–e relationship or the underlying eq. (14).

The demonstrated validity of eqs. (1) and (2) leads to a consideration of the validity of eq. (23) where the individual probabilities include the consideration of the possibilities of additions of any of four monomers to a given radical:

$$P_{ab}P_{bc}P_{cd}P_{da} = P_{ad}P_{dc}P_{cb}P_{ba} \tag{23}$$

For instance

$$P_{ab} = \frac{K^{ab}[A\cdot][B]}{K^{ab}[A][B] + K^{aa}[A\cdot][A] + K^{ac}[A\cdot][C] + K^{ad}[A\cdot][D]}$$

$$= \frac{(B/r_{12})}{(B/r_{12}) + A + (C/r_{13}) + (D/r_{14})} \tag{24}$$

In the system of four monomers styrene–methyl methacrylate–acrylonitrile–vinylidene chloride, reactivity ratios for all binary combinations are known.   Assuming equimolar ratios, eq. (23) reduces

$$\left(\frac{r_{13}r_{14}}{r_{13}r_{14} + r_{12}r_{13}r_{11} + r_{12}r_{14} + r_{12}r_{13}}\right)\cdot\left(\frac{r_{21}r_{24}}{r_{21}r_{24} + r_{21}r_{23}r_{24} + r_{23}r_{24} + r_{21}r_{23}}\right)$$

$$\left(\frac{r_{31}r_{32}}{r_{31}r_{32} + r_{31}r_{32}r_{34} + r_{32}r_{34} + r_{31}r_{34}}\right)\cdot\left(\frac{r_{42}r_{43}}{r_{42}r_{43} + r_{41}r_{42}r_{43} + r_{41}r_{43} + r_{41}r_{42}}\right) =$$

$$\left(\frac{r_{12}r_{13}}{r_{13}r_{14} + r_{12}r_{13}r_{14} + r_{12}r_{14} + r_{12}r_{13}}\right)\cdot\left(\frac{r_{41}r_{42}}{r_{42}r_{43} + r_{41}r_{42}r_{43} + r_{41}r_{43} + r_{41}r_{42}}\right)$$

$$\left(\frac{r_{31}r_{34}}{r_{31}r_{32} + r_{31}r_{32}r_{34} + r_{32}r_{34} + r_{31}r_{34}}\right)\cdot\left(\frac{r_{23}r_{24}}{r_{21}r_{24} + r_{21}r_{23}r_{24} + r_{23}r_{24} + r_{21}r_{23}}\right) \tag{25}$$

On substitution in eq. (25) of values for reactivity ratios in the above system of $r_{12} = 0.52$, $r_{21} = 0.46$, $r_{23} = 1.35$, $r_{32} = 0.18$, $r_{34} = 0.91$, $r_{43} = 0.37$, $r_{13} = 0.41$, $r_{31} = 0.04$, $r_{14} = 1.85$, $r_{41} = 0.085$, one obtains

$$P_{ab}P_{bc}P_{cd}P_{da} = P_{ad}P_{dc}P_{cb}P_{ba}$$

$$(0.326)(0.172)(0.0338)(0.60) = (0.0915)(0.138)(0.169)(0.505) \tag{23}$$

$$0.00114 = 0.00108$$

Hence eq. (25), a special case of eq. (23), appears to be valid for this four-component system.   By analogy with the proven relationship

$$P_{ab}P_{bc}P_{ca} = P_{ac}P_{cb}P_{ba}$$

the more general eq. (23) is probably valid also.   It follows from substitution of reactivity ratios in the general eq. (23) for all monomer proportions that

$$r_{14}r_{43}r_{32}r_{21} = r_{12}r_{23}r_{34}r_{41} \tag{26}$$

It seems likely by way of further analogy that for any multicomponent polymerization

$$a/b = P_{ba}/P_{ab} \tag{27}$$

$$a/c = P_{ca}/P_{ac} \tag{28}$$

and so forth, until

$$a/j = P_{ja}/P_{aj} \tag{29}$$

where j is the final component in the polymerization. Each probability includes the consideration of possibilities of reaction of a given radical with monomers a–j. Thus in the four-component copolymerization of styrene–methyl methacrylate–acrylonitrile–vinylidene chloride studied by Walling and Briggs the premise is considered that

$$a/b = P_{ba}/P_{ab} \tag{30}$$

$$a/c = P_{ca}/P_{ac} \tag{31}$$

$$a/d = P_{da}/P_{ad} \tag{32}$$

The agreement between experimental and new calculated values (Table III) is highly encouraging in view of the great simplification of calculation in eqs. (30)–(32).

TABLE III

| Monomer | Composition, mole-% | Found | Polymer composition, mole-% | |
			Calculated from Walling-Briggs eqs.	Calculated from simplified eqs.
St	25.2	40.7	41.0	42.7
MMA	25.5	25.5	27.3	27.8
AN	25.4	25.8	24.8	23.2
VC	23.9	8.0	6.9	6.1

Substituting in eq. (25) the various reactivity ratios of all possible binary combinations in the four-component system styrene–methyl methacrylate–acrylonitrile–methyl acrylate, one obtains:

$$P_{ab}P_{bc}P_{ad}P_{da} = P_{ad}P_{dc}P_{cb}P_{ba}$$

$$0.00124 = 0.00149$$

This result may be regarded as further proof of the validity of the equality of product probabilities in multicomponent copolymerizations and their utility in predicting monomer reactivity in copolymerizations.

References

1. Ham, G. E., *J. Polymer Sci.*, **A2**, 2735 (1964).
2. Ham, G. E., *J. Polymer Sci.*, **A2**, 4169 (1964).
3. Young, L. J., *J. Polymer Sci.*, **54**, 411 (1961).
4. Ham, G. E., *Copolymerization*, Wiley, New York, 1964, p. 12.

Résumé

On a espéré qu'il existait pour chaque monomère dans une copolymérisation, un paramètre de réactivité, p, tel qu'une probabilité de produit, $\mathcal{P}$, puisse être calculée pour une combinaison quelconque de trois monomères dans une polymérisation binaire ou ternaire $\mathcal{P} = P_{ab}P_{bc}P_{ca} = P_{ac}P_{cb}P_{ba}$. L'accord de cette équation et de son équation dérivée avec le schéma Q–e est démontrée: $r_{12}r_{23}r_{31} = r_{13}r_{32}r_{21}$. Des équations simplifiées sont présentées reliant la composition des monomères et copolymères pour un nombre quelconque de monomères: $a/b = P_{ba}/P_{ab}$, $a/c = P_{ca}/P_{ac}$, etc. jusquà $a/j = P_{ja}/P_{aj}$, où j est la composant dans la copolymérisation et chaque probabilité includes possibilités de réaction d'un radical donné avec des monomères a–j.

Zusammenfassung

Die Annahme, dass für jedes Monomere bei Copolymerisation ein Reaktivitätsparameter p existiert, sodass das Produkt der Einzelwahrscheinlichkeiten $\mathcal{P}$ für jede Kombination der Monomeren in binärer oder ternärer Polymerisation gebildet werden kann, wird untersucht, wobei $\mathcal{P} = P_{ab}P_{bc}P_{ca} = P_{ac}P_{cb}P_{ba}$ ist. Die Übereinstimmung dieser Gleichung und der daraus abgeleiteten Gleichung $r_{12}r_{23}r_{31} = r_{13}r_{32}r_{21}$ mit dem Q–e Schema wird gezeigt. Vereinfachte Gleichungen für die Monomer-und Polymerzusammensetzung werden für eine beliebige Zahl von Monomeren angegeben: $a/b = P_{ba}/P_{ab}$, $a/c = P_{ca}/P_{ac}$ ... usw. bis $a/j = P_{ja}/P_{aj}$ wo j die letzte Komponente in der Copolymerisation ist und jede Wahrscheinlichkeit Reaktionsmöglichkeiten für ein gegebenes Radikal mit den Monomeren a–j beinhaltet.

Penultimate Unit Effects in Terpolymerization

GEORGE E. HAM, *Research Center, Spencer Chemical Company, Merriam, Kansas*

Synopsis

Although the effects of penultimate units in binary copolymerization have been extensively treated, the investigation of these effects in terpolymerization has been neglected. Undoubtedly, this neglect is attributable to the fact that possible effects arising from twenty-seven different propagation possibilities must be considered. Fortunately, for practical purposes, it often occurs that only a few of the penultimate possibilities are important in determining copolymer composition, and that most of the propagating steps can be treated with regard to terminal unit effects alone. Simplified equations are presented which allow for such restrictions. These equations are applied to several experimental examples. In addition, simplified terpolymer equations are derived which allow for the circumstances where one or two homopropagation rate constants approach zero. Furthermore, methods are introduced for assessing K^{32}/K^{31} where K^{33} approaches zero. These methods lead, in turn, to more precise assessments of Q and e for 1,2-disubstituted olefins.

There is an increasing body of evidence that the reactivity of propagating chains, particularly those of the free-radical type with competing monomers, may be substantially influenced by the nature of penultimate units. Penultimate unit effects are already well established in binary copolymerizations.[1-3] A recent paper has pointed out that sequence length distribution and terpolymer composition[4] would be profoundly influenced by such effects.

A complete assessment of penultimate effects in terpolymerization must be regarded as a formidable task. A total of twenty-seven possible propagating reactions may influence sequence distribution and terpolymer composition compared with eight in binary copolymerization. They are as given in eqs. (1)–(27).

$$\sim\!AA\cdot + A \rightarrow \sim\!AAA\cdot \tag{1}$$

$$\sim\!AA\cdot + B \rightarrow \sim\!AAB\cdot \tag{2}$$

$$\sim\!AA\cdot + C \rightarrow \sim\!AAC\cdot \tag{3}$$

$$\sim\!BA\cdot + A \rightarrow \sim\!BAA\cdot \tag{4}$$

$$\sim\!BA\cdot + B \rightarrow \sim\!BAB\cdot \tag{5}$$

$$\sim\!BA\cdot + C \rightarrow \sim\!BAC\cdot \tag{6}$$

$$\sim\!CA\cdot + A \rightarrow \sim\!CAA\cdot \tag{7}$$

$$\sim\!CA\cdot + B \rightarrow \sim\!CAB\cdot \tag{8}$$

$$\sim CA\cdot\ +\ C\ \rightarrow\ \sim CAC\cdot \tag{9}$$

$$\sim BB\cdot\ +\ B\ \rightarrow\ \sim BBB\cdot \tag{10}$$

$$\sim BB\cdot\ +\ A\ \rightarrow\ \sim BBA\cdot \tag{11}$$

$$\sim BB\cdot\ +\ C\ \rightarrow\ \sim BBC\cdot \tag{12}$$

$$\sim AB\cdot\ +\ B\ \rightarrow\ \sim ABB\cdot \tag{13}$$

$$\sim AB\cdot\ +\ A\ \rightarrow\ \sim ABA\cdot \tag{14}$$

$$\sim AB\cdot\ +\ C\ \rightarrow\ \sim ABC\cdot \tag{15}$$

$$\sim CB\cdot\ +\ B\ \rightarrow\ \sim CBB\cdot \tag{16}$$

$$\sim CB\cdot\ +\ C\ \rightarrow\ \sim CBC\cdot \tag{17}$$

$$\sim CB\cdot\ +\ A\ \rightarrow\ \sim CBA\cdot \tag{18}$$

$$\sim CC\cdot\ +\ C\ \rightarrow\ \sim CCC\cdot \tag{19}$$

$$\sim CC\cdot\ +\ A\ \rightarrow\ \sim CCA\cdot \tag{20}$$

$$\sim CC\cdot\ +\ B\ \rightarrow\ \sim CCB\cdot \tag{21}$$

$$\sim AC\cdot\ +\ C\ \rightarrow\ \sim ACC\cdot \tag{22}$$

$$\sim AC\cdot\ +\ A\ \rightarrow\ \sim ACA\cdot \tag{23}$$

$$\sim AC\cdot\ +\ B\ \rightarrow\ \sim ACB\cdot \tag{24}$$

$$\sim BC\cdot\ +\ C\ \rightarrow\ \sim BCC\cdot \tag{25}$$

$$\sim BC\cdot\ +\ A\ \rightarrow\ \sim BCA\cdot \tag{26}$$

$$\sim BC\cdot\ +\ B\ \rightarrow\ \sim BCB\cdot \tag{27}$$

Where only terminal effects operate in terpolymerization, nine propagation reactions are of consequence, expressed as six reactivity ratios in the Alfrey-Goldfinger equations:[5]

$$\frac{a}{b} = \frac{A\left[(A/r_{31}r_{21}) + (B/r_{21}r_{32}) + (C/r_{31}r_{23})\right]\left[A + (B/r_{12}) + (C/r_{13})\right]}{B\left[(A/r_{12}r_{31}) + (B/r_{12}r_{32}) + (C/r_{32}r_{13})\right]\left[B + (A/r_{21}) + (C/r_{23})\right]} \tag{28}$$

$$\frac{a}{c} = \frac{A\left[(A/r_{31}r_{21}) + (B/r_{21}r_{32}) + (C/r_{31}r_{23})\right]\left[A + (B/r_{12}) + (C/r_{13})\right]}{C\left[(A/r_{13}r_{21}) + (B/r_{23}r_{12}) + (C/r_{13}r_{23})\right]\left[C + (A/r_{31}) + (B/r_{32})\right]} \tag{29}$$

Where for a given terminal monomer unit in the propagating chain a penultimate effect operates the reactivity ratios in the eqs. (28) and (29) may be replaced on the basis of the following rules.

(1) Where r_{ij} occurs and j is a higher number than i, replace r_{ij} with $r_{ij}'[r_{ij}(I/J) + 1]/[r_{ij}'(I/J) + 1]$, where I and J are the appropriate molar monomer fractions, and $r_{ij} = K^{iii}/K^{iij}$ and $r_{ij}' = K^{jii}/K^{jij}$.

(2) Where r_{ij} occurs and j is a lower number than i, replace r_{ij} with $r_{ij}'[r_{ij} + (I/J)]/[r_{ij}' + (I/J)]$.

(3) For those six propagation reactions which yield the various possible combinations of ABC: ABC, ACB, BAC, CAB, BCA, and CBA, there is obviously no substitution possible, since all of the reactivity ratios in the Alfrey-Goldfinger equation include propagation rate constants for homogeneous addition. At present no equations or modifications are offered which weigh contributions of these propagation reactions to terpolymer

composition. We can accordingly treat only those cases where these resulting sequence combinations are not influenced by penultimate effects.

Our problem may be appreciably simplified by utilizing instead of the Alfrey-Goldfinger equations, the simplified equations due to Ham[4] as a base point. These equations are as follows:

$$\frac{a}{b} = \frac{P_{ba}}{P_{ba}} = \left[\frac{A}{r_{21}}\left(\frac{B}{r_{12}} + A + \frac{C}{r_{13}}\right)\right]\bigg/\left[\frac{B}{r_{12}}\left(\frac{A}{r_{21}} + B + \frac{C}{r_{23}}\right)\right] \quad (30)$$

$$\frac{a}{c} = \frac{P_{ca}}{P_{ac}} = \left[\frac{A}{r_{31}}\left(\frac{C}{r_{13}} + A + \frac{B}{r_{12}}\right)\right]\bigg/\left[\frac{C}{r_{13}}\left(\frac{A}{r_{31}} + C + \frac{B}{r_{32}}\right)\right] \quad (31)$$

There are many terpolymerizations wherein penultimate effects only occur in one of the three binary combinations operating. Thus, terpolymers of styrene (A) and acrylonitrile (C) (which exhibit penultimate effects)[5] with methyl methacrylate, methyl acrylate, vinyl chloride, vinylidene chloride, or the like would fall in this category. Following the rules set forth above the following eqs. (32) and (33) weighing such penultimate effects result from eqs. (30) and (31).

$$\frac{a}{b} = \frac{\dfrac{A}{r_{21}}\left(\dfrac{B}{r_{32}} + A + \dfrac{C/\{r_{13}'[r_{13}(A/C)+1]\}}{r_{13}'(A/C)+1}\right)}{\dfrac{B}{r_{12}}\left(\dfrac{A}{r_{21}} + B + \dfrac{C}{r_{23}}\right)} \quad (32)$$

$$\frac{a}{c} = \frac{\left\{\dfrac{A}{r_{31}'[r_{31}+(A/C)]/[r_{31}'+(A/C)]}\right\}\left\{\dfrac{C/\{r_{13}'[r_{13}(A/C)+1]\}}{r_{13}'(A/C)+1} + A + \dfrac{B}{r_{12}}\right\}}{\dfrac{C/\{r_{13}[r_{13}(A/C)+1]\}}{r_{13}'(A/C)+1}\left\{\dfrac{A}{r_{31}'[r_{31}+(A/C)]/[r_{31}'+(A/C)]} + C + \dfrac{B}{r_{32}}\right\}} \quad (33)$$

Taking the system styrene–methyl methacrylate–acrylonitrile and values for reactivity ratios as follows:[4] $r_{13} = 0.30$, $r_{13}' = 0.45$, $r_{31} = 0.04$, $r_{31}' = 0.114$, $r_{12} = 0.52$, $r_{21} = 0.46$, $r_{23} = 1.35$, $r_{32} = 0.18$, initial terpolymer compositions were calculated and the predictions of the Alfrey-Goldfinger equations, the simplified equations [eqs. (30) and (31)], the new penultimate modifications compared with the actual experimental values[7] (Table I).

The agreement is regarded as demonstrating the utility of the penultimate modifications (Eqs. 32–33) in predicting terpolymer composition.

Further confirmation of the utility of eqs. (32)–(33) is shown in consideration of the system styrene–vinyl chloride–acrylonitrile (Table II). Since

TABLE I
Styrene (ST)–Methyl Methacrylate(MMA)–Acrylonitrile (AN)

Charge			A/B, mole-%				A/C, mole-%			
ST	MMA	AN	Found	Penultimate modification	Simplified eq., $r_{31} = 0.114$	A-G eq., $r_{31} = 0.04$	Found	Penultimate modification	Simplified eq., $r_{31} = 0.114$	A-G eq., $r_{31} = 0.04$
0.359	0.360	0.281	1.70	1.47	1.44	1.49	1.53	1.47	1.50	1.60
0.532	0.265	0.203	2.60	2.30	2.26	2.27	1.93	2.135	2.28	2.21
0.283	0.282	0.435	1.67	1.74	1.76	1.82	0.995	1.035	1.01	1.16
0.278	0.520	0.202	0.898	0.85	0.84	0.84	1.58	1.58	1.58	1.89

the simplified equations, eqs. (30) and (31), are predicated on the assumption:[4]

$$P_{ab}P_{bc}P_{ca} = P_{ac}P_{cb}P_{ba}$$

The applicability to this system may be justified by testing the dependent equality:[4]

$$r_{13}r_{32}r_{21} = r_{12}r_{23}r_{31}$$

$$(0.41)\ (3.7)\ (0.067) = (35)\ (0.074)\ (0.04)$$

$$0.1015 = 0.1035$$

The agreement is excellent; however, r_{13} and r_{31} disregard penultimate effects. Applying the penultimate modifications, eqs. (32)–(33), satisfactory agreement with experimental data[8] results.

TABLE II
Styrene(St)–Vinyl Chloride(VC)–Acrylonitrile (AN)

Charge			A/B, mole-%		A/C, mole-%	
				Pen-ultimate		Pen-ultimate
St	VC	AN	Found	eq.	Found	eq.
0.200	0.200	0.600	10.1	7.60	1.045	.823
0.202	0.598	0.202	12.55	20.2	1.37	1.20

For these calculations r_{31}' was taken as 0.114. However, if r_{31} is taken as 0.04 and r_{31}' calculated from the experimental A/C ratio of the first experiment, by eq. (33) a value for r_{31}' of 0.075 results. Similarly, from the second experiment a calculated value for r_{31}' of 0.094 results. However, uncertainties in the values of the other reactivity ratios in this system prevent firm conclusions about the precise value of r_{31}' from these data.

It is of interest to consider ternary systems, such as those including α-methylstyrene, where there are antepenultimate effects.[3] In the case of α-methylstyrene in copolymerization, sequences of more than three units of α-methylstyrene are excluded by steric considerations (probably in the transition stage, since poly-α-methylstyrene of high molecular weight is readily produced by cationic polymerization). To treat antepenultimate effects where there are significant differences in value among $r_1 = K^{aaaa}/K^{aaab}$, $r_1' = K^{baaa}/K^{baab}$, and $r_1'' = K^{baa}/K^{bab}$ the reactivity ratios (r_{ij}) exhibiting such differences in eqs. (28) and (29), the Alfrey-Goldfinger equations, are replaced by

$$r_{ij}'' \frac{\left\{ \dfrac{r_{ij}'(I/J)[r_{ij}(I/J) + 1]}{r_{ij}'(I/J) + 1} + 1 \right\}}{r_{ij}''(I/J) + 1}$$

where I and J are the appropriate molar monomer fractions.   In the case of α-methylstyrene terpolymers r_{ij}, where i refers to a radical ending in α-methylstyrene, may be replaced by

$$\frac{r_{ij}''\left[\dfrac{r_{ij}'(I/J)}{r_{ij}'(I/J)+1}+1\right]}{r_{ij}''(I/J)+1}$$

since $r_1 = K^{aaaa}/K^{aaab} = 0$.   In α-methylstyrene copolymers such as those with methacrylonitrile and probably methyl methacrylate, $r_1' = r_1''$, so r_{ij} may be replaced by

$$\frac{r_{ij}''\left[\dfrac{r_{ij}''(I/J)}{r_{ij}''(I/J)+1}+1\right]}{r_{ij}''(I/J)+1}$$

Further simplifications may be effected if $P_{ab}P_{bc}P_{ca} = P_{ac}P_{cb}P_{ba}$ and eqs. (30) and (31) may be used as base points.   It was shown earlier that the relationship $r_{13}r_{32}r_{21} = r_{12}r_{23}r_{31}$ tests this hypothesis.   In the terpolymer system styrene–α-methylstyrene–methyl methacrylate:

$$r_{13}r_{32}r_{21} = r_{12}r_{23}r_{31}$$

$$(1.18)(0.14)(0.46) = (0.52)(0.50)(0.36)$$

$$0.076 = 0.0935$$

so we are probably justified in applying eqs. (30) and (31).   Since two of the three binary systems involved include α-methylstyrene the equations are modified as follows:

$$\frac{a}{b} = \frac{\left|\dfrac{r_{21}''\left[\dfrac{r_{21}''(B/A)}{r_{21}''(B/A)+1}+1\right]\Big/[r_{21}''(B/A)+1]}{A}\right|\left(\dfrac{B}{r_{12}}+A+\dfrac{C}{r_{13}}\right)}{\dfrac{B}{r_{12}}\left|r_{21}''\left[\dfrac{r_{21}''(B/A)}{r_{21}''(B/A)+1}+1\right]\Big/[r_{21}''(B/A)+1]\right|+B+} \tag{34}$$

$$\left|r_{23}''\left[\dfrac{r_{23}''(B/C)}{r_{23}''(B/C)+1}+1\right]\Big/[r_{23}''(B/C)+1]\right|$$

$$\frac{a}{c} = \frac{\dfrac{A}{r_{31}}\left(\dfrac{C}{r_{13}}+A+\dfrac{B}{r_{12}}\right)}{\dfrac{C}{r_{13}}\left(\dfrac{A}{r_{31}}+C+\dfrac{B}{r_{32}}\right)} \tag{31}$$

It is of interest that the second equation remains the same, since no additions to α-methylstyrene free radical influence the ratio of styrene/methyl methacrylate.

Terpolymerizations Where One or More Propagation Constants Approach Zero

By now the substantial equality of product probabilities where one or more reactivity ratios approach zero has been demonstrated. Undoubtedly, there may be instances when steric hindrance may prevent self-propagation; although a few recalcitrant systems such as maleic anhydride have been shown to homopolymerize. The product probabilities $P_{ab}P_{bc}P_{ca}$ and $P_{ac}P_{cb}P_{ba}$ become indeterminate if any self-propagation rate constants disappear, so equality cannot be tested for systems where the relative reactivity ratios are too small to be measured. However, it is believed that the evidence favors equality, even under these conditions. If one accepts this hypothesis, then Eq. 30 and 31 may be modified to accommodate those instances where C in a three-component polymerization cannot add to itself, i.e., where $K^{33} = 0$ and, accordingly, r_{31} and r_{32} are equal to zero. Such monomers are crotonic acid, dichloroethylene, and citraconic acid. It is not necessary to modify eq. (30), since the ratio a/b is not dependent on additions to C.

$$\frac{a}{b} = \left[\frac{A}{r_{21}}\left(\frac{B}{r_{12}} + A + \frac{C}{r_{13}}\right)\right] \Big/ \left[\frac{B}{r_{12}}\left(\frac{A}{r_{12}} + B + \frac{C}{r_{23}}\right)\right] \tag{30}$$

However, as K^{33} approaches zero, eq. (31) may be modified by multiplying numerator and denominator by r_{32} and becomes in the limit:

$$\frac{a}{c} = \left[AR\left(\frac{C}{r_{13}} + A + \frac{B}{r_{12}}\right)\right] \Big/ \left[\frac{C}{r_{13}}(AR_1 + B)\right] \tag{35}$$

where

$$R = K^{31}/K^{32}$$

A single terpolymer experiment is required along with knowledge of r_{12} and r_{13} to complete the data necessary for evaluating R. Then any new compositions can be predicted.

For those cases where B and C have vanishing rates of self-propagation and can add to one another, eq. (30) becomes, on multiplication of numerator and denominator by r_{23},

$$\frac{a}{b} = \left[AR_1\left(\frac{B}{r_{12}} + A + \frac{C}{r_{13}}\right)\right] \Big/ \left[\frac{B}{r_{12}}(AR_1 + C)\right] \tag{36}$$

where

$$R_1 = K^{21}/K^{23}$$

and eq. (31) becomes, as in eq. (35),

$$\frac{a}{c} = \left[AR_2\left(\frac{C}{r_{13}} + A + \frac{B}{r_{12}}\right)\right] \Big/ \left[\frac{C}{r_{13}}(AR_2 + B)\right] \tag{37}$$

where

$$R_2 = K^{31}/K^{32}$$

A single terpolymer experiment yields sufficient information (a/b and a/c) to determine R_1 and R_2. Equations (30), (35), (36), and (37) can be readily modified by the rules described in the earlier section to embrace penultimate and antepenultimate effects.

An extension of the equation

$$r_{13}r_{32}r_{21} = r_{12}r_{23}r_{31}$$

is of particular interest in terpolymers, since it provides information on the reactivity of radicals derived from 1,2-disubstituted monomers with two other unlike monomers. Thus, both sides of the equation may be divided by r_{32} to yield

$$r_{13}r_{21} = r_{21}r_{23}(K^{32}/K^{31}) \tag{38}$$

Now if K^{33} is allowed to approach zero, the validity of eq. (38) is not affected. Accordingly, K^{32}/K^{31} may be estimated if one knows the values of r_{13}, r_{23}, r_{12}, and r_{21}.

$$1/R_2 = K^{32}/K^{31} = r_{13}r_{21}/r_{23}r_{12} \tag{39}$$

In a similar way K^{23}/K^{21} may be estimated:

$$1/R_1 = K^{23}/K^{21} = r_{12}r_{31}/r_{13}r_{32} \tag{40}$$

R_1 and R_2 so estimated might be substituted in eqs. (36) and (37) for prediction of terpolymer compositions where B and C have vanishing rates of self-propagation and yet can add to one another.

By means of eq. (39) the reactivity of a given monomer with a radical such as that derived from maleic anhydride may be compared with the reactivity of a standard monomer such as methyl acrylate taken as 1.0 (Table III).

It should be cautioned that the reactivity ratios employed in these calculations neglect the effects of penultimate and more remote units on radical reactivity.

The value of K^{32}/K^{31} may also be estimated from Q and e values for the various monomers. Thus the appropriate equation may be derived from the equation[8]

$$K_{ij} = P_i Q_j \exp\{-e_i e_j\}$$

TABLE III
Relative Reactivities of Monomers with Maleic Anhydride

Monomer	Relative reactivity
Styrene	1170
Methyl methacrylate	2.04
Methyl acrylate	1.0
Acrylonitrile	0.1873
Vinylidene chloride	0.145
Vinyl chloride	0.087
Vinyl acetate	0.066

which underlies the Q–e scheme:

$$K_{32}/K_{31} = (Q_2/Q_1) \exp\{-e_3(e_2 - e_1)\}$$

For the case that $K^{33} \to 0$ it is necessary to estimate K^{32}/K^{31} from eq. (39) for a particular combination of three monomers. Then, if Q_1, Q_2, e_1, and e_2 are known, e_3 may be determined. Once e_3 is known, K^{32}/K^{31} can be estimated for any other combination of three monomers. It is interesting that the value of Q_3 is not required for this calculation. However, Q_3 can be determined by substitution of e_3 in the appropriate equation for binary systems

$$r_1 = \frac{K^{11}}{K^{13}} = (Q_1/Q_3) \exp\{-e_1(e_1 - e_3)\}$$

where K^{11}/K^{13} is determined from copolymerization experiments of monomers 1 and 3. This method of determining Q and e values for 1,2-disubstituted olefins does not have the obvious drawbacks of that based on assuming a very small but finite value for K^{33}/K^{31} where the Q and e values determined are extremely sensitive to the value of K^{33}/K^{31} chosen.

References

1. Fordyce, R. G., and G. E. Ham, *J. Am. Chem. Soc.*, **73**, 1182 (1951).
2. Barb, W. G., *J. Polymer Sci.*, **11**, 117 (1953).
3. Ham, G. E., *J. Polymer Sci.*, **45**, 169 (1960).
4. Ham, G. E., *J. Polymer Sci.*, **A2**, 2735 (1964).
5. Alfrey, T., Jr., and G. Goldfinger, *J. Chem. Phys.*, **12**, 322 (1944).
6. Ham, G. E., *J. Polymer Sci.*, **14**, 87 (1954).
7. Walling, C., and E. R. Briggs, *J. Am. Chem. Soc.*, **67**, 1774 (1945).
8. Alfrey, T., Jr., and L. J. Young, in *Copolymerization*, G. E. Ham, Ed. Wiley, New York, 1964, Chap. 2.

Résumé

Bien que les effets des unités antépénultièmes dans une copolymérisation d'un système linéaire aient été traités abondamment, l'étude de ces effets dans la terpolymérisation a été négligée. Cette négligence est sans aucun doute due au fait que les effets possibles, provenants de 27 différentes possibilités de propagation, doivent être prisés en considération. Heureusement, dans la pratique, quelques possibilités dues à l'unité antépénultième, sont seulement importantes du point de vue de la détermination de la composition du copolymère, et la plupart des étapes de propagation peuvent être traitées en tenant compte des effets de l'unité terminale uniquement. Des équations simplifiées, qui conviennent à de telles restrictions sont présentées. Ces équations sont appliquées à plusieurs exemples expérimentaux. En plus, des équations de terpolymérisation sont présentées, qui conviennent dans le cas ou une ou deux constantes de vitesse d'homopolymérisation tendent vers zéro. Des méthodes sont également introduites pour évaluer K^{32}/K^{31} dans le cas où K^{33} tend vers zéro. Ces méthodes conduisent; en outre, à de plus précises évaluations de Q et de e pour des oléfines-1,2 disubstituées.

Zusammenfassung

Obwohl der Einfluss der vorletzten Kettenglieder bei binärer Kopolymerisation ausführlich behandelt wurde, ist die Untersuchung dieser Einflüsse bei Terpolymerisation

vernachlässigt worden. Zweifellos ist die Ursache der Tatsache zuzuschreiben, dass die durch siebenundzwanzig Wachstumsmöglichkeiten bedingten möglichen Einflüsse berücksichtigt werden müssen. Glücklicherweise sind für praktische Zwecke nur wenige dieser Möglichkeiten zur Bestimmung der Kopolymerzusammensetzung von Bedeutung und die meisten Wachstumsschritte können ausschliesslich auf Grundlage der Endgruppeneinflüsse behandelt werden. Vereinfachte Gleichungen unter Berücksichtigung dieser Beschränkungen werden mitgeteilt. Diese Gleichungen werden an verschiedenen experimentellen Beispielen angewendet. Zusätzlich werden vereinfachte Terpolymergleichungen abgeleitet, die jene Fälle berücksichtigen, bei welchen eine oder zwei Homopropagationsgeschwindigkeitskonstanten Null werden. Weiters werden Methoden zur Berechnung von K^{32}/K^{31}, wenn K^{33} gegen Null geht, angeführt. Diese Methoden führen andrerseits auch zu einer genaueren Berechnung von Q und c für die 1,2-disubstituierten Olefine.

Prediction of Ionic Copolymerization Reactivity Ratios

KENNETH F. O'DRISCOLL, *Villanova University,*
Villanova, Pennsylvania

Synopsis

It is shown that it is possible to predict the reactivity ratios for the copolymerization of a given monomer pair if each monomer has been separately copolymerized with a third monomer, and the product of the reactivity ratios of one of these separate copolymerizations is equal to unity.   This latter condition is frequently met in ionic copolymerizations and is sometimes true in free radical copolymerizations.   Literature data for five trios of monomer are examined to show the validity of the predictions.

Detailed experimental studies of ionic copolymerizations of vinyl monomers are being published with ever increasing frequency.   It therefore becomes desirable to find a method of correlating existing data and to use the correlation to predict copolymerization behavior for untried pairs of monomers.   The development of such a correlation for ionic copolymerization, analogous, perhaps, to the Q–e scheme in radical copolymerization, has been hindered by the strong dependence of reactivity ratios on experimental conditions, and by the misleading "copolymerization" data which can be obtained from monomers differing widely in electronegativity.   The former point has been the subject of a number of studies using anionic or cationic initiators.   From these works it is possible to state categorically that reactivity ratios are strongly dependent on the initiator, solvent, and temperature used in the ionic copolymerization of a given monomer pair. In spite of these difficulties it is necessary to develop some sort of general understanding of ionic copolymerizations.   It is the purpose of this paper to start such a development, with the use as a basis of the one observation that has been consistently made about ionic copolymerizations: the product of the reactivity ratios is often unity:

$$r_{12}r_{21} = 1 \tag{1}$$

This observation has recently been explored,[1] and it was shown that a simple thermodynamic identity is necessary and sufficient for eq. (1) to hold:

$$F_{12}^{\ddagger} - F_{11}^{\ddagger} = F_{22}^{\ddagger} - F_{21}^{\ddagger} \tag{2}$$

where $F_{ij}^{\ddagger}$ refers to the absolute value of the free energy of the activated complex formed when monomer j adds to a chain ending in monomer i.

Ham has suggested[2] that a route to further understanding of copolymerization can be found in the equation governing terpolymerization. He defines the probability in terpolymerization of monomer j (M_j) adding to a chain ending in monomer i (M_i^*) as

$$P_{ij} = \frac{k_{ij}[M_i^*][M_j]}{k_{ij}[M_i^*][M_j] + k_{ii}[M_i^*][M_i] + k_{ik}[M_i^*][M_k]} \tag{3}$$

when i, j, k, have values of 1, 2, or 3.

Although derived for free radical polymerizations, Ham's equations are valid in ionic systems if steady-state concentrations of chain ends can be assumed. Let us consider the unique possibility that

$$P_{13} = P_{23} \tag{4}$$

Substituting the proper forms of eq. (3), one obtains at equimolar concentrations of the three monomers:

$$k_{13}/(k_{11} + k_{12}) = k_{23}/(k_{22} + k_{21}) \tag{5}$$

If the rate constant k_{ij} is considered, as previously,[1] in terms of absolute reaction rate theory, it can be shown that

$$\exp\{F_{M_1} - F_{M_2}\}(\exp\{F_{13}^{\ddagger} - F_{11}^{\ddagger}\} - \exp\{F_{23}^{\ddagger} - F_{21}^{\ddagger}\})$$
$$= \exp\{F_{23}^{\ddagger} - F_{22}^{\ddagger}\} - \exp\{F_{13}^{\ddagger} - F_{12}^{\ddagger}\} \tag{6}$$

Equation (6), and therefore eq. (4), can be true if

$$(F_{13}^{\ddagger} - F_{11}^{\ddagger}) = (F_{23}^{\ddagger} - F_{21}^{\ddagger})$$

and

$$(F_{23}^{\ddagger} - F_{22}^{\ddagger}) = (F_{13}^{\ddagger} - F_{12}^{\ddagger}) \tag{7}$$

Equation (7) can be rearranged so as to reduce to two conditions, one of which is the same as eq. (2). These two conditions can be stated in terms of rate constants as:

$$k_{11}/k_{21} = k_{12}/k_{22} = k_{13}/k_{23} \tag{7a}$$

It is quite possible then that if the product of the binary reactivity ratios of two monomers is unity, the probability of a third monomer adding to chains ending in either of these will be the same, i.e., if eq. (1) is true, eq. (4) may also be true.

With this last statement in mind it is possible to take advantage of the simple relations proven by Ham[2] for all terpolymerizations which obey steady-state conditions:

$$d[M_i]/d[M_j] = P_{ji}/P_{ij} \tag{8}$$

$$r_{ik}r_{ji}r_{kj} = r_{ij}r_{ki}r_{jk} \tag{9}$$

When eq. (4) holds, it can be shown from the particular forms of eq. (8) that

$$P_{31}/P_{32} = P_{21}/P_{12} \tag{10}$$

TABLE I

Prediction of Ionic Reactivity Ratios at 30°C.

Method	Monomers		i	j	k	r_{ij}	r_{ji}	Product	r_{ik} Predicted	r_{ik} Observed	r_{ki} Predicted	r_{ki} Observed
Cationic	Styrene	M_1	1	2	3	0.20	4.2	0.84	1.3	2.5	0.80	0.45
	p-Methylstyrene	M_2	3	1	2	0.45	2.5	1.1	0.09	0.19	10.5	6.5
	p-Chlorostyrene	M_3	2	3	1	6.5	0.19	1.2	2.9	4.2	0.47	0.20
Cationic	2-Chloroethyl vinyl ether	M_1	1	2	3	45	5	>1	—	—	—	—
	p-Methylstyrene	M_2	3	1	2	11	2	>1	—	—	—	—
	p-Methoxystyrene	M_3	2	3	1	0.30	4.3	1.3	3.3	5	8.6	45
Anionic	Styrene	M_1	1	2	3	0.12	8.0	1.0	0.32	0.14	3.1	7.0
	Isoprene	M_2	3	1	2	7.0	0.14	1.0	0.87	0.38	1.2	2.6
	Butadiene	M_3	2	3	1	2.6	0.38	1.0	18.2	8.0	0.053	0.12

TABLE II

Prediction of Free Radical Reactivity Ratios at 60°C.

Monomers		j	k	r_{ij}	r_{ji}	Product	r_{ik} Predicted	r_{ik} Observed	r_{ki} Predicted	r_{ki} Observed
2-Fluorobutadiene-1,3	M_1	2	3	1.54	0.64	0.99	0.80	1.55	0.29	0.50
Methyl methacrylate	M_2	1	2	0.50	1.55	0.77	0.77	0.46	0.99	0.52
Styrene	M_3	3	1	0.52	0.46	<1	—	—	—	—
Styrene	M_1	1	3	0.78	1.39	1.08	0.28	0.15	1.33	0.7
Butadiene	M_2	3	2	0.7	0.15	<1	—	—	—	—
Methacrylic acid	M_3	2	1	0.20	0.53	<1	—	—	—	—

Since eq. (1) must also be true when eq. (4) holds, then it can be proved by using the proper forms of eq. (3) that

$$r_{13}/r_{23} = r_{12} \tag{11}$$

or, stated more generally,

$$r_{ik}/r_{jk} = r_{ij} \tag{12}$$

if $r_{ij}r_{ji} = 1$. The utility of eq. (12) is almost obvious. If any three monomers are considered, three possible pairs can be copolymerized. If the condition of eq. (1) is satisfied for any of the pairs, then knowledge of the reactivity ratios for only two of the pairs is necessary in order to predict the reactivity ratios of the third pair from eqs. (9) and (12). Since so many ionic copolymerizations satisfy eq. (1), eq. (12) ought to have wide applicability.

Experimental verification of eq. (12) requires ionic copolymerization data for trios of monomers, all obtained under the same experimental conditions. Existing literature data rarely satisfy this requirement, but two such sets of cationic data[3] and one of anionic data[1] have been examined and are presented in Table I. The examination takes the form of making predictions from eqs. (12) and (9) of r_{ik} and r_{ki} assuming the other four reactivity ratios to be known, wherever the reactivity ratio product for the monomer pair M_i–M_j is equal to unity. The agreement between the predicted and observed values is reasonable in the light of the usual imprecision in experimental reactivity ratio data.

Obvious extensions of this predictive ability would be toward its use for predicting ionic terpolymerization behavior, when only two of the three possible pairs have been copolymerized. It would also be useful to predict the magnitude of ionic reactivity ratios when they are so small or large as to defy experimental determination. In particular, it may be of use in Ziegler polymerizations of ethylene–propylene and a third monomer.

Although the ideas presented above have been developed with ionic copolymerization in mind, they can also be applied to free radical copolymerizations where the condition of eq. (1) is satisfied. Most interestingly, this is true for the pair styrene–butadiene at 60°C. Two free radical predictions based on data taken from Young's compilation[4] are shown in Table II.

The results in both Table I and II tend to confirm the hypothesis set forth by Ham[2] that "a logical approach to the problem of general monomer reactivity must lie in a consideration of terpolymerization."

Further work to test eq. (12) is in progress. It is hoped that other workers will apply these equations to suitable systems for which they may have data.

References

1. O'Driscoll, K. F., and I. Kuntz, *J. Polymer Sci.*, **61**, 19 (1963).

2. Ham, G., paper presented at 145th National Meeting, American Chemical Society, New York, Sept. 1963; *Polymer Preprints*, **4**, No. 2, 224 (1963).

3. Kanoh, N., A. Gotoh, T. Higashimura, and S. Okamura, *Makromol. Chem.*, **63**, 106 (1963).

4. Young, L. J., *J. Polymer Sci.*, **54**, 411 (1961).

Résumé

On a montré qu'il est possible de prédire les rapports de réactivité de copolymérisation d'une paire de monomères données si chaque monomère a été séparément copolymérisé avec un troisième monomère et si le produit des rapports de réactivité d'une de ces copolymérisations séparées est égale à l'unité. Cette dernière condition est fréquemment rencontrée dans les copolymérisations ioniques et est quelquefois valide dans les copolymérisations radicalaires. Les données de la littérature pour cinq trios de monomères ont été examinées et ont montré la validité de ces prédictions.

Zusammenfassung

Es wird die Möglichkeit einer Vorhersage der Reaktivitätsverhältnisse für die Copolymerisation eines gegebenen Monomerenpaares gezeigt, unter der Voraussetzung, dass jedes Monomere allein mit einem dritten Monomeren copolymerisiert wurde und dass das Produkt der Reaktivitätsverhältnisse einer dieser getrennten Copolymerisationen gleich eins ist. Letztere Bedingung ist bei ionischen Copolymerisationen häufig und sie ist manchmal bei radikalischen Copolymerisationen anzutreffen. Literaturangagen für fünf Trios von Monomeren werden untersucht, um die Richtigkeit der Vorhersage zu zeigen.

On Correlation of Data in Copolymerization

FRANK R. MAYO, *Stanford Research Institute, Menlo Park, California*

Synopsis

Equation (3) is potentially useful for bringing out inconsistencies between experimental data and theoretical correlations and predictions of behaviors of monomers in copolymerizations. Equation (3) is a modification of Ham's eq. (1). His eqs. (1) and (4) are approximations which are sometimes quite good, and sometimes very poor.

1. Introduction

I had an opportunity to examine carefully before publication two papers by Dr. George E. Ham.[1,2] Some criticisms of his papers are presented in Section 3. However, the principal positive contribution of the present paper is to discuss a new and different application of one of his relations:

$$r_{12}r_{23}r_{31} = r_{13}r_{32}r_{21} \tag{1}$$

Here, r_{12} is the monomer reactivity ratio for an A· radical in copolymerization of monomers A and B, and so on.   Equation (1) was derived first from Ham's novel eq. (4), discussed in Section 3, but it also follows directly from the Alfrey and Price relations[3] such as

$$r_1 = k_{11}/k_{12} = (Q_1/Q_2) \exp \left\{ -e_1(e_1 - e_2) \right\} \tag{2}$$

and also from those of Bamford and Jenkins.[4] *   Both sets of relations have been useful in making semiquantitative predictions of the behavior of two monomers in copolymerization from their respective copolymerizations with a third monomer, either directly or indirectly.   All of these relations are based on the same underlying approximations: that monomer reactivity ratios for any pair of monomers are constant over a wide range of feeds at a given temperature, that steric and penultimate effects are negligible, and that any special (polar) interactions between A· and B and between B· and A (and so on) are symmetrical.

I propose that eq. (1) be used as a test of the adequacy of all three theoretical approaches when experimental data are available for all three pairs of a system of three monomers.   I shall show that the two sides of eq.

---

* Ready conversion of the equations of Bamford and Jenkins[4] to eq. (1) requires use of their relation, $\alpha = -\mu^2\sigma$. Dr. Jenkins has pointed out to me that this approximation is unnecessary when σ values are known.[4]   In such cases, polar interactions need not be symmetrical; eq. (1) need not apply, and H values differing from unity may be expected.

(1) are generally not equal and that there is some pattern in the discrepancies. Therefore, eq. (1) is recast as

$$r_{12}r_{23}r_{31}/r_{13}r_{32}r_{21} = H \tag{3}$$

When experimental data and theory are perfectly consistent, $H = 1$. In other cases, whether H is greater or less than one depends on which monomer is taken as A (or B). I therefore always choose H to be less than one; the smaller is H, the poorer is the agreement between theory and experiment. The monomer reactivity ratios employed come from Ham's papers[1,2] or the compilation of Young.[5]

2. Discussion of H Factors

Table I lists essentially all the systems considered by Ham[1,2] and my calculations of the H factors. These range from 0.07 to 1.0, and any one may vary considerably when a choice of experimental data is available.

Let us examine first system 3, which has the smallest H value, 0.07. Substitution of the monomer reactivity ratios into eq. (1) gives

$$0.75 \times 9 \times 0.01 = 55 \times 0.1 \times 0.18$$

The ratios 55 and 0.01 for styrene and vinyl acetate fall on opposite sides of the equation. This great difference in reactivity is not adequately compensated for in the copolymerizations of these monomers with methyl acrylate and the "equality" (1) fails by a factor of 14. All of the ratios above were determined by my collaborators (the principal ones here being F. M. Lewis and C. Walling) after we had accumulated considerable experience in such work. The 55 might be in error by up to 30% and the 0.01 might be in error by a factor of as much as 3. With the most favorable choices of these errors, the "equality" still fails by a factor of three to four, too large to be ascribed wholly to errors in the other four reactivity ratios, even if all the errors are in the most favorable directions. Similar considerations apply to system 2. Again, all the reactivity ratios were determined by my associates (some here by K. W. Doak) and the H factor of 0.2 is probably good within a factor of 2.

System 4 probably has the most accurately known set of reactivity ratios in Table I. The data are all from my associates; none of the reactivity ratios is too far from one; precipitation during copolymerization is no problem; the analyses are easy, but $H = 0.55$. Similar considerations apply to system 5, where $H = 0.57$.

Further examination of Table I suggests some correlations of H factors. For seven systems of three conjugated monomers or vinylidene chloride, (systems 1, 4–9) and two systems of three unconjugated monomers (15,16) seven of the nine H values lie between 0.55 and 1.0. If we omit the vinylidene chloride systems, all but two fall between 0.7 and 1.0. This result means that Ham's eq. (1) and the two other theoretical relations[3,4] are usually consistent within a factor of two or less for these systems, often

TABLE I

Correlations of Three Copolymerizations of Three Monomers

System no.	Monomers A,B,C, resp.[a]	$P_{ab}P_{bc}P_{ca} = P_{ac}P_{cb}P_{ba}$[b]	$\dfrac{r_{12}r_{23}r_{31}}{r_{13}r_{32}r_{21}}$	H[c]
1	St, MM, AN	0.053 = 0.0454	0.0281/0.0331	0.85
2	St, MA, VCl	0.00504 = 0.00435	0.45/0.52	0.86
		0.0157 = 0.00284[d]	0.066/0.367[d]	0.18
3	St, MA, VAc	0.0084 = 0.00058	0.0675/0.99	0.068
4	St, MM, VCl$_2$	0.042 = 0.023	0.112/0.205	0.55
5	MM, AN, VCl$_2$	0.0262 = 0.0467	0.295/0.168	(0.57)
6	St, MM, VP	0.051 = 0.0562	0.233/0.218	(0.94)
7	St, MM, MA	0.0348 = 0.046	0.215/0.162	(0.75)
8	St, AN, AA	0.0491 = 0.0199	0.024/0.060	0.40
		0.0164 = 0.085[e]	0.036/0.0069[e]	(0.19)
9	St, MA, AN	0.050 = 0.0122[f]	0.0285/0.115[f]	0.248
10	MM, MA, VAc	0.0087 = 0.00282	0.31/0.94	0.33
11	MM, MA, VCl	0.00782 = 0.0055	0.415/0.585	0.71
		0.0131 = 0.00315[d]	0.201/0.84[d]	0.42
12	AN, MA, VCl	0.0168 = 0.0167[h]	0.92/0.292[g]	(0.32)
13	VCl, VAc, AN		0.466/0.266	(0.57)
			0.133/0.266	0.50
		0.00615 = 0.00641[i]	0.200/0.191[i]	(0.96)
		0.00564 = 0.0128[j]	0.406/0.180[j]	(0.44)
14	VCl, VAc, MA	0.00326 = 0.00552[i]	0.485/0.289[i]	(0.60)
		0.00293 = 0.0106[j]	1.62/0.447[j]	(0.28)
15	VAc, VBz, NVP	0.0451 = 0.0461[f]	0.508/0.498[f]	(0.98)
16	VCl, VAc, VCr	0.0162 = 0.0222[f]	0.648/0.468[f]	(0.72)

[a] AA = acrylic acid; AN = acrylonitrile; MA = methyl acrylate; MM = methyl methacrylate; NVP = N-vinylpyrrolidone; St = styrene; VAc = vinyl acetate; VBz = vinyl benzoate; VCl = vinyl chloride; VCl$_2$ = vinylidene chloride; VCr = vinylene carbonate; VP = 2-vinylpyridine.

[b] Calculated for terpolymerization of equimolar mixtures; see Section 3.

[c] H factors, reciprocals in parentheses to make $H < 1$.

[d] MA–VCl by Marvel and Schwen, others by Doak.

[e] AN–AA from Ito and Suzuki, St–AA from Chapin, Ham, and Mills, both instead of unpublished data by Young.

[f] Other available experimental data would give different results.

[g] Using Ham's choice of data and the $r_{12} = 1.4$ which he chose for system 9.

[h] After recalculation of r_{12} by Ham.

[i] Ham's values based on monomer reactivity ratios for vinyl stearate.

[j] My calculations based on VAc data which are said to establish "equivalence" of VAc and vinyl stearate; otherwise same as i.

within experimental error. However, for two of the nine systems (8 and 9), the relations fail by factors of 4 to 5 (my first choice of data). Several sets of data (none by my co-workers) are available for the acrylic acid copolymerizations (8) and for the acrylonitrile–methylacrylate system (9), and I cannot say whether the low H factors arise mostly from errors in the experiments or in the underlying approximations.

For all the systems containing combinations of both conjugated and unconjugated monomers other than vinylidene chloride, the values fall be-

tween 0.06 and 0.50 (my first choice of data). This means that eq. (1) and the theoretical relations are inconsistent with experimental data by factors of at least two and of as much as 14. Most of these discrepancies seem well beyond experimental error. Since there is no reason to think that experimental errors produce consistently low H values, the contrast with wholly conjugated and wholly unconjugated systems seems significant. From the results with styrene and vinyl acetate, where polar, steric, and penultimate effects seem to be small, the major difficulty seems to be that the Q scale in the Alfrey and Price equation cannot accommodate large differences in general reactivity. In general, as any one monomer reactivity ratio of a set approaches zero, H approaches zero; if two ratios approach zero, H may become indeterminate. In either case, the Alfrey-Price equations are unable to make predictions.

In view of the apparent inconsistencies in both the theoretical relations and in some of the experimental data, and the possible errors in isolated data, the initial effort of Thompson and Raines[6] to obtain better data seems much more useful on a long-term basis than several efforts to revise the base points[7] for the Alfrey-Price relations. I hope that the combination of better data and use of the H factor will help to clarify and advance our understanding of copolymerization.

3. Criticism of Ham's Papers

This section summarizes some of my views on Ham's papers.[1,2] The foundations of his first paper are that consideration of terpolymerization is "a logical approach to the problem of general monomer reactivity" and that "terpolymer compositions are much more sensitive to sequence distribution and reactivity ratios than binary systems, so offer an unusual chance to check on questionable reactivity ratios."[1] No justification for this statement is offered, and I know of none. He then proposes that

$$P_{ab}P_{bc}P_{ca} = P_{ac}P_{cb}P_{ba} \ (= \mathcal{P})$$ (4)

where P_{ab} is the probability that monomer A will be followed by monomer B in a terpolymerization of A, B, and C and so on. By definition

$$P_{ab} = \frac{k_{ab}[A \cdot][B]}{k_{aa}[A \cdot][A] + k_{ab}[A \cdot][B] + k_{ac}[A \cdot][C]}$$ (5)

In an equimolar mixture of the three monomers

$$P_{ab} = \frac{1/r_{12}}{1 + 1/r_{12} + 1/r_{13}}$$ (6)

and so on. Equation (4) says that the probability of finding an ABCA sequence (counting an A sequence as one A and so on) in a terpolymerization of the three monomers is the same as the probability of finding the reverse ACBA sequence. In a two-monomer system, the analog of eq. (4) holds perfectly for infinite chains. If terpolymerizations followed a simple

and regular pattern, eq. (4) would apply there. Table I shows that it usually does not. Through substitutions like eqs. (5) and (6), eqs. (1) and (4) can be shown to be equivalent.

Ham's papers are not really much concerned with terpolymerizations; they are concerned primarily (after an unsuccessful attempt to establish them) with the applications of eqs. (4) and (1) to predicting reactivity ratios in binary systems. Thus, if the four reactivity ratios for A and B and for A and C are known, the ratio r_{23}/r_{32} for B and C can be calculated if eq. (1) applies. Equation (4), based on complex functions of monomer reactivity ratios (i.e., probabilities), represents an effort to separate r_{23} and r_{32}, not possible from eq. (1). The indications of success are at least partly illusory.

In both theory and practice, the relations (1) and (4) miss equality by exactly the same percentage; thus eq. (1) can be used to check the longer calculations for eq. (4). If the left side of eq. (4) is larger than the right, the ratio is exactly reversed in eq. (1). Table I shows that evaluations of products of three reactivity ratios, i.e., the values of the numerators and denominators in eq. (3), range from 0.007 to 1.62 while the products of three probabilities have a much smaller arithmetic range, from 0.0006 to 0.09. The form of eq. (6) assures that all the terms in eq. (4) will be smaller than the corresponding terms in eq. (1). On an arithmetic scale, all the probability products are compressed into a smaller range than the reactivity ratio products, but the *ratio* of the largest to the smallest product is about the same for probabilities as for reactivity ratios, and the percentage errors in the "equalities" for each system are identical.

Ham claims that his calculations (essentially all his systems are listed in Table I along with my calculations) show that either side of eq. (4) is usually equal to either 0.037 (for systems of three conjugated or three unconjugated monomers) or 0.006 (for systems containing both types of monomers). The actual average of Ham's values for systems 1, 6, and 7 is 0.048 with a mean deviation of 0.005. If we count vinylidene chloride as a conjugated monomer (as he does, although the "equality" becomes poorer), $\mathcal{P}$ averages 0.042 with a mean deviation of 0.008. Ham picked 0.037 because this value of $\mathcal{P}$ would apply to three monomers of equal reactivity. However, normal alternating tendencies in copolymerization increase this value, which seems to be a minimum value for wholly conjugated systems. For predicting monomer reactivity ratios in systems of three conjugated monomers, Ham's relations are nearly as accurate as the Alfrey-Price relations and they are much easier to apply. Equation (4) should give exactly the same ratio of r_{23}/r_{32} as the Alfrey-Price equation for the same experimental data, but choice of an arbitrary and somewhat uncertain $\mathcal{P}$ introduces some additional error. For systems of three unconjugated monomers, systems 15 and 16 are inadequate to establish any pattern.

For systems of one unconjugated and two conjugated monomers, Table I shows that $\mathcal{P}$ values are fairly well scattered from 0.0006 to 0.017 (a ratio of 28) and that the two sides of eqs. (1) and (4) are far from equal in most

cases.   From this range of values Ham picks $\mathcal{P} = 0.006$, "also in good agreement with experiment."[2]   "This value is the average of a large number of systems with relatively little spread when obtained from reliable data."[2]   This statement must mean either that a factor of three to five is "relatively little spread," or that the great bulk of the literature data, including those of my former associates, are less reliable than Ham's relations.   To me, both meanings are unacceptable.   The products of the monomer reactivity ratios range from 0.07 to 0.99, a larger arithmetic, but a smaller proportional, spread than for the probability ratios.   For reasons which are not clear to me, there is a clear gap between the products of probability ratios for wholly and partially conjugated systems (narrowed if vinylidene chloride is counted as conjugated) but some overlap for the corresponding products of reactivity ratios.   The only two systems in Table I with one conjugated and two unconjugated monomers (13 and 14) give results which depend on the choice of monomer reactivity ratios. The primary data (see below) make Ham's relations look the poorest. The uncertainties in $\mathcal{P}$ values for all these mixed systems make Ham's relations less accurate in predicting monomer reactivity ratios than the Alfrey-Price relations which apply poorly in such systems anyway.

Most of the space in Ham's two papers is concerned with recalculating experimental reactivity ratios so that they agree with his eqs. (1) and (4) and his $\mathcal{P}$ values.   The first portion of my paper showed that the most critical experimental data are more reliable than his equations.

As Ham states in the last paragraph of his second paper, some data were selected to give better agreement with his relations.   Some of these selections are interesting.   For r_{23} in system 2, four values are available:[5] 4.0, 4.4, 5.0, and 9.   Ham chose his own value, 9, for his calculation.   I chose 4.4 for my first test.   The effect on our calculations is substantial, as shown in Table I.   Ham got a much better fit for his probability products and used them to support his assignment $\mathcal{P} = 0.006$.   In his second paper, he recalculates r_{23} from different data as 20, without applying it to system 2 again.   In considering systems 13 and 14 in his second paper, he uses the data of Witnauer, Watkins, and Port[8] to show the "equivalence" of vinyl acetate and vinyl stearate in copolymerizations with acrylonitrile and methyl acrylate.   He then neglects their primary data on the acetate and employs their rather different data on the stearate (differing by factors up to 3) for his vinyl acetate calculations.   "Excellent agreement resulted. Similarly, product probabilities were very close."[2]   For system 8, Ham elected to use some unpublished value of Young instead of his own published ones.

Without detailing further criticisms of Ham's paper, I express the hope that his novel equations will prove useful in the form of eq. (3).

References

1. Ham, G. E., *J. Polymer Sci.*, **A2**, 2735 (1964); Division of Polymer Chemistry, *Preprints*, **4**, No. 2, 224 (September, 1963).

2. Ham, G. E., *J. Polymer Sci*, **A2**, 4169 (1964).

3. Alfrey, T., Jr., and C. C. Price, *J. Polymer Sci.*, **2**, 101 (1947); T. Alfrey Jr., J. J. Bohrer, and H. Mark, *Copolymerization*, Interscience, New York, 1952, Chap. 3.

4. Bamford, C. H., and A. D. Jenkins, *Trans. Faraday Soc.*, **59**, 530 (1963).

5. Young, L. J., *J. Polymer Sci.*, **54**, 411 (1961).

6. Thompson, B. R., and R. H. Raines, *J. Polymer Sci.*, **41**, 265 (1959).

7. Kawabata, N., T. Tsuruta, and J. Furkawa, *Makromol. Chem.*, **51**, 70, 80 (1962); R. D. Burkhardt and N. L. Zutty, *J. Polymer Sci.*, **A1**, 1137 (1963); C. C. Price, *ibid.*, **B1**, 433 (1963); K. Fukui, *Bull. Chem. Soc. Japan*, **36**, 47 (1963).

8. Witnauer, L. P., N. Watkins, and W. S. Port, *J. Polymer Sci.*, **20**, 213 (1956).

Résumé

L'équation (3) est virtuellement utile pour mettre en évidence les différences entre les résultats expérimentaux et les relations et previsions théoriques au sujet du comportement des monomères dans les copolymérisations. L'équation (3) est une modification de l'équation (1) de Ham. Ces équations (1) et (4) sont des approximations qui sont parfois assez et parfois très manvaises.

Zusammenfassung

Gleichung (3) kann zur Ermittlung von Inkonsistenzen zwischen Versuchsdaten und theoretischen Korrelationen und Voraussagen über das Verhalten von Momoneren bei der Copolymerisation herangezogen werden. Gleichung (3) ist eine Modifikation der Gleichung (1) von Ham. Seine Gleichungen (1) und (4) sind Näherungen, die manchmal recht gut, aber manchmal schlecht zutreffen.

Kinetics and Mechanism of the Trialkylboron-Catalyzed Polymerization of Methyl Methacrylate in the Presence of Oxygen

RICHARD L. HANSEN, *Central Research Laboratories, Minnesota Mining & Manufacturing Company, St. Paul, Minnesota*

Synopsis

The rate of the bulk polymerization of methyl methacrylate catalyzed by triethylboron–oxygen was investigated. The rate was studied as a function of initial triethylboron and oxygen concentrations as well as temperature. The effect of hydroquinone was determined. The polymerization rate was also investigated using several other trialkylboranes. The initial rate of the triethylboron-catalyzed polymerization was found to depend on the square root of the oxygen concentration and on the square root of the difference between the triethylboron and oxygen concentrations. The rates at higher conversions were consistent with an initiation mechanism requiring consideration of reactions at all three boron–carbon bonds. An initiation mechanism involving oxidation to peroxide followed by a reduction utilizing unoxidized boron–carbon bonds is advanced. Ethyl radical, produced in this reduction, is the initiating species. The overall activation energy taken from initial rates was 2.4 ± 0.3 kcal./mole in the range 0–$45°C$. A very slow polymerization with triethylboron was observed in the absence of oxygen. Hydroquinone behaved as a typical inhibitor for the aerobic polymerization but did not inhibit the polymerization in the absence of oxygen.

The recent publication[1] of an investigation of the polymerization of methyl methacrylate catalyzed by triethylboron/oxygen prompts the presentation of the results of a similar study conducted in this laboratory. In much of the early work on organoborane-catalyzed polymerizations the role of oxygen was not fully appreciated.[2,3] Somewhat later the profound influence of oxygen was recognized,[4,5] and it is now generally agreed that these polymerizations are typical free radical processes.[6,7] The initiating radicals are thought to arise from oxidation of the borane by molecular oxygen to produce a peroxide, R_2BOOR, which then disproportionates into free radicals[8] or is induced to decompose by excess borane.[1] This latter view is supported by the observation that neither the peroxide nor the borane alone is capable of initiating vinyl polymerization at room temperature in the absence of air.[7,9]

Bawn et al. have studied the rate of polymerization of methyl methacrylate in benzene using tributylboron and the peroxide derived from it.[9] Apparently, only two kinetic investigations have been reported wherein oxygen was used as a reactant. Vinyl chloride was the subject of work by

Talamini and Vidotto,[10] while Welch used methyl methacrylate.[1]   Both of these researches suffered from experimental limitations in that there was some doubt as to the amount of oxygen actually in solution and it was not possible to use a wide range of oxygen concentrations.   Welch was able to confirm the square-root oxygen dependence implied by the work of Bawn et al. but was unable to obtain the kinetic order with respect to the borane. Talamini and Vidotto reported an approximately square-root dependence on the borane concentration in agreement with Bawn and co-workers. They did not, however, report the order with respect to oxygen.   Welch's reported activation energy of 4 kcal./mole is in disagreement with the 12.9 kcal./mole given by Bawn et al.   Both Bawn and Welch reported that their polymerizations were characterized by an inordinately sharp decrease in polymerization rate with conversion.   No explanation has been advanced for this phenomenon.

Furukawa et al. observed that hydroquinone behaved as an accelerator for borane-catalyzed polymerizations.[11]   This has not been re-examined under conditions where oxygen was carefully controlled.   Finally, although the reactions leading to the primary radicals seem to be the only really unique features in these reactions, these steps remain obscure.

This paper describes a study of the bulk polymerization kinetics of methyl methacrylate using oxygen and triethylboron as well as several other alkylboranes.   An attempt is made to answer some of the questions raised or left unanswered by previous work.

EXPERIMENTAL

Materials

Commercial methyl methacrylate containing 60 ppm hydroquinone was stirred for several hours over calcium hydride and distilled through a simple Vigreaux column into a flask containing granular copper.   Subsequent monomer purification is described below.

Triethylboron, a Callery Chemical Co. product, was purified by conventional vacuum techniques involving trap-to-trap distillation at $\sim 10^{-5}$ mm. in a four-trap train.   The purity of the fraction retained was ascertained by vapor pressure measurements (12 mm. at 21°C) and by the linearity of a logarithmic vapor pressure versus $1/T$ plot.   The pure borane was stored in a sealed serum bottle in a continuously flushed dry nitrogen box.   The nitrogen box was monitored with an MSA oxygen indicator.   All transfers of the boranes were made in the box.

Tri-n-hexylboron and tricyclohexylboron were prepared by the hydroboronation procedure of Brown and Subba Rao.[12]   The n-hexyl compound boiled at 97–98.5°C./0.2 mm. (reported[13] b.p. 128–130/2 mm.).   The cyclohexyl compound melted at 117–119°C. (reported[14] m.p. 118°C.).   Tridodecyl and tri-n-butylboron were Callery Chemical Co. products and were used without purification.

The oxygen was U.S.P. quality, and the nitrogen was the dry, high purity grade. All of the other chemicals were commercial products and were used without purification.

Procedure

The vacuum apparatus used in these experiments is illustrated in Figure 1. The rates of polymerization were determined dilatometrically, but the scale of the equipment was larger than normally employed in this kind of study. The dilatometer bulb contained 96.22 ml., and the graduated tube was constructed from a 10 ml. microburet. Volume contractions were easily followed without a cathetometer. The equipment was designed specifically to allow accurate measurement of both the borane and oxygen concentrations and to allow a wide variation in the amounts used. Provisions were made so that actual oxygen concentrations in solution could be determined. A port was provided near the top of the dilatometer bulb capable of receiving a sealed ampule containing a measured amount of the borane. The entire bulb was thermostatted at constant temperature, and the polymerization was initiated on adding the borane as described below. In this way it was possible to obtain data on the initial rate since it was not necessary to bring the reaction mixture to temperature after the components had been mixed. Flushing lines were provided so that at the end of a run the reaction mixture could be quenched without exposure to the atmosphere. The components of the dilatometer assembly were joined with ball and socket joints to permit easy cleaning of the apparatus.

For each experiment, the previously distilled monomer was degassed on the vacuum line by alternately freezing, pumping, thawing, and stirring for five cycles. The system was pumped down to $\sim 10^{-5}$ mm. at the end of this procedure. The degassed monomer was fractionated by trap-to-trap distillation, and the pure fraction (vapor pressure 40 mm. at 30°C.) was transferred to a steel cylinder for overnight storage under vacuum at -78°C.

A small glass ampule (Fig. 1a) was loaded with the desired amount of borane in the nitrogen box by means of an Agla micrometer syringe, sealed with a soft neoprene septum, and removed from the box. The loaded ampule was inserted in the dilatometer bulb, replacing a dummy present initially. The system was pumped down to $\sim 10^{-5}$ mm. and the dilatometer assembly was isolated from the rest of the vacuum line. The bulb was then filled almost to capacity with methyl methacrylate. This was accomplished under vacuum simply by inverting the steel cylinder and allowing the thawed monomer to flow by gravity. The monomer was stirred to temperature equilibrium as indicated by a constant pressure at the manometer. Stirring was then stopped, and a measured volume of oxygen was added to the system from a gas buret. The pressure was noted at the manometer, and stirring was begun to dissolve the desired amount of oxygen. The final pressure was recorded. The amount of oxygen in solution was calculated from the known amount added to the
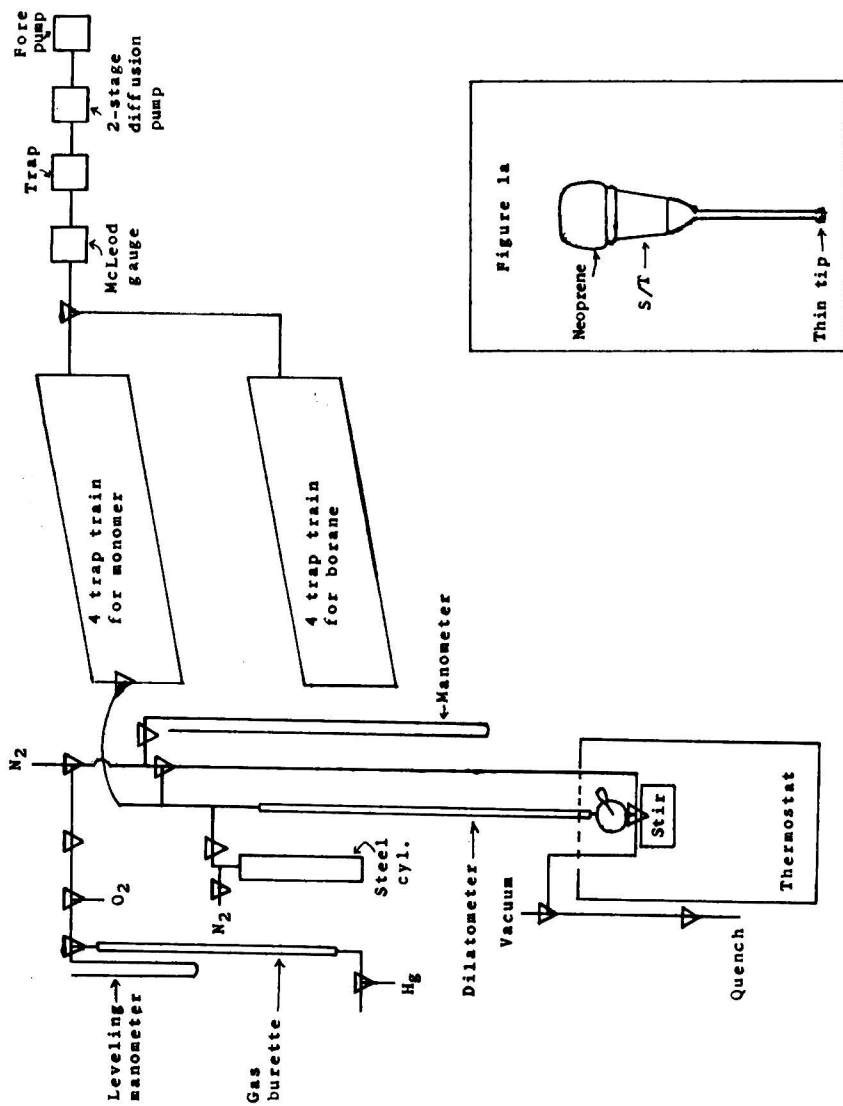
Fig. 1. Apparatus.

system and the decrease in oxygen partial pressure at the manometer. The Perfect Gas Law and Dalton's Law were assumed to be applicable. Monomer was added as before to a convenient level in the graduated tube. Nitrogen was then admitted above the liquid to barometric pressure.

The monomer was stirred at 350 rpm. When thermal equilibrium had been attained the reaction was initiated. The ampule was pressurized with nitrogen by using a Hamilton gas-tight syringe inserted through the neoprene septum of the ampule. The borane was then added by puncturing the thin-walled ampule tip with a stiff wire plunger.

The polymerizations were usually carried to about 15% conversion. The reaction mixture was flushed out by applying nitrogen pressure, and a 5 ml. sample was quenched by precipitation in 50 ml. of a 9/1 solution (by volume) of methanol/ammonium hydroxide. The liquid was evaporated and the polymer was dried to constant weight at 60°C.

The volume contraction was related to the extent of polymerization by using the equations as well as the monomer and polymer specific volumes reported by Schulz and Harborth.[15] Intermittent checks indicated that calculated conversions agreed well with those obtained by actually isolating and weighing the polymer.

Inherent viscosities in benzene were determined at 25°. Intrinsic viscosities were calculated from the equation:[16]

$$[\eta] = \langle\eta\rangle + 0.13\langle\eta\rangle^2 c$$

The $\bar{M}_v$ were obtained from the relation:[17]

$$0.76 \log \bar{M}_v = \log[\eta] + 4.244$$

Number-average molecular weights were determined in methyl ethyl ketone at 25°C. by using a Stabin osmometer with an Utracella membrane.

All absorption spectra were obtained on a Beckman DK-2A spectrophotometer.

RESULTS

The polymerization rate was determined at a constant triethylboron concentration over a wide range of oxygen concentrations. The results are shown in Figure 2. Contrary to another report,[1] a slow polymerization occurred in the absence of added oxygen. A very slow, spontaneous polymerization was also observed when neither oxygen nor borane was present. The rate of this latter reaction was so small that this cannot account for the polymerization in the presence of the borane. The possibility that the reaction was due to traces of oxygen remaining in the monomer cannot be completely ruled out, but is rendered unlikely by more complete studies.[18] The results of inhibition studies described below suggest that the polymerization in the absence of added oxygen may take place by a different mechanism than the aerobic reaction.

Fig. 2. Polymerization of methyl methacrylate at 30.0°C. with $[Et_3B]_0 = 7.18 \times 10^{-3}M$ and varying $[O_2]_0$: (1) $3.63 \times 10^{-3}M$; (2) $1.97 \times 10^{-3}M$; (3) $4.47 \times 10^{-3}M$; (4) $1.14 \times 10^{-3}M$; (5) $5.40 \times 10^{-3}M$; (6) $6.65 \times 10^{-3}M$; (7) $0.51 \times 10^{-3}M$; (8) $7.89 \times 10^{-3}M$; (9) 0.0.
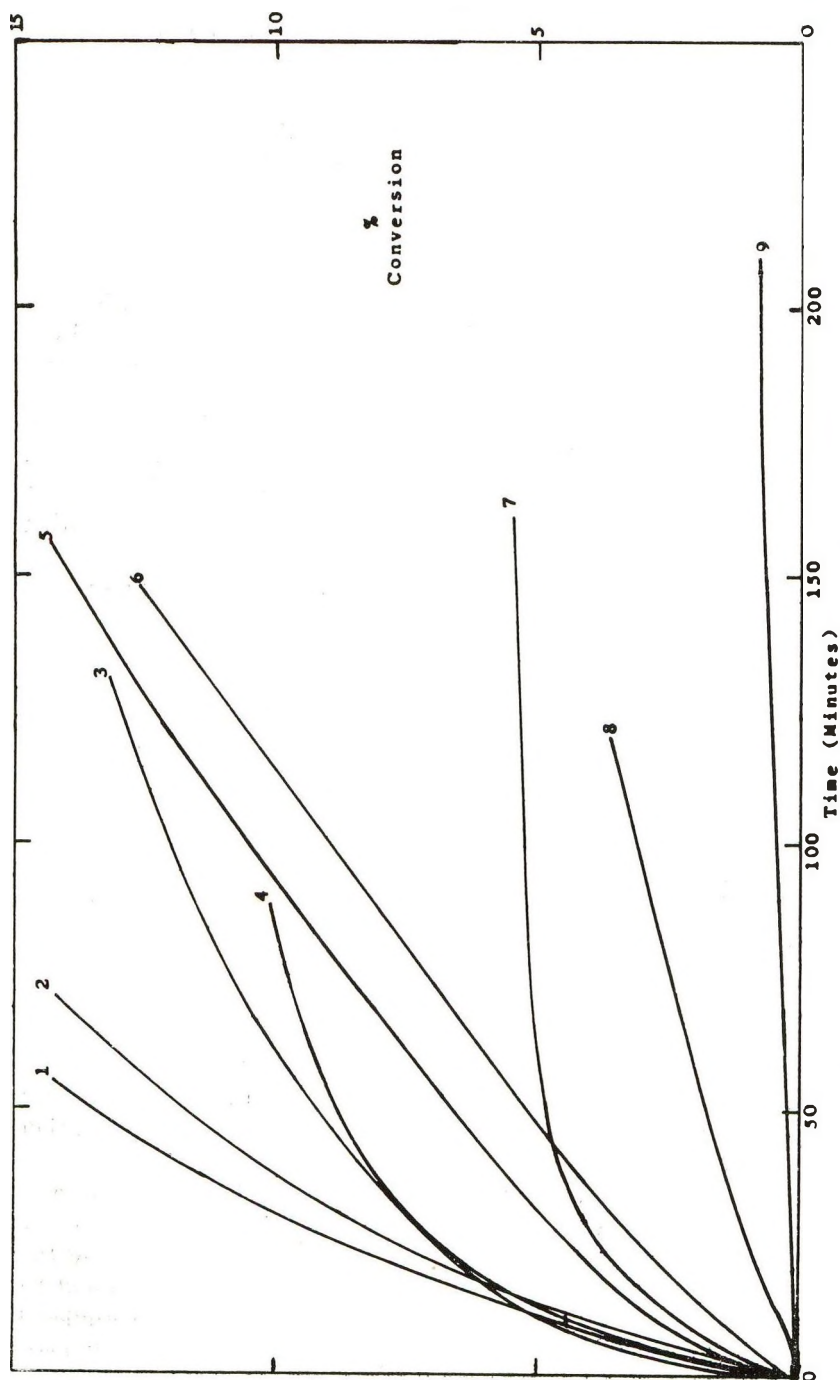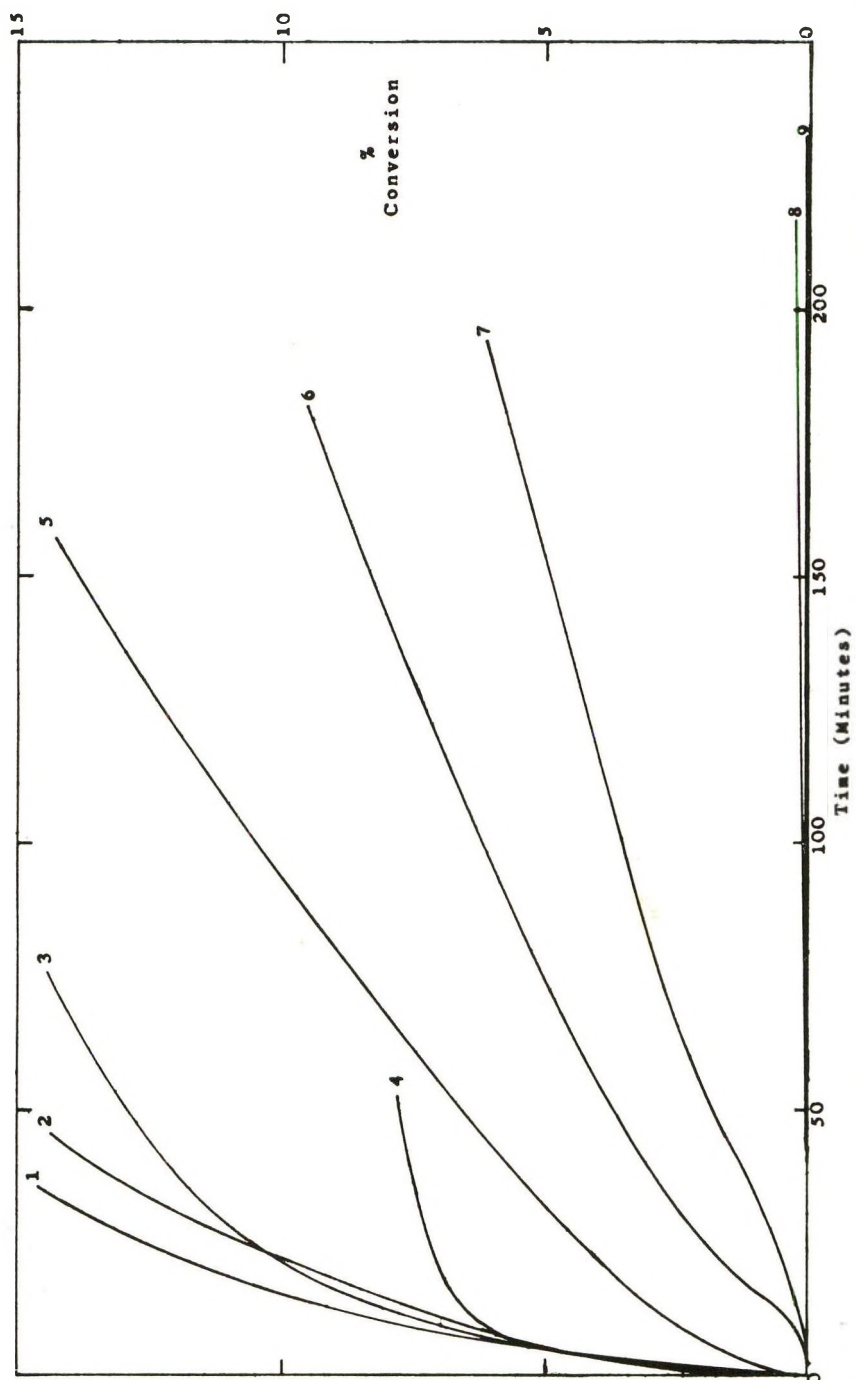
Fig. 3. Polymerization of methyl methacrylate at 30.0°C. with $[O_2]_0 = 5.4 \times 10^{-3}M$ and varying $[Et_3B]_0$: (1) $21.5 \times 10^{-3}M$; (2) $71.8 \times 10^{-3}M$; (3) $14.3 \times 10^{-3}M$; (4) $35.5 \times 10^{-3}M$; (5) $7.18 \times 10^{-3}M$; (6) $5.38 \times 10^{-3}M$; (7) $3.60 \times 10^{-4}M$; (8) $1.43 \times 10^{-3}M$; (9) 0.0. (See Table II.)
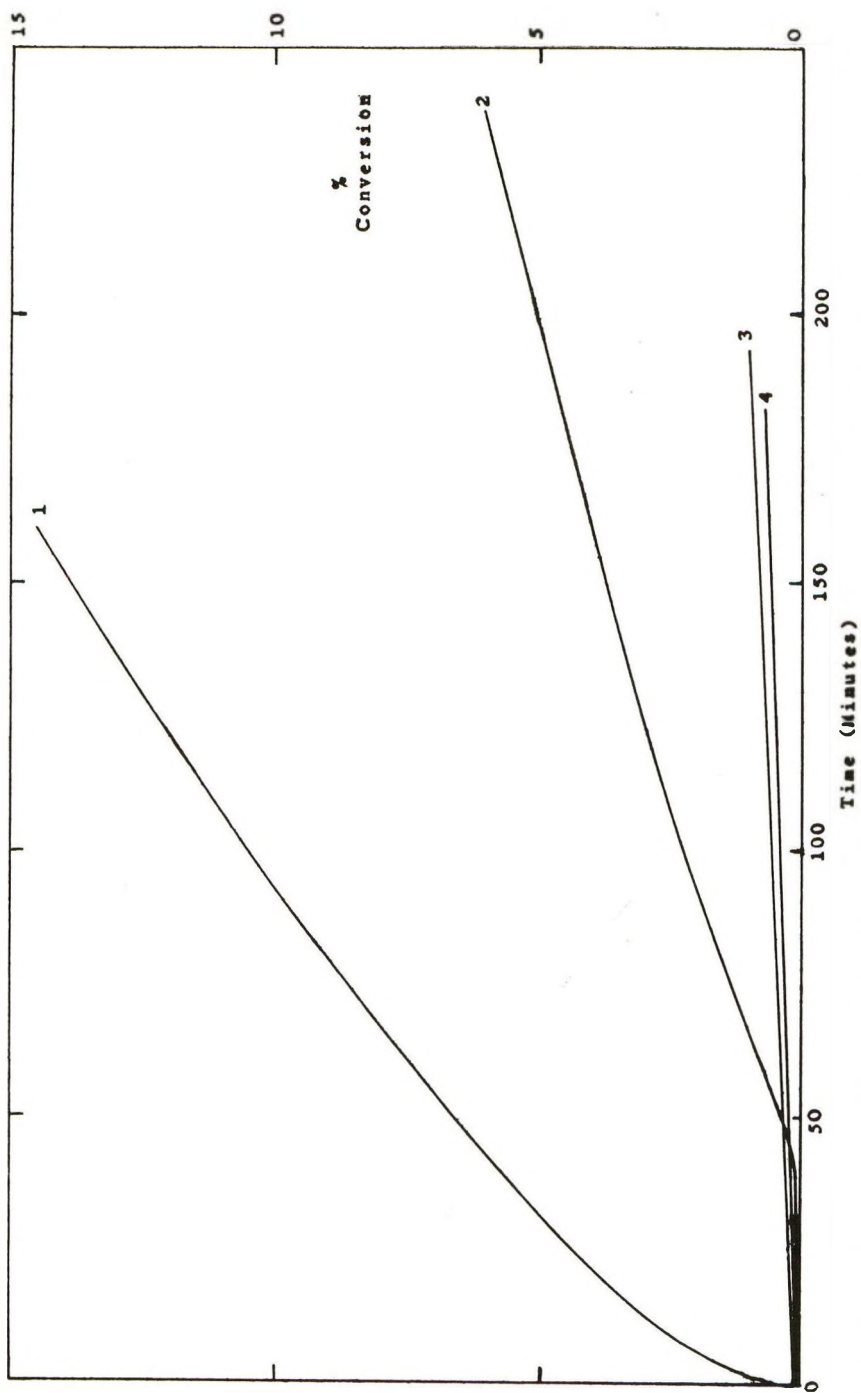
Fig. 4. Effect of hydroquinone (HQ) on the polymerization of methyl methacrylate at $[Et_3B]_0 = 7.18 \times 10^{-3}M$; $30.0°C.$: (1) $[O_2]_0 = 5.40 \times 10^{-3}M$; (2) $[O_2]_0 = 5.50 \times 10^{-3}M$; $[HQ] = 7 \times 10^{-3}M$; (3) $[O_2]_0 = 0.0$; $[HQ] = 7 \times 10^{-4}M$; (4) $[O_2]_0 = 0.0$.

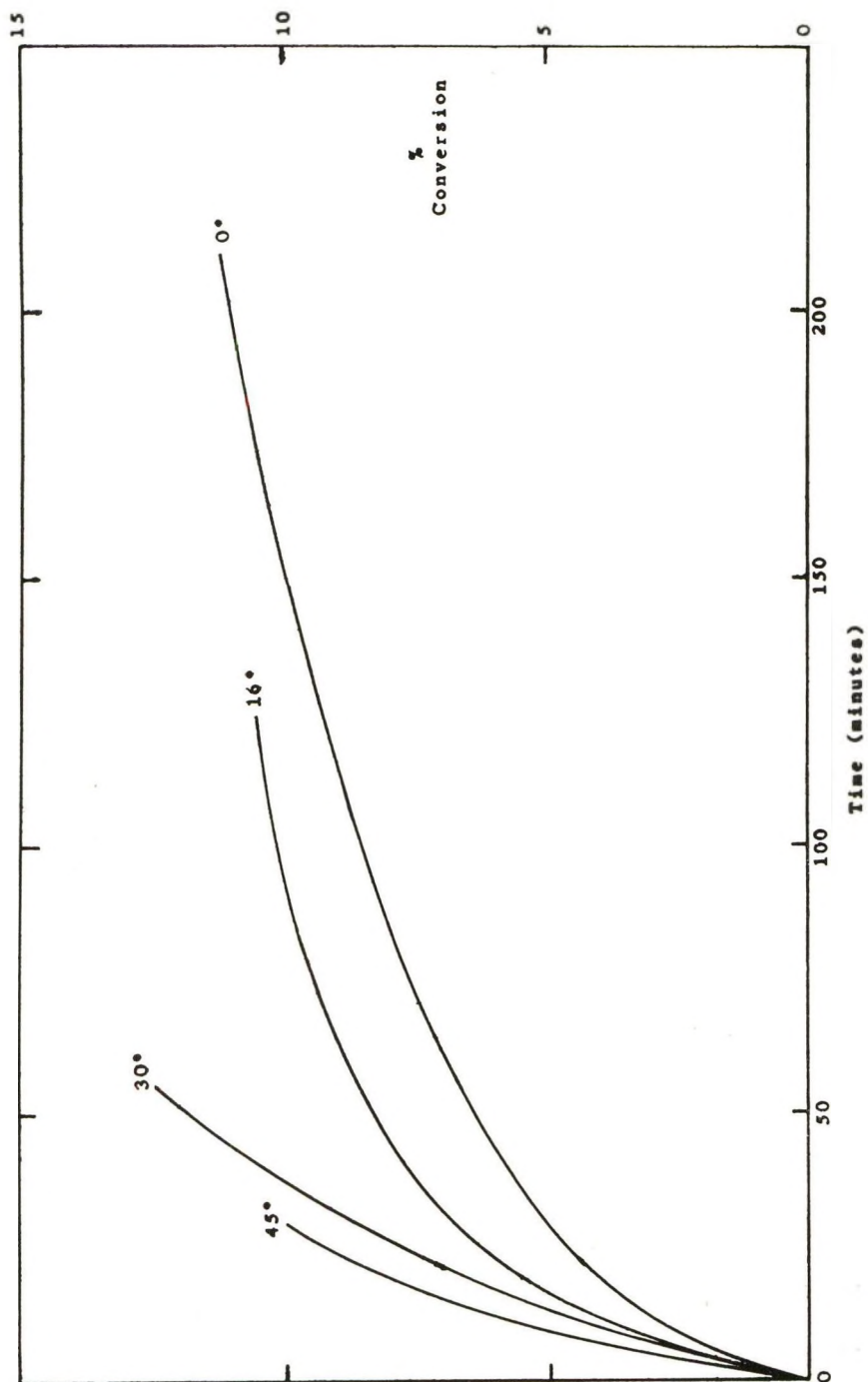Fig. 5. Effect of temperature on the polymerization of methyl methacrylate with $[Et_3B]_0 = 7.18 \times 10^{-3}M$, $[O_2]_0 = 2 \times 10^{-3}M$. (See Table III.)

A definite maximum in the initial rate was discovered as the oxygen concentration was increased. The polymerizations exhibited at least one of the characteristics reported by Welch.[1] In those cases in which the triethylboron concentration exceeded that of oxygen a sharp decrease in polymerization rate occurred at fairly low conversions. In the case that oxygen was in excess, however, a short induction period was observed.

The polymerization rate was also obtained under conditions in which the triethylboron concentration was varied at a constant oxygen level. The results are shown in Figure 3. The characteristics described above were again apparent in this series of experiments. In addition, it was found that when very high borane concentrations relative to oxygen were used, the initial rate was insensitive to the amount of borane. The conversion at which the rate sharply decreased was dependent upon the amount of triethylboron, however.

The results of a brief investigation of the effect of hydroquinone on the polymerization rate are given in Figure 4. A typical induction period was observed for the aerobic polymerization. The polymerization in the absence of added oxygen, on the other hand, was neither inhibited nor markedly accelerated by hydroquinone. A spectroscopic study of triethylboron—hydroquinone mixtures in degassed hexane/dioxane gave no indication of reaction between them.

The effect of temperature on the polymerization rate was determined between 0 and 45°C. The results constitute Figure 5. The initial rate of polymerization was found to be remarkably insensitive to temperature, in substantial agreement with Welch.[1]

The polymerization rate was found to be almost the same when several other trialkylboranes were used in place of triethylboron. Tri-n-butyl-boron produced a slightly larger initial rate than triethylboron, while tri-dodecylboron gave the lowest rate of the compounds studied (See Table IV and the discussion for an explanation of the table).

DISCUSSION

The results obtained in this work, coupled with those reported by Welch[1] and by Bawn and co-workers,[9] indicate that, although the borane/oxygen-catalyzed polymerizations are free radical processes, the reactions are considerably more complex than typical vinyl polymerizations. The quantitative interpretation of the polymerization rates seems to require a more detailed understanding of the reaction steps leading to the formation of initiating primary radicals than has been obtained by studying gross polymerization kinetics. The oxidation of trialkylboranes to form peroxides has been studied.[19-21] Kinetic studies, however, have not been reported for the oxidation itself. The manner in which the intermediate peroxide is decomposed is even more vague. A kinetic study has been undertaken to obtain data on these reactions separately.[22] Some of the results form a basis upon which the polymerization kinetics may be judged.

At the concentration ranges employed in the polymerizations described here, the half-life for the second-order reaction between triethylboron and oxygen to form monoperoxide was less than 15 sec. at 30°C. Subsequent oxidations at the second and third boron–carbon bonds were much slower than this. The reaction between triethylboron and ethylperoxydiethylboron was a 1:1 reaction with a half-life of about 3–10 min. at 30°C. at concentrations in the range expected in the polymerizations. The triethylboron was consumed in this reaction and behaved as a reducing agent for the peroxide. There was evidence that at least two different reduction mechanisms were operative. One of these processes produced ethyl radicals. Approximately one ethyl radical was formed for every two peroxide units reduced. Peroxide reductions brought about by boron–carbon bonds in partially oxidized triethylboron were slower.

It is likely that ethyl, produced by the peroxide reduction, was the initiating primary radical species in the polymerizations. Quantitative emission spectra on ashed polymethyl methacrylate obtained in the present work and twice recrystallized from 2-butanone/methanol showed approximately one boron atom per five polymer chains of known molecular weight. This suggests that very few chains were initiated by radicals containing a boron atom. The reaction,

$$R_3B + R_2BOOR \rightarrow R_3B + R_2BO\cdot + RO\cdot$$

suggested by Welch[1] as the source of primary radicals in probably incorrect.[22]

Since the oxidation of the first boron–carbon bond is so rapid as to be nearly instantaneous, the absence of a gradual increase in the polymerization rate as peroxide is formed can be accounted for. For polymerization with $[Et_3B]_0 > [O_2]_0$, monoperoxide equivalent to the oxygen concentration was present at the start of all practical purposes. Further, since reduction of monoperoxide by triethylboron is also quite rapid, this reaction should be substantially complete in 10–30 min. Polymer which was formed after this period must be due to secondary oxidations and reductions by partially oxidized triethylboron.

These preliminary considerations lead to the conclusion that, in the general case, the rate at which primary radicals are produced is very complicated mathematically. The system of differential equations describing the various oxidations and reductions at all three boron–carbon bonds could not be solved and even an approximate analysis became very difficult. A single equation describing the rate of polymerization over the entire course of the reaction could not be obtained. If one is willing to consider only the initial polymerization rates for those cases where $[Et_3B]_0 > [O_2]_0$, a very simple rate law results. Only first boron–carbon bond oxidation and reduction is important initially and the usual steady-state treatment leads to

$$(\ln [M]_0/[M])_{\text{initial}} = K[O_2]_0^{1/2} ([R_3B]_0 - [O_2]_0)^{1/2}t$$

where the oxidation has been assumed to be instantaneous. This equation is formally analogous to that used by Bawn, Margerison, and Richardson.[9]

TABLE I

Effect of Oxygen Concentration on the Rate of Polymerization of Methyl Methacrylate at $[Et_3B]_0 = 7.18 \times 10^{-3}M$, Temperature 30.0°C.[a]

$[O_2]_0$, mole/l. $\times 10^3$	Initial slope, min.$^{-1} \times 10^3$	K, l./mole-min.	$\bar{M}_v$ $\times 10^{-5}$	$\bar{M}_n$ $\times 10^{-5}$
0	0.04	---	7.60	2.90
0.51	2.82	1.52	4.83	1.35
1.14	5.00	1.90	3.99	---
1.97	4.72	1.47	3.62	3.17
3.63	6.00	1.67	2.04	1.47
4.47	6.35	1.82	3.11	---
5.40	4.55	1.47	4.93	1.85
6.65	1.84	0.99	4.05	---
7.89	0	---	---	---

[a] See Fig. 2.

TABLE II

Effect of Triethylboron Concentration on the Rate of Polymerization of Methyl Methacrylate at $[O_2]_0 \cong 5.4 \times 10^{-3}M$, Temperature 30.0°C.[a]

$[Et_3B]_0$, mole/l. $\times 10^3$	$[O_2]_0$, mole/l. $\times 10^3$	Initial slope, min.$^{-1} \times 10^3$	K, l./mole-min.	$\bar{M}_v$ $\times 10^{-5}$	$\bar{M}_n$ $\times 10^{-5}$
0	5.30	0			
1.43	5.19	0			
3.60	5.20	0		10.1	7.85
5.38	5.50	0		6.21	5.06
7.18	5.40	4.55	1.47	3.62	3.17
14.3	5.50	10.7	1.54	3.15	
21.5	5.40	11.7	1.25	1.07	0.59
35.6	5.40	12.0	0.94	2.85	
71.8	5.50	13.0	0.68	1.20	0.59

[a] See Fig. 3.

The usual first-order plots were made for those polymerizations wherein $[Et_3B]_0 > [O_2]_0$. The initial slopes were linear in each case. These slopes are recorded in Tables I–IV for the applicable experiments. Values of K, the composite rate constant, are also shown where these could be computed.

The values of K given in Table I are practically constant at 1.64 ± 0.16 l./mole-min. A somewhat smaller K of 0.99 was obtained for the experiment in which the initial triethylboron and oxygen concentrations were nearly equal. This is consistent with a slower production of primary radicals in this case due to monoperoxide reduction by partially oxidized triethylboron. The rate law predicts a maximum initial rate for the case that $[Et_3B]_0 = 2[O_2]_0$. This was observed within the listed uncertainty as indicated by the initial slopes in Table I. The dependence of the initial rate on the square root of the oxygen concentration is consistent with the work of others.[1,9,10] A kinetic dependence on the square root of the excess

borane concentration was also implied in the results of Bawn and co-workers.[9]

Table II, which is companion to Figure 3, shows initial slopes and rate constants calculated for several experiments in which a vast excess of triethylboron was used. At $[Et_3B]_0/[O_2]_0 > 3$ a further increase in the triethylboron concentration caused only a slight increase in the initial rate and a corresponding progressive decrease in the computed rate constant. The reasons for this are not certain, but it is probably due to increasing amounts of primary radical coupling and termination in these experiments. The instantaneous primary radical concentration should be larger at higher peroxide reduction rates.

Although it was not possible to interpret rigorously the polymerization kinetics beyond the initial rates, the following semiquantitative explanations are offered for the shapes of the conversion vs. time curves at higher extents of reaction. In the cases where $[Et_3B]_0 > [O_2]_0$ only monoperoxide was formed. Where $[Et_3B]_0 > 2[O_2]_0$, enough triethylboron was present to rapidly reduce the peroxide. This led to a rapid initial polymerization followed by a sharp reduction in rate and cessation of polymerization due to complete peroxide reduction. In those cases where $[O_2]_0 < [Et_3B]_0 < 2[O_2]_0$, a rapid initial rate due to reduction by triethylboron was followed by a slower though sustained rate. This was due to monoperoxide reduction by partially oxidized triethylboron.

In the case where nearly equal concentrations of triethylboron and oxygen were used a rapid initial rate was not observed but a slower and more sustained reaction resulted from monoperoxide reduction by partially oxidized borane.

Finally, where excess oxygen was employed, the rapid formation of the monoperoxide left residual oxygen which inhibited polymerization until it was consumed in formation of ethyldiethylperoxyboron. Peroxide reduction by partially oxidized borane then led to a relatively slow polymerization.

Although Welch used oxygen concentrations in excess of the triethylboron in several experiments, he did not report evidence for an apparent induction period. This may have been due to experimental difficulties in obtaining initial rates since his reaction mixtures were apparently brought to temperature after mixing. Also, actual oxygen concentrations in solution were not accurately known.

Welch found that an inverse linear relation existed between the initial rate and the number average degree of polymerization as calculated from intrinsic viscosities.[1] The data used for this correlation were all obtained with $[Et_3B]_0 > 2[O_2]_0$. Under these conditions the entire polymerization was probably due to monoperoxide reduction by unoxidized triethylboron and the reaction was relatively uncomplicated. The correlation seems valid even though the rates were taken from initial slopes and the polymer was not isolated until conversions up to 15% were attained. A similar, though less perfectly linear, correlation was obtained from the present data.

By using number-average molecular weights no assumptions about the molecular weight distribution were required. The correlation was, however, obtained only when experiments with $[Et_3B]_0 > 2[O_2]_0$ were considered. When other data were included, only a cluster of scattered points resulted. This might have been expected in trying to correlate initial rate of formation with a final polymer property when the polymer was produced by several, essentially different, modes of initiation. Because of this, the molecular weight data in the tables is not very satisfying. Generally speaking, the lowest molecular weights resulted when $[Et_3B]_0 \cong 2[O_2]_0$, as expected from the initial rate alone. At very high $[Et_3B]_0/[O_2]_0$ the molecular weights were significantly lower. Since the initial rates were not exceptionally high, the view that primary radical coupling and termination were important finds support. The runs which exhibited an induction period, those with an oxygen excess, consistently gave higher molecular weight polymer. This probably reflects the slow rate of primary radical production in those instances.

No evidence was found that hydroquinone can accelerate polymerizations with triethylboron, either in the presence or in the absence of added oxygen. The early report by Furukawa et al. was not substantiated.[11] Perhaps oxygen occluded in the solid hydroquinone caused the apparent acceleration. The present inhibition studies suggest that triethylboron in the

TABLE III

Effect of Temperature on the Rate of Polymerization of Methyl Methacrylate at $[Et_3B]_0 = 7.18 \times 10^{-3}M$

Temp., °C.	$[O_2]_0$, mole/l. $\times 10^3$	Initial slope, min.$^{-1} \times 10^3$	K, l./mole-min.	$\bar{M}_v$ $\times 10^{-5}$
0.3 ± 0.1	2.07	3.50	1.08	
15.9 ± 0.1	1.97	4.29	1.34	3.40
30.0 ± 0.1	1.97	4.72	1.64[a]	3.17
45.0 ± 0.1	2.18	6.73	2.04	2.58

[a] Average taken from Table I.

TABLE IV

Effect of Trialkylboron Structure on the Rate of Polymerization of Methyl Methacrylate at $[R_3B]_0 = 7.18 \times 10^{-3}M$, Temperature $= 30.0°C$.

Borane	$[O_2]_0$, mole/l. $\times 10^3$	Initial slope, min.$^{-1} \times 10^3$	K, l./mole-min.	$\bar{M}_v$ $\times 10^{-5}$
$(C_2H_5)_3B$	1.97	4.72	1.47	2.04
$(n\text{-}C_4H_9)_3B$	2.07	5.87	1.80	2.13
$(n\text{-}C_6H_{13})_3B$	2.07	4.12	1.27	2.02
$(Cyclo\text{-}C_6H_{11})_3B$[a]	2.18	4.95	1.59	2.75
$(n\text{-}C_{12}H_{25})_3B$	1.97	2.84	0.89	2.62

[a] $[R_3B]_0 = 6.62 \times 10^{-3}M$ in this experiment.

absence of oxygen may induce a slow, perhaps ionic, polymerization of methyl methacrylate. This reaction is not fully understood.

When the initial rate constants of Table III were treated in the usual way and a plot of ln K versus $1/T$ was constructed, the expected straight line was obtained. The least squares slope was calculated and an Arrhenius activation energy, $E_a = 2.4 \pm 0.3$ kcal./mole was obtained (50% confidence limits).[23] This is only slightly smaller than the value of 4 ± 1 kcal./mole reported by Welch[1] but significantly lower than the value obtained by Bawn et al. for tributylboron.[9] Since the propagation for methyl methacrylate has an activation energy of 6.3 kcal./mole,[24] the activation energy for the initiation process must be extremely small or even negative. The implications of this as regards the mechanism of initiation are described elsewhere.[22]

References

1. Welch, F. J., *J. Polymer Sci.*, **61,** 243 (1962).

2. Kolesnikov, G. S., and N. V. Klimentova, *Vysokomol. Soedin.*, **1,** 362 (1959). See also references to previous Russian work cited therein.

3. Furukawa, J., T. Tsuruta, and S. Inone, *J. Polymer Sci.*, **26,** 234 (1957).

4. Ashikari, N., *J. Polymer Sci.*, **28,** 641 (1958).

5. Furukawa, J., and T. Tsuruta, *J. Polymer Sci.*, **28,** 227 (1958).

6. Fordham, J. W., and C. L. Sturm, *J. Polymer Sci.*, **33,** 504 (1958).

7. Zutty, N. L., and F. J. Welch, *J. Polymer Sci.*, **43,** 445 (1960).

8. Inone, S., T. Tsuruta, and J. Furukawa, *Makromol. Chem.*, **40,** 13 (1961).

9. Bawn, C. E., H. D. Margerison, and H. M. Richardson, *Proc. Chem. Soc.*, **1959,** 397.

10. Talamini, G., and G. Vidotto, *Makromol. Chem.*, **50,** 129 (1961); *ibid.*, **53,** 21 (1962).

11. Furukawa, J., T. Tsuruta, T. Imada, and H. Fukutani, *Makromol. Chem.*, **31,** 122 (1959).

12. Brown, H. C., and B. C. Subba Rao, *J. Am. Chem. Soc.*, **81,** 6428 (1959).

13. Brown, H. C., and B. C. Subba Rao, *J. Am. Chem. Soc.*, **81,** 6423 (1959).

14. Köster, R., *Ann.*, **618,** 31 (1958).

15. Schulz, G. V., and G. Harborth, *Angew. Chem.*, **A59,** 90 (1947).

16. Shultz, A. R., *J. Phys. Chem.*, **65,** 967 (1961).

17. Flory, P. J., *Principles of Polymer Chemistry*, Cornell Univ. Press, Ithaca, N. Y., 1953, p. 312.

18. Schultz, D. R., *J. Polymer Sci.*, **B1,** 613 (1963).

19. Davies, A. G., and D. G. Hare, *J. Chem. Soc.*, **1959,** 438.

20. Merviss, S. B., *J. Am. Chem. Soc.*, **83,** 3051 (1961).

21. Zutty, N. L., and F. J. Welch, *J. Org. Chem.*, **25,** 861 (1960).

22. Hansen, R. L., and R. R. Hamann, *J. Phys. Chem.*, **67,** 2868 (1963).

23. Bennett, C. A., and N. L. Franklin, *Statistical Analysis in Chemistry and the Chemical Industry*, Wiley, New York, 1954, p. 38.

24. Matheson, M. S., E. E. Auer, E. B. Bevilacqua, and E. J. Hart, *J. Am. Chem. Soc.*, **71,** 497 (1949).

Résumé

La vitesse de la polymérisation en masse du méthacrylate de méthyle, catalysée par le triéthylbore-oxygène, a été étudiée. La vitesse a été étudiée en fonction de la concentration initiale en triéthylbore et de l'oxygène ainsi qu'en fonction de la température. L'influence de l'hydroquinone a été déterminée. La vitesse de polymérisation a aussi été étudiée en employant plusieurs autres trialcoylboranes. On a trouvé que la vitesse initiale de la polymérisation, catalysée par le triéthylbore dépend de la racine carrée de la concentration en oxygène et de la racine carrée de la différence entre les concentrations en trialcoylbore et oxygène. Les vitesses à de taux de conversions plus élevés sont compatibles avec un mécanisme d'initiation exigeant l'examen de réactions aux trois liaisons bore-carbon. Un mécanisme d'initiation, impliquant l'oxydation en peroxyde suivi par une réduction par les liaisons bore-carbone non-oxydeés, est proposé. Le radical éthyle, formé dans cette réduction est le groupement initiateur. L'énergie d'activation totale, calculée à partir des vitesses initiales est de 2,4 ± 0.3 Kcal/mole dans un intervalle de 0° à 45°C. Une polymérisation très lente avec le triéthylbore a été observée, en absence d'oxygène ajouté. L'hydroquinone se comporte comme un inhibiteur typique pour les polymérisations à l'air mais n'a pas d'effet inhibiteur en absence d'oxygène.

Zusammenfassung

Die Geschwindigkeit der durch Triäthylborsauerstoff katalysierten Polymerisation in Substanz von Methylmethacrylat wurde untersucht. Die Geschwindigkeit wurde sowohl als Funktion der Triäthylbor- und Sauerstoffausgangskonzentration als auch der Temperatur untersucht. Der Einfluss von Hydrochinon wurde bestimmt. Die Polymerisationsgeschwindigkeit wurde auch unter Verwendung verschiedener anderer Trialkylborane untersucht. Die Anfangsgeschwindigkeit der Triäthylbor-katalysierten Polymerisation war von der Quadratwurzel der Sauerstoffkonzentration und von der Quadratwurzel der Differenz der Triäthylbor- und Sauerstoffkonzentration abhängig. Die Geschwindigkeit bei höherem Umsatz liess sich mit einem Startmechanismus unter Teilnahme von Reaktionen an allen drei Bor–Kohlenstoffbindungen darstellen. Ein Startmechanismus unter Oxydation zu Peroxyd gefolgt von einer Reduktion mit nicht oxydierten Bor–Kohlenstoffbindungen wird vorgeschlagen. Der Starter ist ein bei dieser Reaktion entstandenes Äthylradikal. Die Bruttoaktivierungsenergie aus den Anfangsgeschwindigkeiten beträgt 2,4 ± 0,3 kcal/Mol im Bereich von 0° bis 45°C. Ohne Zusatz von Sauerstoff wurde mit Triäthylbor eine sehr langsame Polymerisation beobachtet. Hydrochinon verhielt sich als typischer Inhibitor der aerobischen Polymerisation, inhibierte die Polymerisation bei Abwesenheit von Sauerstoff jedoch nicht.

Ionic Copolymerization of Styrene and
p-Methylstyrene

B. D. PHILLIPS, T. L. HANLON, and A. V. TOBOLSKY, *Frick Chemical Laboratory, Princeton University, Princeton, New Jersey*

Synopsis

The copolymerization of styrene and *p*-methylstyrene has been initiated by Friedel-Crafts metal halides, benzoyl peroxide, a Ziegler catalyst from triethylaluminum and titanium tetrachloride, alkali metal dispersions, and alkali metal–naphthalene complexes in a variety of polar and nonpolar solvents. The composition of the initial copolymer from an equimolar monomer mixture was used as the basis for comparison of these systems. By a suitable choice of initiator and solvent, the copolymer composition was varied within the range 25–79 wt.-% styrene. Cationic catalysts yield copolymers with low styrene contents while anionic and electron transfer initiators produce copolymers with high styrene contents. The compositions of the initial copolymers are briefly discussed in relation to the ionic character of the growing polymer–gegenion ion pair and the polarity of the reaction medium.

INTRODUCTION

When ionic initiators are employed, the composition of the initial copolymer from a particular monomer pair is dependent on the ionic character of the initiator and on the nature of the solvent in which the reaction is performed. A strict correlation between copolymer composition and ionic character of the polymerization system has yet to be achieved in the case of cationic catalysts, but this has been possible to some extent for anionic initiators.[1] In assessing the effect of a solvent on its ability to ionize the growing polymer–gegenion ion pair, such factors as complexing ability dielectric constant, and acid or base strength are important.

The early literature on cationic copolymerization reveals that only small changes occur in the values of the monomer reactivity ratios when the dielectric of the medium or the initiator is varied. Thus Florin[2,3] reported only small variations in the values of r_1 and r_2 in the cationic copolymerization of styrene and 3,4-dichlorostyrene for different initiator–solvent systems. Overberger did not observe any major changes in the reactivity ratios for the monomer pair, styrene–*p*-chlorostyrene in mixtures of carbon tetrachloride and nitrobenzene, or in the pure solvents.[5] It was suggested that the lack of a solvent effect was due to the similarity in structure of the monomer pair.

The cationic copolymerization of α-methyl-styrenes with 2-chloroethyl vinyl ether in benzene and nitrobenzene has been reported by Marvel,[6] and, in spite of the variation in the structure of the monomers, only in the case of α-methylstyrene itself was a change observed in the monomer reactivity ratios.

Recently, Overberger and Kamath have reported wide fluctuations in the values of the reactivity ratios for the monomer pair isobutylene (M_1)–p-chlorostyrene (M_2),[7,8] and, to a lesser extent, for the styrene (M_1)–chloroprene (M_2) system[8] when both initiator and solvent are varied. In the main, an increase in the dielectric constant of the medium resulted in an increase in the value of r_1 and a decrease in r_2. This phenomenon was explained on the basis of preferential solvation of the growing ion pair by the more polar monomer (M_2) in nonpolar solvents.

This concept of preferential solvation successfully explains the observation of Marvel,[6] the solvent effects reported by Okamura,[9,10] and the results of copolymer studies on the monomer pairs, styrene–p-substituted styrenes, performed in these laboratories.[11]

In previous publications from this laboratory, it was reported that the composition of an isoprene–styrene copolymer from anionic initiation depended on the ionic character of the growing ion pair.[1,12–14] Using an equimolar monomer mixture, lithium in toluene gave a copolymer containing 16 wt.-% styrene while reaction in tetrahydrofuran resulted in 80 wt.-% styrene. A further increase in the ionic character of the growing ion pair, by use of cesium naphthalene in tetrahydrofuran, gave almost 100 wt.-% styrene.

Similar data were obtained for this same monomer pair initiated by ethyllithium[15] and an analogous situation was reported for styrene–butadiene.[15,16] Investigations of other monomer pairs[17,18] have also shown that an increase in the ionic character of the growing ion pair, by choice of initiator or solvent, results in the more reactive monomer being favored in the initial copolymer.

Homopolymerization studies of the monomers, styrene, isoprene, and butadiene, initiated by n-butyllithium in benzene, have shown the following decreasing order of reactivity: styrene > isoprene > butadiene.[19–21] Copolymerization of these monomers under identical conditions revealed that in each case butadiene is the favored monomer in the initial copolymer. This "inversion" of reactivities led to the idea that butadiene was preferentially solvating the growing ion pair. Recent work[22] has shown this anomalous behavior to be the direct consequence of a low absolute rate of cross propagation, and the concept of preferential solvation need not be envoked, as was pointed out theoretically by Kuntz and O'Driscoll.[23]

A preliminary study by Tobolsky and Boudreau[11] of the monomer pair styrene–p-methylstyrene revealed that the copolymer obtained from an equimolar monomer mixture, by cationic and anionic initiators, had a composition within the range 20–70 wt.-% styrene. This system is thus suitable for a study of a wide range of initiators in a variety of solvents.

In this present paper the composition of the initial copolymer from an equimolar monomer feed was chosen as the basis for comparison of various catalyst–solvent systems in order to avoid the errors which accompany determination of monomer reactivity ratios and the possible inapplicability of the copolymer composition equation in certain systems.[24,25]   A wider range of catalyst–solvent systems was studied than in the preliminary study.[11]   As far as possible an attempt was made to recheck all catalyst–solvent systems previously reported.

EXPERIMENTAL

Purification of Materials

Styrene and *p*-methylstyrene were washed with aqueous potassium hydroxide, repeatedly with water, and dried over anhydrous magnesium sulfate.   They were further refluxed over calcium hydride under an atmosphere of nitrogen and finally fractionated at 8–10 mm. Hg.   Both monomers were purged with dry nitrogen in a dry box and stored under nitrogen in capped bottles at $-20°$C.

n-Heptane and toluene were refluxed over sodium, fractionally distilled, and filtered in the dry box through a column packed with anhydrous silica gel.

Ethylene dichloride and nitrobenzene were refluxed and fractionated from calcium hydride.   In addition, the ethylene dichloride was filtered through a column of silica gel.

Tetrahydrofuran was refluxed over potassium hydroxide, distilled, and further refluxed over molten potassium.   A small amount of naphthalene, added during the final stages of refluxing, produced the green-black color of potassium naphthalene.   The ether was finally fractionally distilled.

All solvents were further purged with dry nitrogen in the dry box and stored in capped bottles.

Aluminum chloride, antimony trichloride, and trichloroacetic acid were sublimed and stored under vacuum in an all-glass apparatus.

Aluminum bromide, antimony pentachloride, boron trifluoride etherate, and stannic chloride were distilled and stored under vacuum in an all-glass apparatus.

Titanium tetrachloride was purified by the method of Evans and Owen.[26]

Triethylaluminum was distilled under vacuum and diluted with toluene previously dried over Na/K alloy.

Benzoyl peroxide was used as supplied without further purification.

A commercial sample of *n*-butyllithium in *n*-heptane was pressure-filtered under nitrogen and estimated by the double titration method of Gilman.[27]

The lithium dispersion contained 30% lithium by weight in heavy mineral oil, with a small amount of oleic acid as stabilizer.

The sodium dispersion contained 50% sodium by weight in mineral oil, with 2% aluminum stearate as stabilizer.

Potassium and cesium dispersions were prepared in the laboratory by adding a known weight of the metal to a known weight of mineral oil, previously dried by distillation from the metals at reduced pressure.

The dispersions were achieved by fast agitation of the metal–oil mixture at a temperature slightly above the melting point of the metals. A small amount of oleic acid was added as stabilizer.

The alkali metal–naphthalene complexes were prepared under argon from a known weight of resublimed naphthalene, tetrahydrofuran freshly distilled from potassium, and excess of the appropriate alkali metal. The mixtures were pressure-filtered under argon, stored in capped bottles, and estimated by acid titration.

Polymerization

Copolymerizations initiated by cationic, free radical, and Ziegler catalysts were performed in a dry box under an atmosphere of dry nitrogen. Reaction vessels consisted of 2–4 oz. bottles fitted with self-sealing rubber gaskets, polyethylene seals, and screw caps. Liquids were measured by means of hypodermic syringes and solids were weighed in capped bottles under nitrogen. Reaction solutions were comprised of 5 ml. of an equimolar comonomer mixture, sufficient initiator–solvent solution to ensure convenient reaction times, and sufficient solvent to give a total reaction solution of 15 ml. The initiator–solvent solution was added last, except when a Ziegler catalyst was used. In this latter case, the catalyst was prepared *in situ* and the comonomer aliquot was added last.

Two methods were used for copolymerization initiated by anionic type catalysts.

When reaction times were small, e.g., in tetrahydrofuran, copolymerizations were performed in capped bottles under argon. For soluble initiator solutions, reaction mixtures were prepared as described previously. In the case of the metal dispersions, known weights were added to 10 ml. of solvent, followed by addition of 5 ml. of comonomer mixture.

For reaction times of longer duration, e.g., lithium dispersion in toluene preliminary experiments were conducted under high vacuum. However, identical results were obtained using the method previously described, and therefore subsequent studies were performed using this more convenient technique.

All reactions were agitated by means of metal-in-glass or Teflon-covered magnetic stirrers, and reactions were terminated by the addition of methanol. The copolymers were precipitated in methanol containing a few drops of hydrochloric acid. After filtration they were dried in a vacuum oven at 45°C., weighed, reprecipitated from chloroform solution, and again dried prior to analysis for styrene content.

Analytical Methods

The composition of the styrene–p-methylstyrene copolymers was determined by ultraviolet spectrophotometry. A Beckman D. U. spectro-

photometer, operating at a slit width of 0.3 mm., was employed to measure the absorptivities at 275 mμ of chloroform solutions of the copolymers, contained in 1 cm. quartz cells. Table I lists the absorptivities of the homopolymers. Agreement is excellent between the present results and a previous more exact study.[28] In duplicate analyses performed on a series of copolymers with known compositions varying from 18 to 90 wt.-% styrene, a standard deviation of 0.52 wt.-% styrene was obtained.[28]

TABLE I

Polymer	Absorptivity at 275 mμ, a_{275}	
	Literature[a]	This work
Polystyrene	0.21 ± 0.02	0.20
Poly-*p*-methylstyrene	3.71 ± 0.04	3.67

[a] Data of Boudreau.[28]

The molecular weights of the copolymers obtained by cationic initiation were determined in chloroform solution by using a Mechrolab vapor pressure osmometer, model 301A. Precision is $\pm 5\%$ for molecular weights in the region of 10^4.

RESULTS AND DISCUSSION

The molecular weights of the copolymers listed in Table II show that, with the exception of the system trichloroacetic acid–ethylene dichloride, the average degree of polymerization of the copolymers lies within the range 40–120. These values, although low, show that the copolymer compositions can be regarded as a true reflection of the propagation reaction. The low value of the molecular weight of the copolymer from initiation by trichloroacetic acid in ethylene dichloride may contribute to the discrepancy observed in the composition trend. It is interesting to

TABLE II
Molecular Weights of Copolymers from Initiation by Cationic Catalysts in Various Solvents

Initiator	Molecular weights $\times 10^{-3}$		
	In $C_6H_5CH_3$	In $(CH_2Cl)_2$	In $C_6H_5NO_2$
$AlBr_3$	4.0	9.0	—
$AlCl_3$	5.2	6.5	11.7
$BF_3 \cdot Et_2O$	8.6	11.4	9.4
Cl_3CCO_2H	—	2.6	7.6
$SbCl_3$	—	—	7.6
$SbCl_5$	—	—	3.4
$SnCl_4$	4.1	11.3	8.9
$TiCl_4$	4.1	8.9	9.6

note that the molecular weights increase as the dielectric constant of the medium increases, as was observed by Pepper.[32] Variations can be explained by differences in initiator concentration, as in the case of boron trifluoride etherate.

TABLE III

Copolymerization Initiated by Cationic Catalysts at Room Temperature

Initiator	No. of runs	Initiator concn. mole/l.	Solvent	Conversion, %	Styrene, wt. -%[a]
AlBr$_3$	3	2.6×10^{-4}	n-Heptane	4.1–5.8	35.9 ± 0.7
	3	4.3×10^{-4}	C$_6$H$_5$CH$_3$	5.8–10.3	35.6 ± 0.2
	3	5.6×10^{-4}	(CH$_2$Cl)$_2$	7.8–10.2	35.0 ± 0.9
	3	1.6×10^{-3}	C$_6$H$_5$NO$_2$	5.4–5.8	28.3 ± 0.5
AlCl$_3$	3		C$_6$H$_5$CH$_3$	5.0–7.5	32.4 ± 0.2
	2	3.6×10^{-4}	(CH$_2$Cl)$_2$	6.5–6.9	32.8 ± 0.6
	2	1.6×10^{-3}	C$_6$H$_5$NO$_2$	10.7–11.3	28.6 ± 0.2
BF$_3$·Et$_2$O	3	5.3×10^{-3}	C$_6$H$_5$CH$_3$	6.8–12.5	29.1 ± 0.3
	2	1.3×10^{-3}	(CH$_2$Cl)$_2$	6.4–7.7	27.7 ± 0.1
	2	5.0×10^{-3}	C$_6$H$_5$NO$_2$	5.5–6.5	26.6 ± 0.3
Cl$_3$CCO$_2$H	2	6.4×10^{-1}	C$_6$H$_5$CH$_3$–(CH$_2$Cl)$_2$, 1:1	0.6–0.8	33.7 ± 0.4
	2	3.7×10^{-1}	(CH$_2$Cl)$_2$	3.3–4.0	26.8 ± 0.1
	3	5.0×10^{-1}	C$_6$H$_5$NO$_2$	8.0–9.9	29.9 ± 0.5
SbCl$_3$	2	2.9×10^{-1}	(CH$_2$Cl)$_2$	14.3–16.1	29.0 ± 0.1
	3	3.5×10^{-1}	C$_6$H$_5$NO$_2$	4.6–8.2	28.0 ± 0.7
SbCl$_5$	3	6.7×10^{-2}	C$_6$H$_5$CH$_3$	1.9–4.2	46.5 ± 0.5
	3	6.7×10^{-2}	(CH$_2$Cl)$_2$	1.2–2.8	25.4 ± 0.3
	3	1.3×10^{-2}	C$_6$H$_5$NO$_2$	14.0–14.4	27.9 ± 1.7
SnCl$_4$	2	6.7×10^{-3}	C$_6$H$_5$CH$_3$	10.4–11.3	26.6 ± 0.2
	3	6.7×10^{-3}	(CH$_2$Cl)$_2$	7.0–13.9	25.2 ± 0.6
		6.7×10^{-3}	C$_6$H$_5$NO$_2$	2.0–6.2	26.0 ± 1.4
			C$_6$H$_5$NO$_2$–CCl$_4$, 1:1		38.4[b]
TiCl$_4$		6.7×10^{-3}	n-Heptane	9.0	29.6
		6.7×10^{-3}	n-Heptane/C$_6$H$_5$CH$_3$	14.0	27.1
	2	6.7×10^{-3}	C$_6$H$_5$CH$_3$	7.0–24.0	27.4 ± 0.2
TiCl$_4$	2	6.7×10^{-3}	(CH$_2$Cl)$_2$	9.0–11.0	27.8 ± 0.2
	3	3.3×10^{-3}	C$_6$H$_5$NO$_2$	2.2–11.4	28.4 ± 0.7
			C$_6$H$_5$CH$_3$[c]		22.8[b]
			C$_6$H$_5$CH$_3$[d]		39.0[b]
			CCl$_4$		35.9[b]
			C$_6$H$_5$NO$_2$		41.8[b]

[a] The ± values indicate the maximum deviation from mean.

[b] Data of Tobolsky and Boudreau.[11]

[c] At 0°C.

[d] At −78°C.

Overberger has shown that, under conditions similar to those employed in the present investigation, the Lewis acids used as initiators do not yield any alkylation products.[8] True copolymers and not mixtures of homopolymers have been obtained from isobutylene–p-chlorostyrene,[8] and we

have assumed that this is also true for the monomer pair under investigation.

It has previously been reported for the polymerization of styrene initiated by Friedel-Crafts metal halides in these solvents, that, with the exception of antimony pentachloride, no solvent or catalyst fragments are introduced into the polymer.[5]

Antimony pentachloride can function as a chlorinating agent under these conditions, and errors introduced as a result of this side reaction can be important when copolymer compositions are estimated by elemental analysis.[5] The influence of this chlorination reaction on copolymer compositions determined spectrophotometrically has not been investigated and it is possible that this side reaction might affect the composition of the copolymer obtained from antimony pentachloride reported in Table III.

The copolymer obtained from initiation by trichloroacetic acid will contain trichloroacetate terminal groups.[33] The presence of such groups might introduce small errors in the analysis of the copolymer composition, especially if the copolymers are of low molecular weight.

The composition of the initial copolymers cited in Table III shows only small variations as the initiator/solvent system changes, but we feel that these variations are real for the initiator systems, $AlBr_3$, $AlCl_3$, BF_3Et_2O and $SbCl_5$. The data for each initiator system show that as the dielectric of the medium increases, the initial copolymer contains an increased percentage of the monomer more susceptible to cationic catalysis, i.e., p-methylstyrene. The results of Overberger,[3] Marvel,[6] and Okamura[10] show a similar trend.

In the case of isobutylene–p-chlorostyrene in a hydrocarbon solvent,[8] the p-chlorostyrene, being the more polar monomer, is thought to solvate preferentially the growing ion pair. This would result in an envelope of p-chlorostyrene around the active center which would hinder attack by the isobutylene monomer. The percentage of p-chlorostyrene in the copolymer would thus be greater in a hydrocarbon solvent than in a polar solvent such as nitrobenzene where the solvation contribution of this monomer would be negligible.

The present results are inconsistent with this concept of preferential solvation unless styrene would solvate the growing ion pair more easily than would p-methylstyrene, whereas the reverse is probably true.

The results for the system styrene–p-methylstyrene initiated by titanium tetrachloride previously published from this laboratory,[11] are at variance with the present data. Previous values for the styrene content of the copolymer were 22.8 wt.-% in toluene, 35.8 wt.-% in carbon tetrachloride and 41.8 wt.-% in nitrobenzene, while the present values are 28 ± 11 wt.-% styrene in n-heptane, toluene, ethylene dichloride, and nitrobenzene. A similar discrepancy occurs for initiation by stannic chloride in nitrobenzene and in a carbon tetrachloride–nitrobenzene mixture, where the

styrene content of the copolymer would be expected to approximate that in pure nitrobenzene.[8]

In the earlier study[11] monomer reactivity ratios were determined and it is possible that the composition of the initial copolymers cited in Table III, calculated from the values given by Tobolsky and Boudreau,[11] reflect the errors which accompany such determinations. However, the differences cited in the previous paragraph are probably too large to be accounted for on this basis. We have no explanation at the present time for the discrepancies found with some cationic systems. By contrast, few discrepancies were found for anionic systems.

Monomer reactivity ratios for styrene (M_1)–p-methylstyrene (M_2) initiated by the weak cationic initiator, iodine,* in ethylene dichloride have recently been reported.[36] The values show that an equimolar monomer charge would yield an initial copolymer containing 16.8 wt.-% styrene. This value is considerably lower than that observed with the use of stronger cationic initiators.

Values for the absolute rate constants of homopolymerization were also reported and, with the reactivity ratios, allowed the rate constants of cross propagation to be calculated (Table IV).

TABLE IV

		k_{ij}, l./mole min.
$r_1 = k_{11}/k_{12} = 0.2$		$k_{11} = 0.22, k_{12} = 1.1$
$r_2 = k_{22}/k_{21} = 4.2$		$k_{22} = 5.7, k_{21} = 1.4$

If p-methylstyrene does in fact preferentially solvate the growing ion pair, a change in polarity of the reaction medium would be expected to affect the ratio k_{22}/k_{12} only slightly, but markedly change the ratio k_{21}/k_{11}. This could be used as a criterion for a solvent effect. Before any conclusions can be made however, values for the rate constants in solvents such as carbon tetrachloride and nitrobenzene are needed, together with the monomer reactivity ratios for these systems.

The use of copolymer compositions as a basis of comparison between polymerization systems is limited, in that it is the overall effect from changes in four variables, namely the rate constants of propagation. As more data on rate constants of cationic copolymerization become available, it is possible that variations in copolymer compositions for each initiator–solvent system will be explicable in terms of the absolute rates of propagation, particularly cross propagation, without recourse to special solvation effects.

It was thought worthwhile to conduct the free radical-initiated copolymerization of styrene and p-methylstyrene in order to compare the com-

* Tentative experiments with iodine were irreproducible because of an apparently random incorporation of iodine in the copolymer. The irreproducibility did not warrant inclusion of the results in Table III.[34,35]

position of the initial copolymer obtained and estimated by the present techniques with that calculated from the monomer reactivity ratios reported recently.[29] Using labeled styrene and benzoyl peroxide as initiator, Wiley and Davis obtained values of $r_1 = 0.83$ and $r_2 = 0.96$ by means of an ionization chamber assay technique, while a direct counting method gave $r_1 = 0.99$ and $r_2 = 0.94$. The former values were considered to be the more reliable, but the results from this investigation, presented in Table V, are in closer agreement with the latter values.

TABLE V
Copolymerization Initiated by Free Radical Catalysts at 60°C.

Initiator	Initiator concn., wt.-%	Solvent	Conversion, %	Styrene, wt.-%
$(C_6H_5CO)_2O_2$	0.2	Toluene	3.9	50.0
			7.2	49.8
		Bulk	~7	45.2[a]
				47.4[a]

[a] Data of Wiley and Davis.[29]

As can be seen from Table VI, the composition of the copolymer obtained by a Ziegler catalyst at a low Al/Ti ratio, where a cationic mechanism is considered to operate, approximates closely to the values in Table III, where conventional cationic initiators are employed. At higher Al/Ti ratios, there is good agreement between the results from this study and those of Natta[30] and Overberger.[31] The copolymer from initiation by a catalyst with a 3:1 ratio of Al/Ti is not homogeneous, as judged by solvent extraction.

TABLE VI
Copolymerization Initiated by Ziegler-Type Catalysts

Al/Ti (molar ratio)	Solvent	Conversion, %	Styrene, wt.-%
1.2:1[a]	Toluene	6	31.9
		10	28.8
2:1[a]	Toluene	1	32.8
3:1[a]	Toluene	5	43.8 (MEK-soluble)
			50.0 (MEK-insoluble)
3:1[b]	Hydrocarbon		41.3[d]
3:1[c]	Heptane		46.8[e]

[a] $Al(C_2H_5)_2$–$TiCl_4$ catalyst at 50°C.
[b] $Al(C_2H_5)_2$–$TiCl_4$ catalyst at 40°C.
[c] $Al(i-C_4H_9)_3$–$TiCl_3$ catalyst at 70°C.
[d] Data of Natta et al.[30]
[e] Data of Overberger and Ang.[31]

The work of Overberger and Ang[31] showed that styrene–p-methyl-styrene gave true copolymers which were amorphous. On fractionation, the copolymers revealed an intrinsic viscosity and composition distribution which suggested the presence of more than one type of copolymer and a polyactivity of the catalyst. It is probable that a similar situation exists in the case of the present initiator system, and this accounts for the difference in styrene content and solution properties of the two fractions listed in Table VI.

Table VII shows that isotactic polystyrene is obtained under conditions identical to those used for the copolymerization. This infers that the copolymer fraction, insoluble in methyl ethyl ketone, might possibly possess some degree of stereoregularity.

TABLE VII

Homopolymerization of Styrene at 50°C. with $Al(C_2H_5)_3$–$TiCl_4$
Catalyst Prepared *in situ*

Al/Ti Ratio	Solvent	Conversion, %	Polymer solubility
1:1	Toluene	9–14	>90% MEK-soluble
2:1	Toluene	Low	Mostly MEK-soluble
3:1	Toluene	~10	Completely MEK-insoluble

It is interesting to note that the antimony pentachloride–toluene system (Table III) gave a copolymer whose composition approximated that obtained from free radical initiation, and from a Ziegler catalyst at an Al/Ti ratio of 3:1. The possibility of the copolymer from the antimony pentachloride system having resulted from free radical initiation, either thermally or by light, was excluded by control blank experiments. Because of the similarity between the copolymer compositions from this cationic initiator system and the Ziegler system, it was thought worthwhile to determine if the former system possessed any stereoregulating ability. However, attempts to obtain stereoregular polystyrene were unsuccessful.

Table VIII shows that, for copolymerization initiated by n-butyl-lithium, as the basicity of the reaction medium is increased, the initial copolymer contains an increased amount of the monomer more susceptible to anionic propagation, i.e., styrene. The styrene content of the copolymer from reaction in toluene is identical with that calculated from the monomer reactivity ratios published previously.[11] This observed solvent effect is analogous to that reported for other monomer pairs copolymerized by this same initiator.[1]

A study of the initiating ability of the alkali metals reveals that lithium behaves anomalously. Sodium, potassium, and cesium dispersions in toluene yield copolymers with a styrene content of 73 ± 2 wt.-%. Although variation is small, the highest styrene content is obtained from

TABLE VIII
Copolymerization Initiated by Anionic and Electron Transfer
Initiators at Room Temperature

Initiator	No. of runs	Solvent	Conversion, %	Styrene, wt.-%[a]
n-BuLi		Toluene	6.9	70.3
			9.2	68.9
			25.7	67.3
				70.9[b]
		THF	1.9	74.5
			2.1	75.6
			6.5	78.3
Li		Bulk	0.7	55.7
			1.0	62.6
			2.8–13.6	71.1 ± 0.4
		Toluene	1.4	56.3
			2.2	70.0
	4		3.0–32.2	70.4 ± 1.6
		THF	1.0	64.3
			2.9	64.4
			6.6	63.8
			11.0	62.9
			31.0	61.9
				51.5[b]
Na		Toluene	1.8	73.1
			2.8	71.7
			6.2	71.2
			25.3	69.2
		THF	3.0	67.9
			4.5	69.6
			5.5	70.1
				65.5[b]
K	4	Toluene	1.9–7.0	70.9 ± 1.1
		THF	2.7	62.3
			5.3	62.2
			13.1	61.5
			22.1	60.0
Cs		Toluene	3.1	74.9
			6.1	74.3
			9.7	73.9
			20.3	71.8
		THF	3.5	68.2
			4.4	66.5
			6.9	66.0
			20.3	63.8
LiC$_{10}$H$_{10}$	5	THF	0.9–16.4	77.2 ± 1.8
NaC$_{10}$H$_{10}$	4	THF	1.2–14.8	77.5 ± 1.8
KC$_{10}$H$_{10}$	5	THF	3.3–26.4	76.5 ± 1.6

[a] The ± indicates the maximum deviation from mean.
[b] Data of Tobolsky and Boudreau.[11]

initiation by cesium, where the ionic character of the growing ion pair is greatest. However, lithium, in bulk or toluene, produces a copolymer which contains 56 wt.-% styrene at very low conversions. This can be explained by the radical-anion concept of Tobolsky and O'Driscoll.[37] Radical-anion propagation has been discussed by Tobolsky and Hartley,[38] and a rapid decrease in the radical growth was predicted as conversion increased. The styrene content of the copolymer, listed in Table VIII, quickly approaches that for anionic propagation alone and this is in good agreement with the earlier predictions.

A change from the nonpolar solvent toluene to the more basic solvent tetrahydrofuran produces a decrease in the styrene content of the initial copolymer varying from 5 to 9 wt.-% in the case of Na, K, and Cs. The reason for this unexpected result is not apparent. A similar unexpected result was observed for the monomer pair styrene–butadiene initiated by lithium naphthalene and cesium naphthalene in tetrahydrofuran,[14] and again the reason was not apparent.

Although the variation in the copolymer compositions from initiation by the alkali metals in tetrahydrofuran is small, the styrene content is higher in the case of cesium, where the ionic character of the metal–carbon bond is high, than for lithium, where the bond is probably of lower ionicity. There is fair agreement between the result in Table VIII for sodium in tetrahydrofuran and that calculated from monomer reactivity ratios for the same system.[11] There is no evidence for any radical-anion growth from initiation by lithium in tetrahydrofuran.

The compositions of the copolymers from initiation by the alkali metal-naphthalene complexes approximate to the same value of 77 ± 1 wt.-% styrene. This suggests that the ionic character of the growing ion pair is virtually the same for the alkali metals in tetrahydrofuran, when a soluble initiator is used. The copolymer compositions are almost identical with that obtained from initiation by n-butyllithium in tetrahydrofuran, and the values might approximate to a limiting anionic composition for this monomer pair at room temperature.

The composition of the copolymers obtained by the alkali metals in tetrahydrofuran, and the alkali metal–naphthalene complexes in tetrahydrofuran, might be expected to be identical because the ionic character of the growing ion pair should be approximately equal for both these systems. However, in the case of the metal dispersions, the reaction medium is heterogeneous, and propagation of the growing polymer is probably associated with the surface of the metal.

There again, initiation is instantaneous for the alkali metal–naphthalene complexes in tetrahydrofuran, whereas excess alkali metal is always present and results in continuous initiation. These two differences probably account for the discrepancy between the systems.

Values for the absolute rates of propagation and monomer reactivity ratios for styrene–p-methylstyrene in tetrahydrofuran, with a Na^+ counterion have recently been reported[39,40] and are recorded in Table IX.

An equimolar monomer mixture would yield an initial copolymer containing (1) 73.2 wt.-% styrene and (2) 82.2 wt.-% styrene. The latter value is likely to be more correct as it is the most recently determined result.

TABLE IX

Absolute Rate Constants of Propagation for Styrene–p-Methylstyrene[a]

r_1[b]	r_2[c]	k_{11}	k_{12}	k_{22}	k_{21}	Reference
			k_{ij}l./mole sec.			
3.1	0.22	550	180	220	1000	39
5.3	0.18	950	180	210	1150	40

[a] Solvent: THF; Na$^+$ counterion; Temperature: 25°C.; [living ends] = 3 × 10^{-3} mole./l.; [M] < [living ends].

[b] $r_1 = k_{11}/k_{12}$.

[c] $r_2 = k_{22}/k_{21}$.

The agreement between this value and that cited in Table VIII for the sodium naphthalene–tetrahydrofuran system is excellent, considering the differences in reaction conditions.

CONCLUSIONS

By a judicious choice of initiator and solvent, the composition of the initial copolymer from an equimolar mixture of styrene and p-methylstyrene can be varied within the range 25–79 wt.-% styrene. The low styrene contents are obtained by cationic catalysts, while anionic initiators yield the higher values. The approximate coincidence of the copolymer compositions obtained from free radical initiation and from a Ziegler catalyst is probably fortuitous and a similarity of reaction mechanism is not inferred.

It is not possible to envoke a unique concept to explain all the results. However, the overall pattern which emerges from this study indicates that as the ionic character of the growing polymer–gegenion ion pair is enhanced, whether by choice of initiator or solvent, the more reactive monomer is incorporated into the initial copolymer to a greater extent. An exception to this pattern arises when the alkali metals are used as initiators in tetrahydrofuran and the explanation for this unexpected result is not apparent.

The discrepancies between the compositions of the copolymers from initiation by the alkali metal dispersions and by the alkali metal–naphthalene complexes in tetrahydrofuran, probably arise from the heterogeneity and continuous initiation of the former systems as opposed to the homogeneity and instantaneous initiation of the latter systems.

References

1. Tobolsky, A. V., and J. D. Kelly, *J. Am. Chem. Soc.*, **81**, 1597 (1959).
2. Florin, R. E., *J. Am. Chem. Soc.*, **73**, 4468 (1951).
3. Florin, R. E., paper presented at 12th International Congress of Pure and Applied Chemistry, New York, 1951.
4. Overberger, C. G., L. H. Arond, and J. J. Taylor, *J. Am. Chem. Soc.*, **73**, 5541 (1951).
5. Overberger, C. G., R. E. Ehrig, and D. Tanner, *J. Am. Chem. Soc.*, **76**, 772 (1954).
6. Marvel, C. S., and J. F. Dunphy, *J. Org. Chem.*, **25**, 2209 (1960).
7. Overberger, C. G., and V. G. Kamath, *J. Am. Chem. Soc.*, **81**, 2910 (1959).
8. Overberger, C. G., and V. G. Kamath, *J. Am. Chem. Soc.*, **85**, 446 (1963).
9. Okamura, S., and T. Higashimura, *Kobunshi Kagaku*, **17**, 635 (1960).
10. Okamura, S., T. Higashimura, and K. Takeda, *Kobunshi Kagaku*, **18**, 389 (1961).
11. Tobolsky, A. V., and R. J. Boudreau, *J. Polymer Sci.*, **51**, S53 (1961).
12. Tobolsky, A. V., D. J. Kelley, K. F. O'Driscoll, and C. E. Rogers, *J. Polymer Sci.*, **28**, 425 (1958).
13. Tobolsky, A. V., and C. E. Rogers, *J. Polymer Sci.*, **38**, 205 (1959).
14. Rembaum, A., F. R. Ells, R. C. Morrow, and A. V. Tobolsky, *J. Polymer Sci.*, **61**, 155 (1962).
15. Spirin, Yu. L., A. A. Arest-Yakubovich, D. K. Polyakov, A. R. Gantmakher, and S. S. Medvedev, *J. Polymer Sci.*, **58**, 1181 (1962).
16. Korotkov, A. A., paper presented at IUPAC International Symposium on Macromolecular Chemistry, Prague, Sept. 1957; *Angew. Chem.*, **70**, 85 (1958).
17. Inoue, S., T. Tsuruta, and J. Furukawa, *Makromol. Chem.*, **42**, 12 (1960).
18. Dawans, F., and G. Smets, *Makromol. Chem.*, **59**, 163 (1963).
19. Rakova, G. V., and A. A. Korotkov, *Dokl. Akad. Nauk SSSR*, **119**, 982 (1958).
20. Korotkov, A. A., and N. N. Chesnokova, *Polymer Sci. USSR*, **2**, 284 (1961).
21. Kuntz, I., *J. Polymer Sci.*, **54**, 569 (1961).
22. Morton, M., and F. R. Ells, *J. Polymer Sci.*, **61**, 25 (1962).
23. Kuntz, I., and K. F. O'Driscoll, *J. Polymer Sci.*, **61**, 19 (1962).
24. Graham, R. K., D. L. Dunkelberger, and W. E. Goode, *J. Am. Chem. Soc.*, **82**, 400 (1960).
25. O'Driscoll, K. F., *J. Polymer Sci.*, **57**, 721 (1962).
26. Evans, A. G., and E. D. Owen, *J. Chem. Soc.*, **1959**, 4123.
27. Gilman, H., and A. H. Haubein, *J. Am. Chem. Soc.*, **66**, 1515 (1944).
28. Boudreau, R. J., Ph.D. Thesis, Princeton University, 1961.
29. Wiley, R. H., and B. Davis, *J. Polymer Sci.*, **46**, 423 (1960).
30. Natta, G., F. Danuso, and D. Sianesi, *Makromol. Chem.*, **30**, 238 (1959).
31. Overberger, C. G., and F. Ang, *J. Am. Chem. Soc.*, **82**, 929 (1960).
32. Pepper, D. C., *Trans. Faraday Soc.*, **45**, 397 (1949).
33. Brown, C. P., and A. R. Mathieson, *J. Chem. Soc.*, **1957**, 3620.
34. Eley, D. D., and A. W. Richards, *Trans. Faraday Soc.*, **45**, 425 (1949).
35. Perry, E., and C. S. Feldman, *J. Polymer Sci.*, **54**, 818 (1961).
36. Kanoh, N., A. Gotoh, T. Higashimura, and S. Okamura, *Makromol. Chem.*, **63**, 106 (1963).
37. Tobolsky, A. V., and K. F. O'Driscoll, *J. Polymer Sci.*, **31**, 123 (1958).
38. Tobolsky, A. V., and D. B. Hartley, *J. Polymer Sci.*, **A1**, 15 (1963).
39. Smid, J., and M. Szwarc, *J. Polymer Sci.*, **61**, 31 (1962).
40. Shima, M., D. N. Bhattacharyya, J. Smid, and M. Szwarc, *J. Am. Chem. Soc.*, **85**, 1306 (1963).

Résumé

On a initié la copolymérisation du styrène et du *p*-méthylstyrène avec des halogénures de métaux du type Friedel-Crafts, un peroxyde de benzoyle, un catalyseur de Ziegler

obtenu à partir de triéthylaluminium et de tétrachlorure de titane, des dispersions de métaux alcalins et des complexes métal alcalin-naphtalène, dans une variété de solvants polaires et non-polaires.   La composition du copolymère initial obtenu d'un mélange équimoléculaire des deux monomères a été employé comme base de comparaison de ces systèmes.   Le choix approprié de l'initiateur et du solvant permet d'obtenir des compositions du copolymère variant de 25 à 79% en poids de styrène.   Les catalyseurs cationiques donnent des copolymères avec une teneur basse en styrène, tandis que les initiateurs anioniques et les initiateurs de transfert électronique produisent des copolymères avec une teneur élevée en styrène.   Les compositions des copolymères initiaux sont discutées brièvement du point de vue du caractère inoique de la paire ionique: polymère- "gegen-ion" et de la polarité du milieu réactionnel.

Zusammenfassung

Die Kopolymerisation von Styrol und p-Methylstyrol wurde mit Friedel-Crafts-Metallhaliden, Benzoylperoxyd, einem Ziegler-Katalysator aus Triäthylaluminium und Titantetrachlorid, Alkalimetalldispersionen und Alkalimetallnaphthalinkomplexen in verschiedenen polaren und nichtpolaren Lösungsmitteln gestartet.   Die Zusammensetzung des Anfangskopolymeren aus einer äquimolaren Monomermischung wurde als Grundlage des Vergleichs dieser Systeme genommen.   Durch geeignete Wahl von Starter und Lösungsmittel konnte die Kopolymerzusammensetzung in den Grenzen von 25 bis 79 Gewichtsprozenten Styrol variiert werden.   Kationische Katalysatoren liefern Kopolymere mit niedrigem, anionische und Elektronübertragunsstarter dagegen Kopolymere mit einem hohen Styrolgehalt.   Die Zusammensetzung der Anfangskopolymeren wird in bezug auf den ionischen Charakter des Ionenpaares wachsendes Polymeres-Gegenion und der Polarität des Reaktionsmittels kurz diskutiert.

Free-Radical Polymerization of Olefins*

GEORGE A. MORTIMER and LLOYD C. ARNOLD, *Plastics Division, Monsanto Chemical Co., Texas City, Texas*

Synopsis

Propylene, butene-1, isobutylene, 3,3-dimethylbutene-1, and tetradecene-1 were polymerized at high pressures at 130–150°C. with di-*tert*-butyl peroxide initiator to give low molecular weight polymers.   Free radical copolymerization of propylene and isobutylene was also demonstrated.   Facile chain transfer to give relatively stable radicals was blamed for the low rates and degrees of polymerization.   The molecular weights were shown to be controlled by chain transfer.

Introduction

Free radical polymerization of olefins other than ethylene has received very little attention.   Exposure of propylene,[1] isobutylene,[2] hexene-1,[3] diisobutylene,[4] and hexadecene-1[5] at low pressures, in the liquid phase, to ionizing radiation has been shown to give low molecular weight polymers. Although the exact mechanism is unknown, it is now certain that these polymerizations did not go by a free radical path.[1,2]   Irradiation of isobutylene with α-rays in the vapor phase also gave low polymers, and again a nonradical mechanism was indicated.[6]

The numerous studies made of the reactions of alkyl free radicals in the presence of olefins at high temperatures at vacuum pressures have clearly shown that addition to olefins takes place.[7]   Thus, polymerization of propylene was observed, and claimed to be similar to polymerization of ethylene, both being carried out above 300°C. with azomethane as the radical source.[8]   An attempt to polymerize hexadecene-1 with azobisisobutyronitrile at 80°C. was successful to the extent that 0.1% of a product having a degree of polymerization (DP) of 2.0 was isolated.[5]   An instance of benzoyl peroxide initiated polymerization of octene-1 to a polymer of DP = 5 has also been reported.[17]

In view of our success in copolymerizing α-olefins with ethylene at high pressure,[9] it became of interest to study the reactions of the olefins alone at high pressure in the presence of a free-radical initiator.   As this work was drawing to a close, Brown and Wall[10] published an account of the polymerization of propylene at pressures ranging from 74,000 to 240,000 psi initiated by γ-rays.   A free-radical mechanism was clearly indicated from their work.[11]

Experimental

The olefin plus di-*tert*-butyl peroxide (DTBP) in a small amount of benzene were pumped into a preheated, steel autoclave until the desired pressure was reached. The pressure and temperature were held constant during the reaction, which was terminated by carefully opening the valve on the bottom of the autoclave and discharging the contents into an open 4-liter, heavy-walled Erlenmeyer flask. After practice, this operation could be performed without loss of nonvolatile material. The autoclave and flask were thoroughly washed with benzene. The benzene (and unchanged monomer when it, too, was condensable) were removed at reduced pressure by using a rotary film evaporator until no more material distilled. The polymeric product remained as a viscous, colorless to pale yellow liquid. Number-average molecular weights were determined in toluene with a Mecrolab vapor pressure osmometer. All other evaluations were performed in the standard ways.

The propylene used was polymerization grade, nominally 99.9% pure, and was not analyzed. Analyses of the other olefins by gas chromatography were as follows: butene-1: total butenes 99.79%, butadiene 0.16%, isobutane 0.01%, propylene 0.03%, propane 0.01%; isobutylene: isobutylene 99.14%, butene-2 0.41%, isobutane 0.30%, *n*-butane 0.03%, propylene 0.11%, propane 0.02%, butadiene 0.00%, total C_5's 2.99%; 3,3-dimethylbutene-1: 3,3-dimethylbutene-1 92.5%, 2-methylbutene-2 4.1%, other olefins 0.7%, total alkanes 2.6%, unidentified 0.1%. A C_{11}-C_{15} α-olefin mixture (Oronite Chemical Co.) was determined to have $\overline{M}_n = 204$ by our method, and will be referred to hereafter as tetradecene-1 mixture.

Copolymerization experiments were carried out with C^{14}-labeled monomers. The polymer composition was determined by scintillation counting.

Results

It was found that all of the olefins studied homopolymerize to give low molecular weight amorphous polymers. From Table I, it is seen that, at

TABLE I

Polymerization Rates and Degrees of Polymerization at 20,000 psi, 130°C.

Olefin	Rates $\times 10^3$, in (l./mole/sec.)$^{1/2}$ [a]	$\overline{DP}$
Ethylene	370.	10,000
Propylene	4.3	19
Butene-1	0.63	7
Isobutylene	2.1	14
3,3-Dimethylbutene-1	1.2	4
Tetradecene-1 (mixture)	3.7	3

[a] Calculated as $R_p/[M](k_d[I])^{1/2}$, where R_p = rate of polymerization, M = monomer, and k_d = rate of decomposition of the initiator I.

the specified conditions, all these olefins polymerize more slowly (about 100 times) than ethylene and give polymers of much lower degree of polymerization than ethylene.

The effect of increasing reaction pressure is to increase both the polymerization rate and molecular weight. This behavior is illustrated with data for propylene in Table II, and is similar to that found for ethylene.[12] The effect of increasing temperature is seen from Table III to be the same as for any peroxide-initiated vinyl polymerization. Thus, the high pressure polymerization of olefins appears to be a typical, high pressure vinyl polymerization.

Once homopolymerization of these olefins was established, it became of interest to examine the copolymerization of two olefins of different structure. The results, shown in Table IV, indicate that copolymerization of

TABLE II
Polymerization of Propylene at 130°C, 0.112 mole/l. DTBP

Pressure, psi	Rate, %/hr.	$\bar{M}_n$
10,000	1.5	668
20,000	2.1	—
20,000	1.4	737
30,000	4.2	888
40,000	5.0	1070

TABLE III
Polymerization at 20,000 psi, 0.112 mole/l. DTBP

Monomer	Temperature, °C.	$\bar{M}_n$
Propylene	130	737
Propylene	150	676
Isobutylene	130	771, 778
Isobutylene	148	588

TABLE IV
Propylene–Isobutylene Copolymerization at 20,000 psi, 130°C., 0.112 mole/l. DTBP

Feed composition		Polymer composition			
Propylene, mole-%	Isobutylene, mole-%	Propylene, wt.-%	Isobutylene, wt.-%	Rate, %/hr.	$\bar{M}_n$
100	0	100	0	1.4	737
100	0	100	0	2.1	—
93	7	—	5.4	2.8	781
91	9	—	6.7	2.7	806
25	75	13.8	—	1.6	588
0	100	0	100	1.0	771
0	100	0	100	—	778

propylene and isobutylene takes place as readily as homopolymerization. In fact, both the rate and the $\bar{M}_n$ show an apparent maximum with respect to composition in the vicinity of 8% isobutylene. Because of low $\overline{DP}$ of the copolymers, copolymerization reactivity ratios were not calculated.

Discussion

These polymerizations appear to be completely controlled by chain transfer. Evidence for this conclusion is strong. First, infrared and nuclear magnetic resonance spectra indicated substantial amounts of polymer structural features that could not arise except by chain transfer. Second, the molecular weights of polymer made at varying temperatures and initiator concentrations are inconsistent with the kinetics of termination-controlled polymerization but completely consistent with the kinetics of transfer-controlled polymerization. This situation was expected, since olefins containing hydrogen atoms α to the double bond have been shown to be strong chain-transfer agents in ethylene polymerization.[9] Severe rate retardation was also found in olefin-modified ethylene polymerization,[9]

TABLE V
Partial Infrared Spectra of Olefin Polymers

Monomer	CH₃ bending	Vinylidene CH bending	Vinyl CH bending	trans-Vinylene CH bending	CH₂ rocking
Propylene	1370 (S)	887 (W)	908 (W)	969 (M)	735 (W)
Butene-1	1370 (S)	883 (VW)	906 (M)	961 (M)	759 (W), 719 (W)
Isobutylene	1378 (S), 1360 (VS)	884 (W)	Absent	Absent	Absent
3,3-Dimethylbutene-1	1382 (S), 1360 (VS)	887 (W)	908 (VW)	970 (M)	Absent

ᵃ The spectra were so taken that the C=C stretching band at ca. 1640 cm.⁻¹ was weak (W) and the CH₂ bending peak at ca. 1460 cm.⁻¹ was very strong (VS). The other symbols are strong (S), medium (M), and very weak (VW).

TABLE VI
Relative Amounts of Unsaturation in Olefin Polymers

| Monomer | Relative unsaturationᵃ | | |
	Vinylidene	Vinyl	trans-Vinylene
Propylene	1	1	5
Butene-1	0.25	1	1.5
Isobutylene	Present	Absent	Absent
3,3-Dimethylbutene-1	7	1	14

ᵃ For each polymer, vinyl was arbitrarily set at unity. No attempt was made to determine the relative amounts of unsaturation between different polymers.

and it is felt that extensive chain transfer to form relatively stable radicals is the reason that polymerization rates and degrees for the olefins of this study are so much lower than for ethylene (see Table I).

Tables V and VI present the salient features of the infrared spectra of the homopolymers. The 735 cm.$^{-1}$ band in the propylene is assigned as n-propyl endgroups, which could arise if the growing polymer chain abstracted a hydrogen atom (presumably from the monomer). The presence of —CH$_2$CH$_2$-units in about the right amount to be terminal propyl groups was also detected by nuclear magnetic resonance. Vinyl endgroups were also detected.

The polybutene-1 showed the 760 cm.$^{-1}$ band characteristic of pendant ethylene groups in polybutenes.[13] The band at 720 cm.$^{-1}$ is usually ascribed to long —CH$_2$-sequences,[14] and is probably due to endgroups resulting from hydrogen abstraction. The 1.5:1 ratio of internal to vinyl unsaturation is close to the 2:1 ratio found to be due to chain transfer in butene-modified polyethylenes.[9]

The polyisobutylene shows only vinylidene unsaturation, the only type that can arise from chain transfer to isobutylene. The occurrence of chain transfer for these three monomers seems established beyond question.

Inasmuch as it had been shown previously that chain transfer occurs primarily by abstraction of the hydrogen atoms α to the double bond,[9] it was of interest to study the polymerization of 3,3-dimethylbutene-1 which has no α-hydrogen atoms. If both the rate and $\overline{DP}$ of olefins with α-hydrogens are low because of rapid chain transfer and consequent formation of very stable radicals, then dimethylbutene should form high polymers at fast rates. Unfortunately, the dimethylbutene experiments were not definitive. The large amounts of vinylidene and *trans*-vinylene unsaturation found are evidence of extensive chain transfer to the 2-methylbutene-2 impurity. Hence, the $\overline{M}_n$ and rate are depressed by an unknown amount. The values given in Table I for dimethylbutene are therefore not representative of the pure monomer.

The expression for the kinetic chain length of an initiated radical polymerization, as given in a standard text,[15] is

$$\nu = k_p \, [\mathrm{M}]/2(fk_dk_t \, [\mathrm{I}])^{1/2} \tag{1}$$

If one substitutes the simple Arrhenius expressions for the rate constants of eq. (1), it can be shown that, at two different temperatures, indicated here by the subscripts 1 and 2, that

$$\frac{\overline{DP}_2}{\overline{DP}_1} = \frac{[\mathrm{M}_2]}{[\mathrm{M}_1]} \exp\left\{ \frac{1}{2R} \, (2E_p{}^* - E_t{}^* - E_d{}^*) \left(\frac{1}{T_1} - \frac{1}{T_2} \right) \right\} \tag{2}$$

if the polymer molecular weight is controlled by chain termination.

The E^* quantities refer to the activation energies of polymerization propagation and termination, and initiator decomposition respectively. If the differences in molecular weights shown in Table III were due to

termination control, $E_p{}^*$ would have to be about 18 kcal./mole for propylene and 15 kcal./mole for isobutylene. It has been shown that the polymerization of ethylene at high pressure has about the same activation energy as addition of radicals to ethylene at vacuum pressure.[16] By analogy, we should expect the same to be true for the olefins of this study, which would place $E_p{}^*$ at 6–8 kcal./mole.[7] Hence, the molecular weight changes observed in this study are inconsistent with termination control of molecular weight.

If the molecular weight is controlled by chain transfer to monomer, it can be shown by reasoning identical to that above, that at two temperatures

$$\frac{\overline{DP}_2}{\overline{DP}_1} = \exp\left\{\frac{\Delta E^*}{R}\left(\frac{1}{T_2} - \frac{1}{T_1}\right)\right\} \tag{3}$$

where ΔE^* is the activation energy for chain transfer minus the activation energy for propagation. Solving this equation by using the data of Table III gives ΔE^* as 1.5 kcal./mole for propylene and 4.7 kcal./mole for isobutylene. These values are in the range of values obtained in vacuum work.[7] Although these ΔE^* values probably contain an uncertainty of about ±1.5 kcal./mole, they do show that the molecular weight changes are consistent with transfer-controlled kinetics.

As a further check on the foregoing, the 30,000 psi run of Table II was repeated with the use of 0.062 mole/l. of initiator instead of 0.112 mole/l. If the molecular weight were termination-controlled, an increased $\overline{M}_n$ of 1200 would be expected because of the lower radical concentration. If transfer were controlling, no increase in $\overline{M}_n$ would be expected. The measured $\overline{M}_n$ was 820, within experimental error of the value in Table II.

References

1. Wagner, C. D., and D. O. Geymer, in *Proceedings of the International Symposium on Radiation-Induced Polymerization and Graft Polymerization*, Battelle Memorial Institute, Nov. 29–30, 1962, p. 56.

2. Davison, W. H. T., S. H. Pinner, and R. Worrall, *Chem. Ind., (London)*, **1957,** 1274.

3. Chang, P. C., N. C. Yang, and C. D. Wagner, *J. Am. Chem. Soc.*, **81,** 2060 (1959).

4. de Gaudemaris, G., and E. de Gorsky, *Compt. Rend.*, **247,** 2131 (1958); *ibid.*, **248,** 969 (1958).

5. Collinson, E., F. S. Dainton, and D. C. Walker, *Trans. Faraday Soc.*, **57,** 1732 (1961).

6. Mund, W., and P. Huyskens, *Bull. Classe Sci., Acad. Roy. Belge*, **36,** 610 (1950).

7. Kerr, J. A., and A. F. Trotman-Dickenson, in *Progress in Reaction Kinetics*, G. Porter, Ed., Pergamon Press, New York, 1961.

8. Sickman, D. V., and O. K. Rice, *J. Chem. Phys.*, **4,** 609 (1936).

9. Boghetich, L., G. A. Mortimer, and G. W. Daues, *J. Polymer Sci.*, **61,** 3 (1962).

10. Brown, D. W., and L. A. Wall, paper presented to Division of Polymer Chemistry,

142nd Meeting American Chemical Society, Atlantic City, N. J., September 1962: *Preprints*, **3**, 393 (1962).

11. Brown, D. W., and L. A. Wall, *J. Phys. Chem.*, **67**, 1016 (1963).

12. Symcox, R. O., and P. Ehrlich, *J. Am. Chem. Soc.*, **84**, 531 (1962).

13. Harvey, M. C., and A. P. Ketley, *J. Appl. Polymer Sci.*, **5**, 247 (1961).

14. Tobin, M. C., *J. Phys. Chem.*, **64**, 216 (1960).

15. Flory, P. J., *Principles of Polymer Chemistry*, Cornell Univ. Press, Ithaca, N. Y., 1953, pp. 133, 138.

16. Gilchrist, A., in *The Physics and Chemistry of High Pressures*, Gordon & Breach, New York, 1963, p. 219.

17. Kharasch, M. S., and A. Fono, *J. Org. Chem.*, **23**, 324 (1958).

Résumé

On a polymérisé le propylène, le butadiène-1, l'isobutylène, le 3,3-diméthylbutadiène-1, et le tétradécène-1 sous pression élevée à 130–150°C en présence de peroxyde de di-*t*-butyle comme initiateur, pour donner des polymères de bas poids moléculaire. Ainsi on a mis en évidence la copolymérisation par radicaux libres du propylène avec l'isobutylène. Un transfert de chaîne facile donnant des radicaux relativement stables, est responsable des vitesses et degrés de polymérisation très bas. On démontre que le poids moléculaire est contrôlé par transfert de chaîne.

Zusammenfassung

Propylen, Buten-1, Isobutylen, 3,3-Dimethylbuten-1 und Tetradecen-1 wurden bei hohem Druck und 130–150°C unter Verwendung von Di-*t*-butylperoxyd als Starter zu niedrigmolekularen Polymeren polymerisiert. Auch radikalische Kopolymerisation von Propylen und Isobutylen wurde nachgewiesen. Leicht eintretende Kettenübertragung unter Bildung relativ stabiler Radikale wurde für die niedrige Geschwindigkeit und den niedrigen Polymerisationsgrad verantwortlich gemacht. Es wird gezeigt, dass das Molekulargewicht durch die Kettenübertragung bestimmt wird.

BOOK REVIEW

N. G. GAYLORD, Editor

Newer Methods of Polymer Characterization (Polymer Reviews, Vol. 6), B. KE, Editor, Interscience, New York, 1964. xii + 722 pp., $24.50.

The editorially stated objective of the "Polymer Reviews" series is to provide a review of a field while it is still in a process of development, and the latter requirement is certainly adequately met by a number of subjects in the area of polymer characterization. In this volume of the series, the Editor has maintained a fairly standard level of treatment that avoids repetition of theory and descriptions of apparatus and methods that are available in other reference works. This is not to say that these are lacking. A brief (in most cases) review of theory is given, then a description of apparatus and methods, and finally examples of application and potential use. The emphasis varies within this format, however, as must be inevitable both from the multi-authorship and the inherent variation in the subjects. In some, the review is concerned with the application of one physical tool to the solution of a variety of polymer problems, such as the use of DTA (B. Ke) and small-angle x-ray diffraction (W. O. Statton). Other chapters attack one problem in a variety of ways, e.g., orientation by wide angle x-ray, infrared dichroism, briefringence, and light scattering from solids (R. S. Stein). In others, one problem is considered from the standpoint of one method: fractionation by column methods (R. M. Screaton) and number-average molecular weight by elasto-osmometry (J. J. Hermans) are cases in point. There is also a difference in emphasis given to experimental methods on the one hand, and a review of applications on the other. The contribution on microtacticity (W. R. Krigbaum), a problem of great current interest, is one of the latter type. The treatment is excellently conceived here, bypassing much of the detail in favor of a critical evaluation of the various solid state and solution methods. A companion chapter on high-resolution NMR (D. W. McCall and W. P. Slichter) elaborates in a similar vein on this method as applied to configuration and structure problems. Little experimental commentary is provided but much on interpretation. In other cases, the primary departure from previous publications is newer experimental techniques, as in the treatment of light scattering and osmometry at elevated temperatures (R. Chiang).

While most of the methods covered have in one way or another found fairly wide use with important classes of synthetic polymers, optical rotatory dispersion (J. T. Yang) has been applied mainly to proteins and polypeptides. However, the synthesis of optically active polymers in recent years and the prospects for preferred helical configurations of synthetic polymers in solution in certain cases suggests that this tool will become of greater importance. A chapter is also included on the relatively little explored (only 11 references cited) topic of thermal changes taking place in a specimen undergoing deformation (B. Ke). Fluorescence techniques (G. Oster and Y. Nishijima) also have not been widely applied as yet. Remaining chapters are on deuteration and polarization in infrared (C. Y. Liang), electron diffraction (E. W. Fischer), flow birefringence (V. N. Tsvetkov), and monomolecular films (N. Beredjick). The authors are all well known in their subject areas, and the treatments reflect this closeness. (At one point, however, ebullioscopy as a MW method is dismissed as ineffective beyond a value of 20,000, while in reality, reliable values to 30,000 are obtainable and a method useful to 100,000 has been described.)

In total, the book should accomplish its goal of presenting the newest methods and refinements in the subject areas covered in such a way as to lay out the current level of accomplishment along with an indication of the potential for future use. All the chapters contain references up to 1962, routinely, and occasionally to 1963. There is occasional overlap with other, and only slightly earlier, review articles. Written by experts, the book will be useful to other experts for what it suggests for future polymer research and encouragement to developments in the lesser used fields covered. To the polymer chemist whose work interests lie other than primarily in characterization, the book will serve as a valuable statement of what the newer methods can do and how they might be useful as applied to his own work. In an age where the river of research literature has become a raging torrent, a critical and relatively concise review of the more important parts of the stream becomes ever more important despite the speed of the current, especially to the concerned nonexpert. Volume 6 is a valuable addition to the "Polymer Reviews" series.

W. R. Sorenson

Continental Oil Company
Ponca City, Oklahoma

NOTES

The Application of Schofield's Equation to the Uptake of Electrolytes by a Cation Exchange Resin

In a recent article,[1] Shone derived the Schofield's equation[2] and expressed it in the convenient form

$$\frac{C_0 - C^-}{C_0} \cong \frac{1}{X}\left[\frac{q}{(z\beta C_0)^{1/2}} - \frac{4}{z\beta\tau}\right] \tag{1}$$

where C_0 is the external electrolyte concentration (equiv./l. solution), C^- the concentration of anion in the cation resin phase (equiv./l. solution in the resin phase), X the half distance (cm.) between two parallel plane charged surfaces, z the valency of the attracted ion, and τ the equivalent surface charge density in the diffuse double layer (mequiv./cm.²). β is given by $8\pi F^2/1000\epsilon RT$, where F, ϵ, R, and T have their usual significance. For water at 30°C., $\beta = 1.09 \times 10^{15}$ cm./mequiv. The factor q depends on the ratio of the valencies of the diffusible ions; for symmetrical electrolytes (e.g., NaCl, NaBr) $q = 2$; for 1:2 electrolytes (e.g., Na_2CO_3) $q = 2.4495$, and for 1:3 electrolytes [e.g., $Na_3C_6H_5O_7$ (citrate)] $q = 2.65$.

In applying the above equation to the consideration of results obtained for a phenol-formaldehyde sulfonate cation exchange resin, Shone assumed that (1) the resin was an assemblage of flat, parallel charged surfaces spaced 2X cm. and (2) the space between the charged surfaces was filled with the solution of diffusible ions. On the basis of this model, he found the average distance of separation of surfaces to be 60 A. and the surface charge density to be 2.23×10^{-7} mequiv./cm.².

Lakshminarayanaiah[3] has used a similar cation exchange resin in his studies on the sorption of various electrolytes (NaCl, NaBr, Na_2CO_3, and $Na_3C_6H_5O_7$) by the resin. As the properties of the resin described by him satisfy the requirements of the model, an analysis of his results is carried out in the light of the above equation.

The data of Lakshminarayanaiah, have been converted suitably to conform to eq. (1) and plotted in Figure 1.

Equation (1) is applicable provided C_0 is small enough to be treated as an ideal solution. A value of 0.1N is considered the upper limit for ideal behavior;[4] still Schofield and Talibuddin[4] and Shone[1] have used results of electrolyte uptake up to $C_0 = 1.0$ for the evaluation of values for the important parameter X. In terms of eq. (1), X is given by the reciprocal of the slope of the linear part of the plot of $(C_0 - C^-)/C_0$ against $q/(z\beta C_0)^{1/2}$. Shone has shown that the plot of $(C_0 - C^-)/C_0$ against $q/(z\beta C_0)^{1/2}$ is linear for values of C_0 from 0.08 to 1.0 equiv./l. in the case of KCl electrolyte. The data of Lakshminarayanaiah are very sparse between $C_0 = 0.1$ and 1.0 for any given electrolyte to compute a reliable value for X. However, fulfillment of a particular demand of the theory, viz., that the linear parts of the plots of $(C_0 - C^-)/C_0$ against $q/(z\beta C_0)^{1/2}$ for different electrolytes should be parallel, makes it possible to utilize the data to derive a meaningful value for X.

Straight lines were therefore drawn (Fig. 1) through the three points ($C_0 = 0.1$, 0.5, and 1.0) for each of the four electrolytes in such a way as to make them run parallel to one another. The reciprocal of the slope of these lines gave a value of 60 A. for X. With an average value of 1.3 equiv./l. water filled internal volume as the exchange capacity E, of the resin, τ has a value of 7.8×10^{-7} mequiv./cm.². There will thus be 47×10^{13} charges/cm.² of internal surface. If these charges are assumed to be distributed uni-

formly, the distance between any two charges will be about 5 A. In sharp contrast to the resin material used by Shone, the resin used by Lakshminarayanaiah has a distance of separation between flat surfaces of two times, and a distance of separation between charges of nearly one-half times, the respective distances found by Shone for his material and therefore it has more pore volume and increased charge distribution.

It is relevant to observe that the concentration scale in which the important parameters of the resin phase (E, C^-) are expressed is at variance with the molality or molarity scale accepted for ion exchange resin systems.[5] But the precepts of the Schofield theory both demand and justify this adopted deviation from usage.
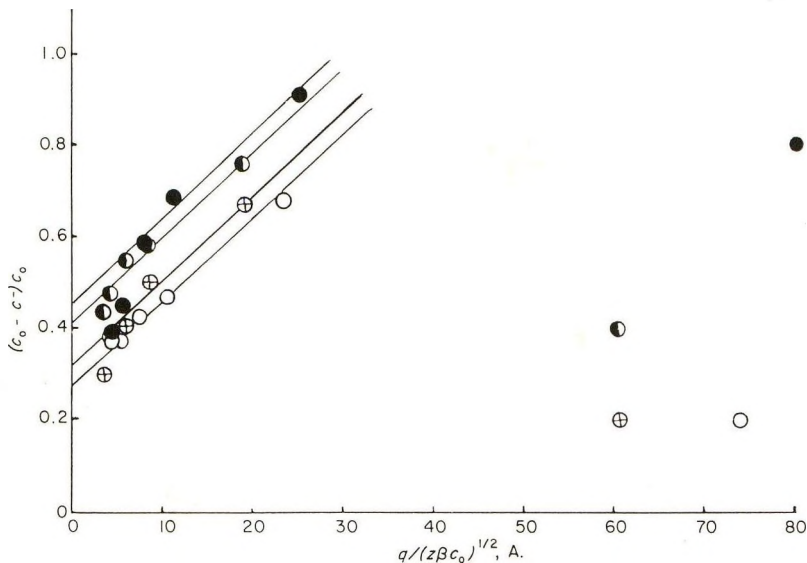

Fig. 1. The plot of $(C_0 - C^-)/C_0$ against $q/(z\beta C_0)^{1/2}$ for the electrolytes: O Na_2CO_3, ⊕ $NaCl$, ◐ $NaBr$, ● $Na_3C_6H_5O_7$.

The above analysis, although very informative, is very restricted in its overall application. The scatter of experimental points in Figure 1 points to the fact that the linear portion of the curve, from which the value of X is derived, is limited to the concentration range 0.1–1.0N. Below 0.1, the theory is completely inapplicable and this has been attributed to an overlapping of double layers by Shone. In the case of sodium citrate electrolyte, even though a straight line is drawn through three points to satisfy the theory, these points seem to be more on a curve than on the straight line, unlike corresponding points connected with the other three electrolytes. This curvature implies that either the theory is completely inapplicable or that it has a limited applicability in the neighborhood of 0.1N for 1:3 electrolyte.

The relative positions of the straight lines emphasize the effectiveness of the attracted ion in excluding the repelled anions from the resin phase. In the concentration range in which the Schofield theory is applicable (i.e., linear parts of the curves) the Na^+ ion excludes the other anions in the order $C_6H_5O_7^{-3} > Br^- > Cl^- > CO_3^{-2}$.

References

1. Shone, M. G. T., *Trans. Faraday Soc.*, **58**, 805 (1962).
2. Schofield, R. K., *Nature*, **160**, 408 (1947).
3. Lakshminarayanaiah, N., *J. Polymer Sci.*, **A1**, 139 (1963).
4. Schofield, R. K., and O. Talibuddin, *Disc. Faraday Soc.*, **3**, 51 (1948).
5. Helfferich, F., *Ion Exchange*, McGraw-Hill, New York, 1962, p. 76.

N. Lakshminarayanaiah

Department of Pharmacology
School of Medicine
University of Pennsylvania
Philadelphia, 4, Pennsylvania

ERRATA

An Evaluation of Column Thermal Diffusion as a Means of Polymer Characterization

(article in *J. Polymer Sci.*, A2, 611–625, 1964)

By DAVID L. TAYLOR

The Institute of Paper Chemistry, Appleton, Wisconsin

On page 611, Synopsis, line 9: for 40°C./cm. read 400°C./cm.

On page 612, line 36: for 250°C. read 25°C.

On page 614, Equation (5) should read:

$$(1/r)(\partial/\partial r)(rD'c\theta + rD\ \partial c/\partial r) = v_z\ \partial c/\partial z$$

Equation (6) should read:

$$\frac{d^2P}{dr^2} + \left(\frac{\theta D'}{D} + \frac{1}{r} + \frac{\theta}{D}\frac{\partial D}{\partial T}\right)\frac{dP}{dr} + \left(\frac{\gamma v_z}{D} + \frac{\theta D'}{rD} + \frac{\theta^2}{D}\frac{\partial D'}{\partial T}\right)P = 0$$

On page 620, line 3: $-\alpha c/\alpha r$ should read $-\partial c/\partial r$

line 5: $\alpha^2 c/\alpha r^2$ should read $\partial^2 c/\partial r^2$

line 8: $\alpha^2 c/\alpha r^2$ should read $\partial^2 c/\partial r^2$, also d^2p/dr^2 should read d^2P/dr^2

line 19: dc/dr should read $\partial c/\partial r$

On page 621, line 5: $\alpha^2 c/\alpha r^2$ should read $\partial^2 c/\partial r^2$

line 20: for radical read radial

line 26: $\alpha c/\alpha r$ should read $\partial c/\partial r$

line 35: $\alpha c/\alpha r$ should read $\partial c/\partial r$

line 36: $\alpha^2 c/\alpha r^2$ should read $\partial^2 c/\partial r^2$

Polymerization Behavior of Aziridines with 1,2-Epoxides

(article in *J. Polymer Sci.*, A2, 2481–2487, 1964)

By C. G. OVERBERGER and MARTIN TOBKES

Department of Chemistry, Polytechnic Institute of Brooklyn, Brooklyn, New York

On page 2481, under the heading RESULTS AND DISCUSSION, the subheading should read:

Polymers Derived from 2-Ethylaziridine and 1,2-Epoxides

On page 2485, 7th text line from the top, read "alkaline saturated" instead of "alka-line-saturated." The solution was saturated sodium chloride which was made alkaline rather than saturated alkali to which sodium chloride was added.

On page 2485, 3rd heading, should read "Epoxide" rather than "Epoxyde."

On page 2485, 5th heading, should read "BF₃" rather than "Bf₃."

On page 2486, 5th line of the Résumé, read "l'époxide" rather than "l'eposide."